Journal of Biological Regulators & Homeostatic Agents

Volume 27, Number 1, January-March 2013

CONTENTS

EDITORIAL

COMPARISON OF BENEFICIAL ACTIONS OF NON-STEROIDAL ANTI-INFLAMMATORY DRUGS TO FLAVONOIDS

P. CONTI[1], G. VARVARA[2], G. MURMURA[2], S. TETÈ[2], G. SABATINO[3], A. SAGGINI[4], M. ROSATI[5], E. TONIATO[1], A. CARAFFA[6], P. ANTINOLFI[6], F. PANDOLFI[7], G. POTALIVO[6], R. GALZIO[8], G. MACCAURO[9] and T. C. THEOHARIDES[10]

[1]Immunology Division, Department of Cancer and Neuroscience, University of Chieti, Chieti, Italy; [2]Dental School, University of Chieti, Italy; [3]Neonatology Division, University of Chieti, Italy; [4]Dermatology Department, University Tor Vergata, Rome, Italy; [5]Gynecology Division, Santo Spirito Hospital, Pescara, Italy; [6]Orthopedics Division, University of Perugia, Perugia, Italy; [7]Department of Medicine, Catholic University of Rome, Rome, Italy; [8]Department of Health Sciences, University of L'Aquila, Italy; [9]Department of Orthopedics, Catholic University, Rome, Italy; [10]Molecular Immunopharmacology and Drug Discovery Laboratory, Department of Molecular Physiology and Pharmacology, Tufts University School of Medicine, Boston, MA, USA

Received September 15, 2012 - Accepted January 25, 2013

Inflammation is involved in increasing number of diseases necessitating the development of new, effective and safe treatments. Non steroidal anti-inflammatory drugs (NSAIDs) have been helpful in many instances, but they only inhibit cyclooxygenase (COX), but not the generation or actions of cytokines. Instead, some natural flavonoids have multiple anti-inflammatory effects, including COX inhibition, and a much safer profile. Increasing evidence indicates that inflammation plays a critical role in the pathogenesis of many diseases that also involve mast cells (1-3) (Table I). Consequently, the need for new, effective and safe anti-inflammatory drugs is all the more urgent. Corticosteroids are quite potent, but have many adverse effects such as increased risk of infections, osteoporosis, glaucoma and depression (4-8). Biological agents such anti-TNF are useful in certain conditions, such as rheumatoid arthritis and psoriasis, but has been associated with increased risk of infection and leukemia.

Non-steroidal anti-inflammatory drugs (NSAIDs)

Non-steroidal anti-inflammatory drugs (NSAIDs) have proved useful in numerous settings (9-14). However, they can lead to gastrointestinal (GI) bleeding and the COX2 inhibitors have been associated with increased risk of myocardial infarctions (15-18). Moreover, a recent study reported that using NSAIDs, such as ibuprofen, together with selective serotonin re-uptake inhibitors (SSRIs) reduces the antidepressant effect of the latter (19-21), while increasing the risk of GI bleeding with SSRIs (22-25).

Flavonoids

Some naturally occurring flavonoids such as quercetin, and its closely structurally related luteolin, have potent anti-oxidant and anti-inflammatory activity (26-29). Flavonoids are very lipophilic

Key words: inflammation, non steroid anti-inflammatory drugs, flavonoids

Mailing address: Theoharis C. Theoharides, M.S., Ph.D., M.D., Molecular Immunopharmacology and Drug Discovery Laboratory, Department of Molecular Physiology and Pharmacology, Tufts University School of Medicine, Suite J304, 136 Harrison Avenue, Boston, MA 02111, USA
Tel.: +1 617 636-6866 Fax: +1 617 636-2456
e-mail: theoharis.theoharides@tufts.edu

0393-974X (2013)

Table I. *Diseases involving sterile inflammation.*

Disease
Asthma
Atopic dermatitis
Autism
Chronic fatigue syndrome
Coronary artery disease
Fibromyalgia/myalgic encephalopathy
Inflammatory bowel disease
Interstitial cystitis/bladder pain syndrome
Multiple sclerosis
Psoriasis

Table II. *Anti-inflammatory actions of luteolin and NSAIDs.*

Actions	**Luteolin**	**NSAIDs***
Cyclooxygenase inhibitor	X	X
Anti-oxidant	X	-
Anti-inflammatory	X	-
Mast cell inhibitor	X	-
Microglial inhibitor	X	-
Cytokine release inhibitor	X	-
Blood vessel stabilizer	X	-
Neuroprotective	X	-
Metal chelator	X	-
T effector cell inhibitor	X	Stimulates

**Induce gastritis, exacerbate asthma, decrease antidepressant action of SSRIs*

with oral absorption less that 10% (30-32). The main metabolism of luteolin is by glucoronidation, methylation, and sulphation (30;33-36). One also has to be aware of unspecified sources of luteolin as the cheapest sources are peanut shells that could induce allergic reactions in susceptible individuals, or from fava beans that could lead to hemolytic anemia in those patients of Mediterranean origin lacking the enzyme glucose-6 phosphate dehydrogenase (G6PD).

Increasing evidence indicates that certain flavonoids have potent antioxidants, free radical scavengers, anti-inflammatory and mast cell inhibitory activity (37-42). Quercetin and its structural analogue luteolin are potent mast cell inhibitors (43-46). Quercetin and luteolin can also inhibit the release of histamine, leukotrienes (LTs) and PGD_2 (47), as well as IL-6, IL-8, TNF and tryptase from human cultured mast cells (43). Luteolin also inhibits mast cell cytokine release (48-52), and mast cell-dependent stimulation of activated T cells (53-59). Luteolin also inhibits auto-immune T cell activation (19, 53, 56). Quercetin also has potent COX2 inhibitory activity (60-63) as does the structurally related kampferol (64-67).

Luteolin and quercetin are generally safe (68-75), and can even protect against chemically-induced hepatotoxicity (76). A dietary supplement with "liposomal luteolin" using olive kernel oil in soft gel capsules, that increases oral absorption, was used for 4 months in a preliminary case-series of 37 autistic children and led to significant benefit with minmal adverse effects (77).

CONCLUSION

The available evidence indicates that certain flavonoids, especially luteolin, have a better anti-inflammatory and saftey profile than NSAIDs, making it attractive for further development.

ACKNOWLEDGEMENTS

Aspects of the work discussed were funded in part by the Autism Research Institute, the National Autism Association, Safe Minds and Theta Biomedical Consulting & Development Co., Inc.

Disclosures**:** TCT is the inventor of US patents No. 6,624,148; 6,689,748; 6,984,667, and EPO 1365777, which cover methods and compositions of mast cell blockers, including flavonoids for inflammatory diseases, as well as US patents No. 7,906,153 and 8,268,365 for treatment of neuro-inflammatory conditions. NeuroProtek® hsas US tadermark 3,225,924. All patents and trademarks have been assigned to Theta Biomedical Consulting and Development Co., Inc. (www.thetabiomed.com).

REFERENCES

1. Theoharides TC, Alysandratos KD, Angelidou A, et al. Mast cells and Inflammation. Biochim Biophys Acta 2010; 1822:21-33.
2. Ruiz-Pérez MV, Sánchez-Jiménez F, Quesada AR, Medina MA. A re-evaluation of the mitogenic effect of serotonin on vascular endothelial cells. J Biol Regul Homeost Agents 2011; 1:13-20.
3. Maccauro G, Tripodi D, Saggini A, et al. Calcium ionophore A23187 and compound 48/80 induce PGD2 and tryptase in human cord blood-derived mast cells: lack of effect of IL-18. Eur J Inflamm 2012; 10:33-43.
4. De BK, Haegeman G, Elewaut D. Targeting inflammation using selective glucocorticoid receptor modulators. Curr Opin Pharmacol 2010; 10:497-504.
5. Spies CM, Bijlsma JW, Burmester GR, Buttgereit F. Pharmacology of glucocorticoids in rheumatoid arthritis. Curr Opin Pharmacol 2010; 10:302-7.
6. Mirzaei K, Hossein-Nezhad A, Mokhtari F, Najmafshar A, Khoshniat Nikoo M. VISFATIN/ NAMPT/PBCEF and cytokine concentration in multiple sclerosis patients compared to healthy subjects. Eur J Inflamm 2011; 9:31-7.
7. Di Muzio G, Perricone C, Ballanti E, et al. Complement system and rheumatoid arthritis: relationships with autoantibodies, serological, clinical features, and anti-TNF treatment. Int J Immunopathol Pharmacol 2011; 24:357-66.
8. Cantarini L, Iacoponi F, Lucherini OM, et al. Validation of a diagnostic score for the diagnosis of autoinflammatory diseases in adults. Int J Immunopathol Pharmacol 2011; 24:695-702.
9. Lee I, Cryer B. Epidemiology and role of nonsteroidal antiinflammatory drugs in causing gastrointestinal

bleeding. Gastrointest Endosc Clin N Am 2011; 21:597-612.
10. Roth SH. Coming to terms with nonsteroidal anti-inflammatory drug gastropathy. Drugs 2012; 72:873-9.
11. Tsoucalas G, Karamanou M, Androutsos G. Travelling through time with aspirin, a healing companion. Eur J Inflamm 2011; 9:13-6.
12. Impellizzeri D, Mazzon E, Di Paola R, Get al. PBS-1086, a Rel inhibitor of NF-kB, ameliorates collagen-induced arthritis in mice. Eur J Inflamm 2012; 10:51-9.
13. Tsoupras AB, Chini M, Tsogas N, Mangafas N, Demopoulos CA, Lazanas MC. *In vivo* effects of a *Ginkgo biloba* extract on platelet activating factor metabolism in two asymptomatic HIV-infected patients. Eur J Inflamm 2011; 9:107-16.
14. Veda P. Why are neutrophils polymorphonuclear? Eur J Inflamm 2011; 9:85-93.
15. Hinz B, Brune K. Cyclooxygenase-2--10 years later. J Pharmacol Exp Ther 2002; 300:367-75.
16. Drazen JM. COX-2 inhibitors--a lesson in unexpected problems. N Engl J Med 2005; 352:1131-2.
17. De Pita O, Nardis C, Lupi F, Luci CA, Frezzolini A, Pallotta S. Modulation of Toll-like receptors in psoriatic patients during therapy with adalimumab. Int J Immunopathol Pharmacol 2011; 24:185-8.
18. Galliera E, De Girolamo L, Randelli P, et al. High articular levels of the angiogenetic factors VEGF and VEGF-receptor 2 as tissue healing biomarkers after single bundle anterior cruciate ligament reconstruction. J Biol Regul Homeost Agents 2011; 1:85-91
19. Warner-Schmidt JL, Vanover KE, Chen EY, Marshall JJ, Greengard P. Antidepressant effects of selective serotonin reuptake inhibitors (SSRIs) are attenuated by antiinflammatory drugs in mice and humans. Proc Natl Acad Sci U S A 2011; 108:9262-7.
20. Belloli L, Carlo-Stella N, Ughi N, Marasini B. Cancer in Italian patients with systemic sclerosis. Eur J Inflamm 2011; 9:151-156.
21. Trellakis S, Farjah H, Bruderek K, Dumitru CA, Hoffmann TK, Lang S, Brandau S. Peripheral blood neutrophil granulocytes from patients with head and neck squamous cell carcinoma functionally differ from their counterparts in healthy donors. Int J Immunopathol Pharmacol 2011; 24:683-93.
22. Theoharides TC, Asadi S, Weng Z, Zhang B. Serotonin-selective reuptake inhibitors and nonsteroidal anti-inflammatory drugs-important considerations of adverse interactions especially for the treatment of myalgic encephalomyelitis/chronic fatigue syndrome . J Clin Psychopharmacol 2011; 31:403-5.
23. De Amici M, Villani MA, Milanesi E, Rossini B, Barco S, Gerletti M, Ciprandi G. Adverse reactions to anaesthetics prevented by the use of specific laboratory tests Eur J Inflamm 2011; 9:79-81
24. Migueres M, Fontaine JF, Haddad T, Grosclaude M, Saint-Martin F, Bem David D, Crestani B. Characteristics of patients with respiratory allergy in France and factors influencing immunotherapy prescription: a prospective observational study (REALIS). Int J Immunopathol Pharmacol 2011; 24:387-400.
25. Boyaci H, Pala A, Argun Bariş S, Başyigit I, Yildiz F, Ilgazli A. The effects of inhaled steroid and theophylline on systemic inflammation in COPD. Eur J Inflamm 2011; 9:241-248.
26. Middleton E, Jr., Kandaswami C, Theoharides TC. The effects of plant flavonoids on mammalian cells: implications for inflammation, heart disease and cancer. Pharmacol Rev 2000; 52:673-751.
27. Armogida M, Spalloni A, Amantea D, Nutini M, Petrelli F, Longone P, Bagetta G, Nisticò R, Mercuri NB. The protective role of catalase against cerebral ischemia in vitro and in vivo. Int J Immunopathol Pharmacol 2011; 24:735-47.
28. Scaramuzzo L, Manicone PF, Graci C, Muratori F, Spinelli MS, Damis G, Raffaelli L, Maccauro G. Morphological modifications in osteoarthritis: a scanning electron microscopy study Eur J Inflamm 2011; 9:73-78
29. Chatzovoulos P, Tsoupras AB, Samiotaki M, Panayotou G, Demopoulos CA, Dotsika E. PAF metabolic enzymes and PAF-like activity in *L. infantum* and *L. major* promastigotes. Eur J Inflamm 2011;9:231-239.
30. Walle T. Absorption and metabolism of flavonoids. Free Radic Biol Med 2004; 36:829-37.
31. Hossein-Nezhad A, Mirzaei K, Aslani S, Tootee A, Karimi F. MIF expression in induced peripheral blood mononuclear cells by vitamin D3 and its

potential correlation with resting metabolic rate in obesity. Eur J Inflamm 2011; 9:125-134.
32. Wu KG, Li TH, Chen CJ, Cheng HI, Wang TY. Correlations of serum Interleukin-16, total IgE, eosinophil cationic protein and total eosinophil counts with disease activity in children with atopic dermatitis. Int J Immunopathol Pharmacol 2011; 24:15-23.
33. Manach C, Donovan JL. Pharmacokinetics and metabolism of dietary flavonoids in humans. Free Radic Res 2004; 38:771-85.
34. Belizário JE. Pathogens and dead cells cooperate with cytokines in activating the innate and adaptive response. Eur J Inflamm 2011; 9:1-11.
35. Borrello S, Nicolò C, Delogu G, Pandolfi F, Ria F. TLR2: a crossroads between infections and autoimmunity? Int J Immunopathol Pharmacol 2011; 24:549-56.
36. Marotta F, Chui DH, Jain S, Polimeni A, Koike K, Zhou L, Lorenzetti A, Shimizu H, Yang H. Effect of a fermented nutraceutical on thioredoxin level and TNF-α signalling in cirrhotic patients. J Biol Regul Homeost Agents 2011; 1:37-45.
37. Kimata M, Shichijo M, Miura T, Serizawa I, Inagaki N, Nagai H. Effects of luteolin, quercetin and baicalein on immunoglobulin E-mediated mediator release from human cultured mast cells. Clin Exp Allergy 2000; 30:501-8.
38. Buonsenso D, Pirronti T, Genovese O, Gargiullo L, Ranno O, Valentini P. Side effects of the immune system: lessons from tuberculosis-related immune reconstitution inflammatory syndrome. Eur J Inflamm 2012; 10:1-10.
39. Park JA, Pak JJ, Kim J, Lee EY, Lee YJ, Song YW, Lee EB. Adenosine A2A receptor polymorphisms in Korean patients with systemic sclerosis. Int J Immunopathol Pharmacol 2011; 24:505-8.
40. Bellisai F, Morozzi G, Scaccia F, Chellini F, Simpatico A, Pecetti G, Galeazzi M. Evaluation of the effect of Bosentan treatment on proinflammatory cytokine serum levels in patients affected by Systemic Sclerosis. Int J Immunopathol Pharmacol 2011; 24:261-4.
41. Rosato E, Rossi C, Molinaro I, Giovannetti A, Pisarri S, Salsano F. Long-term N-acetylcysteine therapy in systemic sclerosis interstitial lung disease: a retrospective study. Int J Immunopathol Pharmacol. 2011; 24:727-33.
42. Tammaro A, Narcisi A, Persechino S, De Marco G, Camplone G. Contact allergy to disperse blue dye in goggles for swimming-bath. Eur J Inflamm 2011; 9:83-4.
43. Kempuraj D, Madhappan B, Christodoulou S, Boucher W, Cao J, Papadopoulou N, Cetrulo CL, Theoharides TC. Flavonols inhibit proinflammatory mediator release, intracellular calcium ion levels and protein kinase C theta phosphorylation in human mast cells. Br J Pharmacol 2005; 145:934-44.
44. Mazzoccoli G. The timing clockwork of life. J Biol Regul Homeost Agents 2011; 1:137-43.
45. Rigante D, Zampetti A, Bersani G, et al. Serum interleukin-18 in children with Henoch-Schönlein purpura: a promising marker of disease activity. Eur J Inflamm 2011; 9:157-68.
46. Yeh JL, Hsu JH, Hong YS, Wu JR, Liang JC, Wu BN, Chen IJ, Liou SF. Eugenolol and glyceryl-isoeugenol suppress LPS-induced iNOS expression by down-regulating NF-kappaB AND AP-1 through inhibition of MAPKS and AKT/IkappaBalpha signaling pathways in macrophages. Int J Immunopathol Pharmacol 2011; 24:345-56.
47. Kimata M, Shichijo M, Miura T, Serizawa I, Inagaki N, Nagai H. Effects of luteolin, quercetin and baicalein on immunoglobulin E-mediated mediator release from human cultured mast cells. Clin Exp Allergy 2000; 30:501-8.
48. Asadi S, Theoharides TC. Corticotropin-releasing hormone and extracellular mitochondria augment IgE-stimulated human mast-cell vascular endothelial growth factor release, which is inhibited by luteolin. J Neuroinflam 2012; 9:85.
49. Menghini L, Leporini L, Scanu N, Pintore G, La Rovere R, Di Filippo ES, Pietrangelo T, Fulle S. Effect of phytochemical concentrations on biological activities of cranberry extracts. J Biol Regul Homeost Agents 2011; 1:27-35.
50. Migliore A, Massafra U, Bizzi E, Vacca F, Martin-Martin LS, Granata M, Tormenta S, Laganà B. Efficacy and safety profile of intra-articular administration of Jointex® in patients suffering from symptomatic hip osteoarthritis: an open, prospective study with a 12-month follow-up. Eur J Inflamm

2011; 9:269-276.
51. Drago L, Vassena C, Dozio E, Corsi MM, De Vecchi E, Mattina R, Romanò C. Procalcitonin, C-reactive protein, interleukin-6, and soluble intercellular adhesion molecule-1 as markers of postoperative orthopaedic joint prosthesis infections. Int J Immunopathol Pharmacol 2011; 24:433-40.
52. Vignini A, Sartini D, Morganti S, Nanetti L, Luzzi S, Provinciali L, Mazzanti L, Emanuelli M. Platelet amyloid precursor protein isoform expression in Alzheimer's disease: evidence for peripheral marker. Int J Immunopathol Pharmacol 2011; 24:529-34.
53. Kempuraj D, Tagen M, Iliopoulou BP, et al. Luteolin inhibits myelin basic protein-induced human mast cell activation and mast cell dependent stimulation of Jurkat T cells. Br J Pharmacol 2008; 155:1076-84.
54. Suzuki K, Setoyama Y, Yoshimoto K, Tsuzaka K, Abe T**,** Takeuchi T. Decreased mRNA expression of two FOXP3 isoforms in peripheral blood mononuclear cells from patients with rheumatoid arthritis and systemic lupus erythematosus. Int J Immunopathol Pharmacol 2011; 24:7-14.
55. Savastano S, Balato N, Gaudiello F, Di Somma C, Brancato V, Colao A, Ayala F, Tarantino G. Insulin-like growth factor-1, psoriasis, and inflammation: a ménage à trois? Eur J Inflamm 2011; 9:277-83.
56. Verbeek R, Plomp AC, van Tol EA, van Noort JM. The flavones luteolin and apigenin inhibit in vitro antigen-specific proliferation and interferon-gamma production by murine and human autoimmune T cells. Biochem Pharmacol 2004; 68:621-9.
57. Saggini A, Maccauro G, Tripodi D, et al. Allergic inflammation: role of cytokines with special emphasis on IL-4. Int J Immunopathol Pharmacol 2011; 24:305-11.
58. Binici DN, Güneş N, Kayataş K, Pişkinpaşa N. The effects of interferon-α2b on intestinal flora in peritoneal fibrosis. Eur J Inflamm 2011; 9:135-9.
59. El-Hashim AZ, Renno WM, Abduo HT, Jaffal SM, Akhtar S, Benter IF. Effect of inhibition of the ubiquitin-proteasome-system and IκB kinase on airway inflammation and hyperresponsiveness in a murine model of asthma. Int J Immunopathol Pharmacol 2011; 24:33-42.
60. Xiao X, Shi D, Liu L, Wang J, Xie X, Kang T, Deng W. Quercetin suppresses cyclooxygenase-2 expression and angiogenesis through inactivation of P300 signaling 1. PLoS ONE 2011; 6:e22934.
61. Guillén D, Millán O, Brunet M. *In vitro* studies of the immunomodulatory effects of statins alone and in combination with immunosuppressive drugs. Eur J Inflamm 2011; 9:117-24.
62. Caporale CM, Notturno F, Pace M, et al. CD1A and CD1E gene polymorphisms are associated with susceptibility to multiple sclerosis. Int J Immunopathol Pharmacol 2011; 24:175-83.
63. Perricone C, De Carolis C, Giacomelli R, Greco E, Cipriani P, Ballanti E, Novelli L, Perricone R. Inhibition of the complement system by glutathione: molecular mechanisms and potential therapeutic implications. Int J Immunopathol Pharmacol 2011; 24(1):63-8.
64. Mahat MY, Kulkarni NM, Vishwakarma SL, et al. Modulation of the cyclooxygenase pathway via inhibition of nitric oxide production contributes to the anti-inflammatory activity of kaempferol. Eur J Pharmacol 2010; 642:169-76.
65. Almerigogna F, Fassio F, Giudizi MG, et al. Natural killer cell deficiencies in a consecutive series of children with herpetic encephalitis. Int J Immunopathol Pharmacol 2011; 24:231-8.
66. Berardi D, De Benedittis S, Scoccia A, Perfetti G. Evaluation of neridronate on the osseointegration process of endeous titanium implants in animal models. Eur J Inflamm 2011; 9:141-9.
67. Pozzi V, Mazzotta M, Lo Muzio L, et al. Inhibiting proliferation in KB cancer cells by RNA interference-mediated knockdown of nicotinamide N-methyltransferase expression. Int J Immunopathol Pharmacol 2011; 24:69-77.
68. Formica JV, Regelson W. Review of the biology of quercetin and related bioflavonoids. Food Chem Toxicol 1995; 33:1061-80.
69. Placido R, Auricchio G, Gabriele I, Galli E, Brunetti E, Colizzi V, Battistini L, Mancino G. Characterization of the immune response of human cord-blood derived gamma/delta T cells to stimulation with aminobisphosphonate compounds. Int J Immunopathol Pharmacol 2011; 24:101-10.
70. Harwood M, nielewska-Nikiel B, Borzelleca JF, Flamm GW, Williams GM, Lines TC. A critical

review of the data related to the safety of quercetin and lack of evidence of in vivo toxicity, including lack of genotoxic/carcinogenic properties. Food Chem Toxicol 2007; 45:2179-205.

71. Migliore A, Bizzi E, Massafra U, Vet al. A new chance to maintain remission induced by anti-TNF agents in rheumatoid arthritis patients: CYnAR study II of a 12-month follow-up. Int J Immunopathol Pharmacol 2011; 24:167-74.
72. Failli A, Legitimo A, Mazzoni A, Urbani L, Scatena F, Mosca F, Consolini R. The combination of immunosuppressive drugs with 8-methoxypsoralen and ultraviolet a light modulates the myeloid-derived dendritic cell function. Int J Immunopathol Pharmacol 2011; 24:89-99.
73. Kawanishi S, Oikawa S, Murata M. Evaluation for safety of antioxidant chemopreventive agents. Antioxid Redox Signal 2005; 7:1728-39.
74. Li L, Gu L, Chen Z, Wang R, Ye J, Jiang H. Toxicity study of ethanolic extract of Chrysanthemum morifolium in rats. J Food Sci 2010; 75:T105-T109.
75. Mazzoccoli G, Vendemiale G, De Cata A, Tarquini R. Change of γδTCR-expressing T cells in healthy aging. Int J Immunopathol Pharmacol 2011; 24:201-9.
76. Domitrovic R, Jakovac H, Milin C, Radosevic-Stasic B. Dose- and time-dependent effects of luteolin on carbon tetrachloride-induced hepatotoxicity in mice. Exp Toxicol Pathol 2009; 61:581-9.
77. Theoharides TC, Asadi S, Panagiotou JP. Effect of a luteolin formulation (NeuroProtek) on autism spectrum disorders-A case series. Int J Immunopathol and Pharmacol 2012; 25:317-232.

EDITORIAL

THE TRANSCRIPTIONAL REGULATORS, THE IMMUNE SYSTEM AND THE CIRCADIAN CLOCK

M. VINCIGUERRA[1], M. BORGHESAN[2], V. PAZIENZA[3], A. PIEPOLI[3], O. PALMIERI[3], R. TARQUINI[4], M.F. TEVY[5], A. DE CATA[6], and G. MAZZOCCOLI[6]

[1]University College London, Institute for Liver and Digestive Health, Division of Medicine, Royal Free Campus, London, United Kingdom; [2]Institute of Hepatology, Foundation for Liver Research, London, United Kingdom; [3]Department of Medical Sciences, Research Laboratory and Division of Gastroenterology, IRCCS Scientific Institute and Regional General Hospital "Casa Sollievo della Sofferenza", San Giovanni Rotondo (FG), Italy; [4]Division of Internal Medicine, University of Florence, Florence, Italy; [5]CSS-Mendel Institute, Rome, Italy; [6]Department of Medical Sciences, Division of Internal Medicine and Chronobiology Unit, IRCCS Scientific Institute and Regional General Hospital "Casa Sollievo della Sofferenza", San Giovanni Rotondo (FG), Italy

Received June 22, 2012 – Accepted November 6, 2012

The immune system function oscillates with a 24-hour period driving circadian rhythmicity of immune responses. A circadian timing system comprising central and peripheral oscillators entrains body rhythmicity of physiology and behavior to environmental cues by means of humoral signals and autonomic neural outputs. In every single cell an oscillator goes ticking through a molecular clock operated by transcriptional/translational feedback loops driven by the rhythmic expression of circadian genes. This clock gene machinery steers daily oscillations in the regulation of immune cell activity, driving the periodicity in immune system function. The transcriptional networks that regulate temporal variation in gene expression in immunocompetent cells and tissues respond to diverse physiological clues, addressing well-timed adjustments of transcription and translation processes. Nuclear receptors comprise a unique class of transcriptional regulators that are capable of gauging hormones, metabolites, endobiotics and xenobiotics, linking ligand sensing to transcriptional responses in various cell types through switching between coactivator and corepressor recruitment. The expression of coregulators is highly responsive to physiological signals, and plays an important role in the control of rhythmic patterns of gene expression, optimizing the switch between nycthemeral patterns, and synchronizing circadian rhythmicity with changing physiological demands across the light-dark cycle. The nuclear receptors and transcription factors expressed in the immune components contribute to the cross-talk between the circadian timing system, the clock gene machinery and the immune system, influencing transcriptional activities and directing cell-type specific gene expression programs linked to innate and adaptive immune responses.

Immune system function is characterized by biological rhythms in different frequency ranges, and in the healthy organism this multifrequency time structure comprises among the others rhythms

Key words: transcriptional regulator, clock gene, circadian rhythm, immunity

Mailing address: Gianluigi Mazzoccoli, M.D.,
Department of Medical Sciences,
Division of Internal Medicine and Chronobiology Unit,
Scientific Institute and Regional General Hospital
"Casa Sollievo della Sofferenza", Cappuccini Avenue,
San Giovanni Rotondo (FG), 71013 Italy
e-mail: g.mazzoccoli@operapadrepio.it

0393-974X (2013)

of the same frequency, prevalently with a period of approximately 24 hours and defined circadian (from the latin *circa*, about, and *dies*, a day), which may have the same phase or different phases and usually show a well-defined time-relation to each other (1). Circadian rhythmicity hallmarks immune system function in plants, insects, animals and humans, as well as the levels of humoral factors and cellular effectors: nycthemeral variations characterize phagocytic, complement, lysozyme and peroxidase activity in innate immunity, and antibody and cytokine production, leukocyte trafficking, proliferation and apoptosis in adaptive immunity (2-5).

The pattern of circadian rhythmicity of immune responses seems to be dependent on species, strain of animals, and type of immune cells and their specific functions. In humans, lymphocyte subpopulations present circadian variation of some of their subsets, with prevalence of cytotoxic function in the activity span and helper function in the resting span of the light/dark cycle, and this variation may influence magnitude and expression of the immune responses (6). The circadian variation of lymphocyte subsets has been related to circadian changes in cell production, release and destruction and to cell redistribution to the bone marrow, mobilization and migration to lymphoid and non-lymphoid organs and peripheral tissues. The phenomenon of lymphocyte subpopulation redistribution may involve several hormones (cortisol, prolactin, growth hormone, thyroid stimulating hormone), autonomic nervous system and monoamines (epinephrine, melatonin), cyto/chemochines, and may represent one of the crucial manifestation of neuro-endocrine-immune system interaction (7-9).

The existence of biological clocks in immune system components has been highlighted by studies performed on cells of the innate immune system and peripheral blood mononuclear cells (5, 10-14). Circadian clocks drive immune responses such as granzyme B and perforin production in rat natural killer cells, and the response to lipopolysaccharide stimulation in mouse peritoneal macrophages (5). Furthermore, circadian T cell immune responses are timed by a self-sustained oscillator, and the nuclear factor κB (NF-kB) pathway links the transcriptional processes to nycthemeral rhythmicity driven by the circadian clock (8).

The circadian clock circuitry

The nycthemeral variations of physiological and behavioral phenomena (sleep/wake, rest/activity- and fasting/feeding cycles) are controlled by a multipart circadian timing system comprising a master oscillator in the suprachiasmatic nuclei (SCN) of anterior hypothalamus, which are entrained by environmental timing cues, principally the light-dark cycle perceived/conveyed by the retino-hypothalamic system, and drive extra-SCN cerebral clocks and peripheral oscillators by means of outputs that may be humoral (cortisol, melatonin) or neural (autonomic nervous system) (15). At the molecular level, circadian rhythms are driven by transcriptional-translational feedback loops (TTL) generated by a set of interplaying genes, called clock genes, and their coded proteins, and the same as many peripheral tissues and cells, leukocytes also rhythmically express clock genes (5, 8, 10-12).

Genes belonging to the basic helix-loop-helix/Per-Arnt-Simpleminded (bHLH-PAS) domain family, encoded by *CLOCK* (or its paralog *NPAS2*) and *BMAL1/2* genes, play a central role in the molecular clock machinery. Heterodimers of the trascription factors CLOCK/BMALl/2 and NPAS2/BMALl/2 bind to Enhancer Box (E-box) DNA sequences in promoter regions and drive the transcription of *PERIOD* (*PER*) and *CRYPTOCHROME* (*CRY*) genes. After translation in the cytoplasm, PER and CRY proteins heterodimerize, translocate to the nucleus, and negatively regulate the trascriptional activity, completing the TTL. As a consequence, expression levels for these two sets of genes display anti-phasic oscillatory profiles with respect to one another, and the TTL completes a cycle in approximately 24 hours (15).

Core clock proteins undergo post-translational modifications (PTMs), and the serine/threonine protein kinases casein kinase (CK) 1 δ/ε and CK2, encoded by CSNK1D, CSNK1E and CSNK2 genes, are key regulators of the clock machinery. CK1 δ/ε and CK2 bind to and phosphorylate multiple circadian substrates, in particular the PERIOD proteins. Mammalian PERIOD proteins act as a scaffold with distinct domains that simultaneously bind CK and CRY, which is phosphorylated by CK only when both proteins are bound to mammalian PERIOD proteins (16).

The robustness and amplitude of the core TTL is increased and driven by the nuclear receptors (NRs) REV-ERBs and RORs. Transcription of *REV-ERBα/β* and *RORα/β/γ* is activated by CLOCK/BMAL1 heterodimer and produces REV-ERBs and RORs with negative and positive regulatory effects on *BMAL1* transcription, respectively: REV-ERBα/β bind ROR specific response elements (RORE) in clock gene promoters, and preventing the binding of the positive transcription regulator RORα, act as negative transcriptional regulators (17) (Fig. 1).

CLOCK/BMAL1 heterodimers regulate the transcription of circadian effector genes, including those encoding the proline-and acidic amino acid-rich domain basic leucine zipper (PAR-bZIP) transcription factors, including DBP (albumin gene D-site binding protein), TEF (thyrotroph embryonic factor), and HLF (hepatic leukaemia factor), and the bHLH transcription factors differentially expressed in chondrocytes protein (DEC)1 and DEC2, whereas the nuclear factor interleukin 3 regulated protein (NFIL3, also known as adenoviral E4 protein–binding protein, E4BP4) is encoded by *Nfil3/E4bp4* gene through the interplay of REV-ERBs with RORs on RORE and oscillates in opposite phase with respect to DBP (18).

Inhibitor of DNA binding genes (*Id1-Id4*) encode bHLH transcriptional repressors that are rhythmically expressed with circadian pattern and phase-locked relationship with canonical clock genes in multiple tissues including the SCN, suggesting that the ID proteins may be important for entrainment and

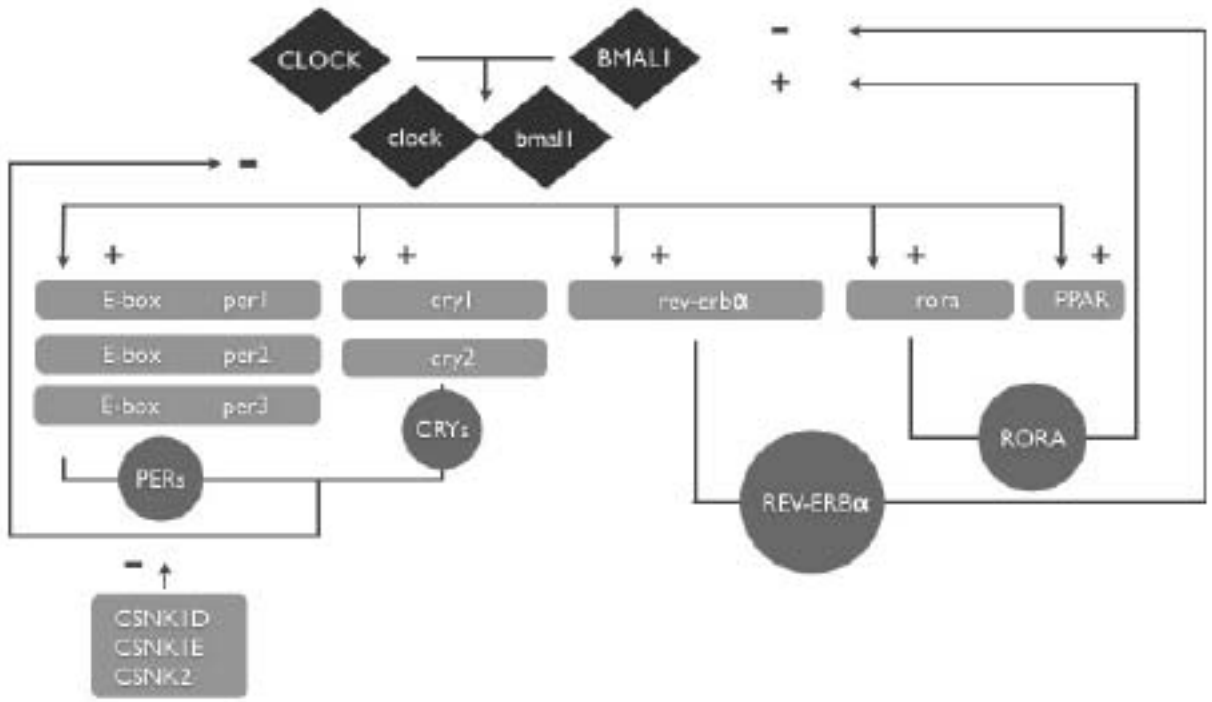

Fig. 1. *Description of the clock gene machinery. CLOCK, BMAL1 and RORα act as transcriptional activators, whereas PER, CRY, and REV-ERBα as transcriptional repressors, and casein kinase 1 and 2 are involved in posttranslational modifications. Heterodimers of the trascription factors CLOCK/BMALl bind to Enhancer Box (E-box) DNA sequences in promoter regions and drive the transcription of PERIOD (PER) and CRYPTOCHROME (CRY) genes. After translation in the cytoplasm, PER and CRY proteins heterodimerize, translocate to the nucleus, and negatively regulate the trascriptional activity, completing the TTL. Circadian proteins undergo post-translational modifications through the casein kinase (CK) 1 δ/ε and CK2, encoded by CSNK1D, CSNK1E and CSNK2 gene, The nuclear receptors REV-ERBs and RORs drive and increase robustness and amplitude of the core TTL, as transcription of REV-ERBα/β and RORα/β/γ is activated by CLOCK/BMAL1 heterodimer and produces REV-ERBs and RORs with negative and positive regulatory effects on BMAL1 transcription, respectively: REV-ERBα/β bind ROR specific response elements (RORE) in clock gene promoters, and preventing the binding of the positive transcription regulator RORα, act as negative transcriptional regulators. CSNK= casein kinase*

functioning of the mammalian circadian system, potentially acting through inhibition of the transactivation potential of CLOCK/BMAL1 on core clock and clock-controlled gene activity (19).

The role of the transcriptional regulators in the cross-talk between the circadian clock and the innate immune system

The immune system is directed to sites of infection by inflammation, an adaptive host response that is involved also in tissue repair processes. At the cellular level, genes that mediate inflammatory responses must be kept tightly repressed under normal conditions, but must also be rapidly and highly induced in the setting of infection or injury. Many of these genes are under the transcriptional control of signal-dependent transcription factors that include members of the NF-κB, activator protein 1 (AP-1, a heterodimer composed of c-Fos/c-Jun family members), and interferon regulatory factor (IRF) families of transcription factors. The activities and/or expression of these factors can be induced by a large number of receptor systems, including pattern recognition receptors for pathogen-associated molecules (Toll-like receptors, TLR), and receptors for cell-derived inducers of inflammation, such as IL1β, TNFα, and interferons. Upon activation, NF-κB, AP-1, and IRF proteins are capable of inducing the expression of hundreds of genes in diverse cell types that initiate and amplify inflammatory processes and promote the development of acquired immunity (20, 21).

Studies performed on homozygous *Clock* mutant mice have highlighted decreased expression of immune-related genes and dampened circadian rhythmicity of leukocyte variation in the peripheral blood (5). The levels of the proinflammatory cytokines interferon IL-1β and (IFN)-γ in the serum are considerably decreased in *Per2*$^{-/-}$ mice following lipopolysaccharide (LPS) challenge, while production of TNFα, IL-6, and IL-10 is conserved, and *Per2*$^{-/-}$mice are more resistant to LPS-induced endotoxic shock compared to control wild-type mice, suggesting that *mPer2* is an important regulator of NK cell function (22).

Studies performed in *Cry1*$^{-/-}$*Cry2*$^{-/-}$ cells have demonstrated that absence of the circadian protein cryptochrome (CRY) unlocks its inhibition on cAMP production, elevates cAMP and increases protein kinase A (PKA) signaling, with increased phosphorylation of p65 at S276 residue and activation of NF-κB signaling and ultimately constitutive elevation of proinflammatory cytokines in a cell-autonomous manner, suggesting a patho-physiological connection between disruption of the circadian clock circuitry and increased susceptibility to chronic inflammatory diseases (23).

Phagocytes are important components of the innate immune system, and one of the defense mechanisms through which phagocytes destroy pathogens is phagocytosis. The circadian protein TIMELESS controls the nychthemeral variations of bacterial phagocytosis in Drosophila melanogaster, and influences survival and sensitivity to infection mediated by changes in resistance through control of microbial load (4). Furthermore, circadian rhythmicity in phagocytic activity has been reported in endothermic and ectothermic vertebrates, but the precise timing of acrophase varies in different animals (24). Melatonin is implicated in the regulation of diurnal variation in phagocytic activity of leucocytes, based on correlation between circadian pattern of plasma melatonin and phagocytosis. In ectothermic vertebrates melatonin suppresses the phagocytic activity (24), whereas in endothermic diurnal or nocturnal vertebrates a positive correlation between levels of plasma melatonin and phagocytic activity of leukocytes has been reported. Furthermore, melatonin biosynthesis has been described in human peripheral blood mononuclear leukocytes, mouse and human bone marrow cells, and human lymphocytes (25). On the other hand, circulating hormones secreted under the control of the hypothalamic–pituitary–adrenal axis (corticotropin-releasing factor, CRF, adrenocorticotropic hormone, ACTH, and cortisol) regulate macrophage gene expression through binding to glucocorticoid receptor (GR) (26).

Studies performed on mice have shown that the promoter region of *mPer1* gene is characterized by a functional glucocorticoid-responsive element (GRE) essential and adequate for glucocorticoid signaling to cause a rapid increase in the level of *mPer1* mRNA: the elevation of the *mPer1* mRNA in response to stressors is dependent on the concentration of serum corticosterone suggesting that *mPer1* can be

considered a potential stress marker (27).

Mouse macrophages in spleen, lymph nodes, and peritoneum contain intrinsic circadian clockworks that operate autonomously and drive circadian rhythmicity in inflammatory and innate immune functions and in TNF-alpha and IL-6 secretion after stimulation with bacterial endotoxin at different circadian times (5). More than 8% of the macrophage transcriptome oscillates in a circadian fashion, including many important regulators for pathogen recognition and cytokine secretion, and these variations are not driven by systemic glucocorticoid oscillation nor by circadian recirculation of different cell types in the spleen, but are operated by autonomous cellular oscillators in splenic macrophages (10).

On the other hand, TNF-α influences the clock gene machinery interfering with the expression of the clock genes and in particular of *PER3*, and suppressing the expression of DBP, TEF and HLF. This interference may underlie the ''inflammatory clock gene response'', providing the link between the activation of innate immunity and fatigue associated with inflammatory/autoimmune diseases (28, 29).

In the connection between the circadian clock circuitry and the immune system a key role is played by the NRs, which encompass a family of ligand-regulated transcription factors operating as receptors for small lipophilic ligands (metabolites, hormones, drugs, environmental compounds), which influence their transcriptional activities, and in that way direct cell-type specific gene expression programs linked to physiological processes. A number of NRs are expressed in immune system tissues, in particular in the spleen and thymus, and may contribute to the cross-talk between the clock gene machinery and immune system regulation and function (30) (Fig. 2).

Furthermore, PER2 interacts with NRs and

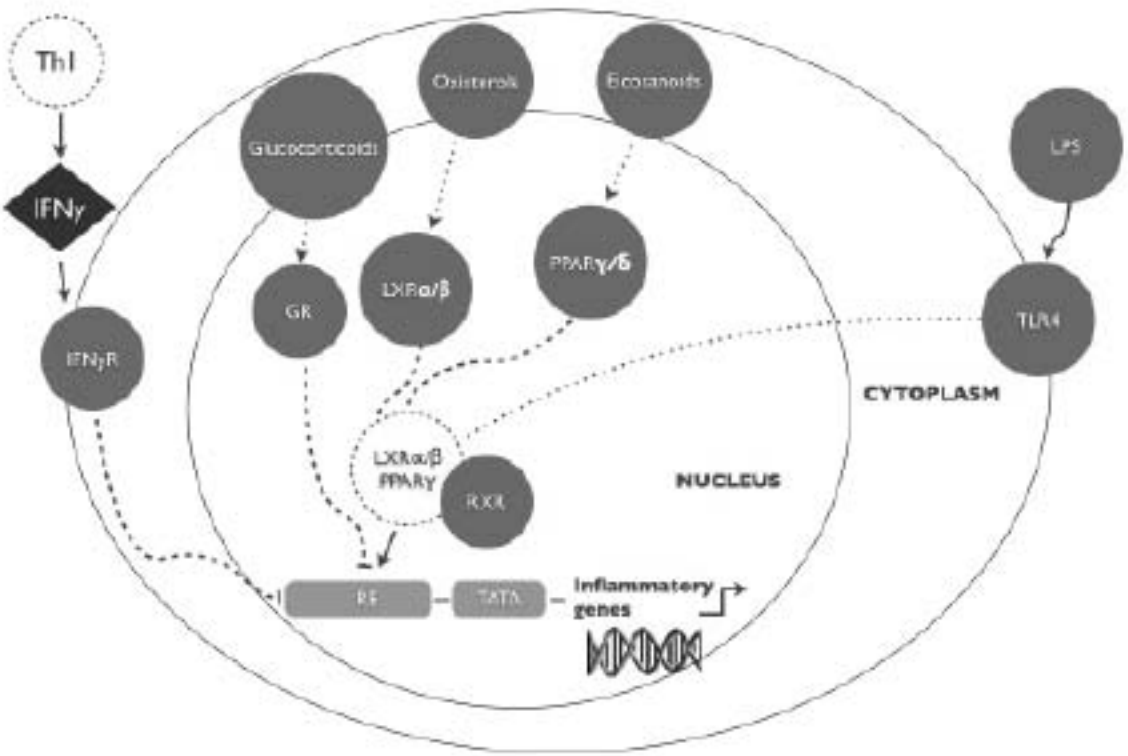

Fig. 2. *Schematic representation of the effects induced in macrophages by PPAR and LXR stimulation. In macrophages inflammatory response genes are inhibited by PPARs, LXRs and GR. Circulating hormones secreted under the control of the hypothalamic–pituitary–adrenal axis regulate macrophage gene expression through binding to GR. PPARs and LXRs regulate gene expression by responding to locally produced ligands. In addition LXR activation turns off inflammatory gene expression triggered by stimuli such as TLR ligands and cytokines. TLR4, toll-like receptor 4; IFN-γ, interferon-γ; LPS, lipopolysaccharide; Th1, T helper cells; RE, response element.*

functions as a coregulator of NR-mediated transcription, modulating *in vivo* the expression of NRs target genes. The rhythmic binding of PER2 at the promoters of NR target genes can coordinate the circadian output with the biological oscillator. In this way clock controlled and output (tissue specific) genes can be driven by the core clock genes and by mediators represented by rhythmically expressed transcriptional regulators. PER2 modulates circadian NR activity at the protein rather than the transcriptional level, contributing a rapid way to modulate rhythmic gene expression and avoiding the problems that could derive from the rigid expression of nuclear receptors. The physical interaction of PER2 with different NRs allows a rapid adaptation of the underlying transcriptional network to changes in the milieu and a clear-cut and advantageous tuning of cellular responses to environmental cues (31).

Macrophages are important regulators of innate immunity and provide temporal gating of proinflammatory cytokine secretion and systemic immune responses, displaying circadian oscillation in the expression of clock genes and genes responsible for pathogen recognition and cytokine production. Studies performed on mutant mice and human macrophage cells have demonstrated that the temporal gating of the innate immune response to endotoxin depends on REV-ERBα control of a set of genes involved in innate immunity, including *IL6*. *Rev-erbα*$^{-/-}$ mice maintain normal circadian function but loss this temporal gating, corroborating the evidence that REV-ERBα plays a key role in the cross-talk between circadian and inflammatory pathways (32).

Moreover, the sequence of activation of the core clock genes in the different compartments of the immune system has been assessed investigating their expression in mouse spleen, thymus and peripheral blood. The comparison of acrophases indicates that gene expression peaks almost always coincide for spleen and thymus, whereas gene expression pattern in the peripheral blood is generally out of phase compared to the one found in the central and peripheral lymphoid tissues. An exception is represented by the gene expression profiles of REV-ERBα showing evident phase similarities among spleen, thymus and blood, suggesting that the expression of this NR may represent a coordinating hinge in the sequence of core clock gene expression in the different compartments of the immune system (11, 12).

As stated above, a component of the innate immune system is represented by the acute phase response (APR), related to the rapid reprogramming of gene expression and metabolism in response to inflammatory cytokine signaling. Hepatocyte derived acute phase proteins (APPs) play a central role in restoring tissue homeostasis, but the connection of chronically elevated APP levels to metabolic syndrome disorders and the emergent role of lipid sensing nuclear receptors (liver X receptor, LXR, liver receptor homolog-1, LRH-1, peroxisome proliferator-activated receptor, PPAR, farnesoid X receptor, FXR) in conjunction with anti-inflammatory genomic and pre-genomic pathways, imply APR as a scaffold for the cross-talk between metabolic and inflammatory pathways. These connections are well rendered by the syncretic neologism "*metaflammation*" and could relate to adverse metabolic and inflammatory disturbances, particularly those affecting lipoprotein properties, cholesterol metabolism and atherogenesis (33). Several metabolic NRs such as PPARs (receptors for fatty acids), FXRs (receptors for bile acids) and LXRs (receptors for oxysterols), interact for transcriptional interference with other signaling pathways and in particular with the inflammatory signal-dependent activation of proinflammatory transcription factors such as NF-kB [homo- or heterodimer composed of p50 and p65 (RelA)], signal transducers and activators of transcription (STATs) and AP-1 family members (33, 34). This crosstalk is capable of inhibiting the activities of other classes of transcription factors in a ligand-dependent manner, repressing inflammatory gene expression in *trans*, with a mechanism termed transrepression that does not require DNA binding by the NR and results in the removal of the NR–proinflammatory transcription factors complexes from genomic binding sites (34). In the absence of ligand, a subset of NRs heterodimerize with retinod X receptor (RXR), and actively repress target genes by binding to hormone response elements (HREs) (35-40).

PPAR and LXR, unlike GR, need to be post-translationally modified by members of the small ubiquitin-related modifier (SUMO) family to enter

the transrepression pathway. SUMOylation is a posttranslational modification process involving three enzymatic steps that proceed sequentially and by which SUMO (~20 kDa) is covalently conjugated to the ε-amino group of lysine residues on target proteins, by forming an isopeptide bond between SUMO and a lysine side chain. Modification of transcription factors by SUMOylation has been proposed as a mechanism to modulate the transactivation and/or transrepression potential of several transcription factors (33, 35).

NR activation by ligands promotes the specific conjugation of SUMO-1 or SUMO-2/3 to the ligand-binding domain of the respective NRs (36). SUMOylation triggers NR targeting (docking) to corepressor complexes containing the core subunits nuclear receptor corepressor (N-CoR), transducin b1-related protein 1 (TBLR1; coregulator exchange factor linked to ubiquitin ligase complexes), G-protein pathway suppressor 2 (GPS2), coronin 2A (CORO2A) and histone deacetylase 3 (HDAC3), at the promoters of proinflammatory transcription factors -regulated genes, and prevents release (locking) of these complexes in response to inflammatory signaling, resulting in maintenance of the repressed state. SUMOylated or not SUMOylated NRs actively recruit corepressor complexes to proinflammatory transcription factors-regulated genes operating

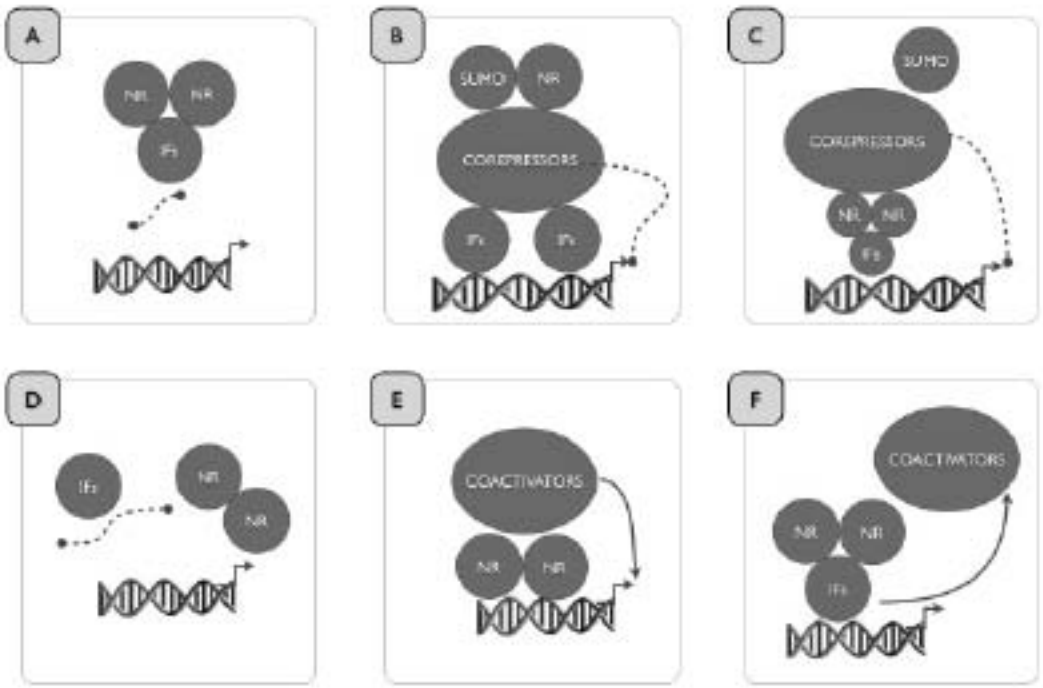

Fig. 3. *Molecular mechanisms by which glucocorticoid receptors (GRs), peroxisome proliferator-activated receptors (PPARs) and liver X receptors (LXRs) operate an anti-inflammatory crosstalk in different cell-types of the immune system controlling the expression of inflammatory genes. PPARs and LXRs interact for transcriptional interference with other signaling pathways and in particular with the inflammatory signal-dependent activation of proinflammatory transcription factors (IFs). This crosstalk is capable of inhibiting the activities of other classes of transcription factors in a ligand-dependent manner, repressing inflammatory gene expression in trans, with a mechanism termed transrepression that does not require DNA binding by the NR and results in the removal of the NR–IF complexes from genomic binding sites (**A**). PPAR and LXR, unlike GR, need to be post-translationally modified by members of the small ubiquitin-related modifier (SUMO) family to enter the transrepression pathway. SUMOylation triggers NR targeting (docking) to corepressor complexes and prevents release (locking) of these complexes in response to inflammatory signaling, resulting in maintenance of the repressed state (**B**). SUMOylated or not SUMOylated NRs actively recruit corepressor complexes to IF-regulated genes operating corepressor recruitment (**C**). Another mechanism is represented by coactivator interference, in which NR binding prevents the recruitment of coactivators to IFs or displaces them from activated IFs (**D**). On the other hand, NRs can directly induce the expression of anti-inflammatory cytokines and mediators (**E**), or may inhibit inflammatory signaling at pre-genomic steps operating signaling interference (**F**)*

corepressor recruitment (36). Another mechanism is represented by coactivator interference, in which NR binding prevents the recruitment of coactivators to proinflammatory transcription factors or displaces them from activated proinflammatory transcription factors. On the other hand, NRs can directly induce the expression of anti-inflammatory cytokines and mediators, or may inhibit inflammatory signaling at pre-genomic steps operating signaling interference (33) (Fig. 3).

The NR superfamily includes a large number of orphan receptors for which ligands have not been identified, and also includes receptors for steroid hormones, such as the GR, estrogen (ER), and vitamin D (VDR), receptors for nonsteroidal ligands, such as the thyroid hormone (TR) and retinoic acid (RAR), and for oxidized forms of cholesterol [oxysterols, such as 24(S)-hydroxycholesterol and 22(R)-hydroxycholesterol] or intermediates of the cholesterol biosynthetic pathway [24(S),25-epoxycholesterol] such as LXR (36).

PPARs are a subfamily of the NR superfamily of transcriptional factors comprising three members, PPAR*α*, PPAR*β*/*δ* and PPAR*γ,* which are expressed with circadian rhythmicity and possess distinct biological activities. PPAR*α* is mainly involved in lipid metabolism, PPAR*γ* is a master regulator of adipogenesis and fat storage, whereas the function of PPAR*β*/*δ* is not completely defined (26).

The clock gene machinery and the nuclear receptors show tight interconnections that may mediate clock entrainment in different tissues: PER2 negatively regulates *Pparg* expression and inhibits PPARγ recruitment to target promoters. On the other hand, PPAR*γ* positively regulates *Bmal1* transcription, there is a reciprocal positive regulation of *Bmal1* expression by PPARα, and *Ppara* expression by BMAL1, and CLOCK directly controls the circadian expression of *Pparα* (38).

The PPARγ gene is transcribed into three different mRNA molecules: PPARγ1 and PPARγ2, which are transcribed from the same promoter by differential promoter usage and subsequent alternative mRNA splicing, and PPARγ3, which is transcribed from an independent promoter (35).

PPARs bind diverse products of lipid metabolism, such as eicosanoids produced by metabolism of arachidonic acid and other long chain polyunsaturated fatty acids [(leukotriene (LT)B4 and 8(S)-hydroxyecosatetraenoic acid (HETE)] for (PPAR) α, and [15-deoxy-D12,14-p rostaglandin J2 (15d-PGJ2), 15-HETE and 13-hydroxyoctadecadienoic acid (HODE)] for PPAR γ, (36). Ligand binding to PPARs triggers a conformational change which allows the dissociation of corepressors and recruitment of coactivators, many of which are known to be histone acetyltransferases (HATs), resulting in transcription activation of target genes (38). In the absence of ligand, PPARs form a multicomponent complex with corepressors, such as Nuclear receptor corepressor 1(NCoR1), silencing mediator of retinoic acid and thyroid hormone receptor (SMRT), small heterodimer partner (SHP), receptor-interacting protein 140 (RIP140), and SIRT-1, which interact with PPAR-RXR heterodimers, inhibiting transcriptional transactivation driven by active PPAR-RXR. Histone deacetylase 3 (HDAC3), a histone modification enzyme, is recruited and stably bound to the repressor complex through a conserved deacetylase activation domain (DAD) in NcoR1, and remodels chromatin in a way less favorable for access by basal transcriptional machinery, leading to the repression of PPAR-mediated transcription activation (38).

A number of NRs (GRα, VDR, RARs, and LXRs) are constitutively expressed in macrophages, whereas ERα and PPARγ expression increases during macrophage differentiation (35, 36). An immunomodulatory role for PPARγ has been described in the monocyte/macrophage, a cell type critical to the innate immune system. Furthermore, PPARγ expression is upregulated during the inflammatory response, and can be induced *in vitro* by IL-4 and other immunoregulatory molecules. In contrast, IFN-γ and lipopolysaccharide (LPS) repress the expression of PPARγ (36).

REV-ERBα expressed in vascular wall cells influences the inflammatory response, up-regulating the expression of IL-6 and cyclooxygenase-2 (41). In particular, REV-ERBα is expressed in primary human macrophages present in vascular wall and is induced by synthetic ligands for the LXRs, which control cholesterol homeostasis, inflammation, and the immune response in macrophages. LXRα induces transcriptional expression binding to a specific response element in the human *Rev-erba* promoter.

LXR activation also increases the response against bacteria in human macrophages via induction of TLR-4 expression. Furthermore, REV-ERBα binds as a monomer to a response element site overlapping with the LXR response element site in the TLR-4 promoter and acts as a negative regulator of LXR transactivation on TLR-4 expression (42).

The circadian clock drives the expression of the pattern recognition receptor TLR-9, an immune system protein that can sense bacterial and viral DNA, and this regulation turns into daily variations in TLR-9 responsiveness as measured by cytokine response and expression of costimulatory molecules. This evidence is corroborated by the influence of a non-functional *Per2* gene on TLR-9 expression, TLR-9 responsiveness, and absolute levels of the adaptive response in a vaccination model using TLR-9 ligand as adjuvant and mice immunized at the time of enhanced TLR-9 responsiveness, presenting weeks later with an improved adaptive immune response. Mice immunized when TLR-9 is most responsive exhibit an enhanced immune response, and in the sepsis mouse model, disease severity is dependent on the timing of sepsis induction, which directly correlated with cyclical changes in TLR-9 (43).

NCoR and SMRT corepressors are required for nearly all of the transrepression activities of LXRs in a combinatorial, corepressor-based strategy for integration of inflammatory and anti-inflammatory signals that play essential roles in immunity and homeostasis (20, 44, 45).

The role of the transcriptional regulators in the cross-talk between the circadian clock and the adaptive immune system

CD4+ T cells (effector or T-helper cells) play critical roles in adaptive immune responses producing cytokines and chemokines, helping B cells make antibodies, activating macrophages, and recruiting neutrophils, eosinophils, and basophils to sites of infection and inflammation. CD4+ naïve helper T cells (Th), regulated by the coordination of signal transduction and a transcription factor network, may selectively differentiate in a series of distinct cell populations, represented by Th1, Th2, Th17 and induced regulatory T (iTreg) cells (46). The biological clock regulates a number of transcription factors implicated in the development of immunocompetent cells, such as STAT, GATA-3, NF-AT, NF-kB, and AP-1 (18).

Th1 cells mediate immune responses against intracellular pathogens, their principal cytokine products are IFNγ, lymphotoxin α (LTα), and IL-2. Transcription factors involved in Th1 differentiation are represented by T-bet, STAT 4, eomesodermin, Hlx and Runx3. On the other hand, Th2 cells mediate host defense against extracellular parasites including helminthes and are important in the induction and persistence of asthma and other allergic diseases. Th2 cells produce IL-4, IL-5, IL-9, IL-10, IL-13, IL-25, and amphiregulin. The production of Th2 cytokines is controlled by several transcription factors including STAT6, GATA-3, NF-AT, NF-kB, c-Maf, and AP-1.

Th cell differentiation is a specific and dynamic process accompanied by changes in concomitant expression patterns of thousands of genes at different stages, and once initiated, T cells develop a number of mechanisms to reinforce this program until epigenetic modifications are established in certain gene loci that lead to the acquisition of a stable and specific phenotype. DEC1 and DEC2 are transcription factors that have been found to oscillate with circadian rhythmicity in peripheral blood mononuclear cells and to play a key role in Th fate and function (47). DEC1-deficient mice exhibit defects in T lymphocyte activation and ineffective elimination of activated T and B cells. DEC2 is preferentially expressed in Th2 cells, is progressively induced during the course of Th2 differentiation, especially at the later stage, and the up-regulated DEC2 can strongly promote Th2 development under Th2-inducing conditions (47). DEC2 functions as an important modulator of IL-2Rα expression and plays a synergistic role in regulating IL-2 signaling with IL-4 to drive Th2 cell differentiation: DEC2 is induced at a late stage of Th2 differentiation and in turn enhances this process by increasing IL-2 signaling (47). The enhanced Th2 development is at least in part due to substantial up-regulation of CD25 expression elicited by DEC2 upon *Stat6* activation, thereby resulting in hyperresponsiveness to IL-2 stimulation. DEC2, induced by IL-4 signaling, promotes Th2 differentiation through enhanced IL-2R mediated signalling: unlike GATA3, DEC2 alone

is not sufficient to achieve Th2 differentiation and its function is restricted to a Th2-priming environment, facilitating Th2 polarization as characterized by an increase in the production of the entire set of Th2 cytokines (47). The dramatic induction of DEC2 expression at the late stage of Th2 differentiation exactly matches the time window for requirement of IL-2 signaling to reinforce Th2 differentiation. DEC2 helps to maintain a high level of IL-2R, and in combination with GATA3, activated Stat5 through IL-2 signaling may maintain the accessibility of the *Il4* gene and maximize its transcription (47).

Another key regulator of Th2 responses is represented by the transcription factor NFIL3/E4BP4, which is highly expressed in Th2 cells and regulates their cytokine production and effector function. NFIL3/E4BP4 expression is very low in many cell types and is induced in response to cytokines and hormones, is minimal in B cells and T cells, where is strongly induced by IL-4 stimulation, and is highly expressed in natural killer (NK) cell and NKT cells (48).

Studies performed by using murine helper T cell clones and freshly isolated splenocytes have shown that T cells express PPARγ1, whose overexpression mediated by ligands (15d-PGJ2, thiazolidinedione agents) inhibits proliferative responses of both the T cell clones directly at the level of the T cell and not at the level of the macrophage/antigen presenting cell (APC) (49). Besides, PPARγ mediates inhibition of IL-2 secretion by the T cell clones while not inhibiting IL-2-induced proliferation of such clones, and its activation in CD4+ T cells selectively suppresses Th17 differentiation, but not differentiation into Th1, Th2, or regulatory T cells (49). PPARγ also inhibits IL-4 production, and ligand-mediated suppression of IL-4 production in CD4+ T cells may involve both inhibition of the nuclear factor of activated T cells (NF-AT)-DNA interactions and competitive recruitment of transcription integrators between NF-AT and PPAR-γ (50). Unliganded PPARα has the ability to negatively regulate the transcription of T-bet, via a DNA-binding independent mechanism, mediated through the ability to repress the phosphorylation of p38 mitogen activated protein (MAP) kinase following T cell activation. Besides, by controlling the initiation of T-bet transcription, PPARα is able to indirectly influence the level of activation- induced IFN-γ produced by CD4+ T cells (51). Furthermore, androgens modify the equilibrium from pro-inflammatory Th1 cytokines to anti-inflammatory Th2 cytokines, and testosterone increases PPARα expression that accordingly is higher in male compared with female T cells, influencing their inflammatory activities and suppressing the production of IFNγ and TNF, through inhibition of binding of transcription factors NF-κB and c-Fos to the promoters of these cytokine genes (52).

Th17 cells mediate immune responses against extracellular bacteria and fungi. They are responsible for, or participate in, the induction of many organ-specific autoimmune diseases. Th17 cells produce IL-17a, IL-17f, IL-21 and IL-22. The transcription factors involved in Th17 differentiation are represented by RORγt, RORα (53), STAT3, and Interferon regulatory factor–4 (IRF4). RORγt is important in Th17 cell differentiation, acting as the key transcription factor that orchestrates the differentiation of Th17 cell lineage (54), RORα is also up-regulated in Th17 cells, and deficiency or suppression of the receptors' transcriptional activity in both RORγt and RORα completely abolishes IL-17 production (55). RORα has been suggested as a mediator of nuclear melatonin signaling and the identification of melatonin as a natural modulator of RORα suggests the involvement of the pineal hormone in the molecular switch implicated in the mutually exclusive generation of Th17 and Treg cells (56). RORα is also important for the development of the nuocytes, cytokine-secreting cells that play a key role in diseases mediated by type 2 immune responses, such as asthma and allergy, and may share a developmental lineage with natural helper cells (57).

Naive CD4 T cells stimulated by TGF-β in the absence of proinflammatory cytokines develop into iTreg cells. Treg cells play a critical role in maintaining self-tolerance as well as in regulating immune responses. The transcription factors important for Treg differentiation are FOXP3 and STAT5. Overexpression of *Foxp3* in conventional T cells converts them to a Treg phenotype and endows them with anergy and suppressive activity. A transcription factor of the bHLH/PAS family Aryl hydrocarbon receptor (AhR) regulates the biochemical and toxic

effects of environmental chemicals, and modulates the differentiation of *Foxp3*(+) Tregs as well as Th17 cells (58). AhR expression levels exhibit diurnal oscillation in many tissues and the circadian variation of AhR drives time qualified pharmacological effects of AhR agonists (59). Studies conducted in mammals have put in evidence a crosstalk between the AhR signaling pathway and the molecular clock system, and in immune competent cells AhR activation promotes epigenetic regulation inducing reciprocal differentiation of Tregs and Th17 cells (58).

Regarding CD8+ T cells, ID2 and ID3 have important roles in effector and memory CD8+ T cell development, inhibiting the DNA-binding activity of E protein transcription factors. ID2 supports the survival of effector CD8+ T cells early during the naive to effector cell transition, whereas ID3 supports their survival later during the effector to memory cell transition (60).

On the other hand, cells of the B lymphocyte lineage (B cells) are the key players in humoral immunity, and studies performed in mice have evidenced that BMAL1 down-regulation reduces B-cell development (5). Besides, IgA(+) memory B cells express the transcription factor RORα, suggesting that divergent transcriptional regulators dynamically maintain subset integrity to promote specialized immune function in class-specific memory B cells (61).

CONCLUSION

The circadian clock circuitry and the immune system contribute to bidirectional interaction and in immune organ and tissue cell-autonomous biological oscillators may integrate both environmental cues and bodily physiological cues derived from other tissues. Nuclear receptors settle reciprocal communications between molecular clocks and various physiological processes through countless transcriptional circuits, and play a key role in the cross-talk between the circadian clock circuitry and the immune system linking biological clockwork components to circadian regulation of immunity. A systematic knowledge at the molecular level of the factors involved in the cross-talk between the circadian clock circuitry and the immune system will afford understanding of the physiological mechanisms underlying the time related variations of immune system parameters and function, and will allow us to unravel the pathophysiological phenomena involved in immune system derangement in a number of diseases and in chronodysruption.

ACKNOWLEDGEMENTS

We apologize for not commenting on all the pertinent references and relevant studies due to space limitation. This work was supported by "Italian Ministry of Health" grant RC1203ME46 through Department of Medical Sciences, Division of Internal Medicine and Chronobiology Unit, IRCCS Scientific Institute and Regional General Hospital "Casa Sollievo della Sofferenza", Opera di Padre Pio da Pietrelcina, San Giovanni Rotondo (FG), Italy.

REFERENCES

1. Haus E, Smolensky MH. Biologic rhythms in the immune system. Chronobiol Int 1999; 16:581-622.
2. Wang W, Barnaby JY, Tada Y, Li H, Tör M, Caldelari D, Lee DU, Fu XD, Dong X. Timing of plant immune responses by a central circadian regulator. Nature 2011; 470:110-14.
3. Wang X, Reece SP, Van Scott MR, Brown JM. A circadian clock in murine bone marrow-derived mast cells modulates IgE-dependent activation in vitro. Brain Behav Immun 2011; 25:127-34.
4. Stone EF, Fulton BO, Ayres JS, Pham LN, Ziauddin J, Shirasu-Hiza MM. The circadian clock protein timeless regulates phagocytosis of bacteria in Drosophila. PLoS Pathog 2012; 8(1):e1002445.
5. Logan RW, Sarkar DK. Circadian nature of immune function. Mol Cell Endocrinol 2012; 349:82-90.
6. Mazzoccoli G, Sothern RB, De Cata A, Giuliani F, Fontana A, Copetti M, Pellegrini F, Tarquini R. A timetable of 24-hour patterns for human lymphocyte subpopulations. J Biol Regul Homeost Agents 2011; 25:387-95.
7. Dimitrov S, Lange T, Born J. Selective mobilization of cytotoxic leukocytes by epinephrine. J Immunol 2010; 184:503-11.
8. Bollinger T, Leutz A, Leliavski A, et al. Circadian clocks in mouse and human CD4+ T cells. PLoS One

2011; 6:e29801
9. Mazzoccoli G, De Cata A, Greco A, Carughi S, Giuliani F, Tarquini R. Circadian rhythmicity of lymphocyte subpopulations and relationship with neuro-endocrine system. J Biol Regul Homeost Agents 2010; 24:341-50.
10. Keller M, Mazuch J, Abraham U, Eom GD, Herzog ED, Volk HD, Kramer A, Maier B. A circadian clock in macrophages controls inflammatory immune responses. Proc Natl Acad Sci USA 2009; 106:21407-12.
11. Mazzoccoli G, Sothern RB, Greco G, Pazienza V, Vinciguerra M, Liu S, Cai Y. Time-related dynamics of variation in core clock gene expression levels in tissues relevant to the immune system. Int J Immunopathol Pharmacol 2011; 24:869-79.
12. Mazzoccoli G, Cai Y, Liu S, et al. REV-ERBalpha and the clock gene machinery in mouse peripheral tissues: a possible role as a synchronizing hinge. J Biol Regul Homeost Agents. 2012; 26(2):265-76.
13. Ebisawa T, Numazawa K, Shimada H, et al. Self-sustained circadian rhythm in cultured human mononuclear cells isolated from peripheral blood. Neurosci Res 2010; 66:223-27.
14. Nakamura Y, Harama D, Shimokawa N, et al. Circadian clock gene Period2 regulates a time-of-day-dependent variation in cutaneous anaphylactic reaction. J Allergy Clin Immunol 2011; 127:1038-45.
15. Mazzoccoli G, Pazienza V, Vinciguerra M. Clock genes and clock controlled genes in the regulation of metabolic rhythms. Chronobiol Int 2012; 29(3):227-51.
16. Eide EJ, Vielhaber EL, Hinz WA, Virshup DM. The circadian regulatory proteins BMAL1 and cryptochromes are substrates of casein kinase Iε. J Biol Chem 2002; 277:17248-54.
17. Cho H, Zhao X, Hatori M, et al. Regulation of circadian behaviour and metabolism by REV-ERB-α and REV-ERB-β. Nature 2012; 485(7396):123-7.
18. Bozek K, Relógio A, Kielbasa SM, Heine M, Dame C, Kramer A, Herzel H. Regulation of clock-controlled genes in mammals. PLoS One 2009; 4(3):e4882.
19. Ward SM, Fernando SJ, Hou TY, Duffield GE. The transcriptional repressor ID2 can interact with the canonical clock components CLOCK and BMAL1 and mediate inhibitory effects on mPer1 expression. J Biol Chem 2010; 285:38987-9000.
20. Ghisletti S, Huang W, Jepsen K, Benner C, Hardiman G, Rosenfeld MG, Glass CK. Cooperative NCoR/SMRT interactions establish a corepressor-based strategy for integration of inflammatory and anti-inflammatory signaling pathways. Genes Dev 2009; 23:681-93.
21. Marcello M, White MR. Spatial and temporal information coding and noise in the NF-κB system. Biochem Soc Trans 2010; 38:1247-50.
22. Liu J, Malkani G, Shi X, Meyer M, Cunningham-Runddles S, Ma X, Sun ZS. The circadian clock Period 2 gene regulates gamma interferon production of NK cells in host response to lipopolysaccharide-induced endotoxic shock. Infect Immun 2006; 74(8):4750-6.
23. Narasimamurthy R, Hatori M, Nayak SK, Liu F, Panda S, Verma IM. Circadian clock protein cryptochrome regulates the expression of proinflammatory cytokines. Proc Natl Acad Sci USA 2012; 109(31):12662-7
24. Roy B, Singh R, Kumar S, Rai U. Diurnal variation in phagocytic activity of splenic phagocytes in freshwater teleost Channa punctatus: melatonin and its signaling mechanism. J Endocrinol 2008; 199:471-80.
25. Carrillo-Vico A, Lardone PJ, Ferna´ndez-Santos JM, Martı´n-Lacave I, Calvo JR, Karasek M, Guerrero JM. Human lymphocyte-synthesized melatonin is involved in the regulation of the interleukin-2/interleukin-2 receptor system. J Clin Endocrinol Metab 2005; 90:992-1000.
26. Li MD, Yang X. A Retrospective on Nuclear Receptor Regulation of Inflammation: Lessons from GR and PPARs. PPAR Res 2011; 2011:742785.
27. Yamamoto T, Nakahata Y, Tanaka M, et al. Acute physical stress elevates mouse period1 mRNA expression in mouse peripheral tissues via a glucocorticoid-responsive element. J Biol Chem 2005; 280:42036-43.
28. Cavadini G, Petrzilka S, Kohler P, Jud C, Tobler I, Birchler T, Fontana A. TNF-alpha suppresses the expression of clock genes by interfering with E-box-mediated transcription. Proc Natl Acad Sci USA 2007; 104:12843-48.
29. Petrzilka S, Taraborrelli C, Cavadini G, Fontana A, Birchler T. Clock gene modulation by TNF-alpha

depends on calcium and p38 MAP kinase signaling. J Biol Rhythms 2009; 24:283-94.
30. Bookout AL, Jeong Y, Downes M, Yu RT, Evans RM, Mangelsdorf DJ. Anatomical profiling of nuclear receptor expression reveals a hierarchical transcriptional network. Cell 2006; 126:789-99.
31. Schmutz I, Ripperger JA, Baeriswyl-Aebischer S, Albrecht U. The mammalian clock component PERIOD2 coordinates circadian output by interaction with nuclear receptors. Genes Dev 2010; 24:345-57.
32. Gibbs JE, Blaikley J, Beesley S, et al. The nuclear receptor REV-ERBα mediates circadian regulation of innate immunity through selective regulation of inflammatory cytokines. Proc Natl Acad Sci USA 2012; 109:582-7.
33. Venteclef N, Jakobsson T, Steffensen KR, and Treuter E. Metabolic nuclear receptor signaling and the inflammatory acute phase response. Trends Endocrinol Metab 2011; 22:333-43.
34. Nijmeijer RM, Gadaleta RM, van Mil SW, et al; Dutch Initiative on Crohn, Colitis (ICC). Farnesoid X Receptor (FXR) Activation and fxr genetic variation in inflammatory bowel disease. PLoS ONE 2011; 6(8): e23745.
35. Majdalawieh A, Ro HS. PPARgamma1 and LXRalpha face a new regulator of macrophage cholesterol homeostasis and inflammatory responsiveness, AEBP1. Nucl Recept Signal 2010; 8:e004.
36. Treuter E. New wrestling rules of anti-inflammatory transrepression by oxysterol receptor LXR revealed. Cell Res 2011; 21:711-14.
37. Glass CK, Saijo K. Nuclear receptor transrepression pathways that regulate inflammation in macrophages and T cells. Nat Rev Immunol 2010; 10:365-76.
38. Charoensuksai P, Xu W. PPARs in rhythmic metabolic regulation and implications in health and disease. PPAR Res 2010; 2010:pii 243643.
39. Chawla A. Control of macrophage activation and function by PPARs. Circ Res 2010; 106:1559-69.
40. Xu L, Shen S, Ma Y, et al. 25-Hydroxycholesterol-3-Sulfate (25HC3S) Attenuates inflammatory response via PPARgamma signaling in human THP-1 Macrophages. Am J Physiol Endocrinol Metab 2012; 302:E788-E799.
41. Migita H, Morser J, Kawai K. Rev-erb alpha upregulates NF-kappaB-responsive genes in vascular smooth muscle cells. FEBS Lett 2004; 561:69-74.
42. Fontaine C, Rigamonti E, Pourcet B, Duez H, Duhem C, Fruchart JC, Chinetti-Gbaguidi G, Staels B. The nuclear receptor Rev-erbalpha is a liver X receptor (LXR) target gene driving a negative feedback loop on select LXR-induced pathways in human macrophages. Mol Endocrinol 2008; 22:1797-811.
43. Silver AC, Arjona A, Walker WE, Fikrig E. The circadian clock controls toll-like receptor 9-mediated innate and adaptive immunity. Immunity 2012; 36(2):251-61.
44. Escoubet-Lozach L, Benner C, Kaikkonen MU, et al. Mechanisms establishing TLR4-responsive activation states of inflammatory response genes. PLoS Genet 2011; 7:e1002401.
45. Huang W, Ghisletti S, Perissi V, Rosenfeld MG, Glass CK. Transcriptional integration of TLR2 and TLR4 signaling at the NCoR derepression checkpoint. Mol Cell 2009; 35:48-57.
46. Zhu J, Paul WE. CD4 T cells: fates, functions, and faults. Blood 2008; 112:1557-69.
47. Liu Z, Li Z, Mao K, et al. Dec2 promotes Th2 cell differentiation by enhancing IL-2R signaling. J Immunol 2009; 183:6320-29.
48. Kashiwada M, Cassel SL, Colgan JD, Rothman PB. NFIL3/E4BP4 controls type 2 T helper cell cytokine expression. EMBO J 2011; 30:2071-82.
49. Klotz L, Burgdorf S, Dani I, et al. The nuclear receptor PPAR gamma selectively inhibits Th17 differentiation in a T cell-intrinsic fashion and suppresses CNS autoimmunity. J Exp Med 2009; 206:2079-89.
50. Chung SW, Kang BY, Kim TS. Inhibition of interleukin-4 production in CD4+ T cells by peroxisome proliferator-activated receptor-gamma (PPAR-gamma) ligands: involvement of physical association between PPAR-gamma and the nuclear factor of activated T cells transcription factor. Mol Pharmacol 2003; 64:1169-79.
51. Jones DC, Ding X, Zhang TY, Daynes RA. Peroxisome proliferator-activated receptor alpha negatively regulates T-bet transcription through suppression of p38 mitogen-activated protein kinase activation. Immunol 2003; 171:196-203.
52. Dunn SE, Ousman SS, Sobel RA, et al. Peroxisome proliferator–activated receptor (PPAR)α expression

in T cells mediates gender differences in development of T cell–mediated autoimmunity. J Exp Med 2007; 204:321-30.

53. Jetten AM. Retinoid-related orphan receptors (RORs): critical roles in development, immunity, circadian rhythm, and cellular metabolism. Nucl Recept Signal 2009; 7:e003.
54. Rauen T, Juang YT, Hedrich CM, Kis-Toth K, Tsokos GC. A novel isoform of the orphan receptor RORγt suppresses IL-17 production in human T cells. Genes Immun 2012; 13:346-50.
55. Solt LA, Kumar N, Nuhant P, et al. Suppression of TH17 differentiation and autoimmunity by a synthetic ROR ligand. Nature 2011; 472:491-94.
56. Lardone PJ, Guerrero JM, Fernández-Santos JM, Rubio A, Martín-Lacave I, Carrillo-Vico A. Melatonin synthesized by T lymphocytes as a ligand of the retinoic acid-related orphan receptor. J Pineal Res 2011; 51:454-62.
57. Wong SH, Walker JA, Jolin HE, et al. Transcription factor RORα is critical for nuocyte development. Nat Immunol 2012; 13:229-36.
58. Singh NP, Singh UP, Singh B, Price RL, Nagarkatti M, Nagarkatti PS. Activation of aryl hydrocarbon receptor (AhR) leads to reciprocal epigenetic regulation of FoxP3 and IL-17 expression and amelioration of experimental colitis. PLoS One 2011; 6(8):e23522.
59. Shimba S, Watabe Y. Crosstalk between the AHR signaling pathway and circadian rhythm. Biochem Pharmacol 2009; 77(4):560-5.
60. Kaech SM, Cui W. Transcriptional control of effector and memory CD8(+) T cell differentiation. Nat Rev Immunol 2012; Oct 19. doi: 10.1038/nri3307. [Epub ahead of print]
61. Wang NS, McHeyzer-Williams LJ, Okitsu SL, Burris TP, Reiner SL, McHeyzer-Williams MG. Divergent transcriptional programming of class-specific B cell memory by T-bet and RORα. Nat Immunol 2012; 13(6):604-11.

OBESTATIN INHIBITS LIPOGENESIS AND GLUCOSE UPTAKE IN ISOLATED PRIMARY RAT ADIPOCYTES

E. PRUSZYŃSKA-OSZMAŁEK[1], D. SZCZEPANKIEWICZ[1], I. HERTIG[1], M. SKRZYPSKI[1,2], M. SASSEK[1,2], P. KACZMAREK[1], P. A. KOŁODZIEJSKI[1], P. MAĆKOWIAK[1], K.W. NOWAK[1], M.Z. STROWSKI[2] and T. WOJCIECHOWICZ[1]

[1]Department of Animal Physiology and Biochemistry, Poznań University of Life Sciences, Wołyńska, Poznań, Poland; [2]Medizinische Klinik mit Schwerpunkt Hepatologie und Gastroenterologie, Charité-Universitätsmedizin, Berlin, Deutschland

Received December 29, 2011 – Accepted January 8, 2013

The first two authors contributed equally to this work.

Ghrelin and obestatin are encoded by the preproghrelin gene and originate from post-translational processing of the preproghrelin peptide. Obestatin is mainly present in the stomach, but its action is focused on appetite inhibition in opposition to ghrelin function. Recently, it has been presented that obestatin may regulate adipocyte metabolism and influence fat content. However, obestatin action is still poorly understood. Therefore, we aimed to investigate obestatin function on adipocyte metabolism in the rat. We studied changes in the mRNA expression of active and inactive isoforms of obestatin receptors. In addition, we analyzed influence of obestatin on lipogenesis, lipolysis and glucose transport in isolated adipocytes. Moreover, we also performed analysis of obestatin action on lipolysis in differentiated rat preadipocytes with silenced obestatin receptor. We found significantly higher expression of the obestatin receptor *Gpr39-1a* active form at an mRNA level following adipocytes incubation with obestatin. We did not observe expression changes in the inactive form of obestatin receptor *Gpr39-1b*. Additionally, we found significant changes in *Gpr39-1a* expression following obestatin receptor silencing in cells incubated with obestatin in comparison to control. Obestatin inhibited both, basal and insulin-stimulated lipogenesis and glucose transport in adipocytes. Furthermore, obestatin potentiated adrenalin-stimulated lipolysis. We also found reduced glycerol release following obestatin incubation in adipocytes with silenced *Gpr39* gene. Our results indicate that obestatin acts via the GPR39 receptor in isolated adipocytes, and that through this mechanism obestatin influences lipid accumulation, glucose uptake and lipolysis.

Obestatin is a 23 amino acid aminated peptide first described in 2005 by Zhang et al. and produced mainly by stomach and spleen (1). It was demonstrated that this peptide is encoded by the same gene that also encodes ghrelin. However, obestatin exerts an opposite effect to ghrelin by inhibiting food intake, gastric emptying and decreasing body weight gain (1-2). On the other hand, several studies indicate that obestatin is not involved in the regulation of these processes (3-5).

Key words: obestatin receptors, lipolysis, lipogenesis, glucose transport

Mailing address: Ewa Pruszyńska-Oszmałek PhD, Department of Animal Physiology and Biochemistry, Poznań University of Life Sciences, Wołyńska 35 St. 60-637 Poznań, Poland
Tel.: +48 618 466084
Fax: +48 618 487197
e-mail ewaprusz@up.poznan.pl

0393-974X (2013)

Recently, it was reported that obestatin acts via the GPR39 receptor (1) which belongs to the ghrelin receptor subfamily (1). Similar to ghrelin, the presence of two isoforms of obestatin receptors has been discovered: an active form containing 7 transmembrane domains (GPR39-1a) and an inactive form consisting of 5 domains (GPR39-1b) (6). However, several studies reported that obestatin may also act trough other receptors (7-9).

Work published by Zhang et al. demonstrated that obestatin acts through the GPR39 receptor and that this receptor is expressed in white adipose tissue as well as in preadipocytes (10). GPR39 expression was also reported in brown fat tissue (6). They also found expression of GPR39 in mouse embryo fibroblast (MEF) cell lines during differentiation into white and brown adipocytes. These results suggest that obestatin influences adipose tissue metabolism. In addition, obestatin may regulate the differentiation of precursor cells into white or brown adipose tissue.

The latest data from Granata and co-workers (15) indicates that obestatin increases insulin-induced glucose transport in the murine adipocyte cell line 3T3-L1 and human adipocytes. Moreover, they found that obestatin enhanced triglyceride content in 3T3-L1 adipocytes and human adipocytes isolated from subcutaneous fat pads. They also found that obestatin increased adipogenesis in adipocytes from omental fat pads.

In our study we aimed to demonstrate the impact of obestatin on adipocytes metabolism through the GPR39 receptor. To address this issue, we conducted a study of GPR39 expression, lipolysis, lipogenesis and glucose transport changes in rat adipocytes following obestatin incubation.

MATERIALS AND METHODS

Animals

In this study adult male Wistar rats (270±20 grams and 100±5 grams) were used. Rats were kept under standard conditions (12h dark/12h light; 21°C). Rats were sacrificed by decapitation and epididymal fat pad tissue was immediately collected for adipocytes isolation. The Local Ethics Committee for Experiments on Animals approved the experimental protocol.

Adipocytes isolation

Adipocytes were isolated from epididymal fat pad of Wistar rats according to the method of Rodbell with some modifications (11-12).

Tissue (15±2 grams) was collected from five rats. After removal of blood vessels, tissue was dried and minced by scissors. Fragmented tissue was digested in Krebs-Ringer bicarbonate buffer (118 mM NaCl, 4.8 mM KCl, 1.3 mM $CaCl_2$, 1.2 mM KH_2PO_4, 1.2 mM $MgSO_4$, 24.8 mM $NaHCO_3$) containing collagenase type II (3mg/1g tissue), 3% bovine serum albumin (BSA), 5 mM glucose and 10 mM Hepes for 45 min. at 37° in shaking water bath. Afterwards cells were filtered through a nylon mesh (250 μm) and rinsed four times with warm KRB without collagenase. Isolated adipocytes were counted using Bürker-Türk counter chamber. Each experiment was performed in four repeats for each concentration of obestatin (1, 10, 100 nM). These doses were chosen based on our previous results. All reagents (unless otherwise indicated) were purchased from Sigma-Aldrich Corp., USA.

Rat preadipocytes isolation

For white preadipocyte isolation (100±5 grams rats) the epidydymal fat pads (3±0.5 grams) were removed and immediately placed into sterile Krebs solution. Blood vessels and any remains of other tissues were removed and tissue was washed 3 times in sterile Krebs solution. The tissue was then minced with scissors to obtain fine pulp and placed in a tube containing sterile collagenase solution (250 U/mg). The tissue was incubated 30 min. in 37°C in a shaker water bath. After 30 min. the digestion was stopped by adding the same volume (1:1 vv) of cold Krebs buffer. The suspension was then left for 30 min. until mature adipocytes formed a floating layer. Adipocytes were removed and the suspension containing preadipocytes was spun down, treated with erythrocyte-lysis buffer for 10 min. and filtered through a 250 μm and 25 μm nylon mesh. Subsequently the cells were centrifuged 10 min. (700 g), resuspended in DMEM containing 10% FBS and cultured until confluent. All reagents (unless otherwise indicated) were from Sigma-Aldrich Corp., USA.

Differentiation of rat preadipocytes

Primary WAT preadipocytes were cultured in DMEM containing 10% FBS until confluent in 24 well plates. When confluent, cells were cultured in the differentiation medium composed of DMEM without FBS, supplemented with insulin (17 nM), T3 (2 nM) and dexamethasone (100 nM) for 9 days. During this period cells accumulated lipid droplets. Differentiated adipocytes were then incubated with DMEM in the presence of obestatin (1, 10, 100 nM) and obestatin and siRNA for 36 h, after which cells were washed twice with PBS and lyzed in Trizol for RNA

isolation. All reagents (unless otherwise indicated) were from Sigma-Aldrich Corp., USA.

Gpr39 silencing in differentiated rat adipocytes

Prevalidated siRNA targeting rat *Gpr39*, non-targeting siRNA and transfection reagent were purchased from SABiosciences Qiagen Company, Frederick, MD, USA. Mixes of either siRNA targeting rat *Gpr39* or non-targeting siRNA (40 nmol/l) with SureFect Transfection reagent were prepared and incubated for 20 min. at room temperature. Medium was then replaced with a medium containing prepared mix according to the manufacturer protocol. Adipocytes (10^5cells/wells) were incubated with siRNA or with non-targeting siRNA for 12 hours in 24-well plates. Medium was then removed and replaced with a fresh medium containing siRNA complex and obestatin (1, 10, 100 nM) and cells were incubated for 24 hours. The efficiency of gene silencing was measured by real-time PCR.

Oil red O

After 36 hours, wells with control and *Gpr39* silenced cells were washed with PBS and fixed for 10 min. with a 10% formalin. Cells were then washed with 60% isopropanol and air-dried. Cells were stained with ORO for 10 min. Excess of ORO was washed three times with water. Images were taken by LSM 510 microscopy (Carl Zeiss, Germany) operated by LSM 510 v. 3.2 SP1 software. For quantification, ORO was eluted from the cells using 100% isopropanol and the absorbance of the eluate was determined at 520 nm wave length against isopropanol as a blank. All reagents (unless otherwise indicated) were from Sigma-Aldrich Corp., USA.

RNA isolation and reverse transcription

For RNA isolation isolated adipocytes were incubated for 10 hours with obestatin (1, 10, 100 nM). Total RNA from adipocytes was isolated using Tripure Reagent (Roche Diagnostic, Penzberg, Germany) according to the manufacturer's protocol. After RNA isolation, DNase digestion using RQ1 RNase-Free DNase (Promega Corp., Madison, WI, USA) was performed. RNA amount and quality was analyzed using NanoDrop spectrophotometer (Thermo Scientific, Wilmington, DE, USA). One μg of total RNA was used to perform RT-PCR analysis. Reverse transcription was executed using ImProm-II Reverse Transcription System (Promega Corp., Madison, WI, USA). A negative control lacking reverse transcriptase was also prepared.

Real-Time PCR

Primers and probes for *Gpr39-1a*, *Gpr39-1b* and internal standard *Gapdh* (Roche Diagnostic, Penzberg, Germany) were designed using Roche software (accessible online at www.roche-applied-science.com/sis/rtpcr/upl/index.jsp?id=uplct_030000) to allow amplification of regions that span introns. Primers sequences and Roche universal probes numbers are presented in Table I. Since *Gpr39-1b* is a non-intronic gene, DNase digestion was necessary to remove genomic DNA. Multiplex real–time expression analysis was performed using a Light Cycle 2.0 instrument (Roche Diagnostic, Penzberg, Germany) and LightCycler TaqMan Master Kit (Roche Diagnostic). After initial optimization of the experimental conditions, products were recovered from capillaries and resolved on 2% agarose gel. Molecular weight was estimated based upon the signals obtained with a DNA molecular weight standard (Promega Corp., Madison, WI, USA). Products were photographed and analyzed using Gel Logic 100 Imaging System and Kodak 1D Analysis Software v.3.6 (Estman Kodak Company, New Haven, CT, USA) to verify a correct product size.

Analysis of *Gpr39-1a* and *Gpr39-1b* relative expression level was made using LightCycler Software Version 4.5 based on the relative quantification method with efficiency correction (standard curve method). Color compensation analysis was taken into consideration. Results are presented as a ratio of detected gene expression relative to expression of the house-keeping gene *Gapdh*.

Protein isolation and western blotting

Total protein was isolated from control mature adipocytes and adipocytes after i) incubation with 10 nM of obestatin and ii) obestatin incubation after *Gpr39* silencing by use of Ripa buffer (50 mM Tris-HCI pH 7.4, 1% NP40, 0,1% SDS, 150 mM NaCl, 2 mM EDTA, 50 mM NaF). Protease inhibitor (Roche Diagnostic Penzberg Germany) was used. Protein quantity was analyzed using Pierce BCA protein assay kit (Thermo Scientific Inc.) and measured on a Synergy 2 microplate reader (BioTek Corp.). Equal amounts of protein (15 μg) were used in the analysis. Samples were mixed with XT Sample Buffer and XT Reducing Agent (Bio-Rad, USA) and boiled at 95°C for 5 min. before loading onto a 12% Criterion XT Precast Gel (Bio-Rad, USA). Protein electrophoresis was performed using Bio-Rad Criterion apparatus in electron transfer XT Mops Running Buffer (Bio-Rad, USA). Wet electrotransfer of proteins from the gel to PVDF membranes was then performed (Millipore Billerica, MA USA) for 90 min. at 75V in 4ºC using Trans-Blott Cell (Bio-Rad, USA). Transfer efficiency was verified by incubating membranes in Ponceau Red solution (Sigma-Aldrich Inc.). Non-specific protein binding was reduced during 1 h incubation in 5% milk in TBST buffer. The membranes were incubated with specific, rabbit derived anti-GPR39 antibodies (1:400 dilution) (Phoenix Pharmaceuticals

Inc.) overnight in 4ºC in 5% milk/TBST. After washing in TBST buffer, membranes were incubated for 2 hours at room temperature with secondary goat-derived anti-rabbit immunoglobulin conjugated to horseradish peroxidase in 5% milk/TBST (1:5000). Immunoreactive complexes were detected with Immobilon Western Chemiluminescent HRP Substrate (Millipore Billerica, MA, USA) after 5 min. incubation at room temperature. Amount of GPR39 protein was normalized to β-actin (1:1000 dilution Sigma-Aldrich Inc.). Western blots were visualized and analyzed using Versa Doc apparatus and QuantityOne 1-D analysis software (Bio-Rad, USA).

Lipogenesis

Lipogenesis was studied by determining incorporation of [U-^{14}C] glucose (PerkinElmer, Massachusetts, USA) into lipids. Adipocytes (10^6 cells/ml) in the same medium as described above were incubated with obestatin (1, 10 and 100 nM) without (basal) or with insulin supplementation (10 nM), in the additional presence of 0.5 μCi [U-^{14}C] glucose for 120 min. at 37ºC in a shaking water bath. Afterwards, Dole's extraction mixture was added to stop the reaction. Tubes with adipocytes were shaken, H_2O and heptan were added and tubes were shaken once again. The upper phase containing lipid fraction was transferred to scintillation liquid for β-counting. All reagents (unless otherwise indicated) were from Sigma-Aldrich Corp., USA.

Glucose transport

Glucose transport was studied by quantifying the amount of 2-deoxy-D-[-1-^{3}H]glucose (GE Healthcare, Poland Distributor) taken up by adipocytes.

Adipocytes were preincubated in glucose-free KRB containing obestatin (1, 10, 100 nM) for 120 min. at 37ºC in a shaking water bath. To stimulate glucose uptake, insulin (100 nM) was added to the medium 30 min. before the end of incubation. Subsequently, 0.5 μCi 2-deoksy-D-[-1-^{3}H]glucose was added to adipocytes for four min. To terminate the reaction, 1.5 mM of cyclochalasin B was added. Cells suspended in KRB were transferred to fresh tubes with silicone oil and centrifuged at 6000 g for 1 min. Adipocytes were transferred to the scintillation vials and the radioactivity was measured using β-counter. All reagents (unless otherwise indicated) were from Sigma-Aldrich Corp. USA.

Lipolysis

Isolated adipocytes (10^6 cells/ml) were incubated with obestatin (1, 10 and 100 nM) in the absence (basal) or presence of adrenalin (1 μM) with KRB containing 5 mM glucose, 10 mM Hepes and 3% BSA. Incubations were carried out at 37ºC in shaking water bath for 120 min. Degree of lipolysis was determined by measuring the amount of released glycerol in the incubation medium (13).

Lipolysis in differentiated adipocytes after obestatin receptor silencing was also prepared according to the same method without adrenalin stimulation (10^5 cells/well). All reagents (unless otherwise indicated) were from Sigma-Aldrich Corp., USA.

Statistical analysis

Each experiment was performed four times in duplicates. Statistical analysis for receptors expression, as well as the changes in degree of lipogenesis, glucose transport and lipolysis were calculated by ANOVA, followed by the Bonferroni test with 99% and 95% confidence intervals. For the analysis of fat contents in adipocytes and protein expression after *Gpr39* silencing, Student's *t*-test was used. Results were shown as means±SEM

RESULTS

Gpr39 receptor expression after obestatin incubation

We demonstrated significantly higher expression of the putative obestatin receptor active form *Gpr39-1a* ($P<0.05$) in adipocytes following incubation with obestatin at the concentrations of 10 and 100 nM (Fig. 1A). On the other hand, we did not observe changes in expression of the obestatin receptor inactive form *Gpr39-1b* (Fig. 1B).

We also presented significantly ($P<0.01$) higher expression of *Gpr39-1a* in differentiated rat preadipocytes (Fig. 1C). However, the active isoform of the obestatin receptor was significantly lower when incubated with 100 nM of obestatin ($P<0.01$). Additionally, we found significantly lower ($P<0.01$) expression of obestatin receptor *Gpr39-1a* after *Gpr39* gene silencing (approx. about 70%) and incubation with obestatin in comparison to the control group and control with NTsiRNA (Fig. 1D).

Expression of *Ghsr-1a* was found to be higher in these cells, yet these changes were not significant (data not shown).

Protein expression after obestatin incubation and Gpr39 gene silencing

Based on the results of *Gpr39-1a* expression on the mRNA level, 10 nM dose of obestatin was utilised for protein expression analysis after *Gpr39* gene silencing. We observed significantly higher expression of GPR39 after incubation with 10 nM

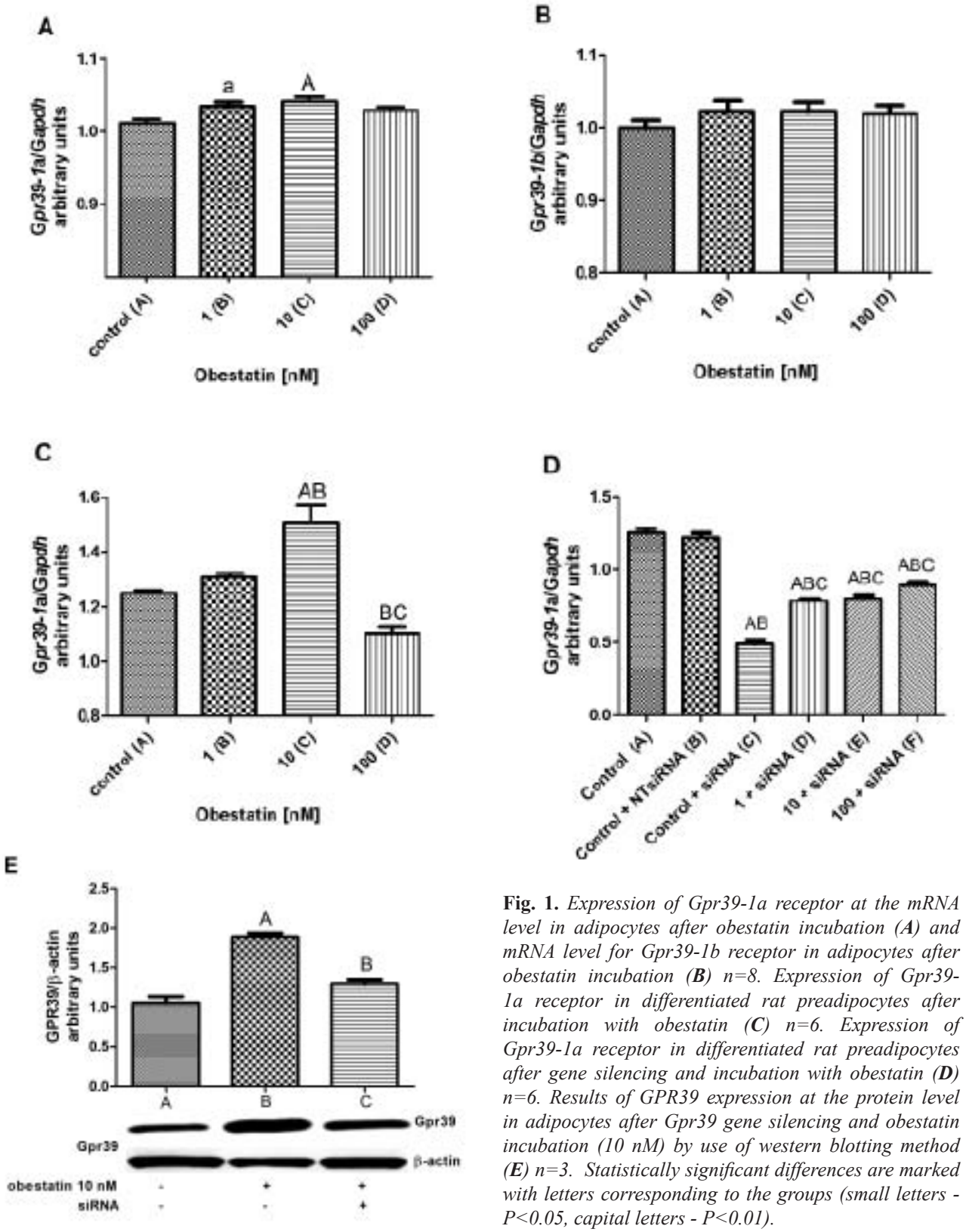

Fig. 1. *Expression of Gpr39-1a receptor at the mRNA level in adipocytes after obestatin incubation (**A**) and mRNA level for Gpr39-1b receptor in adipocytes after obestatin incubation (**B**) n=8. Expression of Gpr39-1a receptor in differentiated rat preadipocytes after incubation with obestatin (**C**) n=6. Expression of Gpr39-1a receptor in differentiated rat preadipocytes after gene silencing and incubation with obestatin (**D**) n=6. Results of GPR39 expression at the protein level in adipocytes after Gpr39 gene silencing and obestatin incubation (10 nM) by use of western blotting method (**E**) n=3. Statistically significant differences are marked with letters corresponding to the groups (small letters - P<0.05, capital letters - P<0.01).*

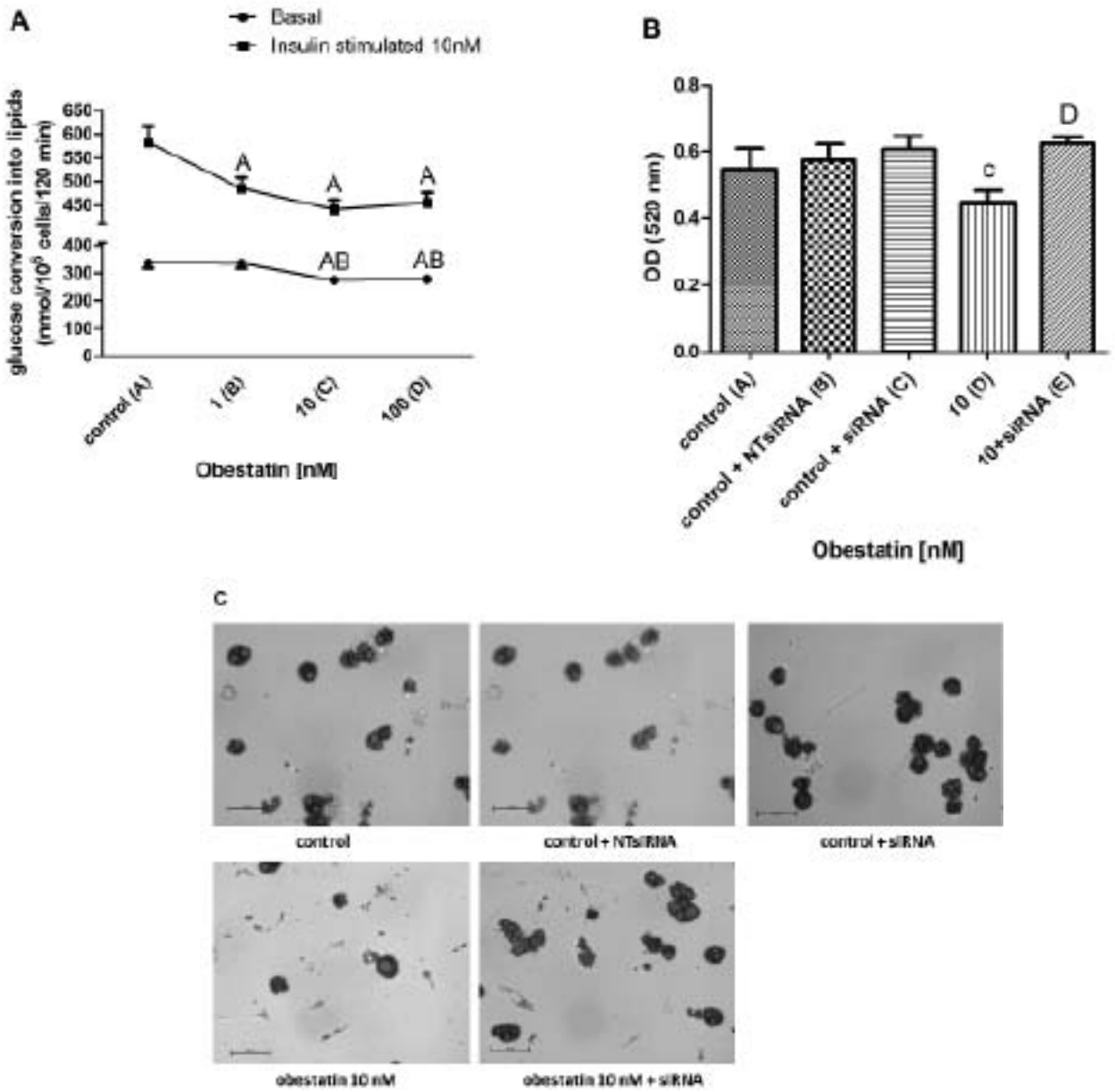

Fig. 2. *Basal and insulin stimulated (10 nM) obestatin effect on lipogenesis (**A**) in isolated rat adipocytes from epididymal fat tissue n=8. Lipid content in differentiated adipocytes after Gpr39 gene silencing (**B**). In this analysis Student's t-test was used. Statistically significant differences are marked with letters corresponding to the groups (small letters - P<0.05, capital letters - P<0.01) n=4. (**C**) Micrographs of adipocytes after obestatin stimulation (10 nM) and Gpr39 gene silencing in differentiated preadipocytes. LSM 510 Meta Confocal Microscope (Carl Zeiss) operated by LSM 510 v. 3.2 SP1 software was used.*

obestatin in comparison to control (P<0.01). After *Gpr39* silencing and incubation with the same dose of obestatin we did not find significant changes in comparison to control adipocytes. However, these changes were significant in comparison to adipocytes incubated with obestatin without silencing of the

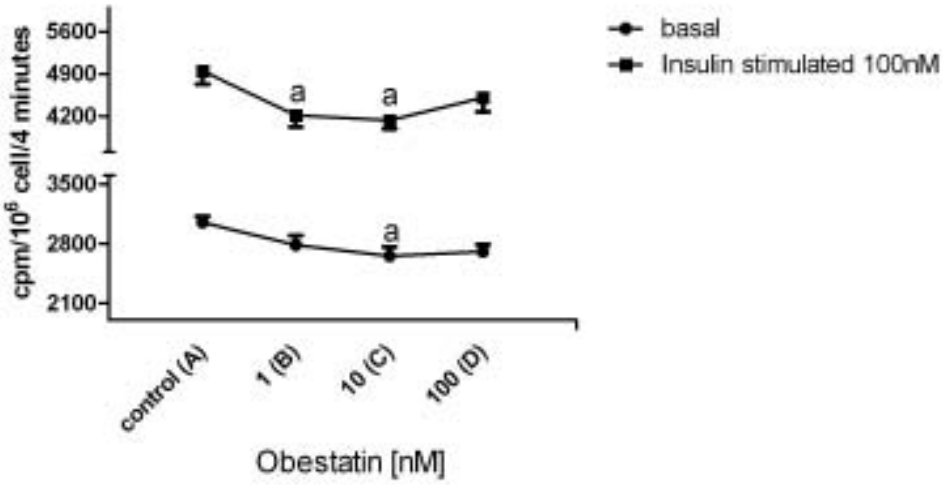

Fig. 3. *Effect of obestatin on basal and insulin stimulated (100 nM) glucose uptake by adipocytes. Statistically significant differences are marked with letters corresponding to the groups (small letters - P<0.05, capital letters - P<0.01) n=8.*

obestatin receptor gene (P<0.01) (Fig. 1D).

Obestatin inhibits basal and insulin stimulated lipogenesis

Obestatin inhibited basal lipogenesis measured as glucose conversion into lipids at the concentrations of 10 and 100 nM (P<0.01 vs. controls) (Fig. 2A). In addition, obestatin inhibited insulin stimulated lipogenesis at all three tested doses (1, 10 and 100 nM) (Fig. 2A). Additionally, we found significantly higher lipid concentration after red-oil staining in differentiated adipocytes after *Gpr39* silencing and incubation with 10 nM of obestatin in comparison to treatment with 10 nM without gene silencing (Fig. 2B). Fig. 3C shows micrographs of mature adipocytes after red-oil staining.

Effect of obestatin on glucose transport

In accordance with the results obtained during lipogenesis experiments, we found that obestatin (at all three tested doses of 1, 10 and 100 nM) significantly inhibited 2-deoxy-D-(-1-3H) glucose uptake by adipocytes (P<0.05) (Fig. 3). In addition, obestatin at 1 nM and 10 nM reduced insulin-stimulated glucose uptake (Fig. 3).

Obestatin action on lipolysis

To investigate if obestatin regulates lipolysis, we exposed adipocytes to obestatin in the absence or presence of adrenalin and measured glycerol release. Obestatin at doses of 10 nM and 100 nM increased adrenalin-stimulated lipolysis (P <0.05). In contrast, when adipocytes were incubated with obestatin only, no stimulation of lipolysis was detected (Fig. 4A).

We also demonstrated significantly higher glycerol release (P<0.05) after obestatin stimulation (10 nM) in differentiated rat preadipocytes (Fig. 4B). However, we found significant decreased glycerol release after obestatin stimulation (P<0.05; P<0.01) in mature preadipocytes with silenced *Gpr39* expression (Fig. 4C).

DISCUSSION

The main finding of our study is that obestatin inhibits glucose uptake and lipid synthesis, whereas it increases lipolysis in isolated rat adipocytes. In addition, obestatin increases the expression of the *Gpr39-1a* receptor isoform, without affecting the expression of *Gpr39-1b* receptor isoform in mature adipocytes. Conversely, in differentiated preadipocytes only 10 nM results in significantly increased expression of *Gpr39-1a* whilst 100 nM obestatin decreases expression at the mRNA level for this receptor. These data are consistent with the results published by Zhang and colleagues (10). They found that obestatin acts through GPR39 to induce c-fos expression and stimulate ERK1/2

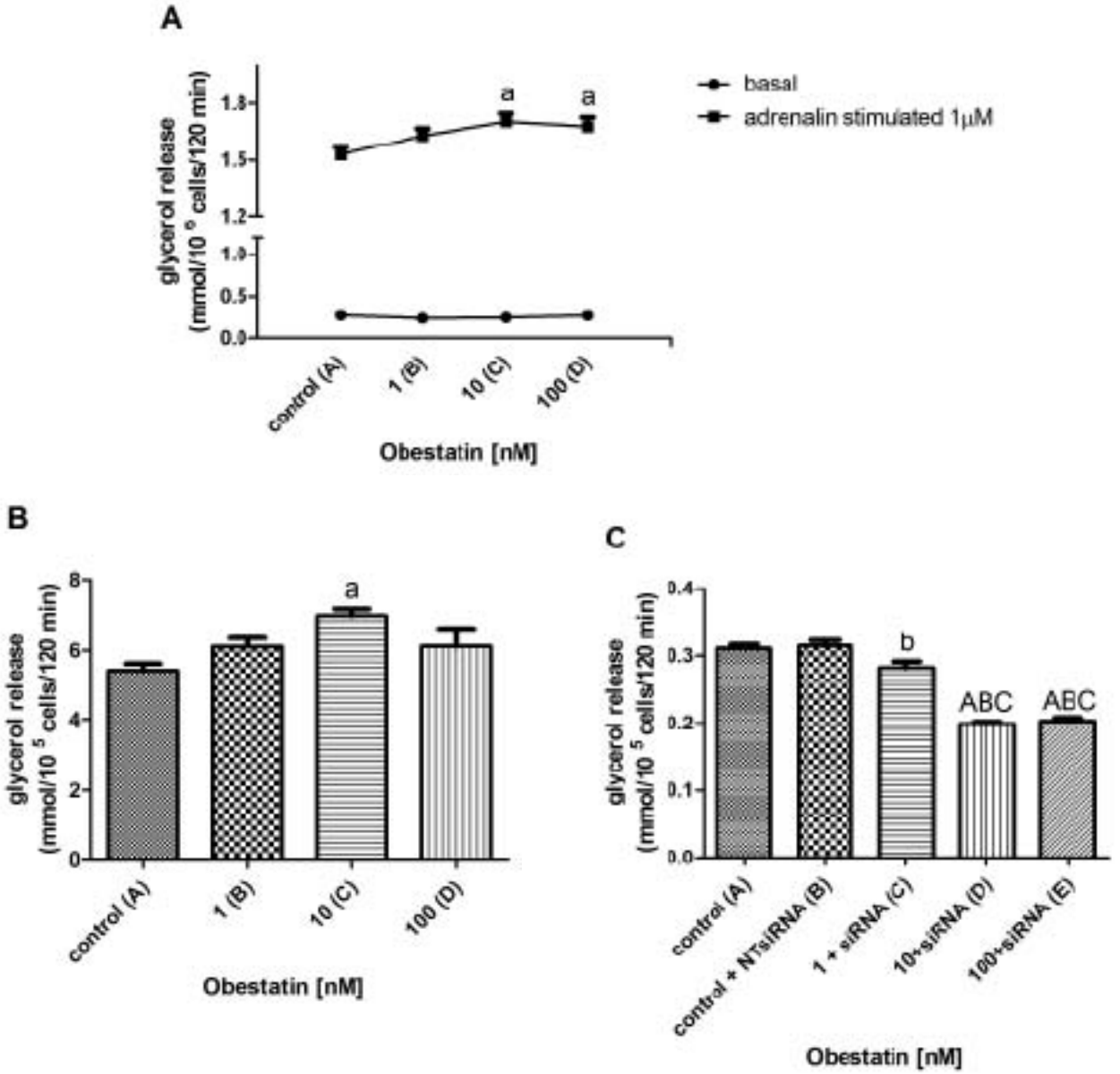

Fig. 4. *Basal and adrenalin stimulated (1 μM) obestatin effect on lipolysis (**A**) n=8. Basal obestatin effect on lipolysis in differentiated rat preadipocytes (**B**) n=6. Obestatin effect on lipolysis in mature rat adipocytes after obestatin receptor gene silencing (**C**) n=6. Statistically significant differences are marked with letters corresponding to the groups (small letters - P<0.05, capital letters - P<0.01).*

phosphorylation in a mouse preadipocyte 3T3-L1 cell line.

On the other hand, Granata and colleagues reported that obestatin can stimulate pancreatic β-cell function by acting on *Glp-1r*. Additionally, the authors reported that exendin, a GLP-1R antagonist, reduced the insulinotrophic effect of obestatin on pancreatic cells (14-15). Granata and co-workers also demonstrated that the ghrelin antagonist, (D-Lys3)-growth hormone releasing peptide-6 [(D-Lys^3)-GHRP-6] and anti-ghrelin antibody blocked obestatin's action on β-cell cell survival

Table I. *PCR primers, probes ID and reaction conditions.*

Gene	Primers sequences	Roche probes ID	Annealing Temp.	Product size (bp)
Gpr39-1a (NM_001114392.1|)	Forward 5' tggtggtcagggtctctctt 3'	#67	61°C	89
	Reverse 5' tcagggacatggctgtgat 3'			
Gpr39-1b (BK005610.1)	Forward 5' ggacagcgagaagacagacc 3'	#115	61°C	68
	Reverse 5' caaagggcccaaaattcc 3'			
Gapdh (ENSRNOT00000025351)	Forward 5' ctgcaccaccaactgcttag 3'	Standard	61°C	92
	Reverse 5' tgatggcatggactgtgg 3'			

(14). These data indicate that obestatin may interact with the receptors for ghrelin (GHSR) and for GLP-1 (GLP-1R). Moreover, it was found that obestatin inhibited insulin secretion from the pancreas after glucose stimulation (16) and that this process may be mediated by obestatin via ATP-dependent K+ channels (15).

Based on the results published by Granata and co-authors (14) we also performed analysis of ghrelin receptor mRNA level in adipocytes exposed to obestatin. Granata et al. (14) reported that (D-Lys^3)-GHRP-6, prevented obestatin action on pancreatic islets and β-cells. This may suggest that obestatin can also act at the ghrelin receptor; during our preliminary study, we found that the level of ghrelin receptor mRNA was elevated after obestatin stimulation (100 nM) in adipocytes with silencing of the *Gpr39* receptor (data not published). However, we did not observe that obestatin affects significantly ghrelin receptor mRNA level. On the other hand, these results may suggest that there is possibility that obestatin may act by ghrelin receptor. This preliminary step may be important for future studies.

Our results and the results obtained by other groups may indicate that obestatin acts via the GPR39 receptor. However, obestatin action via other receptors such as ghrelin receptors should also be taken into account. Mounting evidence implies ghrelin may activate alternative mechanisms of signal transduction (17). These data suggest that obestatin may also use various types of receptors and pathways for signal transduction to the cell.

In our study, we report that obestatin inhibits basal lipogenesis as well as insulin-stimulated lipogenesis. These results are concordant with the observation that obestatin inhibits glucose uptake by adipocytes. Furthermore, we also found that obestatin stimulates lipolysis. However, this was only detectable in adrenalin-treated adipocytes. On the other hand, we found significant decrease in glycerol release in adipocytes with silenced obestatin receptor and incubated with obestatin. Observations reported by Patel et al. (17) indicated that both ghrelin and des-acyl ghrelin have opposite effects to obestatin, significantly increasing insulin-stimulated deoxyglucose uptake in adipocytes isolated from epididymal fat. However, the authors did not determine the effects of obestatin on basal glucose uptake in adipocytes. Moreover, they presented that ghrelin (at concentration 10-1000 nM) and des acyl ghrelin (1000 nM) did not affect basal or insulin-stimulated glucose uptake in adipocytes isolated from peri-renal fat pads (18). Our data indicate that obestatin exerts an opposite action as compared to

ghrelin in regard to regulation of glucose uptake by adipocytes.

A study by Nagaraj et al. found that obestatin and its active fragments (N-terminal and middle fragment) decreased epididymal fat content in CFT Swiss Albino mice (19). Additionally, they found that obestatin and its fragments (C-terminal, N-terminal, middle fragment) decrease perirenal fat content in mice.

Taken together, the results of previous studies published by others and the current findings indicate that obestatin can influence body fat content. However, some of the recent data (20) indicates that both des-acyl ghrelin and obestatin decrease glycerol release in mouse adipocytes cell line 3T3-L1. These authors also found that there is no effect on glucose uptake in these cells. Furthermore, Miegueu et al. (19) also demonstrated that obestatin, active ghrelin, des-acyl ghrelin and GHRP-6 significantly increased lipid content in differentiated cell lines. The latest data obtained by Granata and colleagues (15) indicated that obestatin increased insulin-induced 2-deoxyglucose uptake in 3T3-L1 cell line as well as in adipocytes isolated from human fat tissue. They also found that 100 nM obestatin increased glucose uptake in the absence of insulin. Results obtained by these authors are in contrast to those obtained by our group.

These differences may be partially related to the use of different cell lines (preliminary rat adipocytes vs. mouse cell line 3T3-L1 and human adipocytes). However, contradictory results indicate the need for further studies on this subject.

In summary, we demonstrate that obestatin regulates the metabolism of fat cells by influencing lipogenesis, glucose transport and lipolysis. In addition, obestatin exerts its effect through GPR39 receptor.

ACKNOWLEDGEMENTS

This study was supported by MS&HE Grant No. N N303 319337 (to Tatiana Wojciechowicz) and Grant No. NN 401 0624 35 (to Przemysław Kaczmarek).

Language revision by Hugh Thomas from the University of Southampton, Institute of Developmental Sciences, Faculty of Medicine, Unit of Human Development and Health, Southampton General Hospital is gratefully acknowledged.

Special thanks go to Joanna Chmielewska PhD from Karolinska Institute, Department of Medicine for technical support.

REFERENCES

1. Zhang JV, Ren PG, Avsian-Kretchmer O, Luo CW, Rauch R, Klein C, Hsueh AJ. Obestatin, a peptide encoded by the ghrelin gene, opposes ghrelin's effects on food intake. Science 2005; 310(5750):996-9.
2. Lagaud GJ, Young A, Acena A, Morton MF, Barrett TD, Shankley NP. Obestatin reduces food intake and suppresses body weight gain in rodents. Biochem Biophys Res Commun 2007; 357(1):264-9.
3. Gourcerol G, Million M, Adelson DW, Wang Y, Wang L, Rivier J, St-Pierre DH, Tache Y. Lack of interaction between peripheral injection of CCK and obestatin in the regulation of gastric satiety signaling in rodents. Peptides 2006; 27(11):2811-9.
4. Gourcerol G, Tache Y. Obestatin--a ghrelin-associated peptide that does not hold its promise to suppress food intake and motility. Neurogastroenterol Motil 2007; 19(3):161-5.
5. Green BD, Irwin N, Flatt PR. Direct and indirect effects of obestatin peptides on food intake and the regulation of glucose homeostasis and insulin secretion in mice. Peptides 2007; 28(5):981-7.
6. Egerod KL, Holst B, Petersen PS, Hansen JB, Mulder J, Hokfelt T, Schwartz TW. GPR39 splice variants versus antisense gene LYPD1: expression and regulation in gastrointestinal tract, endocrine pancreas, liver, and white adipose tissue. Mol Endocrinol 2007; 21(7):1685-98.
7. Chartrel N, Alvear-Perez R, Leprince J, et al. Comment on "Obestatin, a peptide encoded by the ghrelin gene, opposes ghrelin's effects on food intake". Science 2007; 315(5813):766.
8. Lauwers E, Landuyt B, Arckens L, Schoofs L, Luyten W. Obestatin does not activate orphan G protein-coupled receptor GPR39. Biochem Biophys Res Commun 2006; 351(1):21-5.
9. Nogueiras R, Pfluger P, Tovar S, et al. Effects of obestatin on energy balance and growth hormone secretion in rodents. Endocrinology 2007; 148(1):21-6.

10. Zhang JV, Jahr H, Luo CW, et al. Obestatin induction of early-response gene expression in gastrointestinal and adipose tissues and the mediatory role of G protein-coupled receptor, GPR39. Mol Endocrinol 2008; 22(6):1464-75.
11. Rodbell M. Metabolism of Isolated Fat Cells. I. Effects of Hormones on Glucose Metabolism and Lipolysis. J Biol Chem 1964; 239:375-80.
12. Szkudelska K, Nogowski L, Szkudelski T. Genistein affects lipogenesis and lipolysis in isolated rat adipocytes. J Steroid Biochem Mol Biol 2000; 75(4-5):265-71.
13. Foster LB, Dunn RT. Stable reagents for determination of serum triglycerides by a colorimetric Hantzsch condensation method. Clin Chem 1973; 19(3):338-40.
14. Granata R, Settanni F, Gallo D, et al. Obestatin promotes survival of pancreatic beta-cells and human islets and induces expression of genes involved in the regulation of beta-cell mass and function. Diabetes 2008; 57(4):967-79.
15. Granata R, Gallo D, Luque RM, et al. Obestatin regulates adipocyte function and protects against diet-induced insulin resistance and inflammation. FASEB J 2012; 26(8):3393-411.
16. Egido EM, Hernandez R, Marco J, Silvestre RA. Effect of obestatin on insulin, glucagon and somatostatin secretion in the perfused rat pancreas. Regul Pept 2009; 152(1-3):61-6.
17. Camina JP. Cell biology of the ghrelin receptor. J Neuroendocrinol 2006; 18(1):65-76.
18. Patel AD, Stanley SA, Murphy KG, et al. Ghrelin stimulates insulin-induced glucose uptake in adipocytes. Regul Pept 2006; 134(1):17-22.
19. Nagaraj S, Peddha MS, Manjappara UV. Fragments of obestatin as modulators of feed intake, circulating lipids, and stored fat. Biochem Biophys Res Commun 2008; 366(3):731-7.
20. Miegueu P, St Pierre D, Broglio F, Cianflone K. Effect of desacyl ghrelin, obestatin and related peptides on triglyceride storage, metabolism and GHSR signaling in 3T3-L1 adipocytes. J Cell Biochem 112(2):704-14.

EFFECT OF LOW TEMPERATURE CULTIVATION ON INSULIN SECRETORY OF HUMAN PANCREATIC ISLETS

D.M. NIKOLIC[1,2], P.B. DJORDJEVIC[1,2], V.B. LACKOVIC[1,3], V. STOJILJKOVIC[4] and B. STANOJEVIC[5]

[1]University of Belgrade, School of Medicine, Belgrade, Serbia; [2]Clinic for Endocrinology, Diabetes and Metabolic Diseases (Laboratory for cells culture), Clinical Centre of Serbia, Belgrade, Serbia; [3]Department for Histology and Embryology Aleksandar Dj. Kostic, Belgrade, Serbia; [4]Laboratory of Molecular Biology and Endocrinology, Vinca Institute of Nuclear Sciences, University of Belgrade, Belgrade, Serbia; [5]Laboratory for Radiobiology and Molecular Genetics, Institute for Nuclear Research, Vinča, Belgrade, Serbia

Received February 29, 2012 – Accepted January 8, 2013

The experiment compared the physiological function (insulin secretory capacity) and membrane integrity of human adult pancreatic islets incubated in culture at 37°C and 24°C. Pancreatic tissue was digested with Collagenase XI, using a non-automated method. Cultures were incubated at 37°C and 24°C. Secretory capacity of the islets is determined by measuring of the stimulation index (SI) on the 1st, 3rd and 7th day of cultivation. Membrane integrity of the islets was determined by dithizone staining. Both groups of examined cultures show a slight increase in SI during the incubation. However islets incubated at 24°C show higher SI values than those incubated at 37°C on the 1st, 3rd and 7th day of incubation. And on the first day of incubation, this difference was statistically significant ($p < 0.05$). Islets incubated at 37°C showed preservation of membrane integrity, the islets are regular spherical shape, while those incubated at 24°C lose such an organization. During the seven-day cultivation, islets incubated at a standard temperature of 37°C show less preserve physiological functions in relation to cultures incubated at 24°C, but islets incubated at 37°C show more regular morphological forms.

One of the important parameters in pretransplatation preparation is the temperature of cultivation of the islets in vitro. Generally, endocrine pancreas islets are cultivated in standard medium at the normal temperature of 37°C. But there are suggestions by some laboratories for the islet cultivation that islets should be incubated at 24°C, because they show less antigenicity and better preservation of functional ability.

In experiments on rats, it was found that cell recovery and the ability of insulin secretion was a twofold-threefold higher in islets cultured at 24°C compared to those cultivated at 37°C. This may be the result of the reduced oxygen consumption and preservation of the integrity of cell membranes, as well as a consequence of reduced glucose and insulin metabolism. Reduction of glucose metabolism over a long period can lead to a critical decrease of metabolic products such as ATP and NADPH, which affect many enzymatic activities and redox state of rat pancreatic islet cells. It can be assumed that this may cause loss of cell membrane organization and

Key words: low temperature cultivation, human islets, insulin secretion

Mailing address: Nikolic DM. PhD,
Clinic for Endocrinology, Diabetes and Metabolic Diseases,
(Laboratory for cells culture),
Clinical Centre of Serbia, Dr Subotica 13,
11000 Belgrade, Serbia
Tel.: +381 11 3639 765 Fax: +381 11 2685 357
e-mail: dragannikolic8@yahoo.com

0393-974X (2013)

cell connections in the islets themselves. Apoptosis of cells is smaller on the 3rd, 5th and 14th day of cultivation at 24°C compared to 37°C. Reduced antigenicity of the islets cultured at 24°C is caused by reduced expression of MHC class II antigens, less expression of TNF-alpha and expression of IL-1b and IL-10 induced by cytokines (1).

Analysis of the islets obtained from porcine pancreas has been shown that cultivation at 22°C causes peripheral disintegration of the islets; while at 37°C islets form a smooth surface (pseudo membrane) due to a reduction in peripheral cells (50%) and increased central necrosis. Porcine pancreatic islets incubated at 37°C show complete loss of expression of MHC II on vascular endothelium but not on leukocytes and macrophages inside the islets (2). Long term cultivation of porcine pancreatic islets (18-21 days) showed complete preservation of the islets at 22°C, while cultivation at 37°C resulted in the loss of about 50% of the cell. Islets cultured at 22°C demonstrate peripheral disintegration, while cell cultivated at 37°C retain a compact cell organization within the smoothly shaped islets. Analysis of long-term culture of pancreatic islets in rats confirmed the beneficial effect of 24 h incubation at 37°C immediately after isolation and prior to cultivation at low temperature. At low temperatures islets damaged by collagenase and ischemia are better preserved, while at 37°C are subjected to fragmentation and disappearance (3).

It was found that glucose is an important metabolic precursor for phospholipids and also an important stimulus for their biosynthesis. Hypothermia significantly reduces glucose metabolism leading to disorder in the synthesis of phospholipids in cell membranes and thus damaging the integrity of the islets. These assumptions are supported in human culture where lower temperature increases the sensitivity of cultured cells on inflammatory mechanisms (4).

Glucose-stimulated insulin secretion increases oxygen and ATP consumption. This is associated with potassium (K^+)-induced membrane depolarization, leading to rapid entry of Ca^{2+} ions into the cell through voltage-dependent channels. Fusion of secretory granules containing insulin with the cell membrane depends of calcium ions (5). Cooling of mouse islets in culture from 37°C to 24°C inhibits insulin secretion due to marked reduction of exocytosis and slight drop in Ca^{2+} current (6).

Long-term cultivation at 37°C leads to central necrosis, despite the fact that viability of the islets is similar to that of freshly isolated islets. Histological studies confirmed that the central area of the islets is completely atrophic. Isolation of the islets from the pancreas destroys the capillary network and oxygen supply of islets. After only 5 m of ischemia, cellular ATP content was significantly reduced to 50% (7), because anoxia blocks glycolysis as an initial step of oxidation of glucose in the islets (8). Oxygen consumption is correlated with consumption of glucose in the medium (9) which leads to a gradient of concentration of oxygen in the isolated islets. Prolonged hypoxia may cause cell lesions, and therefore necrosis of cells. Detailed analysis of the oxygen concentration inside the islets at 37°C shows that hypoxia occurs in the core of the islets. The diffusion of oxygen into the core of the islets can be further reduced by morphological changes in the surface of the islets cultured at 37°C.

Porcine islets cultivated at 22°C show no signs of necrosis, which may be the result of reduced oxygen consumption as a consequence of reduced glucose and insulin metabolism. Solubility of oxygen in the liquid increases with decreasing temperature, and its concentration in the medium increased at lower temperatures compared to cultivation at 37°C (1) and (2). The capacity of insulin secretion was significantly lower in islets cultured at 22°C compared to 37°C and the freshly isolated islets. Despite the central necrosis of the islets cultivated at 37°C, the capacity of glucose-stimulated insulin secretion of islets is significantly different from the insulin response of freshly isolated ones. The lack of secretory capacity of the central cells is compensated by the peripheral cells. Insulin secretion decreases during 24h incubation at 22°C compared to 37°C, indicating that the biosynthesis of insulin does not cover the loss of insulin secretion in the artificial environment (2).

The aim of this study was to examine the influence of cooling to 24°C compared with standard incubation temperature of 37°C.

MATERIALS AND METHODS

Human adult pancreatic tissue was procured from the Institute for Gastrointestinal Diseases, Clinical Centre of Serbia. Tissue samples were collected from live donors,

after total or subtotal pancreatectomy due to chronic pancreatitis, cysts or tumors (10). In the case of the tumors, healthy tissue was obtained near the line of the resection. All procedures were performed in accordance with the rules of Ethics Committee of the Medical Faculty in Belgrade. Written consent was obtained from all patients.

Pancreatic tissue was transported in physiological solution from the Institute for Gastrointestinal Diseases to the Laboratory for Pancreatic Islets Culture in the Institute for Endocrinology, Diabetes and Metabolic Diseases. The material was kept in the refrigerator at 4°C (cold ischemia). Biometric parameters for pancreatic tissue are presented in Table I.

Digestion of pancreatic tissue

For pancreatic tissue digestion we used Collagenase XI - product number C7657, Sigma Aldrich (activity>1200 collagen digestion units per mg solid; 2-5 FALGPA hydrolysis units per mg solid). This enzyme preparation also contained clostripain, nonspecific neutral protease and tryptic activities. Isolation of pancreatic islets was performed in aseptic conditions in a laminar flow hood by non-automatic method (11). Tissue was transferred to Hanks solution (Sigma-Aldrich) and mechanically chopped. This material was collected with the pipette and put in test tubes containing the Collagenase solution (5mg/ml concentration). The duration of incubation was 30 m at 37°C with occasional mechanical stirring. After incubation, the content of the test tube was centrifuged at 400 g for 10 m at 15°C. Supernatant was decanted and the remaining islets were rinsed several times with Hanks solution to eliminate excess lipids and collagenase.

Separation of the islets from the surrounding acinar tissue on Ficoll gradient was not performed in order to eliminate prolong warm ischemia, which could affect the final results. Than islets were re-suspended in the final medium RPMI 1640 (Sigma-Aldrich) supplemented with 0.1% L-glutamine, 5.5 mM glucose, 25 mM hepes, 100 U/ml penicillin, 100µg/ml streptomycin and 10% fetal calf serum (FCS, Sigma). The islets were incubated in plastic flasks (Falcon 3013, volume 50 cc) in an incubator either at 24°C or at 37°C in a 5% CO_2 and 95% humidity atmosphere for 7 days. Warm ischemia time is the time measured from the beginning of the mechanical mincing of the tissue, including the isolation procedure, to the moment of placing the islets in the culture.

Determination of the isolated human adult islets

Islets were determined by dithizone (DTZ) staining on the 1st, 3rd and 7th day after their isolation.

Preparation of the Dithizone solution

Fifty milligrams of DTZ was dissolved in 10 ml of DMSO and 10 ml of Hanks solution. The solution was sterilized by passage through nylon filters of 0.20 µm pore size. Samples (1 ml of each culture) were stained with 0.2 ml of DTZ solution and incubated in an incubator at 37°C in a 5% CO_2 and 95% humidity atmosphere for 30 m. Stained islets were rinsed in Hanks solution and re-suspended in 1 ml of RPMI medium. Islets were determined with stereo-light microscope in the special counting micro-chambers (12).

Determination of the functional capacity and insulin secretion

To determine preservation of the functional capacity of the isolated islets, glucose-stimulated insulin secretion was measured on the first, third and seventh day of cultivation (13).

A static glucose stimulation assay was performed. Samples were incubated (approximately 1000-2000 islets per culture) for 1 h in low glucose (2.8 mM/L RPMI) medium, then 1 h in high glucose (20 mM/L RPMI) medium, followed by a further 1 h in low glucose medium. After each step of stimulation, cultures were centrifuged at 400G, for 10 m at 15°C. Supernatant was decanted and stored at -18˚C for insulin quantification. Insulin content was determined by radioimmunoassay (RIA INSULIN PEG). Sensitivity of the assay is 0.60 mIU/L and detection range 0.6-300mIU/L. The relative insulin release was expressed as a stimulation index (SI) and calculated as the ratio of insulin release during high glucose stimulation to insulin release during low glucose stimulation.

Statistical analysis

All results are expressed as mean±SD. A P value of less than 0.05 was considered to be statistically significant (Student's *t*-test).

RESULTS

Human adult pancreatic islets were isolated by collagenase digestion (Collagenase XI, Sigma Aldrich). Tissue for the islet cultures (in total 10 samples) was obtained from the patients after resection of pancreatic head tumor. A total of 18 cultures were incubated at 37°C and 19 cultures were incubated at 24°C in standard medium and standard conditions for 7 days. Biometric data on the material and ischemia are given in Table I. The appearance of cultures is shown in Fig. 1, 2 (incubation at 37°C) and Fig. 3, 4 (incubation at 24°C).

Insulin secretion was measured by determination of secretory index (SI) on the 1st, 3rd and 7th day of

Table I. *Biometrical data of material used for the experiment (cultures were incubated at 24 and 37°C).*

Temperature incubation (°C)	Tissue weight (g) mean±SE	Warm ischemia (min) mean±SE	Cold ischemia (min) mean±SE
24	5.84±0.513	126.4±13.388	74.4 ± 15.351
37	5.032 ± 0.57	117.2±17.14	70.2±28.33

Table II. *Mean values of SI and statistical significance in cultures incubated at 24 and 37°C. Statistical significance was compared by days of stimulation within each group.*

Temperature incubation (°C)	Time of cultivation Stimulation index (mean ± SE)			Comparison SI by days of incubation, Statistical significance (P)		
	1st day	3rd day	7th day	1st and 3rd day	1st and 7th day	3rd and 7th day
24	0.973 ±0.135	1.037 ±0.177	0.839 ±0.066	0.777	0.377	0.302
37	0.469 ±0.110	0.752 ±0.160	0.760 ±0.112	0.1656	0.0827	0.9660
Statistical significance (P)	**0.030**	0.342	0.535			

cultivation. SI values and statistical significance are shown in Table II. As for the cultures incubated at 37°C, SI values were the smallest on the first day of stimulation and then increased on the third and seventh day of stimulation (Fig. 5, Table II). There were no statistically significant differences between the results for different days of cultivation ($p \geq 0.05$).

On the other hand, SI values for cultures incubated at 24°C were similar for all three days of stimulation and no statistically significant differences were

observed (Table II).

Comparison of data for incubation at 37°C and 24°C is shown in Fig. 5. Culture cultivated at 24°C had higher SI values during all three days of stimulation, indicating that culture is more stable and has more preserved physiological function of insulin secretion. This difference was the greatest on the first day of stimulation (p less 0.05), while on the third and seventh day of incubation the differences in insulin secretion were not statistically significant (p>0.05).

Islets in cultures incubated at the standard temperature of 37°C have a proper round shape (Figs. 1, 2). Outer cell layer is dense and compact, while interior of the islets is looser. When the islets were incubated at 24°C, they lose the proper form and islets were disintegrated and irregular in shape (Figs. 3, 4).

DISCUSSION

An inevitable step in pretransplatation preparation of human adult pancreatic islets is incubation of the islets at a certain temperature. In this study we investigated the insulin secretory capacity of islets incubated at a standard temperature of 37°C and a lower temperature of 24°C. Lower temperature of incubation is recommended because it reduces antigenicity of the islets (1). Antigenicity of the islets is one of the major obstacles to successful execution of allotransplantation (transplantation between different individuals within a species). But the question is how cooling affects the physiological ability of adult human pancreatic islets to respond adequately to glucose stimulation (i.e. secretory capacity).

Comparison of secretory ability of the islets incubated at higher and lower temperatures (37°C and 24°C, respectively) show marked differences between SI values. These differences were greatest on the first day of incubation (insulin secretion of cultures incubated at lower temperature was about 107% greater), while during further incubation differences between SI values decrease (on the third day of stimulating secretion capacity was up by 37% and on the seventh day increased by 10% in cultures incubated at 24°C). Generally, cultures incubated at lower temperature showed a higher SI values on all three days of stimulation than those incubated at higher temperature.

These findings are in correlation with the results of experiments with rat islets where the secretory

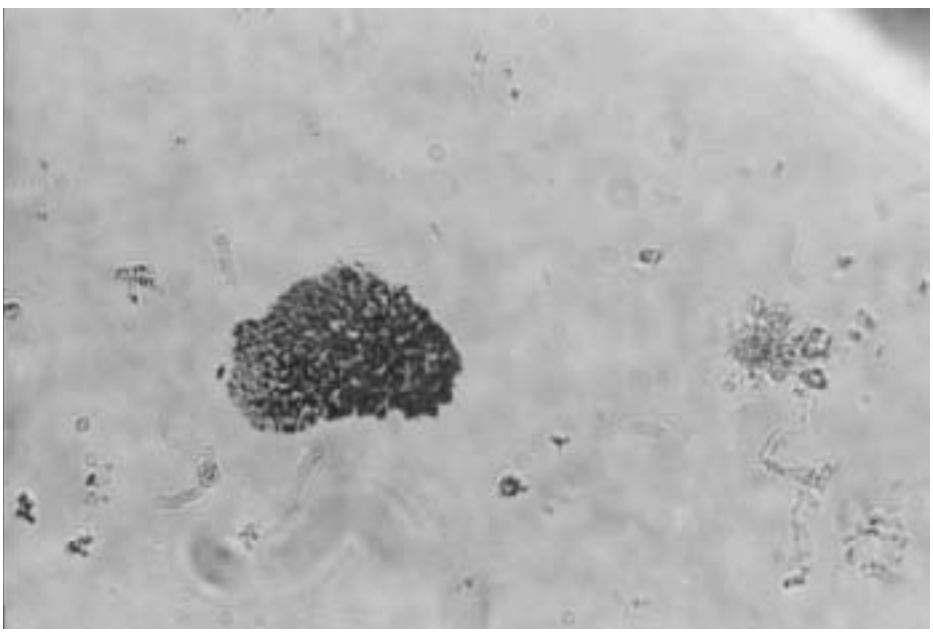

Fig. 1. *Morphological aspects of the islets incubated at 37°C, magnification (40x10), 7th day of incubation.*

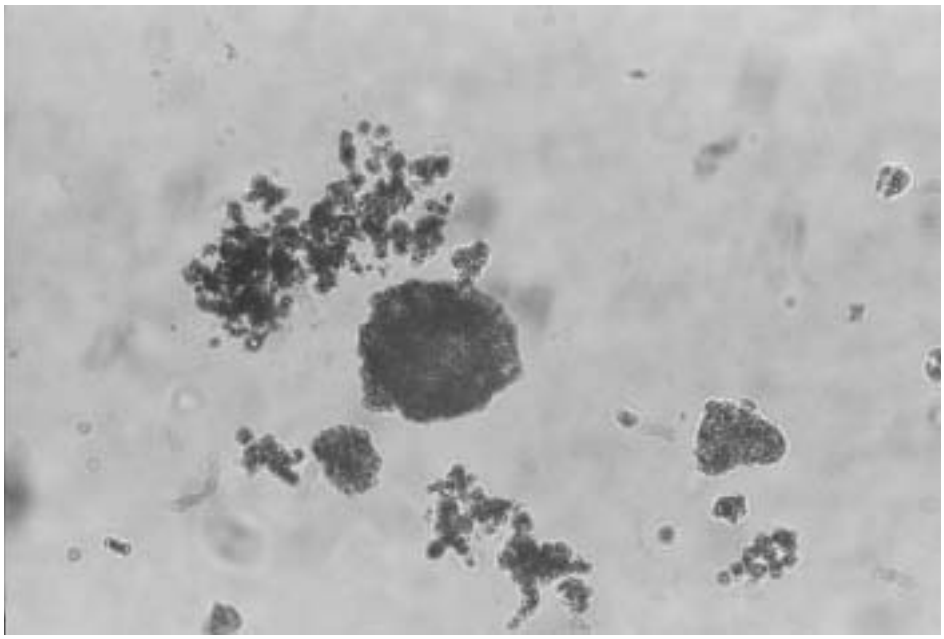

Fig. 2. *Morphological aspects of the islets incubated at 37°C, magnification (32X10), 3rd day of incubation.*

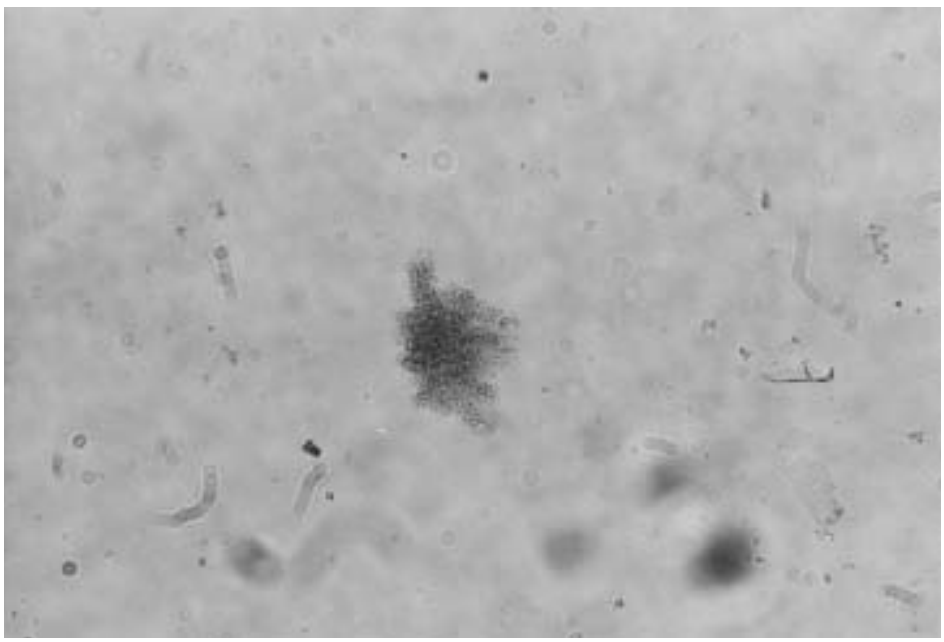

Fig. 3. *Display islet cultures incubated at 24°C, magnification (40x10), 7th day of incubation.*

capacity of islets was even 2 to 3 times higher in cultures incubated at 24°C compared to 37°C (1). But another group of authors got different results in the experiments with porcine islets (2). Secretory capacity was significantly lower in cultures cultivated at 22°C compared to 37°C. Even 24-h basal secretion was lower at 22°C compared to 37°C. At lower temperatures the biosynthesis of insulin does not cover loss of insulin in the artificial environment. Increased and decreased insulin secretion, according to those authors, is associated with the consumption of oxygen and membrane integrity, but these views

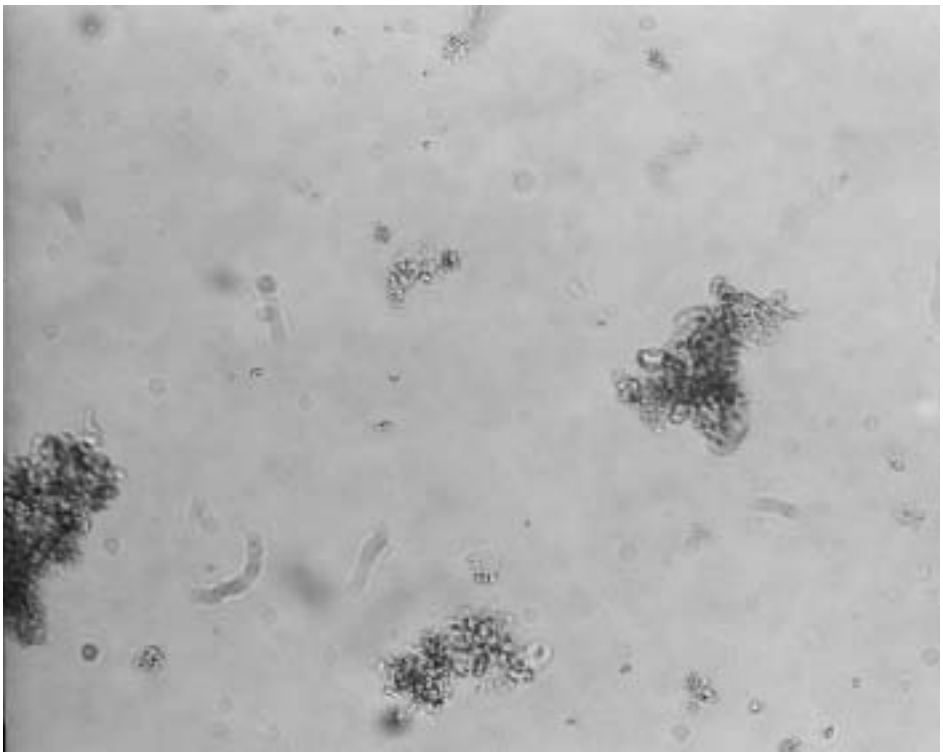

Fig. 4. *Display islet cultures incubated at 24°C, magnification (40x10), 7th day of incubation.*

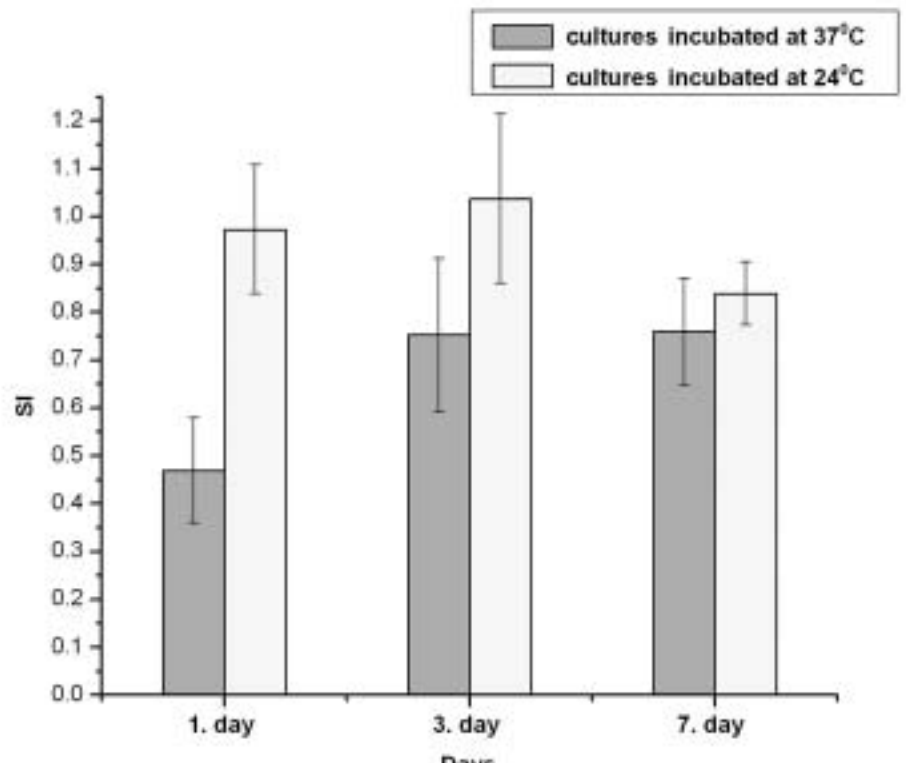

Fig. 5. *Comparative review of secretory indexes (SI) on the first, third and seventh day of incubation. Islet cultures were incubated at 24°C and 37°C. On the first day of stimulation, statistically significant difference between these two groups was observed (p <0.05).*

are very contradictory.

It should be noted that in the culture there was also present acinar tissue of the pancreas as well as ductal cells that can also affect the insulin secretion of islets. Factors related to glucose metabolism are often oscillatory and this includes oxygen consumption (14) and (15), NAD(P)H (16), mitochondrial membrane potential (17) ATP and ATP/ADP ratio (18) and the release of lactate (19).

As for the incubation at lower temperatures, we agree that cooling decreases cell metabolism, which causes reduction in glucose metabolism and this leads to a decrease in ATP and NADPH synthesis affecting many enzymatic processes inside the cell. As a consequence, there is disturbance in the synthesis of phospholipids in the cell membranes and hence impairment of integrity of the islets. Due to impaired integrity of the islets at lower temperature (Fig. 3), oxygen penetrates easier to the central parts of the islets. On the other hand, at higher temperatures oxygen solubility in liquid is reduced and the islets in the medium form a smooth outer membrane which prevents flow of oxygen to the central cell (Fig. 4). Therefore, in islets cultured at lower temperatures, there are reduced apoptosis and necrosis of central cells compared to higher temperature where the loss of cell is up to 50% (7).

Islets of Syrian golden hamsters incubated at 24^{o}C also show disintegration of peripheral layer. Such morphological changes can be mitigated by the presence of acinar trophic tissues and ductal cells that are necessary for the preservation of the morphological organization of the islets (20). Since our cultures were not purified, the presence of these cells has helped to preserve the islet organization.

Decomposition of one molecule of glucose in the glycolytic path gives two molecules of ATP. In order to enter the glycolytic path, glucose has to go through the process of phosphorylation by the action of the enzyme hexokinase. This process needs a certain amount of energy from ATP and Mg^{2+} ions and this process leads to significant loss of energy as heat that is released into the medium. It is possible that temperature in incubation medium may increase in this process. Temperatures higher than 37^{o}C (37-40^{o}C) activate the mitochondrial energy supply but further increase in temperature leads to reduced ATP synthesis (21).

Glucose-stimulated insulin secretion increases consumption of oxygen and ATP which are required for the opening of ion channels and the entry of calcium ions. Calcium ions enable the fusion of insulin secretion granules with the cell membrane and thus insulin secretion by pancreatic islet beta cells. Oxygen consumption in the medium is directly relevant to the consumption of glucose. Lack of oxygen in terms of extended hypoxia may explain the reduced insulin secretion of the cultures incubated at 37^{o}C compared to 24^{o}C. But the response should be sought in the difference of insulin secretion under the influence of low and high glucose concentrations in different temperature conditions of incubation.

During the the second hour of stimulation we added greater concentration of glucose (20 mM) but at 37^{o}C glucose uptake decreases and therefore insulin secretion. In that way the effect of increasing concentrations of glucose did not show the right way. From the formula for calculation of SI is clearly seen that the SI value will be greater if values of insulin secretion during one hour-stimulation with high concentrations of glucose are greater.

However, increased cell loss caused by necrosis and apoptosis and reduction of insulin secretion cannot fully explain the lower SI in cultures incubated at 37^{o}C compared to 24^{o}C. SI represents the ratio between the values of insulin secretion stimulated by high concentration of glucose compared to low concentration. Thus secretory capacity does not depend on the total number of stimulated cells. Although there is a worldwide laboratory practice to associated SI values with strict number of stimulated cells.

The greater value of secretory capacity on the first day of stimulation at 24^{o}C compared to 37^{o}C may be explained by the smaller temperature shock. In fact, after cold ischemia (+4^{o}C) during the process of isolation the islets were already exposed to lower temperature 18^{o}C - 24^{o}C, so that their transfer to the medium and cultivation at 24^{o}C do not represent greater temperature changes. And also residual concentration of collagenase used in the process of islet isolation have decreased enzymatic activity at lower temperatures (digestion is carried out at 37^{o}C) and therefore less pronounced toxic effects on cells.

This article present the initial phase of our investigation in the field of human pancreatic islets

cultivation on temperatures below the standard. This article presents an excellent experimental model as well. We suggest to continue to decrease the temperature of cultivation but very cautiously, until the cells in culture enter the phase of physiological coma (i.e., complete cessation of response upon glucose stimulation). Necrotic and apoptotic cell death processes should be also monitored simultaneously. The goal is to determine the temperature at which the cells can be stored in a state of hibernation which would enable the collection of more donor tissue without freezing

Analysis of the results obtained by testing the degree of preservation of insulin secretion and comparison between cultures that were incubated at standard temperature of 37°C and at low temperature of 24°C, we can conclude the following: During the seven days of cultivation the culture incubated at 24°C show greater ability of insulin secretion on the first, third and seventh day of stimulation and this difference was statistically significant on the first day. Islets incubated at 37°C have proper globular, blackberry-like shape and do not lose their configuration during the cultivation. In contrast, islets incubated at 24°C have an irregular and disorganized morphological shape.

ACKNOWLEDGEMENTS

This work was supported by the Ministry of Sciences and Technological Development of the Republic of Serbia (Grant 41002).

REFERENCES

1. Kim SC, Han DJ, Kim IH, et al. Comparative study on biologic and immunologic characteristics of the pancreas islet cell between 24°c and 37°c culture in the rat. Transplant Proc 2005; 37:3472-5.
2. Brandhorst D, Brandhorst H, Hering BJ, Bretzel RG. Long-term survival, morphology and *in vitro* function of isolated pig islets under different culture conditions. Transplantation 1999; 67:1533-41.
3. Andersson A. Long-term effects of glucose on insulin release and glucose oxidation by mouse pancreatic islets maintained in tissue culture. Biochem J 1974; 140:377-82.
4. Jahr H, Wacker T, Brandhorst H. Seven days culture of human islets at 22°C enhances susceptibility to beta cell injury. Autoimmunity 1995; 21:76-86.
5. Ortsa¨ter H, Liss P, Bergsten P. Oscillations in oxygen tension and insulin release of individual pancreatic ob/ob mouse islets. Diabetologia 2000; 43:1313-8.
6. Renstrom E, Eliasson L, Bokvist K, Rorsman P. Cooling inhibits exocytosis in single mouse pancreatic B-cells by suppression of granule mobilization. J Physiol 1996; 494:41-52.
7. Hellman B, Idahl LA, Sehlin J, Täljedal IB. Influence of anoxia on glucose metabolism in pancreatic islets: lack of correlation between fructose-1,6-diphosphate and apparent glycolytic flux. Diabetologia 1975; 11:495-500.
8. Hellerström C. Effects of carbohydrates on the oxygen consumption of isolated pancreatic islets of mice. Endocrinology 1967; 81:105-12.
9. Ono J, Lacy PE, Michael HEB, Greider MH. Studies of the functional and morphologic status of islets maintained at 24°C for four weeks *in vitro*. Am J Pathol 1979; 97:489-94.
10. White SA, Davies JE, Pollard C, et al. Pancreas resection and islet autotransplantation for end stage chronic pancreatitis. ann surg 2001; 223:423-31.
11. Nikolic DM, Djordjevic PB, Dimitrijevic Sreckovic V, et al. Comparative analysis of Collagenase XI and Liberase H1 for the isolation of human pancreatic islets. Hepato-gastroenterology 2010; 57:1573-8.
12. Nikolic DM, Djordjevic PB, Dimitrijevic Sreckovic V, Paunovic I, Kalezic N, Popovic S, Stefanovic D, Dzingalasevic M. The effect of different concentracions of liberase HI in a nonautomated method for human adult pancreatic islet isolation. Arch Biol Sci 2010; 62:833-40.
13. Mittal K, Toledo-Pereyra H, Sharma M, Ramaswamy K, Puri K, Cortez A. Acute portal hypertension and diseminated intravascular coagulation following pancreatic islet autotransplantation after subtotal pancreatectomy. Transplantation 1981; 31:302-4.
14. Nikolić DM, Djordjević PB, Dimitrijević-Srećković V, Dzingalasević M, Belij S, Kalezić N. Influence of the purification of human adult pancreatic islets on insulin secretion. Vojnosanit Pregl 2010; 67:128-31.
15. Bergsten PJ, Westerlund P, Carlsson O. Primary *in vivo* oscillations of metabolism in the pancreas. Diabetes 2002; 51:699-703.
16. Luciani DS, Misler S, Polonsky KS. Ca2þ controls

slow NAD(P)H oscillations in glucose-stimulated mouse pancreatic islets. J Physiol 2006; 572:379-92.
17. Kindmark H, Kohler M, Berggren PO. Glucose-induced oscillations in cytoplasmic free Ca2þ concentration precede oscillations in mitochondrial membrane potential in the pancreatic b-cell. J Biol Chem 2001; 276:34530-6.
18. Ainscow EK, Rutter GA. Glucose-stimulated oscillations in free cytosolic ATP concentration imaged in single islet b-cells: evidence for a Ca2þ-dependent mechanism. Diabetes 2002; 51:162-70.
19. Chou HF, Berman N, Ipp E. Oscillations of lactate released from islets of Langerhans: evidence for oscillatory glycolysis in b-cells. J Physiol 1992; 262:800-05
20. Ilieva A, Songyang Y, Rennian W, Duguid WP, Rosenberg L. The structural integrity of the islet in vitro: The effect of incubation temperature. Pancreas 1999; 19:297-03.
21. Zukiene R, Nauciene Z, Ciapaite1 J, Mildaz V, Ien E. Acute temperature resistance threshold in heart mitochondria: Febrile temperature activates function but exceeding it collapses the membrane barrier. Int J Hyperthermia 2010; 26:56-66.

EFFECTIVENESS OF OMALIZUMAB IN NON-ALLERGIC SEVERE ASTHMA

C. DOMINGO[1,2], X. POMARES[1,2], N. ANGRILL[1,2], N. RUDI[3], M.J. AMENGUAL[2,4] and R.M. MIRAPEIX[5]

[1]Servei de Pneumologia, Corporació Sanitària Parc Taulí, Sabadell Barcelona, Spain; [2]Departament de Medicina, Universitat Autònoma de Barcelona, (UAB), Barcelona, Spain; [3]Servei de Farmàcia, Corporació Sanitària Parc Taulí, Sabadell, Barcelona, Spain; [4]Servei de Laboratori, Secció d'Immunologia, UDIAT, Corporació Sanitària Parc Taulí, Sabadell Barcelona, Spain; [5]Departament de Ciències Morfològiques, Unversitat Autònoma de Barcelona, (UAB)Barcelona, Spain

Received July 2, 2012 - Accepted January 22, 2013

Omalizumab is an effective drug for allergic asthma. The purpose of this study was to evaluate the effectiveness and tolerance of this drug in non-allergic GINA step V asthma patients. This study was single-centre, prospective, open-label, observational, naturalistic. Non-allergic asthma patients requiring a mean dose of oral prednisolone of at least 5 mg/day during ≥1 year or an accumulated oral corticosteroid dose/year ≥1500 mg were enrolled. At entry and the end of the 12-month follow-up we measured blood eosinophilia and IgE concentration; at every monthly visit a forced spirometry and exhaled fraction of nitric oxide (NO) were carried out. The subjects were seven adult patients (5 female), age range 37-63 years, with the following mean values: IgE: 226.7±176 IU/mL; FVC 74±18%; FEV_1 57±11%; NO: 21.2±7 ppb. The study was approved by the IRB of the hospital. One patient decided to stop treatment after 12 weeks and was excluded from the evaluation. We did not observe changes in eosinophil count, spirometry or NO values. Three patients considered responders did not need prednisolone during the follow-up. The mean daily dose of prednisolone fell from 6.6±8.1 mg/day at entry to 1.5±2.3 mg/day ($p<0.16$) at the end of follow-up. The mean monthly accumulated dose fell from 92±112 to 12±26 mg/month ($p=0.26$). Total blood IgE increased 1.93-fold. Side effects were only local: treatment tolerance was excellent; three out of six patients seemed to slightly benefit from anti-IgE treatment; to date there is no evidence strong enough to systematically prescribe omalizumab in non-allergic asthma patients.

In the last 30 years, a new pathophysiological approach to asthma has emerged that emphasizes the important role of inflammation in this condition. Given the importance of the inflammatory events, designers of asthma management protocols have proposed the administration of anti-inflammatory drugs as first line option in persistent asthma, regardless of the severity of the disease. The consensus documents published by various professional societies support a stepwise therapeutic approach (1, 2). The last update of the Global Initiative for Asthma Treatment (GINA) emphasized the importance of controller medications, among them omalizumab, a murine IgE antibody blocking agent marketed at the end of 2006 (2). Currently, omalizumab is recommended only as add-on therapy for allergic step V asthma patients with concentrations of blood IgE above 30 IU/mL. Although some off-label prescriptions

Key words: non-allergic asthma, omalizumab, oral corticosteroid sparing effect

Mailing address: Dr. Christian Domingo,
Servei de Pneumologia,
Corporació Parc Taulí, Parc Tauli 1,
08208 Sabadell, Barcelona, Spain
Tel.: +34 93 7231010
Fax: +34 93 7160646
e-mail: cdomingo@tauli.cat

0393-974X (2013)

have been evaluated (and have been associated with varying degrees of success) there are no reports in the literature on the effectiveness of omalizumab for severe non-allergic asthma patients. In this paper we describe our long-term experience in a cohort of these patients treated with omalizumab.

MATERIALS AND METHODS

Our hypothesis was that omalizumab would be effective and well tolerated in non-allergic asthma patients with blood IgE concentrations above 30 IU/mL and that the drug would have an oral corticosteroid sparing effect.

Population

Patients were recruited from the out-patient clinic for asthma treatment at our institution (3). The inclusion criteria were: age ≥18 years old; obstructive airway disease with an FEV_1 reversibility ≥12% and 200 mL; steroid-dependence: defined either as a requirement of a mean daily dose of at least 5 mg per day of prednisolone to maintain a forced expiratory volume in the first second (FEV_1) □50% during a period of one year or more, in addition to the best standard care (BSC) provided by GINA (2), or as repeated boosters (≥5/year with an accumulated oral corticosteroid dose ≥300 mg/episode) during the previous year; negative skin-prick test and *in vitro* reactivity (RAST); baseline Immunoglobulin E level ranking between 30-700 IU/mL; patient weight between 25 and 150 kg. The exclusion criteria were: patient refusing treatment; hypersensitivity to omalizumab; patient unable to regularly attend the asthma unit for control and drug administration; previous anti-IgE treatment.

Since this was an off-label treatment, written informed consent as well as the authorization of the Spanish Health Ministry was obtained in all cases. The study was approved by the internal review board (IRB) of the hospital.

Methods

The study design was single-centre, prospective, open-label, and observational naturalistic. The follow-up period considered for evaluation was 12 months. The study was carried out at the Corporació Parc Taulí (CPT) (Sabadell, Catalonia), a 760-bed university hospital.

BSC following the recommendations of the GINA are described elsewhere (4). Prior to starting omalizumab treatment, patients underwent a stabilization period of at least three months. The protocol followed for decreasing oral steroid administration has also been described elsewhere (4).

The dose of omalizumab was calculated according to the dosing tables previously published by the European Medical Agency (5). Patients remained under observation for two hours after the first three omalizumab injections and for one hour after all injections (4).

The primary outcome of effectiveness was the oral corticosteroid sparing capacity, measured as the decrease from the initial to the final oral corticosteroid dose as well as the progressive decrease in the monthly accumulated dose or the absence of boosters of oral corticosteroids during follow-up. The primary safety outcome was the incidence of side-effects, and the second safety outcome was the deterioration of the lung function (FEV_1) and increase in airway inflammation (exhaled nitric oxide).

At each outpatient visit, patients were asked to describe their asthma treatment, and the total monthly oral corticosteroid dose was recorded. In the case of exacerbation, patients were asked to come to the hospital, if possible to the outpatient centre at our pulmonary service during business hours rather than the emergency room (ER) in order to facilitate treatment control. Nonetheless, we were also able to retrieve data on patients who came to the ER and on their treatment after discharge, since the clinical histories at the hospital are computerized.

Pulmonary function testings (PFTs), prick test, exhaled nitric oxide (NO) measurement, blood analysis (including hemogram, IgE level and RAST) and imaging tests were performed as previously described (4). PFTs and exhaled NO were measured at each monthly visit.

Side-effects

Patients were specifically asked about side-effects at each visit. They were also given the telephone number of the outpatient unit of the pulmonary service and told to report any suspected side-effects.

Statistical analysis

Descriptive statistics included means and standard deviations for continuous variables. Parametric tests (student's *t*-test for paired data) were used to compare the initial and end corticosteroid dose, NO, and PFTs. ANOVA test was used for the monthly dose of oral corticosteroid intake comparison. SPSS version 17.0 was used for data compilation and analysis. A p-value <0.05 was considered statistically significant.

RESULTS

Seven patients were included but one dropped out early of her own volition and was excluded from the evaluation. The follow-up period was 12 months. Demographic data, baseline spirometry values, blood eosinophil count, mean initial daily

Table I. *Demographic data as well as initial and end results.*

	Initial	End
Number of patients:	7	6
Age range (years)	37-63	
Sex	5 females, 2 males	
FVC mL (%)	2.730±1.430 (74±18)	2.420±1061 (68±19)
FEV_1 mL (%)	1.520±620 (57±11);	1.391±677 (53±23)
FEV_1/FVC (%)	58,6±8,7	56.2±10.5
Mean IgE concentrations (IU/mL)	226.7±176	437±504
Mean oral corticosteroid dose (mg/day)	6.6±8.1	1.5±2.3
Mean monthly accumulated oral corticosteroid dose (mg/day)	92±112	12±26
Eosinophil count (absolute value)	415±407	311±206
Eosinophil count (%)	4.0±3.5	3.6±2.19

dose of 6-methylprednisolone at the end of the stabilization period and the data at the end of follow-up are shown in Table I. The relations between initial and final oral corticosteroid dose, mean monthly accumulated oral corticosteroid dose, eosinophil count and IgE concentrations are shown in Table I. The IgE concentration showed a 1.93-fold increase. Fig. 1 shows the accumulated monthly dose of oral corticosteroid in every patient. Patients 4, 5 and 6 did not benefit but in patient 2 the monthly dose of oral corticosteroids progressively decreased. Patients 1 and 3 were not taking oral corticosteroids at the beginning of treatment with omalizumab, but they required repeated boosters (as stated in the inclusion criteria); during follow-up they no longer needed these boosters. As a result, patients 1, 2 and 3 were considered responders according to the definition of the primary outcome. Two out of these three patients were taking weekly oral methotrexate, which could be stopped during the follow-up. The monthly individual spirometric results are displayed in Fig. 2. This figure shows that although FEV_1 increased markedly in patient 2, in general the severity of airway obstruction did not worsen. The mean exhaled NO values at entry were 21.2±7 (ppb). Fig. 3 shows the individual mean monthly values of exhaled NO measurements. Exhaled NO values remained quite stable during the follow-up except for a peak value for patient 5 which preceded an increase in the oral corticosteroid dose, thus reflecting an exacerbation. Fig. 4AB show the initial and final eosinophil counts for each patient. The response was quite similar in responder and non-responder groups; in both groups the eosinophil count increased in one patient, decreased in another and did not change in another.

Side-effects

Drug administration was generally well tolerated, despite mild local side-effects. No general side-effects were detected.

DISCUSSION

Until late 2006 oral corticosteroids was the only treatment admitted for severe asthma patients (2). Several immunosuppressors had been tested but, despite the favourable results of some studies (6, 7), no international guideline currently recommends their use. In November 2006 omalizumab, a humanized murine IgG with an IgE blocking effect was marketed. Although it had only been tested in patients with allergic asthma receiving high doses of inhaled corticosteroids, the GINA included it in the highest treatment step as an alternative or add-on therapy for uncontrolled allergic asthma patients requiring oral corticosteroids (2). Since

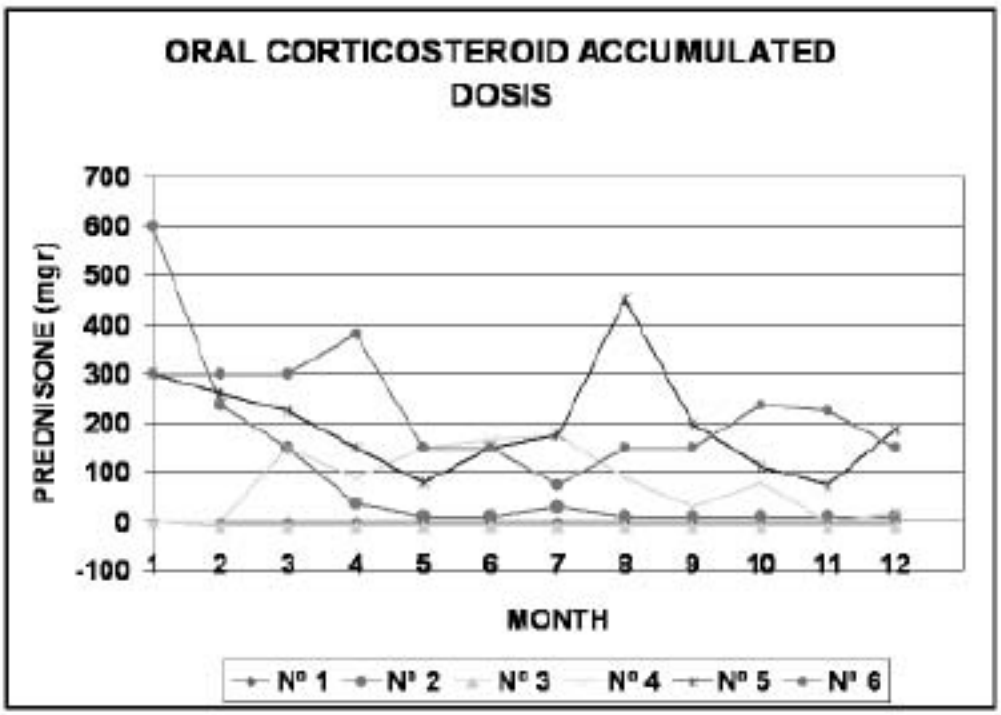

Fig. 1. *Accumulated monthly dose of oral corticosteroid in every patient.*

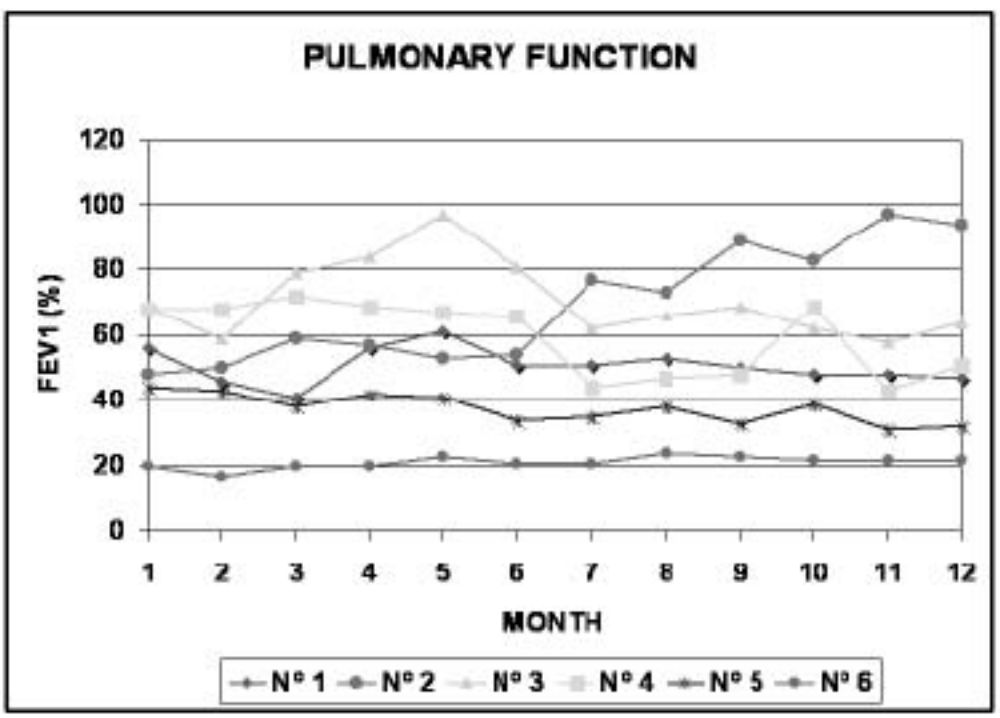

Fig. 2. *Monthly individual spirometric results.*

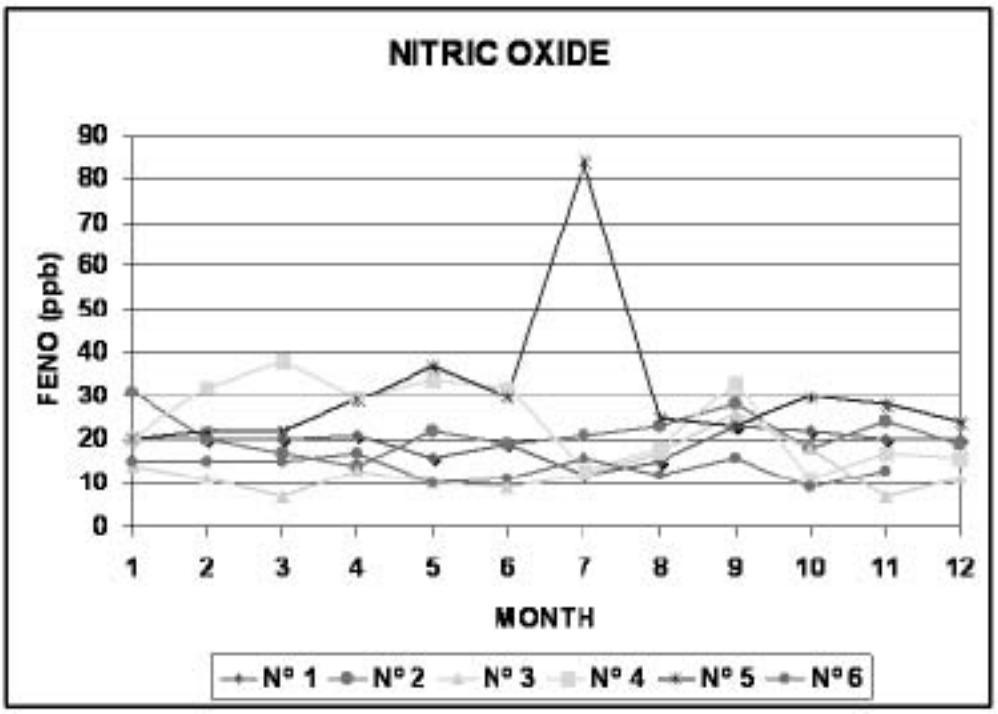

Fig. 3. *Mean monthly results of exhaled nitric oxide measurements.*

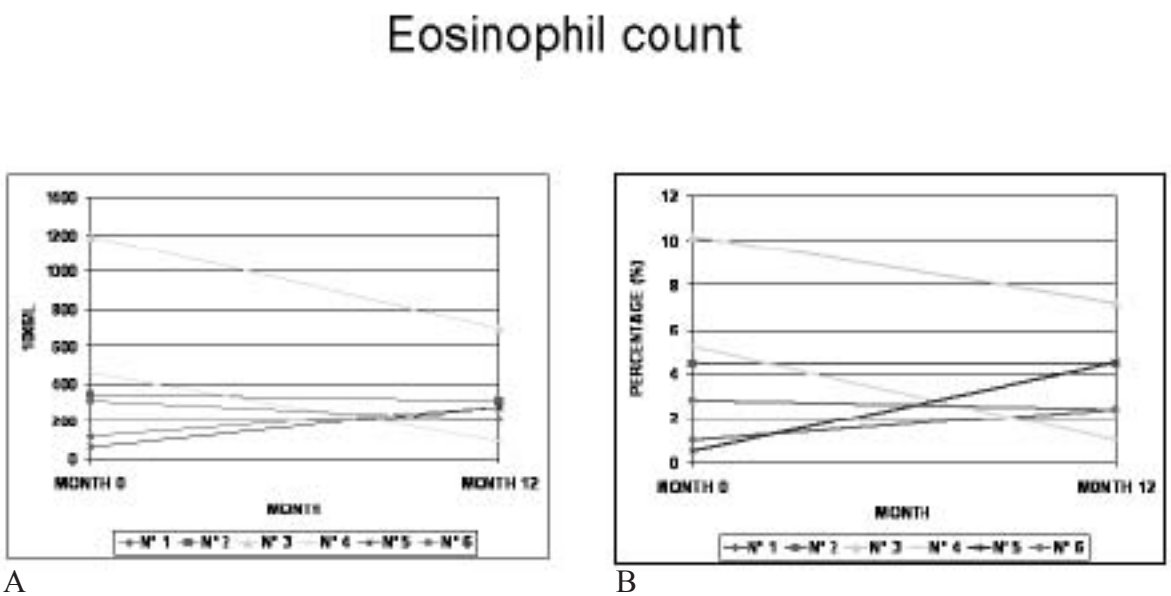

Fig. 4. A and **B)** *Initial and final eosinophil counts for each patient in absolute value and percentage.*

then, reports in the literature have demonstrated the oral corticosteroid sparing effect of omalizumab in allergic asthmatic patients (4, 8). The drug has also been prescribed in off-label situations, although the experience is limited (9-11). It is currently unclear whether omalizumab has a beneficial effect in patients with non-allergic asthma with a blood IgE concentration above 30 IU/mL.

Asthma is a chronic inflammatory disease of the airways caused by the interaction of several types of cells and molecules. The cells involved include mast cells, eosinophils, T-lymphocytes, macrophages and neutrophils. The inflammatory cascade is mediated by cytokines and interleukins. When an atopic individual is exposed to an antigen, the dendritic cells (specialized macrophages located in the organism's epithelium) internalize it, process it and present it to a T-lymphocyte via the major histocompatibility complex. In this process the T-lymphocyte develops a T_h2 or a T_h1 profile. When the type of antigen is an allergen, the lymphocyte differentiates into a T_h2 cell able to produce IL-4 which in turn promotes the synthesis of IgE by the B-lymphocytes (5). IgE-dependent inflammatory phenomena have been studied in depth and are recognized in atopic subjects (12). In these subjects, exposure to high concentrations of allergens, above all dust mites at early ages, leads to a high concentration of serum IgE, which favours the appearance of allergic symptoms. Though the IgE regulation described above is found in atopic subjects, recent publications show that IgE may be produced by B-lymphocytes in non-allergic subjects due to the presentation of the allergen through the mucosa. This IgE may bind to the high affinity receptors on the mast cells or basophils and produce the same type of inflammation as in subjects considered allergic (13, 14).

Some authors have suggested that there are many similarities between allergic and nonallergic asthma since both sets of patients present largely the same type of inflammation in the bronchial mucosa and an increased numbers of eosinophils and mast cells in bronchial biopsies (15, 16). Thus the relatively recent finding that IgE can be produced locally in mucosal tissue, without a marked increase in IgE levels in the blood, somewhat blurs the distinction between non-atopic and atopic diseases such as asthma. Interestingly, an alternative or additional explanation may be provided by the findings of Kalesnikoff et al (17), who observed that by binding to its high-affinity receptor (FcεRI) IgE was able to induce intracellular signaling pathways, resulting in the production of cytokines (e.g. IL-4, IL-6, IL-13, tumor necrosis factor-α) and the enhancement of mast cell survival on its own, without cross-linking by allergens. In addition, IgE can directly bind and activate receptors present on eosinophils, neutrophils, and monocytes (18, 19). As a result, the rationale for the use of omalizumab in non-allergic patients is based on its blocking effect on IgE which inhibits part of T_h2 immune response, thus reducing recruitment and activation of effector cells of the inflammatory process, including eosinophils (20). Because IgE effector cells such as mast cells and basophils are a source of pro-inflammatory chemokines, cytokines, and proteases, anti-IgE therapy may have anti-inflammatory effects in asthma; indeed this role has been suggested in other diseases such as eosinophil-associated gastrointestinal disorders (21).

The use of omalizumab can reduce both the daily and the monthly accumulated oral corticosteroid intake. The total daily and monthly accumulated dose of oral corticosteroids notable decreased (77% and 87% respectively) but the results did not reach a statistically significance; this may have been due to the small number of patients treated, they also somehow reflect that the benefits are much less relevant than in allergic patients (4). We classified the cohort into responders (3 patients) and non-responders (3 remaining patients) according to the oral corticosteroid sparing effect of the drug. Two of the responders (patients 1, 3) had been receiving boosters during the previous year, but they did not need oral corticosteroids during the twelve-month follow-up. Patient 2, who was taking oral corticosteroids, progressively reduced her needs. Finally, these three patients had been prescribed methotrexate for its oral corticosteroid sparing effect, and we were able to withdraw this drug in two of them. Since according to our experience methotrexate has an oral corticosteroid sparing effect (6, 7, 22), this aspect, although difficult to quantify, should also be considered as a clinical benefit observed in these two responder patients. Despite the reduction in oral corticosteroid intake, no patient experienced a deterioration in pulmonary function or exhaled NO, with the exception of patient 5 in which the increase in NO measurement was followed by an increase in the oral corticosteroid dose, reflecting an exacerbation.

Although these data could easily make support the hypothesis that omalizumab exerts anti-inflammatory effects in non-allergic asthma and that the treatment was effective, our experience in

long-term treatment of asthma patients has taught us that these apparent benefits could be due to the long-term effects of oral corticosteroids, rather than to omalizumab. It is well-known that the dose of oral corticosteroids is variable along patients' life and that in some patients considered oral corticosteroid dependent, the oral steroids can temporarily be withdrawn. Thus, in an open observational study one would expect a more dramatic improvement.

Some studies have demonstrated the anti-allergic and anti-inflammatory properties of omalizumab, such as the reduction in circulating and tissue eosinophils (23, 24). More recently, Noga et al. 2006 (23) demonstrated an increase in eosinophil apoptosis and a decrease in granulocyte macrophage colony stimulating factor (GM-CSF, IL-2 and Il-13. Thus one would expect the number of eosinophils in peripheral blood to decrease in this series. The overall evaluation showed a slight decrease in the eosinophil count, both in absolute value and as a percentage of total white cells. The comparison of responders and non-responders evidenced that in both groups the changes occurred randomly, since the number of eosinophils increased in one patient, decreased in another and did not change in the third. Thus, in non-allergic asthma, treatment with omalizumab did not seem to influence the peripheral eosinophil count.

Some authors have suggested that patients with higher levels of serum total IgE will present increased symptoms and more severe airway (25, 26). We could not confirm these hypotheses in our series since the airway obstruction was not related to the IgE level. Moreover, our cohort of patients had slightly lower values of IgE blood concentration than allergic patients, and the increase after omalizumab treatment was also lower (4). Finally, as expected, the tolerance of treatment was excellent (4).

We have found only two case reports in the literature of the use of omalizumab to treat non-allergic asthma. The first one was a patient with Churg-Strauss syndrome (CSS) (20). Although he received omalizumab for recurrences of his CSS, including lung infiltrates and eosinophilia, he presented non-allergic asthma. The second was a recently published pure case (27). Both patients improved after anti-IgE treatment.

Finally, we also found an abstract where the authors intended to identify the subset of non-allergic asthma patients that might benefit from omalizumab; although they observed a shift in cellular FcεRIά in treated patients, no clinical benefits were evidenced (28).

Our study has a number of limitations. The number of patients is low, there is no control group, and neither patients nor physicians were blind to treatment. So the contribution of placebo effects in responder patients cannot be excluded. However, the uncontrolled status of the study could in fact be considered a strength, since it was performed in a naturalistic setting, the ideal way to demonstrate the results of an effectiveness study. Finally, although systemic corticosteroid requirement is one of the major treatment outcomes in severe asthma, symptom control is also important in deciding effectiveness of treatment. Thus symptom assessments of the patients before and after omalizumab treatment by one of the validated questionnaires were not regularly obtained in our study.

To summarize, we believe that although our results seem to somehow show that in some non-allergic asthma patients, omalizumab could have to some extend an oral corticosteroid sparing effect we should be very cautious in the interpretation of these findings. Our results should be considered preliminary and further studies are needed before any conclusion is definitely established. Thus, to date there is no strong enough evidence to systematically prescribe omalizumab in non-allergic asthma patients.

ACKNOWLEDGEMENTS

The authors thank Adela García and Carmen Veigas, nurses at the Service of Pneumology for their clinical assistance, and Michael Maudsley of the University of Barcelona's Language Service for revising the English. This study was partially funded by a grant obtained from the FUCAP (Fundació Catalana de Pneumologia 2007).

REFERENCES

1. International Consensus Report on diagnosis and treatment of asthma. National Heart, Lung and Blood Institute, National Institutes of Health. Bethesda,

Maryland 20892. Eur Respir J 1992; 5:601-41.
2. Global Initiative for Asthma (GINA). Global strategy for asthma management and prevention. NHLBI/WHO workshop report. National Institutes of Health, National Heart, Lung and Blood Institute. NIH publication number 95-3659.
3. Domingo C. Effectiveness and efficiency of an outpatient clinic for corticosteroid-dependent asthmatics. Arch Bronconeumol 2001; 37:274-80.
4. Domingo C, Moreno A, Amengual M.J, Montón C, Suárez D, Pomares J. Omalizumab in the management of oral corticosteroid-dependent IgE-mediated asthma patients. Curr Med Res Opin 2011; 27:145-53
5. Domingo Ch, Pacheco A, Hinojosa M, Bosque M. The relevance of IgE in the pathogenesis of allergy: the effect of an anti-IgE Drug in asthma and other diseases. Recent Patents Inflamm. Allergy Drug Discov 2007; 1:151-64.
6. Comet R, Domingo Ch, Larrosa M, Morón A, Rué M, Amengual MJ, Marín A. Benefits of low weekly doses of methotrexate in steroid-dependent asthmatic patients. a double-blind, randomized, placebo-controlled study. Respir Med 2006; 100:411-9.
7. Domingo Ch, Moreno A, Amengual M.J, Comet R, Luján M. Twelve years' experience with methotrexate for GINA treatment step 5 asthma patients. Curr. Med Res Opin 2008; 25:367-74.
8. Molimard M, Buhl R, Niven T, et al. Omalizumab reduces oral corticosteroid use in patients with sever allergic asthma: Real life data. Respir Med 2010; 104:1381-5.
9. Mankad VS, Burks AW. Omalizumab other indications and unanswered questions. Clin Rev Allergy and Immunol 2005; 29:17-30.
10. Kaya H, Gümüş S, Uçar E, Aydoğan M, Muşabak U, Tozkoparan E, Bilgiç H. Omalizumab as a steroid-sparing agent in chronic eosinophilic pneumonia. Chest 2012; 142:513-6.
11. Domingo C, Pomares, X. Can omalizumab be effective in chronic eosinophilic pneumonia? Chest 2013; 143:274.
12. Owen CE. Immunoglobulin E: Role in asthma and allergic disease: Lessons from the clinic. Pharmacol Ther 2007; 113:121-33.
13. Humbert M, Menz G, Ying S, Corrigan CJ, Robinson DS, Durham SR, Kay AB. The immunopathology of extrinsic (atopic) and intrinsic (non atopic) asthma; more similarities than differences. Immunology Today 1999; 20:528-33.
14. Mehlhop PD, Blake K. Impact of inadequately controlled asthma: a need for targeted therapy? J Clin Pharmacother 2004; 29:189-94.
15. Ying S, Humbert M, Barkans J, et al. Expression of IL-4 and IL-5 mRNA and protein product by CD4 1 and CD8 1 T cells, eosinophils, and mast cells in bronchial biopsies obtained from atopic and nonatopic (intrinsic) asthmatics . J Immunol 1997; 158:3539-44.
16. Humbert M, Durham SR, Ying S, et al. IL-4 and IL-5 mRNA and protein in bronchial biopsies from patients with atopic and nonatopic asthma: evidence against "intrinsic" asthma being a distinct immunopathologic entity. Am J Respir Crit Care Med 1996; 154:1497-504.
17. Kalesnikoff J, Huber M, Lam V, et al. Monomeric IgE stimulates signaling pathways in mast cells that lead to cytokine production and cell survival. Immunity. 2001; 14:801-11.
18. Saffar AS, Alphonse MP, Shan L, Hayglass KT, Simons FE, Gounni AS. IgE modulates neutrophil survival in asthma: role of mitochondrial pathway. J Immunol 2007; 178:2535-41.
19. Bjerke T, Hoffmann HJ, Christensen EI, Poulsen LK, Skjold T, Dahl R. Regulation of FcepsilonARI synthesis in human eosinophils. Int Arch Allergy Immunol 1999; 118:440-42.
20. Gavina Bianchi P, Gavina-Bianchi M, Agondi R, Kalil J. Three months administration of anti-IgE to a patient with Churg-Strauss syndrome. J Allergy Clin Immun 2007; 119:1279.
21. Forough S, Foster B, Kim NY et al. Anti-IgE treatment of eosinophil-associated gastrointestinal disorders. J Allergy Clin Immunol 2007; 120:594-601.
22. Noga O, Hanf G, Kunbel G. Immunological and clinical changes in allergic asthmatics following treatment with omalizumab. Int Arch Allergy Immunol 2003; 131:46-52.
23. Djukanovic R, Wilson SJ, Kraft, M, et al. Effects of treatment with anti-immunoglobulin E antibody omalizumab on airway inflammation in allergic asthma. Am J Resp Crit Care Med 2004; 170:583-93.
24. Beeh KM, Ksoll M, Buhl R. Elevation of total

serum IgE is associated with asthma in nonallergic individuals. Eur Respir J 2000; 16:609-14.

25. Burrows B, Halonen M, Lebowitz MD, Knudson RJ, Barbee RA. The relationship of serum immunoglobulin E, allergy skin tests, and smoking to respiratory disorders. J Allergy Clin Immunol 1982; 70:199-204.
26. van den Berge M, Pauw RG, de Monchy JG, van Minnen CA, Postma DS, Kerstjens HA. Beneficial effects of treatment with anti-IgE antibodies (omalizumab) in a patient with severe asthma and negative skin-prick test results. Chest 2011; 139:190-3.
27. Creticos PS, Saini SS, Scarupa MD, Balcer-Whaley SL, Bieneman AP, Schroeder JT. Effects of omalizumab in non-allergic asthma. J Allergy Clin Immunol 2010; 125(2):AB197.

PROTECTIVE EFFECT OF OLEANOLIC ACID AGAINST β CELL DYSFUNCTION AND MITOCHONDRIAL APOPTOSIS: CRUCIAL ROLE OF ERK-NRF2 SIGNALING PATHWAY

X. WANG[1], H.L. CHEN[1], J.Z. LIU[1], N. LIAO[1], W.H. YU[1], X.D. ZHANG[1], T. ZHANG[1], W.L. LI[1] and C.X. HAI[1]

[1]Department of Toxicology, Shaanxi Key Lab of Free Radical Biology and Medicine, Ministry of Education Key Lab of Hazard Assessment and Control in Special Operational Environment, School of Public Health, Fourth Military Medical University, Xi'an, China

Received August 1, 2012 – Accepted November 21, 2012

The first three authors contributed equally to this work

Pancreatic β cell dysfunction is a hallmark of diabetes. Our previous results have shown that oleanolic acid (OA) has anti-diabetic potential. However, there is little literature reporting the effect of OA on β cell dysfunction. The present study was designed to investigate the protective effect of OA against lipotoxicity and the underlying mechanisms. Lepr (db/db) diabetic mice were subjected to fasting blood glucose measurement, intraperitoneal glucose tolerance test after the administration of OA for two weeks. Histopathological observation was conducted by HE staining and transmission electron microscopy assay. Pancreatic islets were isolated from db/db diabetic mice and C57BL/6J mice. Palmitic acid (PA) was used to induce lipotoxicity *in vitro*. Apoptosis was evaluated in pancreatic islets in diabetic mice and in isolated pancreatic islets and β-TC3 cells by TUNEL assay. Cellular ATP content, mitochondrial function and redox balance were examined. Phosphorylation of c-Jun NH2-terminal kinase (JNK) and extracellular signal-regulated kinase (ERK) and the activation of nuclear erythroid factor 2 p45-related factor 2 (Nrf2) signaling were evaluated by western blotting. In db/db mice, OA significantly protects β cell function against lipotoxicity, evidenced by inhibition of apoptosis and improvement of glucose tolerance. In cells, OA administration may protect against PA-induced apoptosis and decrease of GSIS, in which process the activation of Nrf2 is essential. Once Nrf2 is activated, OA could induce GCLc expression, promote the production of GSH, and thus inhibit JNK phosphorylation and solid the antioxidant defense of mitochondria, leading to the inhibition of mitochondrial apoptosis. ERK signaling pathway is responsible for OA-induced activation of Nrf2 and the protective effect of OA. Overall, our study enhances the understanding of the protective effect of OA on β cell and provides clues for further studies on the underlying mechanisms.

In the last decades, diabetes has become a serious public health problem across the whole world (1, 2), which is characterized by hyperglycemia. A recent report suggests that 92.4 million adults (9.7% of the

Key words: oleanolic acid, β cell dysfunction, nuclear factorerythroid 2 p45-related factor 2, extracellular signal-regulated kinase

Mailing address: C.X. Hai, Ph.D., M.D.,
Department of Toxicology,
School of Public Health,
Fourth Military Medical University,
Xi'an, 710032, China
Tel.: +86 29 84774879 Fax: +86 29 84774879
e-mail: cx-hai@fmmu.edu.cn

0393-974X (2013)

adult population) have diabetes in China (3). Current estimates suggest that by the year 2030, over 350 million people worldwide will be affected by this disease and its conditions (4). β cell dysfunction is a key driver and a hallmark in the pathogenesis of both of type 1 diabetes and type 2 diabetes, contributing to hyperglycemia (5). A large body of evidence has shown that oxidative stress plays a fundamental role in the pathogenesis of β cell dysfunction (6).

In light of the widespread of diabetes, there is urgent need to find out effective strategies. Although various compounds have been testified to reduce insulin resistance and protect β cell function, there are still some limitations to the current treatment options (7). Therefore, exploration of compounds with anti-diabetic properties is still needed. In recent years, great attention has been focused on the pharmacological activities of plants rich in triterpenoid. Oleanolic acid (OA) is a natural triterpenoid and an aglycone of many saponins. OA has been used in Chinese medicine for the treatment of liver disorders for over 20 years. OA exists largely in food products (vegetable oils), and is a constituent of the leaves and roots of Olea europaea, Viscum album L., Aralia chinensis L. and other more than 120 plant species (8). Originally, OA has been shown to protect against a variety of hepatotoxicants such as carbon tetrachloride, cadmium, acetaminophen, and bromobenzene (9, 10). Our previous studies have found that OA possesses a potent antioxidant activity and could protect hepatocytes against oxidative stress (11). Nuclear factor erythroid 2 p45-related factor 2 (Nrf2) may be the target of OA, which is responsible for the antioxidant activity of OA (11, 12). In streptozotocin-induced diabetic rats, we have shown that OA effectively lowered blood glucose, in which process the activation of ERK signaling was involved (13). However, the understanding of the protective effect of OA against diabetes is far from complete and further work is urgently needed to clarify the effect of OA on pancreatic β cell dysfunction.

In the present study, we aimed to investigate the effect of OA on β cell dysfunction in Lepr (db/db) mice and β-TC3 cells. The results showed that in db/db mice, OA administration significantly lowered fasting blood glucose (FBG), ameliorated impairment of glucose tolerance and protected β cell function. In β-TC3 cells, OA could significantly attenuate palmitic acid (PA)-induced apoptosis. Moreover, OA may notably protect against PA-induced insulin secretion deficiency.

The activation of extracellular signal-regulated kinases (ERK)-Nrf2 pathway was involved in the protective effect of OA.

MATERIALS AND METHODS

Chemicals and reagents

GCLc, JNK, P- JNK, ERK, P-ERK and Tubulin α antibodies were purchased from Bioworld Technology. β-actin, cytochrome c and Nrf2 antibodies were purchased from Santa Cruz Biotechnology (Santa Cruz, CA). Most of the other chemicals and reagents used in this study were procured from Sigma.

Animals treatment and pancreatic islet cultures

Animal experiments were approved by University Ethics Committee. 20 db/db mice and 10 wild type littermates were purchased from Model Animal Research Centre, Nanjing University, China. db/db mice were randomly divided into two groups: db/db group and 20 mg/kg OA group. Wild type littermates were used as control. In OA-treating groups, mice were administered with OA (20 mg/kg, i.p.) for two weeks. In other groups, mice were offered with vehicle (2% Tween 80 in sterile saline, i.p.). Part of pancreas was excised from the animals for the pathological histology. db/db mice and C57BL/6J mice were anesthetized with pentobarbital (65 mg/ml, i.p.) and isolated pancreatic islets were obtained by collagenase digestion as described (14). After digestion, the islets were purified by filtration. Pancreatic islets Islets were cultured in DMEM, supplemented with 10% fetal bovine serum, for the determination of insulin secretion.

IPGTT

The intraperitoneal glucose tolerance test (IPGTT) was performed. Prior to the test, mice were fasted for 12 h. Then, a baseline blood sample was taken from their tail and then each mouse received i.p. glucose, 1 g/kg body weight (Novolin R by Novo Nordisk Pharmaceuticals, Princeton, NJ). Tail blood samples were drawn at, 30, 60, and 120 m after the injection and were analyzed immediately for glucose content.

Transmission electron microscopy (TEM) assay

TEM assay was conducted as previously described (15). In brief, pancreas was fixed in 2% glutaraldehyde in 0.1 M PBS (pH 7.4) for 2 h at 4°C. Subsequently, they were post-fixed in 1% osmium tetroxide in 0.1 M PBS

(pH 7.4) for 2 h at 4°C. After that, samples were washed in buffer and dehydrated in a series of water/ethanol mixtures to 100% ethanol. Then they were infiltrated in sequentially increasing concentrations of araldite 618 to 100%, embedded in Beam capsules, and placed in a 60°C oven for 48 h. Ultrathin sections were stained with lead citrate and rinsed with distilled water. Finally, section samples were viewed with transmission electron microscope (JEM-2000EX, Japan).

Cell culture and treatment

β-TC3 cells were obtained from the China Center for Type Culture Collection (CCTCC; Wuhan, China). β-TC3 cells were cultured in DMEM medium containing 5.5 mM glucose and 10% fetal bovine serum. They were maintained in a humidified 5% CO_2 atmosphere at 37°C. In all analyses, PA was first dissolved in 100% ethanol at a concentration of 100mM, then freshly diluted with serum-free DMEM with 2% fatty acid-free BSA as we previously reported (16), to the appropriate concentration. The final concentration of ethanol was <0.1%. Culture medium with ethanol and 2% fatty acid-free BSA served as the control in each PA-treating experiment. After pre-incubation overnight in the presence of 5.5 mM glucose and 10% fetal bovine serum, cells were washed three times with PBS and exposed to 400 μM PA in the presence or absence of 10 μM OA for 48 h.

Determination of β cell apoptosis

Cell apoptosis of pancreatic islets was evaluated by TUNEL (Beyotime Institute of Biotechnology) assay according to the manufacture's instruction. Islets and β cells were fixed in 4% (wt/vol.) phosphatebuffered paraformaldehyde. Cell apoptosis was quantified by staining islets and β cell with TUNEL and anti-insulin antibody. Histological assessment of β cell apoptosis was carried out by a single investigator who was blinded to experimental treatment for each sample. An average of 15 islets per experimental condition was analyzed. The proportion of apoptotic β cells was calculated by manually counting the number of TUNEL-positive cells in insulin-positive cells.

Evaluation of insulin secretion

In brief, cells were washed three times and pre-incubated for 1 h in glucose-free Krebs-Ringer HEPES buffer (KRH) (17) composed of 135 mM NaCl, 3.6 mM KCl, 10 mM Hepes (pH 7.4), 0.5 mM $MgCl_2$, 1.5 mM $CaCl_2$, 0.5 mM NaH_2PO_4, and 0.1% (w/v) BSA in a 37°C humidified incubator. Subsequently, cells were incubated in the same buffer containing 5.5 or 25 mM glucose for 1 h, and the medium was collected were spun for 2 m at 13,000 RPM to pellet any detached cells and 100 μl was removed and used to determine insulin concentration. Insulin was measured using the Rat Insulin ELISA kit (CUSABIO BIOTECH), using mouse insulin as a standard. Values for secreted insulin were normalized to the total protein content in each lysate.

Mitochondrial membrane potential (MMP)

MMP was assessed by the retention of Rhodamine 123 (Rho123) (18), a specific fluorescent cationic dye that is readily sequestered by active mitochondria, depending on their transmembrane potential. In brief, at the end of the experiment, cells were stained by 10 μM Rho123 (kept in the dark, 4ºC) for 30 m. Then, cells were examined with a laser scanning confocal microscope (Olympus, Tokyo, Japan) and MMP was expressed as percentage fluorescence intensity of control.

ATP determination

For ATP measurement, a commercially available firefly luciferase assay kit (Beyotime Institute of Biotechnology, China) was used. Briefly, β-TC3 cells were treated with PA and OA for 48 h and then collected. After a single wash with ice-cold PBS, cells were lysed with the somatic cell ATP-releasing reagent provided by the kit. Then, Luciferin substrate and luciferase enzyme were added and bioluminescence was assessed by a spectroflurometer. The level of cellular ATP was converted to percentage of control.

Isolation of mitochondria

Intact mitochondria were isolated from cultured β-TC3 cells by a commercial kit (KeyGEN Biotech, China) following the manufacturer's instructions. Mitochondria and cytoplasm was isolated, respectively. Cytoplasmic protein was lysed for western blotting detection of cytochrome C release. The resulting mitochondria pellet was re-suspended in storage buffer. Mitochondria suspensions were kept on ice, and all experiments were performed within 6 h.

Mitochondrial ROS measurement

Maximal mitochondrial ROS production was measured using dichlorodihydrofluorescein diacetate in the presence of horseradish peroxidase as described (19). As a cell permeant indicator for intracellular ROS, DCF is nonfluorescent until the acetate groups are removed by intracellular esterases and oxidation occurs within the cell. Using a fluorescence plate reader (excitation 485 nm, emission 528 nm), ROS in isolated mitochondria was estimated. Data were expressed as arbitrary fluorescence units (RFU).

Mitochondrial GSH and GSSG determination

GSH and GSSG were determined as we previously

described. For GSH, fluorescence at 425nm was determined with the excitation at 350 nm. For GSSG, fluorescence at 422nm was determined with the excitation at 338 nm. Mitochondrial GSH and GSSG were expressed as nmol/mg protein.

siRNA treatment

Short interfering RNAs (siRNA) of Nrf2 targeting four positions (siRNA-1: Sense: 5'-GCAAGAAGCCAGAUACAAAUU-3', Antisense: 5'-PUUUGUAUCUGGCUUCUUGCUU-3': siRNA-2: Sense: 5'-GAGAUGAGCUUAGGGCAAAUU-3', Antisense: 5'-PUUUGCCCUAAGCUCAUCUCUU-3'; siRNA-3: Sense: 5'-AGACUCAAAUCCCACCUUAUU-3', Antisense: 5'-PUAAGGUGGGAUUUGAGUCUUU-3'; siRNA-4: Sense: 5'-AGGCAGCCAUGACUGAUUUUU-3', Antisense: 5'-PAAAUCAGUCAUGGCUGCCUUU-3') of the mouse Nrf2 mRNA were synthesized at Dharmacon. In brief, β-TC3 cells were plated the day before transfections and grown up to 30-50% confluence in 6-well plates. Transfections were carried out with Lipofectamine 2000 (Invitrogen, Carlsbad, CA, USA) following the manufacturer's instructions. Transfected cells were grown for 48 h in a 37°C incubator with 5% CO_2 before treatments were conducted. Thus the cells were cultured with indicated concentrations of PA in the presence or absence of OA for 48 h.

Western blotting

Western blotting was conducted as described previously (16). Briefly, protein extractions were separated by using SDS-PAGE on 10% polyacrylamide gels, and transferred to nitrocellulose membranes (Millipore, Billerica, MA, USA). After blocking for 1 h with 8% skimmed milk in TBS buffer (10 mM Tris, 150 mM NaCl), the membrane was incubated with indicated primary antibodies overnight at 4°C. After the membrane was washed four times for 15 m each with TBST buffer (10 mM Tris, 150 mM NaCl, and 0.1% Tween-20), it was incubated in the appropriate HRP-conjugated secondary antibody (diluted 1:5 000 in TBST) at 37°C for 30 m. The protein bands were visualized using chemiluminescent reagents according to the manufacturer's instructions and quantified using an image analyzer Quantity One System (Bio-Rad, Richmond, CA, USA). The protein quantifications were adjusted for the corresponding Tubulin α or β-actin level, which was not consistently changed by the different treatment conditions.

Statistical analysis

All experiments were performed at least three times, and results were expressed as the means±SD. The results were analyzed by one-way ANOVA followed by a SNK-q test for multiple comparisons. All analyses were performed using the Statistical Package for the Social Sciences (SPSS) software. Data were considered statistically significant for $p < 0.05$. More specific indices of statistical significance are indicated in individual figure legends.

RESULTS

OA protects β cell function in vivo and in vitro

In the present study, db/db mice, isolated pancreatic islets and β-TC3 cells were used to evaluate the protective effect of OA against lipotoxicity. As shown in Fig. 1A, 20 mg/kg OA significantly lowered FBG in db/db mice. IPGTT was conducted to assess the function of pancreatic islets. As shown in Fig. 1B, following i.p. glucose load, the blood glucose of db/db mice increased to 30.33±1.72 mmol/l from a baseline value of 19.00±0.46 mmol/l before slowly declining to 21.00±0.78 mmol/l after 120 m. Following i.p. glucose load, the blood glucose of 20 mg/kg OA-treating mice increased to 22.97±0.50 mmol/l from a baseline value of 16.30±0.72 mmol/l before slowly declining to 17.63±1.03 mmol/l after 120 m (Fig. 1B). Additionally, the area under the curve (AUC), which is a measure of impaired glucose tolerance, proved that the administration of OA significantly decreased AUC of IPGTT and thus resulted in improvement of impaired glucose tolerance (Fig. 1C).

In response to glucose, β cell secrets insulin, which process is also called glucose-stimulated insulin secretion (GSIS), which represents the function of β cell. PA is a C16:0 saturated fatty acid which is the most abundant FFAs in serum. We evaluated the effect of PA and OA on GSIS in vitro. Pancreatic islets were isolated from C57BL/6J mice and exposed to 400 μM PA and 10 μM OA for 48 h to evaluate the effect of PA on GSIS. In Fig. 1D, we showed that in control group, high concentration of glucose incubation resulted in a significant increase of insulin secretion. However, in the presence of 400 μM PA, the GSIS was notably inhibited (Fig. 1D). The administration of OA significantly inhibited PA-induced decrease of GSIS (Fig. 1D). Moreover, we also determined GSIS in β-TC3 cells and the results further confirmed that OA could protect insulin-secreting capability in β cell (Fig. 1E). These results

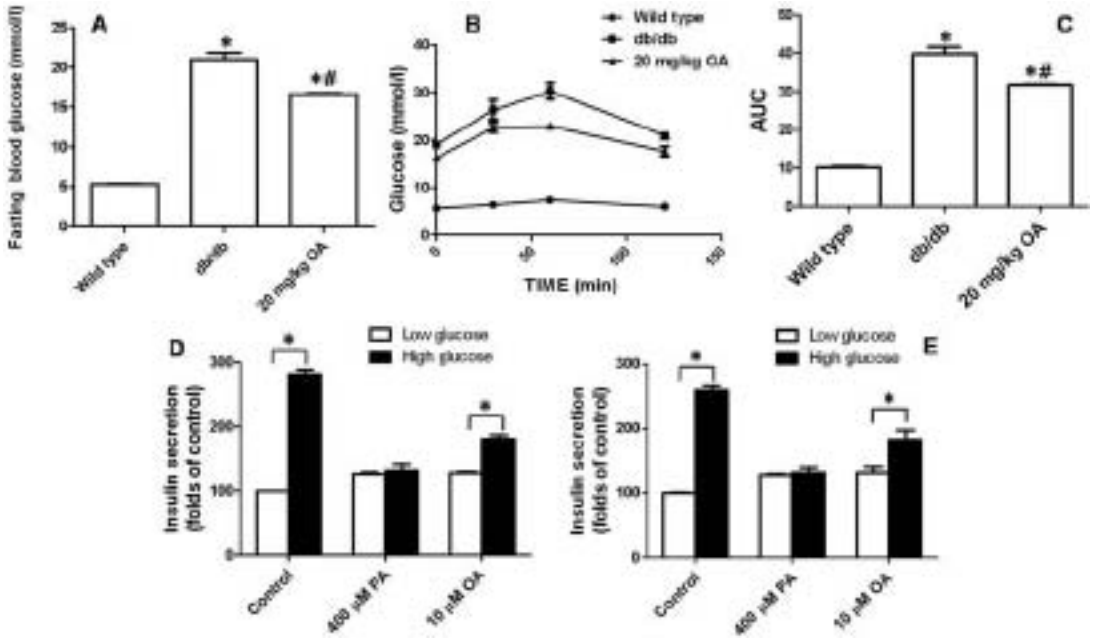

Fig. 1. *The effect of OA on β cell function in vivo and in vitro(**A**). The effect of OA on FBG in db/db diabetic mice (**B**). The effect of OA on glucose tolerance in db/db diabetic mice. db/db mice were administrated with 20 mg/kg OA for 2 weeks. At the end, FBG (**A**) and IPGTT (**B** and **C**) were measured. For clarity of display, standard error bars were omitted (**B**). AUC was calculated to measure impaired glucose tolerance (**C**) *p<0.05, compared with wild type mice; #p<0.05, compared with db/db mice. (D and E) The effect of OA on PA-induced β cell dysfunction in cultured pancreatic islets and β-TC3 cells. Isolated pancreatic islets (**D**) and β-TC3 cells (**E**) were incubated with 400 μM PA in the presence or absence of 10 μM PA OA for 48 h. Then, glucose-stimulated insulin secretion was assessed by an ELISA kit. *p<0.05, compared with corresponding control.*

demonstrated that OA may protect β cell function against lipotoxicity *in vivo* and *in vitro*.

OA protects β cell against apoptosis

In pancreatic islets of db/db mice, dissolved cytoplasm and vacuolar cells were observed (Fig. 2A). According to microscopic examinations, severe lesions of pancreatic islets were remarkably reduced by OA (Fig. 2A). OA markedly inhibited β cell apoptosis in db/db mice, evidenced by decreased number of TUNEL-positive cells in insulin-positive cells (Fig. 2B). In order to detect the effect of OA on β cell apoptosis under the stress of chronic FFAs exposure, isolated pancreatic islets and β-TC3 cells were incubated with PA in the presence or absence of 10 μM OA for 48 h. As shown in Fig. 2C, 48 h culture of pancreatic islets with 400 μM PA significantly increased cell apoptosis. In the presence of OA, cell apoptosis in pancreatic islets induced by PA was evidently inhibited (Fig. 2C). In addition, the results also showed that in β-TC3 cells, OA inhibited PA-induced increase of apoptotic cells (Fig. 2D). Furthermore, TEM assay was used to observe ultramicroscopic morphological changes of pancreatic β cell. Fig. 3A was a TEM of apoptotic β cell with condensed and peripheralized chromatin and vacuole in cytoplasm. When OA was present, condensation and peripheralization of chromatin and vacuole in cytoplasm was significantly reduced (Fig. 3A). These results demonstrated that OA may protect β cell against lipotoxicity-induced apoptosis.

Inhibition of mitochondrial dysfunction is involved in the protective effect of OA

Mitochondria play key roles in activating apoptosis in mammalian cells. Then, we determined whether the protective effect of OA was dependent on mitochondria. As shown in Fig. 3A, in pancreatic β cells of db/db mice, the density of mitochondria was significantly decreased and the mitochondria

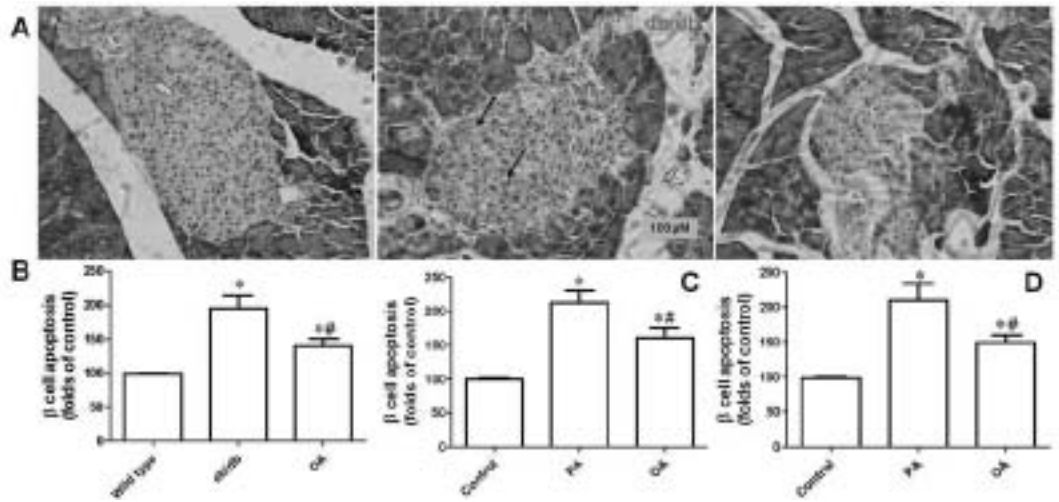

Fig. 2. *The effect of OA on lipotoxicity-induced β cell apoptosis.* ***A****) The effect of OA on histopathology of pancreas in db/db mice. Hematoxylin/eosin staining, magnification 400×.* ***B****,* ***C*** *and* ***D****) The effect of OA on β cell apoptosis in db/db mice (****B****), cultured pancreatic islets (****C****) and β-TC3 cells (****D****). Data were expressed as percentage of control. *p<0.05, compared with wild type mice or control; #p<0.05, compared with db/db mice or PA-treating group.*

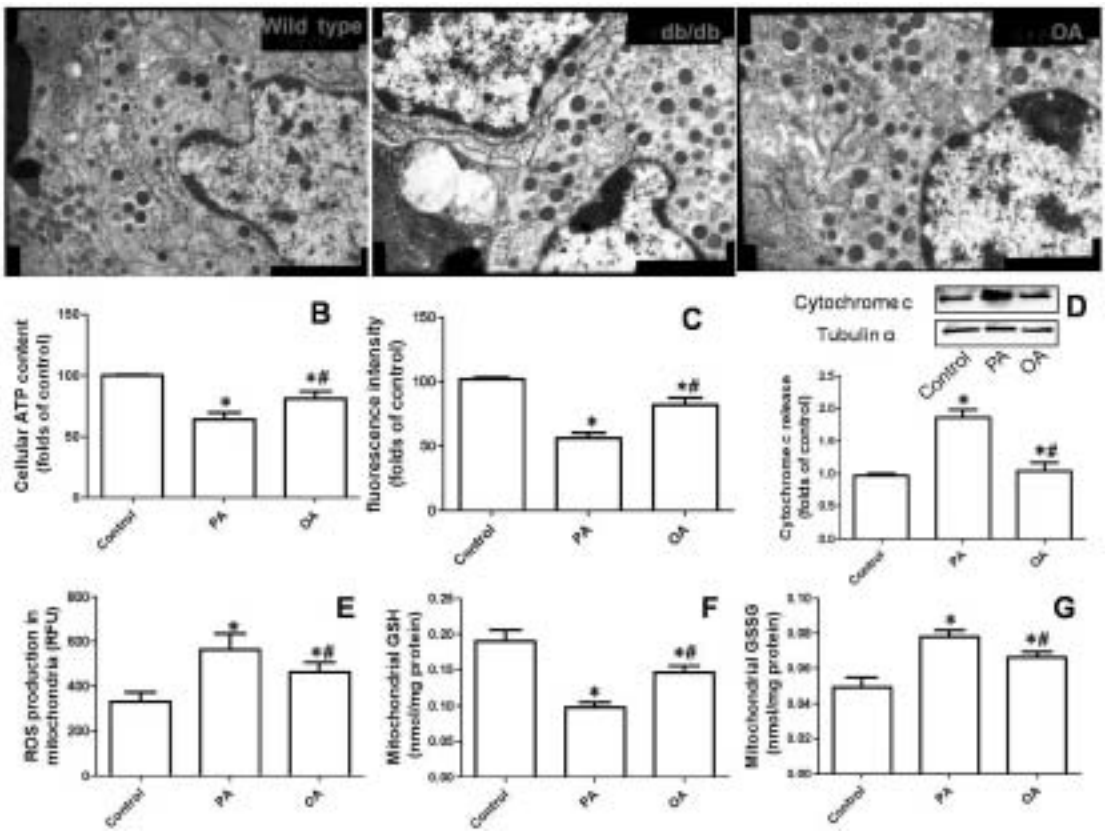

Fig. 3. *The effect of OA on mitochondrial function and redox balance.* ***A****) Transmission electron micrographs of pancreatic islets in db/db mice after the administration of OA.* ***B****) Cellular ATP content in β-TC3 cells treated by PA and OA was assayed by a commercial kit.* ***C****) MMP in β-TC3 cells treated by PA and OA was detected by Rho123.* ***D****) Cytoplasmic expression of cytochrome c in β-TC3 cells treated by PA and OA was determined by western blotting.* ***E****) Mitochondrial ROS production in β-TC3 cells treated by PA and OA was measured by DCF.* ***F*** *and* ***G****) Mitochondrial GSH (****F****) and GSSG (****G****) content were detected. *p<0.05, compared with control; #p<0.05, compared with PA-treating group.*

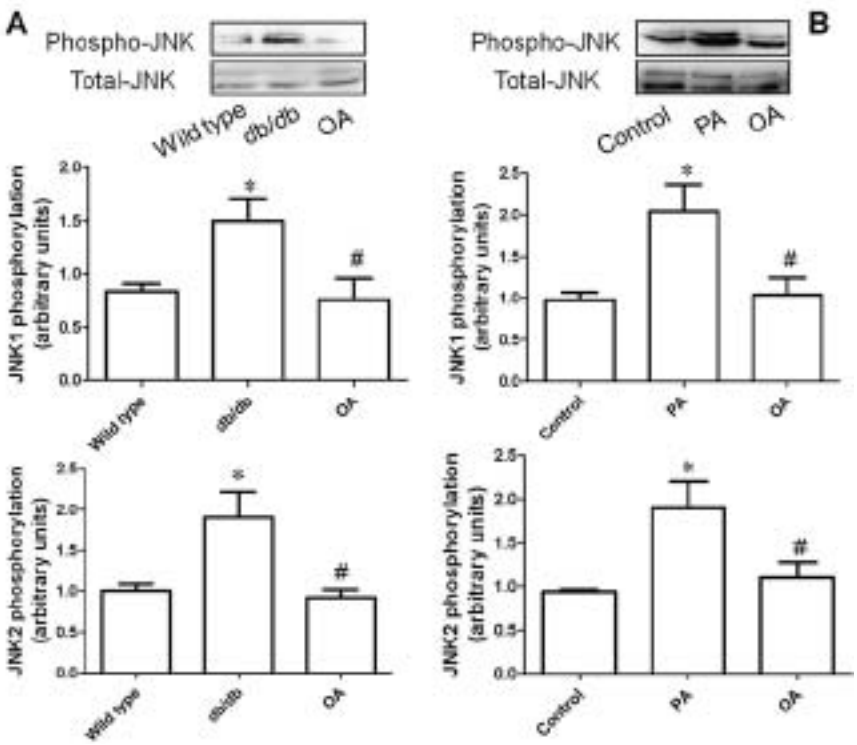

Fig. 4. *The effect of OA on JNK phosphorylation in vivo and in vitro. JNK phosphorylation in pancreatic islets (**A**) and β-TC3 (**B**) was determined by western blotting. Representative blot was shown. The values from densitometry of phosphorylated JNK were normalized to the level of total JNK protein. *p<0.05, compared with wild type mice or control; #p<0.05, compared with db/db mice or PA-treating group.*

were dramatically swollen. Moreover, mitochondrial function was further evaluated. As shown in Fig. 3B, after the treatment of PA, ATP content in β-TC3 cells was reduced, and OA inhibited the decrease of ATP significantly. Mitochondrial membrane potential (MMP) was detected by the probe of rhodamine (Rho 123). In Fig. 3C, we showed that when β-TC3 cells were exposed to PA for 48 h, MMP was markedly decreased, as reflected by the decrease of fluorescence intensity. In contrast, OA significantly inhibited the injury of MMP (Fig. 3C). The release of cytochorome c to cytoplasm is a key step of mitochondrial apoptosis. Thus, we next detected the release of cytochorome c by extraction of cytoplasmic protein. As expected, incubation of cells with PA remarkably promoted cytoplasmic expression of cytochorome c, which was blocked by OA (Fig. 3D).

Mitochondria are main targets of oxidative injury in a cell. In the present study, ROS production in isolated mitochondria was determined by a DCF probe. As shown in Fig. 3E, mitochondrial ROS level was increased by the incubation of PA, as evidenced by the increase of fluorescence intensity. OA treatment could significantly down-regulated the level of ROS induced by PA (Fig. 3E). Glutathione (GSH)/GSSG (glutathione, oxidized form) ratio plays a key role in keeping mitochondrial redox balance. We then measured the level of GSH and GSSG in mitochondria. In Fig. 3F and 3G, the results showed that in the presence of PA, mitochondrial GSH was reduced and GSSG was increased, both of which were inhibited by OA treatment.

Inhibition of JNK is involved in the protective effect of OA

Previous studies indicated that stress-related signaling pathways were involved in mitochondrial apoptotic cell death (20, 21). In the present study, we evaluated the level of an important stress-sensitive kinase, c-Jun NH2-terminal kinase (JNK). In Fig.

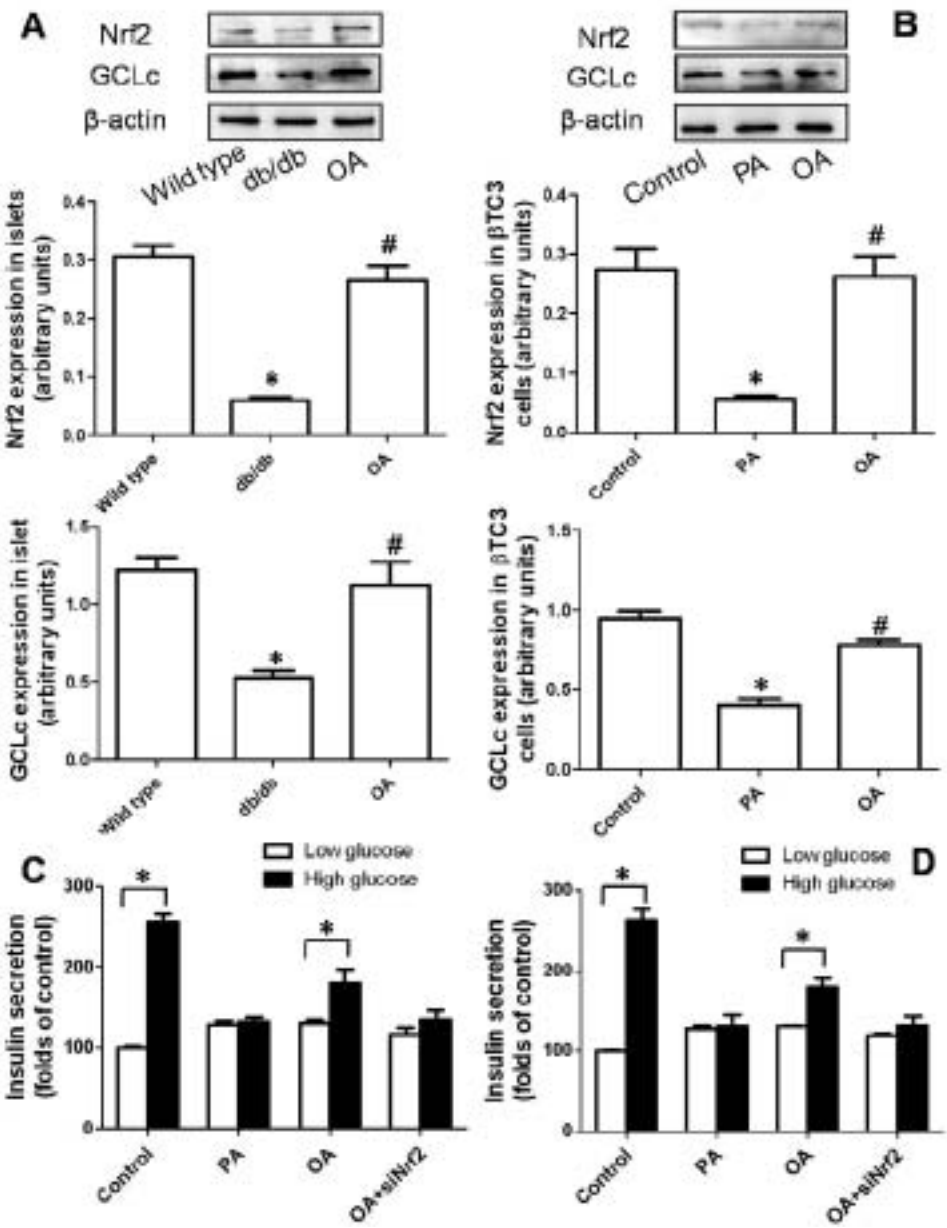

Fig. 5. *Role of Nrf2 in the protective effect of OA.* ***A*** *and* ***B****) Nrf2 and GCLc expression in pancreatic islets of db/db mice (****A****) and β-TC3 cells treated by PA and OA was determined by western blotting. Representative blot was shown. The values from densitometry of Nrf2 and GCLc were normalized to the level of β-actin protein. *p<0.05, compared with wild type mice or control; #p<0.05, compared with db/db mice or PA-treating group.* ***C*** *and* ***D****) The effect of OA on PA-induced β cell dysfunction in cultured pancreatic islets and β-TC3 cells. Isolated pancreatic islets (****C****) and β-TC3 cells (****D****) were incubated with 400 μM PA in the presence or absence of 10 μM PA OA with or without siNrf2 for 48 h. Then, glucose-stimulated insulin secretion was assessed by an ELISA kit. *p<0.05, compared with corresponding control.*

4A, we showed that the phosphorylation of JNK1 and JNK2 was increased in pancreatic islets in db/db mice and OA administration could block the activation of JNK. Consistent with the results in db/db mice, PA increased the phosphorylatory level of JNK1 and JNK2, which was blocked by OA treatment (Fig. 4A).

The activation of Nrf2-signaling pathway is responsible for the protective effect of OA

Oxidative stress plays a fundamental role in

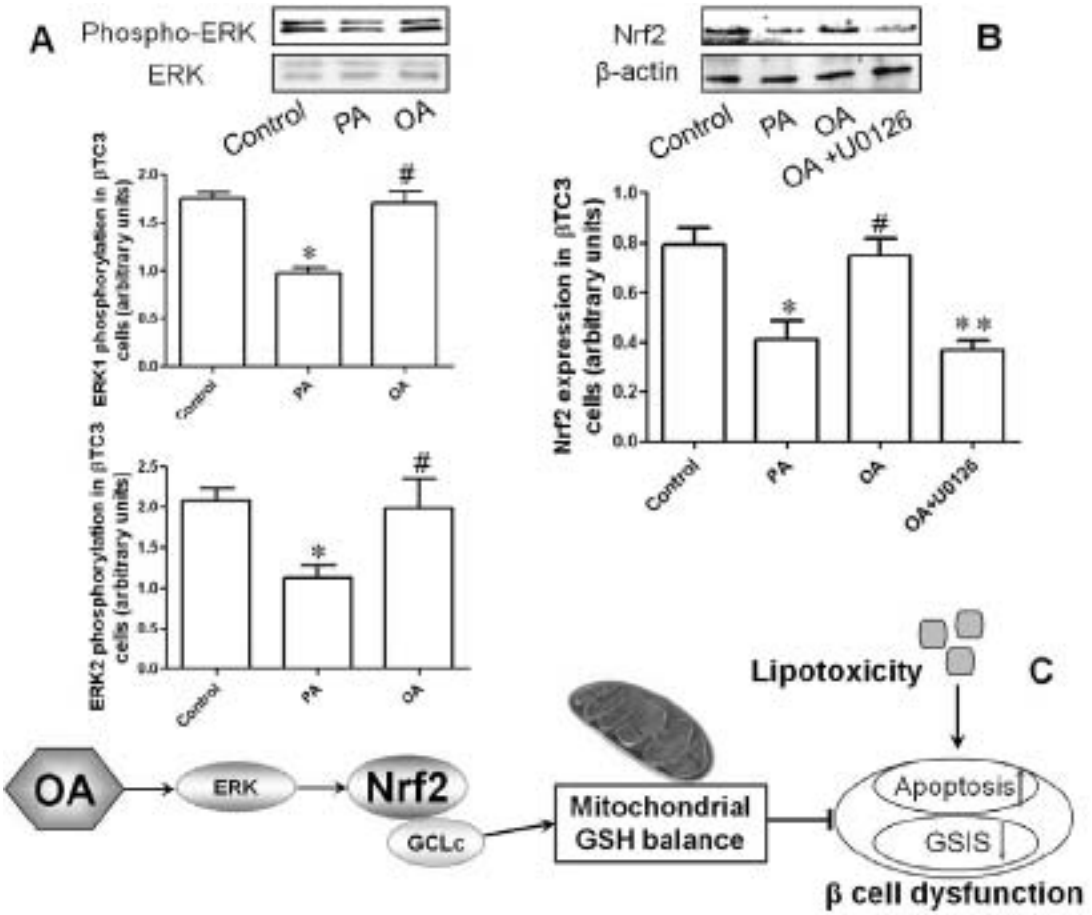

Fig. 6. *Role of ERK in OA-induced activation of Nrf2 in β-TC3 cells.* ***A****) ERK phosphorylation in β-TC3 cells treated by PA and OA was determined by western blotting. Representative blot was shown. The values from densitometry of phosphorylated ERK were normalized to the level of total ERK protein.* ***B****) Nrf2 expression in β-TC3 cells treated by PA and OA in the presence or absence of U0126, an inhibitor of ERK, was determined by western blotting. Representative blot was shown. The values from densitometry of Nrf2 were normalized to the level of β-actin protein. *p<0.05, compared with control; #p<0.05, compared with PA-treating group; *p<0.05, compared with PA+OA-treating group.* ***C****) Schematic figure of the potential effect of OA on β cell dysfunction and the underlying mechanism.*

various types of β cell dysfunction. In db/db mice, the expression of Nrf2 in pancreatic islets, a pivotal transcription factor responsible for the induction of various antioxidant enzymes, was assayed by western blotting. As shown in Fig. 5A, compared with wild type mice, the expression of Nrf2 in pancreatic islets of db/db mice was significantly down-regulated. OA administration notably inhibited the down-regulation of Nrf2 (Fig. 5A). In order to further determine the effect of PA and OA on redox balance in β cells, β-TC3 cells with PA and OA. As shown in Fig. 5B, the expression of Nrf2 was significantly reduced by PA. In contrast, OA notably inhibited the effect of PA on Nrf2 expression (Fig. 5B). Moreover, the expression of glutathione cysteine ligase catalytic subunit (GCLc) was reduced in pancreatic islets of db/db mice and β-TC3 treated by PA, which phenomenon was inhibited by indicated concentrations of OA (Fig. 5A and 5B). To further determine the role of Nrf2 in the protective effect of OA, siRNA of Nrf2 was introduced in the present experiment. β-TC3 cells were pre-cultured with siNrf2 for 48 h and then exposed to PA in the presence or absence of 10 μM OA. The results showed that siNrf2 treatment could significantly suppress the protective effect of OA on GSIS both in pancreatic islets (Fig. 5C) and in

β-TC3 cells (Fig. 5D). These results indicated that Nrf2 plays a crucial role in the protective effect of OA against lipotoxicity in β cell.

ERK signaling is responsible for OA-induced protective effect

To further explore the possible signaling pathways, which may be involved in the protective effect of OA, the phosphorylation of ERK were also determined by western blotting. As shown in Fig. 6A, in PA-treating group, the phosphorylation of ERK1 and ERK2 was inhibited. OA treatment significantly increased the phosphorylation of ERK1 and ERK2 (Fig. 6A). To examine the role of ERK signaling in OA-induced activation of Nrf2, Nrf2 expression was examined by western blot (Fig. 6B) in the presence or absence of indicated inhibitor. As shown in Fig. 6B, U0126, an inhibitor of mitogen-activated protein kinase kinase (MEK)/ERK, could reduce the protective effect of OA on Nrf2 expression. The results implicated that ERK signaling pathway was involved in OA-induced activation of Nrf2 and thus the protective effect on β cell function.

DISCUSSION

Recently, our studies have shown that OA has potent antioxidant activity and could effectively lower blood glucose (11, 13). In addition, there is also other evidence that show the anti-diabetic potential of OA. Ngubane et al. have shown that STZ-induced diabetic rats exhibited depleted glycogen levels and low activities of glycogenic enzymes in muscle and hepatic tissues and OA administration restored these biochemical alterations to near normalcy (22). The findings of Mapanga et al. (23) suggest that OA may have beneficial effects on some processes associated with renal derangement of STZ-induced diabetic rats. de Melo et al. (24) have reported that OA ameliorates visceral adiposity and improves glucose tolerance in mice and thus has an antiobese potential through modulation of carbohydrate and fat metabolism. And a couple of literature has shown the anti-diabetic potential of OA extracted from various natural substances (23, 25). However, to date, little is known about the effect of OA on β cell function. The present study was designed to investigate the protective effect of OA against chronic lipotoxicity-induced β cell dysfunction and to gain insight into possible molecular mechanisms.

In db/db diabetic mice, OA administration could lower FBG, protect glucose tolerance and inhibit β cell apoptosis (Fig. 1). Co-culture of isolated pancreatic islets or β-TC3 cells with PA and OA could significantly inhibit PA-induced decrease of GSIS (Fig. 1), which is consistent with a previous study. In 2008, Teodoro et al. (26) investigated the effect of OA on insulin secretion and content in pancreatic β cells and rat islets. They showed that OA significantly enhanced insulin secretion in INS-1 cells and enhanced acute GSIS in isolated rat islets (26). Chronic treatment with OA increased total cellular insulin protein and mRNA levels (26). The evidence suggests that OA could protect β cell against lipotoxicity and contribute to the anti-diabetic properties of this natural product.

It is well-known that apoptosis participates in the pancreatic β cell destruction. In the current study, we determined whether the protective effect of OA on β cell function was dependent on inhibition of apoptosis. As expected, OA administration ameliorated histopathological changes of β cell in db/db diabetic mice (Fig. 2). Moreover, OA inhibited β cell apoptosis both in db/db diabetic mice and in isolated pancreatic islets and β-TC3 cells induced by chronic FFAs incubation (Fig. 2). The mitochondria act at the core of the apoptotic pathway by providing many important factors including those that induce caspase activation and chromosome fragmentation (27). We next detected the changes of the number and morphology of mitochondria in vivo and in vitro. Ultramicroscopic observations showed that OA administration increased the density of mitochondria and ameliorated mitochondrial swelling (Fig. 3A). Furthermore, mitochondrial function was significantly protected by OA treatment, as reflected by inhibition of the decrease of ATP content and MMP induced by chronic FFAs incubation (Fig. 3B and C). The reduction of cytochrome c release by OA (Fig. 3D) further indicated that FFAs-induced apoptosis was dependent on mitochondrial dysfunction and the protective effect of OA may be due to the protection on mitochondria.

Previous studies have revealed that the lipotoxicity to β cell is accompanied by increased production of ROS (28, 29). Compared with other

tissues, islets contained relatively lower activities of major antioxidant enzymes, including SOD1, SOD2, GPx (30). Up-regulation of endogenous antioxidant enzymes was reported to protect β cells against oxidative stress in vitro and in vivo (31). In normal cells, ROS is mainly derived from mitochondrial oxidative phosphorylation and mitochondria are the main target of oxidative injury, leading to mitochondria-dependent apoptosis. In our study, OA reduced ROS generation in mitochondria of β-TC3 cells treated by FFAs (Fig. 3E). It has reported that cellular GSH/GSSG plays an important role in apoptotic signaling, mitochondrial GSH loss is related to enhanced cytotoxicity (32). The results in the present study demonstrated that mitochondrial oxidative stress and related apoptotic signaling were related with loss of mitochondrial GSH. And the protective effect of OA against mitochondrial apoptosis may possibly be due to the effect on GSH redox balance (Fig. 3F, G).

As a typical stress-sensitive kinase, JNK has been reported to be related to mitochondrial apoptosis through the activation of p53 (20). When diabetic mice and FFAs-treated cells were give OA, activated JNK was significantly reduced (Fig. 4). Nrf2, a pivotal regulator of the cellular redox homeostasis, plays an important role in protecting cells against ROS damage and keeping redox balance, through its capacity to induce the expression of antioxidant enzymes and other antioxidant proteins (11). Upon recognition of signals imparted by oxidative stimuli and a number of antioxidants, Nrf2 escapes proteosomal degradation and translocates to the nucleus to induce various genes (33-35). Our previous results have shown that OA could induce several antioxidant enzymes through activating Nrf2 (11). Reisman et al. (12) have also found that OA facilitates Nrf2 nuclear accumulation, causing induction of Nrf2-dependent genes. In the current study, the role of antioxidant activity in the protective effect of OA was evaluated. As expected, OA could inhibit lipotoxicity-induced down-regulation of Nrf2 both in pancreatic islets and β-TC3 cells (Fig. 5A, B). Moreover, inhibition of Nrf2 with siRNA could significantly reduce the protective effect of OA on insulin secretion in response to glucose (Fig. 5C, D). γ-Glutamylcysteine ligase (GCL) is the rate-limiting enzyme in the first of two steps of GSH synthesis, which is composed of a catalytic or heavy subunit (GCLc) and a modulatory or light subunit (GCLm) subunit. In the present study, consistent with the changes of Nrf2, OA significantly inhibited the decrease of GCLc expression in pancreatic islets in diabetic mice and β-TC3 cells treated by FFAs (Fig. 5A, B). The results indicated that the restore of mitochondrial GSH redox balance may probably be due to OA-induced Nrf2-GCLc signaling. The data suggested that the protective effect of OA against apoptosis is dependent on the maintenance of mitochondrial GSH redox balance mediated by the activation of Nrf2-GCLc signaling.

To investigate the signaling pathways that may be responsible for OA-induced activation of Nrf2 and related antioxidant defense, U0126, the inhibitor of MEK/ERK signaling pathway, was introduced in the current experiment. The results showed that OA could reverse PA-induced phosphorylation of ERK and inhibition of the phosphorylation of ERK could significantly reduce OA-activated Nrf2 expression (Fig. 6A, B), which is concomitant with our previous results (11, 13). In addition, in rat vascular smooth muscle cells, ERK/Nrf2 pathways have been shown to be involved in OA-induced HO-1 expression (36). These results indicate that MEK/ERK pathway may be the general pathway responsible for OA-induced activation of Nrf2.

In conclusion, the present study examined the protective effect of OA against lipotoxicity in β cells in vivo and in vitro (Fig. 6C). In db/db mice, OA significantly protects β cell function against lipotoxicity, evidenced by inhibition of apoptosis and improvement of glucose tolerance. In vitro, OA administration may protect against lipotoxicity-induced apoptosis and decrease of GSIS, in which process the activation of Nrf2 is essential. Once Nrf2 is activated, OA could induce the expression of GCLc, which may promote the production of GSH and solid the antioxidant defense of mitochondria, leading to the inhibition of mitochondrial apoptosis (35). ERK signaling pathway is responsible for OA-induced activation of Nrf2 and the protective effect of OA. Overall, our study enhances the understanding of the anti-diabetic potential of OA and elucidates the importance of ERK-Nrf2 pathways in the protective effect of OA in β cells, and provides clues for further studies on the underlying mechanisms.

ACKNOWLEDGEMENTS

This work was supported by Program for Changjiang Scholars, Innovative Research Team in University (PCSIRT) and National Natural Science Foundation of China (No. 30872135). The Study was also supported by Natural Science Foundation of Shaanxi Province (No. S2013JC10314). Doctoral Thesis Science Foundation of Fourth Military Medical University (2010D06).

REFERENCES

1. Khoury MJ, Valdez R, Albright A. Public Health Genomics Approach to Type 2 Diabetes. Diabetes 2008; 57:2911-4.
2. Leelayuwat N, Tunkumnerdthai O, Donsom M, Punyaek N, Manimanakorn A, Kukongviriyapan U and Kukongviriyapan V. An alternative exercise and its beneficial effects on glycaemic control and oxidative stress in subjects with type 2 diabetes. Diabetes Res Clin Pract 2008; 82:8.
3. Yang WY, Lu JM, Weng JP, et al. Prevalence of diabetes among men and women in China. N Engl J Med 2010; 362:1090-101.
4. Seghrouchni I, Drai J, Bannier E, Rivière J, Calmard P, Garcia I, Orgiazzi J, Revol A. Oxidative stress parameters in type I, type II and insulin-treated type 2 diabetes mellitus; insulin treatment efficiency. *C*linica Chimica Acta 2002; 321:89-96.
5. Fridlyand LE, Philipson LH. Does the glucose-dependent insulin secretion mechanism itself cause oxidative stress in pancreatic beta-cells? Diabetes 2004; 53:1942-8.
6. Wang X, Hai CX. ROS Acts as a Double-Edged Sword in the Pathogenesis of Type 2 Diabetes Mellitus: Is Nrf2 a Potential Target for the Treatment? Mini-Reviews in Medicinal Chemistry 2011; 11:1082-92.
7. Cheng AY, Fantus IG. Oral antihyperglycemic therapy for type 2 diabetes mellitus. CMAJ 2005; 172:213-26.
8. Perez-Camino M, Cert A. Quantitative determination of hydroxy pentacyclic triterpene acids in vegetable oils. *J.* Agric. Food Chem 1999; 47:1558-62.
9. Xinpeng B, Aiyong Q, Junjun G, Zhongping S. Antioxidant and protective effect of an oleanolic acid-enriched extract of A. deliciosa root on carbon tetrachloride induced rat liver injury. Asia Pac J Clin Nutr 2007; 16:169.
10. Liu J. Pharmacology of oleanolic acid and ursolic acid. J Ethnopharmacol 1995; 49:57-68.
11. Wang X, Ye XL, Liu R, et al. Antioxidant activities of oleanolic acid in vitro: possible role of Nrf2 and MAP kinases. Chem Biol Interact 2010; 184:328-37.
12. Reisman SA, Aleksunes LM, Klaassen CD. Oleanolic acid activates Nrf2 and protects from acetaminophen hepatotoxicity via Nrf2-dependent and Nrf2-independent processes. Biochem Pharmacol 2009; 77:1273-82.
13. Wang X, Li YL, Wu H, et al. Antidiabetic Effect of Oleanolic Acid: A Promising Use of a Traditional Pharmacological Agent. Phytother Res 2011; 25:1031-40.
14. Zhang CY, Baffy G, Perret P, et al. Uncoupling protein-2 negatively regulates insulin secretion and is a major link between obesity, b cell dysfunction, and type 2 diabetes. Cell 105 745–755. Cell 2001; 105:745-55.
15. Ye Y, Liu J, Xu J, Sun L, Chen M, Lan M. Nano-SiO2 induces apoptosis via activation of p53 and Bax mediated by oxidative stress in human hepatic cell line. Toxicology In Vitro 2010; 24:751-8.
16. Wang X, Liu JZ, Hu JX, Wu H, Li YL, Chen HL, Bai H, Hai CX. ROS-activated p38 MAPK/ERK-Akt cascade plays a central role in palmitic acid-stimulated hepatocyte proliferation. Free Radic Biol Med 2011; 51:539-51.
17. Affourtit C, Jastroch M, Brand MD. Uncoupling protein-2 attenuates glucose-stimulated insulin secretion in INS-1E insulinoma cells by lowering mitochondrial reactive oxygen species. Free Radic Biol Med 2011; 50:609-16.
18. Baracca A, Sgarbib G, Solaini G, Lenaz G. Rhodamine 123 as a probe of mitochondrial membrane potential: evaluation of proton flux through F0 during ATP synthesis. Biochimica et Biophysica Acta 2003; 1606:137-46.
19. Andrews ZB, Liu Z, Walllingford N, et al. UCP2 mediates ghrelin's action on NPY/AgRP neurons by lowering free radicals. Nature 2008; 454:846-51.
20. Reyes-Zurita FJ, Pachon-Pena G, Lizarraga D, Rufino-Palomares EE, Cascante M, Lupianez JA. The natural triterpene maslinic acid induces

apoptosis in HT29 colon cancer cells by a JNK-p53-dependent mechanism. Bmc Cancer 2011; 11:154-67.

21. Yuan H, Zhang X, Huang X, et al. NADPH oxidase 2-derived reactive oxygen species mediate FFAs-induced dysfunction and apoptosis of beta-cells via JNK, p38 MAPK and p53 pathways. PLoS One 2010; 5:e15726.
22. Ngubane PS, Masola B, Musabayane CT. The effects of Syzygium aromaticum-derived oleanolic acid on glycogenic enzymes in streptozotocin-induced diabetic rats. Ren Fail 2011; 33:434-39.
23. Mapanga RF, Tufts MA, Shode FO, Musabayane CT, Renal effects of plant-derived oleanolic acid in streptozotocin-induced diabetic rats. Ren Fail 2009; 31:481-91.
24. de Melo CL, Queiroz MG, Fonseca SG, Bizerra AM, Lemos TL, Melo TS, Santos FA, Rao VS. Oleanolic acid, a natural triterpenoid improves blood glucose tolerance in normal mice and ameliorates visceral obesity in mice fed a high-fat diet. Chem Biol Interact 2010; 1016:28.
25. Gao D, Li Q, Li Y, et al. Antidiabetic potential of oleanolic acid from Ligustrum lucidum Ait. Can J Physiol Pharmacol 2007; 85:1076-1083.
26. Teodoro T, Zhang L, Alexander T, Yue J, Vranic M, Volchuk A. Oleanolic acid enhances insulin secretion in pancreatic [beta]-cells. Febs Letters 2008; 582:1375-80.
27. Wang C, Richard JY. The Role of Mitochondriain Apoptosis. Annu Rev Genet 2009; 43:95-118.
28. Carlsson C, Borg LA, Welsh N. Sodium palmitate induces partial mitochondrial uncoupling and reactive oxygen species in rat pancreatic islets in vitro. Endocrinology 1999; 140:3422-8.
29. Zhang X, Bao Y, Ke L, Yu Y. Elevated circulating free fatty acids levels causing pancreatic islet cell dysfunction through oxidative stress. J Endocrinol Invest 2010; 33:388-94.
30. Grankvist K, Marklund SL, Taljedal IB. CuZn-superoxide dismutase, Mnsuperoxide dismutase, catalase and glutathione peroxidase in pancreatic islets and other tissues in the mouse. Biochem J 1981; 199:393-8.
31. Gier B, Krippeit-Drews P, Sheiko T, Aguilar-Bryan L, Bryan J, Düfer M, Drews G. Suppression of KATP channel activity protects murine pancreatic b cells against oxidative stress. J Clin Invest. 2009; 119:3246-56.
32. Circu ML, Rodriguez C, Maloney R, Moyer MP. Aw TY. Contribution of mitochondrial GSH transport to matrix GSH status and colonic epithelial cell apoptosis. Free Radic Biol Med 2008; 44:768-78.
33. Kensler TW, Wakabayashi N, Biswal S. Cell survival responses to environmental stresses via the Keap1-Nrf2-ARE pathway. Ann Rev Pharmacol Toxicol 2007; 47:89-116.
34. Zipper LM. Mulcahy RT. Inhibition of ERK and p38 MAP kinases inhibits binding of Nrf2 and induction of GCS genes. Biochem Biophys Res Commun 2000; 278 484-92.
35. Wang X, Tao L. Hai CX. Redox-regulating role of insulin: The essence of insulin effect. Mol Cell Endocrinol 2011; 349:111-27.
36. Feng J, Zhang P, Chen X, He G. PI3K and ERK/Nrf2 pathways are involved in oleanolic acid-induced heme oxygenase-1 expression in rat vascular smooth muscle cells. J Biochem 2011; 112:1524-31.

COMPARATIVE EVALUATION OF GASTRIC GHRELIN CELLS AND LEVELS OF HORMONE IN THE SERUM OF HEALTHY WOMEN AND MEN

I. KASACKA[1], M. ARCISZEWSKI[1], I. JANIUK[2] and W. ŁEBKOWSKI[3]

[1]Department of Histology and Cytophysiology, Medical University, Bialystok, Poland; [2]Department of Vertebrates Morphology, Siedlce University of Natural Sciences and Humanities, Siedlce, Poland; [3]Department of Neurosurgery, Medical University, Bialystok, Poland

Received September 29, 2011 - Accepted April 2, 2012

Due to difficulties in obtaining human material, most of the data concerning the site of occurrence and synthesis of ghrelin are based on animal studies. There are only few reports describing ghrelin-containing cells in the human digestive tract, based on the limited human material obtained during surgery or biopsy. The aim of this study was to compare and evaluate the distribution and morphology of ghrelin cells in the stomach and the levels of hormone in the serum of healthy men and women. The study included 18 subjects with normal gastric mucosa (12 men and 6 women). Immunohistochemistry was performed using rabbit anti-ghrelin (human) antiserum. Ghrelin level in serum was measured by ELISA. The total number of ghrelin positive cells was greater in the stomach of women than men. Ghrelin-immunoreactive cells were more elongated and larger in the stomach of women. The serum ghrelin level was higher in men than in women. Ghrelin concentration in serum correlates negatively with body mass index and weight in both genders, whereas the correlation between ghrelin level and age was positive in women and negative in men. The number of cells containing ghrelin in the stomach does not reflect the serum hormone levels. The differences in gastric ghrelin cells and ghrelin levels in serum between women and men, indicate that secretion of hormone can be under control sex hormones or other unknown factors.

As shown in the *in vivo* and *in vitro* model carried out on different species, ghrelin fulfills a number of functions, acting both as a hormone and locally as an autocrine or paracrine factor in many organs (1, 2). Ghrelin is involved in a wide range of endocrine and non-endocrine actions linking the gastrointestinal activities with organism functions. One of the physiological actions of hormone is its effect on different levels of the hypothalamic-pituitary-gonadal axis (3).

The 28-amino acid peptide was isolated from the stomach, where its expression is higher than in any other tissue (4). In humans, rats, and domestic animals, expression of ghrelin mRNA and the ghrelin peptide have been primarily detected in specific endocrine cells of the fundic gland in the stomach and have now been renamed ghrelin cells (5). They are second in terms of density the population of gastric endocrine cells and are located mainly in the mucous layer of gastric fundus (6).

The cells secreting ghrelin are also present in the small intestine and in minor amounts in the colon, lungs, thyroid, heart, placenta and gonads (7). Receptors for ghrelin (GHS-R) were found in

Key words: ghrelin cells, stomach, serum, human

Mailing address: Prof dr hab. Irean Kasacka,
Department of Histology and Cytophysiology,
Medical University of Białystok,
ul. Kilińskiego 1, 15-089 Białystok, Poland
Tel.: +48 85 7485458
Fax: +48 85 7485516
e-mail: kasacka@umb.edu.pl

0393-974X (2013)

high number in hypothalamus, specifically in the arcuate nucleus where the region of appetite control is located (8). The main regulator of serum ghrelin levels in human body is food intake. Circulating ghrelin levels decrease postprandial and increase before meals (2).

The hormone level is altered in a variety of gastrointestinal disorders. An increase of ghrelin concentration in serum has been observed in humans with anorexia, cachexia, diabetes type 1 (9, 10). Moreover in patients after a gastric surgery, there is a significant reduction of hormone levels in serum (11).

Ghrelin participates in many biological processes influencing the activity not only the gastrointestinal tract, but also many other systems. It stimulates secretion of growth hormone (GH) and prolactin, modulates carbohydrate metabolism and function of the immune system as well as controls endocrine function of the pancreas islets (1, 12). In nervous system hormone is responsible for normal physiological state of sleep and wakefulness (13). The main role of ghrelin in the human gastrointestinal tract (GI-tract) is gastric acid secretion, acceleration of gastric emptying and stimulation of ileal peristalsis (4, 6).

Substances produced and secreted by different structures in our body have an impact on ghrelin excretion and its activity. Cholecystokinin is one of the major substances which increase levels of ghrelin in blood while glucose, insulin, NPY (neuropeptide Y), PYY-36 (peptide tyrosine tyrosine) and leptin reduces its concentration (6, 14).

Ghrelin levels in the human body also depend on anthropometric and metabolic factors such as body mass index, weight, percentage of fat or age (15-17). Literature data on the differences in serum ghrelin levels related with gender are often contradictory. According to Nanjo et al., concentration of hormone in serum depends on gender (15), while Tschop et al. found no such relationship between sex and ghrelin levels (17). Ariyasu et al. noticed higher levels of ghrelin in men serum (6), whereas Aydin et al. showed greater concentration of hormone in women (14).

Difference in serum ghrelin levels between sexes according to Ingellson et al. may be caused by different endocrine function of reproductive glands, steroid hormones, appetite or some unknown factors in our body (16). Immunohistochemical studies revealed the presence of ghrelin-producing cells and ghrelin receptors in some structures within gonads. In women ghrelin was found in the mature and fading corpus luteum, placenta and endometrium (3, 18), whereas in men hormone was detected in mature Leydig and Sertoli cells and in the germ cells, mainly in the pachytene spermatocytes (3, 19). Disparity in ghrelin levels in serum can also be caused by gonadal hormones (estrogens and testosterone) which modify concentration of hormone (20, 21).

Distribution of ghrelin cells in stomach was described in rat, mouse or pig (5), while the knowledge about the presence of ghrelin cells (Ghr-IR) in the human stomach and its level in serum is limited mostly to data from different pathological cases (obesity, anorexia nervosa) (9, 10, 17, 22). This limitation is due to the difficulty in obtaining material for the study from healthy human subjects.

The aim of this study was comparative evaluation of distribution and morphology of ghrelin cells in the stomach and levels of hormone in serum of healthy men and women.

MATERIALS AND METHODS

Sample collection

Eighteen subjects (donors of organs) with normal alimentary tract were used in the study. There were 12 men with a mean age of 43.1 years; the age range was from 21 to 65 years old, with mean body weight of 82.63 kg and mean BMI (body mass index) of 26.42, and 6 women with a mean age of 45.2 years; the age range was from 19 to 58 years old, with mean body weight of 63.2 kg and mean BMI of 23.06.

Each of the subjects which presented clinical symptoms of brain death, were considered to be organ donors. Irreversible brain damage was confirmed by special clinical examination and angiography (no blood flow within the brain arteries). After brain death was diagnosed and individual death was confirmed by doctors, stomach samples, about 1 cm long (the same part of the cardia, fundus and pylorus), were collected from each body after other organs (kidneys, heart, liver) for transplantation were harvested.

Samples of the stomach were immediately fixed in Bouin's solution and routinely embedded in paraffin. Specimens were stained with hematoxylin and eosin for general histological examination and processed by immunohistochemistry for ghrelin detection.

Ethical issues

The study protocol was approved by the Ethics Committee

at the Medical University of Białystok (R-I-002/345/2007) and a written informed consent had previously been obtained from each subject or from his/her family member(s).

Immunohistochemistry

Paraffin blocks were cut into 4-μm sections (3 sections from each subject) and attached to positively charged glass slides. Immunohistochemistry was performed, using an EnVision Plus-HRP Rabbit Detection Kit (K4011; Dako, Glostrup, Denmark) (23). Immunostaining was performed by the following protocol: paraffin-embedded sections were deparaffinized and hydrated in pure alcohols. For antigen retrieval, the sections were subjected to pretreatment in a pressure chamber heated for 1 min at 21 psi (one pound force per square inch (1 psi) equates to 6.895 kPa, the conversion factor was provided by the United Kingdom National Physical Laboratory) at 125°C, using Target Retrieval Solution Citrate pH=6,0 (S 2369; Dako, Glostrup, Denmark). After cooling down to room temperature, the sections were incubated with Peroxidase Blocking Reagent (S 2001; Dako, Glostrup, Denmark) for 10 min to block endogenous peroxidase activity. The sections with the primary antibody to ghrelin (No H-031-30; Phoenix Pharmaceuticals Inc., Mountain View, CA, USA) (1:10,000 dilution) were incubated overnight at 4°C in a humidified chamber. The ghrelin antiserum, a rabbit polyclonal, exhibits 100% cross-reactivity with the human ghrelin. The antiserum was diluted in Antibody Diluent (S 0809, Dako, Glostrup, Denmark), followed by incubation with secondary antibody (conjugated to horseradish peroxidase-labeled polymer). The bound antibodies were visualized by 1 min incubation with liquid 3,3'-diaminobenzidine (DAB) substrate chromogen. The sections were finally counterstained in QS haematoxylin (H-3404; Vector Laboratories, Inc., 30 Ingold Road, Burlingame, CA 94010 U.S.A.), mounted and evaluated under light microscope.

Appropriate washing with Wash Buffer (S 3006; Dako, Glostrup, Denmark) was performed between each step. Specificity tests, performed for the ghrelin antibody included: negative control, where the antibodies were replaced by normal rabbit serum (S-5000; Vector Laboratories, Inc., 30 Ingold Road, Burlingame, CA 94010 USA) at respective dilution and a positive control was prepared from specific tissue (neuroendocrine cells of human pylorus) as recommended by the manufacturer.

Histological preparations were subjected to a visual analysis using an Olympus B 50x light microscope with digital camera and a PC computer with NIS Elements AR 3.10 NIKON software for microscope image analysis (Fig. 1).

Quantitative analysis

Ghrelin immunopositive cells were counted in ten randomly selected microscopic fields, each field of 0.785 mm^2, in magnification of 200x (20x the lens and 10x the eyepiece). Five sections of each subject from each parts of the stomach were analyzed. The numbers of positively stained cells were presented as mean values per visual field.

Also length (μm) and the surface (μm^2) of Ghr-IR cells with similar shape were measured.

ELISA

The ghrelin concentrations of each blood sample were found according to the protocol of Millipore Human Ghrelin (Total) ELISA kit (Cat. No EZGRT-89K; EMD Millipore Corporation, Billerica, MA, USA). The final step in the ELISA assay required the use of a spectrophotometer which analyzed the samples at different wavelengths to determine ghrelin concentrations in pg/mL.

Statistical analysis

Results from morphometric analysis and ELISA are shown as mean±SD. The relationships between serum ghrelin levels and various anthropometric variables were examined by linear regression and Spearman's correlation coefficient analyses. Differences in results calculated for morphometric parameters of cells, ghrelin levels in serum, weight and body mass index between genders were examined by non-parametric Mann-Whitney test for two independent groups. $P<0.05$ was considered statistically significant. All of the analyses were performed using Statistica system, version 10.

RESULTS

Routine studies (H+E staining) showed no microscopic pathological changes in the stomachs of men and women.

The mean values of age, body weight, body mass index (BMI) and serum ghrelin concentration in group of men (M) and women (F), are presented in Table I. The age of men and women in our study was similar while other investigated parameters were higher in men. Differences in weight ($Z= -3.05$, $P<0.05$) and BMI ($Z= -2.77$, $P<0.05$) between genders was statistically significant. Concentration of ghrelin in serum was higher in men than women, but this differences was not significant ($Z= -1.24$, $P<0.05$), (Table I).

Immunohistochemistry

The immunohistochemical studies revealed a positive reaction in the cytoplasm of neuroendocrine

Table I. *Age (year), weight (kg), BMI (body mass index – kg/m^2) and ghrelin level in the serum (pg/mL) of men (M) and women (F) expressed as mean±SD. Statistically significant differences (P <0.05) in parameters between genders are linked.*

Parameter / Sex	Age	Weight	BMI	Ghrelin level
M	43.1 ± 15	**82.63 ± 4.1**	**26.42 ± 0.58**	255.931 ± 59.533
F	45.2 ± 15	**63.2 ± 5.8**	**23.06 ± 2.73**	214.421 ± 55.006

Table II. *Morphometric parameters of Ghr-IR cells: number, length (μm) and surface (μm^2) in the different stomach parts and whole gastric of men (M) and women (F) expressed as mean±SD. Statistically significant differences (P <0.05) in morphometric parameters between sexes are linked.*

Parameter	Cardia		Fundus		Pylorus		Total	
	M	F	M	F	M	F	M	F
Cell number	10 ± 5	14 ± 6	25 ± 9	29 ± 6	17 ± 6	21 ± 8	52 ± 7	64 ± 7
Cell length [μm]	3.33 ± 0.65	4.08 ± 1.22	3.99 ± 0.5	4.12 ± 0.48	**3.73 ± 0.66**	**4.27 ± 0.77**	11.05 ± 0.33	12.47 ± 0.1
Cell surface [μm^2]	7.87 ± 3.4	8.41 ± 2.93	8.28 ± 1.95	8.31 ± 1.52	**8.61 ± 2.54**	**9.89 ± 3.16**	24.76 ± 0.37	26.61 ± 0.88

cells in all studied parts of the stomach in all subjects. There was no immunoreactivity when the primary antibodies were omitted from the staining procedure. The positive control tissue showed good positive staining of neuroendocrine cells from human pylorus.

The neuroendocrine cells were characterized on the basis of cytoplasmic staining. All the immunoreactive (IR) cells showed a dark brown color and were easy to identify. The nuclei were located in the middle part of cell body and showed a spherical shape. Ghr-IR cells surrounded by other cells of the gastric epithelium were distinctive by shape, usually round or oval but sometimes they were irregular in shape. Ghrelin containing cells were localized in the basal region of the gastric mucosa although single cells were observed in upper parts. IR-cells mainly displayed strong staining of ghrelin, (Fig. 2).

Higher number of cells with positive reaction to antibody against ghrelin was found in the women than in the men in all regions of the stomach (Fig. 2 and Table II). The highest Ghr-IR cell numbers were observed in the fundus (Fig. 2C, D and Table II), while the least ghrelin-containing cell numbers occurred in cardia (Fig. 2A, B and Table II).

Morphometry

The mean number of Ghr-IR cells and their morphometric parameters (length and surface) are presented in Table II.

Number of ghrelin positive cells was higher in

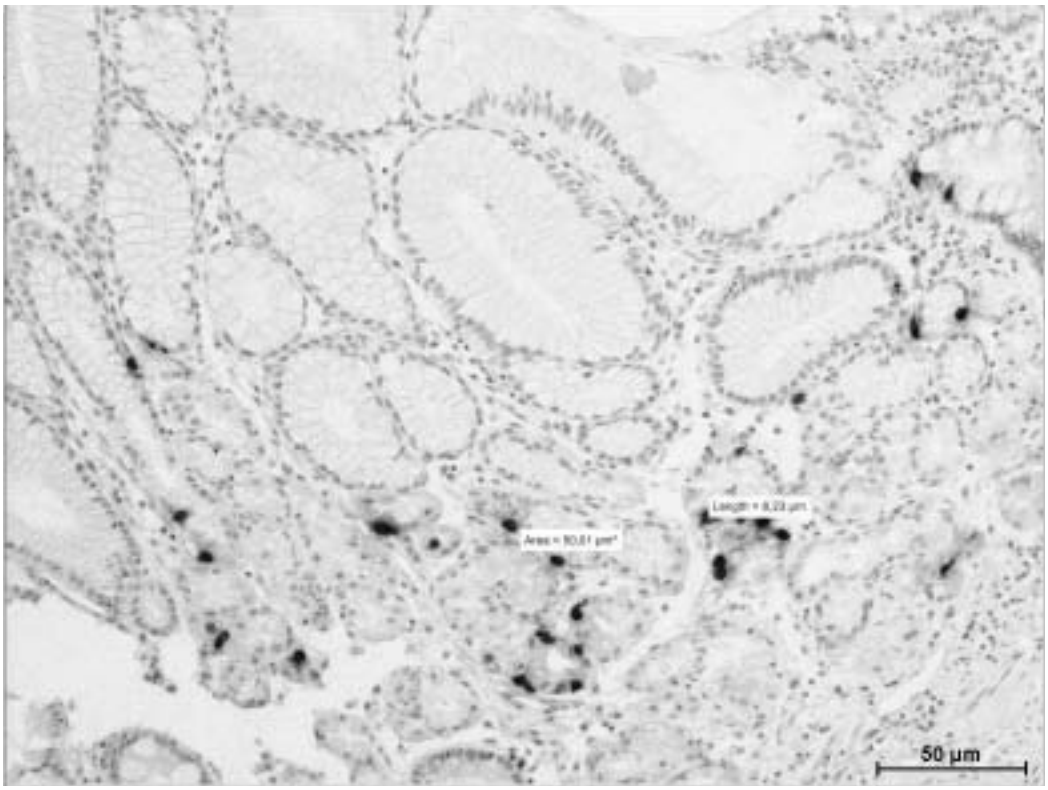

Fig. 1. *Morphometric analysis of ghrelin-IR cells in the human stomach. Scale bars=50 µm.*

all parts of stomach in women than in men. Cells in all regions of women gastric were more elongated and had larger surface. Difference in length (Z= 3.32, P<0.05) and surface (Z= 2.04, P<0.05) of the ghrelin positive cells between genders was statistically significant only in the pylorus (Table II).

ELISA

The mean content of ghrelin in the serum was higher in men than women (Table I). A negative correlation between ghrelin levels in serum and BMI in both sexes was noticed, however this interconnection was not statistically significant in both studied groups (M: r= -0.2787, P= 0.4066; F: r= -0.3637, P= 0.5473) (Fig. 3).

Correlation between serum ghrelin level and BMI in entire group of our subjects (men and women together) was positive (r= 0.0841, P= 0.7567) (Fig. 4).

Results of analysis revealed a statistically significant negative correlation between ghrelin levels in serum and weight in men (r= -0.7232, P= 0.0119). In women this interaction was similar however no statistically significant correlation was found (r= -0.5901, P= 0.2949) (Fig. 5).

It was found a negative correlation between ghrelin levels in serum and age in men (r= -0.0858, P= 0.802) and positive correlation in women (r= 0.6805, P= 0.2061), however this dependence was not statistically significant in both groups (Fig. 6).

DISCUSSION

Ghrelin affects many functional aspects of the gastrointestinal tract, including exocrine secretion, epithelial protection and motility (1, 2). Besides its effects on the gastrointestinal tract, ghrelin has a vast range of physiological functions, thus the abnormality in its secretion leads to multiple organs dysfunction and metabolic syndromes, such as hypo- or hyperglycemia, obesity, cardiovascular diseases, immune or reproduction disorders and many other pathological changes (3, 9, 10).

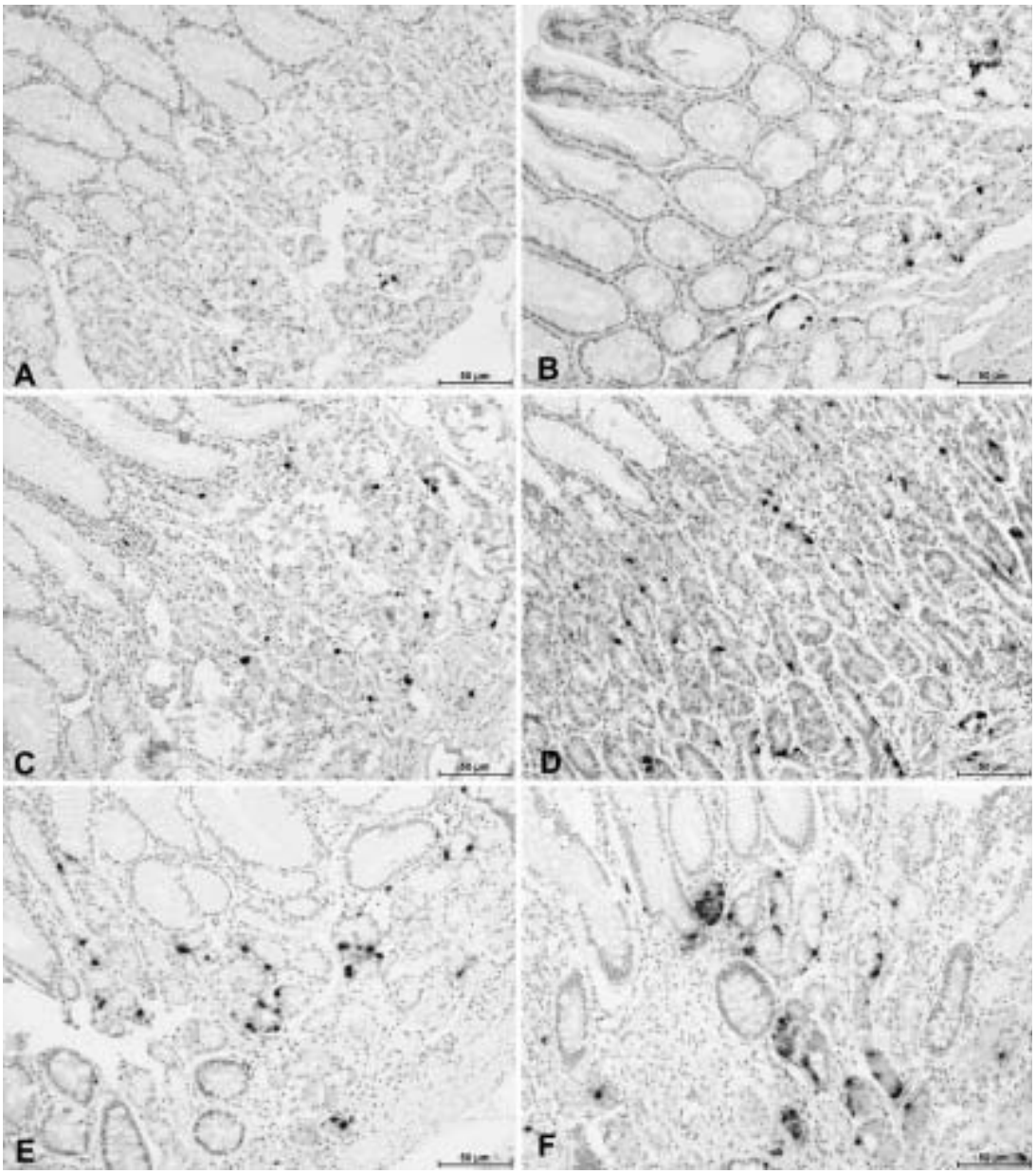

Fig. 2. *Immunolocalization of ghrelin cells in cardia, fundus and pylorus of the stomach of men (A, C, E) and women (B, D, F). Scale bars=50 µm.*

Although numerous results about the function of ghrelin in physiological and pathological conditions have been reported, the current understanding of the mechanisms of regulation of the ghrelin expression and secretion is only beginning to emerge, with much discrepancy among studies (6, 12, 13, 16).

This is the first report of comparative morphometric characterization of gastric ghrelin cells and serum ghrelin levels in healthy men and women.

Our study revealed the presence of ghrelin cells in all regions of the gastric mucosa in men and women. We found that gastric ghrelin cells in humans are mainly located in lower parts of gastric mucosa in all parts of the stomach, with the highest number in fundus and the lowest density in cardia in both

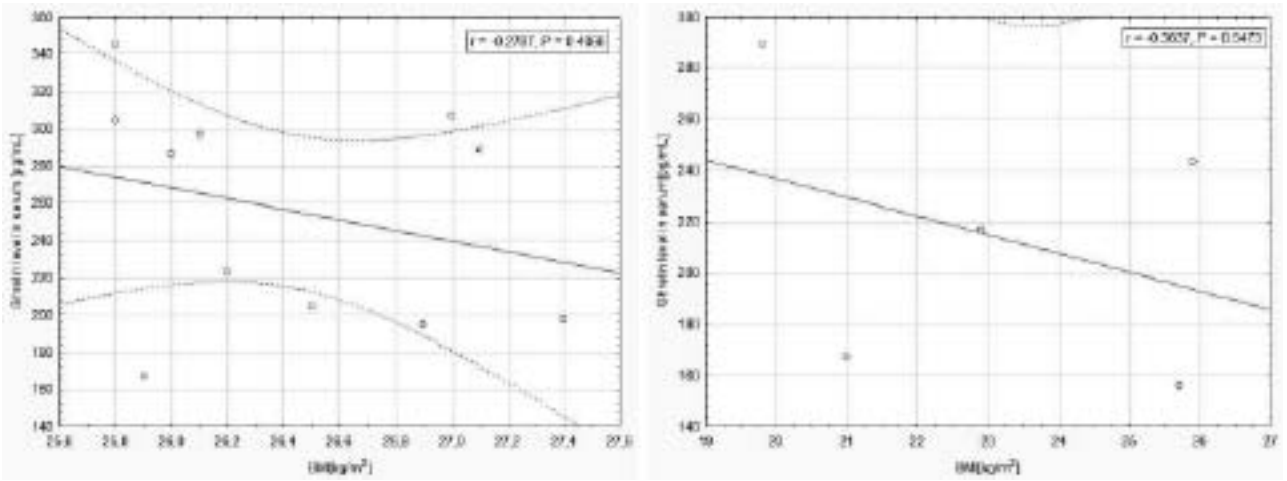

Fig. 3. *Correlation between ghrelin serum level and BMI in men (r= -0.2787, P= 0.4066) and women (r= -0.3637, P= 0.5473).*

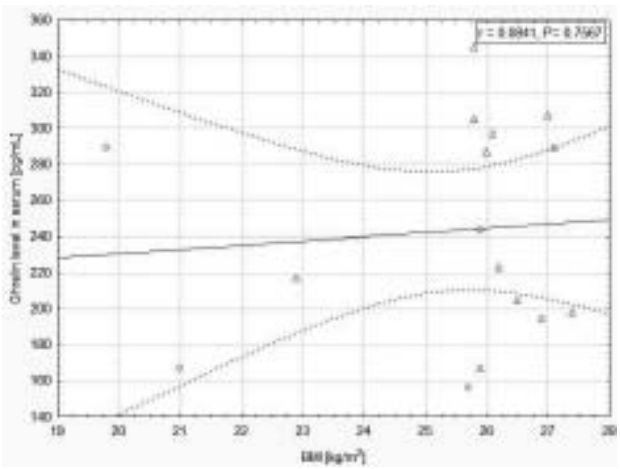

Fig. 4. *Plasma ghrelin levels in the same 18 subjects are positively correlated with BMI (△men, ◇women). Correlation between serum ghrelin level and BMI in entire group of our subjects (men and women) (r= 0.0841, P= 0.7567).*

genders. Similar manner of distribution and density of Ghr-IR cells was described by Dadan et al. in the stomach of obese people (24).

It was found that circulating ghrelin levels decreased over 65%, after gastrectomy in humans, suggesting that the main source of ghrelin in the organism is the stomach (11). Our results confirmed that fundus is a major region of ghrelin synthesis in human stomach. Most of the cells containing ghrelin do not communicate with the lumen of the stomach, but, they are positioned adjacent to capillaries, indicating that the hormone is secreted primarily into blood vessels (7).

In this study, ghrelin cells were more abundant in women than in men. In the literature no evidence for a difference in the number of these cells in relation to human sex was found, while the experimental results are often contradictory. Gualillo et al. showed that stomach-derived ghrelin mRNA levels exhibit no significant sex differences (25), whereas Zhao et al. in the study conducted on gastric mucosa of rats found larger number of ghrelin cells in females than in males (26). This sexual dimorphism of ghrelin cells density, is explained by the authors by different rate of cells maturation and the effect of sex hormones, especially estrogens, which can modify secretion of ghrelin in the stomach.

The present study demonstrated that gastric ghrelin cells in women, were not only more abundant, but also more elongated and had larger surface than in men.

The difference between mentioned morphometric parameters of the cells may suggest their different activity in the stomach of women and men.

The serum ghrelin level depends on the nutrition level, lifestyle and other factors. Some previous studies showed that ghrelin concentration depends on sex suggesting that ghrelin synthesis is modulated by sex hormones (15, 16).

Greater number of ghrelin cells in the stomach of women in our study doesn't reflect level of hormone in serum. In our study we noticed higher ghrelin levels in men than in women. Data on differences

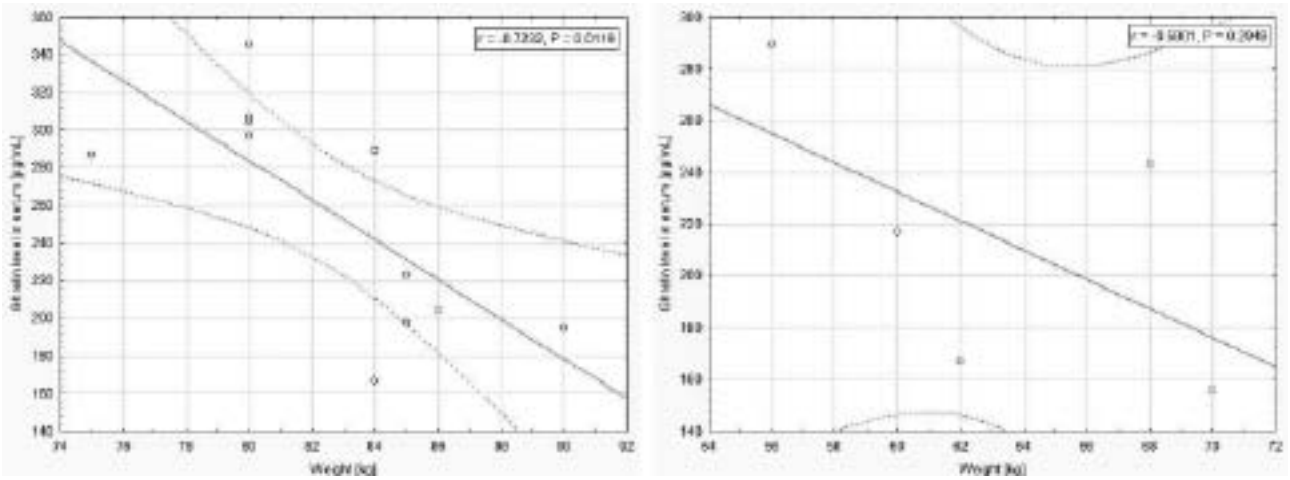

Fig. 5. *Correlation between ghrelin serum level and weight in men (r= -0.7232, P= 0.0119) and women (r= -0.5901, P= 0.2949).*

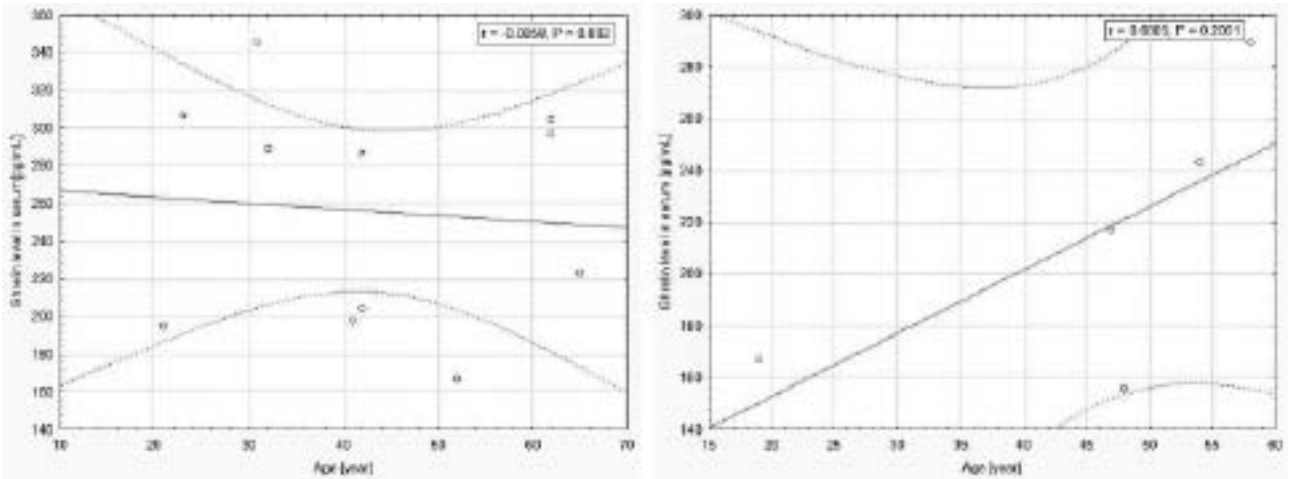

Fig. 6. *Correlation between ghrelin serum level and age in men (r= -0.0858, P= 0.802) and women (r= 0.6805 P= 0.2061).*

in the levels of ghrelin in human based on gender are often contradictory. Tschop et al. found no sexual difference in ghrelin levels between human genders (17), while Ariyasu et al. examining serum of normal healthy volunteers found greater ghrelin levels in men than in women (6). Contradictory results were reported by Aydin et al., who demonstrated higher levels of ghrelin concentrations in women than in men (14). Both authors suggest that sex hormones are responsible for disparity in ghrelin levels between genders. The mechanism which is responsible for sexual disparity in human ghrelin levels in serum is still unknown.

Ingellson et al. suggested that this difference can be caused by: steroid hormones, different number of structures in gonads which show ghrelin expression, appetite or unknown substances (16). Other studies also showed that level of ghrelin is under the influence of sex hormones. In hypogonadal men, testosterone therapy causes increase in ghrelin concentration as compared to normal values (21). Additionally, in postmenopausal women after hysterectomy, estrogen therapy cause increase of ghrelin level in serum (20). It is known that ghrelin has an effect on the hypothalamic-pituitary-ovarian axis (1, 3).

Conflicting evidence exists on the direct effect of ghrelin on gonadotropins production *in vivo*, e.g. injections of ghrelin had no effect on FSH (follicle-

stimulating hormone) and LH (luteinizing hormone) secretion in humans (3). Other studies have shown that ghrelin has an impact on the gonadotropin level in serum (27).

The presence of ghrelin in the testis was found in the Leydig and Sertoli cells as well as in pachyten spermatocytes (19), while in the ovaries expression of ghrelin was observed only in corpus luteum (18). Lower number of structures showing expression of ghrelin in women gonads, might explains difference in levels of hormone between genders.

Sexual disparity in ghrelin levels can be caused by other peptide hormone e.g. leptin, which is a major antagonist of ghrelin. Leptin suppresses expression of ghrelin mRNA in the stomach and decreases levels of the peptide in serum (6, 14). Our study showed higher levels of leptin (four times higher) in serum of examined women than men (unpublished data). Leptin probably can also modulate transcription of ghrelin mRNA, resulting in lower ghrelin concentration in the serum. However, this hypothesis needs to be confirmed in our further experiments. Many reports show that ghrelin level in human is under the influence of different anthropometric factors e.g. BMI, weight or age (9, 15, 17). We confirmed that ghrelin correlates negatively with body mass index and weight. Similar observation was made by Tschop et al. on a group of lean and obese subjects (17).

It is not well established whether ghrelin concentration is associated with age in humans. In our study we noticed negative correlation between age and serum ghrelin levels in men, while in women this correlation was positive. This finding is in agreement with data published previously by Nanjo et al. in men (15) and by Ingellson et al. in a group of women (16).

The results of this study may lead to the identification of other, still unknown, roles of ghrelin in physiological and pathological conditions.

In summary, ghrelin is a peptide hormone mainly secreted from the stomach into the circulation, but it can be also synthesized by other tissues e.g. gonads as a potential additional autocrine/paracrine factor. Ghrelin is involved in a wide range of endocrine and non-endocrine actions linking the gastrointestinal activities with organism functions. Thus, this peptide could operate as a novel regulator of energy balance and reproductive function in women and men.

The present results support previous evidence that the stomach is a major place of ghrelin synthesis in human body. The differences in gastric ghrelin cells and ghrelin levels in serum between women and men, indicate that its secretion can be under control of sex hormones or other unknown factors.

The correlation between the number and immunoreactivity of gastric ghrelin cells and ghrelin levels in serum, however, requires further research to draw firm conclusions.

REFERENCES

1 Ghigo E, Broglio F, Arvat E, Maccario M, Papotti M, Muccioli G. Ghrelin. More than a natural GH secretagogue and/or an orexigenic factor. Clin Endocrinol 2005; 62:1-17.

2. Ueno H, Yamaguchi H, Kangawa K, Nakazato M. Ghrelin. A gastric peptide that regulates food intake and energy homeostasis. Regul Pept 2005; 126:11-9.

3. Lorenzi T, Meli R, Marzioni D, et al. A metabolic signal affecting the reproductive system. Cytokine Growth Factor Rev 2009; 20:137-52.

4. Kojima M, Hosoda H, Date Y, Nakazato M, Matsuo H, Kangawa K. Ghrelin is a growth-hormone-releasing acylated peptide from stomach. Nature 1999; 402:656-60.

5. Hayashida T, Murakami K, Mogi K, et al. Ghrelin in domestic animals: distribution in stomach and its possible role. Domest Anim Endocrinol 2001; 21:17-24.

6. Ariyasu H, Takaya K, Tagami T, et al. Stomach is a major source of circulating ghrelin, and feeding state determines plasma ghrelin-like immunoreactivity levels in humans. J Clin Endocrinol Metab 2001; 86:4753-8.

7. Rindi G, Necchi V, Savio A, et al. Characterisation of gastric ghrelin cells in man and other mammals: studies in adult and fetal tissues. Histochem Cell Biol 2002; 117:511-9.

8. Bagnasco M, Tulipano G, Melis MR, Argiolas A, Cocchi D, Muller EE. Endogenous ghrelin is an orexigenic peptide acting in the arcuate nucleus in response to fasting. Regul Pept 2003; 111:161-7.

9. Carlson JJ, Turpin AA, Wiebke G, Hunt SC, Adams TD. Pre- and post- prandial appetite hormone levels

in normal weight and severely obese women. Nutr Metab 2009; 6:32.
10. Isomoto H, Ueno H, Nishi Y, et al. Circulating ghrelin levels in patients with various upper gastrointestinal diseases. Dig Dis Sci 2005; 50:833-8.
11. Tymitz K, Engel A, McDonough S, Hendy MP, Kerlakian G. Changes in ghrelin levels following bariatric surgery: review of the literature. Obes Surg 2011; 21:125-30.
12. Chmielewska J, Szczepankiewicz D, Skrzypski M, Kregielska D, Strowski MZ, Nowak KW. Ghrelin but not obestatin regulates insulin secretion from INS1 beta cell line via UCP2-dependent mechanism. J Biol Regul Homeost Agents 2010; 24:397-402.
13. Steiger A, Dresler M, Schüssler P, Kluge M. Ghrelin in mental health, sleep, memory. Mol Cell Endocrinol 2011; 340:88-96.
14. Aydin S, Halifeoglu I, Ozercan IH, et al. A comparison of leptin and ghrelin levels in plasma and saliva of young healthy subjects. Peptides 2005; 26:647-52.
15. Nanjo Y, Adachi H, Hirai Y, et al. Factors associated with plasma ghrelin level in Japanese general population. Clin Endocrinol 2011; 74:453-8.
16. Ingelsson E, Larson MG, Yin X, et al. Circulating ghrelin, leptin, and soluble leptin receptor concentrations and cardiometabolic risk factors in a community-based sample. J Clin Endocrinol Metab 2008; 93:3149-57.
17. Tschöp M, Weyer C, Tataranni PA, Devanarayan V, Ravussin E, Heiman ML. Circulating ghrelin levels are decreased in human obesity. Diabetes 2001; 50:707-9.
18. Gaytan F, Barreiro ML, Chopin LK, et al. Immunolocalization of ghrelin and its functional receptor, the type 1a growth hormone secretagogue receptor, in the cyclic human ovary. J Clin Endocrinol Metab 2003; 88:879-87.
19. Gaytan F, Barreiro ML, Caminos JE, et al. Expression of ghrelin and its functional receptor, the type 1a growth hormone secretagogue receptor, in normal human testis and testicular tumors. J Clin Endocrinol Metab 2004; 89:400-9.
20. Kellokoski E, Pöykkö SM, Karjalainen AH, Ukkola O, Heikkinen J, Kesäniemi YA, Hörkkö S. Estrogen replacement therapy increases plasma ghrelin levels. J Clin Endocrinol Metab 2005; 90:2954-63.
21. Pagotto U, Gambineri A, Pelusi C, et al. Testosterone replacement therapy restores normal ghrelin in hypogonadal men. J Clin Endocrinol Metab 2003; 88:4139-43.
22. Gale SM, Castracane VD, Mantzoros CS. Energy homeostasis, obesity and eating disorders: recent advances in endocrinology. J Nutr 2004; 134:295-8.
23. Herman GE, Elfont EA. The taming of immunohistochemistry: the new era of quality control. Biotech Histochem 1991; 66:194-9.
24. Dadan J, Hady HR, Zbucki RL, Iwacewicz P, Bossowski A, Kasacka I. The activity of gastric ghrelin positive cells in obese patients treated surgically. Folia Histochem Cytobiol 2009; 47:307-13.
25. Gualillo O, Caminos JE, Kojima M, Kangawa K, Arvat E, Ghigo E, Casanueva FF, Diéguez C. Gender and gonadal influences on ghrelin mRNA levels in rat stomach. Eur J Endocrinol 2001; 144:687-90.
26. Zhao Z, Sakai T. Characteristic features of ghrelin cells in the gastrointestinal tract and the regulation of stomach ghrelin expression and production. World J Gastroenterol 2008; 14:6306-11.
27. Kluge M, Schüssler P, Schmidt D, Uhr M, Steiger A. Ghrelin suppresses secretion of luteinizing hormone (LH) and follicle-stimulating hormone (FSH) in women. J Clin Endocrinol Metab 2012; 97:448-51.

JAGGED-1–HES-1 SIGNALING INHIBITS THE DIFFERENTIATION OF TH17 CELLS VIA ROR γt

P. YOU[1], F. XING[1,2], C. MAO[1], Z. CHEN[1], H. ZHANG[3], Y. WANG[4], J. XU[5], J. DI[1], S. ZENG[1] and J. LIU[6]

[1]Institute of Tissue Transplantation and Immunology, Department of Immunobiology, Jinan University, Guangzhou, China; [2]Key Laboratory of Functional Protein Research of Guangdong, Higher Education Institutes, Jinan University, Guangzhou, China; [3]Institute of Human Virology, Zhongshan School of Medicine, Sun Yat-sen University, China; [4]Guangdong Provincial Key Laboratory of Bioengineering Medicine, Department of Cellular Biology, Jinan University, Guangzhou, China; [5]School of Pharmaceutical Sciences, Sun Yat-sen University, China; [6]Department of Stomatology, Jinan University, Guangzhou, China

Received October 10, 2012 – Accepted February 4, 2013

P.Y., C.M. and Z.C. contributed equally to this work

Notch signaling plays an important role in differentiation of T cells. However, little is known as to action of it in differentiation of Th17 cell subset. In this study, a soluble Jagged-1/Fc chimera protein (Jagged-1) was directly used to activate Jagged-1–Notch signaling, while Hes-1-targeting siRNA was used to knock down *Hes-1* gene to investigate effect of Jagged-1–Hes-1 signaling on the differentiation of CD4$^+$ T cells into Th17 cells. The results showed that Jagged-1 could promote the expression of Hes-1 and Deltex-1 mRNAs and the expression of NICD, Hes-1 and Deltex-1 proteins, which might be significantly blocked by DAPT, a specific inhibitor of Notch signaling. Jagged-1–Hes-1 signaling resulted in the markedly decreased in situ expression of RORγt in the CD4$^+$ T cells induced by IL-6 plus TGF-β. Flow cytometric analysis showed the reduction of IL-17 production in CD4$^+$ T cells by Jagged-1, but the enhancement of it by Hes-1-targeting siRNA. The level of IL-10 produced by the treated cells was also enhanced, whereas the expression of IL-17 was prominently attenuated, which could be offset by anti-Jagged-1 antibody or DAPT. The results indicate that Jagged-1–Hes-1 signaling can suppress the skewing of CD4$^+$ T cells toward Th17 cells via RORγt, for which Hes-1 may be crucial.

A novel CD4$^+$ T cell subset has been discovered from lyme arthritis, rheumatoid arthritis, experimental autoimmune encephalomyelitis, other autoimmune diseases and allergen-specific reaction, which produces mainly IL-17 and is called Th17 cells discriminated from Th1 and Th2 (1-4). Th17 cells may play an essential role in protection against certain extracellular pathogens, chronic inflammation and autoimmunity diseases (5). However, the mechanism of their differentiation remains unclear. Notch signaling not only regulates T/B cell lineage commitment, but also

Key words: Jagged-1, Hes-1, siRNA, Th17, differentiation

Mailing address:
Dr. Feiyue Xing or Jing Liu,
Institute of Tissue Transplantation and Immunology,
Department of Immunobiology,
Jinan University, Guangzhou 510632, China
Tel.: +86 20 85220723
e-mail: tfyxing@jnu.edu.cn, tjliu@jnu.edu.cn

0393-974X (2013)

the differentiation and function of peripheral T cells (6, 7). Inactivation of Notch1 in bone marrow induces a blockade of T cell development at a early stage, while B cell development is promoted in the thymus (8). This proves that Notch1 is essential for T cell lineage commitment and inhibitory for B cell lineage. Vertebrates have multiple homologs of Notch ligands, Delta homolog is known as Delta or Delta-like(Dll) and Serrate homolog is known as Jagged (Jagged-1 and Jagged-2) (9, 10). The two types of Notch ligands play a different role in the differentiation of naive $CD4^+$ T cells. $CD4^+$ T cells develop in the presence of Delta-1, only producing IFN-γ (11) , while $CD4^+$ T cells develop in the presence of Jagged-1, mainly yielding IL-4. This indicates that Delta ligands promote naïve $CD4^+$ T cells to differentiate into Th1 cells, while Jagged-1 promotes Th2 differentiation (12). *Hes* gene is a homolog of hairy/E (spl) gene family, which encodes a transcriptional regulator containing the basic helix-loop-helix motif (13). This protein plays a key role in Notch signaling that regulates differentiation and proliferation of many types of cells. There are seven homologs of Hes found at present. If there is lack of Hes-1 in process of T cell development, it may arrest in a $CD4^-CD8^-$ stage. Mukherjee et al. found that dendritic cells (DCs) were activated by toll like receptor (TLR)-specific signals, and delta-like 4 (Dll4) up-regulated Rorc expression in T cells and that both Rorc and *il17* gene promoters were direct transcriptional notch targets that further enhanced the differentiation of Th17 cell population, while an anti-Dll4 antibody significantly inhibited the differentiation (14). Toshihiro Ito *et al*. showed that TLR-9-deficient mice challenged with a mycobacterium antigen displayed an altered Th17 cytokine profile, decreased accumulation of granuloma associated myeloid DCs, and profoundly impaired dll4 Notch ligand expression, suggesting dll4 plays an important role in promoting Th17 effector activity during a mycobacterium challenge (15). Notch3 Abs could down-regulate expression of IL-17 on experimental autoimmune encephalomyelitis. These show that Dll-Notch signaling may be involved in the differentiation of Th17 cells (16). Since it has been revealed that Dll-Notch signaling and Jagged-Notch signaling exert the different roles in differentiation of T and B cells, whether or how does Jagged-Notch signaling affect differentiation of Th17 cells? Moreover, our previous studies showed that a soluble Jagged-1/Fc chimera protein (Jagged-1) might be directly used to induce the in vitro differentiation of lymph node cells into $CD4^+CD25^+$ regulatory T cells (17) It is speculated that Jagged-1–Notch signaling might influence differentiation of Th17. Therefore, in the current study, activation of Jagged-1–Notch signaling, blockage of Jagged-1–Notch signaling and know-down of critical *Hes-1* gene in the Jagged-1–Notch signaling pathway were employed as major strategies to explore effect of the Jagged-1–Hes-1 signaling on the differentiation of Th17 cells.

MATERIALS AND METHODS

Mice

Male BALB/c mice were purchased from the Guangdong Medical Animal Center (Guangzhou, China). Eight week-old animals weighing 20.0 to 22.0 g were used. All animals were bred and maintained under specific pathogen-free conditions. All animal handling and experiment procedures were approved by the Animal Care and Use Committee of Guangdong Medical Animal Center.

Immunomagnetic bead isolation and cell culture

Lymphocytes from peripheral and mesenteric lymph nodes in the mice were segregated, triturated mechanically, and filtered through a stainless wire net with 200 meshes, followed by passing through nylon fiber column. Then they were collected, washed with phosphate buffered saline (PBS), and re-suspended at the density of 1×10^6 cells/ml. The cell culture was performed in RPMI 1640 complete medium supplemented with 10% (v/v) fetal bovine serum (Gibco BRL, Gaithersburg, MD, USA), and maintained at 37℃ in an incubator containing 5% CO_2 for the experiments below.

$CD4^+$ T cells were isolated from the above separated lymphocytes using EasySep Mouse $CD4^+$ T cell enrichment kit (Stem Cell Technologies, Canada) which negatively depletes non-$CD4^+$ T cells. The lymphocytes were suspended at a concentration of $1x10^8$ cells/ml in PBS containing 2% FBS and 5% Normal Rat Serum in a polystyrene tube. $CD4^+$ T Cell Enrichment Cocktail, Biotin Selection Cocktail and Magnetic Nano particles were added into the tube, respectively, according to the manufacturer's instructions. The magnetically labeled and unwanted cells were discarded, and $CD4^+$ T cells were enriched in suspension. The harvested $CD4^+$ T cells were

cultured in the complete medium and maintained at 37°C in an incubator containing 5% CO_2 for below experiments.

RNA interference and cell treatment

The sense sequences of Hes-1-siRNA and mismatch Hes-1 siRNA (M- Hes-1-siRNA) with point mutations were 5'-CGAGGUGACCCGCUUCCUGdTdT-3' and 5'-CGAGGUCACCCGGUUCCUGdTdT-3' (the mutated nucleotides are underlined), respectively, which had been proved to be working (18). The siRNA duplexes were synthesized and purified by Guangzhou RiboBio Biotechnology Co., Ltd (RiboBio, Guangzhou, China). They were diluted in Opti-MEM medium with reduced serum (Gibco BRL, Gaithersburg, MD, USA) and mixed with SunBio™Trans-EZ siRNA Transfection Agent (SunBio, Shanghai, China) that was pre-diluted by Opti-MEM, according to the manufacturer's instructions. After being stood at room temperature for 20 min, 100 µl of complex was added into each well containing the cells in a 12-well plate (1×10^7 cells/well). Then, the transfected or untransfected cells were treated for 48 or 72 h respectively by 5 mg/L immobilized anti-CD3 plus 2 µg/ml soluble anti-CD28 (eBioscience, San Diego, CA, USA), 2 ng/ml TGF-β, 10 ng/ml IL-1-β, 20-40 µg/ml IL-6 (PeproTech, Rocky Hill, NJ, USA), 5 µg/ml anti-mouse IL-4, 5 µg/ml anti-mouse IFN-γ (eBioscience, San Diego, CA, USA) and 40 ng/ml IL-23 (PeproTech, Rocky Hill, NJ, USA), with or without 0.5-1.0 µg/ml Jagged-1 or 500 ng/ml of an anti-Jagged-1 antibody (R&D Systems, Minneapolis, MN, USA) or 10 µmol/L of DAPT (N-[N-(3,5- difluorophenacetyl)-l-alanyl]-S-phenylglycinet-butyl ester) (Sigma-Aldrich, St. Louis, MO, USA) 1.5 h before adding Jagged-1. Six hours before the end of the treatment, the cells were stimulated with 10 ng/ml of phorbol-12-myristate-13-acetate (PMA) (Sigma-Aldrich, St. Louis, MO, USA) plus 1 µg/ml of ionomycin (Alexis, Lausen, Switzerland) for below experiments.

RT-PCR

Total RNA in the cells was extracted at day 1, 2, 3 and 5 after the treatment using a Trizol RNA Extraction Reagent (Invitrogen, Carlsbad, CA, USA) according to the manufacturer's instructions. The extracted RNAs from the different groups were quantified by spectrophotometry for absorbance at OD260. The primer pairs for Hes-1 mRNA were 5'-ACCGATCACTAAGTAGCCCTAA-3' (forward) and, 5'-TATTCTTGCCCTTCGCCTC-3' (reverse) with 454 bp of PCR product. The primer pairs for β-actin mRNA were 5'-AACAGTCCGCCTAGAAGCAC-3' (forward) and 5'-CGTTGACATCCGTAAAGACC-3' (reverse) with 281 bp of PCR product. For measuring the level of Hes-1 mRNA expression in the treated cells at the indicated time, a reverse transcriptase-polymerase chain reaction (RT-PCR) was performed with a QIAGEN OneStep RT-PCR Kit (QIAGEN GmbH, Hilden, Germany) according to the manufacturer's instructions. 25 µl of RT-PCR mixture contained 10 µl of RNase free H_2O, 5 µl of 5× Buffer, 2 µl of 10 mM dNTP, 100 nmol/L of each primer and 1 µg RNA. The RT-PCR reaction was amplified with the following profile: 50°C for 30 min, 92°C for 15 min, 95°C for 30 s, 58°C for 30 s, 72°C for 1 min, and 30 recycles in total, with a final extension step for 10 min at 72°C. The amplified products were size-fractionated by electrophoresis on 1.5% agarose gel, and analyzed by a FluorChem 8000 system (Alpha Innotech, Santa Clara, CA, USA).

Western blotting

The cells were treated with Hes-1-siRNA (30, 60, 100, 200 and 250 nmol/L), M-Hes-1 siRNA (100 nmol/L), Jagged-1 (10, 50, 100, 250 and 500 µg/ml), DAPT (10 µmol/L) and 500 ng/ml of an anti-Jagged-1 antibody for 12 to 96 h. The treated cells were washed with PBS twice before being lysed with radio-immunoprecipitation assay (RIPA) lysis buffer (BioColors, Shanghai, China) containing phenylmethanesulfonyl fluoride. Concentration of the extracted protein was quantified with a Bicinchoninic Acid (BCA) Protein Assay Kit (Beyotime, Beijing, China). Equal amount of the protein in the different groups was separated by SDS-PAGE and transferred on a nitrocellulose membrane (Amersham Biosciences, Piscataway, NJ, USA). The membrane was blocked in 5% skim milk dispensed with Tris-buffered saline containing 0.05% Tween-20 (TBST) for 1 h at room temperature. The membrane was incubated overnight with a rabbit anti-cleaved Notch-1 (NICD) primary antibody (Cell Signaling, Danvers, MA, USA) (1:1000 dilution in 5% skim milk TBST) for determining NICD protein, washed 3 times using TBST, and then incubated for an additional hour with a HRP-conjugated goat anti-rabbit IgG secondary antibody (Cell Signaling, Danvers, MA, USA) (1:2000 in 5% skim milk TBST) for 1 h. For the detection of Hes-1 and Deltex-1, the membrane was probed with a goat anti-Hes-1 or a goat anti-Deltex-1 primary antibody (Santa Cruz biotechnology, Santa Cruz, CA, USA) (1:500 dilution in 5% skim milk TBST) overnight, respectively, then a HRP-conjugated donkey anti-goat IgG secondary antibody (Santa Cruz biotechnology, Santa Cruz, CA, USA) (1:10000 in 5% skim milk TBST) for 1 h at room temperature. The specific bands on the membranes were visualized by an Enhanced Chemiluminescence Detection Kit (Amersham Biosciences, Piscataway, NJ, USA) according to the manufacturer's instructions. The band density was quantified by a FluorChem 8000 system (Alpha Innotech, Santa Clara, CA, USA).

Flow cytometry

Four hours before the end of the above treatment, 10 μg/ml of brefeldin A (BioVision, San Francisco Bay area, USA) was added to the cells. The cells were washed twice, fixed with 2% paraformaldehyde for 30 min, and then permeabilization buffer (eBioscience, San Diego, CA, USA) was added for another 30 min at 4°C. After washed with PBS, the cells were incubated for extracellular and intracellular staining with FITC-conjugated anti-mouse CD4 (0.125 μg per million cells), PE-conjugated anti-mouse IL-17 (0.05 μg per million cells) and FITC-conjugated anti-mouse IFN-γ (0.25 μg per million cells) (eBioscience, San Diego, CA, USA) according to the manufacturer's instructions. Finally, they were analyzed on a FAC-Scalibur Flow Cytometer with a CellQuest software (Becton Dickinson, Franklin Lakes, NJ, USA).

Immunofluorescence staining

Detection of in situ expression of RORγt in the above treated $CD4^+$ T cells was performed using immunofluorescence staining. In brief, the treated cells were fixed in cold methanol at 4°C for 15 min and blocked with 5% BSA in PBS for 30 min. Then, the blocked cells were incubated with an anti-mouse RORγt antibody (Santa Cruz Biotechnology, Santa Cruz, CA, USA) for 2 h at room temperature. Subsequently, the cells were washed 3 times with PBS, and incubated with Alexa Fluor®488 Conjugate Anti-Rabbit IgG (Cell Signaling, Danvers, MA, USA) for 1 h at the same temperature, followed by 6-diamidino-2-phenylindole (DAPI) staining for 5 minutes. Finally, the cells were examined under a DMRA2 fluorescence microscope (Leica, Germany) with a FW 4000 software (Leica, Germany).

ELISA

Supernatants from the treated cells were collected at 24-96 h after the above treatment of Jagged-1, DAPT and anti-Jagged-1, respectively, or at 36 and 48 h after the above transfection of Hes-1 siRNA and M-Hes-1 siRNA, respectively. The concentrations of IL-4, IL-6, IL-10 and IL-17 were assessed via an enzyme linked immunosorbent assay (ELISA) with a Mouse IL-4 ELISA Kit, a Mouse IL-6 ELISA Kit, a Mouse IL-10 ELISA Kit and a Mouse IL-17 ELISA Kit (Bender MedSystems, Burlingame, CA, USA) according to the manufacturer's instructions. Absorbance value was measured at 450 nm on a 680 type microplate reader (BIO-RAD, Berkeley, CA, USA). The concentrations of IL-4, IL-6, IL-10 and IL-17 were quantified according to the corresponding standard curves.

Statistical analysis

Means±SD of independent experiments were analyzed by SPSS 13.0 statistical package. One way ANOVA was used for multiple comparisons and Student's paired *t*-test was followed for paired datum comparison and a *P* value of less than 0.05 was considered statistically significant.

RESULTS

Increases of Hes-1 and Deltex-1 mRNA expression by stimulation of Jagged-1

To investigate a hypothesis that activation of Jagged-1–Hes-1 signaling may impact Th17 cell differentiation, we need to confirm as a first step whether direct usage of Jagged-1 can induce the activation of Jagged-1–Hes-1 signaling in the treated cells. As shown in Fig. 1, Jagged-1 induced the augment of Hes-1 and Deltex-1 mRNA levels in the lymphocytes, compared with the control. The Hes-1 mRNA level was most significantly increased on day 3 after the stimulation of Jagged-1, and the Deltex-1 mRNA level peaked on day 2 after the stimulation of Jagged-1. On the contrary, the increase of the Hes-1 and Deltex-1 mRNA levels by the stimulation of Jagged-1 was blocked by DAPT, a specific inhibitor of a Notch signaling pathway at the most observed time-points. These results show that the direct use of Jagged-1 protein can activate the Jagged-1–Hes-1 pathway through up-regulating the expression of the Hes-1 and Deltex-1 mRNA.

Increases of NICD, Hes-1 and Deltex-1 protein expression by stimulation of Jagged-1

To further confirm that direct usage of Jagged-1 can induce the activation of Jagged-1–Hes-1 signaling, we tested effect of Jagged-1 at the different doses and the different time on expression of NICD, Deltex-1 and Hes-1 proteins in the cells. As shown in Fig. 2, Jagged-1 significantly increased the expression of NICD, Deltex-1 and Hes-1 proteins. It seemed to be in a dose-dependent manner (Fig. 2A, C, E). Compared to the control, the enhancement of the NICD and Deltex-1 protein expression occurred mainly on day 1 to 3 after the treatment of Jagged-1, but the enhancement of the Hes-1 protein expression mainly on day 3 after the treatment of Jagged-1 (Fig. 2B, D, F). The role of Jagged-1 can be reversed by DAPT or an anti-Jagged-1 antibody, respectively. The data support that the Jagged-1–Hes-1 signaling pathway is indeed activated by the direct use of Jagged-1 protein.

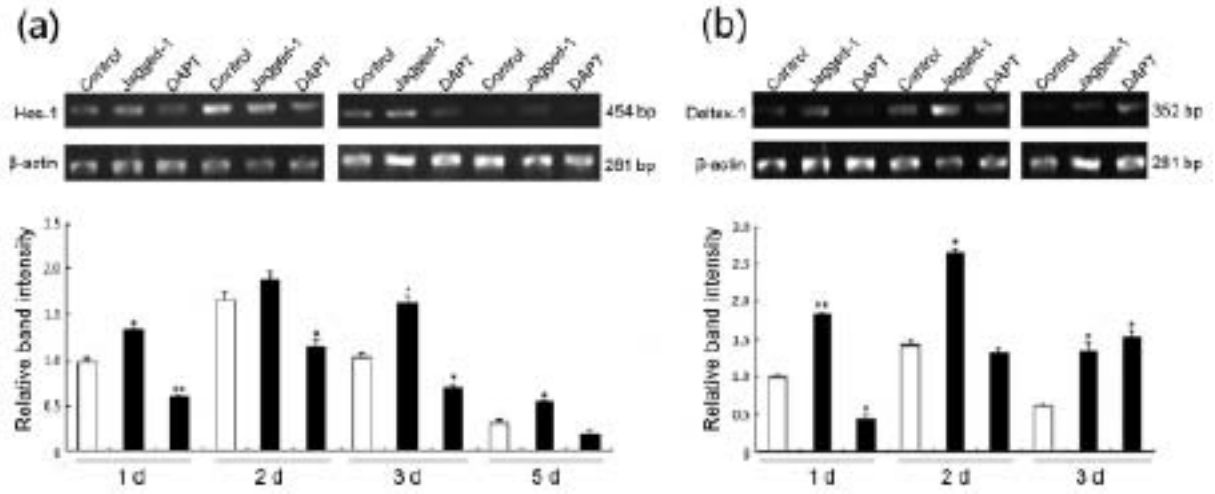

Fig. 1. *Jagged-1 up-regulates the levels of both Hes-1 and Deltex-1 mRNA in the T cells.* ***A****) The cells were stimulated with 500 ng/ml of Jagged-1 or 10* μmoL*/L of DAPT at 1.5 h before the addition of Jagged-1 for 1, 2, 3 and 5 d, respectively. After the stimulation, the expression of Hes-1 mRNA was evaluated by RT-PCR.* ***B****) The cells were stimulated with the same dose of Jagged-1 or DAPT for 1, 2 and 3 d, respectively. After the stimulation, the expression of Deltex-1 mRNA was evaluated by RT-PCR. The primers for RT-PCR were described in "Materials and Methods". The PCR products were separated by electrophoresis on a 1.5% agarose gel. The results are representative of three independent experiments. *P<0.05, **P<0.01 vs the corresponding control.*

Decrease of Hes-1 protein expression by interference of Hes-1-targeting siRNA

Simultaneously, Hes-1-targeting siRNA was employed to knock down *Hes-1* gene (a potentially critical gene) in the Notch signaling pathway. Influence of Hes-1-targeting siRNA on the expression of Hes-1 protein in the cells was examined at the different doses and the different time. The result revealed that 250 nmol/L of Hes-1 siRNA exerted the down-regulation of Hes-1 protein, which could be abrogated by a mutant of Hes-1 siRNA, i.e. M-Hes-1 siRNA. The opposite influence was observed in only Jagged-1-treated group. 100–200 nmol/L of Hes-1 siRNA could result in the decrease of Hes-1 protein expression in the cells, but there were statistical differences, compared with the control (Fig. 3A). The expression of Hes-1 protein began to increase at 24 h post the treatment of Jagged-1, reached peak at 36 h, maintained until 48 h and finally returned nearly to the level of the control at 72 h (Fig. 3B-F). The data suggest that Hes-1-targeting siRNA inhibits the activation of the Jagged-1–Hes-1 signaling pathway through knocking down *Hes-1* gene in this pathway.

Reduction of $CD4^+IL\text{-}17^+$ T cells by stimulation of Jagged-1

To examine effect of the activation of the Jagged-1–Hes-1 signaling pathway on the polarization of Th17 cells, their phenotypes were analyzed by flow cytometry. As shown in Fig. 4, treated with the different concentrations of Jagged-1 for 48 h. Percentage of $CD4^+IL\text{-}17^+$ T cells was reduced with the increased doses of Jagged-1, appearing in a dose-dependent manner (Fig. 4A, B). If calculated, percentage of $CD4^+IL\text{-}17^+$ T cells in the total $CD4^+$ T cells was also diminished significantly(Fig. 4C). The reduction of the $CD4^+IL\text{-}17^+$ T cells occurred within days 4 after the treatment of Jagged-1 (Fig. 4D, E). This reduction could be reversed by DAPT and abrogated by the anti-Jagged-1 antibody (Fig. 4F). Consistent with the tendency of the $CD4^+IL\text{-}17^+$ T cell change, percentage of $IFN\text{-}\gamma^+IL\text{-}17^+$ cells was also decreased by Jagged-1, seeming to be in a dose-dependent manner, which could be blocked by DAPT and abrogated by the anti-Jagged-1 antibody as well (Fig. 4F, G). The data indicate that the activation of the Jagged-1 signaling can inhibit the polarization of

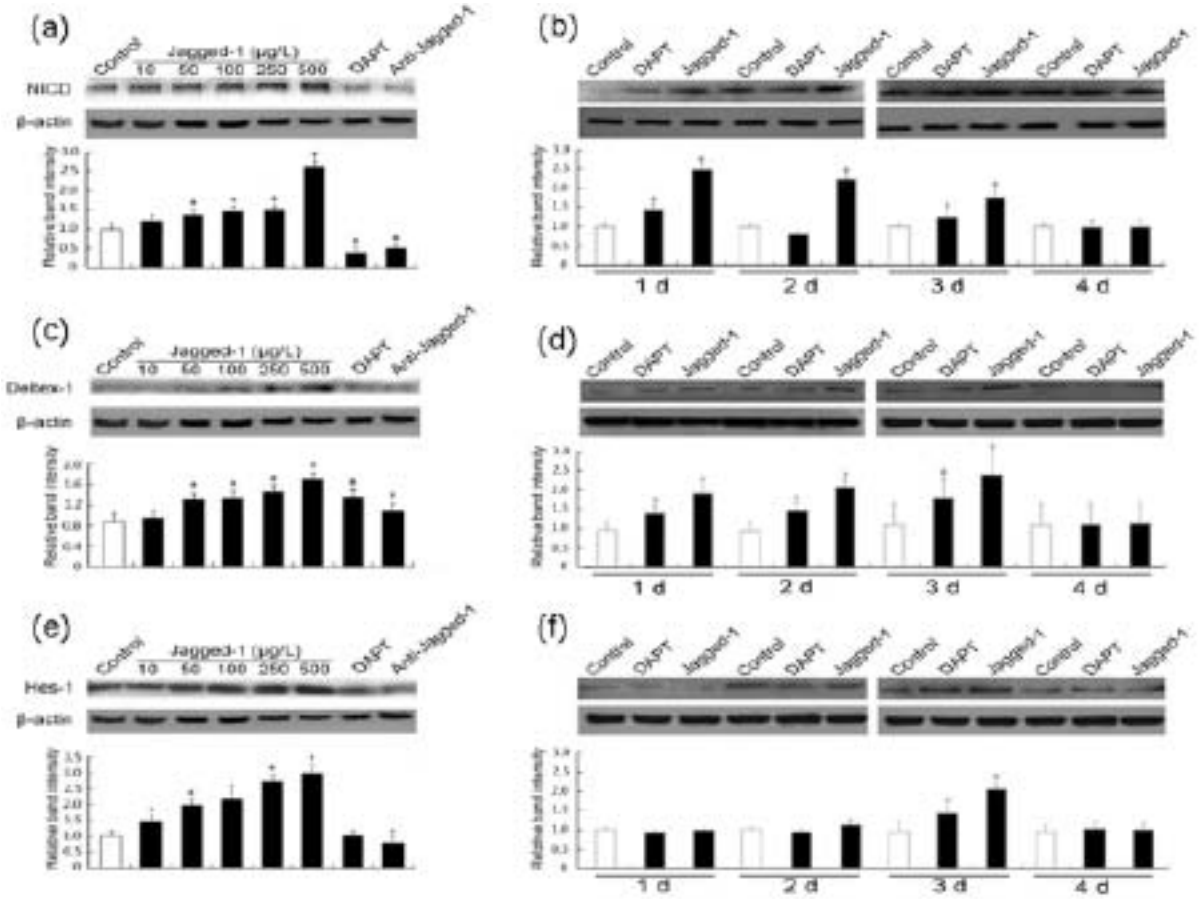

Fig. 2. *Jagged-1 promotes the expressions of NICD, Hes-1 and Deltex-1 proteins in the T cells (**A, B**). The cells were treated with the indicated concentrations of Jagged-1 for 48 h. 10* μmoL*/L of DAPT was used to block Jagged-1–Notch signaling in the cells at 1.5 h before the addition of Jagged-1. 500 ng/ml of anti-Jagged-1 antibody served as a neutralizing role and an equivalent volume of PBS was used as a normal control (**A**). Simultaneously, the cells were treated with 500 ng/ml of Jagged-1 for the different time and 10* μmol*/L DAPT was used for the same purpose as described above (**B**). Then, the cytoplasm protein in the differently treated cells was extracted and quantified at the indicated time after the treatment. Finally, Western blot for NICD was performed (**C, D**). As described in (**A**), the cells were treated with the indicated concentrations of Jagged-1 (**C**). The cells were treated with 500 ng/ml of Jagged-1 at the indicated time (**D**). Then, the cytoplasm protein in the differently treated cells was extracted and quantified at the indicated time after the treatment. Finally, Western blot for Deltex-1 was performed(**E, F**). As described in (**A**), the cells were treated with the indicated concentrations of Jagged-1 (**E**). The cells were treated with 500 ng/ml of Jagged-1 at the indicated time (**F**). Then, the cytoplasm proteins in the differently treated cells were extracted and quantified at the indicated time after the treatment. Finally, Western blot for Hes-1 was performed. The results are representative of three independent experiments. *P<0.05, vs the corresponding control.*

Th17 cells.

Enhancement of $CD4^+IL\text{-}17^+$ T cells by interference of Hes-1-targeting siRNA

Hes-1-targeting siRNA was employed to knock down *Hes-1* gene in the Notch signaling pathway further to confirm a possible role of the Jagged-1–Hes-1 signaling in differentiation of Th17 cells. Compared with the control, Hes-1-siRNA caused the increased percentage of $CD4^+IL\text{-}17^+$ T cells, consistent with that of the cells treated with IL-6 plus TGF-β as a positive control. This action of Hes-1-siRNA could be blocked by DAPT and abrogated by M-Hes-1-siRNA (Fig. 5A, 6A, B). Hes-1 siRNA also resulted in the augment of percentage of $IFN\text{-}\gamma^+IL\text{-}17^+$ cells, having the similar tendency with

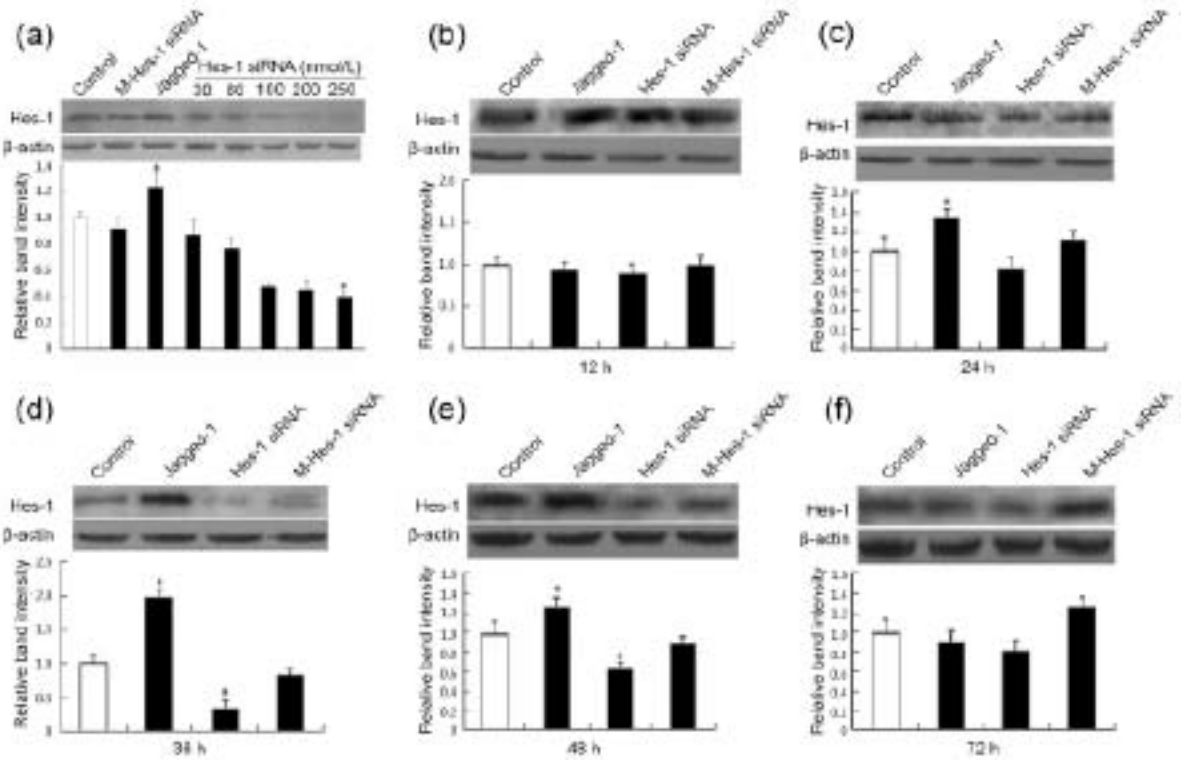

Fig. 3. *Hes-1-targeting siRNA down-regulates the expressions of Hes-1 protein in the T cells (**A**). The cells were treated with the indicated concentrations of Hes-1-siRNA to knock down Hes-1 gene. 500 ng/ml of Jagged-1 was utilized to activate the Notch–Jagged-1 signaling pathway as a positive control. 100 nmol/L of mutated Hes-1-siRNA (M-Hes-1-siRNA) was used as a negative control and an equivalent volume of PBS as a normal control (**B-F**). The cells were treated with 100 nmol/L of Hes-1-siRNA at the indicated time. The used doses of Jagged-1 and M-Hes-1-siRNA were the same as above. Then, the cytoplasm proteins in the differently treated cells were extracted and quantified at the indicated time after the treatment. Finally, Western blot for Hes-1 was performed. The results are representative of three independent experiments. *P<0.05, vs the corresponding control.*

the $CD4^+IL\text{-}17^+$ T cell change (Fig. 5B). The data further support that the activation of Jagged-1–Hes-1 signaling pathway may inhibit the differentiation of $CD4^+$ T cells into Th17 cells and that Hes-1 may be a key target molecule in this pathway.

Jagged-1–Hes-1 signaling inhibits the in situ expression of RORγt in the $CD4^+$ T cells induced by IL-6 plus TGF-β

CD4+ T cells were treated for 72 h with 1 μg/ml of Jagged-1, 100 nmol/L of Hes-1-siRNA, 40 ng/ml of IL-6 and 2 ng/ml of TGF-β to further find out effect of Jagged-1–Hes-1 signaling on the in situ expression of RORγt in the $CD4^+$ T cells. Compared with the control, both IL-6 and TGF-β could eminently increase the in situ expression of RORγt in the $CD4^+$ T cells. But Jagged-1 or Hes-1-siRNA could decrease the in situ expression of RORγt in the $CD4^+$ T cells induced by IL-6 plus TGF-β. The expression of RORγt was mainly found in the nuclei of the $CD4^+$ T cells. These findings indicate that Jagged-1–Hes-1 signaling inhibits the in situ expression of RORγt in the $CD4^+$ T cells induced by IL-6 plus TGF-β (Fig. 7).

Reduction of the specific cytokine for Th17 cells by Jagged-1–Hes-1 signaling

Cytokines secreted from subsets of T cells are considered as functional markers representative of different T cell subsets. Therefore, extracellular levels of IL-17, IL-4, IL-6 and IL-10 were examined by ELISA. The concentration of IL-17 was reduced with the increased concentration of Jagged-1, which could be blocked by DAPT and abrogated by anti-

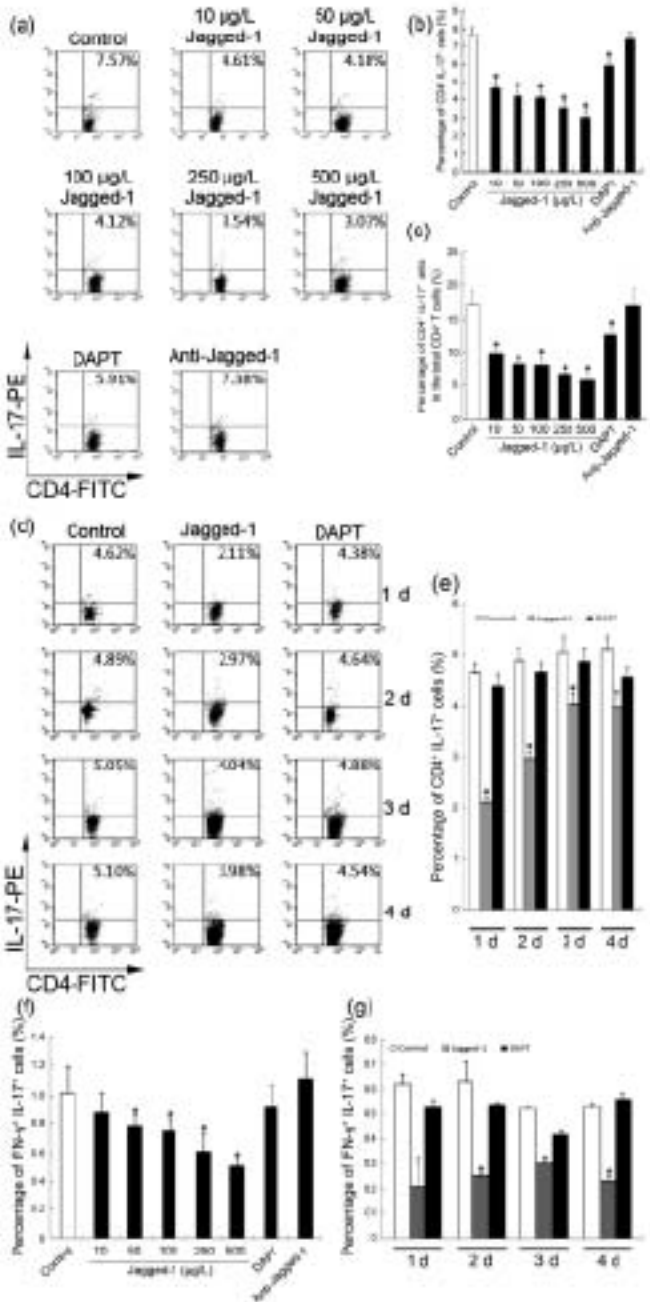

Fig. 4. *Jagged-1 inhibits the differentiation of the T cells into Th17 cells. The T cells were treated for 48 h with the different concentrations of Jagged-1, 10* μmoL*/L of DAPT to block Notch–Jagged-1 signaling in the cells at 1.5 h before the addition of Jagged-1, 500 ng/ml of an anti-Jagged-1 antibody and an equivalent volume of PBS as a normal control (**A, B, C**). The intracellular IL-17 in $CD4^+$ T cells was assayed by flow cytometry 48 h post the treatment of the different concentrations of Jagged-1 (**A**). Then, the percentage of $CD4^+IL\text{-}17^+$ T cells (**B**) and the percentage of $CD4^+IL\text{-}17^+$ T cells in the total $CD4^+$ T cells (**C**) were quantitatively analyzed, respectively (**D, E**). The intracellular IL-17 in $CD4^+$ T cells was assayed by flow cytometry at the indicated time after the treatment of 500 ng/ml of Jagged-1 (**D**) and its quantitative analysis was performed (**E**). Simultaneously, intracellular IL-17 and IFN-γ production in the treated cells was assayed by flow cytometry 48 h post treatment (**F, G**). The percentage of $IFN\text{-}\gamma^+IL\text{-}17^+$ cells was quantitatively analyzed after the treatment of the different concentrations of Jagged-1 (**F**) or at the indicated time after the treatment of 500 ng/ml of Jagged-1(**G**). Results are representative of three independent experiments. *$P<0.05$, vs the corresponding control.*

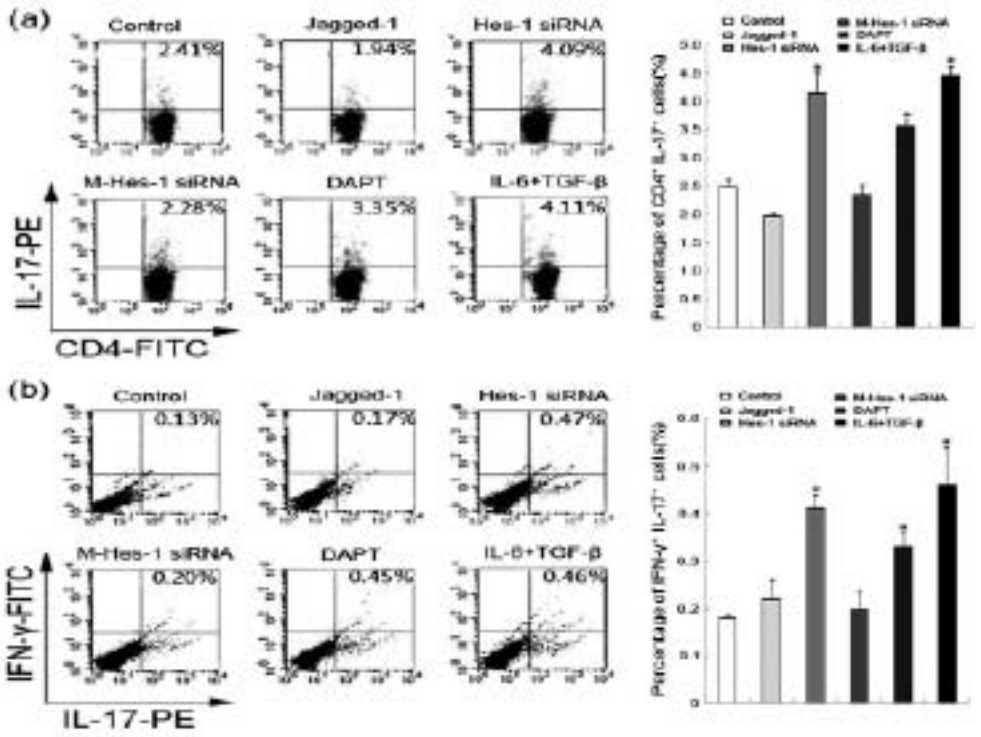

Fig. 5. *Hes-1-targeting siRNA promotes the differentiation of the T cells into Th17 cells. The T cells were treated for 48 h with 100 nmol/L of Hes-1-siRNA or M-Hes-1-siRNA, 500 ng/ml of Jagged-1, 10* μmoL*/L of DAPT at 1.5 h before the addition of Jagged-1, 20 ng/ml IL-6 plus 2 ng/ml TGF-β to serve as a positive control and an equivalent volume of PBS to do as a normal control (**A**). The intracellular IL-17 in $CD4^+$ T cells was assayed by flow cytometry 48 h post treatment of Hes-1-siRNA, and the percentage of $CD4^+IL\text{-}17^+$ T cells was quantitatively analyzed (**B**). Simultaneously, intracellular IL-17 and IFN-γ production in the treated cells was assayed by flow cytometry 48 h post treatment of Hes-1-siRNA. Then, the percentage of $IFN\text{-}\gamma^+IL\text{-}17^+$ cells was quantitatively analyzed. Results are representative of three independent experiments. *P<0.05, vs the corresponding control.*

Jagged-1 antibody (Fig. 8A). The reduction of it was maintained on day 4 after the treatment of Jagged-1. Interestingly, the level of IL-17 in the control was increased with extension of cell culture time without any treatment, indicating that conventionally *in vitro* culture conditions may affect the differentiation of IL-17 (Fig. 8B). On the contrary, Hes-1-targeting siRNA brought about marked increase of IL-17 at 36 h and 48 h post treatment, which was abrogated by its mutant. IL-6 plus TGF-β as a positive control promoted the cells to produce IL-17 significantly at 48 h post the treatment (Fig. 8C). The concentration of IL-4 was reduced with the increased dose of Jagged-1, which was maintained on day 4 after the treatment, whereas the expression of IL-6 did not change dramatically, compared with the control. Interestingly, DAPT not only reversed the action of Jagged-1, but also enabled the level of IL-4 to greatly surpass that in the control on day 4 post the treatment (Fig. 8D, E). The level of Il-10 was up-regulated by 500 ng/ml of Jagged-1, especially on day 3 and 4 after the treatment (Fig. 8F, G). The results suggest that the activation of the Jagged-1–Hes-1 signaling pathway may impact differentiation of Th17 other than Th2 cells.

DISCUSSION

Jagged-1, a single trans-membrane glycoprotein, is one of the main ligands for Notch receptors on mammalian cell membrane, expressing on numerous cells including bone marrow, fetal liver stroma and thymus epithelium, and participates in controlling growth and development of numerous tissues,

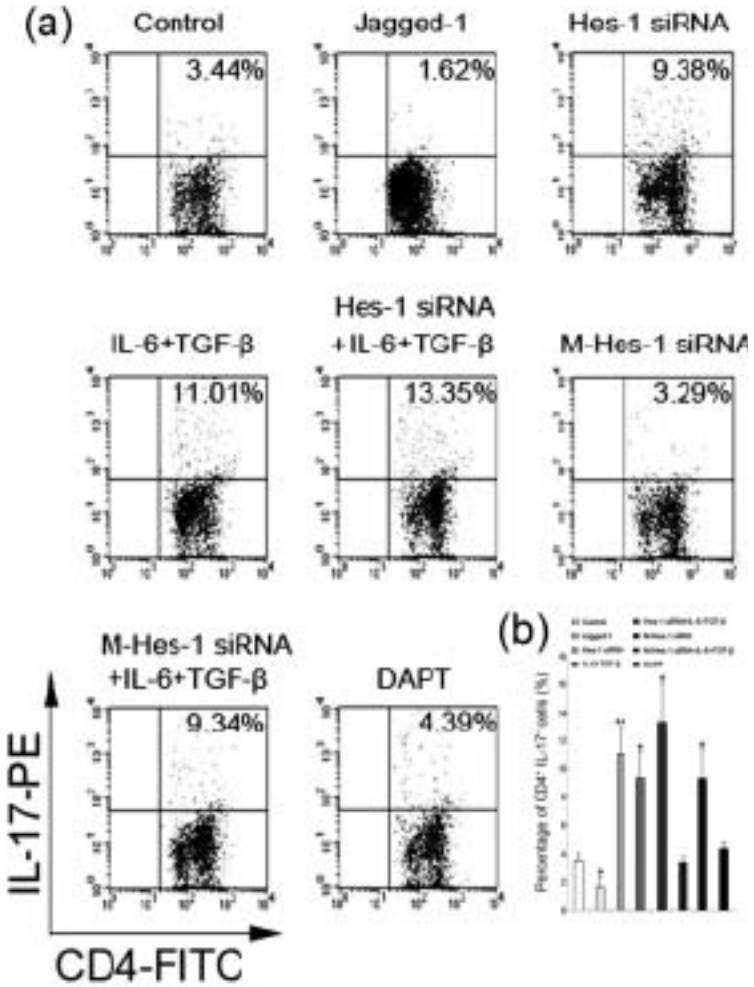

Fig. 6. *Hes-1-targeting siRNA promotes the differentiation of the CD4⁺ T cells into Th17 cells. The CD4⁺ T cells were treated for 72 h with 1* μg*/ml of Jagged-1, 10* μmoL*/L of DAPT, 100 nmol/L of Hes-1-siRNA or M-Hes-1-siRNA, 40 ng/ml of IL-6, 2 ng/ml of TGF-β, 40 ng/ml of IL-23, 10 ng/ml of IL-1-β, 5* μg*/ml of anti-mouse IL-4 and 5* μg*/ml of anti-mouse IFN-γ, respectively (**A**). The intracellular IL-17 in CD4+ T cells was assayed by flow cytometry 72 h post the treatment of Hes-1-siRNA (**B**). Simultaneously, the percentage of CD4⁺IL-17⁺ T cells was quantitatively analyzed. Results are representative of three independent experiments. *P<0.05, **P<0.01 vs the control group.*

maintaining renewal and differentiation of normal haemopoietic stem cells (19). Dendritic cells decide differentiation fate of T cell subsets, mediating immune response or tolerance dependant on a mature extent of DCs. Jagged-1 also expresses highly on the surface of DCs and T cells (20). Jagged 1 was found to promote the maturation of DCs (21). Notch signaling was proved to maintain and control the differentiation of $CD8^-$ DCs (22). Eagar's experiment demonstrated that Notch 1 signaling might play an important role in regulating naive T cell activation and homeostasis (23). Furthermore, it was reported that T cell hypo-responsiveness was promoted by Jagged-1, whereby primary T cell proliferation and cytokine secretion were potently inhibited (24).

What subsets of T cells are mainly affected by Jagged-1–Notch signaling? Amsen et al showed that Jagged-1 instructs naïve $CD4^+$ T cells to differentiate into the Th2 lineage by increasing the expression of IL-4 of naïve T cells. Th2 differentiation induced by antigen presenting cells is abrogated in T cells lacking RBP-Jκ. Notch directs Th2 differentiation by

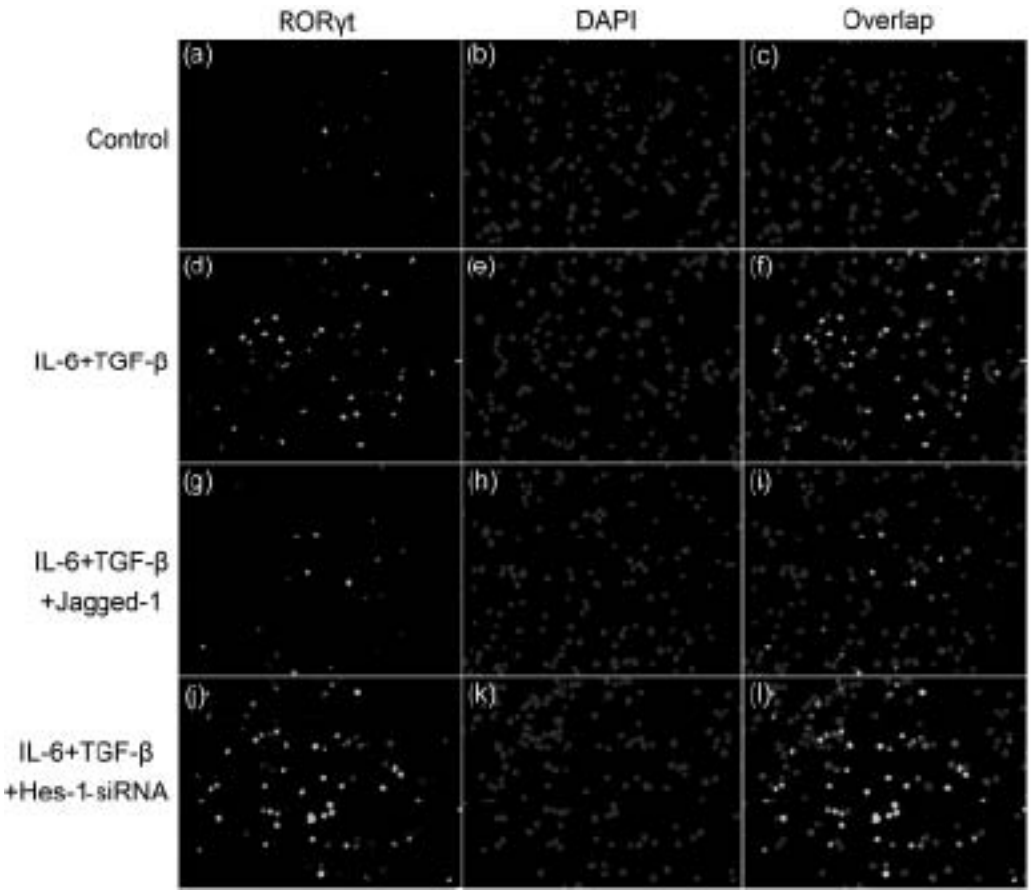

Fig. 7. *Jagged-1–Hes-1 signaling inhibits the in situ expression of RORγt in the CD4⁺ T cells induced by IL-6 plus TGF-β. The CD4⁺ T cells were treated for 72 h with 1* μg*/ml of Jagged-1, 100 nmol/L of Hes-1-siRNA, 40 ng/ml of IL-6, 2 ng/ml of TGF-β, 40 ng/ml of IL-23, 10 ng/ml of IL-1-β, 5* μg*/ml of anti-mouse IL-4 and 5* μg*/ml of anti-mouse IFN-γ, respectively. The cells were incubated with an anti-mouse RORγt antibody for 2 h, and then combined with Alexa Fluor®488 Conjugate Anti-Rabbit IgG for 45 min, followed by DAPI staining for 5 min. Finally, the cells were observed under a fluorescence microscope with a FW 4000 software for in situ expression and distribution of RORγt (**A-C**). The in situ expression of RORγt was shown in the control cells (**D-F**). The in situ expression of RORγt was shown in the cells treated with IL-6 plus TGF-β (**G-I**). The in situ expression of RORγt was shown in the cells treated with IL-6 and TGF-β plus Jagged-1 (**J-L**). The in situ expression of RORγt was shown in the cells treated with IL-6 plus TGF-β after the transfection of Hes-1-siRNA. All the images are at magnification ×200. Results are representative of two independent experiments.*

inducing GATA3 and by directly regulating *il4* gene transcription through RBP-Jκ sites in a 3' enhancer (25). Other research groups found that Jagged-1 directly activated Jagged-1–Notch signaling pathway, inducing naïve peripheral T cells to differentiate into regulatory T cells (Treg) (17, 26, 27). Moreover, Ito, et al. found both in mice and in vitro that Dll-4, another member of Notch ligands, would improve the secretion of Th17 type cytokines such as IL-17A and IL-17F. Dll4 influences the generation of IL-17-producing T cells in the presence of both IL-6 and TGF-β (15). In the absence of notch signals, IL-17 production was significantly inhibited even under specific skewing conditions, demonstrating that Dll4 up-regulates Rorc expression in T cells and that both Rorc and *Il17* gene promoters are direct transcriptional notch targets that further enhance the differentiation of Th17 cell populations (28).

Since Jagged-1–Notch signaling may impact the maturation status of DCs to stimulate development and differentiation of effector T cells, and Dll-Notch signaling may affect the differentiation of Th17 sub-

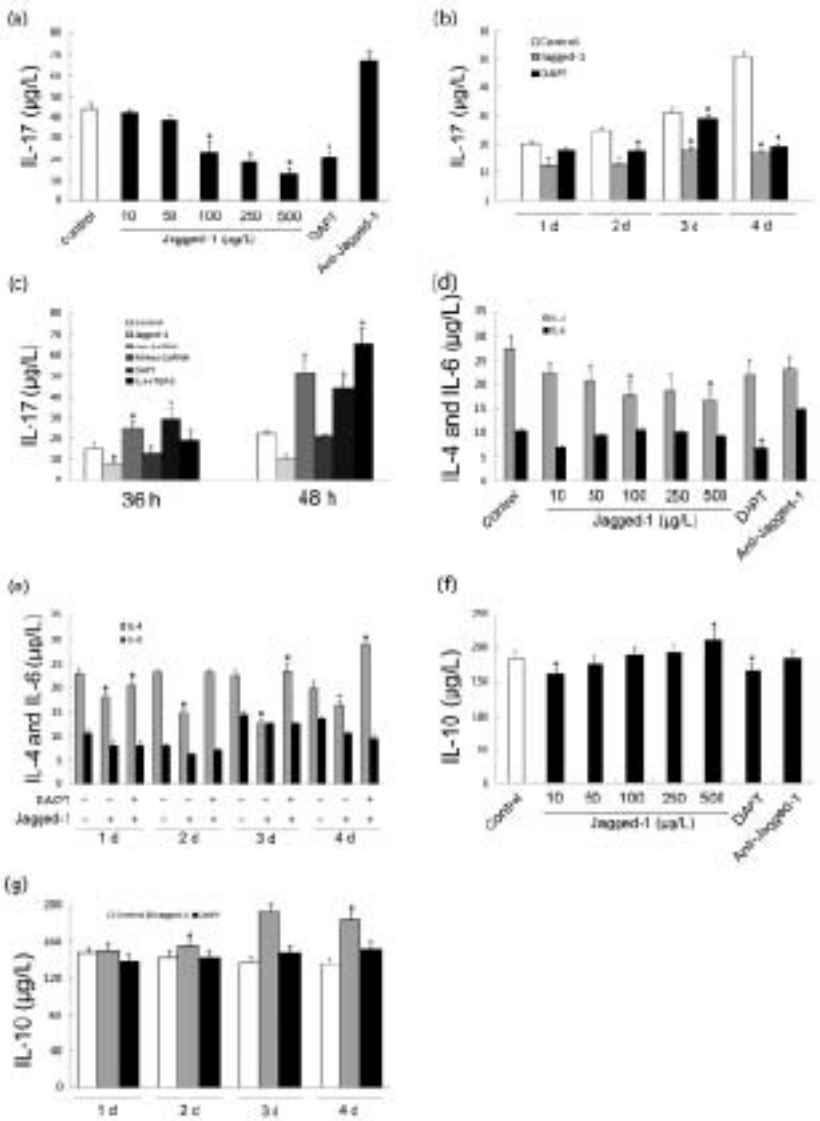

Fig. 8. *Activation of Jagged-1 signaling and knock-down of Hes-1 gene produce the opposite influences on the production of IL-17 in T cells. The T cells were treated for 48 h as below. Then, the cell culture supernatants were harvested to be assayed for cytokines by ELISA (**A**). The T cells were treated with the different concentrations of Jagged-1, 10 μmoL/L of DAPT at 1.5 h before addition of Jagged-1, 500 ng/ml of anti-Jagged-1 antibody and an equivalent volume of PBS as a normal control. The cell culture supernatants were harvested to be assayed for IL-17 (**B**). The cells were treated with 500 ng/ml of Jagged-1 at the indicated time and 10* μmol*/L of DAPT. The cell culture supernatants were harvested to be assayed for IL-17, too (**C**). The cells were treated with 100 nmol/L of Hes-1-siRNA or M-Hes-1-siRNA, 500 ng/ml of Jagged-1, 10* μmoL*/L of DAPT at 1.5 h before the addition of Jagged-1, 20 ng/ml of IL-6 plus 2 ng/ml of TGF-β and an equivalent volume of PBS as a normal control. The cell culture supernatants were harvested at the indicated time to be assayed for IL-17 (**D-G**). The cells were treated as described in (**A**) and (**B**). The cell culture supernatants were harvested to be assayed for IL-4, IL-6 and IL-10, respectively. The results are representative of three independent experiments. *P<0.05 vs the corresponding control.*

population that is critically involved in inflammatory immune responses, it is reasonably speculated that Jagged-1–Hes-1 signaling might influence differentiation of Th17 cells. However, little is, to date, known as to effects of Jagged-1–Hes-1 on differentiation of $CD4^+$ T cells into Th17 cells. In

another aspect, many events of *Hes* gene expression are regulated by Notch signaling, which mediates cell to cell communication (29). Applying the Hes-1 siRNA technology, David A. found that the expression of Hes-1 protein was obviously decreased in 3T3-L1 cells, and the cells' differentiation was also inhibited, revealing Hes-1 plays an important role in adipocyte development (30). Nevertheless, this technology has not yet been used to study effect of Notch signaling on differentiation of Th17 cells until now. Our results showed that direct usage of a soluble Jagged-1 could inhibit the differentiation of $CD4^+IL\text{-}17^+$ T cells, which could be offset by DAPT or anti-Jagged-1 antibody. On the contrary, Hes-1-gargeting siRNA to knock-down *Hes-1* gene in Jagged-1–Notch pathway could promote the differentiation of $CD4^+IL\text{-}17^+$ T cells. In addition, Jagged-1–Hes-1 signaling prominently inhibited the in situ expression of RORγt in the $CD4^+$ T cells induced by IL-6 plus TGF-β. The decrease of $CD4^+IL\text{-}17^+$ T cells was related to the activation of Hes-1 in Jagged-1–Hes-1 signaling pathway downstream with the up-regulation of IL-10 level and the down-regulation of both IL-4 and IL-17 levels. Therefore, these findings strongly prove that the activation of Jagged-1–Hes-1 signaling inhibits the differentiation of $CD4^+$ T cells into Th17 cells through Hes-1. Generally speaking, IL-4 and Il-10 are representatives of Th2-associated cytokines. And IL-10 is able to inhibit the differentiation of Th1. But IL-6 plays an important role in the inflammatory response. Combining all the above results, we consider that activation of Jagged-1–Hes-1 signaling pathway might involve regulation of the differentiation balance among Th1, Th2, Treg and Th17 cells, and that Delta and Jagged might play opposite roles in the differentiation of Th17 cells. Additionally, as for the expression of NICD and Deltex-1 induced by Jagged-1, DAPT is able to almost completely inhibit the former, but partially the latter in our experiment, suggesting that there might be other signaling pathways to take part in the regulation of expressing Deltex-1.

The development of the IL-17-secreting phenotype in Naive $CD4^+$ T cells isolated from $Stat3^{CD4-/-}$ mice was greatly decreased. Stat3 is required for programming the TGF-β1 plus IL-6 and the IL-23-stimulated IL-17-secreting phenotype. Moreover, retroviral transduction of a constitutively active Stat3 into differentiating T cells enhances IL-17 production from these cells, suggesting that Stat3 may directly regulate the forming of Th17 cells (31). Studying the multi-potent progenitor cells derived from the central nervous system, Tanigaki, et al. found that the activated Notch did not stimulate phosphorylation of STAT3 directly, but it may activate ERK1/2. Activated ERK1/2 may be associated with the expression of p-Stat3 (32). Inhibiting the expression of ERK1/2 can increase the phosphorylation levels of Stat3(33). Another literature reported that the activation of Jagged-1–Hes-1 signaling and ERK1/2 signaling may be correlated each other (34). As a result, it can be speculated that Stat3 may also play a role in Th17 differentiation through the correlation of ERK1/2 signaling with Jagged-1–Hes-1 signaling, and the detailed mechanism needs further study.

Analyzing related reports that are less, we noticed that there seems to be inconsistent findings. Higashi, et al. utilized a mixed lymphocyte reaction between human monocyte-derived DCs and allogeneic naive $CD4^+$ T cells to show that curdlan, one of β-glucans, had the ability to induce DC-mediated Th17 differentiation. Jagged-1 mRNA is up-regulated by curdlan, suggesting Notch pathway may be related to the differentiation of Th17. Thus, the authors speculated that curdlan might induce the DCs to express Jagged-1. But there lacked determination for the phenotype of Th17 cells in their experiment (35). Bugeon also showed that $CD25^+$ cells cultured with Jagged-1-conditioned DCs produced very high levels of IL-17 in an IL-2-dependent fashion (36). Compared with the above used models, there exists a main difference from our using one. In the first model, the change of Jagged-1 looks only a concomitant event. It needs to be confirmed whether there is a cause-effect relationship in the process of DC differentiation. In another model, Th17 cell formation was observed through Jagged-1-conditioned DCs. Based on known knowledge, jagged-1-conditioned DCs possibly exert to direct Th17 cell differentiation through their interaction with naïve T cells or their producing cytokines. Obviously, this is entirely different from inducing T cell differentiation by directly using a soluble Jagged-1 ligand to bind corresponding Notch receptors on T cell membrane, realizing influence on T cell differentiation. It is well

known that surfaces of DCs and T cells have rich Notch receptors and relevant ligands. Therefore, we consider that it is important to further find out role of Jagged- or Delta-Notch signaling in $CD4^+$ T cell polarization directed by DCs.

ACKNOWLEDGEMENTS

This work was supported by the National Natural Science Foundation of China (No 30971465, No 81172824, No 30471635) and "211" project grant.

REFERENCES

1. Infante-Duarte C, Horton HF, Byrne MC, Kamradt T. Microbial lipopeptides induce the production of IL-17 in Th cells. J Immunol 2000; 165(11):6107-15.
2. Harrington LE, Hatton RD, Mangan PR. Interleukin 17-producing CD4(+) effector T cells develop via a lineage distinct from the T helper type 1 and 2 lineages. Nat Immunol 2005; 6(11):1123-32.
3. Langrish CL, Blumenschein WM, Mattson J, Basham B, Sedgwick JD, McClanahan T, Kastelein RA, Cua DJ. IL-23 drives a pathogenic T cell population that induces autoimmune inflammation. J Exp Med 2005; 201(2):233-40.
4. Park H, Li ZX, Yang XO, et al. A distinct lineage of CD4 T cells regulates tissue inflammation by producing interleukin 17. Nat Immunol 2005; 6(11):1133-41.
5. Bettelli E, Korn T, Kuchroo VK. Th17: the third member of the effector T cell trilogy. Curr Opin Immunol 2007; 19(6):652-7.
6. Radtke F, Wilson A, MacDonald HR. Notch signaling in T- and B- cell development. Curr Opin Immunol 2004; 16(2):174-9.
7. Tanigaki K, Honjo T. Regulation of lymphocyte development by Notch signaling. Nat Immunol 2007; 8(5):451-6.
8. Han H TK, Yamamoto N, Kuroda K, Yoshimoto M, Nakahata T, Ikuta K, Honjo T. Inducible gene knockout of transcription factor recombination signal binding proein-J reveals its essential role in T versus B lineage decision. Int Immunol 2002; 14(6):637-45.
9. Fleming RJ. Structural conservation of Notch receptors and ligands. Semin Cell Dev Biol 1998; 9(6):599-607.
10. Lewis J. Notch signaling and the control of cell fate choices in vertebrates. Semin Cell Dev Biol 1998; 9(6):583-9.
11. Nyfeler Y, Kirch RD, Mantei N, et al. Jagged1 signals in the postnatal subventricular zone are required for neural stem cell self-renewal. Embo J 2005; 24(19):3504-15.
12. Amsen D BJ, Lee GR, Tanigaki K, Honjo T, Flavell RA. Instruction of distinct CD4 T helper cell fates by different notch ligands on antigen-presenting cells. Cell 2004; 117(4):515-26.
13. Feder JN JL, Jan YN. A rat gene with sequence homology to the Drosophila gene hairy is rapidly induced by growth factors known to influence neuronal differentiation. Mol Cell Biol 1993; 13(1):105-13.
14. Mukherjee S, Schaller MA, Neupane R, Kunkel SL, Lukacs NW. Regulation of T Cell Activation by Notch Ligand, DLL4, Promotes IL-17 Production and Rorc Activation. J Immunol 2009; 182(12):7381-8.
15. Ito T, Schaller M, Hogaboam CM, et al. TLR9 regulates the mycobacteria-elicited pulmonary granulomatous immune response in mice through DC-derived Notch ligand delta-like 4. J Clin Invest 2009; 119(1):33-46.
16. Jurynczyk M, Jurewicz A, Raine CS, Selmaj K. Notch3 inhibition in myelin-reactive T cells down-regulates protein kinase C theta and attenuates experimental autoimmune encephalomyelitis. J Immunol 2008; 180(4):2634-40.
17. Xing FY, Liu J, Yu Z, Ji YH. Soluble Jagged-1/Fc chimera protein induces the differentiation of lymphonode cells into CD4(+) CD25(+) T cells. Prog Biochem Biophys 2008; 35(6):676-83.
18. Kamakura S, Oishi K, Yoshimatsu T, Nakafuku M, Masuyama N, Gotoh Y. Hes binding to STAT3 mediates crosstalk between Notch and JAK-STAT signalling. Nat Cell Biol 2004; 6(6):547-54.
19. Cheng P, Nefedova Y, Miele L, Osborne BA, Gabrilovich D. Notch signaling is necessary but not sufficient for differentiation of dendritic cells. Blood 2003; 102(12):3980-8.
20. Yamaguchi E, Chiba S, Kumano K, Kunisato A, Takahashi T, Hirai H. Expression of Notch ligands, Jagged1, 2 and Delta1 in antigen presenting cells in

mice. Immunol Lett 2002; 81(1):59-64.
21. Weijzen S, Velders MP, Elmishad AG, et al. The Notch ligand Jagged-1 is able to induce maturation of monocyte-derived human dendritic cells. J Immunol 2002; 169(8):4273-8.
22. Caton ML, Smith-Raska MR, Reizis B. Notch-RBP-J signaling controls the homeostasis of CD8- dendritic cells in the spleen. J Exp Med 2007; 204(7):1653-64.
23. Eagar TN, Tang QZ, Wolfe M, He YP, Pear WS, Bluestone JA. Notch 1 signaling regulates peripheral T cell activation. Immunity 2004; 20(4):407-15.
24. Kostianovsky AM, Maier LM, Baecher-Allan C, Anderson AC, Anderson DE. Up-regulation of gene related to anergy in lymphocytes is associated with Notch-mediated human T cell suppression. J Immunol 2007; 178(10):6158-63.
25. Amsen D, Blander JM, Lee GR, Tanigaki K, Honjo T, Flavell RA. Instruction of distinct CD4 T helper cell fates by different notch ligands on antigen-presenting cells. Cell 2004; 117(4):515-26.
26. Vigouroux S, Yvon E, Wagner HJ, et al. Induction of antigen-specific regulatory T cells following overexpression of a Notch ligand by human B lymphocytes. J Virol 2003; 77(20):10872-80.
27. Yvon ES, Vigouroux S, Rousseau RF, et al. Overexpression of the Notch ligand, Jagged-1, induces alloantigen-specific human regulatory T cells. Blood 2003; 102(10):3815-21.
28. Mukherjee S, Schaller MA, Neupane R, Kunkel SL, Lukacs NW. Regulation of T cell activation by Notch ligand, DLL4, promotes IL-17 production and Rorc activation. J Immunol 2009; 182(12):7381-8.
29. Kageyama R, Ohtsuka T, Kobayashi T. The Hes gene family: repressors and oscillators that orchestrate embryogenesis. Development 2007; 134(7):1243-51.
30. Ross DA, Rao PK, Kadesch T. Dual roles for the notch target gene Hes-1 in the differentiation of 3T3-L1 preadipocytes. Mol Cell Biol 2004; 24(8):3505-3513.
31. Mathur AN, Chang HC, Zisoulis DG, et al. Stat3 and Stat4 direct development of IL-17-secreting Th cells. J Immunol 2007; 178(8):4901-7.
32. Tanigaki K, Nogaki F, Takahashi J, Tashiro K, Kurooka H, Honjo T. Notch1 and Notch3 instructively restrict bFGF-responsive multipotent neural progenitor cells to an astroglial fate. Neuron 2001; 29(1):45-55.
33. Li YJ CW, Tian ZJ, Hao YM, et al. Crosstalk between ERK1/2 and STAT3 in the modulation of cardiomyocyte hypertrophy induced by cardiotrophin-1. Chin Med J 2004; 117(8):1135-42.
34. Campos AH, Wang WL, Pollman MJ, Gibbons GH. Determinants of Notch-3 receptor expression and signaling in vascular smooth muscle cells - Implications in cell-cycle regulation. Cir Res 2002; 1(11):999-1006.
35. Higashi T HK, Takagi R, Mizuno Y, Okazaki Y, Tanaka Y, Matsushita S. Curdlan induces DC-mediated Th17 polarization via Jagged1 activation in human dendritic cells. Allergol Int 2010; 59(2):161-6.
36. Bugeon L GL, Rose A, Gentle M, Dallman MJ. Cutting edge: Notch signaling induces a distinct cytokine profile in dendritic cells that supports T cell-mediated regulation and IL-2-dependent IL-17 production. J Immunol 2008; 181(12):8189-93.

IMMUNE RESPONSES TO TETANUS VACCINATION IN ITALIAN HEALTHY SUBJECTS AND CHILDREN WITH RECURRENT INFECTIONS

S. GRAZIANI[1], M.L. ROMITI[1], C. CAPPONI[2], S. DI CESARE[1], S. CORRENTE[1], E. MONTEFERRARIO[1], A. DI PAOLO[3], C. DE MARCHIS[4], L. CHINI[1] and V. MOSCHESE[1].

[1]Department of Pediatrics, Policlinico of Tor Vergata, University of Rome Tor Vergata, Rome, Italy; [2]Laboratory of Immunology, Bambino Gesù Children's Research Hospital, Rome, Italy; [3]Department of Pediatrics, S. Eugenio Hospital, Rome, Italy; [4]Department of Neonatology, S. Eugenio Hospital, Rome, Italy

Received June 11, 2012 – Accepted November 20, 2012

The ability of vaccine antigen to generate protection is a challenge that cannot be restricted to the antibody response; however, the contribution of T cell-mediated mechanisms has not been extensively analyzed. Age and administration to specific categories of patients, i.e. children with recurrent infections (RI), are some of the factors that might affect the vaccine immune response. We investigated the humoral and cellular response to tetanus toxoid (TT) vaccine in 104 healthy children (HC), 11 newborns and 22 healthy adults to characterize the status of immunity according to age and compared it to 118 RI children. Humoral and cellular responses varied in both groups according to age and doses of TT administered. The prevalence of antibody and cellular response was similar in both cohorts (HC 88% and 82% versus RI 86% and 85%), however, TT antibody values were significantly higher in 12-18 months old RI children compared to HC (median: 5 IU/ml *vs* 1.10 IU/ml) (p = 0.02). The lack of an efficient immune response was observed in 12-15% of children from both cohorts. Our data showed that specific antibodies were responsible for early protection, whereas cell-mediated mechanisms may contribute to the generation of long-term immunity after an appropriate vaccine recall. The occurrence of higher TT antibody values in 12-18 months old RI children deserves additional research to determine whether they are caused by different infectious agents and/or by other environmental factors. Clarification of this issue is important for categorizing patients into an optimal vaccine policy.

Tetanus toxoid (TT), a T cell dependent antigen, has been used to immunize against tetanus in different vaccine formulations (1). Although this vaccine has been very significant in reducing morbidity and mortality associated with tetanus disease throughout the world, its long-term protection has not yet been established (2). In Italy, the administration of TT is part of the childhood immunization program that includes 3 doses given at 3, 5 and 12 months of age. At 6 and, since 2005, 12 years of age, an additional booster has been given; booster doses are recommended every 10 years throughout the patient's life, with further tetanus prophylaxis in the case of deep wounds. However, these booster immunizations are not regularly performed: patients either underestimate the importance of boosters

Key words: childhood immunization, immune response, vaccine, tetanus toxoid

Mailing address: Viviana Moschese, MD, PhD, Associate Professor of Pediatrics, Università di Roma Tor Vergata, Policlinico Tor Vergata, Viale Oxford, 81, 00133, Roma, Italy
Tel.: +39 0620900525 Fax: +39 0620900530
e-mail: moschese@med.uniroma2.it

0393-974X (2013)

or forget to have them because of the time lapse between each administration (3).

The antibody response to tetanus vaccination has been extensively studied; it has been shown that the degree and duration of immunity increases with the number of doses of TT received, but antibody titers decrease gradually the older the patient is (4, 5). A tetanus antitoxin titer of 0.1 IU/ml is considered to be protective, although tetanus cases have been reported in individuals with antibody titers higher than this value (6-9). *In vitro* lymphocyte proliferation to TT represents a useful test to identify, characterize and quantify antigen-specific T cells which are very important in the immunization response. However, there is only limited data available on long-term cellular immunity after a tetanus vaccine (4).

During childhood recurrent respiratory infections represent a burden on children and their families and a cause of morbidity and hospitalization with an average incidence estimated from five to seven episodes a year (10). A variety of risk factors has been associated with these recurrent infections such as increased exposure to infectious agents due to environmental factors during early childhood (11) and/or highly variable kinetics of maturation of the immune system. The immunological impact of vaccination on children affected by recurrent respiratory infections is poorly investigated and more information is needed.

We analyzed specific antibody production and lymphocyte proliferative immune responses following scheduled routine tetanus vaccinations both in healthy children and in children affected by recurrent infections to characterize the status of immunity according to age. The evaluation of immunization programs and the development of appropriate guidelines for some groups of patients, i.e. children with recurrent infections, might benefit from the contribution of this study.

MATERIALS AND METHODS

Patients

Our Italian study population consisted of 104 healthy children, ranging from 6 months to 14 years and 6 months of age (median age 4 $^{5/12}$ years), who were asymptomatic and enrolled during a screening work-up for family history of allergic diseases. Eleven newborns and 22 adults (aging from 24 to 79 years, median age 40 $^{6/12}$ years) were also tested. Moreover, we evaluated 118 children, admitted to our Outpatient Paediatric Immunology Unit at the Policlinico Tor Vergata, Rome, Italy, for a clinical history of recurrent infections. Their ages ranged from 1 year to 14 years and 8 months of age (median age 3 $^{11/12}$ years). To classify a child affected by recurrent respiratory infections we applied the criteria established in 1970 by the Immunology Study Group of the Italian Pediatric Society. These criteria consist of the absence of any underlying pathologic condition (primary or secondary immunodeficiency, cystic fibrosis, airway malformation, immotile-cilia syndrome) justifying the recurrence of infections and the presence of at least one of the following conditions: 1) six or more annual diseases due to respiratory infections; 2) one or more monthly diseases due to respiratory infections from October to February; 3) three or more annual diseases due to lower airway respiratory infections (12-14). No adults were enrolled in the population of patients with recurrent infections since our centre is a Paediatric Unit. All healthy subjects and patients were selected on the basis of regular vaccinations according to the National Immunization Program (3 doses given at 3, 5 and 12 months of age; then an additional booster given at 6 and, since 2005, at 12 years of age), regularly checked against their vaccine record forms during the immunological consultation. All subjects had normal immunoglobulin values, lymphocyte subsets and lymphocyte proliferative immune responses to mitogens such as PHA, PWM and OKT3. All samples were obtained when subjects were infection-free .

Patients with immunodeficiencies and/or allergies were excluded from this study. Informed consent was obtained from the children's parents and adults. The study was approved by the Ethic Committee of the Hospital.

Tetanus humoral response

A commercially available test kit (VaccZyme™, The Binding Site Ltd, Birmingham, UK) was used for measuring specific tetanus antibodies, according to the manufacturer's instructions. Briefly, pre-diluted human serum at concentrations of 7.00, 2.33, 0.78, 0.26, 0.09, 0.03 and 0.01 IU/ml was used for calibration. This serum itself was calibrated against the human tetanus anti-toxin 76/589, obtained from the National Institute for Biological Standards and Control (NIBSC). Wells were incubated for 30 min. with pre-diluted (1/100) test serum or calibrators, washed three times, and subsequently incubated with purified peroxidase labelled antibody to human IgG for 30 min. The optical density generated after incubation of the wells with TMB substrate for 30 min. was measured in a spectrophotometer at 450 nm. The concentrations of IgG tetanus toxoid-specific antibodies were determined from the calibration curve. The results were expressed as IU/ml. Antitoxin levels higher than 0.1 IU/ml were considered protective.

Proliferative assay

Peripheral Blood Mononuclear Cells (PBMC) obtained by Ficoll-Hypaque (Pharmacia, Uppsala, Sweden) density gradient centrifugation from post-vaccination heparinized blood samples were tested in lymphoproliferative assay. Cell cultures were prepared in triplicate in microtitre 96-well plates (Falcon). Two hundred thousand patients' PBMC per well were stimulated with tetanus toxoid (1:50 of Lot 48 UBT 1348 kindly provided by Chiron, Siena, Italy). Lymphocytes were incubated for 7 days at 37°C in a complete culture medium consisting of RPMI 1640 with L-glutamine (Sigma, Milan, Italy) supplemented with 10% AB human serum (SIGMA), 50 IU/ml Penicillin and 50 µg/dl of Streptomycin (Sigma, Milan, Italy), then pulsed with 0.5 µCi/well 3H-thymidine for additional 6 h and harvested into glass fiber filters (Packard, Milan, Italy).

Proliferation was measured by 3H-thymidine incorporation and analyzed by B-counter scintillator (Canberra Packard Instrument Company, Meriden, CT, USA). Data were calculated as count per minute (cpm) and expressed as a stimulation index (SI) representing the ratio between the average count of stimulated and unstimulated PBMC; SI = proliferation of PBMC with mitogen or antigen/spontaneous proliferation of PBMC.

For categorical analyses, a SI $\geq$ 3 was considered a positive response for tetanus toxoid and other antigens, as previously reported (15, 16).

IFN-γ and IL-4 quantification

IFN-γ and IL-4 cytokines were quantified in supernatant of stimulated cells and measured by standard sandwich ELISA kits by following the manufacturer's instructions (both PERBIO, ENDOGEN, Woburn, MA, USA). IFN-γ and IL-4 values were expressed referring to a standard curve constructed by assaying serial dilutions of standard cytokine. The assay cut-off level of both cytokines was 2 pg/ml. Antigen-specific cytokine secretion was obtained by subtracting the cytokine content of the supernatants of negative control.

Statistical analysis

The analysis of the relationship between humoral and cellular immunity in both populations was performed by using Student's *t*-test. A p value of less than 0.05 was considered significant.

RESULTS

Humoral and cellular response to tetanus vaccination in healthy subjects

The TT vaccine response was evaluated according to age and the study population of healthy children (HC) was within reason divided into 6 groups (group N: newborns, group 1: 6-12 months, group 2: 12-18 months, group 3: 18-36 months, group 4: 3-6 years, group 5: 6-9 years, group 6: 9-14 years). To represent the time course of the humoral response to TT satisfactorily, 11 healthy newborns (group N), 11 adults younger than 40 years (group A1), and 11 adults older than 40 years of age (group A2) were included.

In this population, the prevalence of the antibody response (³ 0.1 IU/ml) was 88% with the following distribution by age stratum: 100% for group 1 and 2, 88% for group 3, 81% for group 4 and 5, and 94% for group 6. In groups N, A1 and A2, the coverage percentages were 100%, 91% and 91% respectively (Fig. 1A).

As reported in Fig. 1B, the highest levels of TT-specific antibodies were observed in groups 2-3 and 5-6 (group 2: median 1.10 IU/ml, range 0.20-5 IU/

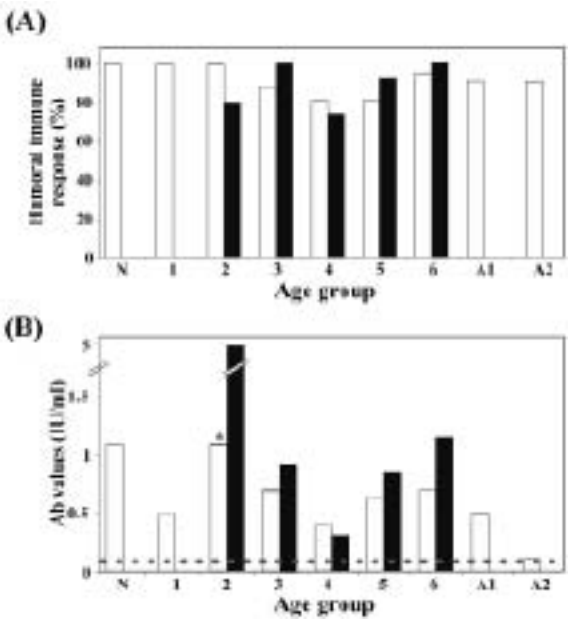

Fig. 1. ***A)*** *Distribution of tetanus antibody response by age in HC (white bars) and RI children (black bars). Each bar indicates the percentage of individuals providing protective antibody values (≥ 0.1 IU/ml) within each age group.* ***B)*** *Stratification of tetanus antibody values (IU/ml) according to age. The bars express the median values and dashed line indicates the serological value of protection (0.1 IU/ml). The significant difference between the two cohorts is expressed by *p=0.02.*

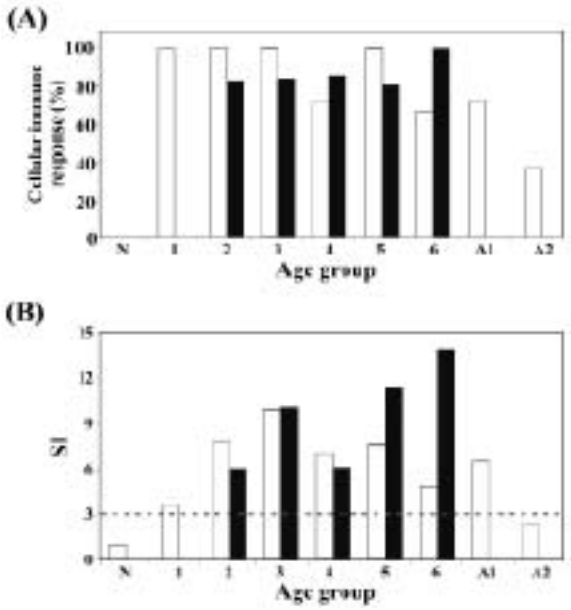

Fig. 2. ***A****) Distribution of cellular immune response to tetanus toxoid vaccine according to age in HC (white bars) and RI children (black bars). Each bar indicates the percentage of individuals with a positive response to tetanus toxoid antigen (SI≥3) within each age group.* ***B****) Stratification of T-cell proliferation in response to tetanus toxoid antigen according to age. The bars express the median values and the dashed line indicates SI=3.*

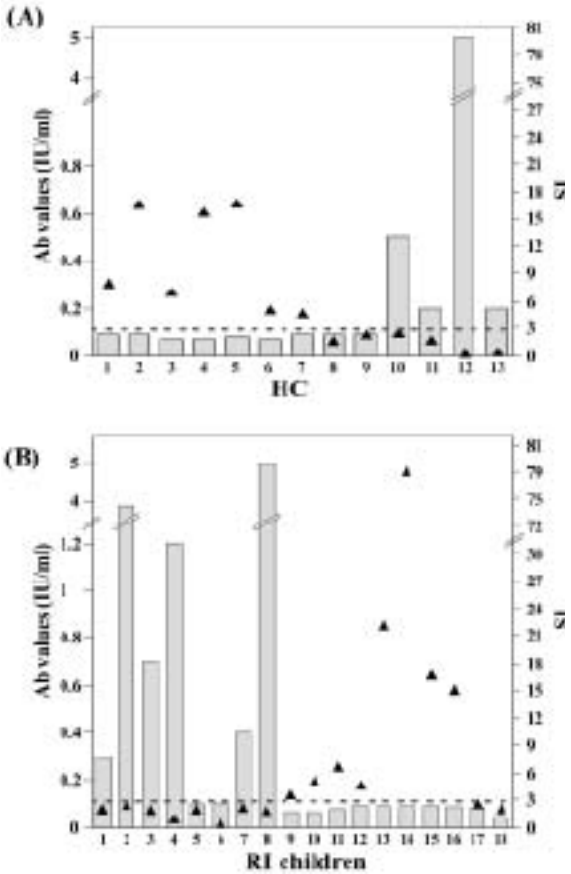

Fig. 3. *Humoral (grey bars) and cellular (black triangles) immune response in (****A****) 13 HC and (****B****) 18 RI children with reduced TT specific antibodies and/or lymphoproliferation. The antibody values and the stimulation index are indicated on the left and right axis, respectively. The dashed line expresses the cut-off values of serological (0.1 IU/ml) and cellular (SI=3) immune response to tetanus toxoid. In each group, two children (pts. 8 and 9 in Fig. 3A; pts. 17 and 18 in Fig. 3B) were unable to produce specific antibodies and to lymphoproliferate to tetanus toxoid.*

ml; group 3: median 0.7 IU/ml, range 0.10-5 IU/ml; group 5: median 0.65 IU/ml, range 0.07-5 IU/ml; group 6: median 0.7 IU/ml, range 0.07- 4.30 IU/ml). No significant differences of the antibody titers were observed between groups 1 and 2, despite the different number of tetanus vaccine doses administered (two versus three respectively); however, as expected, lower levels were found in group 1. Not surprisingly, the lowest values were identified in group 4 (median: 0.40 IU/ml, range 0.07-5 IU/ml), representing the age group before receiving the TT booster. At six years of age, after the booster, titers slightly increased up to 14 years of age, then they tended to decline towards adulthood with borderline protective values only at older ages (group A1: median 0.5 IU/ml, range 0.05-1.7 IU/ml; group A2: median 0.1 IU/ml, range 0.09-0.7 IU/ml). In group N, TT-antibody levels were protective with median values of 1.1 IU/ml.

Cellular responses to TT-antigen were evaluated in 33 subjects randomly selected from 104 HC, 11 newborns and 22 adults. A positive stimulation index (SI) (≥3) was identified in 82% of the children population with values ranging from 67% in group 6 to 100% in groups 1, 2, 3 and 5. As expected, in groups A1 and A2, the rate of response was lower, 73% and 36% respectively, and no response was observed in newborns (Fig. 2A). As reported in Fig. 2B, the course of cellular response showed an

increase of the SI from group 1 to 2-3, followed by a slight decrease in group 4. This value was maintained in group 5, followed by a gradual decrease in group 6. In adulthood, a protective cellular response was lost from group A1 (median SI: 6.5, range 1.45-28.21) to group A2 (median SI: 2.31, range 0.91-4.5).

When cellular and humoral responses to tetanus were simultaneously compared in 33 HC, a good humoral and cellular protection was observed in 20/33 (61%), whereas 13/33 (39%) children, with a variable age-distribution, showed a defect in humoral and/or cellular immunity. In particular, 7/13 (54%) had low antibody titers with a normal SI, 4/13 (31%) had normal antibody values with a low SI and 2/13 (15%) of the children resulted in being unable to produce either specific antibodies or to proliferate to TT (Fig. 3A).

Briefly, specific antibodies in HC are responsible for early protection whereas cell-mediated mechanisms contribute to the maintenance of long-term protection following an appropriate vaccine recall.

Humoral and cellular response to tetanus vaccination in children with recurrent infections

An analysis of antibody responses to tetanus was also performed in 118 children with recurrent infections (RI). Due to the peculiarity of the condition, RI children ranged from 1 to 14 years of age and, accordingly, were divided into 5 age-related groups (group 2 to 6). In this population, the prevalence of antibody responses corresponded to 86%, with values ranging from 74% in group 4 to 100% in groups 3 and 6 (Fig. 1A). As shown in Fig. 1B, antibody titers reached a peak in groups 2 (median: 5 IU/ml, range 0.09-5 IU/ml) and 6 (median: 1.15 IU/ml, range 0.30-3.40 IU/ml). In particular, antibody levels were significantly higher in the group 2 of RI cohort compared to the age-matched HC ($p=0.02$). No differences were observed in the other age groups, although antibody titers of RI patients tended to be higher than in HC (Fig. 1B).

Cellular responses to TT-antigen were evaluated in 66 RI children. Adequate SI values were identified in 85% of them, with values ranging from 80% in group 5 to 100% in group 6 (Fig. 2A). The course of cellular response was similar to that seen in the HC cohort; an increase of the SI from group 2 (SI: 6.1) to group 3 (SI: 9.9), followed by a slight decrease in group 4 while, an increase in groups 5 and 6 was observed (Fig. 2B). Within each age group, no significant difference in SI was observed between RI and HC cohorts.

When cellular and humoral responses to tetanus were compared in 66 RI children, good humoral and cellular protection was observed in 48/66 (73%), conversely 18/66 (27%) of the children showed a defect in humoral and/or cellular immunity. In particular, 8/18 (44%) had low antibody titers with normal SI, 8/18 (44%) had normal antibody values with low SI and, as reported for HC, only 2/18 (12%) of the children resulted in being unable to produce either specific antibodies or to proliferate to TT **(**Fig. 3B**)**.

Cytokine response primed by immunization

TT-stimulated IFN-γ and IL-4 production was investigated in 16 HC and 31 RI children. High *in vitro* IFN-γ values (>2 pg/ml) were found in 62.5% (10/16) HC and in 42% (13/31) RI patients, respectively. Moreover, no significant differences were found in IFN-γ values between HC (median: 160.92 pg/ml, range 97.7-840.4 pg/ml) and the RI population (median: 72.07 pg/ml, range 9.07-1200 pg/ml). When low IFN-γ values (<2 pg/ml) were observed, low antibody titers and/or low SI showed different combinations. Only 2 HC showed a simultaneous defect of IFN-γ, antibody titers and SI. No significant amount of IL-4 cytokine was detected in any of the HC and RI children tested: this was most likely due to lower supernatant concentrations than the Elisa kit sensibility (data not shown).

DISCUSSION

Currently, immunization is the most cost-effective strategy in preventing needless morbidity and mortality. In this context, it would be useful to develop a combined vaccine with the aim of immunizing against several diseases reducing the number of shots required, particularly in high-risk age groups (17, 18). The measurement of serum antibody levels and the evaluation of the lymphoproliferation after stimulus may be considered good practice in monitoring the effectiveness of any vaccination strategy (5).

Nowadays, TT is a prototypical recall antigen

to evaluate both cellular and humoral responses in patients with primary or acquired immunodeficiency and in populations at high-risk of infections in developing countries (19). Indeed, immunological correlates to TT have been analyzed in HIV young patients after HAART treatment and in children infected with *Schistosoma haematobium*, supporting the role of TT response as a marker of immune protection (15, 20). In our study, the humoral and cellular responses to TT after vaccination were investigated in a healthy paediatric cohort and compared to children with recurrent infections to better ascertain the type, grade and timing of protection provided by the vaccine. Therefore, our results need to be extended and further investigated.

In HC the course of humoral response showed a curve reaching a nadir below 6 years of age, followed by an increase up to 14 years of age. With age, the antibody response decreased, in particular among adults over 40 years of age, this in accordance with previous reports, despite the variation in methods used for testing antibody concentrations and booster schedules (21, 22).

Interestingly, the analysis of 11 newborns showed a protective average level of 1.1 IU/ml, most likely due to maternal IgG placental transfer. The presence of protective antibody levels in this group confirmed maternal antibody transfer as an efficient immunological experience passively transmissible in soluble form (23). Indeed, the level of protective antibodies and the passive transfer of immunity to tetanus were shown to be directly dependent on the level of tetanus antitoxin in the maternal serum (24, 25). Recently, it was proposed that minimal maternal antibody level of 0.1 IU/ml ensured protective antibody level in infants (26). Although we were not able to evaluate the correspondent maternal values, we observed protective TT antibody titers in 10 healthy females of childbearing age (age range: 25-40 yrs; median value: 0.45 IU/ml) supporting the idea that the vaccination of women represented an excellent way of exerting a protective effect on the newborn.

The course of humoral response in the RI cohort was similar to the response of the healthy age-matched subjects, showing a trend towards higher concentrations from 6 to 14 years of age, possibly ascribed to concomitant vaccinations containing tetanus toxoid as a protein carrier. Furthermore, significant higher antibody levels were observed in the RI group 2 compared to the same group of HC ($p=0.02$). This may be attributed to a multifactorial pathogenesis at an early age, including genetic and environmental determinants. Moreover, children with RI may be more prone to respond to optional prophylactic vaccines such as *Meningococcal C* conjugate and *Haemophilus Influentiae* vaccines which commonly contain TT as protein carriers (27). Clinical trial data with *Meningococcal C* vaccine in pre-school children (3-4 years) and adolescents (13-17 years) clearly showed that the TT conjugates induced a high response to tetanus (27). Indeed, we had previously observed that children and adults, not revaccinated with TT vaccine, but exposed to TT contained in *Haemophilus Influentiae* vaccines, showed an increase in both tetanus and *Haemophilus Influentiae* antibody titers (personal observation). Since the introduction of these TT conjugates containing vaccines induced a response to tetanus comparable to that induced by the tetanus itself, further monitoring is mandatory for a better evaluation of the immunization policy.

No significant differences according to age were observed in the RI versus HC in the course of cellular responses. When comparing humoral versus cellular responses, the lowest values of antibody titers and SI were observed in group 4, representing the age group prior to receiving the TT booster. The absence of lymphoproliferation in newborns may be due to the lack of previous TT antigen exposure. Indeed, our data confirmed the observation of Zinkernagel et al. that T cells cannot be transmitted from mother to offspring because of mutual immunological rejection (23). A possible explanation for the decreased anti-tetanus cellular immunity in older age groups may be due to the lack of compliance with the immunization schedule, especially with booster doses.

Interestingly, a inverse relationship between humoral and cellular response has been observed in some subjects (16/18 RI children and 11/13 HC) (Fig. 3A, 3B). Although we did not find evidence of correlation to age or to vaccine booster, further investigation of potential contributing factors could be informative.

In line with previous reports (4, 7, 22), our study confirms that 12-15% of children lack an

immunological response to TT, precisely negative TT immune reactions are higher for cellular immune response (15-18%) than antibody response (12-14%); however, the absence of tetanus disease leads us to postulate that genetic, environmental and socio-economic factors might contribute to the various immunization rates reported from different countries (7, 28). Nowadays the incidence of tetanus disease varies throughout the world, but it is still a major cause of mortality in areas of the world with inadequate hygiene and immunization programs (29). Furthermore, although neonatal tetanus is rare in industrialized countries, it still causes an estimated 200,000-500,000 deaths annually in developing countries (30), supporting once again the importance of vaccination campaigns with special focus on women during childbearing age. Moreover, further studies are needed to investigate the inter and intrapopulation variability in response to a specific vaccine.

Cellular response to vaccination or infection is characterized by the cytokine production of activated peripheral blood lymphocytes or monocytes (31, 32). Although cytokine production has frequently been evaluated in neonates and children with various diseases (33, 34), surprisingly few comparative studies of cytokine production in healthy children and adults have been conducted (35). In our study we analyzed cytokine production in order to evaluate the lymphocyte subsets involved in the response to TT stimulus. Even though obtained from a limited cohort of healthy and RI children, the observation of the IFN-γ production confirms a significant Th1 involvement in the TT immune response (36).

To summarize, our results indicate that T-cell responses may contribute to the generation of long-term immunity upon appropriate vaccine recall. The prevalence and intensity of immune response to tetanus vary according to age and, in our healthy cohort, the National Immunization Program is appropriate. However, more extensive investigations are required in RI children, confirming an optimal effective vaccine formulation, dose requirements and schedules. Moreover, the identification of partial or no-responders may lead to improved vaccination strategies and to the characterization of those mechanisms by which the immune system induces a diverse qualitative and quantitative protective response. The goal is fitting each category of patients to the most appropriate vaccine in the very near future.

ACKNOWLEDGEMENTS

The authors would like to thank Dr. P. Ciaffi, G. Bonelli, our Head Nurse R. Reggi and her staff at the Department of Pediatrics, University of Rome Tor Vergata, for their clinical and technical support. Moreover, a special thanks to Dr. R. Addario, Dr. F. Melia and Dr. S. Linton who revised the English version of the manuscript.

This study was supported by the Master in Advanced Pediatric Allergy and Immunology of the University of Rome, Tor Vergata.

REFERENCES

1. Wassilak SGF, Roper MH, Murphy TV, Orenstein WA. Tetanus toxoid. In: Plotkin SA, Orenstein WA, eds. Vaccines. Saunders 2004; 745-81.
2. Dietz V, Galazka A, van Loon F, Cochi S. Factors affecting the immunogenicity and potency of tetanus toxoid: implications for the elimination of neonatal and non-neonatal tetanus as public health problems. Bull World Health Organ 1997; 75:81-93.
3. Gindi M, Oravitz P, Sexton R, Shpak M, Eisenhart A. Unreliability of reported tetanus vaccination histories. Am J Emerg Med 2005; 23:120-2.
4. Schatz D, Ellis T, Ottendorfer E, Jodoin E, Barrett D, Atkinson M. Aging and the immune response to tetanus toxoid: diminished frequency and level of cellular immune reactivity to antigenic stimulation. Clin Diagn Lab Immunol 1998; 5:894-6.
5. Galazka AM. The immunological basis for immunization series. Module 3: tetanus. Document no. WHO/EPI/GEN/93.13. World Health Organization, Geneva.
6. Crone NE, Reder AT. Severe tetanus in immunized patients with high antitetanus titres. Neurology 1992; 42:761-4.
7. Gergen PJ, McQuillan GM, Kiely M, Ezzati-Rice TM, Setter RW, Virella G. A population-based serologic survey of immunity to tetanus in the United States. N Engl J Med 1995; 332:761-6.

8. McQuillan GM, Kruszon-Moran DM, Deforest A, Chu SY, Wharton M. Serologic immunity to diphtheria and tetanus in the United States. Ann Intern Med 2002; 136:660-6.
9. Brabin L, Fazio-Tirrozzo G, Shahid S, et al. Tetanus antibody levels among adolescent girls in developing countries. Trans R Soc Trop Med Hyg 2000; 94:455-9.
10. Gruber C, Keil T, Kulig M, et al. History of respiratory infections in the first 12 yr among children from a birth cohort. Pediatr Allergy Immunol 2008; 19:505-12.
11. Griffin MR, Walker FJ, Iwane MK, Weinberg GA, Staat MA, Erdman DD. New Vaccine Surveillance Network Study Group. Epidemiology of respiratory infections in young children: insights from the new vaccine surveillance network. Pediatr Infect Dis J 2004; 23(S):188-92.
12. Galli L, De Martino M, Muccioli AT. Biological response modifiers in children with recurrent respiratory infections. J Chemother 1991; 3:196-202.
13. De Martino M, Rossi ME, Muccioli AT, Vierucci A. T lymphocytes in children with recurrent respiratory infections: effect of the use of thymostimulin on the alterations of T-cell subsets. Int J Tissue React 1984; 6:223-8.
14. De Martino M, Galli L, Vierucci A. The child with recurrent respiratory infections. In Aiuti F. eds. Pathogenesis and control of viral infections. New York Raven Press 1989; 225-31.
15. Ching N, Deville JG, Nielsen KA, et al. Cellular and humoral immune responses to a tetanus toxoid booster in perinatally HIV-1-infected children and adolescents receiving highly active antiretroviral therapy (HAART). Eur J Pediatr 2007; 166:51-6.
16. Palma P, Romiti ML, Cancrini C, et al. Delayed early antiretroviral treatment is associated with an HIV-specific long-term cellular response in HIV-1 vertically infected infants. Vaccine 2008; 26(40):5196-201.
17. André FE. Vaccinology: past achievements, present roadblocks and future promises. Vaccine 2003; 21:593-95.
18. Siegrist CA, Aspinal R. B-cell responses to vaccination at the extremes of age. Nat Rev Immunol 2009; 9:185-94.
19. Nookala S, Srinivasan S, Kaliraj P, Narayanan RB, Nutman TB. Impairment of tetanus-specific cellular and humoral responses following tetanus vaccination in human lymphatic filariasis. Infect Immun 2004;72(5):2598-604.
20. van Riet E, Retra K, Adegnika AA, Jol-van der Zijde CM, Uh HW, Lell B et al. Cellular and humoral responses to tetanus vaccination in Gabonese children. Vaccine 2008; 26:3690-5.
21. Caglar K, Karakus R, Aybay C. Determination of tetanus antibodies by a double-antigen enzyme-linked immunosorbent assay in individuals of various age groups. Eur J Clin Microbiol Infect Dis 2005; 24:523-8.
22. Maple PA, Jones CS, Wall EC, et al. Immunity to diphtheria and tetanus in England and Wales. Vaccine 2001; 19:167-73.
23. Zinkernagel RM. On natural and artificial vaccinations. Annu Rev Immunol 2003; 21:515-46.
24. Einhorn MS, Granoff DM, Nahm MH, Quinn A, Shackelford PG. Concentrations of antibodies in paired maternal and infant sera: relationship to IgG subclass. J Pediatr 1987; 111:783-8.
25. Sangpetchsong V, Vichaikummart S, Vichitnant A, Podhipak A. Transfer rate of transplacental immunity to tetanus from non-immunized and immunized mothers. Southeast Asian J Trop Med Public Health 1984; 15:275-80.
26. Maral I, Cirak M, Aksakal FN, Baykan Z, Kayikcioglu F, Bumin MA. Tetanus immunization in pregnant women. Serum levels of antitetanus antibodies at time of delivery. Eur J Epidemiol 2001; 17:661-5.
27. Richmond P, Goldblatt D, Fusco PC, et al. Safety and immunogenicity of a new Neisseria meningitides serogroup C-tetanus toxoid conjugate vaccine in healthy adults. Vaccine 2000; 18: 641-6.
28. Van Loveren H, Van Amsterdam JGC, Vandebriel RJ, et al. Vaccine-induced antibody responses as parameters of the influence of endogenous and environmental factors. Environ Health Perspect 2001; 109:757-64.
29. Brook I. Current concepts in the management of Clostridium tetani infection. Expert Rev Anti Infect Ther 2008; 6:327-36.
30. Vandelaer J, Birmingham M, Gasse F, Kurian M, Shaw C, Garnier S. Tetanus in developing countries: an update on the Maternal and Neonatal Tetanus

Elimination Initiative. Vaccine 2003; 21:3442-5.
31. Sander B, Skansén-Saphir U, Damm O, Håkansson L, Andersson J, Andersson U. Sequential production of Th1 and Th2 cytokines in response to live bacillus Calmette-Guérin. Immunology 1995; 86:512-8.
32. Ward BJ, Griffin DE. Changes in cytokine production after measles virus vaccination: predominant production of IL-4 suggests induction of a Th2 response. Clin Immunol Immunopathol 1993; 67:171-7.
33. Neuhaus TJ, Wadhwa M, Callard R, Barratt TM. Increased IL-2, IL-4 and interferon-gamma (IFN-gamma) in steroid-sensitive nephrotic syndrome. Clin Exp Immunol 1995; 100:475-9.
34. Lilic D, Cant AJ, Abinun M, Calvert JE, Spickett GP. Chronic mucocutaneous candidiasis. I. Altered antigen-stimulated IL-2, IL-4, IL-6 and interferon-gamma (IFN-gamma) production. Clin Exp Immunol 1996; 105:205-12.
35. Lilic D, Cant AJ, Abinun M, Calvert JE, Spickett GP. Cytokine production differs in children and adults. Pediatr Res 1997; 42:237-40.
36. Rowe J, Macaubas C, Monger TM, Holt BJ, Harvey J, et al. Antigen-specific responses to diphtheria-tetanus-acellular pertussis vaccine in human infants are initially Th2 Polarized. Infect Immun 2000; 68:3873-7.

CURCUMIN INDUCES APOPTOSIS IN BREAST CANCER CELL LINES AND DELAYS THE GROWTH OF MAMMARY TUMORS IN NEU TRANSGENIC MICE

L. MASUELLI[1], M. BENVENUTO[2], M. FANTINI[2], L. MARZOCCHELLA[2], P. SACCHETTI[1], E. DI STEFANO[1], I. TRESOLDI[2], V. IZZI[2], R. BERNARDINI[3], C. PALUMBO[2], M. MATTEI[3], F. LISTA[4], F. GALVANO[5], A. MODESTI[2] and R. BEI[2]

[1]Department of Experimental Medicine, University of Rome "Sapienza", Rome, Italy; [2]Department of Clinical Sciences and Translational Medicine, University of Rome "Tor Vergata", Rome, Italy; [3]STA, University of Rome "Tor Vergata", Rome, Italy; [4]Histology and Molecular Biology Section, Army Medical and Veterinary Research Center, Rome, Italy; [5]Department of Drug Sciences, Section of Biochemistry, University of Catania, Catania, Italy

Received December 4, 2012 – Accepted February 11, 2013

Breast cancer is a leading cancer in women and despite the benefits of the current therapies a significant number of patients with this tumor is at risk of relapse. Some of the alterations taking place in breast cancer cells are currently exploited by molecularly targeted drugs. Different drugs have been developed which target a single molecule but, given that the tumor originates from the dysregulation of many genes, there is the need to find new drugs that have more than one molecular target. Curcumin [1,7-bis-(4-hydroxy-3-methoxyphenyl)-1,6-heptadiene-3,5-dione] (CUR), a polyphenolic compound found in the spice turmeric, is a pleiotropic molecule able to interact with a variety of molecular targets and has antitumor, anti-inflammatory, antioxidant, immunomodulatory and antimicrobial activities. Here we demonstrate that CUR inhibits the growth of breast cancer cell lines in a dose dependent manner, with IC50 values in the micromolar range, and induces an increase in the percentage of cells in sub-G0 phase, representing the apoptotic cell population. The activation of apoptosis was confirmed by PARP-1 cleavage and by the increased ratio between the pro-apoptotic Bax and the anti-apoptotic Bcl-2 protein. In addition, in CUR-treated cells the activity of ERK1/ERK2 MAP kinases was down-regulated. The cytotoxic effects of CUR were observed in breast cancer cells expressing either high or low levels of ErbB2/neu. The *in vivo* antitumor activity of CUR was tested in BALB-*neu*T mice transgenic for the neu oncogene, which develop atypical hyperplasia of the mammary gland at 6 weeks of age and invasive carcinoma at 16 weeks of age. CUR, administered to mice both early and in an advanced stage of mammary carcinogenesis, induced a significant prolongation of tumor-free survival and a reduction of tumor multiplicity. In addition, CUR administration was safe, since no modification of hematological and clinical chemistry parameters could be observed in BALB-*neu*T and BALB/c mice treated with this compound for several weeks. These findings support further studies on the therapeutic potential of CUR in combination with standard therapies in breast cancer patients.

Breast cancer is a leading cancer in women with more than 1 million new cases each year (1).

Key words: curcumin, breast cancer, polyphenol, apoptosis, neu transgenic mice

Mailing address: Prof. Roberto Bei,
Department of Clinical Sciences and Translational Medicine,
Faculty of Medicine, University of Rome "Tor Vergata",
Via Montpellier 1, 00133 Rome,
Tel.: + 39 06-72596522
Fax: + 39 06-72596506
e-mail: bei@med.uniroma2.it

0393-974X (2013)

Different subtypes of breast cancers that show different survival outcomes for patients have been identified (1). All this and the severe risk of disease recurrence have led to the development of targeted therapies with clinically proven efficacy (2, 3). Major target proteins in breast cancer are ErbB receptors (EGFR and ErbB2) and Vascular Endothelial Growth Factor (VEGF). Different drugs have been developed to target these molecules, but there is the need to find new drugs that have more than one molecular target, given that the tumor originates from the dysregulation of many genes (2, 4). In fact, a significant proportion of patients with breast cancer has recurrent disease, clearly demonstrating the need to study the specific subtypes of disease in order to improve the existing therapeutic results and solve the problem of therapeutic resistance (1, 3).

Flavonoids are a large group of polyphenolic compounds, which are ubiquitously expressed in plants. In the last years, epidemiological studies have shown the association between the consumption of a diet rich in polyphenols and the prevention of human diseases, including cancer (5-8). Accordingly, an increased interest in studying the effects of these compounds as protective agents for human health has emerged (5, 6, 8). Curcumin [1,7-bis-(4-hydroxy-3-methoxyphenyl)-1,6-heptadiene-3,5-dione] (CUR), a polyphenol compound found in the spice turmeric, a product of the plant *Curcuma longa,* has been widely employed for centuries in Asia as a food additive as well as in cosmetic and herbal medicine. CUR is a pleiotropic molecule able to interact with a variety of molecular targets and signal transduction pathways, and has been revealed to have antitumor, anti-inflammatory, antioxidant, immunomodulatory and antimicrobial activities both in rodents and humans (8). Due to its ability to modulate the activity of multiple targets involved in carcinogenesis through direct interaction or modulation of gene expression, CUR is considered a "dirty drug" (8). The multiple targets modulated by CUR comprise transcription factors, genes involved in apoptosis and cell proliferation, growth factors and their receptors, cytokines and enzymes (8). In particular, the antitumor effect of CUR has been attributed to the inhibition of cell proliferation and to the induction of apoptosis in several tumor models both *in vitro* and *in vivo* (8).

The aim of this study was to evaluate the *in vitro* effect of CUR on cell proliferation, apoptosis, cell cycle regulation and MAP kinase (Mitogen Activated Protein kinase) activation in human (MDA-MB-231, MDA-MB-435, MDA-MB-453, MDA-MB-468, T-47D, MCF7, BT-474, SK-BR-3) and mouse (TUBO) breast cancer cell lines, and in mouse fibroblasts (NIH3T3) stably transfected with the sequence coding for human ErbB2 (LTR-ErbB2) or for rat ErbB2/neu (LTR-NeuN). In addition, the effect of CUR on the growth of breast tumors arising in BALB-*neu*T mice, which are transgenic for the neu oncogene (9), was evaluated for the first time. Finally, to determine whether CUR had side effects, hematological and clinical chemistry parameters were measured in mice before and after several weeks of CUR administration. Our results support both the *in vitro* and *in vivo* antitumor effect of CUR, coupled to the absence of side effects.

MATERIALS AND METHODS

Reagents

DMSO, curcumin from *Curcuma Longa* (CUR) and sulforhodamine B (SRB) were purchased from Sigma Aldrich (Milano, Italy). Rabbit polyclonal anti-Bax and mouse monoclonal anti-Bcl-2 antibodies were obtained from BD Pharmingen (BD Biosciences). Antibodies against ERK1/2 (C-14), phospho-ERK (E-4) and PARP-1 (F-2) were obtained from Santa Cruz Biotechnology (CA, USA). Anti-ErbB2 antiserum was provided by Dr. M.H. Kraus (University of Alabama, Birmingham, USA) (10). Rabbit polyclonal antibody against actin and peroxidase-conjugated goat anti-mouse or -rabbit IgG were from Sigma Aldrich.

Cell lines and treatments

BALB-*neu*T mammary cancer cells (H-2^d) (TUBO) overexpressing activated rat ErbB2/neu were kindly provided by Prof. G. Forni (University of Turin, Italy) (9). Mouse fibroblasts (NIH3T3) overexpressing human ErbB2 (LTR-ErbB2) or normal rat ErbB2/neu (LTR-NeuN) were previously described (11) and provided by Dr. M.H. Kraus (University of Alabama, Birmingham, USA) and Dr. E. Di Marco (Istituto Tumori di Genova, Italy). Human (MDA-MB-231, MDA-MB-435, MDA-MB-453, MDA-MB-468, T-47D, MCF7, BT-474, SK-BR-3) and mouse (TUBO) breast cancer cell lines, and mouse fibroblasts (NIH3T3, LTR-ErbB2, LTR-NeuN) were maintained in RPMI containing 10% fetal bovine serum, 100 U/ml penicillin and 100 μg/ml streptomycin

(complete medium). Cells were grown at 37°C in a humidified incubator with 5% CO_2.

CUR was dissolved in DMSO. For treatments, cells were incubated for the indicated times in the presence of CUR (dose range 6-50 μM) or vehicle control (DMSO ≤ 0.1%).

Sulforhodamine B (SRB) assay

Cells were seeded at 4 x 10^3/well in 96-well plates and incubated at 37°C to allow cell attachment. After 24 h, the medium was changed and the cells were treated with CUR or DMSO and incubated for 24 or 48 h. Cells were then fixed with cold trichloroacetic acid (final concentration 10%) for 1 h at 4°C. After 4 washes with distilled water, the plates were air-dried and stained for 30 min with 0.4% (wt/vol) SRB in 1% acetic acid. After 4 washes with 1% acetic acid to remove the unbound dye, the plates were air-dried and cell-bound SRB was dissolved with 200 μl/well of 10 mM unbuffered Tris base solution. The optical density (O.D.) of the samples was determined at 540 nm using a spectrophotometric plate reader. The percentage survival of the cultures treated with CUR was calculated by normalization of their O.D. values to those of control cultures treated with DMSO (12). The experiments were performed in triplicate and repeated three times. The concentrations of CUR required to reduce cell survival by 50% (IC50) were calculated from dose response data using GraphPad Prism software.

FACS analysis

Asynchronized, log-phase growing cells (60% confluent, about 2.5 x 10^5/well in 6-well plates) were treated with CUR or DMSO in complete culture medium. After 48 h, adherent as well as suspended cells were harvested, centrifuged at 1500 rpm for 10 min and washed twice with cold phosphate buffered saline (PBS). Cell pellets were resuspended in 70% ethanol and incubated for 1 h at -20°C. Cells were then washed twice with cold PBS, centrifuged at 1500 rpm for 10 min, incubated for 1 h in the dark with propidium iodide (25 μg/ml final concentration in 0.1% citrate and 0.1% Triton X-100) and analyzed by flow cytometry using a FACSCalibur flow cytometer through CellQuest software (12).

Preparation of cell lysates and western blotting

About 1 x 10^6 cells were seeded in 100 mm tissue culture dishes 24 h prior to the addition of 25 μM of CUR or vehicle control. After a 48 h incubation, the cells were harvested, washed twice with cold PBS and lysed in RIPA lysis buffer (Triton X-100 1%, SDS 0.1%, NaCl 200 mM, Tris HCl 50 mM pH 7.5, PMSF 1 mM, NaOV 1 mM). After 30 min at 4°C, the mixtures were centrifuged at 12,000 g for 15 min and the supernatants were analyzed by Western blotting (13). For immunoblot analysis, 50 μg of cell lysates were resolved in 10% SDS-PAGE and then transferred to nitrocellulose membranes (14). After blocking, the membranes were incubated with specific primary antibodies at the concentration of 1-2 μg/ml overnight at 4°C. After washing, the filters were incubated with goat anti-mouse or -rabbit IgG, peroxidase-conjugated antibodies and developed by chemiluminescence as previously described (15-16). Densitometric analysis of autoradiographic bands was performed using the Image J software (National Institutes of Health, USA) after blot scanning (17).

Transgenic BALB-neuT mouse colony

Transgenic BALB-*neu*T male mice were routinely mated with BALB/c females (H-2^d; Charles River, Calco, Italy) in the animal facilities of Tor Vergata University (18). Founder male BALB-*neu*T mice were kindly provided by Prof. G. Forni (University of Turin, Italy) (9). Progenies were confirmed for presence of the transgene by PCR (9). Individually tagged virgin females were used in this study. Mice were bred under pathogen-free conditions and handled in compliance with European Union and institutional standards for animal research.

CUR treatment of BALB-neuT mice

Groups of female BALB-*neu*T mice (5 mice per group) were treated per os with CUR (2 mg in 50 μl of corn oil), corn oil (50 μl) or water (50 μl) for 3 times a week. Mice were treated starting at the age at which they displayed atypical breast hyperplasia (6 weeks) or invasive breast carcinoma (16 weeks) and until the 30th week. Mice were sacrificed at the first signs of distress. All experiments were approved by the Institutional Animal Care and Use Committee (IACUC) and carried out according to the Italian rules (D.L.vo 116/92; C.E. 609/86). A veterinary surgeon was present during the experiments. Animal care, before and after the experiments, was carried out only by trained personnel.

Analysis of CUR antitumor activity in vivo

Mammary glands were checked weekly and tumors recorded at 3 mm in diameter. Tumor growth was monitored until all mammary glands displayed a palpable tumor or tumor mass exceeding 15 mm in diameter (18). At this point mice were killed. The time of tumor appearance was recorded and tumor multiplicity for each treatment group was expressed as mean ± standard deviation (SD) (18).

Measurement of hematological and clinical chemistry parameters

All blood samples were collected in animals under

i.p. anesthesia (20 µl/g.b.w. of 1.2% Avertin-2,2,2-tribromoethanol, 2.4% 2-methyl-2-butanol; Sigma-Aldrich). For determination of hematological parameters, 20 µl of whole blood, collected in K2EDTA microtainers (Becton, Dickinson and Company, USA), where analyzed using the commercially available automated cell counter "Simply cell" (BPC BioSed s.r.l., Italy). For cytomorphological examination, each sample from peripheral blood smears was prepared using the differential staining Diff-Quick (Dade SpA, Italy) and analyzed under optical microscopy. For determination of clinical chemistry parameters, blood samples were collected in SST microtainers (Serum Separator Tube; Becton, Dickinson and Company) and centrifuged in a microcentrifuge (5415R model; Eppendorf s.r.l., Italy) at 13,000 rpm for 7 min to separate the serum. Cholesterol (CHOL), triglycerides (TRI), glutamic oxaloacetic transaminase (GOT), glutamic pyruvic transaminase (GPT), blood urea nitrogen (BUN) and lactate dehydrogenase (LDH) were measured using the automatic analyzer Keylab (BPC BioSed s.r.l., Rome, Italy).

Statistical analysis

Data distribution of cell survival and FACS analyses were preliminarily verified by the Kolmogorov-Smirnov test, and data sets were analyzed by one-way analysis of variance (ANOVA) followed by Newman-Keuls test. Survival curves and tumor multiplicity were estimated using the Kaplan–Meier method and compared by the log-rank test with calculation of the SD according to the method of Greenwood. Differences were regarded as significant when p value was ≤ 0.05.

RESULTS

Inhibition of breast cancer cells survival by CUR

Survival of human (MDA-MB-231, MDA-MB-435, MDA-MB-453, MDA-MB-468, T-47D, MCF7, BT-474, SK-BR-3) and mouse (TUBO) breast cancer cells was quantified after exposure to increasing doses of CUR (6 to 50 µM) or vehicle control (DMSO) for 24 and 48 h. CUR induced a dose-dependent decrease of cell survival in all cell lines (Table I). The concentration of CUR required to reduce cell survival by 50% (IC50) after 48 h of treatment ranged between about 10 and 20 µM for 7 out of 9 cell lines, the remaining 2 cell lines having an IC50 of about 40 µM (MDA-MB-453) and >50 µM (BT-474) (Table II).

Induction of breast cancer cells apoptosis by CUR

In order to evaluate the effect of CUR on apoptosis and cell cycle distribution, FACS analysis of DNA content was performed on breast cancer cells treated for 48 h with increasing doses of CUR or with DMSO vehicle. The mean results of three independent experiments are reported in Fig. 1. All cell lines, including the mouse cell line TUBO bearing activated ErbB2/neu, were susceptible to the

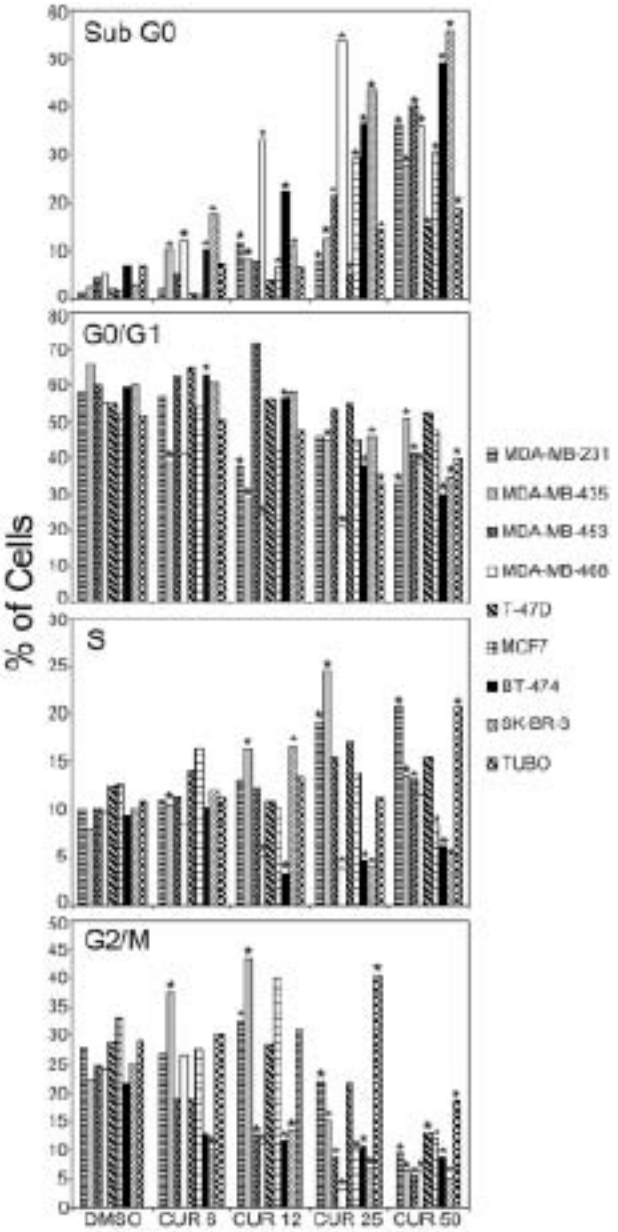

Fig. 1. *Effects of CUR on apoptosis and cell cycle distribution of breast cancer cells. FACS analysis of DNA content was performed on breast cancer cells treated for 48 h with CUR or DMSO in complete culture medium. *p≤0.05 vs DMSO-treated cells.*

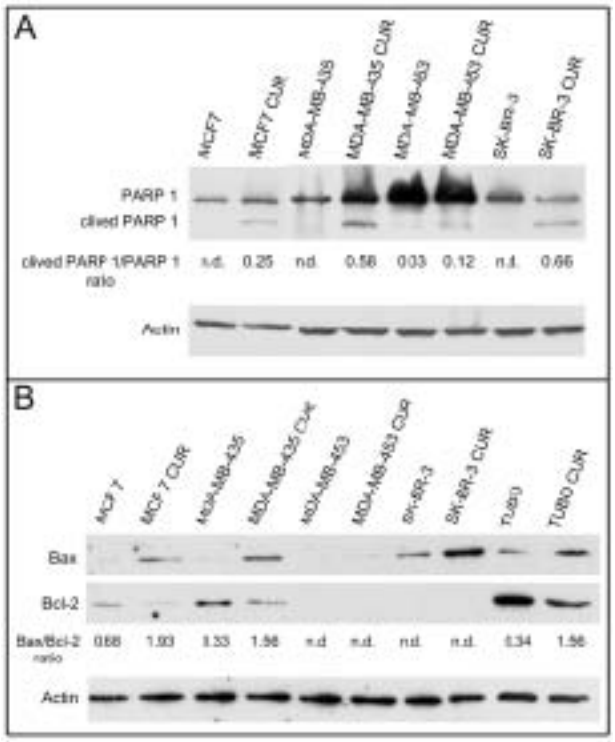

Fig. 2. *Cleavage of PARP-1 and Bax/bcl-2 expression ratio in CUR-treated breast cancer cell lines. Western blotting was performed on cells treated with CUR 25 μM or DMSO vehicle for 48 h. Panel **A**: PARP-1 cleavage. Panel **B**: Bax/Bcl-2 expression ratio. n.d: not determined.*

pro-apoptotic effect of CUR, as demonstrated by the increase in the percentage of cells at sub-G0, which are cells with a hypodiploid DNA content typical of apoptosis. Pooling the data from all 9 cell lines, the percentage of cells in sub-G0 ranged from 1.6 to 7.0% in cultures treated with DMSO, from 3.9 to 33.3% in cultures treated with CUR 12 μM and from 15.0 to 55.8% in cultures treated with CUR 50 μM.

Depending on the cell line, the increase of the sub-G0 fraction was associated with a decrease of the percentage of cells in G0/G1 and/or G2/M, and with either an increase or a decrease of the percentage of cells in the S phase. Thus, while CUR induced apoptosis in all cell lines investigated, its effects on cell cycle distribution appeared more cell context-dependent.

To corroborate that the effect of CUR on the increase of cells in sub-G0 was due to the induction of apoptosis, the cleavage of poly (ADP-ribose) polymerase-1 (PARP-1) as well as Bax/Bcl-2 expression ratio were analyzed by Western blotting in sub-panels of breast cancer cell lines treated with 25 μM CUR or with DMSO for 48 h. During the apoptotic process PARP-1, an enzyme involved in the control of DNA repair, as well as cell cycle progression and cell death, is cleaved by caspases. Such cleavage was detected by Western blotting using a specific antibody that recognizes both the full-length and the C-terminal cleavage product of PARP-1. As shown in Fig. 2, Panel A, treatment with CUR induced the cleavage of PARP-1 in all four breast cancer cell lines analyzed. Interestingly, an increase in the amount of uncleaved PARP-1 was observed in two (MCF7 and MDA-MB-435) of the four cell lines treated with CUR. Of note, PARP-1 has been reported to be up-regulated in association with increased cell death in various conditions (19). As for the apoptosis regulatory proteins Bax and Bcl-2, the amount of the pro-apoptotic Bax was increased by CUR in all five breast cancer cell lines investigated (Fig. 2, Panel B). Conversely, the anti-apoptotic Bcl-2, which was not detected in MDA-MB-453 and SK-BR-3 cells, was reduced by CUR in all other three cell lines, i.e. MCF7, MDA-MB-435 and TUBO (Fig. 2, Panel B).

Inhibition of the MAP kinase ERK1/ERK2 signal transduction pathway by CUR

One of the main signal transduction pathways aberrantly activated in cancer cells is that of the MAP kinases (Mitogen Activated Protein kinases) ERK1 and ERK2. In order to verify whether CUR was able to interfere with the activation of this signaling pathway, the amounts of phosphorylated ERK1 and ERK2 proteins were compared with those of total ERK proteins in lysates from breast cancer cells treated with 25 μM CUR or with DMSO for 48 h. As shown in Fig. 3, CUR inhibited the activation of ERK1/ERK2 in MCF7 cells, and completely abolished it in MDA-MB-453 and SK-BR-3 cells. ERK1/ERK2 phosphorylation was also moderately reduced by CUR treatment in TUBO cells. By contrast, in MDA-MB-435 cells CUR was found to activate both these MAP kinases.

Expression of ErbB2/neu in breast cancer cell lines

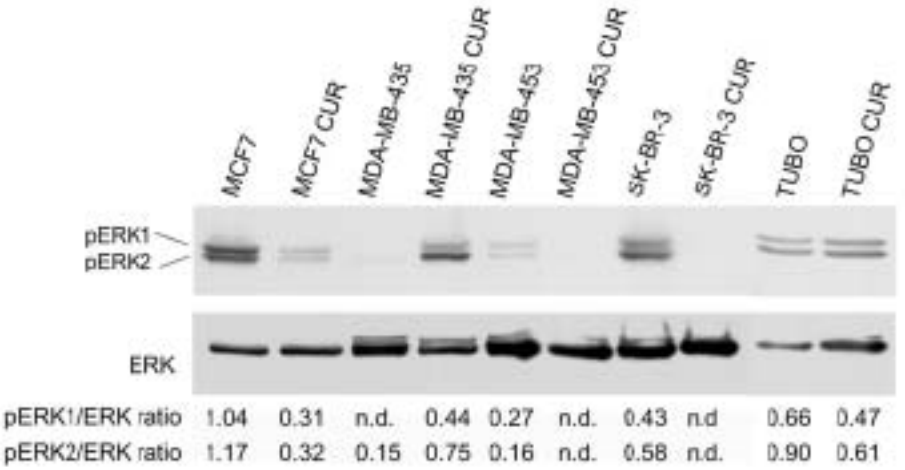

Fig. 3. *ERK1/ERK2 phosphorylation status in CUR-treated breast cancer cell lines. Western blotting was performed on cells treated with CUR 25 μM or DMSO vehicle for 48 h. The levels of phosphorylated ERK1/ERK2 were compared with those of total ERK proteins. n.d=not determined*

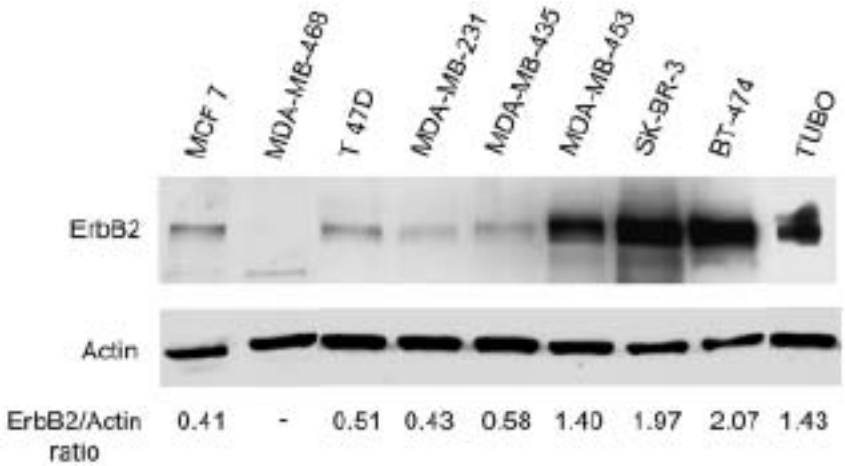

Fig. 4. *Expression of ErbB2/neu in breast cancer cell lines. Western blotting analysis. 50 μg of cell lysates were resolved in 10% SDS-PAGE and then transferred to nitrocellulose membranes After blocking, the membranes were incubated with specific anti-ErbB2 antibody overnight at 4°C. Densitometric analysis of autoradiographic bands was performed using the Image J software. Numbers represent ErbB2/actin expression ratio by Western blotting.*

susceptible to the cytotoxic effect of CUR and cell survival inhibition in ErbB2/neu-overexpressing fibroblasts

ErbB2/neu overexpression found in 15-25% of breast cancers, is associated with an aggressive phenotype and can confer apoptosis resistance to tumor cells (1). Accordingly, we wanted to investigate ErbB2/neu protein levels in human and mouse breast cancer cell lines sensitive to the cytotoxic effect of CUR. ErbB2/neu was expressed heterogeneously in the different cell lines: it was not detectable in MDA-MB-468 cells, weakly expressed in MCF7, T-47D, MDA-MB-231 and MDA-MB-435 cells and expressed at high levels in MDA-MB-453, SK-BR-3, BT-474 and TUBO cells (Fig. 4) These results, coupled with those of cell survival studies (Table I) and FACS analysis (Fig. 1), demonstrate that CUR was able to inhibit cell survival and induce apoptosis

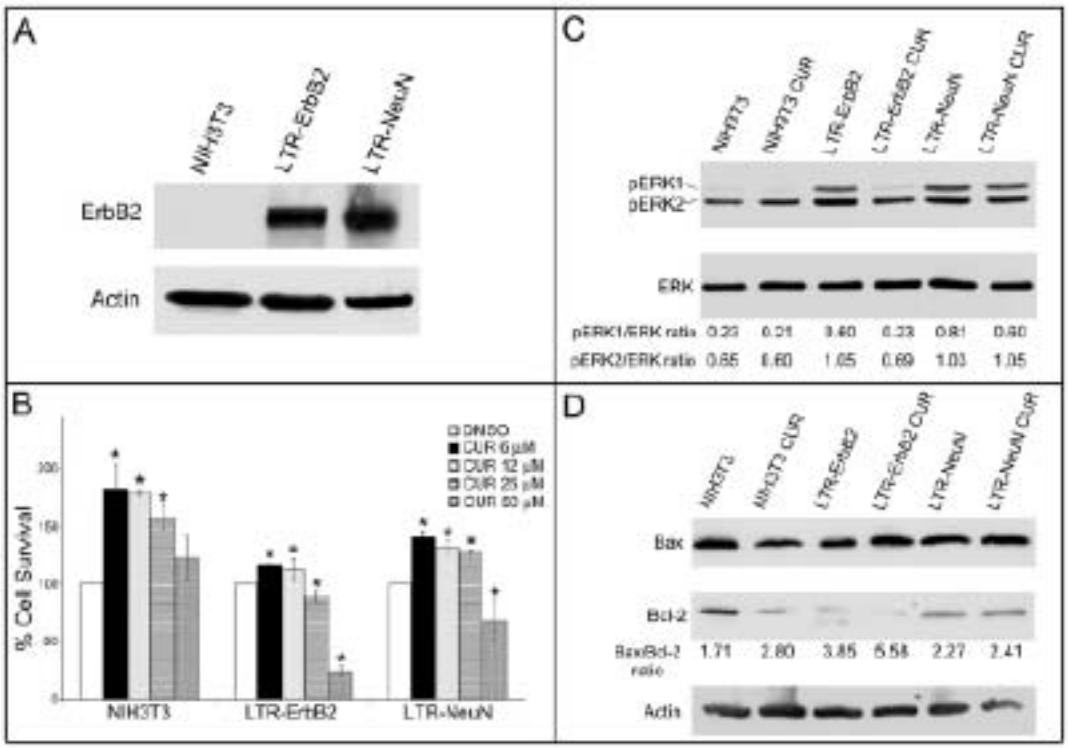

Fig. 5. *Effects of CUR on NIH3T3 mouse fibroblasts and on NIH3T3 cells overexpressing human ErbB2 (LTR-ErbB2) o rat ErbB2/neu (LTR-neuN). Panel **A**: Expression of ErbB2/neu in NIH3T3, LTR-ErbB2 and LTR-neuN by Western blotting. Panel **B**: Effect of CUR on cell survival (*p≤0.05 vs. DMSO-treated cells). Panel **C**: ERK1/ERK2 phosphorylation in cells treated with 25 µM CUR or DMSO for 48 h. Panel **D**: Bax/Bcl-2 expression ratio by Western blotting in cells treated with 25 µM CUR or DMSO for 48 h.*

in breast cancer cells expressing either high or low levels of ErbB2/neu.

Furthermore, the effects of CUR on survival of transformed mouse fibroblasts overexpressing human ErbB2 (LTR-ErbB2) or rat ErbB2/neu (LTR-NeuN) were investigated and compared to those induced by the compound on wild type, non-transformed NIH3T3 fibroblasts (Fig. 5, Panel A). In normal NIH3T3, treatment with CUR 6-50 µM for 48 h did not reduce, but instead increased cell survival, in particular at the lower concentrations (Fig. 5, panel B). In contrast, survival of LTR-ErbB2 and LTR-NeuN cells was reduced by the highest CUR concentration (Fig. 5, panel B). On the other hand, the sensitivity of the transfected cells to CUR was quite different, since 50 µM CUR inhibited the growth of LTR-ErbB2 cells more strongly than that of LTR-NeuN cells (by about 75 and 30%, respectively; p≤0.001). Moreover, at 25 µM CUR was effective in reducing cell survival in LTR-ErbB2 cells only, whereas in LTR-NeuN the lower CUR concentrations increased cell survival similarly to wild type NIH3T3 (Fig. 5, panel B).

As for the effects on CUR on the MAP kinase pathway, inhibition of ERK1/ERK2 was observed in CUR-treated LTR-ErbB2 and a modest inhibition of ERK1 was detected in CUR-treated LTR-NeuN cells. CUR did not affect ERK1/ERK2 phosphorylation in NIH3T3 (Fig. 5, Panel C). Finally, CUR treatment increased the ratio between Bax and Bcl-2 in NIH3T3 and LTR-ErbB2 but not in LTR-NeuN cells (Fig. 5, Panel D).

In summary, in breast cancer cells the effects of CUR were not associated with ErbB2 expression levels. In non-transformed NIH3T3 fibroblasts CUR did not reduce cell survival and activity of MAP kinases. On the other hand, following ErbB2/neu overexpression and cell transformation, NIH3T3 fibroblasts became sensitive, albeit with a different profile, to CUR inhibitory effects in terms of both cell survival and MAP kinases activity.

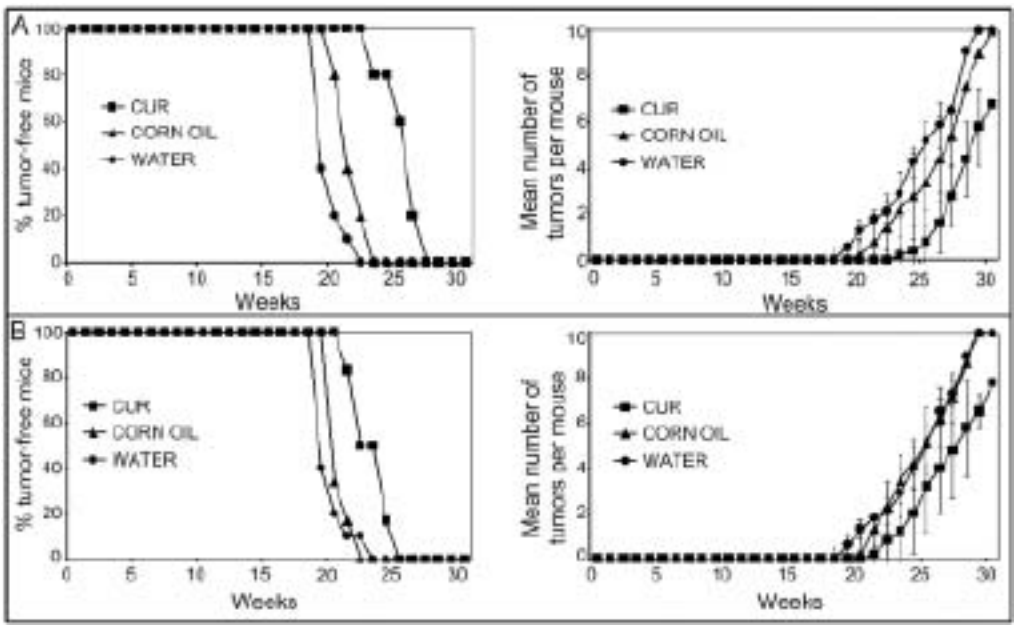

Fig. 6. *Delay of tumor growth in BALB-neuT mice treated with CUR. CUR administration (3 times a week) was initiated at 6 weeks (Panel **A**) and 16 weeks of age (Panel **B**), that is when mammary glands displayed atypical hyperplasia or invasive carcinoma, respectively. Reported are the time of tumor appearance (left graphs) and tumor multiplicity expressed as mean ± standard deviation of incidental tumors (right graphs).*

Delay of tumor growth in BALB-neuT mice treated with CUR

To evaluate the antitumor effect of CUR on ErbB2/neu-mediated carcinogenesis in BALB-*neu*T mice, groups of female BALB-*neu*T (5 mice per group) were treated with CUR dissolved in corn oil or, as negative controls, corn oil or water. Treatment was initiated at 6 and 16 weeks of age, when BALB-*neu*T female mice develop mammary atypical hyperplasia or invasive breast carcinoma, respectively. When the treatment was started at 6 weeks, all BALB-*neu*T mice subjected to mock treatments had palpable tumors by week 22 (water-treated group) or 23 (corn oil-treated group). Tumor multiplicity was 2.1 and 2.2, respectively for the mice to which was administered water and corn oil. By contrast, none of the CUR-treated mice exhibited signs of tumor growth at week 22, indicating specific interference of the compound with tumor development ($p \leq 0.01$) (Fig. 6, Panel A). Indeed, in the CUR-treated group palpable tumors appeared at week 23 and affected all mice only at week 27. In addition, at week 27, the multiplicity of tumors in corn oil- and water-treated mice was 5.4 and 5.9 respectively, while that of CUR-treated mice was 2.8 ($p \leq 0.05$) (Fig. 6, Panel A). Our results indicate that CUR induced a significant prolongation of tumor-free survival and a reduction of tumor multiplicity when treatment was started at the stage of mammary atypical hyperplasia.

When the treatment was started at 16 weeks, 100% of water- and corn oil-treated mice had palpable tumors by 23 and 22 weeks. Tumor multiplicity was 2.9 (water-treated group) and 3.5 (corn oil-treated group) (Fig. 6, Panel B). In comparison, only 50% of the CUR-treated mice displayed tumors at 23 weeks, indicating a specific interference of the compound with tumor growth also in an advanced stage of carcinogenesis ($p \leq 0.05$) (Fig. 6, Panel B). At week 25, tumors had affected all CUR-treated mice. However, while tumor multiplicity in corn oil- and water-treated mice was 5.0 and 6.2 respectively, that of CUR-treated mice was 3.2 only ($p \leq 0.05$) (Fig. 6, Panel B).

Hematological and clinical chemistry parameters in mice treated with CUR

To determine whether the administration of CUR had side effects, BALB-*neu*T females (3-5 mice per

Table I. *Percentage survival[1] of breast cancer cells treated with CUR.*

Cell line	Treatment	24 hours	48 hours
MDA-MB-231	CUR 6[2]	92.5	82.6
	CUR 12	90.5	53.6
	CUR 25	70.0	38.0
	CUR 50	60.5	17.3
MDA-MB-435	CUR 6	80.0	57.5
	CUR 12	75.5	48.0
	CUR 25	63.0	38.0
	CUR 50	57.0	34.0
MDA-MB-453	CUR 6	89.0	85.0
	CUR 12	76.0	78.3
	CUR 25	75.0	61.0
	CUR 50	69.0	43.3
MDA-MB-468	CUR 6	89.5	93.3[3]
	CUR 12	74.5	62.0
	CUR 25	45.0	37.3
	CUR 50	62.5	34.3
T-47D	CUR 6	96.0	85.0
	CUR 12	79.0	56.0
	CUR 25	66.5	41.0
	CUR 50	63.5	37.0
MCF7	CUR 6	93.5[3]	79.0
	CUR 12	74.5	50.0
	CUR 25	57.0	35.0
	CUR 50	61.0	32.0
BT-474	CUR 6	80.5	77.0
	CUR 12	86.5	87.5
	CUR 25	85.5	60.5
	CUR 50	67.0	61.0
SK-BR-3	CUR 6	87.0	74.0
	CUR 12	81.0	60.6
	CUR 25	63.3	38.3
	CUR 50	67.6	49.3
TUBO	CUR 6	96.0[3]	83.0
	CUR 12	86.5	74.0
	CUR 25	83.0	47.0
	CUR 50	73.5	34.0

[1]The percentage survival of the cultures treated with CUR was calculated by normalization of their O.D. values to those of control cultures treated with DMSO vehicle; results reported are mean values from three experiments performed in triplicate. [2]doses of CUR are in μM. The effects of CUR reached statistical significance ($p \leq 0.05$) at all doses tested, except when indicated by 3.

group) were treated with CUR, corn oil or water for 4 and 8 weeks starting from the 6th or 16th week of age, and clinical parameters were measured in each group before the beginning of treatment and after its completion. In particular, the analysis included hematological (complete blood count) and clinical chemistry parameters (cholesterol, triglycerides, serum glutamic oxaloacetic transaminase, serum glutamic pyruvic transaminase, blood urea nitrogen, lactate dehydrogenase). Values of individual mice appeared very heterogeneous within each group.

When the treatment was started on the 6th week,

Table II. *CUR concentrations (μM) required for 50% inhibition of breast cancer cell survival (IC50) after 48 hours of treatment.*

Cell line	IC_{50}[1]
MDA-MB-435	10.7 ± 0.5
MCF7	12.6 ± 1.4
MDA-MB-231	15.0 ± 1.1
T-47D	15.9 ± 5.8
MDA-MB-468	18.2 ± 1.0
SK-BR-3	18.4 ± 0.9
TUBO	23.7 ± 0.2
MDA-MB-453	40.2 ± 8.7
BT-474	> 50

[1] *Mean ± SD of three independent experiments.*

the post-treatment measurements were performed at 10 and 14 weeks of age. In this case, no significant differences were observed between the parameters measured before and after treatment in each group of mice (data not shown). On the other hand, when the treatment was started at week 16, that is when mice have already tumors of the mammary gland, although still not palpable, the post-treatment measurements performed at week 20 and 24 revealed alterations in some clinical parameters in each group of mice. Still, such alterations were less pronounced in the CUR-treated groups than in the corn oil- or water-treated groups. Indeed, at 24 weeks of age CUR-treated mice displayed only a slight and not significant decrease in the percentage of lymphocytes and an

Table III. *Lack of side effects of CUR in BALB/c mice: complete blood count (CBC) and clinical chemistry parameters.*

CBC	Reference values	Mean ± SD pre-treatment	Mean ± SD 4 weeks post-treatment	Mean ± SD 8 weeks post-treatment
RBC (10^6/mm^3)	6.0-12.0	11.8 ± 0.8	11.0 ± 0.5	11.2 ± 0.1
MCV (μm^3)	43.0-58.0	45.4 ± 2.1	47.6 ± 0.7	47.8 ± 1.8
HCT (%)	35.0-60.0	53.5 ± 1.1	52.2 ± 1.4	53.1 ± 1.8
PLT (10^3/mm^3)	250-1200	909 ± 72	897 ± 40	788 ± 76
MPV (μm^3)	4.0-7.0	5.9 ± 0.1	6.1 ± 0.1	5.9 ± 0.4
WBC (10^3/mm^3)	5.0-12.0	9.4 ± 1.3	11.0 ± 0.1	9.8 ± 1.3
HGB (g/dl)	9.0-19.0	16.9 ± 0.1	17.0 ± 1.0	16.9 ± 0.2
MCH (Pg)	15.0-19.0	14.4 ± 0.8	15.5 ± 0.3	15.2 ± 0.3
MCHC (g/dl)	34.0-39.0	31.7 ± 0.4	32.5 ± 1.0	31.9 ± 0.8
RDW (%)	0-99.9	16.7 ± 0.4	15.9 ± 0.6	15.1 ± 0.4
LYM (%)	50.0-75.0	60.7 ± 0.9	62.1 ± 0.5	65.0 ± 2.4
MID (%)	5.0-15.0	8.2 ± 1.1	6.4 ± 0.3	6.1 ± 0.6
GRAN (%)	15.0-40.0	31.2 ± 0.2	31.6 ± 0.8	28.9 ± 1.8
LYM (10^3/mm^3)	4.0-10.0	5.7 ± 0.6	6.8 ± 0.1	6.4 ± 1.1
MID (10^3/mm^3)	0-2.0	0.9 ± 0.4	0.7 ± 0.1	0.7 ± 0.1
GRAN (10^3/mm^3)	0.5-6.0	2.9 ± 0.4	3.5 ± 0.1	2.8 ± 0.1
PCT (%)	0-99.9	0.5 ± 0.0	0.5 ± 0.0	0.5 ± 0.1
PDW (%)	0-99.9	8.7 ± 0.1	9.1 ± 0.1	8.6 ± 0.7
Clinical Chemistry				
CHOL (mg/dl)	50-120	118 ± 14	152 ± 23	122 ± 14
TRI (mg/dl)	80-200	106 ± 42	124 ± 1	122 ± 37
GOT (U/l)	20-250	192 ± 215	234 ± 167	118 ± 20
GPT (U/l)	20-100	73 ± 74	113 ± 24	18 ± 1
BUN (mg/dl)	10-40	28 ± 6	34 ± 9	32 ± 11
LDH (U/l)	300-900	780 ± 42	824 ± 48	878 ± 74

Abbreviations: SD: Standard Deviation; RBC: Red Blood Cells; MCV: Mean Corpuscular Volume; HCT: Hematocrit; PLT: Platelets; MPV: Mean Platelet Volume; WBC: White Blood Cells; HGB: Hemoglobin; MCH: Mean Corpuscular Hemoglobin; MCHC: Mean Corpuscular Hemoglobin Concentration; RDW: Red Cell Distribution Width; LYM: Lymphocytes; MID: Minimum Inhibitory Dilution; GRAN: Granulocytes; PCT: Plateletcrit; PDW: Platelet Distribution Width; CHOL: cholesterol; TRI: triglycerides; GOT: serum Glutamic Oxaloacetic Transaminase; GPT: serum Glutamic Pyruvic Transaminase; BUN: Blood Urea Nitrogen; LDH: Lactate Dehydrogenase.

increase in that of granulocytes, with both values remaining within the normal range of reference. Conversely, in mice treated with corn oil or water were observed: a decrease in the number of red blood cells and hematocrit ($p \leq 0.05$ *vs* pre-treatment values), although still within the normal range of reference; a decrease in the percentage of lymphocytes (reference values 50-75%; pre-treatment *vs* post-treatment values: 69 *vs* 20% in water-treated mice and 79 *vs* 32% in corn oil-treated mice; $p \leq 0.05$); an increase in the percentage of granulocytes (reference values 15-40%; pre-treatment *vs* post-treatment values: 21 *vs* 73% in water-treated mice and 15 *vs* 42% in corn oil-treated mice; $p \leq 0.05$). In water-treated mice the total number of white blood cells was also increased (reference values 5-12 x $10^3/mm^3$; pre-treatment *vs* post-treatment values: 7 *vs* 22 x $10^3/mm^3$; $p \leq 0.05$) as well as the level of blood urea nitrogen (reference values 10-40 mg/dl; pre-treatment *vs* post-treatment values: 27 *vs* 45 mg/dl; $p \leq 0.05$). Collectively, these results demonstrate that CUR treatment does not modify hematological and clinical chemistry parameters and indicate that the alterations observed in corn oil- and water-treated mice at week 24 are likely associated with the advanced neoplastic stage. In fact, at this age 100% of corn oil- and water-treated mice carried tumors, with a multiplicity of about 4. In contrast, at the same age only 83% of CUR-treated mice displayed tumors, with a tumor multiplicity of 2 only.

In order to further demonstrate the lack of side effects of CUR, treatments were performed in BALB/c mice, *i.e.* the wild type strain from which cancer-prone transgenic BALB-*neu*T mice were generated (9). Thus, BALB-c mice aged 16 weeks were treated with CUR for 4 and 8 weeks, and hematological and clinical chemistry parameters were measured before the beginning of treatments and after their completion (Table III). The results obtained confirm that CUR treatment does not lead to any alteration of the parameters analyzed (Table III).

DISCUSSION

Breast cancer patients show different survival outcomes according to the neoplasia biological behavior which, in turn, is dependent on the molecular alterations occurring in cancer cells (1). Some of the alterations taking place in breast cancer cells are currently exploited by molecularly targeted drugs. However, despite the benefits of the current therapies a significant number of patients with breast cancer is at risk of relapse (3). In this context, a mono-targeted therapy, which is used in many cases in conjunction with traditional therapies, has the limit to counteract the action of a single molecular target (4, 8). On the other hand, cancer transformation arises by dysregulation of a multitude of genes, and a multi-targeted therapy has the advantage to simultaneously inhibit multiple signaling pathways involved in carcinogenesis (8).

Nutraceuticals (derived by the words nutrition and pharmaceutical) are food substances or food ingredients that provide medical and health benefits by behaving as multi-targeted therapy drugs. Among other nutraceuticals, CUR is regarded as a multi-targeted drug due to its ability to inhibit cancer growth through the interaction with multiple signaling pathways (8).

In light of these considerations, the purpose of our study was to evaluate first the *in vitro* effect of CUR on proliferation, apoptosis and cell cycle of breast cancer cell lines. Our results demonstrate that CUR inhibits the growth of breast cancer cells in a dose dependent manner, with IC50 values in the micromolar range. In addition, treatment with CUR induced a dose-dependent increase in the percentage of cells in sub-G0 phase, representing the apoptotic cell population. The activation of apoptosis was confirmed by the observation that CUR was able to induce the cleavage of PARP-1. Further, following CUR treatment an increase of the ratio between the pro-apoptotic Bax and the anti-apoptotic Bcl-2 protein was observed in all breast cancer cell lines analyzed. According to these findings, CUR can trigger tumor cell death when used alone and might also improve the effectiveness and tolerability of chemotherapy regimens or mono-targeted therapies by lowering the apoptotic threshold of cancer cells (8).

Hyperactivation of the ERK1/ERK2 MAP kinases signaling pathway is frequent in human cancer and is known to be related with increased cell survival and proliferation (20). MAP kinases are among the intracellular effectors of ErbB receptors (EGFR,

ErbB2, ErbB3 and ErbB4) (21). Approximately 15-25% of human breast tumors overexpress ErbB2/neu, in association or not with gene amplification (1). ErbB2/neu is a transmembrane receptor with tyrosine kinase activity and is involved in the transduction pathways that mediate cell proliferation and differentiation (21). Here we demonstrate that MAP kinases activity is downregulated by CUR in breast cancer cells. In particular, treatment with CUR was able to inhibit the activation of ERK1/ERK2 in MCF7 cells, which express low levels of ErbB2/neu, and to completely abolished it in MDA-MB-453 and SK-BR-3 cells that overexpress ErbB2/neu. By contrast, in MDA-MB-435 cells, which also express low levels of ErbB2/neu, CUR treatment was found to activate ERK1/ERK2 MAP-kinases. Nonetheless, this cell lines was sensitive to the pro-apoptotic effect of CUR, suggesting that in these cells CUR may activate apoptotic signaling pathways which involve MAPK activation. In fact, it has recently been demonstrated that activation of ERK1/ERK2 can contribute to cell death in some cell types (22). Different strategies for inhibiting MAP kinase signaling are evaluated as cancer therapies, including the use of Raf and MEK inhibitors (20). Accordingly, CUR might potentiate the effectiveness of such drugs in tumors sensitive to MAP kinase inhibition.

The potential utility of CUR for the treatment of ErbB2-overexpressing breast cancers, which are characterized by aggressive growth and poor prognosis, is supported by different studies. For instance, it has been reported that CUR inhibits the tyrosine kinase activity of ErbB2/neu (23). In a study performed on breast cancer xenografts overexpressing ErbB2, the combination of CUR with herceptin (a humanized anti-ErbB2 monoclonal antibody) was not better than herceptin alone in reducing tumor size. Still, the combination of taxol and CUR had antitumor effects comparable with those of taxol and herceptin (24). In this context, our results demonstrate that CUR is able to inhibit cell survival and induce apoptosis in breast cancer cells expressing either high or low levels of ErbB2/neu.

In order to further investigate the involvement of ErbB2/neu in modulating cell responses to CUR treatment, the effects of this compound on survival of transformed mouse fibroblasts overexpressing human ErbB2 (LTR-ErbB2) or rat ErbB2/neu (LTR-NeuN) were investigated and compared to those induced on wild type, non-transformed NIH3T3 fibroblasts. In non-transformed NIH3T3 CUR did not reduce cell survival and activity of MAP kinases. On the other hand, following ErbB2/neu overexpression and cell transformation, NIH3T3 fibroblasts became sensitive, albeit with a different profile, to CUR inhibitory effects on both cell survival and MAP kinases activity. Interestingly, a different sensitivity to CUR effects was observed between LTR-ErbB2 and LTR-NeuN: LTR-ErbB2 cells were more sensitive than LTR-NeuN to the cell survival inhibitory effects of CUR; moreover, in LTR-ErbB2 CUR inhibited ERK1/ERK2 MAP kinases activity and increased Bax expression, whereas in LTR-NeuN it moderately reduced ERK1 phosphorylation only. These results indicate that there is a different sensitivity to CUR effects between LTR-ErbB2 and LTR-NeuN that is not dependent on the level of expression of ErbB2/neu.

One of the limits of the nutraceuticals and thus of CUR is their poor bioavailability, which might hinder the *in vivo* effects of the compounds (5, 8). Therefore, the *in vivo* antitumor activity of CUR was tested in BALB-*neu*T mice transgenic for the neu oncogene, a mouse model of aggressive mammary carcinogenesis. Indeed, BALB-*neu*T mice develop atypical hyperplasia of the mammary gland at 6 weeks of age and in situ and invasive carcinoma at 11 and 16 weeks of age, respectively (9). Our data provide evidence that CUR induces a significant prolongation of tumor-free survival and a reduction of tumor multiplicity in BALB-*neu*T mice. Even though the best treatment effects were obtained when the administration of CUR was started early in the mammary gland carcinogenesis process, *i.e.* at the stage of atypical hyperplasia, CUR was able to interfere with tumor growth also when the treatment was started in an advanced stage of carcinogenesis. In addition we demonstrate that CUR administration was safe, since no side effects could be observed both in BALB-*neu*T and BALB/c mice.

Clinical trials using CUR alone or in combination with chemotherapy have been performed (25-28). CUR induced a significant 40% reduction in colorectal aberrant crypt foci number when administered to 41 subjects (25). In addition, it was shown that in patients with monoclonal gammopathy of

undetermined significance and smoldering multiple myeloma CUR therapy decreased the free light-chain ratio and reduced the difference between clonal and non-clonal light-chain, thus suggesting that CUR might have the potential to slow the disease process (26). When CUR was administered alone in patients with pancreatic cancer it was well tolerated and, despite its limited absorption, had biological activity in some patients (27). In addition, among nine advanced and metastatic breast cancer patients treated with the combination of docetaxel and CUR, one patient had only evaluable bone lesions which were stable after six cycles of treatment, five patients had partial response and three patients had stable disease at least 6 weeks after the last cycle of treatment (28). It appears that the best results can be achieved by using CUR in early stages of carcinogenesis and by increasing its bioavailability. In this regard, novel nano-preparations of CUR should overcome the bioavailability drawback (5). A dispute concerning the biological effects of curcumin is related to its ability to behave both as a cytoprotective and a cytotoxic molecule. Curcumin possesses high antioxidant activity, but it also behaves as a pro-oxidant agent in the presence of transition metals, resulting in DNA injuries and apoptotic cell death (29). Among the others CUR has been shown to induce the expression of heme oxygenase 1 (HO-1) (30), a cytoprotective enzyme with anti-oxidant and anti-inflammatory activity, protecting different cell types to oxidative stress and apoptosis. However, this effect appears to be mainly restricted to normal cells such as endothelial cells (30). In addition to the pro-oxidant activity, the main biological effects of CUR rely on its ability to inhibit survival and proliferation of cancer cells by simultaneously suppressing several signaling pathways which are up-regulated in tumor but not in normal cells (8, 29). Furthermore, most cancer cells show lower levels of glutathione than normal cells and, accordingly, are more sensitive to oxidation by CUR (29). Thus, the CUR-mediated induction of phase II enzymes such as HO-1 appears not sufficient to protect tumor cells from CUR pro-oxidant activity, consistent with the cytotoxic rather than cytoprotective effect displayed by this compound (29).

Overall, our results show that CUR has a potent cytotoxic effect on breast cancer cell lines, regardless of the expression of ErbB2/neu. In addition, CUR has antitumor activity *in vivo*, as demonstrated by its ability to interfere with the process of neu-mediated carcinogenesis in BALB-*neu*T mice. These findings support further studies on the therapeutic potential of CUR in combination with standard therapies in breast cancer patients.

ACKNOWLEDGEMENTS

This study was supported by a grant from MIUR, PRIN 2009 (R.B, 2009EWAW4M_002). The authors thank the friend Dr. MH Kraus (University of Alabama, Birmingham, USA) for providing LTR-ErbB2 cells and anti-ErbB2 antibody, Dr. E. Di Marco (Istituto Tumori di Genova, Italy) for providing LTR-NeuN cells and Barbara Bulgarini for editorial assistance in the preparation of the manuscript. We will always be indebted to Prof. G Forni (University of Turin, Italy) for providing founder male BALB-*neu*T mice and TUBO cells, and for all his anti-ErbB2/neu vaccine studies using these mice which have been of help to the entire scientific community.

REFERENCES

1. Blows FM, Driver KE, Schmidt MK, et al. Subtyping of breast cancer by immunohistochemistry to investigate a relationship between subtype and short and long term survival: a collaborative analysis of data for 10,159 cases from 12 studies. PLoS Med 2010; 7:e1000279.
2. Mukai H. Targeted therapy in breast cancer: current status and future directions. Jpn J Clin Oncol 2010; 40:711-6.
3. Gonzalez-Angulo AM, Morales-Vasquez F, Hortobagyi GN. Overview of resistance to systemic therapy in patients with breast cancer. Adv Exp Med Biol 2007; 608:1-22.
4. Palumbo C, Bei R, Procopio A, Modesti A. Molecular targets and targeted therapies for malignant mesothelioma. Curr Med Chem 2008; 15:855-67.
5. Marzocchella L, Fantini M, Benvenuto M, Masuelli L, Tresoldi I, Modesti A, Bei R. Dietary flavonoids: molecular mechanisms of action as anti- inflammatory agents. Recent Pat Inflamm Allergy Drug Discov 2011; 5:200-20.
6. Izzi V, Masuelli L, Tresoldi I, Sacchetti P, Modesti A,

Galvano F, Bei R. The effects of dietary flavonoids on the regulation of redox inflammatory networks. Front Biosci 2012; 17:2396-418.
7. Chiurchiù V, Maccarrone M. Chronic inflammatory disorders and their redox control: from molecular mechanisms to therapeutic opportunities. Antioxid Redox Signal 2011; 15:2605-41.
8. Kunnumakkara AB, Anand P, Aggarwal BB. Curcumin inhibits proliferation, invasion, angiogenesis and metastasis of different cancers through interaction with multiple cell signaling proteins. Cancer Lett 2008; 269:199-225.
9. Rovero S, Amici A, Di Carlo E, et al. DNA vaccination against rat her-2/Neu p185 more effectively inhibits carcinogenesis than transplantable carcinomas in transgenic BALB/c mice. J Immunol 2000; 165:5133-42.
10. Bei R, Pompa G, Vitolo D, et al. Co-localization of multiple ErbB receptors in stratified epithelium of oral squamous cell carcinoma. J Pathol 2001; 195:343-8.
11. Di Marco E, Pierce JH, Knicley CL, Di Fiore PP. Transformation of NIH 3T3 cells by overexpression of the normal coding sequence of the rat neu gene. Mol Cell Biol 1990; 10:3247-52.
12. Masuelli L, Marzocchella L, Quaranta A, et al. Apigenin induces apoptosis and impairs head and neck carcinomas EGFR/ErbB2 signaling. Front Biosci 2011; 16:1060-8.
13. Bei R, Masuelli L, Moriconi E, Visco V, Moretti A, Kraus MH, Muraro R. Immune responses to all ErbB family receptors detectable in serum of cancer patients. Oncogene 1999; 18:1267-75.
14. Masuelli L, Budillon A, Marzocchella L, et al. Caveolin-1 overexpression is associated with simultaneous abnormal expression of the E-cadherin/α-β catenins complex and multiple ErbB receptors and with lymph nodes metastasis in head and neck squamous cell carcinomas. J Cell Physiol 2012; 227:3344-53.
15. Masuelli L, Bei R, Sacchetti P, et al. Beta-catenin accumulates in intercalated disks of hypertrophic cardiomyopathic hearts. Cardiovasc Res 2003; 60:376-87.
16. Masuelli L, Pompa G, Fabrizi M, et al. Patients with peri-implantitis, unlike those with a healthy peri-implant microenvironment, display antibodies to more than one heat shock protein (HSP 27, HSP 65 and HSP 90) linear epitope. Eur J Inflamm 2011; 9:257-67.
17. Ingrosso G, Fantini M, Nardi A, et al. Local radiotherapy increases the level of autoantibodies to ribosomal P0 protein but not to heat shock proteins, extracellular matrix molecules and EGFR/ErbB2 receptors in prostate cancer patients. Oncol Rep 2013; 29:1167-74.
18. Masuelli L, Focaccetti C, Cereda V, et al. Gene-specific inhibition of breast carcinoma in BALB-neuT mice by active immunization with rat Neu or human ErbB receptors. Int J Oncol 2007; 30:381-92.
19. Martín-Oliva D, Ferrer-Martín RM, Santos AM, et al. Simultaneous cell death and upregulation of poly(ADP-ribose) polymerase-1 expression in early postnatal mouse retina. Invest Ophthalmol Vis Sci 2011; 52:7445-54.
20. Pratilas CA, Solit DB. Targeting the mitogen-activated protein kinase pathway: physiological feedback and drug response. Clin Cancer Res 2010; 16:3329-34.
21. Eccles SA. The epidermal growth factor receptor/Erb-B/HER family in normal and malignant breast biology. Int J Dev Biol 2011; 55:685-96.
22. Zhuang S, Schnellmann RG. A death-promoting role for extracellular signal-regulated kinase. J Pharmacol Exp Ther 2006; 319:991-7.
23. Hong RL, Spohn WH, Hung MC. Curcumin inhibits tyrosine kinase activity of p185neu and also depletes p185neu. Clin Cancer Res 1999; 5:1884-91.
24. Lai HW, Chien SY, Kuo SJ, Tseng LM, Lin HY, Chi CW, Chen DR. The potential utility of curcumin in the treatment of HER-2-overexpressed breast cancer: an in vitro and in vivo comparison study with herceptin. Evid Based Complement Alternat Med 2012; 2012:486568.
25. Carroll RE, Benya RV, Turgeon DK, et al. Phase IIa clinical trial of curcumin for the prevention of colorectal neoplasia. Cancer Prev Res 2011; 4:354-64.
26. Golombick T, Diamond TH, Manoharan A, Ramakrishna R. Monoclonal gammopathy of undetermined significance, smoldering multiple myeloma, and curcumin: a randomized, double-blind placebo-controlled cross-over 4g study and an open-label 8g ex-

tension study. Am J Hematol 2012; 87:455-60.
27. Dhillon N, Aggarwal BB, Newman RA, et al. Phase II trial of curcumin in patients with advanced pancreatic cancer. Clin Cancer Res 2008; 14:4491-9.
28. Bayet-Robert M, Kwiatkowski F, Leheurteur M, et al. Phase I dose escalation trial of docetaxel plus curcumin in patients with advanced and metastatic breast cancer. Cancer Biol Ther 2010; 9:8-14.
29. Ravindran J, Prasad S, Aggarwal BB. Curcumin and cancer cells: how many ways can curry kill tumor cells selectively? AAPS J 2009; 11:495-510.
30. Motterlini R, Foresti R, Bassi R, Green CJ. Curcumin, an antioxidant and anti-inflammatory agent, induces heme oxygenase-1 and protects endothelial cells against oxidative stress. Free Radic Biol Med 2000; 28:1303-12.

p63 EXPRESSION IN LARYNGEAL SQUAMOUS CELL CARCINOMA IS RELATED TO TUMOR EXTENSION, HISTOLOGIC GRADE, LYMPH NODE INVOLVEMENT AND CLINICAL STAGE

M. RE[1], G. MAGLIULO[2], L. FERRANTE[3], A. ZIZZI[4], A. SANTARELLI[5], D. STRAMAZZOTTI[4], L. LO MUZIO[6], G. GOTERI[4] and C. RUBINI[4]

[1]Department of Otorhinolaryngology, Polytechnic University of the Marche United Hospitals, Torrette (Ancona), Italy; [2]G Ferreri Department of Otorhinolaryngology, Audiology and Phoniatrics, La Sapienza University, Rome, Italy; [3]Department of Biomedical Sciences and Public Health, Centre of Epidemiology, Biostatistic and Medical Informatics, Polytechnic University of the Marche, Torrette (Ancona), Italy; [4]Department of Biomedical Sciences and Public Health, Section of Pathologic Anatomy and Histopathology, Polytechnic University of the Marche/United Hospitals, Torrette (Ancona), Italy; [5]Department of Specialistic Clinic and Odontostomatological Sciences, Polytechnic University of the Marche, Torrette (Ancona), Italy; [6]Department of Surgical Sciences, University of Foggia, Foggia, Italy

Received July 12, 2012 - Accepted January 8, 2013

To analyse the relationship of the immunohistochemical p63 expression with tumoral extent, histologic grade, lymph node involvement and clinical stage in laryngeal squamous cell carcinoma (LSCC), a series of 81 patients with primary LSCC treated by primary surgery was retrospectively evaluated. Immunohistochemistry was performed on formalin-fixed and paraffin-embedded tissue blocks from surgical samples. Clinicopathologic data were correlated with the p63 staining results. Differences in p63 immunoreactivity between the different groups were compared using both parametric analysis of variance (ANOVA) and non-parametric Kruskal-Wallis test. Statistical significance was set at $p<0.05$. All statistical analyses were performed using the R statistical package. We found a statistically significant association between p63 protein expression and increase of tumor extension (T1 *vs* T3), of histological grading, of level of lymph node involvement (N0 *vs* N1 and N2), and clinical stage (I *vs* IV). Our findings suggest that abnormal expression of p63 may be involved in the early phases of laryngeal tumorigenesis and this oncoprotein might become a useful predictor of clinical outcome.

Laryngeal squamous cell carcinoma (LSCC) is the most common malignancy of the head and neck region in adults, and it accounts for about 1.5% of all cancers (1). The prognosis of LSCCs is defined on the basis of clinical stage (2), site and size of the tumour, histological grading (3), depth of invasion and host reaction (4), although, in absolutely, the most significant prognostic indicator of survival in patients with LSCC is the presence or absence of metastatic cervical nodes (2, 3, 5). LSCC shows heterogeneous biological behaviors in terms of the development of recurrent and/or metastatic disease.

Key words: laryngeal squamous cell carcinoma, prognosis, biomarker, p63 immunostaining

Mailing address: Dr. Massimo Re,
Department of Otorhinolaryngology,
Polytechnic University of Marche,
"Ospedali Riuniti" of Ancona, Via Conca 71,
60020 Torrette, Ancona, Italy
Tel.: +39 071 5964624 Fax: +39 071 5964415
e-mail: remassimo@hotmail.com

0393-974X (2013)

Patients with identical clinicopathological features may have a different clinical course or response to the same therapy. The outcome of advanced stages III and IV in particular is still poor, regardless of the treatment modality chosen. There is the necessity that clinical staging should be supplemented by others factors which would increase our knowledge about the biologic behaviour of these tumours and also would help in deciding on treatment for individual patients. Biological markers capable of distinguishing patients with a good prognosis from those with a worse prognosis are thus needed.

p63 is a cloned p53-related gene mapping to chromosome 3q27-29, which shares structural and functional homologies with the p53 family of transcription factors. It is capable of binding DNA, transactivating p53-responsive genes, and inducing apoptosis (6).

p63 does not seem to play a major role as a tumor suppressor gene, because it is rarely mutated in primary tumours (7, 8) and in cancer cell lines (9). Nevertheless, p63 mRNA and/or protein are overexpressed in a variety of human neoplasms as a result of gene amplifications (10, 11), and gene aberrations are common in squamous cell carcinoma arising in head and neck region (13-22).

These data strongly suggest that p63 gene aberrations may be involved in human tumorigenesis and may play a role in cell invasion and migration, supporting an oncogenic role in head and neck squamous cell carcinoma (SCCHN) (13, 16, 20, 22).

The aim of this study was to determine the prevalence of immunohistochemical p63 expression and the relationship with tumoral extent, histologic grade, lymph node involvement and clinical stage in a cohort of patients with primary LSCCs treated by primary surgery.

MATERIALS AND METHODS

Patients

The medical charts of all patients with primary laryngeal squamous cell carcinoma, consecutively treated by primary surgery at the Department of Otorhinolaryngology, Polytechnic University of Marche, Ancona, Italy, between years 1999 and 2004, were retrospectively retrieved and reviewed. Informed consent had been obtained from each patient included in the study at the time of surgery. Inclusion criteria were: primary surgical treatment of the tumor with complete surgical excision of the tumour by means of partial or total laryngectomy, complete clinical data, uniformity of histogical differentiation throughout the tumor sample, and the availability of sufficient material from the primary tumor for this and other investigations. Patients with previous or synchronous second malignancies or with previous radiation therapy or chemotherapy were excluded from the study. There were 81 patients who met the inclusion criteria. Representative tissue blocks were retrieved from the archives of the Section of Pathological Anatomy, Polytechnic University of Marche, Ancona, Italy.

Diagnosis and assessment of the histological grading (G1, G2, G3) of tumor differentiation, according the the WHO (2005) classification on tumors (23), were made on 4-6 μm thick paraffin tissue sections stained with conventional hematoxylin and eosin. Identification of the anatomical site of the tumors (T from T1 to T4), nodal involvement (N0, N1, N2) and clinicopathologic stage were determined according to the AJCC (2010) TNM classification of malignant tumors (24). Institutional Review Board approval was obtained for our study.

Immunohistochemistry

Serial sections of 4 μm from formalin-fixed, paraffin-embedded blocks of tumor rapresentative areas were cut for each case. Tissue sections were deparaffinized in xylene and rehydrated through a graded ethanol series.

To better unmask antigenic sites, an antigen retrieval solutions was applied, by incubating sections with a Dako Target Retrieval solution High pH (DakoCytomation, Glostrup, Denmark) at 750 KW for 20 m. Endogenous peroxidase activity was quenched incubating the sections in 3% (v/v) hydrogen peroxide for 7 m at room temperature. Sections were then incubated for 60 m with the anti-p63 monoclonal antibody (clone 4A4, dil. 1:400, DakoCytomation, Glostrup, Denmark). Antigen-antibody complex was subsequently visualized using the Envision/HRP™ Detection System kit peroxidase/DAB (DakoCytomation, Glostrup, Denmark). Sections were counterstained with Mayer's Haematoxylin (Bio-Optica SPA, Milano, Italy) and cover-slipped with Paramount.

Normal human prostate was immunohistochemically performed as positive controls. Negative controls were performed by substituting the primary antibody with non-immune serum. The number of p63 immunoreactive nuclei was counted among at least 500 cells in the more representative fields by using a microscope at ×400 magnification and expressed as percentage. The counts were performed by two investigators simultaneously (CR and GG), using a double-headed light microscope. Both examiners had to agree on the count of the positive cells.

Statistical analysis

For each case, tumor extension (T), histological grading of differentiation, lymph node metastasis (N), clinical stage, and immunohistochemical p63 expression were entered in an EXCEL file. When appropriate, analysis of variance (ANOVA) and Tukey *t*-test were performed to compare the distributions of p63 expression among the categories of clinicopathologic variables. To test the ANOVA assumptions, we performed Shapiro-Wilk test to verify the normality of distributions and Bartlett test was applied to verify homoscedasticity of variances. If the ANOVA assumptions were not verified, we performed Kruskal-Wallis non-parametric test for multiple comparisons. Statistical analyses were performed using R statistical program (25). Statistical significance was set at $p<0.05$.

RESULTS

The main clinicopathologic features of the patients are summarized in Table I. The series was composed of 81 patients, 76 males and 5 females, with a mean age of 63.2 years (range 42-85 years). Thirty-one patients were treated with partial (39.5%) and 50 with total laryngectomies (60.5%). The tumors were distributed almost equally at different location, in the supraglottis, glottis and transglottis; a lesser number of cases were localised in the subglottis. Almost half of the cases were limited to the larynx with vocal cord fixation (T3); the remaining cases were either limited to one site with cord mobility (T1) or extended to the adjacent subsite with impaired cord mobility (T2) or were locally advanced (T4). Histopathological evaluation showed that twenty-five tumors were well differentiated (G1- Fig. 1A), thirty-six moderately differentiated (G2) and twenty poorly differentiated (G3- Fig. 1B) LSSCs. lymph node metastases. No patient had tumor in or near (<1 mm) surgical margins. The majority of cases did not display lymph node metastasis (N0); the remaining either showed metastasis in a single ipsilateral lymph node, 3 cm or less in greatest dimension (N1) or metastasis in a single ipsilateral lymph node, more than 3 cm but not more than 6 cm in greatest dimension, or in multiple ipsilateral lymph nodes, none more than 6 cm in greatest dimension, or in bilateral or contralateral lymph nodes, none more than 6 cm in greatest dimension (N2). All the patients did not have evidence of metastasis at diagnosis (M0). The majority of patients exhibited a high clinical stage (III and IV).

Immunoreactivity for p63 was detected in the neoplastic cells of all LSCCs and the positivity was only nuclear (Fig. 2). In all LSCCs, p63 immunostaining was either non-homogeneous or diffuse. The percentage of p63 positive cells ranged from 25% to 80%. Table II shows the means and the

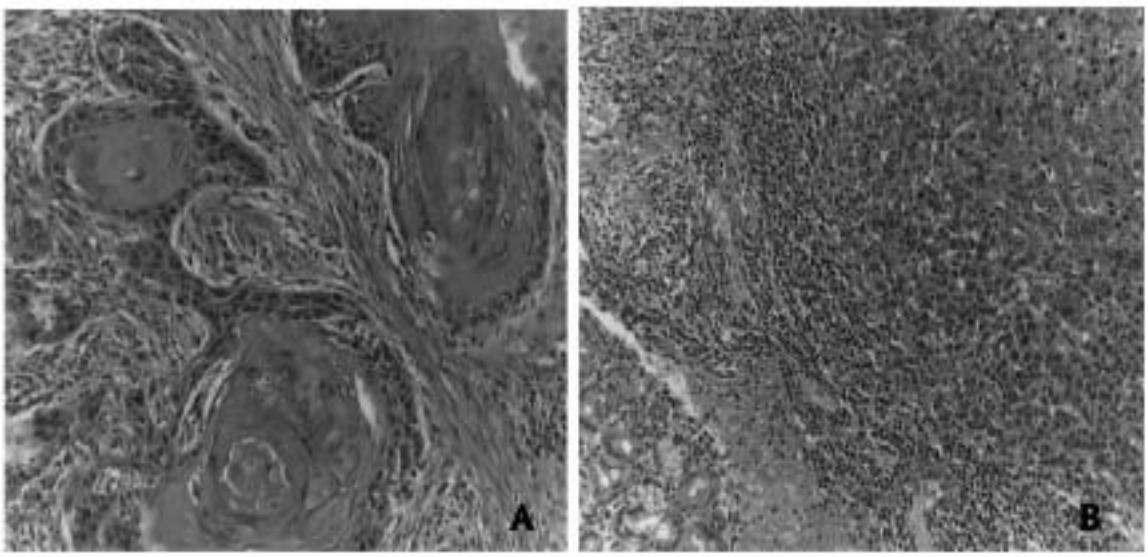

Fig. 1. *Hematoxylin and eosin staining of:* ***A)*** *well differentiated LSCC (G1) with keratin pearls and intratumoral inflammatory infiltrate (original magnification ×250);* ***B)*** *poorly differentiated LSCC (G3) with squamous-like features and moderate peritumoral inflammatory infiltrate (original magnification ×250).*

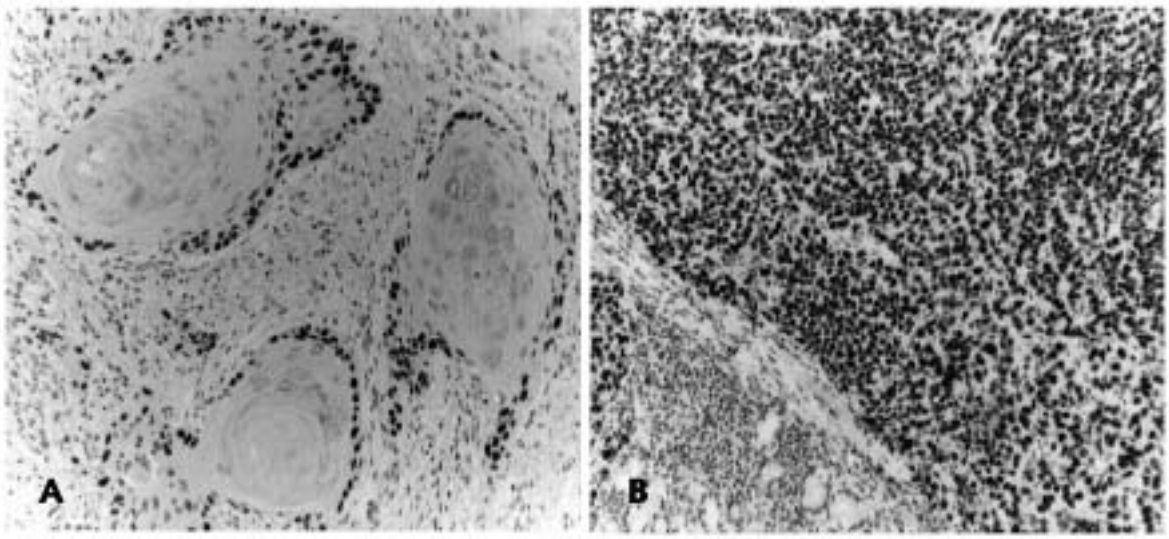

Fig. 2. *Immunohistochemical detection of p63 in: **A**) well differentiated LSCC (G1). (Immunoperoxidase, original magnification ×250); **B**) poorly differentiated LSCC (G3). (Immunoperoxidase, original magnification ×250).*

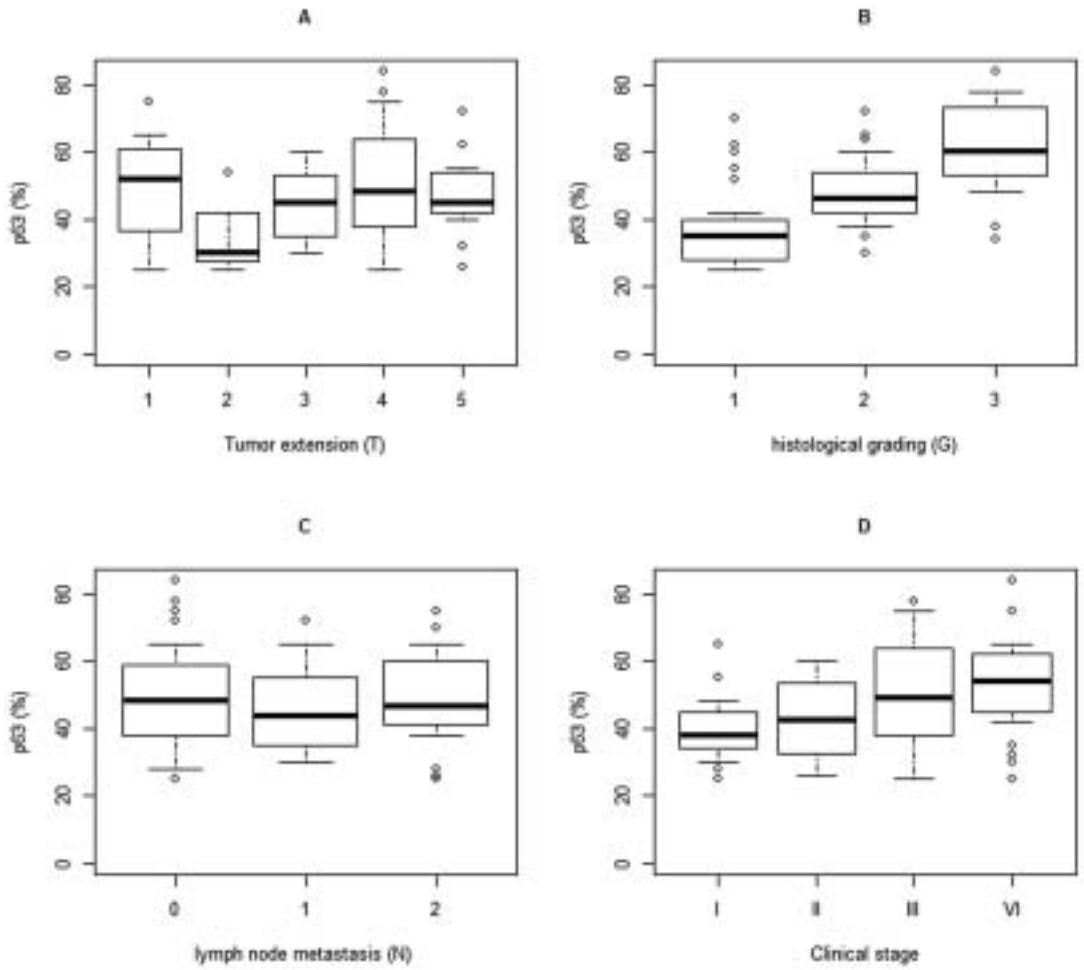

Fig. 3. *Boxplot p63 expression vs**: A**) the categories of clinical stages; **B**) the histological grading (G); **C**) the categories of tumor extension (T); **D**) the categories of lymph node metastasis (N).*

Table I. *Synoptic table of clinicopathologic features of patients with primary LSCC*

Parameters	N. of patients
Total patients	81
Mean age at surgery	63.24 (range 42- 85)
Gender	
M	76 (93.8%)
F	5 (6.2%)
Tumor localization	
Supraglottis	27 (33%)
Glottis	29 (36,3%)
Subglottis	3 (3.7%)
Transglottis	22 (27%)
Histological grading	
G1	25 (30,86%)
G2	36 (44.44%)
G3	20 (24.70%)
T stage	
T1	18 (22,22%)
T2	12 (14,81%)
T3	37 (45,68%)
T4	14 (17,29%)
N stage	
N0	47 (58,02%)
N1	14 (17,28%)
N2	20 (24,70%)
M stage	
M0	81 (100%)
M1	0 (0%)
Clinical stage	
I	18 (22,22%)
II	8 (9.88%)
III	26 (32,10%)
IV	29 (35.80%)

standard deviations of p63 immunostaining when the different categories were considered.

p63 expression (Fig. 3A) for each T category did not result significantly different from the normal distribution (Shapiro-Wilk's test, $p>0.44$) and the p63 immunostainings showed homogeneity of the variances (Bartlett's test, $p=0.37$). ANOVA and Tukey *t*-test pointed out that p63 immunostaining was significantly different ($p=0.002$) only between T1 and T3 patients with an increase of p63 expression of 14.2% (95% confidence interval: 4.1%-24.3%).

The distribution of p63 expression in G1 tumor resulted significantly different from the normal distribution (Shapiro-Wilk's test, $p=0.002$). By Kruskal-Wallis non-parametric ANOVA procedure, the distributions of p63 was significantly different ($p<0.001$, Fig. 3B) among the three categories of G and a nonparametric multiple comparison procedure showed that all three distributions of p63 were significantly different from each other ($p<0.001$).

The distribution of p63 related to N0 (Fig. 3C) did not shown a normal distribution (Shapiro-Wilk: $p=0.03$); by using non parametric Kruskal-Wallis test, we found a significant difference of the p63 immunostaining between N0 patients compared with those N1 ($p=0.029$) and N2 ($p<0.001$), but not between p63 of N1 and N2 patients ($p=0.383$).

The distribution of p63 expression (Fig. 3D) for each category of clinical stage did not result significantly different from the normal distribution (Shapiro-Wilk's test, $p>0.30$) and the p63 expressions showed homogeneity of the variances (Bartlett's test, $p=0.34$). By the ANOVA procedure, although p63 expression increased with clinical stage, Tukey *t*-test showed that p63 immunostaining was significantly different ($p=0.005$) only between stage I and stage IV.

DISCUSSION

Although some of the classic prognostic factors continue to be of great utility in predicting the clinical behavior of a laryngeal tumor, it is still not clear why some patients with laryngeal SCC do better than others with the same type of lesion in terms of histologic characteristics and clinical stage. Conventional clinicopathologic parameters do not accurately reflect the clinical outcome of patients with this tumor, thus the establishment of additional prognostic factors that may improve the understanding of treatment failure is an essential goal.

During recent years there has been increasing

Table II. *p63 immunohistochemical expression in primary LSCC.*

Variable	Groups	N. of patients	% of p63 (mean ± SD)
Clinical Stage	I	18	39.89 ± 10.03
	II	8	42.87 ± 12.24
	III	26	50.15 ± 15.24
	IV	29	53.86 ± 13.83
Histological grading	G1	25	37.72 ± 12.60
	G2	36	49.00 ± 9.66
	G3	20	61.00 ± 13.17
T stage	T1	18	39.89± 10.03
	T2	12	45.42 ± 14.18
	T3	37	54.08 ± 14.75
	T4	14	47.36 ± 12.52
N stage	N0	47	43.17 ± 13.14
	N1	14	52.57 ± 13.26
	N2	20	58.10 ± 12.07

interest in assessing head and neck cancer progression and predicting its course by using different molecular markers (26-36). In this study, we investigated the p63 immunohistochemical expression in a well-characterized series of patients with LSCCs treated by primary surgery. Few studies have determined the expression of p63 in SCCHN (15-20, 22, 37-41), including laryngeal cancer (15, 17-19) and the prognostic relevance is discussed controversially.

Reasons for these discordant results may include the selection of heterogeneous tumor study groups in terms of stage and site, the small number of cases studied, the differences in evaluation methods (cut-off scores), and finally the heterogeneity at the level of tumor sampling.

By subjecting p63-siRNA treated SCCHN cells to microarrays analysis, Gu et al. (22) identified 127 genes in which expression relies on the overexpression of p63. They concluded that their findings indicate an oncologic role for p63 in SCCHN. Lo Muzio et al. (16) studied p63 in ninety-four cases with oral squamous cell carcinoma. They demonstrated that patients with increased p63 expression had poorer survival rates than the group with decreased p63 expression, but did not find a statistically significant correlation between p63 expression and sex, age, tumour size, clinical staging, recurrence or metastasis. They proposed that p63 expression may be useful to identify cases of oral squamous cell carcinoma with a more aggressive and invasive phenotype, providing novel diagnostic and prognostic information relating to individual patient survival with oral cancer.

Ramer et al. (41) demonstrate significantly higher mortality rates in head and neck adenoid cystic carcinoma patients whose tumors had higher p63 expression compared with those with lower p63 expression.

p63 positivity was also found to have prognostic

significance in Merkel cell carcinoma, with positive cases demonstrating a more aggressive clinical course as compared with cases that did not express p63 (42). Conversely, in a study of esophageal squamous cell carcinoma, the 5-year overall survival was significantly longer in p63-positive compared with p63-negative tumors as defined by a specific cutoff value for p63 expression (38).

Few studies have evaluated the prognostic significance of p63 immunolabelling in LSCC (15, 17-19). Recently, Jia et al. (19) reported that the positive over-expression rate of the p63 gene in LSCC and in matched metastatic lymph node was significantly higher than adjacent tissues, non metastatic lymph node and normal tissue. They found no correlation between p63 gene expression and clinical stage of the LSCC. Similary, Wen et al. (17) observed that the expression of p63 was not related to any clinicopathological features.

We found a high p63 expression in all LSCC in agreement with other authors (15, 19). These data suggest that an abnormal status and expression of the p63 may play a pivotal role in the multiple stage model of laryngeal tumorigenesis, and p63 abnormalities may be involved in the very early steps of laryngeal cancer development in a similar manner as for p53.

We also evaluated the clinical implications of p63 deregulation in patients with laryngeal carcinoma. Our data showed a statistically significant association between p63 expression and some clinical parameters. In particular, we noticed that p63 up-regulation was clearly associated with high histological grade laryngeal carcinomas. There was also a significant association between p63 expression and tumor size (p63 expression of T1 patients resulted significantly lower than T3 patients) and clinical stage (p63 expression of stage I patients resulted significantly lower than stage IV patients).

The prognosis for tumours of the upper aerodigestive tract has been shown to be closely related to regional lymph nodes metastases. Lymph nodes metastases constitute the main prognostic factor in laryngeal cancer (2, 3, 5). Our data showed a significant association between p63 overexpression and lymph node metastases in laryngeal squamous cell carcinoma. In particular, p63 immunostaining was higher in N1 and N2 than in N0 patients.

In conclusions, our findings suggest that abnormal expression of p63 may be involved in the early phases of laryngeal tumorigenesis and quantitative assessment of this oncoprotein expression might become a useful predictor of clinical outcome. Although staging continues to play a pivotal role in the management of patients with LSCC, high p63 expression could warrant a more aggressive mode of therapy.

REFERENCES

1. Taxy JB. Upper respiratory tract. In: Damjanov I, Linder J (eds). Anderson's pathology, 10th edn. St. Louis. Mosby 1996; p.1463.
2. Pradier R, Gonzalez A, Matos E, et al. Prognostic factors in laryngeal carcinoma: Experience in 296 male patients. Cancer 1993; 71:2472-6.
3. Pera E, Moreno A, Galindo L. Prognostic factors in laryngeal carcinoma: A multifactorial study of 416 cases. Cancer 1986; 58:928-34.
4. Gallo O, Libonati GA, Gallina E, et al. Langerhans cells related to prognosis in patients with laryngeal carcinoma. Arch Otolaryngol Head Neck Surg 1991; 117:1007-10.
5. Vlachtis K, Nikolau A, Markou K, Fountzilas G, Daniilidis I. Clinical and molecular prognostic factors in operable laryngeal cancer. Eur Arch Otorhinolaryngol 2005; 262:890-8.
6. Levrero M, De Laurenzi V, Costanzo A, Gong J, Wang JY, Melino G. The p53/p63/p73 family of transcription factors: Overlapping and dinstinct functions. J Cell Sci 2000; 113:1661-70.
7. Nishi H, Isaka K, Sagawa Y, et al. Mutation and transcription analyses of the p63 gene in cervical carcinoma. Int J Oncol 1999; 15:1149-53.
8. Tani M, Shimizu K, Kawahara C, et al. Mutation and expression of the p51 gene in human lung cancer. Neoplasia 1999; 1:71-9.
9. Hagiwara K, McMenamin MG, Miura K, Harris CC. Mutation analysis of the p63/p73L/p51/p40/CUSP/KET gene in human cancer cell lines using intronic primers. Cancer Res 1999; 59:4165-9.
10. Barbareschi M, Pecciarini L, Cangi MG, et al. P63, a p53 homologue, is a selective nuclear marker of myoepithelial cells of the human breast. Am J Surg

Pathol 2001; 25:1054-60.
11. Glickman JN, Yang A, Shahsafaei A, McKeon F, Odze RD. Expression of p53-related protein p63 in the gastrointestinal tract and in esophageal metaplastic and neoplastic disorders. Hum Pathol 2001; 32:1157-65.
12. Park BJ, Lee SJ, Kim JI, et al. Frequent alteration of p63 expression in human primary bladder carcinomas. Cancer Res 2000; 60:3370-4.
13. Hibi K, Trink B, Patturajan M, et al. AIS is an oncogene amplified in squamous cell carcinoma. Proct Natl Acad Sci USA 2000; 97:5462-7.
14. Yamaguchi K, Wu L, Caballero OL, et al. Frequent gain of the p40/p51/p63 gene locus in primary head and neck squamous cell carcinoma. Int J Cancer 2000; 86:684-9.
15. Pruneri G, Pignataro L, Manzotti M, et al. p63 in laryngeal squamous cell carcinoma: evidence for a role of TA-p63 down regulation in tumorigenesis and lack of prognostic implications of p63 immunoreactivity. Lab Invest 2002; 82:1327-34.
16. Lo Muzio L, Santarelli A, Caltabiano R, et al. P63 overexpression associates with poor prognosis in head and neck squamous cell carcinoma. Hum Pathol 2005; 36:187-94.
17. Wen X, Gao Y, Ji W. Expression and biological significance of survivin and p63 in laryngeal squamous cell carcinoma (in Chinese). Lin Chuang Er Bi Yan Hou Ke Za Zhi 2005; 19:833-5.
18. Dong P, Li X, Zhu Z, et al. Expression of S-100 positive dendritic cell, TIMP-1 and p63 and its significance in the primary laryngeal carcinoma (in chinese). Lin Chuang Er Bi Yan Hou Ke Za Zhi 2005; 19:311-22.
19. Jia H, Wang J, Shan Y, Hou J. The clinical significance of the expression of p63 gene in laryngeal squamous cell carcinoma (in chinese). Lin Chuang Er Bi Yan Hou Ke Za Zhi 2006; 20(3):119-21.
20. de Oliveira LR, Ribeiro-Silva A, Zucoloto S. Prognostic impact of p53 and p63 immunoexpression in oral squamous cell carcinoma. J Oral Pathol Med 2007; 36:191-7.
21. Westfall MD, Pietenpol JA. P63: molecular complexity in development and cancer. Carcinogenesis 2004; 25:857-64
22. Gu X, Coates PJ, Boldrup L, Nylander K. p63 contributes to cell invasion and migration in squamous cell carcinoma of the head and neck. Cancer Lett 2008; 263:26-34.
23. Cardesa A, Gale N, Nadal A, Zidar N. Squamous cell carcinoma. In: Head and Neck tumors: Pathology & Genetics. World Health Organization Classification on Tumors (WHO) 2005; p118-9.
24. Edge SB, Compton CC. The American Joint Committee on Cancer: the 7th edition of the AJCC Cancer Staging Manual and the future of TNM. Ann Surg Oncol 2010; 17:1471-4.
25. R Development Core Team (2008). R: a language and environment for statistical computing. R Foundation for Statistical Computing Vienna Austria; ISBN 3-900051-07-0
26. Langer CJ. Exploring biomarkers in head and neck cancer. Cancer 2012; 118(16):3882-92.
27. Jin YT, Kayser S, Kemp BL, et al. The prognostic significance of the biomarkers p21, p53 and bcl-2 in laryngeal squamous cell carcinoma. Cancer 1998; 82:2159-65.
28. Friedman M, Lim JW, Manders E, Schaffner AD, Kirshenbaum GL, Tanyeri HM, Caldarelli DD, Coon JS: Prognostic significance of bcl-2 and p53 expression in advanced laryngeal squamous cell carcinoma. Head Neck 2001; 23:280-5.
29. Re M, Magliulo G, Salvolini E, Orciani M, Gioacchini FM, Goteri G, Rubini C. Prognostic significance of p53 and KAI-1 expression in patients with laryngeal squamous cell carcinoma. Anal Quant Cytol Histol 2010; 5(32):247-53.
30. Miyazaki T, Kato H, Shitara Y, et al. Mutation and expression of the metastasis suppressor gene KAI-1 in esophageal squamous cell carcinoma. Cancer 2000; 89:955-62.
31. Re M, Magliulo G, Tarchini P, Mallardi V, Rubini C, Santarelli A, Lo Muzio L. p53 and BCL-2 over-expressionon inversely correlate with hostological differentiation in occupational ethmoidal intestinal type sinonasal adenocarcinoma. Int J Imunopathol Pharmacol 2011; 24:603-609.
32. Uzawa K, Ono K, Suzuki H, Tanaka C, Yakushiji T, Yamamoto N, Yokoe H, Tanzawa H. High prevalence of decreased expression of KAI-1 metastasis suppressor of human oral carcinogenesis. Clin Cancer Res 2002; 8:828-35.

33. Xie X, Clausen OP, De Angelis P, Boysen M. The prognostic value ofspontaneous apoptosis, Bax, Bcl-2, and p53 in oral squamous cell carcinoma of the tongue. Cancer 1999; 86:913-20.
34. Re M., Romeo R, Mallardi V. Paralateral nasal malignant schwannoma with rabdiomyoblastic differentiation (Triton's tumor). Acta Otorhinolaryngol Ital 2002; 22:245-47.
35. Perrone F, Oggionni M, Birindelli S, Suardi S, Tabano S, Romano R. TP53, pl4ARF, p16INK4a and H-ras gene molecular analysis in intestinal-type adenocarcinoma of the nasal cavity and paranasal sinuses. Int J Cancer 2003; 105:196-203.
36. Perez-Ordonez B, Huynh NN, Berean KW, Jordan RC. Expression of mismatch repair proteins, beta catenin, and E cadherin in intestinal-type sinonasal adenocarcinoma. J Clin Pathol 2004; 57:1080-3.
37. LoMuzio L, Campisi G, Farina A, et al. Effect of p63expression on survival in oral squamous cell carcinoma.Cancer Investig 2007; 25:466-9.
38. Takahashi Y, Noguchi T, Takeno S, Kimura Y, Okubo MKawahara K. Reduced expression of p63 has prognostic implications for patients with esophageal squamous cell carcinoma. Oncol Rep 2006; 15:323-8.
39. Oliviera LR, Silva AR, Zucoloto S. Prognostic significance of p53 and p63 immunolocalisation in primary and matched lymph node metastasis in oral squamous cell carcinoma. Acta Histochemica 2007; 109:388-96.
40. Rushing EJ, Olsen C, Man YG. Correlation of p63 immunoreactivity with tumor grade in meningiomas. Int J of Surg Pathol 2008; 16:38-42.
41. Ramer N, Wu HS, Sabo E, Ramer Y, Emanuel P, Orta L, Burstein DE. Prognostic value of quantitative p63 immunostaining in adenoid cystic carcinoma of salivary gland assessed by computerized image analysis. Cancer 2010; 1:77-83.
42. Asioli S, Righi A, Volante M, Eusebi V, Bussolati G. p63 expression: a new prognostic marker in Merkel cell carcinoma. Cancer 2007; 110:640-7.

THREE NOVEL HUMAN SPORADIC MELANOMA CELL LINES: SIGNALING PATHWAYS CONTROLLED BY MC1R, BRAF AND β-CATENIN

P. ZANNA[1], I. MAIDA[1], C. GRIECO[1], S. GUIDA[2], M.C. TURPIN SEVILLA[3], S. DE SUMMA[4], S. TOMMASI[4], G.A. VENA[2], R. FILOTICO[2] and G. GUIDA[1]

[1]Dept. of Basic Medical Sciences, Faculty of Medicine and Surgery, School of Medicine, University of Bari, Italy; [2]Unit of Dermatology and Venereology, Department of Biomedical Sciences and Human Oncology, University of Bari, Italy; [3]Dept. of Biochemistry and Molecular Biology B, Faculty of Medicine and Surgery, School of Medicine, University of Murcia, Spain; [4]National Cancer Research Center "Giovanni Paolo II", Bari, Italy

Received July 20, 2012 – Accepted November 8, 2012

We studied the behaviour of three novel human sporadic melanoma cell lines (hmel1, hmel9, hmel11) extracted from tumors with different degrees of malignancy, concerning the cell signalling pathways controlled by MC1R, BRAF, NRAS and β-catenins. The novel cell lines were compared to metastatic cell lines (HBL, LND1), wild type (wt) for MC1R and BRAF genes, that have been extensively characterised and were used as control. All the novel cell lines have silent or no MC1R mutations even though MC1R signalling is severely impaired. Conversely, they harbour BRAF mutations at the V600 residue. These mutations determine a constitutive ERK phosphorylation in all the three cell lines. Our new melanoma cell lines were BRAF mutated in hetero- and homozygosis, even with a wild type MC1R, and unresponsive to NDP-MSH treatment. Quantity and subcellular localization of β-catenin were analyzed in both novel and control cell lines. In HBL and LND1 there were high levels of β-catenin distributed in the cytoplasm/nucleus, while in the novel melanoma cell lines β-catenins were less abundant and seemed to be located at the plasma membrane/cytoplasm and absent in the nucleus. We sequenced β-catenin cDNA for all the melanoma cell lines, and found mutations in HBL, LND1 and hmel1, while hmel9 and hmel11 were wt. We found that β-catenin levels were not influenced by the RAS/RAF/MAPK pathway because inhibition with PD98059 (a MEK inhibitor) did not produce any effect on β-catenin stability and/or localization.

Melanoma is one of the skin tumours showing an increasing incidence in the general population (1), and is among the particularly severe forms of skin cancers because it is resistant to chemotherapy and has a high metastatic potential.

Recent findings of genetic alterations involving cell cycle regulatory genes and mutations in cell signalling pathways in melanoma have prompted much research with the aim of obtaining novel targeted therapies. Mostly, melanoma is a sporadic disease but a hereditary component has been found. High penetrance genes such as CDKN2A and CDK4 are able to induce melanomas and additional cancers, and are associated to a familial cancer risk (2-3). They are rarely found in the population and they encode for proteins that act as regulators for the

Key words: melanoma, bcatenin, RAS/RAF/MAPK, MC1R

Mailing address: G. Guida, PhD,
Dept. of Basic Medical Sciences,
Faculty of Medicine and Surgery,
School of Medicine,
University of Bari, Italy
Tel.: +39 080 5448556 Fax: +39 080 5448568
e-mail: g.guida@biolgene.uniba.it

0393-974X (2013)

cell cycle.

For sporadic melanoma, the most representative low penetrance gene is MC1R, whose variants are widely distributed in the population (4-5), but a leading role is played by BRAF, a target for therapeutical approaches (6), and β-catenins that seem to control the melanoma potential to metastasize (7-8). The human MC1R gene is highly polymorphic, more than 100 non-conservative variants having been described, and some of its genetic forms (RHC) are characterised by a lower ability to generate cAMP as compared to the wt receptor. The MC1R impairment could be due to a defective cAMP coupling (R294H), or to deficient trafficking to the plasma membrane (R151C, R160W) (9-10). MC1R activation by MSH induces melanogenesis, enhancing tyrosinase expression (11). This enzyme is regulated by MITF, that is modulated by several signalling pathways (12), one of which is the cAMP pathway induced by MSH.

Alterations that determine a constitutive activation of the RAS/RAF/MAPK pathway are commonly detected in melanoma, but are also present in a high percentage of nevi. These mutations seem to be important but not sufficient to induce tumoral transformation (13). The BRAF gene encodes for a key protein in the RAS/RAF/MAPK pathway in melanocytes (14). This pathway controls cell proliferation or differentiation. Most of the BRAF mutations detected in melanoma are located in the BRAF kinase domain, and act by increasing the constitutive activity on MEK and MAPK (15). The most common BRAF activating substitution occurs at the V600 amino acid residue; the most frequent mutations are V600E (1799T>A), followed by V600K (1798_1799delinsAA) and V600R (1798_1799delinsAG) (16).

The Wnt/β-catenin signalling pathway has a leading role in the control of melanocyte proliferation, differentiation and motility. Its activation is determined by binding of Wnt glycoproteins family members to the Frizzled/Low-density-lipoprotein-receptor on the outer cell surface, and this inhibits glycogen synthetase kinase 3β (GSK3β). This inhibition decreases the amount of β-catenin phosphorylated by GSK3β undergoing proteasome degradation, and leads to an accumulation of the unphosphorylated form of β-catenin in the cytoplasm (17). The massive quantity of cytoplasmic β-catenin promotes its translocation to the nucleus, where it interacts with the TCF/LEF1 transcription factor to activate the expression of downstream genes involved in cell proliferation and differentiation, such as CCND1 and others (18). Recent works have reported that in some human melanomas, RAS/RAF/MAPK inhibition in BRAF mutated (V600E) melanoma cells leads to alterations in the Wnt/β-catenin pathway (19). Wnt/β-catenin pathway deregulation has been implicated at various levels in cell growth and tumorigenesis but the effects of its involvement are still unclear.

In this work we studied the behaviour of three novel human sporadic melanoma cell lines, selected in our laboratory, concerning the cell signalling pathways controlled by MC1R, BRAF, NRAS and β-catenins, as compared to metastatic cell lines that have been extensively characterised and were used as control. In this study we focused on the possibility of identifying subsets of sporadic melanomas with a similar behaviour, in order to focus on critical points that could help to devise future targeted therapies.

MATERIALS AND METHODS

Materials

Igepal CA-630, BSA, EDTA, PMSF, PD98059, TPA, and the bicinchoninic acid were from Sigma (St. Louis, MO), as also the synthetic αMSH analogue [Nle^4, D-Phe^7]-aMSH (NDP-MSH). The radioligand ^{125}I-NDP-MSH, specific activity 2000 Ci/mmol, and a cAMP radioimmunoassay kit were from Amersham Pharmacia Biotech (Little Chalfont, Buckinghamshire, UK). Other reagents were from Merck (Darmstadt, Germany) or Sigma (St. Louis, MO). The antibodies were from BD Biosciences (NJ, USA), from Santa Cruz (Santa Cruz Biotechnology, Santa Cruz CA, USA) or Molecular Probes (Invitrogen, Carlsbad, CA, USA).

Cell cultures

The hmel1, hmel9, hmel11 cell lines have been obtained from biopsy samples of a metastasis (hmel1) and two primary sporadic melanomas (hmel9 and hmel11). Hmel1, hmel9 and hmel11 have already been described in Zanna et al. (20). HBL, LND1 were a kind gift of Prof. G. Ghanem (University of Brussels). Cells were harvested at 37°C, in a 5% CO_2 atmosphere and cultured in Dulbecco's modified Eagle's medium enriched with 10% fetal bovine serum, 100 U/ml penicillin, 100 mg/ml streptomycin. The RAS/RAF/

MAPK pathway was stimulated or inhibited using 200 nM TPA or 50 μM PD98059 for the time intervals indicated.

Genotyping

For MC1R, NRAS and BRAF, the DNA/RNA extraction, retrotranscription and sequencing were performed as described in Zanna et al. (20). For bcatenin, the total RNA was extracted as previously described (20) and retrotranscribed using the First strand cDNA syntesis kit (Invitrogen). The cDNA was then amplified using the following primers: Febcat: CAATGGCTACTCAAGCTG; Rebcat: ACAGCTAAAGGATGATTTAC; F2bcat: CTAGTTCAGTTGCTTGTTC; R2bcat: CATAAAACAACACAGAATCC; BCATFw: CTTACTGGCCATCTTTAAG; BCARRv: ATCCCGAGCTAGGATGTG. All the PCR amplicons were analysed by direct sequencing at the National Cancer Research Center "Giovanni Paolo II", Bari, Italy.

Functional assays

All experiments were performed in triplicate dishes. Radioligand binding was carried out using 10^{-10} M ^{125}I-NDP-MSH, as described in Sanchez-Mas et al. (21). Functional coupling assays were performed as previously described (22) using serum-starved cells stimulated for 30 min with 10^{-7} M NDP-MSH. cAMP was measured with a radioimmunoassay kit (Amersham) as per instructions.

Cell fractioning

Cell fractioning was performed as previously described (5), with minor modifications. Cells were harvested to 70% confluence in T25. They were washed twice with ice cold PBS and detached with trypsin, pelletted and resuspended in 0.5 ml of lysis buffer (10 mm Tris-HCl, pH 7.4, 10 mm NaCl, 3 mm $MgCl_2$, 0.3% Igepal, 1 mM phenylmethylsulfonyl fluoride), sonicated, and incubated on ice for 30 min. They were then centrifuged at 500×*g* for 5 min to pellet nuclei. The supernatants were used as the cytosolic fraction after 13000xg centrifugation for 5 min at 4°C. Pellets were washed 5 times in lysis buffer without igepal, and finally resuspended in lysis buffer with 1% igepal and vortexed. Nuclear membranes were lysed by igepal containing lysis buffer and pelletted at 13000xg for 5 min at 4°C. The supernatant was the nuclear fraction. To ensure complete membrane breakage the protein fraction was frozen with liquid nitrogen and thawed to 37°C, 3 times. The purity of the nuclear and cytosolic fractions was verified by the presence or absence of immunoreactive bands corresponding to GAPDH after immunoblotting with anti-GAPDH antibodies (AbD Serotec, MorphoSys, UK).

Western blotting

Treated cells were washed with phosphate buffered saline (PBS) and lysed in solubilization buffer (10 mM phosphate buffer pH 7, 1% Igepal CA-640, 0.1 mM EDTA and 0.1 mM PMSF). The protein concentration in cell lysates was determined by the bicinchoninic acid method. The samples were pelletted at 12000xg for 20 min, at 4°C. Supernatants were used for western blotting. For SDS–PAGE, 30 mg total protein were loaded per lane. Electrophoresis and western blots were performed as described (21, 23). Samples were incubated in sample buffer (60 mM Tris–HCl, pH 6.8, 5% glycerol, 3% SDS, 2.5% bromophenol blue, containing 1M b-mercaptoethanol) and loaded. Detection was performed using anti-βcatenin monoclonal antibodies (BD biosciences), anti-βactin monoclonal antibodies (Sigma) or anti-ERK/anti-pERK polyclonal antibodies (Santa Cruz) as required, and double-stained with HRP-conjugated anti-mouse (Molecular probes) or anti-rabbit secondary antibodies (Santa Cruz) stained with a chemiluminescent substrate (Pierce, Thermoscientific).

Confocal microscopy

Cells grown on coverslips were washed with PBS, fixed with 4% paraformaldehyde, and blocked with 20 mM glycine. They were permeabilized with 0.5% Igepal CA-640 in PBS. The β-catenin was stained with a mouse anti-bcatenin antibody in PBS containing 1% BSA. Rabbit anti-mouse Alexa 568-conjugated antibody (Molecular Probes) was used as secondary antibody, in PBS containing 1% BSA. Incubations were performed at 4°C. Samples were examined with a Nikon confocal microscope (Nikon Corporation, Tokyo, Japan).

RESULTS

MC1R genotype and activity

The hmel1, hmel9 and hmel11 cell lines were screened for their MC1R genotype. All three cell lines were wt for the melanocortin 1 receptor gene. The only mutation found was a silent T314T (nucl. 942 A/G) in heterozygosis in hmel11 and hmel9, while hmel1 was wt/wt (20) (Fig. 1A). MC1R activated cAMP synthesis in response to NDP-MSH stimulation, reaching a maximum at 30 min stimulation, while by 180 min stimulation cAMP levels decreased due to receptor desensitization (24). The ability to generate cAMP in response to NDP-MSH treatment was tested for the still uncharacterized melanoma cell lines. The HBL and LND1 cell lines, wt for MC1R, were used as control and respond efficiently to NDP-MSH activation. The cAMP assay (Fig. 1B) revealed an impaired

a

Cell line	MC1R protein	MC1R cDNA
HBL	WT/WT	-
LND1	WT/WT	-
Hmel1	WT/WT	-
Hmel9	T314T/ T314T	nucl. 942 A/G
Hmel11	T314T/ T314T	nucl. 942 A/G

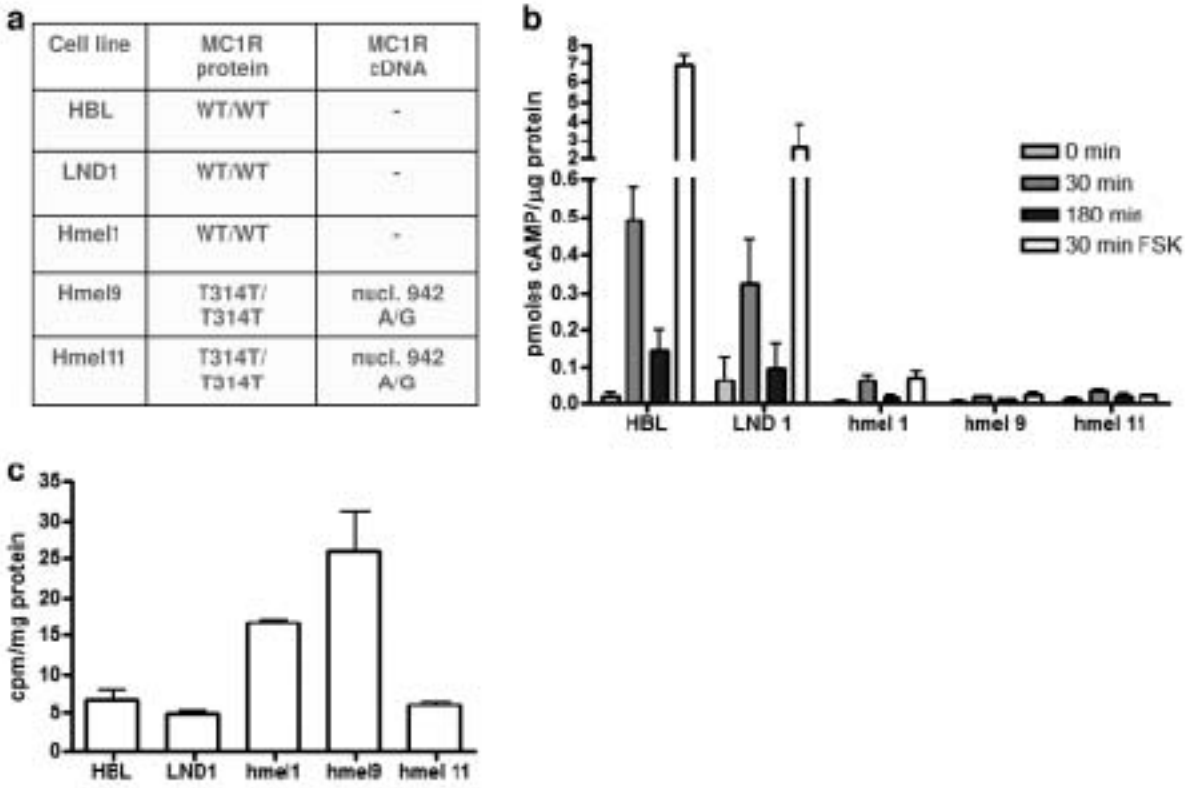

Fig. 1. *MC1R genotype, response to NDP-MSH treatment and ^{125}I-NDP-MSH binding in melanoma cells.* ***A)*** *MC1R genotype of the melanoma cell lines.* ***B)*** *cAMP assay performed on the novel melanoma cell lines hmel1, hmel9, hmel11 and on HBL and LND1, used as controls. Cells were treated with 10^{-7}M NDP-MSH at different time intervals (0 min, 30 min, 180 min) or with 10^{-5}M forskolin (positive control for AC activation) for 3 min. Values are expressed as picomoles cAMP/mg protein.* ***C)*** *^{125}I-NDP-MSH binding to melanoma cell lines. Cells were treated with 10^{-10}M ^{125}I-NDP-MSH and with 10^{-9}M NDP-MSH for 1 h.*

MC1R coupling to the cAMP pathway in all the novel melanoma cell lines, although the receptor was wt. The hmel9 and hmel11 cell lines were not able to respond to NDP-MSH, despite expressing a wt MC1R. Hmel1, although possessing a wt receptor, showed a very low response to NDP-MSH stimulation, with a slight peak of stimulation after 30 min of NDP-MSH treatment and after forskolin (an AC activator) induction. In any case, the hmel1 response featured a very low intensity as compared to that of HBL and LND1.

The MC1R ability to bind to ^{125}I-NDP-MSH was tested to detect whether the MC1R impairment was due to a low level of receptor expression on the plasma membrane, that could determine an impaired binding to the hormone. Fig. 1C shows that hmel1, hmel9 and hmel11 had the highest number of MC1 receptors expressed on the plasma membrane per microgram of protein and a greater MSH binding ability with respect to the HBL and LND1 cell lines. Therefore, these results show that in the cells unresponsive to NDP-MSH treatment (hmel1, hmel9, hmel11), the impaired MC1R coupling to cAMP synthesis was not ascribable to a low quantity of NDP-MSH binding sites exposed on the cell surface.

BRAF exon 15 mutations and activation of the RAS/RAF/MAPK pathway

To detect a constitutive activation of the RAS/

a

Cell line	NRAS	BRAF exon15 protein	BRAF exon15 cDNA
HBL	WT/WT	WT/WT	-
LND1	WT/WT	WT/WT	-
Hmel1	WT/WT	V600K/WT	1798_1799 delinsAA
Hmel9	WT/WT	V600R/V600R	1798_1799 delinsAG
Hmel11	WT/WT	V600R/WT	1798_1799 delinsAG

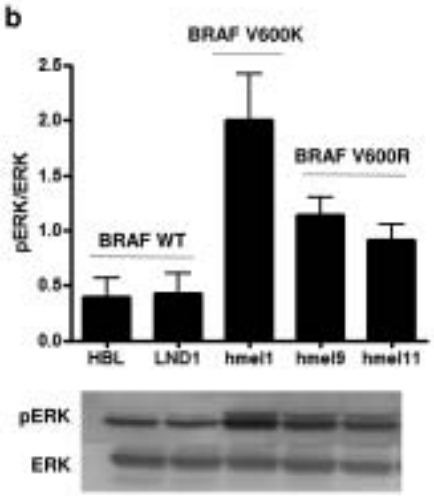

Fig. 2. *The RAS/RAF/MAPK pathway in melanoma cell lines.* ***A)*** *NRAS and BRAF exon 15 genotype in the melanoma cell lines.* ***B)*** *ERK1/2 phosphorylation levels in melanoma cell lines analyzed by western blotting using antibodies against phosphorylated ERK1/2 on Thr202/Tyr204. Their densitometric profiles were normalized for that of the total ERK protein.*

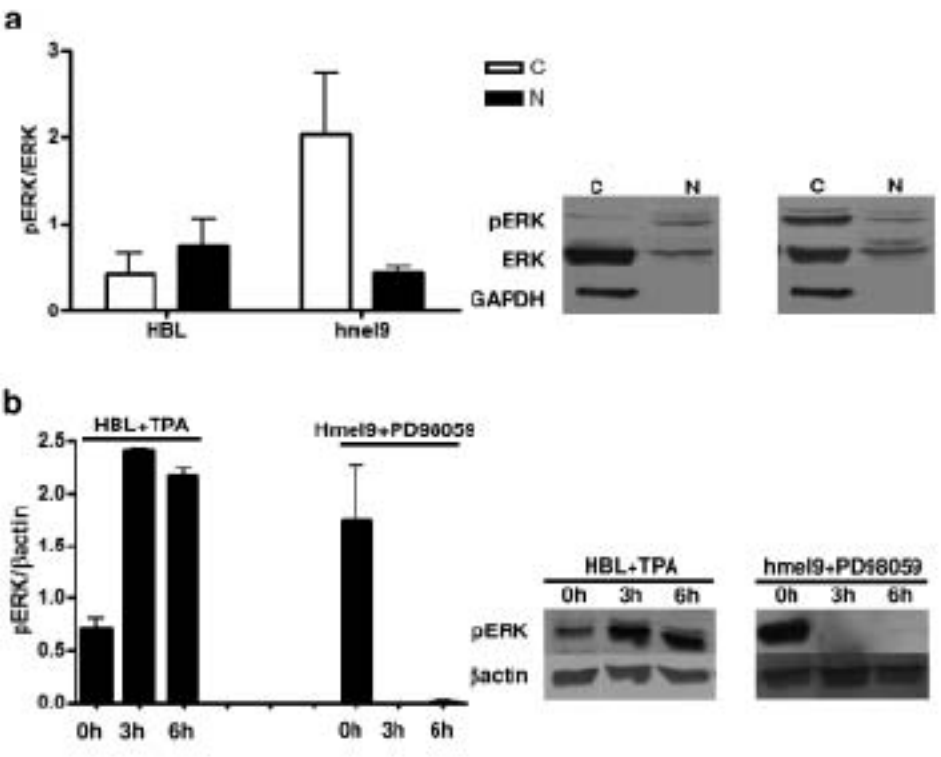

Fig. 3. *pERK analyses on different subcellular fractions of hmel9 and HBL melanoma cell lines and the response to activators or inhibitors.* ***A)*** *pERK western blotting analyses on cytoplasmic and nuclear fractions of hmel9 and HBL melanoma cell lines extracts, normalized for ERK2. The purity of the fractions was determined with anti-GAPDH antibodies against the cytoplasmic fraction.* ***B)*** *The hmel9 melanoma cell line in the presence of MEK inhibitor PD98059 50 μM was analysed as compared to a control (HBL cell line) treated with a RAS/RAF/MAPK pathway activator (TPA 200 nM) at different time intervals (0 h, 3 h, 6 h).*

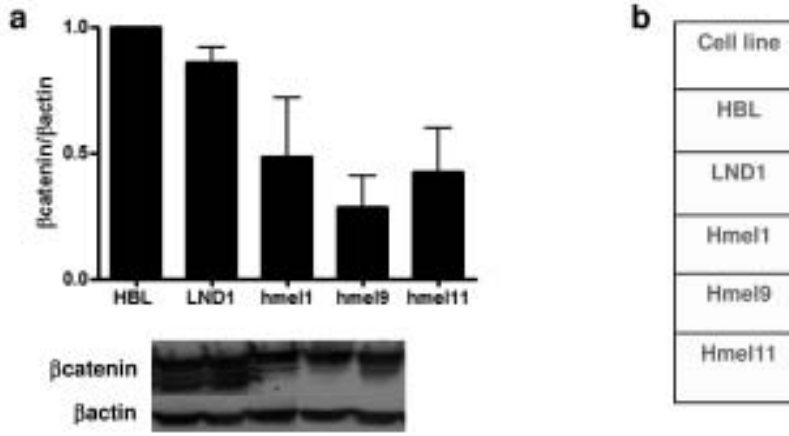

b

Cell line	βcatenin protein	βcatenin cDNA
HBL	S33Y	Nucl. 100 C>A
LND1	S33Y	Nucl. 100 C>A
Hmel1	W383C	Nucl. 1149 G>T
Hmel9	WT/WT	-
Hmel11	WT/WT	-

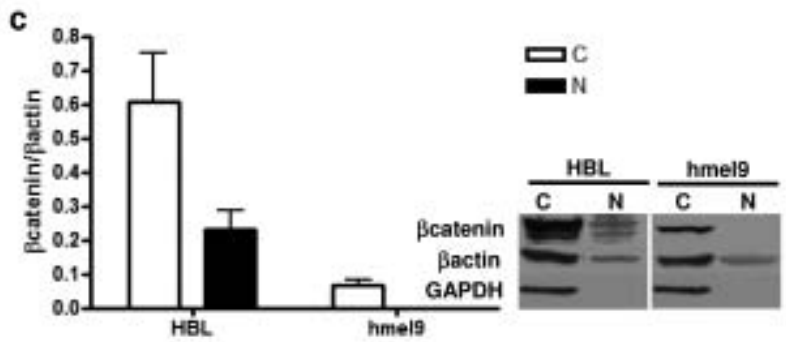

Fig. 4. *Quantification and localization of β-catenin by western blotting and sequence analyses in all the melanoma cell lines.* ***A)*** *β-catenin western blotting densitometric profiles normalised for bactin as reference gene and HBL as control cell line.* ***B****. β-catenin genotype of melanoma cell lines.* ***C)*** *β-catenin western blotting densitometric profiles on cytoplasmic (C) and nuclear (N) fractions obtained from hmel9 and HBL cell lines, normalised for bactin as reference gene. GAPDH was used to control the purity of the fractions.*

RAF/MAPK pathway, we sequenced the BRAF exon 15, where a "hot spot" is found at nucleotides 1798-1799 of the coding sequence, and NRAS in all the cell lines. HBL and LND1 were not mutated in BRAF at the V600 residue and NRAS, while the three novel melanoma cell lines had a BRAF mutation at the V600 residue and were wt for NRAS (Fig. 2A). Hmel1 had a BRAF mutation V600K (1798_1799delinsAA) in heterozygosis, hmel9 had a BRAF mutation V600R in homozygosis (1798_1799delinsAG) (20), like hmel11, that had a mutation V600R (1798_1799delinsAG) in heterozygosis (Fig. 2A).

To determine the effect of BRAF mutations on the overall RAS/RAF/MAPK pathway, the basal levels of phosphorylated ERK1/2 (pERK1/2) were analysed by western blotting using antibodies specific for phosphorylated ERK1/2 on the Thr202/Tyr204 residues. The resulting bands were compared with the total ERK1/2 levels. The ratios obtained are shown in Fig. 2B. In all the cell lines bearing V600 BRAF mutations, the ERK1/2 phosphorylation levels were higher than in the control cell lines HBL and LND1, that did not have mutations in BRAF exon 15 or NRAS. Hmel1, hmel9, and hmel11 showed a high basal ERK1/2 activation and, consequently, a constitutively active RAS/RAF/MAPK pathway.

The BRAF mutations found behave as dominant positive mutations, since the RAS/RAF/MAPK pathway was activated by BRAF V600 mutations

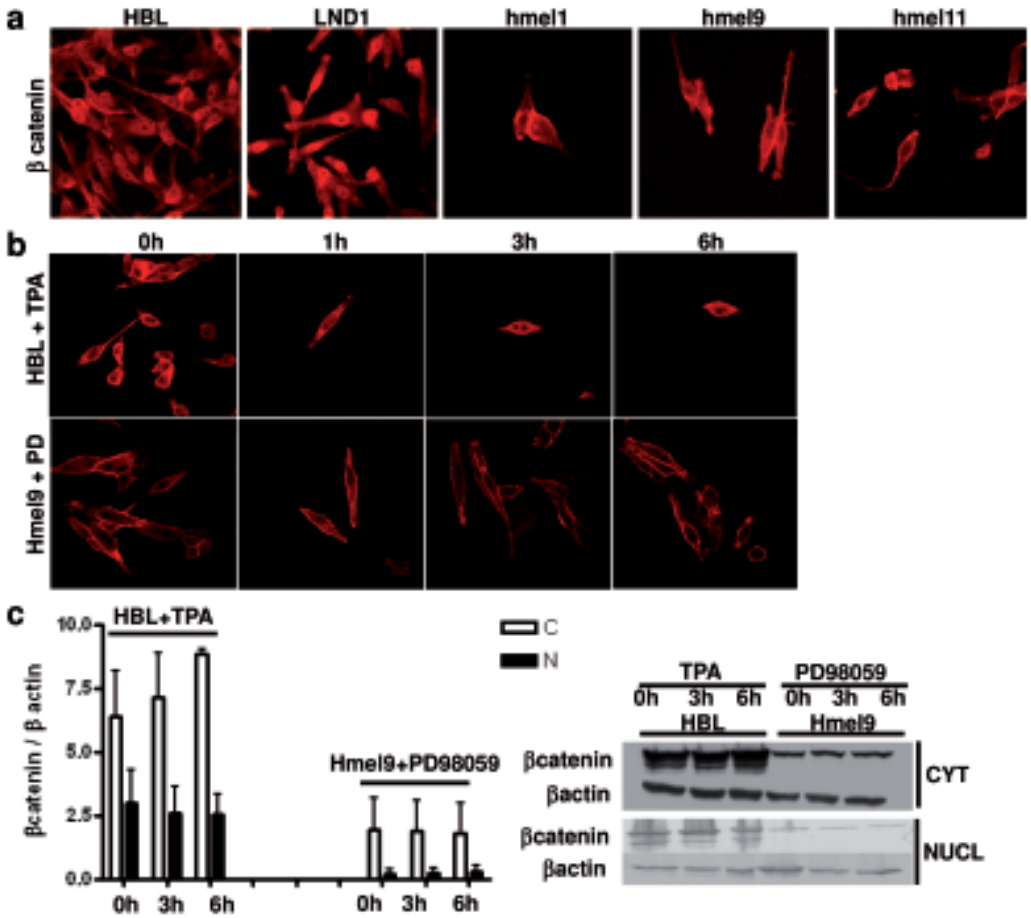

Fig. 5. *β-catenin localization in melanoma cell lines. **A**) Confocal microscopy of β-catenin localization in melanoma cell lines. **B**) Confocal analyses using β-catenin antibodies in hmel9 and HBL, after PD98059 (50 μM) or TPA (200nM) treatment for different time intervals. **C**) Western blotting densitometric profiles using β-catenin antibodies in hmel9 and HBL, after PD98059 (50 μM) or TPA (200 nM) treatment for different time intervals. They were normalized for bactin as reference gene.*

both in heterozygosis and homozygosis. Moreover, the BRAF mutations V600K and V600E seemed to have a more potent effect than V600R in activating ERK1/2 phosphorylation (data not shown).

The ERK and pERK distribution in the nucleus and the cytoplasm was studied by western blotting experiments with anti-ERK and anti-pERK antibodies on the nuclear and cytoplasmic purified fractions. The absence of cytoplasmic contamination on the nuclear fraction was tested by western blotting with an anti-GAPDH antibody and by LDH activity assay (data not shown).

As previously described, HBL and hmel9 behave differently as regards the RAS/RAF/MAPK pathway activation. Moreover, they derive from melanoma lesions with different degrees of aggressiveness, since HBL derived from a metastasis whereas hmel9 was extracted from a primary lesion. For these reasons, only HBL and hmel9 were used to detect whether pERK1/2 had a different subcellular distribution. We found an asymmetrical pERK1/2 distribution in the nucleus as compared to the cytoplasm in the two cell lines examined. In particular, hmel9 showed pERK1/2 localized in the cytoplasm with only a

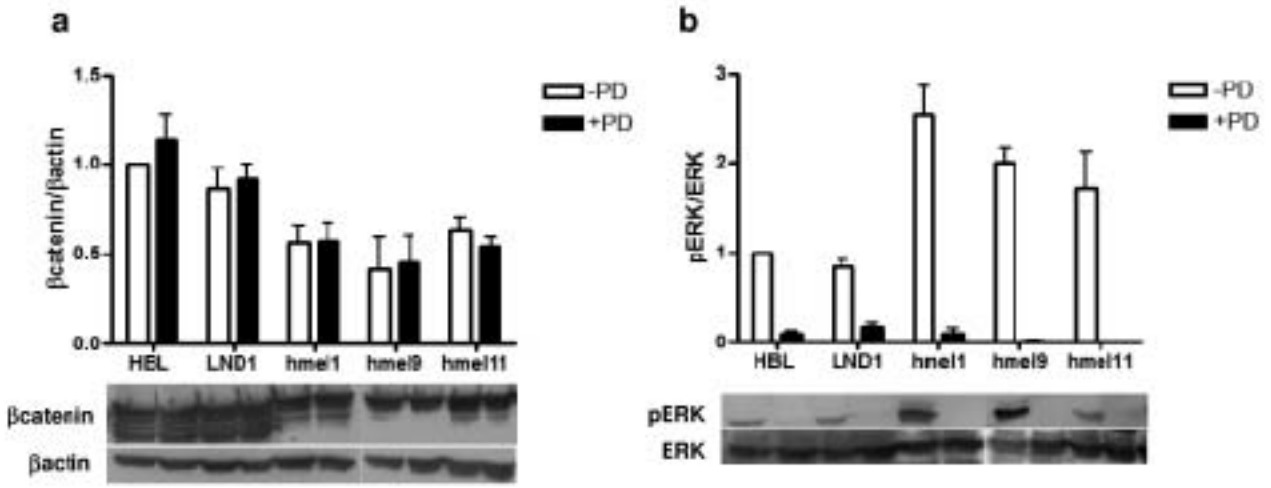

Fig. 6. *Western blotting analyses of β-catenin levels and their relationship with ERK phosphorylation.* ***A)*** *Western blotting using anti-β-catenin antibodies in all the melanoma cell lines in the presence or absence of the MEK inhibitor PD98059 (50 μM). Treatments were performed for 3 h. Values were normalized for bactin as reference gene and for HBL as control cell line.* ***B)*** *Western blotting densitometric profiles using anti pERK antibodies in all the melanoma cell lines in the presence or absence of the MEK inhibitor PD98059 (50 μM). Densitometric profiles were normalized for the total ERK protein and for HBL as control cell line.*

small part in the nucleus, while HBL presented a similar pERK1/2 quantity in both fractions, with a slightly greater localization in the nucleus (Fig. 3A).

Because the BRAF mutation V600R, that constitutively activates hmel9 for the RAS/RAF/MAPK pathway, which is not present in HBL, hmel9 were treated with the MEK inhibitor PD98059 (50 μM), and in HBL the pathway was positively activated using TPA (200nM). The results indicated that both TPA and PD98059 were effective after 3 h of stimulation (Fig. 3B).

β-CATENIN localization and expression

β-catenin localization in our melanoma cell lines was analysed as a marker of its effective role in cell adhesion or transcription. β-catenin abundance and distribution studies were performed by western blotting and confocal microscopy. There were found to be lower β-catenin levels in hmel1, hmel9 and hmel11 total cell extracts than in HBL and LND1 (Fig. 4A). β-catenin cDNA was sequenced for all the melanoma cell lines. We found a β-catenin mutation in HBL and LND1 (Fig. 4B) by a 100C>A transversion in heterozygosis that caused a missense mutation TCT(S33)>TAT(Y33). The Ser33 mutation to Tyr33 abolished a phosphorylation site for GSK3b, reducing its susceptibility to degradation by proteasomes (25), and it was seen to be dominant positive since it increased β-catenins levels in heterozygosis (Fig. 4A). Conversely, hmel1 was mutated in heterozygosis by a 1149G>T transversion, responsible for a missence mutation TGG(W383)>TGT(C383) (Fig. 4B). This amino acid change did not seem to determine any macroscopic effect on protein stability and localization as compared to the wt. This 1149G>T transversion could be considered either a polymorphism or a recessive mutation. Hmel9 end hmel11 were wt for β-catenin.

Western blotting analyses on β-catenin subcellular distribution were performed on HBL (β-catenin mutated) and hmel9 (wt for β-catenin), indicating a different distribution in the nucleus and cytoplasm (Fig. 4C). Confocal microscopy studies on β-catenin localization showed that in all the novel cell lines it was mostly located at the plasma membrane (Fig. 5A). On the contrary, the melanoma cell lines HBL and LND1 had β-catenins located mainly in the nucleus and cytoplasm, suggesting a main transcriptional role for β-catenin in these cells

(Fig. 5A).

To check whether β-catenin differences in localization were due to hyper-phosphorylated ERK in BRAF mutated cell lines, we analyzed β-catenin localization in BRAF mutated and non-mutated cell lines.

Cells with constitutively active RAS/RAF/MAPK (hmel9), in the presence of a MEK inhibitor PD98059, were analysed and compared to a control (HBL) treated with a RAS/RAF/MAPK pathway activator (TPA). In both cases the β-catenin abundance and cellular localization did not seem to change significantly after 1h, 3h and 6h treatment, analyzed by confocal microscopy (Fig. 5B) and by western blotting (Fig. 5C).

We also studied the effects of NDP-MSH on β-catenin quantity and localization. In all the five cell lines analysed by immunocytochemistry, a stimulation time course with 10^{-7} M NDP-MSH (0 min, 30 min, 60 min, 180 min) did not significantly change the β-catenin subcellular localization and its overall abundance (data not shown).

To determine whether β-catenin levels depended on ERK phosphorylation, crude extracts of all the cell lines, previously treated with/without 50 mM PD98059 for 3 h, were analyzed and compared by Western blotting analyses. In all the cell lines β-catenin levels in the crude extracts remained constant even after the complete inhibition of ERK phosphorylation (Fig. 6A). As control, PD98059 treatment efficiently lowered the ERK1/2 phosphorylation levels in all the cell lines (Fig. 6B).

DISCUSSION

Melanocyte differentiation is regulated by various stimuli, many of which drive melanogenesis activation. One of the most important is α-MSH activation of MC1R, that acts through cAMP. This hormone binds on the cell surface to MC1R, a well known low penetrance gene for melanoma. MC1R mutations that abolish this activity have been associated with an increased risk of developing melanoma (26). Even when expressing wt MC1R, as in hmel1, hmel9 and hmel11, the cAMP pathway may be impaired, by still uncharacterised mechanisms. Hmel1, hmel9 and hmel11 had the most impaired MC1R coupling to cAMP synthesis despite showing the highest number of NDP-MSH binding sites on the cell surface (Fig. 1C). For this reason, the impairment was not ascribable to a low MC1R distribution or to a poor NDP-MSH binding on the cell surface. MC1R impairment was described by Dumaz and Marais (27) for cell lines with a constitutively active RAS/RAF/MAPK pathway. Our results confirm this behaviour, showing a BRAF mutation in hetero and homozygosis and an impairment of MC1R coupling to cAMP production, even if our novel sporadic melanoma cell lines expressed a wt MC1R (Fig. 1, 2). Alternatively, the MC1R impairment could be due to a poor functionality of adenylyl cyclase, that could explain the low levels of cAMP production after both NDP-MSH and Forskolin stimulation (Fig. 1B).

Wnt/β-catenin pathway deregulation has been involved at various levels in cell growth, tumorigenesis and migration (28). The β-catenin subcellular localization is important to determine the predominant role of this protein in mediating cell-cell interactions at the level of the plasma membrane or in regulating gene expression in the nucleus.

The mutation of Ser33 that is converted to Tyr33 has been shown by Morin et al. (25) to determine a 6-fold activation of β-catenin-Tcf signalling, probably with a massive bcatenin nuclear localization, by abolishing the GSK-3β phosphorylation site. In the cell lines HBL and LND1 harboring this mutation, the β-catenin levels were higher than in hmel1, hmel9 and hmel11. Moreover, HBL and LND1 β-catenins were mainly localized in the nucleus rather than close to the plasma membrane like in hmel1, hmel9 and hmel11 (Fig. 5A). We found that in hmel1, β-catenin resulted mutated in the residue Trp383 to Cys383. This mutation has never previously been described. This β-catenin variant could be considered either a polymorphism or a recessive mutation.

Treatment of hmel1, hmel9 and hmel11 with NDP-MSH had no effect on the bcatenin quantity and localization (data not shown). This could probably be an effect of the MC1R uncoupling to the cAMP signalling in these cell lines. However, NDP-MSH treatments did not seem to have any effect on β-catenin in the HBL and LND1 cell lines, which produce cAMP in response to NDP-MSH treatment. This treatment should increase β-catenin stability, as described in Bellei et al. (29), through

PKA direct phosphorylation but it was ineffective in the HBL and LND1 cell lines. This could be due to the β-catenin mutation on Ser33 that increases its stability regardless of β-catenin phosphorylation by PKA. Moreover, neither the RAS/RAF/MAPK pathway activation nor inhibition were able to change the β-catenin abundance and localization, indicating that the RAS/RAF/MAPK pathway was unable to influence β-catenin stability in the cell lines analyzed.

In conclusion, we isolated three novel melanoma cell lines and characterized them for some melanogenic and proliferation signaling pathways, in which the common feature was the BRAF mutation V600, the MC1R being wt. Moreover, even if the three novel cell lines present a similar β-catenin quantity and localization, only the hmel1 cell line (extracted from a metastasis) had a β-catenin mutation. According to the literature, it seems that these genes are really important in defining the aggressiveness of melanoma, and that β-catenin has a leading role (28, 30). Due to the extreme heterogeneity of melanoma cells behaviour, these novel cell lines could be a useful tool to test new drugs targeting melanoma because the experimental system is particularly homogeneous.

ACKNOWLEDGEMENTS

The authors would like to thank Dr. G. Ghanem for providing the HBL and LND1 melanoma cell lines, Prof. J.C. García-Borrón for the precious collaboration, and Dr. N. Cassano and Dr. M. Scivetti for technical assistance. Some of the experiments were performed by Dr. Zanna during a UNESCO-L'Oreal FWIS Fellowship. This work was sponsored by grants from "Fondazione Cassa Di Risparmio di Puglia".

REFERENCES

1. Diepgen TL, Mahler V. The epidemiology of skin cancer. Br J Dermatol 2002; 146(61):1-6.
2. Cannon-Albright LA, Goldgar DE, Meyer LJ, et al. Assignment of a locus for familial melanoma, MLM, to chromosome 9p13-p22. Science 1992; 258(5085):1148-52.
3. Healy E, Sikkink S, Rees JL. Infrequent mutation of p16INK4 in sporadic melanoma. J Invest Dermatol 1996; 107:318-21.
4. Box NF, Duffy DL, Irving RE, et al. Melanocortin-1 receptor genotype is a risk factor for basal and squamous cell carcinoma. J Invest Dermatol 2001; 116(2):224-9.
5. Pérez Oliva AB, Fernéndez LP, Detorre C, et al. Identification and functional analysis of novel variants of the human melanocortin 1 receptor found in melanoma patients. Hum Mutat 2009; 30(5):811-22.
6. Ravnan MC, Matalka MS. Vemurafenib in Patients With BRAF V600E Mutation-Positive Advanced Melanoma. Clin Ther 2012. [Epub ahead of print]
7. Damsky WE, Curley DP, Santhanakrishnan M, et al. β-catenin signaling controls metastasis in Braf-activated Pten-deficient melanomas. Cancer Cell 2011; 20(6):741-54.
8. Gallagher SJ, Rambow F, Kumasaka M, Champeval D, Bellacosa A, Delmas V, Larue L. Beta-catenin inhibits melanocyte migration but induces melanoma metastasis. Oncogene 2012; 10:229.
9. Sánchez-Laorden BL, Jiménez-Cervantes C, García-Borrón JC. Regulation of human melanocortin 1 receptor signaling and trafficking by Thr-308 and Ser-316 and its alteration in variant alleles associated with red hair and skin cancer. J Biol Chem 2007; 282(5):3241-51.
10. Sánchez-Laorden BL, Herraiz C, Valencia JC, Hearing VJ, Jiménez-Cervantes C, García-Borrón JC. Aberrant trafficking of human melanocortin 1 receptor variants associated with red hair and skin cancer: Steady-state retention of mutant forms in the proximal golgi. J Cell Physiol 2009; 220(3):640-54.
11. García-Borrón JC, Sánchez-Laorden BL, Jiménez-Cervantes C. Melanocortin-1 receptor structure and functional regulation. Pigment Cell Res 2005; 18(6):393-410.
12. Vance KW, Goding CR. The transcription network regulating melanocyte development and melanoma. Pigment Cell Res 2004; 17(4):318-25.
13. Pollock PM, Harper UL, Hansen KS, et al. High frequency of BRAF mutations in nevi. Nat Genet 2003; 33(1):19-20.
14. Garnett MJ, Marais R. Guilty as charged: B-RAF is a human oncogene. Cancer Cell 2004; 6(4):313-9.

15. Davies H, Bignell GR, Cox C, et al. Mutations of the BRAF gene in human cancer. Nature 2002; 417(6892):949-54.
16. Hocker T, Tsao H. Ultraviolet radiation and melanoma: a systematic review and analysis of reported sequence variants. Hum Mutat 2007; 28(6):578-88.
17. Bullions LC, Levine AJ.The role of beta-catenin in cell adhesion, signal transduction, and cancer. Curr Opin Oncol 1998; 10(1):81-7.
18. Shtutman M, Zhurinsky J, Simcha I, Albanese C, D'Amico M, Pestell R, Ben-Ze'ev A. The cyclin D1 gene is a target of the beta-catenin/LEF-1 pathway. Proc Natl Acad Sci USA 1999; 96(10):5522-7.
19. Delmas V, Beermann F, Martinozzi S, et al. Beta-catenin induces immortalization of melanocytes by suppressing p16INK4a expression and cooperates with N-Ras in melanoma development. Genes Dev 2007; 21(22):2923-35.
20. Zanna P, Maida I, Turpin Sevilla MC, et al. Molecular characterization of novel melanoma cell lines. J Biol Regul Homeost Agents 2011; 25(2):239-47.
21. Sánchez Más J, Olivares Sánchez C, Ghanem G, Haycock J, Lozano Teruel JA, García-Borrón JC, Jiménez-Cervantes C. Loss-of-function variants of the human melanocortin-1 receptor gene in melanoma cells define structural determinants of receptor function. Eur J Biochem 2002; 269(24):6133-41.
22. Sánchez-Más J, Hahmann C, Gerritsen I, García-Borrón JC, Jiménez-Cervantes C. Agonist-independent, high constitutive activity of the human melanocortin 1 receptor. Pigment Cell Res 2004; 17(4):386-95.
23. Sánchez-Laorden BL, Sánchez-Más J, Martínez-Alonso E, Martínez-Menárguez JA, García-Borrón JC, Jiménez-Cervantes C. Dimerization of the human melanocortin 1 receptor: functional consequences and dominant-negative effects. J Invest Dermatol 2006; 126(1):172-81.
24. Sánchez-Más J, Guillo LA, Zanna P, Jiménez-Cervantes C, García-Borrón JC. Role of G protein-coupled receptor kinases in the homologous desensitization of the human and mouse melanocortin 1 receptors. Mol Endocrinol 2005; 19(4):1035-48.
25. Morin PJ, Sparks AB, Korinek V, Barker N, Clevers H, Vogelstein B, Kinzler KW. Activation of beta-catenin-Tcf signaling in colon cancer by mutations in beta-catenin or APC. Science 1997; 275(5307):1787-90.
26. Savage SA, Gerstenblith MR, Goldstein AM, Mirabello L, Fargnoli MC, Peris K, Landi MT. Nucleotide diversity and population differentiation of the melanocortin 1 receptor gene, MC1R. BMC Genet 2008; 9:31.
27. Dumaz N, Hayward R, Martin J, et al. In melanoma, RAS mutations are accompanied by switching signaling from BRAF to CRAF and disrupted cyclic AMP signaling. Cancer Res 2006; 66(19):9483-91.
28. Sinnberg T, Menzel M, Ewerth D, Sauer B, Schwarz M, Schaller M, Garbe C, Schittek B. β-Catenin signaling increases during melanoma progression and promotes tumor cell survival and chemoresistance. PLoS One 2011; 6(8):e23429.
29. Bellei B, Pitisci A, Catricalà C, Larue L, Picardo M. Wnt/β-catenin signaling is stimulated by α-melanocyte-stimulating hormone in melanoma and melanocyte cells: implication in cell differentiation. Pigment Cell Melanoma Res 2011; 24(2):309-25.
30. Biechele TL, Kulikauskas RM, Toroni RA, et al. Wnt/β-catenin signaling and AXIN1 regulate apoptosis triggered by inhibition of the mutant kinase BRAFV600E in human melanoma. Sci Signal2012; 10(206):5.

DIFFERENTIAL ROLE OF EGF AND bFGF IN HUMAN GBM-TIC PROLIFERATION: RELATIONSHIP TO EGFR-TYROSINE KINASE INHIBITOR SENSITIVITY

A. BAJETTO[1], C. PORCILE[2], A. PATTAROZZI[1], L. SCOTTI[3], A. ACETO[3], A. DAGA[4], F. BARBIERI[1] and T. FLORIO[1]

[1]Department of Internal Medicine, Section of Pharmacology and Centre of Excellence for Biomedical Research (CEBR) School of Medicine, University of Genova, Genoa, Italy; [2]Department of Health Sciences, University of Molise, Campobasso, Italy; [3]Department of Biomedical Sciences, University "G. d'Annunzio" of Chieti-Pescara, Chieti, Italy; [4]Laboratory of Gene Transfer, IRCCS-AOU San Martino-IST, Genova, Italy

Received October 15, 2012 – Accepted November 14, 2012

Glioblastoma multiforme (GBM) is among the most devastating human tumors being rapidly fatal despite aggressive surgery, radiation and chemotherapies. It is characterized by extensive dissemination of tumor cells within the brain that hinders complete surgical resection. GBM tumor initiating-cells (TICs) are a rare subpopulation of cells responsible for tumor development, growth, invasiveness and recurrence after chemotherapy. TICs from human GBM can be selected in vitro using the same conditions permissive for the growth of normal neural cells, of which share some features including marker expression, self-renewal capacity, long-term proliferation, and ability to differentiate into neuronal and glial cells. EGFR overexpression and its constitutive activation is one of the most important signaling alteration identified in GBM, and its pharmacological targeting represents an attractive therapeutic goal. We previously demonstrated that human GBM TICs have different sensitivity to the EGFR kinase inhibitors erlotinib and gefitinib, depending on the differential modulation of downstream signaling cascades. In this work we investigated the mechanisms of resistance to erlotinib in two human GBM TIC cultures, analyzing EGF and bFGF individual contribution to proliferation, clonogenicity, and migration. We demonstrated the presence of a small cell subpopulation whose proliferation is supported by EGF and a larger one mainly dependent on bFGF. Thus, insensitivity to EGFR kinase inhibitors as far as TIC proliferation results from a predominant FGFR activation that hides the inhibitory effects induced on EGFR signaling. Conversely, EGF and bFGF induced cell migration with similar efficacy. In addition, unlike neural stem/progenitors cells, the removal of chondroitin sulphate proteoglycans from cell surface was unable to discern EGF- and bFGF-dependent subpopulations in GBM TICs.

Glioblastoma (GBM) is the most aggressive and deadly tumor of the central nervous system (CNS). Despite aggressive conventional therapies, life expectancy after diagnosis is about 14 months. GBM is highly vascularized, infiltrative, and radio- and chemo-resistant and almost invariably recurs even after radical surgical excision (1). One of the distinguishing features of high-grade astrocytic tumors is their infiltrative nature: GBM grows within brain parenchyma as a mass intermingled with normal cells, without well-defined limits. This biological behavior represents the major determinant

Key words: glioblastoma, tumor-initiating cells, EGF; bFGF, tyrosine kinase inhibitors

Mailing address: Dr Tullio Florio,
Department of Internal Medicine,
Section of Pharmacology,
University of Genova,
Viale Benedetto XV 2, 16132 Genoa, Italy
Tel.: +39 010 3538806 Fax: +39 010 3538806
e-mail: tullio.florio@unige.it

0393-974X (2013)

of GBM surgical failure of cure and recurrence from micro-dissemination disease. This unique pattern of invasiveness suggests that GBM cells are adapted to the microenvironment present in the normal CNS (2).

Tumor initiating cells (TICs) are defined as the rare clonogenic subpopulation of tumor cells able to originate cancer. They share many characteristics of embryonic and normal tissue stem cells including the property of multipotential differentiation, unlimited proliferation and self-renewal (3). The cell type(s) from which GBM develops is currently unknown. Mounting evidence supports the hypothesis that transformation of neural stem cells (NSCs) and/or neural progenitors, rather than differentiated CNS cells, may lead to the formation of GBM-initiating cells, responsible of tumor development (4). More recently, it was demonstrated that a restricted, stem-like cell population can repopulate glioma tumor mass, when the bulk of the tumor is wiped out by chemotherapy (5). In glioma, TIC cultures were isolated using the neurosphere culture system, previously developed for culturing NSCs, that requires serum-free medium and the addition of epidermal growth factor (EGF) and basic fibroblast growth factor (bFGF). In these conditions cells can be expanded indefinitely with limited variations in their growth and differentiation characteristics. Removal of growth factors from the medium induces the differentiation of progenitors into neurons, astrocytes and oligodendrocytes (6).

EGF plays an important role in the maintenance of normal and malignant cells of many tumor types, promoting proliferation and survival. EGFR gene amplification, mutation, re-arrangement and subsequent over-expression of EGFR protein are the most common genetic alterations in primary GBMs. Malignant glioma is the only non-epithelial human tumor in which gene amplification, overexpression, mutation or hyper-activation of EGFR has been associated with tumor aggressiveness and reduced patient survival (7, 8). EGFR tyrosine kinase inhibitors (TKIs), such as erlotinib or gefitinib, are small molecules that bind the intracellular TK domain of EGFR, competing with adenosine triphosphate binding, inhibiting kinase activity and downstream signaling. TKIs are among the most clinically relevant EGFR targeted-drugs for the treatment of tumors whose cell growth is strongly dependent on EGF.

We previously reported that both erlotinib and gefitinib cause concentration- and time-dependent growth arrest and cell death of human GBM TICs, displaying individual sensitivity. In fact, despite all TIC cultures analyzed expressed EGFR, two out of seven were insensitive to the antiproliferative effects of erlotinib and gefitinib, although these drugs caused inhibition of EGF-dependent EGFR phosphorylation and ERK1/2 activation (9).

To more closely examine this phenomenon, in this study we analyzed the individual contribution of EGF and bFGF as far as proliferation, clonogenicity and cell migration in two TKI-insensitive TIC cultures. Furthermore, we evaluated the role of chondroitin sulphate glycosaminoglycans (CS-GAGs) on TIC biological behavior in response to EGF and/or bFGF.

MATERIALS AND METHODS

Reagents

Erlotinib-HCl (Selleck Biochem, Munich, Germany), was dissolved in DMSO and then diluted to appropriate concentrations. Recombinant human EGF and bFGF were purchased by PeproTech EC (London, UK), reconstituted in double distilled H_2O, and stored in working aliquots at -20°C.

TIC isolation and growth conditions

Following informed consent, tumor samples, classified as glioma grade IV (GBM) based on the World Health Organization (WHO) criteria, were obtained from two 48 and 67 years old male patients undergoing surgical treatment at the Neurosurgery Department, IRCCS-AOU San Martino-IST (Genova, Italy) following Institutional Ethics Board approval. Patients underwent surgery for the first time and did not received chemotherapy or radiotherapy. Tumors were washed and immediately processed for single cell isolation by mechanical dissociation and plated in matrigel-coated culture flasks (BD Biosciences) in serum-free medium containing: neurobasal 50%, Dulbecco's modified Eagle's medium/F12 50%, B27 supplement (Invitrogen), 2 mM L-glutamine, 100U/ml penicillin/streptomycin, 2μg/ml heparin, 15μg/ml insulin, 20ng/ml bFGF, and 20ng/ml EGF.

Cell survival assay

Cell viability was evaluated measuring the reduction

of 3-(4,5-dimethylthiazol-2-yl)-2, 5, diphenyl tetrazolium bromide (MTT) (Sigma-Aldrich). The cleavage of MTT to a purple formazan product by mitochondrial dehydrogenase was spectrophotometrically quantified (10). In brief, treated and control cells were incubated for 2 h with 0.25 mg/ml MTT solution in culture medium at 37°C; after the removal of the medium, formazan crystals were dissolved in DMSO and absorbance measured at 570 nm.

Cell migration assay

Cell migration was performed using BD FluoroBlock™ (BD Biosciences) inserts containing light-tight PET membrane that blocks light transmission within 490-700 nm, making invisible fluorescent labeled cells remaining in the top chamber of the insert.

Cells were stained with the flourescent dye Vybrant CFDA SE Cell Tracer (Molecular Probes Invitrogen) following manufacturer's instructions and plated at $5x10^4$ per well on 0.8 μM inserts, previously coated with diluted (1:200) matrigel (BD Biosciences) in DMEM/F12 medium. Inserts were placed in 24 multi-well plate in DMEM/F12 medium with or without EGF (20ng/ml) or bFGF (20ng/ml) or both. After 24 h, cells migrated to the bottom of the membranes were quantified by confocal laser-scanning microscope (BioRad MRC 1024 ES) at 10X magnification (11), using the ImageJ software (NIH, Bethesda, USA).

Cloning assay/limiting dilution assay

Single-cell suspensions of TICs, obtained after dissociation of neurospheres, were plated on uncoated 24 and 96 well plates at serial dilutions to obtain 1000, 100, 10, 1 cells/well in free medium (devoid of growth factors) or supplemented with EGF, bFGF, or EGF + bFGF. Plates were fed weekly until clones reached adequate size to be counted.

Statistical analysis

All experiments were performed in quadruplicate and repeated at least three times. Data are expressed as means ±SE. Statistical significance ($P \leq 0.05$) was assessed by the Student's *t*-test for independent groups.

RESULTS

TIC growth's dependence on EGF and BFGF

To understand the possible individual different sensitivity of GBM-TICs to EGFR-TKI treatment, we analyzed, the *in vitro*, growth characteristics of two cultures showing resistance or low sensitivity to EGFR-TKIs when grown in standard medium permissive for TIC proliferation, and containing both EGF and bFGF (complete medium) (Fig. 1A). Preliminary characterization showed that these cultures (hereafter named TICs 1 and TICs 2), isolated from two human GBM specimens, express markers previously identified in GBM stem-like cells (nestin, CD133), are able to form neurospheres, and are tumorigenic when xenotransplanted in NOD-SCID mice (data not shown), thus representing *bona fide* GBM-TICs.

To discriminate the individual contribution of EGF and bFGF to TIC growth, cells were cultured in medium without growth factors (free medium), complete medium, or in medium supplemented with a single growth factor, and proliferation rate was analyzed by MTT assay. TIC proliferation was strongly influenced by the presence of bFGF in the medium, reaching 83% for TICs 1 and 86% for TICs 2 of the growth obtained in complete medium containing both growth factors; EGF contribution of cell growth was limited to 29% for TICs 1 and 47% for TICs 2. (Fig. 1B). These results clearly evidenced that TIC proliferation mainly relies on bFGF, in these cultures.

TICs grow as neurospheres when plated without any coating, or form monolayers when plated on a thin coat of matrigel, maintaining in both cultures phenotypical and biological characteristics of stem cells (9, 12). Since growth factors are present in matrigel composition, we evaluated TIC growth in complete medium also in the absence of matrigel coating, evidencing a reduction of cell growth in the absence of matrigel coating, still maintaining the same growth factor requirement (data not shown).

To analyze whether bFGF-dependence of TIC growth supports the sensitivity to erlotinib treatment, we evaluated the effects of this drug on TIC proliferation, culturing the cells in free medium, complete medium or medium supplemented with single growth factors.

In complete medium, erlotinib was scarcely effective reducing cell growth of 2% and 16% *vs*. untreated cells, for TICs 1 and TICs 2, respectively. However, if the same cells were cultured in medium supplemented with EGF only, proliferation in the presence of erlotinib was reduced of 46% for TICs 1 and 35% for TICs 2 (Fig. 1A). Conversely, in medium supplemented with bFGF only, erlotinib

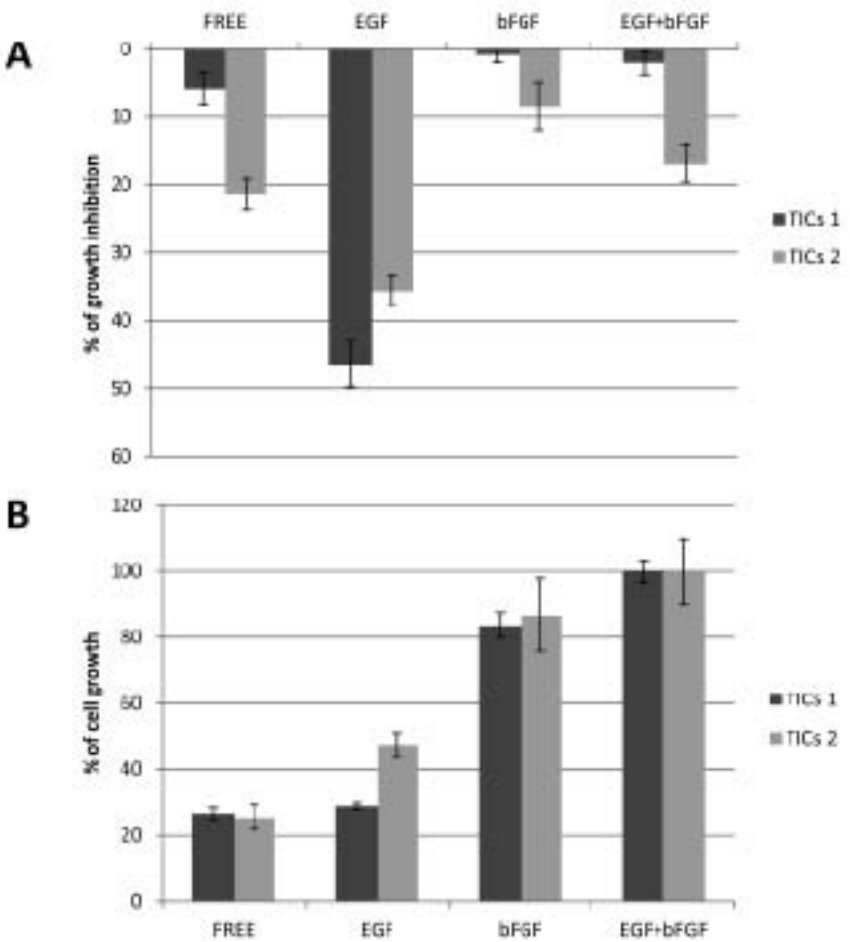

Fig. 1. *In vitro proliferation of TICs1 and TICs 2 and inhibitory effect of erlotinib treatment.* ***A****) TICs 1 and TICs 2 grown in free medium or in the presence of EGF, bFGF, or EGF + bFGF were treated with 5μM of erlotinib for 72h and cell proliferation was evaluated by MTT assay.* ***B****) TICs1 and TICs 2 were cultured in medium free or supplemented with only EGF or bFGF, or with EGF + bFGF. The graph reports the average of four independent experiments performed in triplicate.*

inhibited TICs growth of 1% in TICs 1 and 8% in TICs 2. In addition, we observed that cells cultured in medium without EGF and bFGF, erlotinib treatment reduced TICs 1 and TICs 2 proliferation of 6% and 21%, respectively (Fig. 1A).

Taken together these data suggest that EGFR expressed by TICs is responsive to TKIs if the cells are cultured in the absence of bFGF.

Time and number dependence of TICs growth

Cell growth in the presence of EGF or bFGF was evaluated as function of time and number of plated cells. After three days of culture in medium containing only bFGF, TICs 1 growth reaches 72% of that observed keeping the cells in complete medium, and was reduced to 60% after five days of culture. In medium supplemented with only EGF, TICs 1 growth was 21% after 3 days, further reduced to 6% after 5 days (Fig. 2A). Similarly, TICs 2 proliferation rate in medium supplemented with only bFGF was 88% and 80% of that observed in complete medium after 3 and 5 days of culture, respectively (Fig. 2B). Conversely, cell growth in medium containing only EGF was 47% and 20% (after 3 and 5 days, respectively) of that obtained in complete medium (Fig. 2B). The higher proliferation rate observed at 3 *vs* 5 days in culture with both EGF and bFGF, is likely due to the residual effect of complete medium,

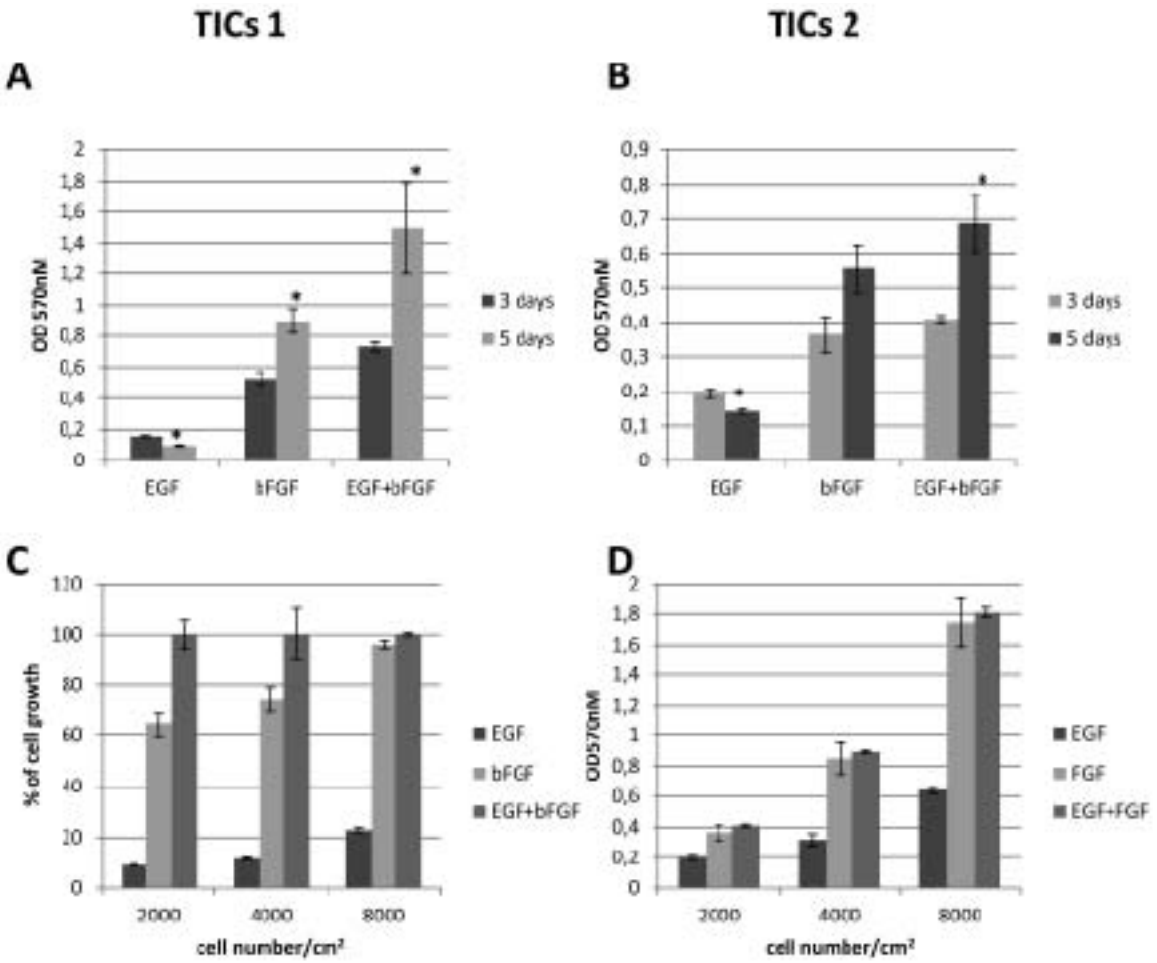

Fig. 2. *Time- and cell density- dependence of TICs proliferation. Time-dependent proliferation of TICs 1 (**A**) and TICs 2 (**B**) in medium supplemented with EGF, bFGF, or both factors, after 3 and 5 days of culture. TICs 1 (**C**) and TICs 2 (**D**) were seeded at $2x10^3$, $4x10^3$ and $8x10^3$ cells/cm^2 and cultured in medium with only EGF, bFGF, or EGF + bFGF for 5 days and cell proliferation was tested by MTT assay. * = P<0.05*

in which the cells were cultured before being shifted to media containing a single growth factor.

Cells, plated at different density, were grown in medium supplemented with either bFGF, EGF or both factors. TICs 1 proliferation in the presence of only bFGF, was 64%, 74%, and 96% of those observed in complete medium, respectively at $2x10^3$, $4x10^3$ and $8x10^3$ cells/cm^2, while in medium supplemented with only EGF cell growth was 9%, 11% and 23% (Fig. 2C). This result, showing a direct relationship between proliferation rate and cell number, is highly suggestive of the activation of paracrine mechanisms *via* stimulatory factors released by the TICs themselves, as observed in previous studies (13, 14). Conversely, the growth of TICs 2 was less influenced by cell number since, in the presence of bFGF, its growth was 88%, 95%, 96% of that observed in complete medium and 47%, 35%, 35% in the presence of only EGF, at $2x10^3$, $4x10^3$ and $8x10^3$ cells/cm^2, respectively (Fig. 2D). These results suggest that the growth of TICs in presence of EGF decreased with time culture and, in TICs 1, it could also be influenced by cell density (Fig. 2A-D).

Growth and clonogenicity

Subsequently, we investigated the individual and combined effects of EGF and bFGF on TICs growth

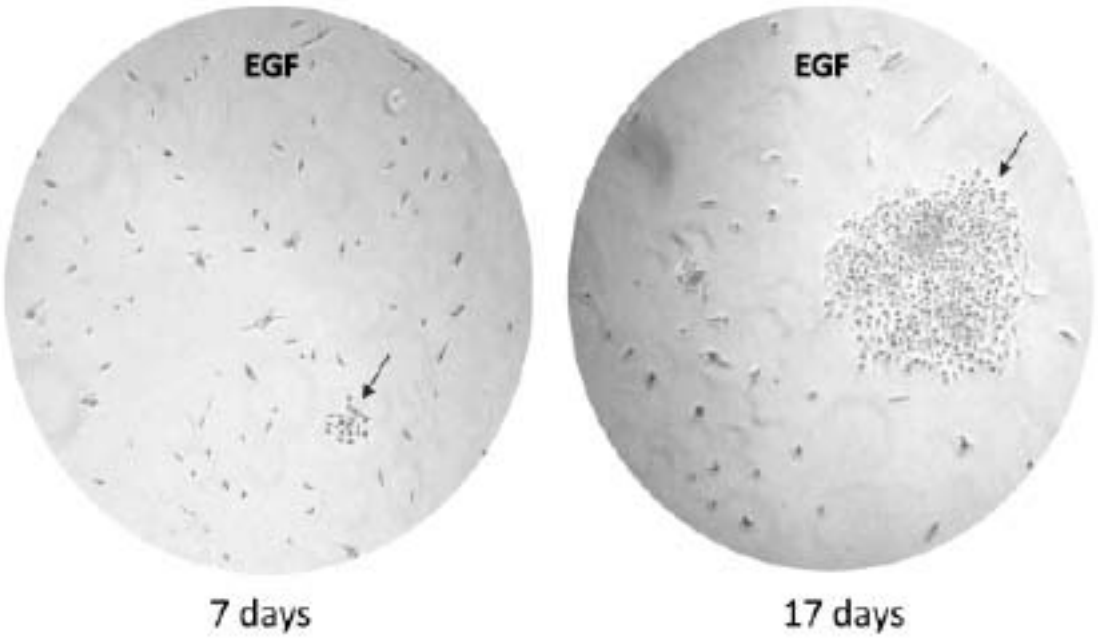

Fig. 3. *Phase-contrast micrographs documenting TICs 1 colony development in medium supplemented with only EGF, after 7 days and 17 days of culture.*

behavior and clonogenicity, after prolonged *in vitro* culture (7-17 days). Only few TICs were able to survive and proliferate in culture medium containing only EGF (Fig. 3). Initially, cells reduced growth rate and, after few days slowly started to proliferate again when cell number increases (Fig. 3). Conversely, TICs, grown in medium supplemented with only bFGF or in complete medium, showed a constant and similar rate of growth (data not shown).

To assess the role of these growth factors in self-renewal, we analyzed the ability of TICs to generate single spheres when cultured at limiting dilution (15, 16) in free medium and in the presence of EGF, bFGF or both peptides (Fig. 4). TICs 1, plated at 10^2 cells/well, generated a mean of 13 neurospheres in medium with only bFGF and 16 in complete medium; when plated at 10 cells/well the mean number of neurospheres was 2.5 in both culture conditions, while 0.1 (bFGF) and 0.6 (complete medium) spheres were observed when TICs 1 were plated at 1 cell/well. In free medium or in medium supplemented with only EGF, TICs 1 failed to generate neurospheres when plated at $<10^2$cells/well (Fig. 4). TICs 2 seeded at 10^2 cells/well gave rise to a mean of 27 neurospheres in complete medium and 28 in presence of only bFGF; 4.5 clones grown when cells were plated at 10 cells/well in both bFGF supplemented or complete medium and 0.8 or 0.6 clones after limiting dilution (1 cell/well). Similarly, TICs 2 did not generate neurospheres when grown in free medium or EGF-supplemented medium. that were observed only when the cells were seeded at higher density ($>10^3$ cells/well) (data not shown).

These results indicate that density of cell seeding and the presence of a specific growth factor are the determinants for neurosphere formation.

Role of EGF and bFGF in cell migration

Finally, we investigated the role of EGF and bFGF in cell migration. TICs were allowed to migrate through 0.8 μM light-tight PET membrane FluoroBlok™ that blocks the transmission of light. Fluorescent labeled cells present on the top chamber of the insert are made invisible by the FluoroBlok™ membrane allowing the detection of only those attached on the underside of the membrane.

Cells were labeled with CFDA SE cell tracer, and plated on inserts coated with a thin film of diluted matrigel in DMEM/F12 medium. The inserts were put in 24-multiwell in DMEM/F12 free medium

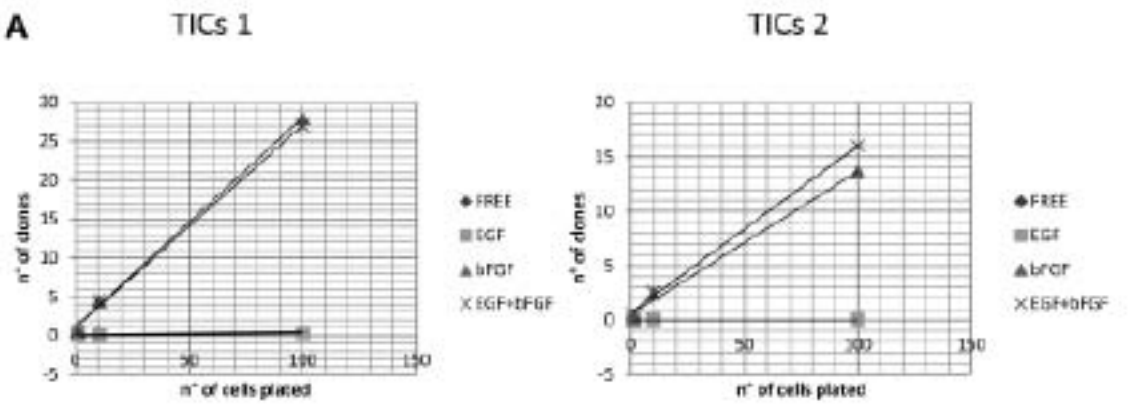

B

Medium	FREE		EGF		bFGF		EGF+bFGF	
n° of cells	TICs 1	TICs 2	TICs 1	TICs 2	TICs 1	TICs 2	TICs 1	TICs 2
1	0	0	0	0	0,1	0,8	0,6	0,6
10	0	0,3	0	0	2,5	4,5	2,5	4,5
100	0	0,5	0	0,3	13,6	18	16	27

Fig. 4. *Neurosphere generation. Number of clones of TICs 1 and TICs 2 generated in free medium or in the presence of EGF, bFGF, or both growth factors related to cells plated at 1, 10, 100 cells/well.*

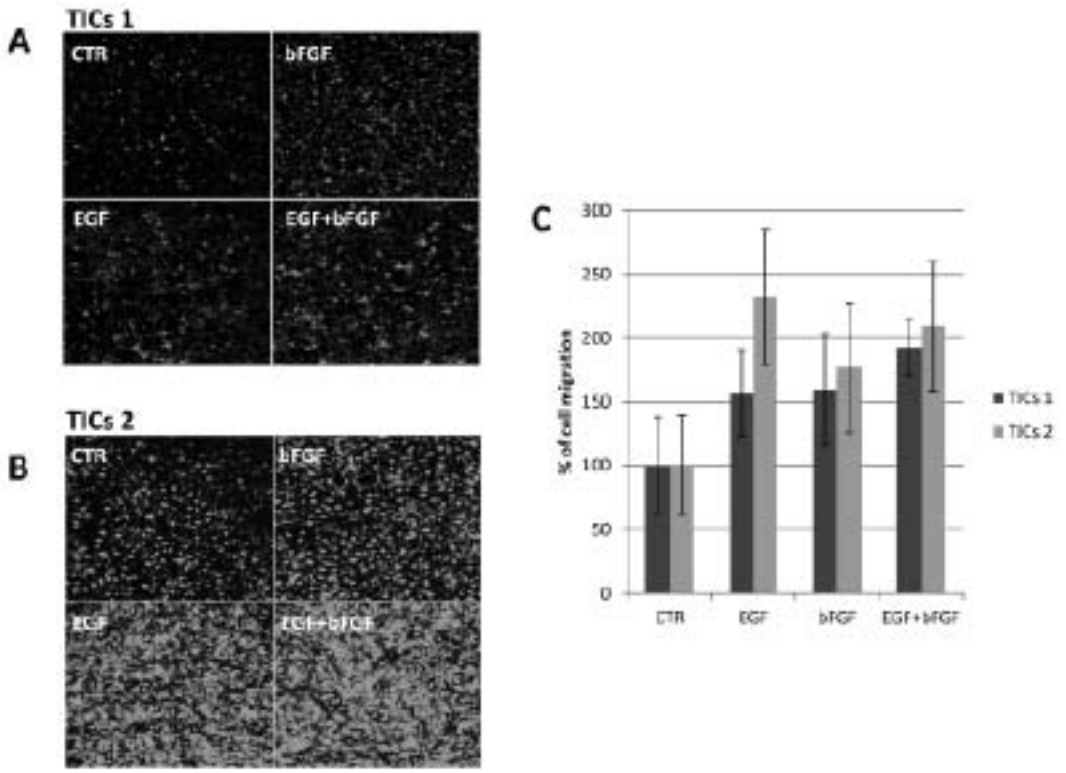

Fig. 5. *Cell migration. **A** and **B**: Representative confocal microscopy images of CFDA-SE labeled TICs 1 and TICs 2 migrated on the underside of FluoroBlok membrane immersed in free medium (CTR) or in medium supplemented with EGF, bFGF or EGF + bFGF. **C**: Quantitative analysis of cell migration, expressed as percentage of cells migrated to the underside of membrane in the presence of growth factors as compared to free medium.*

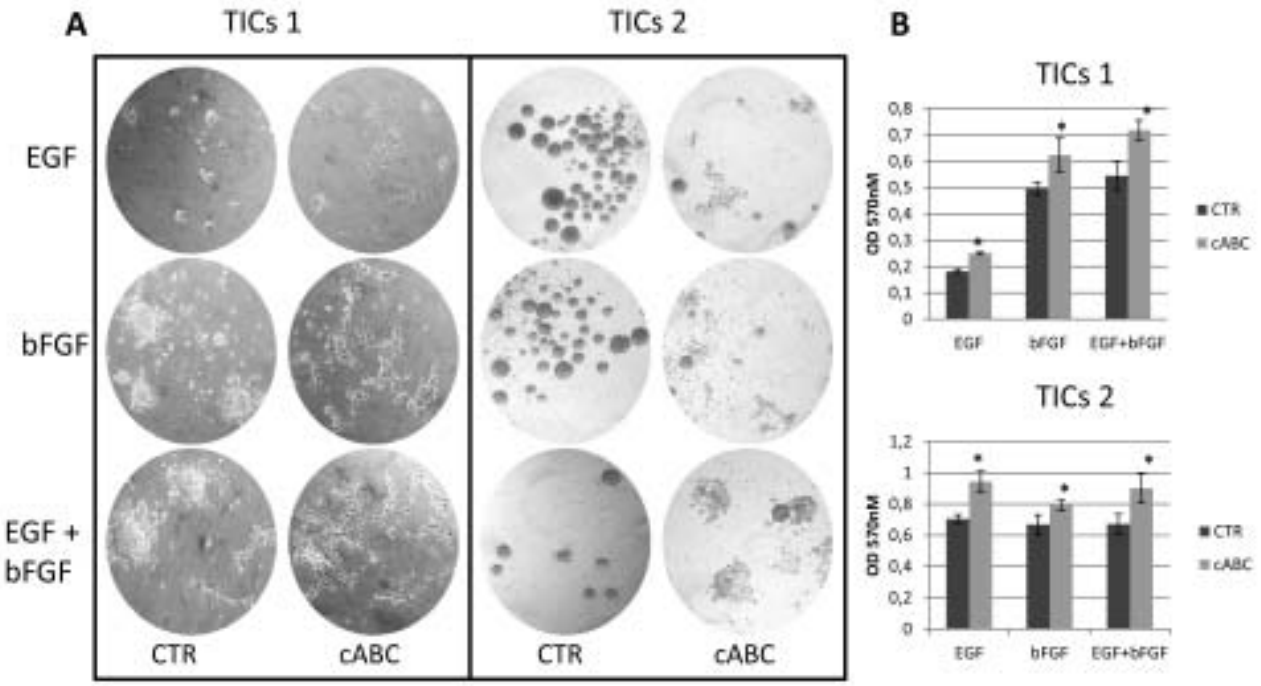

Fig. 6. ***A)*** *Phase-contrast micrographs documenting neurosphere growth and migration of TICs 1 and TICs 2 in medium supplemented with EGF, bFGF, or both factors without and after addition of cABC for 7 days.* ***B)*** *Cell proliferation of TICs 1 and TICs 2, cultured in the presence or absence of cABC, quantified by MTT assay, in comparison with untreated cells; * = P<0.05.*

or containing EGF (20ng/ml), bFGF (20ng/ml), or both factors. After 24 h, cell migration was evaluated by fluorescence confocal microscopy. The results showed that both factors, individually administered, induce TICs migration (Fig. 5A and B). EGF and bFGF caused a similar activation of TICs 1 migration (about 160% of basal) that was slightly increased (about 190%) by the simultaneous presence of both factors. On the other hand, EGF was the main actor in the chemotactic response in TICs 2, inducing a response superimposable to that of the combined treatment with both EGF and bFGF (Fig. 5C).

Role of chondroitin sulphate glycosaminoglycans (CS-GAG) in the recognition of EGF and bFGF subpopulations

It was reported that different cell subpopulations reside in neural stem/progenitor neurospheres, distinguishable by CS-carbohydrate structures-mediated responsiveness to EGF and bFGF (17).

To analyze whether such subpopulations can be identified within GBM-TICs, we used the enzyme chondroitinase ABC (cABC) to selectively degrade the chondroitin sulfate proteoglycans.

TICs were plated in the absence of matrigel, in a medium supplemented with EGF, bFGF or both factors, in the presence or absence of 50mU/ml of ChABC. Cell observation, by light microscope after five days of culture, clearly evidenced an increase of cell adhesion in cABC-treated cultures, in all the different media used (complete or free media) (Fig. 6A). In addition, cABC appears to influence not only cell adhesion, but also cell growth. To confirm this observation, we quantified cell growth in the presence or absence of cABC by MTT reduction test. In these experiments, we evidenced that removal of CS-GAG allows increase in cell growth rate of about 37%, 25%, 31% in TICs 1, and about 33%, 12%, 34% in TICs 2, when the cells were cultured in medium supplemented with only EGF, bFGF or in complete medium, respectively (Fig. 6B).

When the same experiments were performed

in matrigel coated plates, we did not observe any change in cell proliferation and adhesion (data not shown). These data indicate that chondroitin sulfate proteoglycans are involved in molecular bond of TICs into neurospheres and, apart from the presence of growth factors, matrigel untied their interaction. Moreover, this observation suggests that the interaction between cells during sphere formation could have a braking action on cell proliferation.

DISCUSSION

EGFR is a relevant target in several malignant tumors, including GBM, and small molecules inhibiting EGFR-TK were proposed to represent an innovative therapeutic approach for brain tumors. However, although several clinical trials were designed to evaluate the efficacy of gefitinib and erlotinib in numerous malignancies, they did not reach the therapeutical expectations and only modest antitumor activity was reported (18-20, 21). The resistance to EGFR-specific TKIs is an important phenomenon that limits the clinical benefits of these drugs in the control of tumor growth in many cancers of epithelial origin.

In this work we investigated, *in vitro*, possible mechanisms of insensitivity to EGFR-TKI treatment in two GBM TIC cultures, analysing the individual contribution of growth factors (EGF and bFGF) in cell proliferation, clonogenicity and migration, to identify possible determinants of the response to EGFR-TKIs in this stem-like tumor subpopulation. TICs are grown using neural stem cell permissive conditions, in the presence of EGF and bFGF, that maintain *in vitro* stem cell self-renewal and multilineage differentiation potential. In these experimental conditions, we previously demonstrated that TICs, isolated from different human GBMs, show individual EGFR-TKI sensitivity, independently from EGFR expression that was constantly identified (9). Here, we show that GBM-TIC proliferation from cultures insensitive to EGFR-TKI treatment, was mainly dependent on bFGF, while EGF gives only a modest supply to cell proliferation. This observation clearly supports the concept that this behaviour could be the basis for EGFR-TKI resistance of GBM. TICs are mixed population of cancer cells, composed by rare cancer stem cells and by other proliferating cancer cells, originated from stem/progenitor cell populations, having different characteristics of growth, migration and differentiation. Cell concentration, time of culture, and the presence of growth factors are some of the conditions that may influence the expansion of both subpopulations. We demonstrated that, in the GBM TICs used in our experiments, a large number of cells are dependent on bFGF for proliferation, and only a small subpopulation of cells is supported by EGF. However, EGF-dependent proliferation resulted in a minimal growth of both TICs 1 and TICs 2 cultures, although a lower effect was observed in TICs 1 as compared to TICs 2.

Although small variations according to experiments, time of culture, and cell concentrations were detected, EGF-dependent TIC subpopulation always gives a minor or negligible contribution to *in vitro* TICs growth, as compared to bFGF-dependent subpopulation.

Proliferation of the EGF-dependent TIC subpopulation was inhibited by erlotinib, demonstrating that EGFR expressed on these cells was sensitive to TKIs, but, when the cells were grown in complete medium, the presence bFGF reduced the effects of the EGFR-TKI on the EGF-dependent proliferation. In particular, in complete medium TICs 2 showed 16% of growth inhibition after erlotinib treatment, whereas TICs 1 growth was reduced by only 2%, confirming its lower dependence on EGF for the proliferation. We conclude that the resistance to EGFR-TKI treatment manifested in TICs might be due to the presence and activation of an alternative and predominant receptor TK pathway, distinct from EGFR, represented, in this case by FGFR. In agreement with this hypothesis, FGFRs have been identified among the most commonly mutated kinase genes in human cancers (22, 23), and in non-small lung cancer, FGF signaling pathway has been described as one of the mediators of intrinsic and acquired resistance to EGFR TKIs (24).

In addition, we demonstrated that EGFR, expressed on TKI-resistant TICs, was functional since it induces *in vitro* cell migration in response to its cognate ligand EGF. The attractive force exerted by EGF to move TICs was equivalent to that triggered by bFGF, suggesting the ability of growth factors to induce distinct intracellular pathways driving proliferation and cell migration. These data are in

agreement with the ability of EGF to phosphorylate EGFR, also in TK-resistant TICs (9).

Neurosphere generation in limiting dilution experiments is one of the parameters commonly used to demonstrate *in vitro* self-renewal of TICs (16). Neurosphere formation was strongly influenced by bFGF presence and cell density. Neurospheres were obtained also from cells cultured in free medium or supplemented with EGF but only when cells were seeded at $>10^2$ cell/well. Below this density, we observed neurosphere formation only in the presence of bFGF that are still generated also when cells were plated at limiting dilution. Noteworthy, TICs can generate spheres also in the absence of growth factors, suggesting the existence of an autocrine/paracrine pathways, producing factors needed for self-renewal. These notes are in agreement with two reports supporting the ability of human brain tumor stem cells to grow as neurospheres in serum-free medium and to initiate intracranial tumors in immuno-compromised mice, without the requirement of exogenous EGF or bFGF (25, 26). Clonogenicity and tumorigenicity of cells cultured in the absence of growth factors, open the question to identify the better experimental conditions leading to the growth and amplification of cancer stem cells maintaining as much as possible the characteristics of the tumor of origin. In addition, this suggests to evaluate whether the presence of mitogens might favor the expansion of a subpopulation of cells particularly responsive to growth factors.

The current hypothesis proposes that glioma TICs originate from the transformation of neural/progenitor stem cells (4). Recently, three important reports in mouse models of brain, skin and intestinal tumors provided the experimental evidence of the role of TICs in tumor formation (5, 27, 28).

Neural stem cells, able to self-renew and generate both neurons and glia, have been isolated from different regions of embryonic and adult brain (29). EGF and bFGF promote the *in vitro* proliferation of single neural precursors leading to neurosphere formation (30). *In vitro*, bFGF and EGF responsive precursors are lineage-related: bFGF-responsive cells acquire EGF responsiveness and give rise to cells responding to both factors (31). In developing embryo, multipotent stem cells initially generate lineage-restricted progenitors and later differentiate into neurons and glia according to differential niche factor/growth factor stimulation. During early development, neural stem/progenitor cells (NSPCs) proliferate only in response to bFGF and preferentially generate neuronal progeny. At later stages, in addition to bFGF, NSPCs become EGF-responsive and this event has been associated with enhanced gliogenesis (32).

Our study started from the hypothesis that TICs sensitivity to EGF and bFGF might reflect the intrinsic characteristics of the cells that originate individual GBM. Chondroitin sulphate glycosaminoglycans control neurogenesis, as well as radial glia proliferation and differentiation in NSPCs. The removal of chondroitin sulfate glycosaminoglycans with the bacterial enzyme chondroitinase ABC reduced NSPCs proliferation and self-renewal, favoring astroglial formation at expense of neurogenesis (33). In a recent paper, Sirko and coll. showed that CS-GAG removal selectively reduced neurosphere formation, self-renewal and proliferation of cortical NSPCs in response to bFGF but not in response to EGF (17, 34).

In our experiments, treatment of TICs with cABC modified the intercellular adhesion of cells within neurospheres, increasing the cell migration out of the spheres and favoring the adhesion to the plastic support. Similar results were obtained in embryonic forebrain NSPCs, wherein CS-GAGs are required to maintain neurospheres in a free floating status (33). However, in GBM-TICs, this behavior was independent from the presence of either growth factor, suggesting that, differently from NSPCs, CS-GAG removal affects at the same extent bFGF- and EGF-dependent TIC subpopulations. Moreover, CS-GAGs removal favors proliferation of TICs when cultured as free-floating neurospheres, while proliferation rate is not modified when cells were seeded on a thin layer of matrigel. Thus, these results suggest that intercellular binding into spheres generated an environment that reduces cell proliferation rate, perhaps mimicking the niche milieu.

In conclusion, our results demonstrated that resistance to EGFR-TKI treatment can be hidden by TICs proliferation induced by the predominant influence of the bFGF/FGFR pathway, suggesting that, in these conditions, additional receptor tyrosine kinase-dependent pathways must be targeted. The

combined treatment with EGFR- and FGFR-specific TKIs, or, alternatively, the blockade of specific intracellular pathways activated by both receptors, could represent a strategy to prolong or enhance the action of drugs, like erlotinib or gefitinib, toward TIC subpopulations.

ACKNOWLEDGEMENTS

The support of Italian Association for Cancer Research (AIRC) and University of Genova (PRA-2011) was gratefully acknowledged.

REFERENCES

1. Chen J, McKay RM, Parada LF. Malignant glioma: lessons from genomics, mouse models, and stem cells. Cell 2012; 149(1):36-47.
2. Van Meir EG, Hadjipanayis CG, Norden A, Shu HK, Wen PY, Olson JJ. Exciting new advances in neuro-oncology: the avenue to a cure for malignant glioma. CA Cancer J Clin 2010; 60(3):166-93.
3. Florio T, Barbieri F. The status of the art of human malignant glioma management: the promising role of targeting tumor-initiating cells. Drug Discov Today 2012; 17(19-20):1103-10.
4. Alcantara Llaguno S, Chen J, Kwon CH, J, et al. Malignant astrocytomas originate from neural stem/progenitor cells in a somatic tumor suppressor mouse model. Cancer cell 2009; 15(1):45-56.
5. Chen J, Li Y, Yu TS, McKay RM, Burns DK, Kernie SG, Parada LF. A restricted cell population propagates glioblastoma growth after chemotherapy. Nature 2012; 488(7412):522-6.
6. Singh SK, Hawkins C, Clarke ID, et al. Identification of human brain tumor initiating cells. Nature 2004; 432(7015):396-401.
7. Furnari FB, Fenton T, Bachoo RM, et al. Malignant astrocytic glioma: genetics, biology, and paths to treatment. Genes Dev 2007; 21(21):2683-710.
8. Ye F, Gao Q, Cai MJ. Therapeutic targeting of EGFR in malignant gliomas. Expert Opin Ther Targets 2010; 14(3):303-16.
9. Griffero F, Daga A, Marubbi, D, et al. Different response of human glioma tumor-initiating cells to epidermal growth factor receptor kinase inhibitors. J Biol Chem 2009; 284(11):7138-48.
10. Pattarozzi A, Gatti M, Barbieri F, et al. 17beta-estradiol promotes breast cancer cell proliferation-inducing stromal cell-derived factor-1-mediated epidermal growth factor receptor transactivation: reversal by gefitinib pretreatment. Mol Pharmacol 2008; 73(1):191-202.
11. Bajetto A, Barbieri F, Dorcaratto A, et al. Expression of CXC chemokine receptors 1-5 and their ligands in human glioma tissues: role of CXCR4 and SDF1 in glioma cell proliferation and migration. Neurochem Int 2006; 49(5):423-32.
12. Fael Al-Mayhani TM, Ball SL, Zhao JW, Fawcett J, Ichimura K, Collins PV, Watts C. An efficient method for derivation and propagation of glioblastoma cell lines that conserves the molecular profile of their original tumors. J Neurosci Methods 2009; 176(2):192-9.
13. Barbero S, Bonavia R, Bajetto A, et al. Stromal cell-derived factor 1alpha stimulates human glioblastoma cell growth through the activation of both extracellular signal-regulated kinases 1/2 and Akt. Cancer Res 2003; 63(8):1969-74.
14. Barbieri F, Bajetto A, Stumm R, et al. Overexpression of stromal cell-derived factor 1 and its receptor CXCR4 induces autocrine/paracrine cell proliferation in human pituitary adenomas. Clin Cancer Res: 2008; 14(16):5022-32.
15. Dontu G, Al-Hajj M, Abdallah W.M, Clarke M.F, Wicha MS. Stem cells in normal breast development and breast cancer. Cell Prolif 2003; 36 Suppl 1:59-72.
16. Pastrana E, Silva-Vargas V, Doetsch F. Eyes wide open: a critical review of sphere-formation as an assay for stem cells. Cell stem cell 2011; 8(5):486-98.
17. Sirko S, von Holst A, Weber A, Wizenmann A, Theocharidis U, Gotz M, Faissner A. Chondroitin sulfates are required for fibroblast growth factor-2-dependent proliferation and maintenance in neural stem cells and for epidermal growth factor-dependent migration of their progeny. Stem Cells 2010; 28(4):775-87.
18. Barbieri F, Bajetto A, Florio T. Role of chemokine network in the development and progression of ovarian cancer: a potential novel pharmacological target. J Oncol 2010; 2010:426956.

19. Raizer JJ, Abrey LE, Lassman AB, et al. A phase II trial of erlotinib in patients with recurrent malignant gliomas and nonprogressive glioblastoma multiforme postradiation therapy. Neuro-oncology 2010; 12(1):95-103.
20. Raizer JJ, Abrey LE, Lassman AB, et al. A phase I trial of erlotinib in patients with nonprogressive glioblastoma multiforme postradiation therapy, and recurrent malignant gliomas and meningiomas. Neuro-oncology 2010; 12(1):87-94.
21. Favoni RE, Florio T. Combined chemotherapy with cytotoxic and targeted compounds for the management of human malignant pleural mesothelioma. Trends Pharmacol Sci 2011; 32(8):463-79.
22. Brooks AN, Kilgour E, Smith PD. Molecular pathways: fibroblast growth factor signaling: a new therapeutic opportunity in cancer. Clinical cancer research: an official journal of the American Association for Cancer Res 2012; 18(7):1855-62.
23. Turner N,Grose R. Fibroblast growth factor signalling: from development to cancer. Nature reviews. Cancer 2010; 10(2):116-29.
24. Kono SA, Marshall ME, Ware KE, Heasley LE. The fibroblast growth factor receptor signaling pathway as a mediator of intrinsic resistance to EGFR-specific tyrosine kinase inhibitors in non-small cell lung cancer. Drug Resist Updat 2009; 12(4-5):95-102.
25. Li G, Chen Z, Hu YD, Wei H, Li D, Ji H, Wang DL. Autocrine factors sustain glioblastoma stem cell self-renewal. Oncol Rep 2009; 21(2):419-24.
26. Kelly JJ, Stechishin O, Chojnacki A, et al. Proliferation of human glioblastoma stem cells occurs independently of exogenous mitogens. Stem Cells 2009; 27(8):1722-33.
27. Schepers AG, Snippert HJ, Stange DE, Van Den Born M, Van Es JH, Van De Wetering M, Clevers H. Lineage tracing reveals Lgr5+ stem cell activity in mouse intestinal adenomas. Science 2012; 337(6095):730-5.
28. Driessens G, Beck B, Caauwe A, Simons BD, Blanpain C. Defining the mode of tumor growth by clonal analysis. Nature 2012; 488(7412):527-30.
29. Reynolds BA, Weiss S. Generation of neurons and astrocytes from isolated cells of the adult mammalian central nervous system. Science 1992; 255(5052):1707-10.
30. Craig CG, Tropepe V, Morshead CM, Reynolds BA, Weiss S, Van Der Kooy D. In vivo growth factor expansion of endogenous subependymal neural precursor cell populations in the adult mouse brain. J Neurosci 1996; 16(8):2649-58.
31. Ciccolini F. Svendsen CN. Fibroblast growth factor 2 (FGF-2) promotes acquisition of epidermal growth factor (EGF) responsiveness in mouse striatal precursor cells: identification of neural precursors responding to both EGF and FGF-2. J Neurosci 1998; 18(19):7869-80.
32. Ciccolini F. Identification of two distinct types of multipotent neural precursors that appear sequentially during CNS development. Mol Cell Neurosci 2001; 17(5):895-907.
33. Sirko S, Von Holst A, Wizenmann A, Gotz M, Faissner A. Chondroitin sulfate glycosaminoglycans control proliferation, radial glia cell differentiation and neurogenesis in neural stem/progenitor cells. Development 2007; 134(15):2727-38.
34. Sirko S, Akita K, Von Holst A, Faissner A. Structural and functional analysis of chondroitin sulfate proteoglycans in the neural stem cell niche. Methods Enzymol 2010; 479:37-71.

COULD PAST CHLAMYDIAL VASCULAR INFECTION PROMOTE THE DISSEMINATION OF *CHLAMYDIA PNEUMONIAE* TO THE BRAIN?

M. DI PIETRO[1], S. FILARDO[1], S. CAZZAVILLAN[2], C. SEGALA[2], P. BEVILACQUA[2], E. BONOLDI[2], E.S. D'AMORE[2], M. RASSU[3] and R. SESSA[1]

[1]Department of Public Health and Infectious Diseases, "Sapienza" University, Rome; [2]Pathology, and [3]Microbiology and Virology Unit, San Bortolo Hospital, Vicenza, Italy

Received August 2, 2012 – Accepted November 19, 2012

***Chlamydia pneumoniae*, a pathogen responsible for respiratory tract infections, has been associated with atherosclerosis which, along with hypertension, hyperlipidemia, cardiovascular and/or cerebrovascular ischemia and stroke, is a risk factor for chronic neurological disorders. Several studies have demonstrated the ability of *C. pneumoniae* to disseminate from lungs to arteries through peripheral blood mononuclear cells. Once inside the vascular tissue, *C. pneumoniae* infection may disseminate via peripheral monocytes to the brain over the intact blood-brain barrier, and contribute to the development of chronic neurological disorders. The aim of our study was to evaluate whether past *C. pneumoniae* vascular infection may promote the dissemination of this microorganism to the brain, therefore we investigated the presence of *C. pneumoniae* in post-mortem brain tissue specimens of patients with past chlamydial vascular infection. Seventy six post-mortem brain tissue specimens from 19 patients with past chlamydial vascular infection were investigated for the presence of *C. pneumoniae* by immunohistochemistry, polymerase chain reaction, *in situ* polymerase chain reaction and *in situ* reverse transcription polymerase chain reaction. As control, 28 brain tissue specimens were taken from 7 age and sex matched subjects without chlamydial infection. *C. pneumoniae* was detected in 16 (84.2%) out of 19 patients with chlamydial vascular infection whereas it was not detected in control subjects (p= 0.0002). In conclusion, the main result of our study is the evidence that a chlamydial vascular infection can disseminate to the brain. It will be important for current and future researches to perform large-scale prospective studies on cardiovascular patients with chlamydial vascular infection in order to evaluate the long-term pathological alterations of the brain.**

Chlamydia pneumoniae (C. pneumoniae), an intracellular obligate pathogen, is recognized as a common cause of mainly asymptomatic respiratory tract infections.

C. pneumoniae has a unique developmental cycle with two alternating functional and morphological forms: the extracellular infectious elementary body (EB) and the replicating non-infectious reticulate body (RB) (1). Recently a third non replicating and non-infectious form, called persistent form, has been reported to play a role in the development of chronic diseases since it can evade the host immune response and is more difficult to eradicate by antibiotics (2-5).

Cumulative evidence suggests that *C. pneumoniae* can contribute to the pathogenesis of

Key words: *C. pneumoniae, atherosclerosis, neurological disorders*

Mailing address: Prof.ssa Rosa Sessa,
Department of Public Health and Infectious Diseases,
"Sapienza" University, P.le Aldo Moro 5,
00185 Rome, Italy
Tel.: +39 06 49914102
Fax: +39 06 49914634
e-mail: rosa.sessa@uniroma1.it

0393-974X (2013)

DISCLOSURE: ALL AUTHORS REPORT NO CONFLICTS OF INTEREST RELEVANT TO THIS ARTICLE.

the atherosclerosis. These include: the presence of the microorganism inside atherosclerotic plaques (6-12), the recovery of viable *C. pneumoniae* from atherosclerotic plaques (coronary and carotid) and aneurism of abdominal aorta (13), the induction of pro-atherosclerotic cytokines such as Interleukin(IL)-1β, IL-6 and Tumoral Necrosis Factor-α (TNF-α) (14-16) and the acceleration of the atherosclerotic lesion development following intranasal inoculation of *C. pneumoniae* in animal models (11-17).

Therefore, *C. pneumoniae* infection has been associated with functional vascular disorders caused by hypertension, hyperlipidemia, cardiovascular and/or cerebrovascular ischemia and stroke (7, 18-20). The latter, along with the atherosclerosis, have been recognized as risk factors for chronic neurological disorders and contribute to their clinical manifestations and worsening (21, 22).

The involvement of *C. pneumoniae* with extrapulmonary diseases is related to some characteristics of this pathogen, such as the persistent form and its ability to multiply inside a wide range of cell types (macrophages, monocytes, endothelial cells and smooth muscle cells) that allows the spreading to other anatomical sites. Indeed, several studies have provided evidence about systemic dissemination of *C. pneumoniae* from the lung to vasculature via peripheral blood mononuclear cells (PBMC) (17, 23-28).

C. pneumoniae has been implicated in Alzheimer's disease (AD) (29, 30) and in Multiple Sclerosis (MS) (31-33), even though several studies failed to demonstrate a relationship between *C. pneumoniae* and these diseases (34-37).

The ability of *C. pneumoniae* to multiply into PBMC supports the detection of the microorganism into microglial cells, astrocytes and neurons as well (29, 30). Hence, *C. pneumoniae* can possibly use this pathway to enter the brain over an intact blood-brain barrier, contributing to the development of chronic neurological diseases through an intense inflammatory response.

In order to establish whether *C. pneumoniae* vascular infection may promote the dissemination of this microorganism to the brain, we investigated the presence of *C. pneumoniae* in post-mortem brain tissue specimens of patients with past chlamydial vascular infection.

MATERIALS AND METHODS

Brain tissue specimens

The post-mortem brain tissue specimens from the cerebral cortex were collected from 19 patients during the autopsy in the Department of Pathology of San Bortolo's Hospital. The patients were selected from a cohort of 30 patients investigated for the presence of *C. pneumoniae* infection; they were positive to *C. pneumoniae* DNA by PCR targeting *OmpA* gene (38) in atherosclerotic plaques from coronary artery and abdominal aorta.

The patients were aged from 43 to 84 (average 61±20) and included 13 men and 6 women. None of the patients showed any clinical signs of chronic neurological diseases. The causes of death were pulmonary thromboembolism (4 cases), aortic rupture (1 case), acute myocardial infarction (12 cases), cerebral haemorrhage (1 case) and bacterial pneumonia no *C. pneumoniae* related (1 case).

As control, brain tissue specimens were taken from 7 age and sex healthy matched subjects without *C. pneumoniae* infection and died from not cardiovascular disease related causes.

Each specimen was dissected into 5 parts, which were used for histology, immunohistochemistry (IHC), polymerase chain reaction (PCR), *in situ* PCR and *in situ* RT-PCR.

Brain tissue specimens were considered positive to *C. pneumoniae* when it was detected by at least two different methods.

Paraffin embedded brain tissue was used for histology, IHC, *in situ* PCR and *in situ* RT-PCR whereas frozen specimens were used for PCR.

Histology

5 μm paraffin embedded tissue sections were used for haematoxylin/eosin staining performed using standard procedures.

IHC

Immunohistochemical detection of *C. pneumoniae* was performed as previously described (39). Briefly, the 5 μm paraffin-embedded tissue sections were deparaffinized and then rehydrated through graded series of alcohols and PBS.

The sections were incubated in a humidified chamber with anti-chlamydia antibodies, RR402 mouse monoclonal antibodies, against a major outer membrane protein of *C. pneumoniae* (MOMP, dilution 1:5) (DAKO, Denmark) for 60 min at 37°C. Streptavidin –biotin – peroxidase method (Vector Laboratories Inc, Burlingame, CA) was used for detecting monoclonal antibody binding.

Infected HEp-2 cells were used as a positive control and mock-infected HEp-2 cells were used as a negative control.

PCR

DNA was extracted from each brain tissue specimen (500 mg) using the phenol/chloroform method; DNA amplification of the *C. pneumoniae OmpA* gene was performed using a touchdown nested PCR assay as previously described (39). The amplification products were visualized in 3% NuSieve 3:1 Agarose with a Gel Star nucleic acid gel stain (Cambrex, Rockland, Me, USA). Human *C. pneumoniae* TW 183 ATCC (n.WR-2282 type strain RF215335- RF49329) grown in HEp-2 cells was used as a positive control in PCR assays.

In order to assess the presence of possible PCR inhibitors, human β-globin gene was amplified from all clinical DNA specimens.

Extreme care was taken to avoid cross-contamination of the samples in the preparation procedure. In each assay a negative and a positive control were run. Each clinical specimen was analyzed in triplicate. A specimen was considered positive if all of the three assay results were positive in the replicate test.

OmpA gene sequencing

PCR products were purified with Wizard SV Gel and PCR Clean-up System (Promega Corporation, Madison, WI, USA) following manufacturer's instruction. ABI Prism BigDye Terminator v1.1 Cycle sequencing kit (Applied BioSystems, CA, USA) was used for the amplification on GeneAmp 9700 (Perkin Elmer Applied Biosystems).

The primer used was the reverse one (CPD, 5' – ATC TAC GGC AGT AGT ATA GTT – 3') and the final reaction volume was 20 µl. The thermal cycling conditions were 25 cycles of 10 sec at 96°C, 5 sec at 50°C and 4 min at 60°C. The reaction products were purified with Centri-Sep Columns (Princeton Separation) to remove exceeding DyeDeoxyTM terminators before automated sequencing on ABI PRIMS 310 (Genetic Analyzer, CA, USA).

The sequences were analyzed using BLAST 2 (http://www.ncbi.nlm.nih.gov/blast) and compared to the *C. pneumoniae* sequences of the *OmpA* gene available in GeneBank.

In situ PCR

Five µm thick tissue sections were deparaffinized and permeabilized with HCl 0.2 M for 20 m at 37°C. Then the specimens were digested in proteinase K (10 mg/ml) in a buffer containing 0.05 M Tris HCl (pH 9) for 10 m at 37°C and were treated with 20% acetic acid at 4°C. The sections were then dehydrated and air dried.

For the amplification, the primers CPC (5' – TTA TTA ATT GAT GGT ACA ATA – 3') and CPD (5' – ATC TAC GGC AGT AGT ATA GTT – 3') targeting a 207 bp product of the C. *pneumoniae OmpA* gene were used. A single step of amplification was carried out in a reaction volume of 50 µl containing 10 mM Tris HCl pH 8.3, 50 mM KCl, 200 µM dNTPs, 2.5 mM $MgCl_2$, 1 µM of each primer, 5 U ampliTaq DNA polymerase in situ (Applied Biosystems, Foster City, CA) and 2.5 µM digoxigenine-dUTP. The PCR was performed in GeneAmp *in situ* PCR system 1000 (Applied Biosystems, Foster City, CA) under the following conditions: 2.5 m at 94°C followed by 40 cycles consisting of 1 m at 94°C, 1 m at 50°C and 30 s at 72°C.

C. pneumoniae OmpA gene detection was carried out with antidigoxigenin-coniugated alkaline phosphatase (αDigoxigenin-AP, Kreatech Diagnostic) for 30 m at 37°C. The slides were visualized using a bright-field microscopy (Axio Scope Zeiss).

C. pneumoniae infected HEp-2 cells were used as a positive control and mock-infected HEp-2 cells were used as a negative control.

In situ RT-PCR

The digestion was performed as described for *in situ* PCR. DNA degradation was performed incubating the tissue sections with DNase RNase free (0.01 U/µl) for 10 m at 37°C. As for the retrotranscription step, the sections were incubated for 30 m at 42°C with the following reaction mix: 1 mM dNTPs, 25 U RNase inhibitor, 1.25 µM random hexamers, 50 U Multiscribe Reverse Transcriptase (Applied Biosystems, Foster City, CA). The amplification and immunodetection were performed as described for *in situ* PCR.

DEPC water was used for buffers and washings. Controls of complete DNA degradation (sections not retrotranscripted), negative (uninfected HEp-2 cells) and positive controls (*C. pneumoniae* infected HEp-2 cells) were used.

Statistical analysis

Results were subjected to χ^2 analysis (significance at p=0.05), with Yates' correction, to compare frequency distribution. When the minimum expected value was less than 5, the Fisher's exact test was used.

RESULTS

A total of 104 post-mortem brain tissue specimens, 76 obtained from the 19 patients with past chlamydial vascular infection and 28 from the 7 control subjects, were investigated for the presence of *C. pneumoniae* by IHC, PCR, *in situ* PCR and *in situ* RT-PCR.

Overall, *C. pneumoniae* was detected in 16 (84.2%) out of 19 patients while it was not detected

Table I. *The prevalence of C. pneumoniae in the brain tissue specimens from 19 patients with past chlamydial infection by IHC, PCR, in situ PCR and in situ RT-PCR.*

Pts	Cause of death	IHC (MOMP)	PCR (OmpA)	In situ PCR (OmpA)	in situ RT-PCR (OmpA)
1	Pulmonary Thromboembolism	+	+	+	+
2	Acute Miocardial Infarction	+	+	+	+
3	Acute Miocardial Infarction	+	+	+	+
4	Acute Miocardial Infarction	+	+	+	+
5	Acute Miocardial Infarction	+	+	+	+
6	Pulmonary Thromboembolism	+	+	+	+
7	Pulmonary Thromboembolism	+	+	+	+
8	Pulmonary Thromboembolism	+	+	+	+
9	Acute Miocardial Infarction	+	+	+	+
10	Acute Miocardial Infarction	+	+	+	+
11	Acute Miocardial Infarction	+	+	+	+
12	Acute Miocardial Infarction	+	+	+	+
13	Acute Miocardial Infarction	+	+	+	+
14	Cerebral Hemorrhage	+	+	+	+
15	Aorta Dissecting Aneurism	+	-	+	+
16	Acute Miocardial Infarction	+	-	+	+
17	Bacterial Pneumonia No *C.p.* related	-	-	-	-
18	Acute Miocardial Infarction	-	-	-	-
19	Acute Miocardial Infarction	-	-	-	-

Pts: patients; + : C. pneumoniae positive; - : C. pneumoniae negative

in the control subjects (p= 0.0002).

All the *C. pneumoniae* positive patients were deceased from cardiovascular disease related causes, whereas no evidence of neurological disease was observed in all post-mortem brain tissue specimens examined by using histology.

The prevalence of *C. pneumoniae* in the brain tissue specimens from the 19 patients by IHC, PCR, *in situ* PCR and *in situ* RT-PCR is shown in table I. IHC, PCR, *in situ* PCR and *in situ* RT-PCR were concordantly positive in 14 (73.7%) out of 19 patients (Fig. 1-3) whereas they gave negative

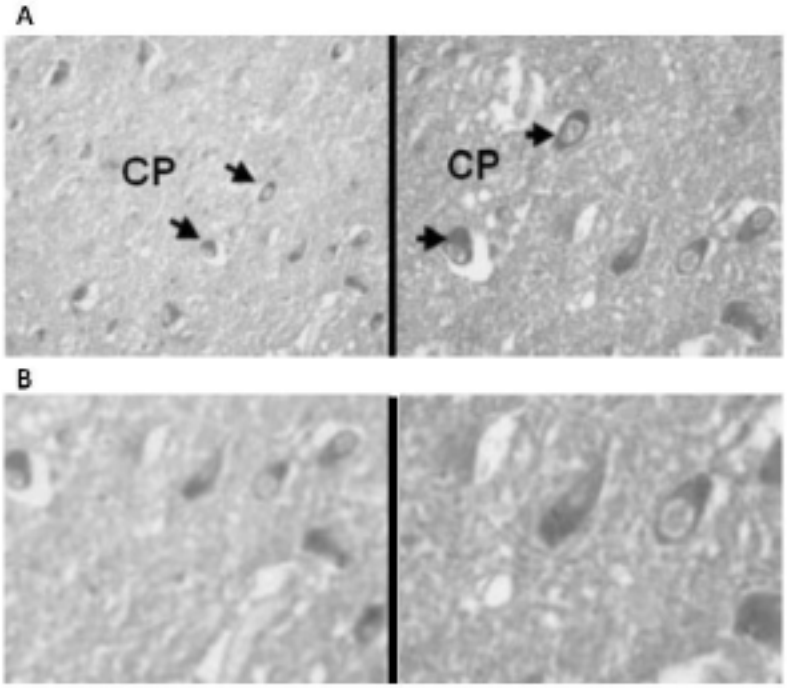

Fig. 1. *IHC detection of C. pneumoniae (CP) in post-mortem brain tissue specimens at two different magnification through light microscopy (left 40X and right 60X). Anti-chlamydia antibodies (RR402 mouse monoclonal antibodies) against a major outer membrane protein (MOMP) were used.* ***A)*** *Positive specimen; the arrows indicate C. pneumoniae infected cells.* ***B)*** *Negative specimen (left 40X and right 60X).*

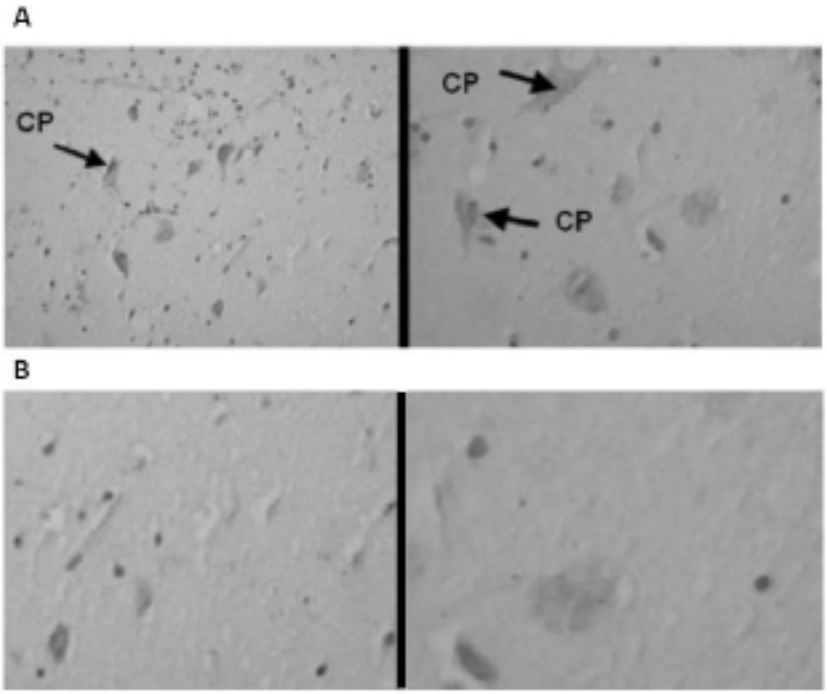

Fig. 2. *In situ PCR detection of C. pneumoniae (CP) in post-mortem brain tissue specimens at two different magnification through bright-field microscopy (left 40X and right 60X). The reaction was performed in GeneAmp in situ PCR system 1000 (Applied Biosystems, Foster City, CA). A pair of primers (CPC, 5'– TTA TTA ATT GAT GGT ACA ATA – 3', and CPD, 5'– ATC TAC GGC AGT AGT ATA GTT – 3') targeting a 207 bp product of the C. pneumoniae OmpA gene was used.* ***A)*** *Positive specimen; the arrows indicate C. pneumoniae infected cells.* ***B)*** *Negative specimen (left 40X and right 60X).*

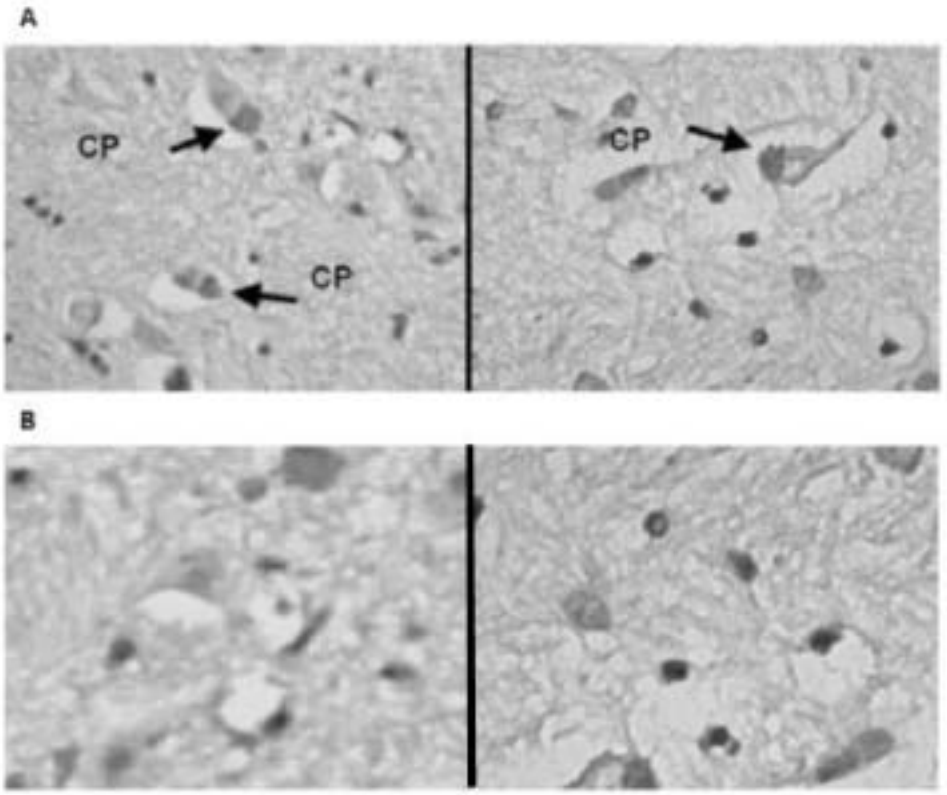

Fig. 3. *In situ RT-PCR detection of C. pneumoniae (CP) in post-mortem brain tissue specimens at two different magnification through bright-field microscopy (left 40X and right 60X). The reaction was performed by a two steps protocol: firstly the retrotranscription which was performed for 30' at 42°C with the reagent mixture including 1 mM dNTPs, 25 U Rnase inhibitor, 1.25 μM random examers, 50 U Multiscribe Reverse Transcriptase (Applied Biosystems, Foster City, CA) and secondly the DNA amplification which was carried out as described for in situ PCR.* ***A)*** *Positive specimen; the arrows indicate C. pneumoniae infected cells.* ***B)*** *Negative specimen (left 40X and right 60X).*

results in 3 patients. Two (10.5%) out of 19 patients were positive to IHC, *in situ* PCR and *in situ* RT-PCR but PCR negative.

By using *in situ* RT-PCR we demonstrated the presence of *C. pneumoniae* in PBMC within small brain vessels and crossing the endothelium (Fig. 4).

The sequencing analysis of all the positive amplification products confirmed the identification of *C. pneumoniae OmpA* gene. No significant difference was found in *C. pneumoniae* positive sequences for TW 183 and those reported by GeneBank.

DISCUSSION

In this report we demonstrate that the past vascular chlamydial infection may promote the spread of *C. pneumoniae* to the central nervous system. Indeed, *C. pneumoniae* was detected in the post-mortem brain tissue specimens from the patients with past chlamydial vascular infection whereas it was not found in the control subjects without chlamydial infection (p= 0.0002). All the *C. pneumoniae* positive brain tissue specimens came from patients deceased from cardiovascular disease related causes and it is well known that *C. pneumoniae* is involved in such diseases which are, moreover, risk factors for chronic neurological disorders (21,22).

These neurological diseases, in recent years, became an increasing problem as more people survive to old age.

The significance of the spread of chlamydial infection to the brain of patients with past vascular infection is intriguing. There have been several studies in animal experimental models showing haematogenic dissemination of *C. pneumoniae* into the brain (40, 41). More interestingly, Little

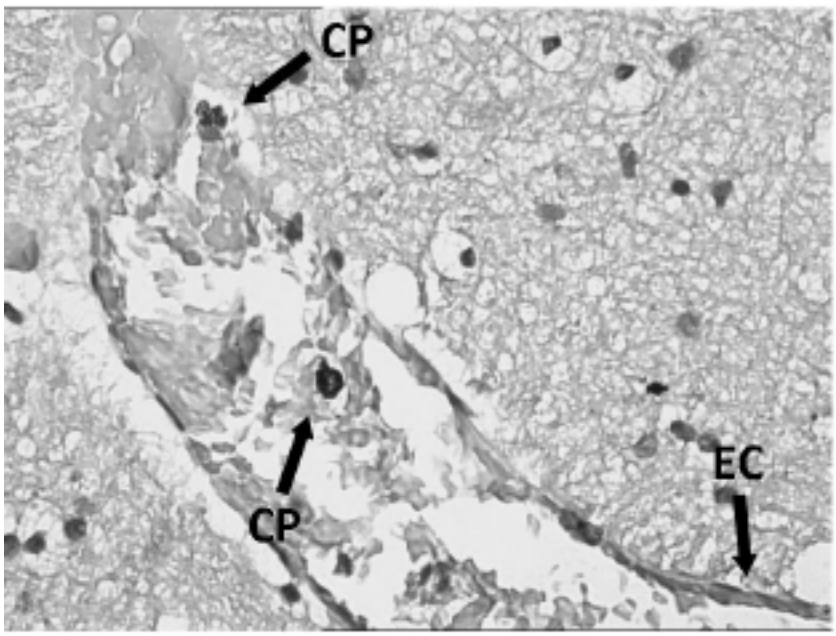

Fig. 4. *Bright-field microscopy of in situ RT-PCR of C. pneumoniae showing a small brain vessel with circulating peripheral blood mononuclear cells which cross the endothelium. A slight positivity can be observed in the endothelium cells (magnification 40X). The arrows indicate the presence of C. pneumoniae RNA in the infected cells and the endothelial cells.*

et al. (42) showed that intranasal inoculation of *C. pneumoniae* was followed initially by the recovery of this microorganism within pulmonary and heart tissues and later into the brain in which a prominent macrophages and monocytes infiltration was not found. Similarly, in our study, a significant leukocyte infiltration was not observed in the brain tissue specimens positive to *C. pneumoniae* and this can be explained by the fact that the central nervous system is an immunoprivileged site. Therefore, following the spread of *C. pneumoniae* to the brain, the eradication of this microorganism by the immune system may be more difficult and such conditions, instead, may favour the development of chlamydial chronic infections through the persistent forms. *C. pneumoniae* persistence has been, indeed, described as a long-term relationship with the host cell, therefore it may induce inflammatory chronic sequelae. Specifically, the presence of the chlamydial persistent forms could be supported by data from *in situ* RT-PCR analyses since they are metabolically active forms.

In addition, some studies have found the presence of *C. pneumoniae* infected macrophages and monocytes in and around blood vessels in AD brain (29, 43). This supports the transmigration of the infected monocytes through brain endothelial cells, as first demonstrated by MacIntyre *et al*. (43). Similarly, we were able to demonstrate, by *in situ* PCR, the presence of *C. pneumoniae* in PBMC within small brain vessels and crossing the endothelium.

Interestingly, in our study, the evidence of *C. pneumoniae* in the atherosclerotic plaques from coronary artery and abdominal aorta and later in the brain tissue from the same patient suggests that vascular *C. pneumoniae* infection may be responsible for the dissemination of the microorganism to the brain. Specifically, the sequence data from the DNA amplified from the brain tissue revealed a similar *OmpA* gene sequence to the DNA amplified from the atherosclerotic plaques of the same patient. As a consequence, it cannot be excluded that the same *C. pneumoniae* serotype could be involved. However, since a genetic typing system has not been established for *C. pneumoniae*, the presence of a genotype with a distinct cerebral pathogenicity should be considered.

Our *C. pneumoniae* positive patients did not show any evidence of pathological alterations of

the brain tissue as well as any clinical neurological diseases. In the literature there is no clear correlation between the pathological findings and the clinical manifestations of these diseases (44). Indeed, some neurological patients with massive pathology have no symptoms whereas symptomatic patients may show little pathology upon post-mortem histopathological examination. Since the response of the brain to the infection may determine the extent of pathology and symptomatology there are many variations in the amount and type of damage in the brain. In this regard, *C. pneumoniae* infection may promote an inflammatory response whereby cytokines, such as IL-1β and TNF-α are secreted and may initiate cellular damage, suggesting that other events may be missing in the pathobiology of chronic neurological diseases. Indeed, *C. pneumoniae* persistence in the central nervous system might indicate the establishment of chronic asymptomatic process. However, we did not have the possibility to determine the early signs and symptoms of the neurological disease of our patients, since it is a progressive disorder and the patients were already deceased.

C. pneumoniae infection could stimulate, as previously described, an inflammatory response that may result in a brain damage. Consequently, two hypotheses can be considered which might explain the putative role of *C. pneumoniae* in the chronic neurological disorders. First, *C. pneumoniae* infection of microglial cells induces the expression of neurotoxic proinflammatory cytokines (IL-1β, IL-6, TNF-α), which accelerate β-amyloid production and deposition or contribute to nerve fibers damage (41, 45, 46). Second, *C. pneumoniae* ability to multiply inside neurons contributes directly to the brain damage through the induction of apoptosis (45).

In conclusion, the main result of our study is the evidence that a chlamydial vascular infection can disseminate to the brain. It will be important for current and future researches to perform large-scale prospective studies on cardiovascular patients with chlamydial vascular infection in order to evaluate the long term pathological alterations of the brain.

ACKNOWLEDGEMENTS

This study was supported by grants from Center for Social Disease Research, "Sapienza" University" Rome, to R. Sessa.

REFERENCES

1. Rockey D. D. & Matsumoto, A. The chlamydial developmental cycle. Prokaryotic Development 2000; 403-425.
2. Wolf K, Fischer E, Hackstadt T. Ultrastructural analysis of developmental events in *Chlamydia pneumoniae*-infected cells. Infect Immun 2000; 68(4):2379-85.
3. Hogan RJ, Mathews SA, Mukhopadhyay S, Summersgill JT, Timms P. Chlamydial persistence: beyond the biphasic paradigm. Infect Immun 2004; 72(4):1843-55.
4. Di Pietro M, Tramonti A, De Santis F, De Biase D, Schiavoni G, Filardo S, Zagaglia C, Sessa R. Analysis of gene expression in penicillin G induced persistence of *Chlamydia pneumoniae*. J Biol Regul Homeost Agents 2012; 26(2):277-84.
5. Sessa R, Di Pietro M, Schiavoni G, et al. *Chlamydia pneumonia* induces T cell apoptosis through glutathione redox imbalance and secretion of TNF-alpha. Int J Immunopathol Pharmacol 2009; 22(3):659-68.
6. Sessa R, Di Pietro M, Santino I, del Piano M, Varveri A, Dagianti A, Penco M. *Chlamydia pneumoniae* infection and atherosclerotic coronary disease. Am Heart J 1999; 137(6):1116-19.
7. Sessa R, Di Pietro M, Schiavoni G, Santino I, Benedetti-Valentini F, Perna R, Romano S, del Piano M. *Chlamydia pneumoniae* DNA in patients with symptomatic carotid atherosclerotic disease. J Vasc Surg 2003; 37(5):1027-31.
8. Sessa R, Di Pietro M, Schiavoni G, et al. Detection of *Chlamydia pneumoniae* in atherosclerotic coronary arteries. Int J Immunophatol Pharmacol 2004; 17:301-306.
9. Sessa R, Di Pietro M, Schiavoni G, et al. *Chlamydia pneumoniae* in asymptomatic carotid atherosclerosis. Int J Immunopathol Pharmacol 2006; 19(1):111-8.
10. Sessa R, Cipriani P, Di Pietro M, Schiavoni G, Santino I, del Piano M. *Chlamydia pneumoniae* and chronic diseases with a great impact on public health. Int J Immunopathol Pharmacol 2008; 21(4):1041-43.
11. Watson C, Alp NJ. Role of *Chlamydia pneumoniae* in atherosclerosis. Clin Sci (Lond) 2008; 114(8):509-31.

12. Sessa R, Nicoletti M, Di Pietro M, Schiavoni G, Santino I, Zagaglia C, Del Piano M, Cipriani P. *Chlamydia pneumoniae* and atherosclerosis: current state and future prospectives. Int J Immunopathol Pharmacol 2009; 22(1):9-14.
13. Apfalter P, Loidl M, Nadrchal R, Makristathis A, Rotter M, Bergmann M, Polterauer P, Hirschl AM. Isolation and continuous growth of *Chlamydia pneumoniae* from arterectomy specimens. Eur J Clin Microbiol Infect Dis 2000; 19(4):305-8.
14. Kern JM, Maass V, Maass M. *Chlamydia pneumoniae* adversely modulates vascular cell properties by direct interaction with signalling cascades. Thromb Haemost 2009; 102(6):1064-70.
15. Di Pietro M, Schiavoni G, del Piano M, et al. *Chlamydia pneumoniae* and atherosclerosis: the role of mast cells. J Biol Regul Homeost Agents 2009; 23(2):65-9.
16. Schiavoni G, Di Pietro M, Ronco C, et al. *Chlamydia pneumoniae* infection as a risk factor for accelerated atherosclerosis in hemodialysis patients. J Biol Regul Homeost Agents 2010; 24(3):367-75.
17. de Kruif MD, van Gorp EC, Keller TT, Ossewaarde JM, ten Cate H. *Chlamydia pneumoniae* infections in mouse models: relevance for atherosclerosis research. Cardiovasc Res 2005; 65(2):317-27.
18. Romano S, Fratini S, Di Pietro M, et al. *Chlamydia pneumoniae* infection in patients with acute coronary syndrome: a clinical and serological 1-year follow-up. Int J Immunopathol Pharmacol 2004; 17(2): 209-18.
19. Romano S, Penco M, Fratini S, Di Pietro M, Sessa R, del Piano M, Fedele F, Dagianti A. *Chlamydia pneumoniae* infection is associated with coronary artery disease but not implicated in inducing plaque instability. Int J Cardiol 2004; 95(1):95-9.
20. Kaperonis EA, Liapis CD, Kakisis JD, Perrea D, Kostakis AG, Karayannakos PE. The association of carotid plaque inflammation and *Chlamydia pneumoniae* infection with cerebrovascular symptomatology. J Vasc Surg 2006; 44(6):1198-204.
21. Breteler MM. Vascular risk factors for Alzheimer's disease: an epidemiologic perspective. Neurobiol Aging 2000; 21(2):153-60.
22. Kalaria RN. The role of cerebral ischemia in Alzheimer's disease. Neurobiol Aging 2000; 21(2):321-30.
23. Rassu M, Lauro FM, Cazzavillan S, et al. Detection of *Chlamydophila pneumoniae* DNA in peripheral blood mononuclear cells of blood donors in the north-east of Italy. Med Microbiol Immunol 2001; 190(3):139-44.
24. Sessa R, Di Pietro M, Schiavoni G, Santino I, Cipriani P, Romano S, Penco M, del Piano M. Prevalence of *Chlamydia pneumoniae* in peripheral blood mononuclear cells in Italian patients with acute ischaemic heart disease. Atherosclerosis 2001; 159(2): 521-25.
25. Sessa R, Schiavoni G, Di Pietro M, et al. *Chlamydia pneumoniae* in PBMC: reproducibility of the OMPA nested touchdown PCR. Int J Immunopathol Pharmacol 2005; 18(1):113-20.
26. Sessa R, Di Pietro M, Schiavoni G, et al. Measurement of *Chlamydia pneumoniae* bacterial load in peripheral blood mononuclear cells may be helpful to assess the state of chlamydial infection in patients with carotid atherosclerotic disease. Atherosclerosis 2007; 195(1):e224-30.
27. Palikhe A, Tiirola T, Puolakkainen M, Nieminen MS, Saikku P, Leinonen M, Sinisalo J. *Chlamydia pneumoniae* DNA is present in peripheral blood mononuclear cells during acute coronary syndrome and correlates with chlamydial lipopolysaccharide levels in serum. Scand J Infect Dis 2009; 41(3):201-5.
28. Di Pietro M, Schiavoni G, Sessa V, Pallotta F, Costanzo G, Sessa R. *Chlamydia pneumoniae* and osteoporosis associated bone loss: a new risk factor? Osteoporos Int 2012. In press (on line, DOI:10.1007/s00198-012-2217-1)
29. Balin BJ, Gérard HC, Arking EJ, Appelt DM, Branigan PJ, Abrams JT, Whittum-Hudson JA, Hudson AP. Identification and localization of *Chlamydia pneumoniae* in the Alzheimer's brain. Med Microbiol Immunol 1998; 187(1):23-42.
30. Hammond CJ, Hallock LR, Howanski RJ, Appelt DM, Little CS, Balin BJ. Immunohistological detection of *Chlamydia pneumoniae* in the Alzheimer'sdisease brain. BMC Neurosci 2010; 11:121.
31. Sriram S, Stratton CW, Yao S, Tharp A, Ding L, Bannan JD, Mitchell WM. *Chlamydia pneumoniae* infection of the central nervous system in multiple

sclerosis. Ann Neurol 1999; 46(1):6-14.
32. Sessa R, Schiavoni G, Borriello G, Zagaglia C, Marinelli F, del Piano M, Pozzilli C. Real time PCR for detection of *Chlamydophila pneumoniae* in peripheral blood mononuclear cells of patients with multiple sclerosis. J Neurol 2007; 254(9):1293-5.
33. Fainardi E, Castellazzi M, Tamborino C, Seraceni S, Tola MR, Granieri E, Contini C. *Chlamydia pneumoniae*-specific intrathecal oligoclonal antibody response is predominantly detected in a subset of multiple sclerosis patients with progressive forms. J Neurovirol 2009; 15(5-6):425-33.
34. Stratton CW, Wheldon DB. Multiple sclerosis: an infectious syndrome involving *Chlamydophila pneumoniae*. Trends Microbiol 2006; 14(11):474-9.
35. Budak F, Keçeli S, Efendi H, Budak F, Vahaboğlu H. The investigation of *Chlamydophila pneumoniae* in patients with multiple sclerosis. Int J Neurosci 2007; 117(3):409-15.
36. Paradowski B, Jaremko M, Dobosz T, Leszek J, Noga L. Evaluation of CSF-*Chlamydia pneumoniae*, CSF-tau, and CSF-Abeta42 in Alzheimer's disease and vascular dementia. J Neurol 2007; 254(2):154-9.
37. Tang YW, Sriram S, Li H, Yao SY, Meng S, Mitchell WM, Stratton CW. Qualitative and quantitative detection of *Chlamydophila pneumoniae* DNA in cerebrospinal fluid from multiple sclerosis patients and controls. PLoS One 2009; 4(4):e5200.
38. Dowell SF, Peeling RW, Boman J, et al. *pneumoniae* Workshop Participants. Standardizing *Chlamydia pneumoniae* assays: recommendations from the Centers for Disease Control and Prevention (USA) and the Laboratory Centre for Disease Control (Canada). Clin Infect Dis 2001; 33(4):492-503.
39. Rassu M, Cazzavillan S, Scagnelli M, et al. Demonstration of *Chlamydia pneumoniae* in atherosclerotic arteries from various vascular regions. Atherosclerosis 2001; 158(1):73-9.
40. Ezzahiri R, Stassen FR, Kurvers HA, van Pul MM, Kitslaar PJ, Bruggeman CA. *Chlamydia pneumoniae* infection induces an unstable atherosclerotic plaque phenotype in LDL-receptor, ApoE double knockout mice. Eur J Vasc Endovasc Surg 2003; 26(1):88-95.
41. Voorend M, van der Ven AJ, Mulder M, Lodder J, Steinbusch HW, Bruggeman CA. *Chlamydia pneumoniae* infection enhances microglial activation in atherosclerotic mice. Neurobiol Aging 2010; 31(10):1766-73.
42. Little CS, Bowe A, Lin R, Litsky J, Fogel RM, Balin BJ, Fresa-Dillon KL. Age alterations in extent and severity of experimental intranasal infection with *Chlamydophila pneumoniae* in BALB/c mice. Infect Immun 2005; 73(3):1723-34.
43. MacIntyre A, Abramov R, Hammond CJ, Hudson AP, Arking EJ, Little CS, Appelt DM, Balin BJ. *Chlamydia pneumoniae* infection promotes the transmigration of monocytes through human brain endothelial cells. J Neurosci Res 2003; 71(5):740-50.
44. Duyckaerts C, Delatour B, Potier MC. Classification and basic pathology of Alzheimer disease. Acta Neuropathol 2009; 118(1):5-36.
45. Mattson MP. Infectious agents and age-related neurodegenerative disorders. Ageing Res Rev 2004; 3(1):105-20.
46. Dreses-Werringloer U, Bhuiyan M, Zhao Y, Gérard HC, Whittum-Hudson JA, Hudson AP. Initial characterization of *Chlamydophila (Chlamydia) pneumoniae* cultured from the late-onset Alzheimer brain. Int J Med Microbiol 2009; 299(3):187-201.

BONE MARROW CONCENTRATED CELL TRANSPLANTATION: RATIONALE FOR ITS USE IN THE TREATMENT OF HUMAN OSTEOCHONDRAL LESIONS

C. CAVALLO[1], G. DESANDO[2], L. CATTINI[1,2], M. CAVALLO[3], R. BUDA[3], S. GIANNINI[3], A. FACCHINI[1,2,4] and B. GRIGOLO[1,2]

[1]SSD Laboratory RAMSES, Rizzoli Orthopedic Institute, Bologna, Italy; [2]SC Laboratory of Immunorheumatology and Tissue Regeneration, Rizzoli Orthopedic Institute, Bologna Italy; [3]SC I Orthopedic and Traumatologic Clinic, Rizzoli Orthopedic Institute, Bologna Italy; [4]Department of Clinical Medicine, University of Bologna, Bologna, Italy

Received September 3, 2012 – Accepted November 30, 2013

Bone marrow is one of the best characterized stem cell microenvironments that contains Mesenchymal Stem Cells (MSCs), a rare population of non-hematopoietic stromal cells. MSCs have been indicated as a new option for regenerative medicine because of their ability to differentiate into various lineages such as bone, cartilage and adipose tissue. However, isolation procedures are crucial for the functional activity of the transplanted cells. The use of concentrated bone marrow cells (BMCs) enables a cell population surrounded by its microenvironment (niche) to be implanted while avoiding all the complications related to the *in vitro* culture. The cells of the niche are able to regulate stem cell behavior through direct physical contact and secreting paracrine factors. The aim of this study was to characterize BMCs *in vitro* to evaluate their ability to differentiate toward mature cells and try to understand whether there are differences in the chondrogenic and osteogenic potential of cells from patients of different ages. Mononuclear Cells (MNCs) isolated by Ficoll were used as control. Both cell populations were grown in monolayers and differentiated with specific factors and analyzed by histological and molecular biology assays to evaluate the expression of some specific extracellular matrix molecules. The present investigations revealed the ability of BMCs to act as isolated cells. They are able to form colonies and differentiate toward chondrogenic and osteogenic lineages, the latter pathway appearing to be influenced by donor age. The results obtained by this study support the use of BMCs in clinical practice for the repair of osteochondral damage, which might be particularly useful for the "one-step" procedure allowing cells to be directly implanted in operating room.

An important problem in orthopaedics is cartilage tissue lesions after injury or that occurs during osteoarthritic processes (1). Several techniques have been used to treat cartilage lesions, such as debridement (2), drilling subchondral bone (3), microfractures (4), periosteal and perichondral transplantation (5) and, in the last decade, autologous chondrocyte transplantation (6). This therapeutic strategy has been improved by the use of suitable scaffolds, which provide a biodegradable three-dimensional structure for tissue development, thus facilitating also the surgical procedure and the

Key words: bone marrow cells, mesenchymal stem cells, transplantation, osteochondral lesions, differentiation

Mailing address: Brunella Grigolo PhD,
SSD RAMSES Laboratory/SC,
Immunorheumatology and Tissue Regeneration Laboratory,
Istituto di Ricerca Codivilla Putti, Istituto Ortopedico Rizzoli,
Via di Barbiano 1/10, 40136 Bologna, Italy
Tel.: +39 051 6366803 Fax: +39 051 6366807
e-mail: brunella.grigolo@ior.it

0393-974X (2013)

expression of specific molecules by the cells (7). The goal is to regenerate a tissue with the structural and mechanical properties of the original one, a result that cannot be obtained by traditional therapeutic approaches. However, the use of mature chondrocytes isolated from articular cartilage and expanded in culture might be displaced by that of Mesenchymal Stem Cells (MSCs), which can be easily isolated from different sources, such as bone marrow (8). The potential of MSCs to produce cartilage and bone-like tissues has been widely shown *in vitro*, in animal and human models (9-11). However, little consensus and in many cases conflicting results regarding the effect of donor age on regenerative potential have been reported (12). A number of authors have reported a decrease in MSCs with increased age and some changes in differentiation, proliferation, attachment, senescence or self-renewal (13), whereas others have not (14). An age-related atrophy of MSCs has been suggested as a cause of decreased number of osteoprogenitor cells and decreased bone formation capacity because of a lack of mature matrix-forming OB (15).

The MSC population contains progenitors capable of *in vitro* proliferation and differentiation in the presence of specific factors such as Transforming Growth Factor-β (TGF-β) and Bone Morphogenic Protein-7 (BMP-7) for cartilage and dexamethasone, β-glycerophasphate (β-GP), and Fibroblast Growth Factor-2 (FGF-2) for bone, which significantly increase the frequency of tissue formation (16). MSCs commit to chondrogenesis and osteogenesis when the proliferation and phenotypic expression of cells are affected and different genes involved in these processes are modulated (17).

Recently, taking into account that MSC activity is due not only to the expression of one or more intrinsic cell capabilities but depends also on the surrounding microenvironment (niche), transplanting concentrated bone marrow cells (BMCs) was hypothesized (18). The concept that a stable, custom microenvironment or niche might control stem cells was initially hypothesized by Schofield (19). In a niche, neighboring subsets of cells and extracellular substrates house stem cells, and provide specialized functions to modulate stem cell self-renewal and progeny production *in vivo* (20). Bone marrow contains not only Hematopoietic Stem Cells (HSCs) and MSCs as a source for regenerating tissues but also accessory cells that support angiogenesis and vasculogenesis by producing several growth factors (21). Following these findings the transplantation of BMCs seems to be an ideal strategy for the regeneration of cartilage lesions that also involve the subchondral bone. Furthermore, the use of total bone marrow might avoid the isolation and expansion phases required to obtain MSCs, the possible malignant transformations of the cells and risks of adverse immune reactions e.g. components of the Foetal Bovine Serum (FBS) added to the culture (22).

To our knowledge, data present in the Literature which are aimed at characterizing bone-marrow-derived cells refer to studies on cells of animal origin which are isolated from bone marrow (23). The aim of the present study was to evaluate human BMCs, obtained by a concentration procedure performed directly in the operating room, by their phenotypical characterization and ability to differentiate towards chondrogenic and osteogenic lineages.

Mononuclear cells (MNCs) from the same patients isolated by synthetic polysaccharid gradient (Ficoll) were used for comparison. Cells were obtained from patients of different age in order to verify the influence of this factor on the differentiation potential.

MATERIALS AND METHODS

Bone marrow harvesting and concentration

Bone marrow was obtained from the iliac crest of 20 patients (mean age 30.35±12.63; 11 women and 9 men) undergoing autologous cell transplantation for the treatment of osteochondral defects. The Ethical Committee of the Institution approved the human protocol for this study. All investigations were conducted in conformity with ethical principles of research, and written informed consent was signed by all the patients enrolled in this research. The bone marrow was harvested from the posterior iliac crest in a sterile regimen, with the patient in prone decubitus and using general or spinal anesthesia. The marrow was aspirated in small fractions from different points to maximize the harvesting of the marrow stromal cells and reduce dilution by peripheral blood. The harvested bone marrow was reduced in volume directly in the operating room, by removing most of the red cells and plasma. Thus, it was possible to obtain a concentrate of nucleated cells, that are stem cells, monocytes, lymphocytes, and other bone marrow

resident cells. The bone marrow was concentrated with a cell separator (Smart PReP®, Harvest Technologies Corp., Plymouth, MA, USA), by a sterile and disposable dedicated kit (BMAC®, Harvest Technologies Corp., Plymouth, MA, USA). Sixty milliliters of bone marrow aspirate was injected into the posterior portion of the double chamber device. This was placed vertically on the rotor of the centrifuge. A 3 min centrifugation at 2500 rpm separated the red cells from the other components with the help of a semi-permeable membrane; then, during a 2 min arrest period, the buffy coat separated from the erythrocytes was transferred into the anterior chamber. Finally, a 9 min phase at 2300 rpm separated the cellular component from the plasma in the anterior chamber; at the end of the entire process the majority of the red cells remained in the posterior chamber of the container and the mononuclear cells were found at the bottom of the anterior chamber of the device, covered by the platelet-poor plasma. The cells were then aspirated with a syringe and re-suspended into platelet-poor plasma up to 6 ml of cell concentrate. Two out of the 6 ml of concentrate was sent to the authors' laboratory for the experiments *in vitro*. 0.5 ml of concentrate was used *in toto* and 1.5 ml was used to isolate mononuclear cells by Ficoll procedure.

MNC isolation

MNCs were isolated from bone marrow concentrate. 1.5 ml of bone marrow was diluted 1:10 with Phosphate Buffer Saline (PBS), collected in 50 ml tubes and isolated by Ficoll gradient (d=1.077 g/ml) (Sigma, St. Louis, MO, USA). The ring was collected and cells were washed twice, re-suspended in alpha-minimal essential medium (α-MEM) (Sigma) with 15% FBS and counted using Turk dye (Farmitalia Carlo Erba, Milano, Italy).

Analyses performed

Cells, both BMCs and MNCs, were analyzed by flow cytometry analysis (FACS) to evaluate their phenotypic expression. *In vitro* self-renewal capacity was demonstrated by Colony-Forming Unit Fibroblast (CFU-F) assays. Moreover, their differentiation capacity toward the osteogenic and chondrogenic lineages was also evaluated by Alcian Blu and Alizarin Red (Sigma) staining and by molecular biology investigations.

Flow cytometric analysis

A total of $10x10^6$ of BMCs and MNCs were used for the evaluation of specific markers by three-colour immunofluorescence. The cells were washed and resuspended with PBS containing 2% FBS and 0.1 % sodium azide (Sigma). Specific binding block was performed by incubating the cells for 10 min at Room Temperature (RT) with immunoglobulins (Dako, Glostrup, Denmark) of the same isotype of the primary antibodies used. $2.5x10^5$ cells for each marker were successively incubated with mouse monoclonal antibody anti-human CD45 conjugated with Tetramethyl Rhodamine Isothiocyanate (TRITC) (Dako), anti-human CD34 conjugated with Phycoerythrin (PE) and anti human CD90, CD105, CD106, CD146 conjugated with Fluorescein Isothiocyanate (FITC) (Serotec, Oxford, UK) at a concentration of 1μg/ml for each antibody in the dark for 30 min on ice. Then, the cells were washed twice and fixed with 1% paraformaldehyde and analyzed with a FACStar Plus (Becton Dickinson, Mountain View, CA). Negative and isotype-matched controls were performed. The percentages of specific markers were evaluated on CD34 and CD45 negative cells.

Colony-Forming Units-Fibroblast (CFU-F) assay

The clonogenic ability of BMCs and MNCs was determined by a low-density CFU-F assay $5x10^4$ cells from the two different populations were seeded in Petri dishes in α-MEM supplemented with 20% FBS. The medium was changed twice a week. At 7 and 14 days the wells were washed with PBS, and the cells were fixed with methanol and stained with Crystal Violet (Sigma). An aggregate of cells containing more than 50 cells was classified as a colony originating from one clonal cell.

Chondrogenic and osteogenic differentiation of BMCs and MNCs

The differentiation potential of both BMCs and MNCs was performed in monolayers. Despite being aware that chondrogenesis should be performed in 3D, in the present experiments pellet cultures could not be obtained from BMCs. $1.5x10^5$/wells of both BMCs and MNCs were seeded onto a 12-well plate in α-MEM supplemented with 15% FBS. For each sample one plate was used for histochemical assay and one for molecular biology analysis. Different plates were used for the experimental times scheduled. For chondrogenic differentiation the medium was replaced after 24 h with complete medium Dulbecco's Modified Eagle Medium (DMEM) (Life Technologies, Grand Island, NY, USA) with high glucose supplemented with ITS Premix: 6.25 μg/mL insulin, 6.25 μg/mL transferrin, 5.33 μg/mL linoleic acid, 1.25 mg/mL Bovine Serum Albumin (BSA) (BD Biosciences, Bedford, MA), 10^{-7} M dexamethasone (Sigma), 37.5 μg/mL ascorbate-2 phosphate (Sigma), 1 mM of sodium pyruvate (Sigma) and 10 ng/mL of TGF-β1 (R&D Systems).

For osteogenic differentiation the initial medium was substituted with: αMEM (Sigma) with 15% FBS (Cambrex) containing 75 μg/mL ascorbate-2 phosphate (Sigma), 0.01 mM β-GP (Sigma), 10^{-7} M dexamethasone

(Sigma).

Complete medium without the specific growth factors was used for chondrogenic and osteogenic control respectively. Cells (for both chondrogenesis and osteogenesis) were maintained in culture up to 28 days and the medium was changed twice a week.

Alcian Blue staining

To assess chondrogenic differentiation Alcian Blue staining was performed at 21 and 28 days. Briefly, cultured cells were washed with PBS, fixed in 10% neutral buffered formalin for 30 min at RT. Then, the cells were incubated for 3 min at RT with a 3% acetic acid solution and stained with 1% Alcian Blue solution for 30 min at room temperature. Stained cells were washed extensively in running tap water and rinsed in Double Deionizer Water (DDW).

Alizarin Red staining

To assess osteogenic differentiation, the calcium deposition was evaluated using Alizarin Red S staining at 21 and 28 days. Briefly, cultured cells were washed with PBS, fixed in 10% neutral buffered formalin for 1 h at room temperature. After washes in DDW, the cells were dehydrated in alcohol graded series and stained with 1% Alizarin red S solution (Sigma) for 2 min. Stained cells were washed extensively with DDW to remove the non-specific precipitation, positive red staining represents calcium deposits on the differentiated cells. Experiments were performed in duplicate wells.

Analysis of mRNAs expression by Real-Time PCR

BMCs and MNCs were analyzed by Real-Time RT-PCR to investigate the expression of specific markers during chondrogenesis and osteogenesis at 0 and 28 days for the former and at 0, 21 and 28 days for the latter. In particular, collagen type II, aggrecan and Sox-9 were evaluated in chondrogenic cells and Alkaline Phosphatase (AP), Bone Sialoprotein (BSP) and osteocalcin (OC), were evaluated in osteogenic cells. $1.5x10^5$ cultured cells were directly lysed by the addition to each well of 0.5 ml of TRIzol reagent (Invitrogen, Life Technologies). RNA was recovered by precipitation with isopropyl alcohol and then treated with DNase I (DNAfree Kit, Ambion, Austin, TX, USA). Total RNA was reverse transcribed using the Multiscribe reverse transcriptase (Applied Biosystems, Courtaboeuf, France), according to the manufacturer's protocol. PCR primers for the selected genes and for the housekeeping gene glyceraldehyde-3-phosphate dehydrogenase (GAPDH) used as an internal control were obtained from published references or designed using the PRIMER3 software (Table I) (24-26). Real-Time PCR was run in a LightCycler Instrument (Roche) using the QuantiTect® SYBRt® Green PCR Kit (Qiagen, GmbH, Germany) following previously described protocols (27). For each target gene, mRNA levels were normalized using the reference gene GAPDH.

Statistical analysis

Spearman's rank correlation analysis was used to test the relationship between age and differentiation and the differences among the follow-up times. The Mann Whitney test was performed to assess differences between means of the 2 types. General linear model for repeated measures with Sidak correction for multiple comparisons and type and age grouping as factors was performed to test differences of the scores at different follow-up times and the influence of age and type. For all tests $p<0.05$ was considered significant. Statistical Analysis was carried out by the Statistical Package for the Social Sciences (SPSS) software version 15.1 (SPSS Inc., Chicago, USA).

RESULTS

Flow cytometric analysis

BMCs and freshly isolated MNCs analyzed by FACS before seeding was positive for CD90, CD105, CD106, CD146 (Fig. 1A). The expression of these markers is similar between the two cell population and is not related to age (data not shown).

Colony-Forming Units-Fibroblast (CFU-F) assay

The functional capacity of BMCs and MNCs was determined by measuring the colony-forming activity. The CFU-F test showed that the mean number of colonies obtained with the two different cell populations was similar (Fig. 1B). No differences were observed among cultures of patients of different ages (data not shown).

Alcian Blue staining

During chondrogenic differentiation, an extracellular matrix deposition was evident on day 28 in both BMC and MNC cells (Fig. 2A). A slight difference was observed among patients of different ages (data not shown).

Alizarin Red staining

During osteogenic differentiation the calcium deposition was evident starting from day 21 and particularly on day 28 in both BMC and MNC cells. An evident difference was observed among patients

Table I. *List of primers used in Real-Time RT-PCR.*

Gene	Primer sequences (5'-3')	Amplicon size (base pairs)	Annealing temperature (°C)	References[a]
Aggrecan	5'-TCG AGG ACA GCG AGG CC 3'-TCG AGG GTG TAG CGT GTA GAG A	85	60	47
Type II collagen	5'-GAC AAT CTG GCT CCC AAC 3'-ACA GTC TTG CCC CAC TTA C	257	60	PRIMER 3
Sox-9	5'-GAG CAG ACG CAC ATC TC 3'-CCT GGG ATT GCC CCG A	118	60	PRIMER 3
ALP	5' GGA AGA CAC TCT GAC CGT 3' GCC CAT TGC CAT ACA GGA	152	60	PRIMER 3
BSP	5' CAGTAGTGACTCATCCGAAG 3'CATAGCCCAGTGTTGTAGCA	158	60	PRIMER 3
OC	5' GCA GCG AGG TAG TGA AGA 3' TCC TGA AAG CCG ATG TGG	148	60	PRIMER 3
GAPDH	5'-TGG TAT CGT GGA AGG ACT CAT GAC 3'-ATG CCA GTG AGC TTC CCG TTC AGC	190	60	46

[a]*Primer sequences were obtained from published references where indicated or designed using PRIMER 3.*

of different ages in a high percentage of cases evaluated (Fig. 2B).

Analysis of mRNAs expression by Real-Time PCR: Chondrogenesis

To investigate the chondrogenic differentiation potential of both BMCs and MNCs, type II collagen, Sox-9 and aggrecan mRNA were analyzed by quantitative RT-PCR on day 0 and 28, since in the authors' experience before this time mRNA chondrogenic-specific markers are very poorly expressed. No significant differences were observed between the two cell groups analyzed at all the experimental times evaluated. Collagen type II mRNA, which was almost undetectable on day 0 in both BMCs and MNCs, showed a very light increase on day 28 in the first group while a more evident, even not significant, expression on the same day in the second one (Fig. 3A). Sox-9, a transcriptional factor of collagen type II, was significantly highly expressed on day 28 compared to day 0 ($p<0.0005$) (Fig. 3B). Aggrecan mRNA was highly expressed on day 28 compared to day 0 with significant values ($p<0.0005$) (Fig. 3C). For these chondrogenic markers no differences were observed among patients of different ages (data not shown).

Analysis of mRNAs expression by Real-Time PCR:Osteogenesis

No difference between BMC and MNC groups was observed for ALP, BSP and OC mRNA expression at all the experimental times evaluated. In general, ALP was significantly higher on day 21 and day 28 compared to day 0 ($p<0.0005$) although it tended to decrease from day 21 until day 28 (Fig. 4A). These differences were influenced by age since the higher increase was evident for younger patients (<25 years) compared to "older ones" (>25 years) as was the decrease which was more evident for the first group ($p=0.037$) (Fig. 4B). BSP increased significantly on day 21 ($p<0.0005$) and 28 ($p<0.013$) compared to day 0 in both cell populations (Fig. 4C). Moreover, inside each group, a significant difference between younger patient and older ones was observed ($p<0.035$) since in the former BSP increased at high levels up to 28 days (Fig. 4D). Osteocalcin mRNA

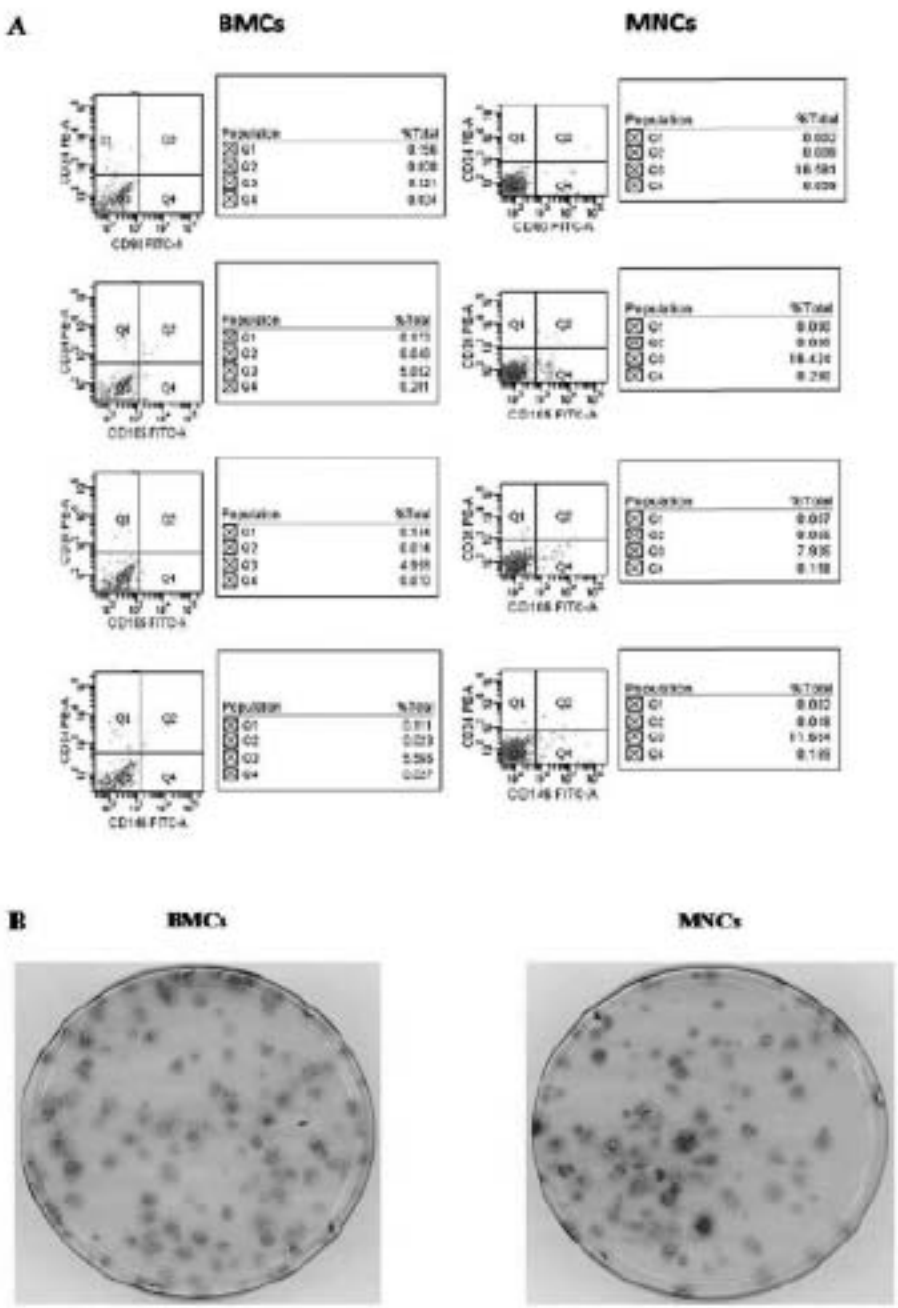

Fig. 1. ***A****) Flow cytometric analyses of CD90+, CD105+, CD106+ and CD146+ evaluated on CD34 and CD45 negative cells.* ***B****) Colonies forming Units. 14 days after initial seeding of 5x10*^{5} *BMCs and MNCs; no differences between the two populations analyzed are present. Two representative colonies in CFU-F assay are shown.*

was slightly highly expressed on day 21 compared to day 0 and significantly more highly expressed on day 28 compared to day 0 ($p<0.049$) (Fig. 4E). No significant differences were observed among patients of different ages (data not shown).

DISCUSSION

Currently, there is no reliable reconstructive technique to repair osteochondral articular defects anatomically (1). Cartilage and bone repair requires a

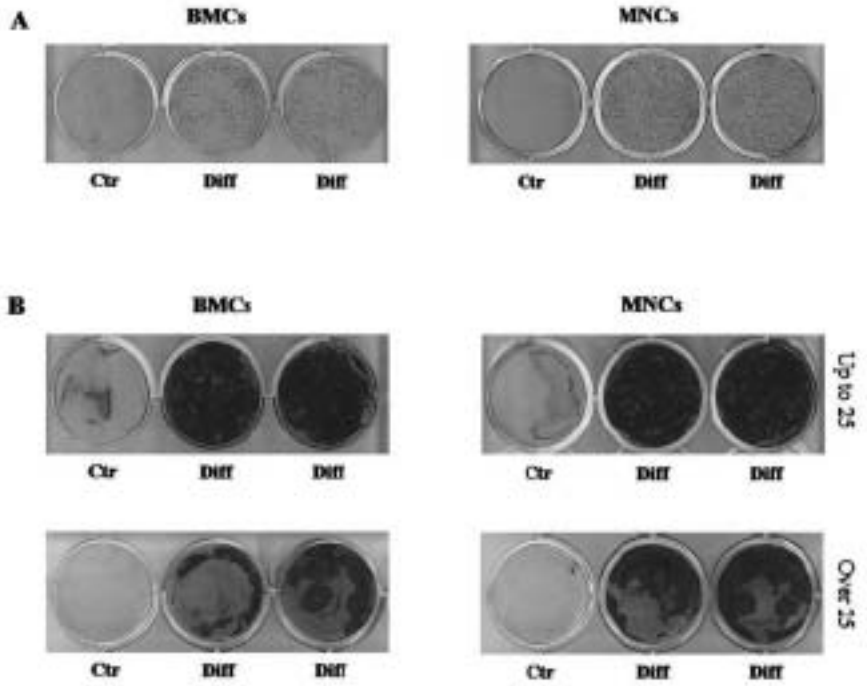

Fig. 2. ***A****) Alcian Blue staining of BMCs and MNCs cultured in the absence (Ctr) or presence of TGF-ß1 (Diff) at 28 days. Diff samples are in duplicate. No differences between BMCs and MNCs are present.* ***B****) Alizarin Red S staining of BMCs and MNCs of representative patients cultured in the absence (Ctr) or presence of ascorbate-2 phosphate, ß-glycerophosphate and dexamethasone (Diff) at 28 days. Diff samples are in duplicate. In the upper panel cells from a patient <25 years were seeded, whereas in the lower panel, cells from a patient >25 years were seeded. There is a visible different staining between the cells from the patients of different ages.*

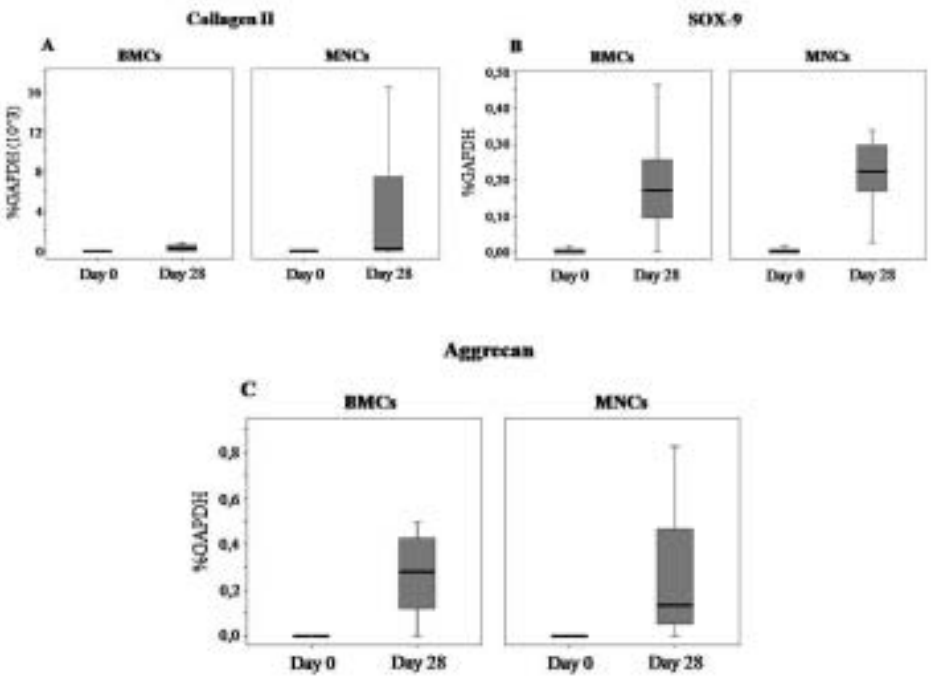

Fig. 3. *Distribution of Type II collagen (****A****), Sox-9 (****B****) and Aggrecan (****C****) messenger RNAs expression in BMCs and MNCs at day 0 and day 28. Sox-9 is more highly expressed at day 28 compared to day 0 (p<0.0005) such as Aggrecan (p<0.0005). Data (mean±standard deviation) were normalized to GAPDH.*

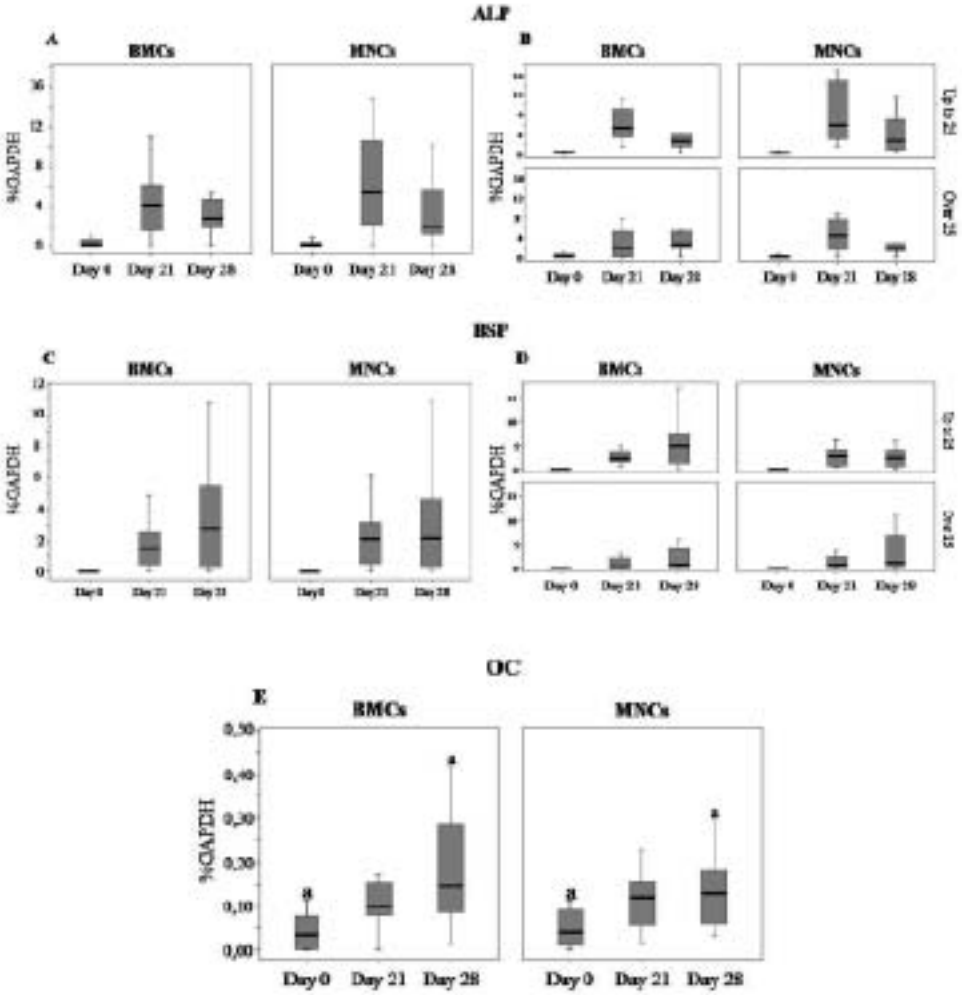

Fig. 4. *Distribution of ALP messenger RNAs expression in BMC and MNC groups at days 0, 21 and 28 (**A**); ALP is more highly expressed at day 21 compared to day 0 ($p<0.0005$) and at day 28 compared to day 0 ($p<0.0005$). Distribution of ALP messenger RNAs expression in the two different age groups: up to 25 and over 25 (**B**); in addition to the significant differences observed in figure 4A, a significant decrease at day 28 compared to day 21 is observed in the group of patient up to 25 ($p<0.037$). Distribution of BSP messenger RNAs expression in BMC and MNC groups at day 0, 21 and 28 (**C**); BSP is more highly expressed at day 21 compared to day 0 ($p<0.0005$) and at day 28 compared to day 0 ($p<0.013$). Distribution of BSP messenger RNAs expression in the two different age groups: up to 25 and over 25 (**D**); in addition to the significant differences observed in figure 4C, a significant decrease at day 28 compared to day 21 is observed in the group of patients up to 25 ($p<0.035$). Distribution of OC messenger RNAs expression in BMC and MNC groups at days 0, 21 and 28 (**E**). OC is slightly more highly expressed at day 21 compared to day 0 and significantly more highly expressed at day 28 compared to day 0 ($p<0.049$). Data (mean±standard Ddeviation) were normalized to GAPDH.*

multistep controlled activation and silencing of genes producing extracellular matrix, growth factors, and adhesion molecules involved in tissue formation (1). The use of autologous chondrocyte transplantation has produced successful results in recent years (28). However, this technique has some limitations, such as requiring two surgical operations for healthy cartilage harvesting and cell implantation and it is not employable in the presence of osteochondral defects which require the regeneration of both cartilage and bone tissues (1). This has led to the search for other cell types that can be obtained from the patient

without performing an arthroscopy procedure.

MSCs are a fascinating source for regenerative medicine because they can be harvested in a less invasive manner, easily isolated and expanded *in vitro*. MSCs have proven to be able to differentiate, after appropriate induction, into several mesodermal tissues including cartilage and bone (29). They provide tissue protection and repair by the release of paracrine molecules including cytokines and growth factors (30). Nevertheless, in bone marrow aspirate, MSCs account for a very small fraction of the total population of nucleated cells; therefore, innovative in-depth research has paved the way for the clinical use of concentrate bone marrow . However, despite the increase in the number of precursor cells obtained by the concentration procedure, the rationale for using total bone marrow resides in its peculiar characteristics that identify it as an orchestra of cells and signals. As reported above, the bone marrow niche which comprises HSCs and MSCs is responsible for the regeneration of tissues. However, it is certain that the composition of cell types and extracellular matrix components in the bone marrow varies extensively over a lifetime. These changes are reflected also by decreased bone formation .

The present study was aimed at characterizing human BMCs, by analyzing their phenotypical and functional features to further support their use for the regeneration of damaged osteochondral tissues. The behavior of these cells was compared to that of MNCs isolated by the Ficoll procedure which is the gold standard but has some important limitations such as the time needed for the procedure and the requirement of Good Laboratory Manufacturing practice (GMP).

Taking into account one of the minimal criteria for defining multi-potent mesenchymal stromal cells, that refers to the expression of specific CD markers (31), our data show that BMCs present the same CD pattern as isolated MNCs. However, being the MSC population extremely low in the two different cell populations a quantitative comparison is quite impossible.

Concerning the clonogenic capacity of BMCs and MNCs, our results demonstrated that both cell populations are able to form CFU-F colonies with a similar ability.

Concerning the differentiation potential, both BMCs and MNCs are able to differentiate *in vitro* towards chondrogenic and osteogenic lineages as testified by the expression of specific extracellular molecules during culture. These results are not be surprising since both groups comprise cells of the same origin, but it had to be shown since the BMC population is heterogeneous. In both cell populations some differences are highlighted among patients of various ages particularly for their ability to differentiate into the osteogenic lineage. Cells from patients up to 25 years old express, during their differentiation process, higher levels of osteogenic markers such as ALP and BSP compared to those of patients over 25 years old. These results are in agreement with other previous data giving further evidence of the effect of donor age on differentiation, particularly towards the osteogenic lineage (13), and confirm the combination of niche microenvironment intrinsic changes and aging. This finding is not related, however, to a specific mesenchymal phenotype since no correlations were observed between the expression of cellular surface markers and that of specific molecules involved in the differentiation processes. Based on the results of this and other similar studies, it is evident that many variables must be taken into account for the choice of an ideal cell source for tissue regeneration and in particular the age of the patients. Despite this, the use of total bone marrow which avoids the expansion of the cells and low the cost of the procedure may be preferred compared to other procedures. The correlation between the present *in vitro* results and the clinical outcome in the follow-up of patients treated with BMCs will be the aim of future studies.

The results obtained by this study support the use of bone marrow concentrate in clinical practice for the repair of osteo-chondral damage, which might be particularly useful for the “One-Step” procedure allowing cells to be directly implanted in the operating room.

ACKNOWLEDGEMENTS

We thank Patrizia Rappini and Graziella Salmi for their assistance in the preparation of the manuscript and Luciano Pizzi for his technical assistance. We also thank Dr Elettra Pignotti for statistical analysis and Dr Keith Smith for the revision of English

language. This work was partially supported by grants from Progetto Regione Emilia-Romagna Università 2007-2009 "Regenerative medicine in osteo-articular diseases".

REFERENCES

1. Buckwalter JA, Rosenberg LC, Hunziker EB. Articular cartilage: composition, structure, response to injury and methods of repair. In Articular cartilage and knee joint function: basic science and arthroscopy. JW Ewing eds Raven Press 1990; p.19.
2. Clarke HD, Scott WN. The role of debridement: through small portals. J Arthroplasty 2003; 18:10-3.
3. Takao M, Ochi M, Naito K, Uchio Y, Kono T, Oae K. Arthroscopic drilling for chondral, subchondral, and combined chondral-subchondral lesions of the talar dome. Arthroscopy 2003; 19:524-30.
4. Steadman JR, Rodkey WG, Rodrigo JJ. Microfracture: surgical technique and rehabilitation to treat chondral defects. Clin Orthop Relat Res 2001; 391:(S)362-9.
5. Ritsilä VA, Santavirta S, Alhopuro S,. Periosteal and perichondral grafting in reconstructive surgery. Clin Orthop Relat Res 1994; 302:259-65.
6. Brittberg M, Lindahl A, Nilsson A, Ohlsson C, Isaksson O, Peterson L. Treatment of deep cartilage defects in the knee with autologous chondrocyte transplantation. N Engl J Med 1994; 331:889-95.
7. Kon E, Verdonk P, Condello V, Delcogliano M, Dhollander A, Filardo G, Pignotti E, Marcacci M. Matrix-assisted autologous chondrocyte transplantation for the repair of cartilage defects of the knee: systematic clinical data review and study quality analysis. Am J Sports Med 2009; 37:156-66.
8. Ronzière MC, Perrier E, Mallein-Gerin F, Freyria AM. Chondrogenic potential of bone marrow- and adipose tissue-derived adult human mesenchymal stem cells. Biomed Mater Eng 2010; 20:145-58.
9. Heng BC, Cao T, Lee EH. Directing stem cell differentiation into the chondrogenic lineage in vitro. Stem Cells 2004; 22:1152-67.
10. Grigolo B, Lisignoli G, Desando G. Osteoarthritis treated with mesenchymal stem cells on hyaluronan-based scaffold in rabbit. Tissue Eng Part C Methods 2009; 15:647-58.
11. Marcacci M, Kon E, Moukhachev V, Lavroukov A, Kutepov S, Quarto R, Mastrogiacomo M, Cancedda R. Stem cells associated with macroporous bioceramics for long bone repair: 6- to 7-year outcome of a pilot clinical study. Tissue Eng 2007; 13:947-55.
12. Chambers SM, Goodell MA. Hematopoietic stem cell aging: wrinkles in stem cell potential. Stem Cell Rev 2007; 3:201-11.
13. Roobrouck VD, Ulloa-Montoya F, Verfaillie CM. Self-renewal and differentiation capacity of young and aged stem cells. Exp Cell Res 2008; 314:1937-44.
14. Oreffo RO, Bennett A, Carr AJ, Triffitt JT. Patients with primary osteoarthritis show no change with ageing in the number of osteogenic precursors, Scand J Rheumatol 1998; 27:415-24.
15. Quarto R, Thomas D, Liang CT. Bone progenitor cell deficits and the age-associated decline in bone repair capacity. Calcif Tissue Int 1995; 56:123-9.
16. Indrawattana N, Chen G, Tadokoro M, Shann LH, Ohgushi H, Tateishi T, Tanaka J, Bunyaratvej A. Growth factor combination for chondrogenic induction from human mesenchymal stem cell, Biochem Biophys Res Commun 2004; 320:914-9.
17. Chimal-Monroy J, Rodriguez-Leon J, Montero JA, Gañan Y, Macias D, Merino R. Analysis of the molecular cascade responsible for mesodermal limb chondrogenesis: Sox genes and BMP signaling. Dev Biol 2003; 257:292-301.
18. Taichman RS. Blood and bone: two tissues whose fates are intertwined to create the hematopoietic stem-cell niche. Blood 2005; 105:2631-9.
19. Schofield R. The relationship between the spleen colony-forming cell and the haemopoietic stem cell. Blood Cells 1978; 4:7-25.
20. Spradling A, Drummond-Barbosa D, Kai T. Stem cells find their niche. Nature 2001; 414:98-104.
21. Velazquez OC. Angiogenesis and vasculogenesis: inducing the growth of new blood vessels and wound healing by stimulation of bone marrow-derived progenitor cell mobilization and homing. J Vasc Surg 2007; 45:39-47.
22. Tonti GA, Mannello F. From bone marrow to therapeutic applications: different behaviour and genetic/epigenetic stability during mesenchymal stem cell expansion in autologous and foetal bovine sera. Int J Dev Biol 2008; 52:1023-32.

23. Bosnakovski D, Mizuno M, Kim G, Takagi S, Okumura M, Fujinaga T. Chondrogenic differentiation of bovine bone marrow mesenchymal stem cells in pellet culture system. Exp Hematol 2004; 32:502-9.
24. Blanco FJ, Geng Y, Lotz M. Differentiation-dependent effects of IL-1 and TGF-β on human articular chondrocyte proliferation are related to inducible nitric oxide synthase expression. J Immunol 1995; 154:4018-26.
25. Martin I, Jakob M, Schäfer D, Dick W, Spagnoli G, Heberer M. Quantitative analysis of gene expression in human articular cartilage from normal and osteoarthritic joints. Ostearthritis Cart 2001; 9:112-8.
26. Rozen S, Skaletsky HJ. Primer3 on the WWW for general users and for biologist programmers. In Bioinformatics Methods and Protocols: Methods in Molecular Biology. Humana 2000; p.365.
27. Cavallo C, Desando G, Columbaro M. Ferrari A, Zini N, Facchini A, Grigolo B. Chondrogenic differentiation of bone marrow concentrate grown onto a hylauronan scaffold: rationale for its use in the treatment of cartilage lesions. J Biomed Mat Res Part A 2012; doi10:1002.
28. Harris JD, Siston RA, Pan X, Flanigan DC. Autologous chondrocyte implantation: a systematic review. J Bone Joint Surg Am 2010; 92:2220-33.
29. Caplan AI. Mesenchymal stem cells. J Orthop Res 1991; 9:641-50.
30. Schutze N, Noth U, Schneidereit J, Hendrich C, Jakob F. Differential expression of CCN-family members in primary human bone marrow-derived mesenchymal stem cells during osteogenic, chondrogenic and adipogenic differentiation. Cell Commun Signal 2005; 31-12.
31. Dominici M, Le Blanc K, Mueller I. Minimal criteria for defining multi-potent mesenchymal stromal cells. The International Society for Cellular Therapy position statement. Cytotherapy 2006; 8:315-7.

EFFECT OF AUTOLOGOUS PLATELET-RICH PLASMA ON DISTRACTION OSTEOGENESIS IN THE MANDIBLE OF RABBITS: A MORPHOLOGIC AND MORPHOMETRIC APPROACH

T. BOU ASSI[1], M. RAHME[2], S. SAGHIEH[3], N. BOU RAAD AZOURY[4], I. ABDALLAH HAJJ HUSSEIN[2, 5], A. LEONE[6] and A. JURJUS[2]

[1]Department of Pathology and Laboratory Medicine, American University of Beirut, Lebanon; [2]Department of Anatomy, Cell Biology and Physiology, American University of Beirut, Lebanon; [3]Department of Surgery, American University of Beirut, Beirut, Lebanon; [4] Faculty of Nursing Al Mana College Of health Science Al-Khobar, Saudia Arabia; [5]William Beaumont School of Medicine, Oakland University, Michigan, USA; [6]Department of Experimental Biomedecine and Neuroscience, Section of Histology and Embryology, University of Palermo, Italy

Received October 30, 2012 – Accepted January 11, 2013

Distraction osteogenesis of the jaw is a common surgical practice in the treatment of pediatric craniofacial deformities. Autologous platelet rich plasma (PRP) has been used to increase the healing potential of bones in humans during distraction osteogenesis. This article aims to study the morphometric and morphologic parameters resulting from the effect of PRP on bone healing after mandibular distraction in rabbits. Right mandibular distraction was performed in 12 rabbits divided equally into 2 groups. PRP and physiological saline were injected, according to a defined protocol, in the callus following distraction of the experimental and control groups respectively. The rabbits were sacrificed after a consolidation period of 45 days and the mandibles were surgically removed. Bone mineral density, radiographic analysis, mechanical properties and histological features of the lengthened bones were assessed using radiographic examination, dual X-ray absorptiometry, biomechanical testing and histology. Results showed that the regenerate bone density, the amount of trabeculation in addition to the bone mineral density and mineral content, as measured by absorptiometry, were better with PRP but not significantly different between groups. Two radiographs revealed a more consistent healing in the experimental mandibles compared with erratic outcomes in corresponding controls. Two of the latter could not be subjected to any mechanical testing because the mandibular parts, connected with fibrous tissue, were separated. Consequently, the biomechanical test depicted greater maximal loads in the experimental group. The histological studies exhibited more ossification and less connective tissue fibers in the experimental group. PRP accelerated healing of mandibles in rabbits following distraction and improved their biomechanical properties. These findings have significant clinical implications on reducing the period of consolidation of the mandibles which may not be immobilized like other bones for long periods of time.

Distraction osteogenesis on the jaw is currently used by maxillofacial surgeons for treating various

Key words: mandibular distraction, platelet-rich plasma, mandible osteogenesis

Mailing address: Dr Angelo Leone. MD,
Sp. Ortho, PGCAPHE,
Sezione di Istologia ed Embriologia Generale,
Facolta' di Medicina e Chirurgia,
Universita' degli Studi di Palermo, Palermo, Italy
Tel.:+39 091 6553581 Fax: +39 091 6553586
e-mail: angelo.leone@unipa.it

0393-974X (2013)

DISCLOSURE: ALL AUTHORS REPORT NO CONFLICTS OF INTEREST RELEVANT TO THIS ARTICLE.

pediatric deformities such as mandibular and maxillary retrognathia (1, 2), lengthening of a short mandibular ramus and widening of a narrow mandible (3). Because of the long consolidation period, the main problem encountered following distraction is bone fracture with an incidence that varies from 3-39% (4). That led researchers to test the effect of some substances on the bone remodeling process.

Accelerating bone healing was mainly tested in tibia and femur, only rare studies addressed the craniofacial complex. The effect of adjuvant on bone healing in the consolidation period can be summarized as acceleration using parathyroid hormone (PTH) (5, 6), growth hormone (GH) (7, 8) and stem cells (9, 10). However, more experiments are needed with Calcitonin (11, 12), Alendronate (12) and Platelet Rich Plasma (PRP) before making final conclusions.

PRP serves as a reservoir of critical growth factors that contribute to bone healing including platelet derived growth factor (PDGF), transforming growth factor (TGF), insulin like growth factor 1 (IGF 1) (13-15). PRP improves the healing potential of femur, tibia and overlying soft tissue and shortens the consolidation period (16-18). In addition, it increases bone density and radiographic maturation rate (19). It is also believed that it produces an advanced state of osteogenic differentiation (20) and PRP improves wound healing in patients with multiple myeloma who developed osteonecrosis of the jaw (21). Furthermore PRP has similar effects on skeletal muscle lesions, it improves muscle regeneration and neovascularization (22).

The possible effect of PRP on the quality and healing potential of a distracted mandible needs further studies. Our objective is to assess the morphometric and morphologic effects of autologous PRP on bone remodeling in the jaws of rabbits. While there is published data on bone formation rate in the appendicular skeleton, there is little such information on the jaws of rabbits.

MATERIALS AND METHODS

Twelve young white New Zealand rabbits weighing 2 kg each and divided into 2 groups of 6, were included in this study. Twelve fixators (M100- Orthofix USA) were inserted in the right mandibles of the rabbits with four 3mm half pins. Group one was injected with physiologic saline in the callus following distraction, while group 2 was injected with autologous PRP. All the rabbits were acquired and maintained in the animal house of the American University of Beirut (AUB) and treated according to guidelines set by the Institutional Animal Care and Use Committee of the American University of Beirut.

Surgical procedure

Following anesthesia by Ketamine (35 mg/kg), Xylazine (10 mg/kg) and Midazolane (2 mg/kg), a longitudinal skin incision was made along the inferior border of the mandible. The underlying muscles and periosteum were reflected to expose the mandibular body and nerve. The mental nerve served as a landmark during the surgery since two of the pins were placed directly anterior to the nerve and the remaining two posterior to it while the corticotomy was performed directly posterior to it.

(a) (b)

Fig. 1. ***A)*** *Inferior view of the distractor fixation on the pins.* ***B)*** *Lateral view of the distractor fixation on the pins.*

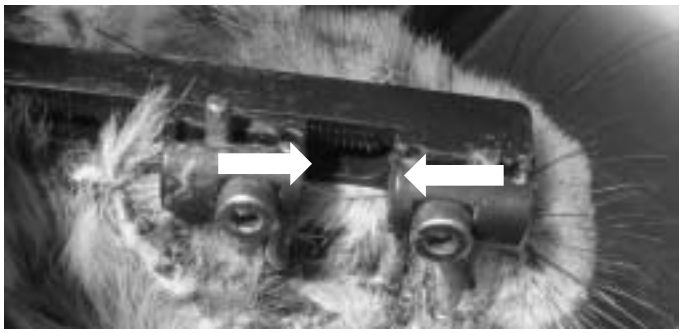

Fig. 2. *Lateral view of the rabbit's mandible showing 10 mm of mandibular distraction (between the white arrows).*

Fig. 3. *Anterior view of the rabbit's teeth showing a 10 mm shift between the maxillary and mandibular midlines upon occlusion as a result of mandibular distraction.*

The pins were checked at the end of the surgery for their parallelism. After insertion of the pins, the corticotomy was performed using an abrasive disc engaged in a rotary instrument. The corticotomy was performed between the mental nerve and the pin posterior to it. Penicillin was locally injected and then the wound sutured over the pins. Finally, the distractor was fixed on the pins with screws (Fig. 1).

Injection of antibiotics (streptomycin/penicillin 0.1 ml/Kg) and analgesics (tramal 10 mg/kg) were performed every 8 h for 3 days following surgery. The recovery period (latency period) was set for 5 days following distractor placement. During this period, 2 rabbits died in the first 2 days of the latency period due, most probably, to a severe bleeding during the surgery. They were replaced by 2 new rabbits on which new surgeries were performed.

Protocol of distraction

After the recovery period, the distraction phase started at a rate of 1 mm per day for a total of 10 days, corresponding to 10 mm of bone distraction and callus formation (Fig. 2).

Checking the amount of distraction was performed by observing the occlusion between the maxillary and mandibular incisors. Normally, the incisors should be overlapping and the maxillary midline is aligned with the mandibular midline, however, following distraction we could clearly see the amount of shift between midlines (Fig. 3).

PRP preparation

Following the distraction phase, PRP was prepared according to the method described by Gimeno et al (23). Under general anesthesia, 12 ml of whole blood was collected from each rabbit then centrifuged for 15 m at 4°C with a 70g speed. The resulting 5 ml supernatant plasma was further centrifuged at 4°C for 5 m at 1010 g, resulting into two parts; the upper 4.7 ml were poor-platelet plasma (PPP) and the lower pellet was of 0.3 ml of platelet-rich plasma (PRP). Then, 4 drops of a 5% calcium chloride

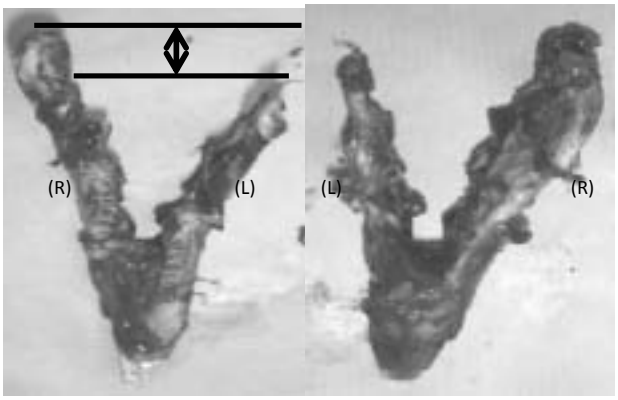

(a) Upper view (b) Lower view

Fig. 4. *Removed mandibles of both experimental and control groups after the consolidation period (day 60). Note the 10 mm length difference between right distracted mandibular part (R) and left non distracted mandibular part (L) (Black arrow).*

(CaCl2) solution were added to the PRP that became to transform into a gel like solution.

Injection of PRP and Physiologic Saline

Following blood withdrawal, 0.3 ml of PRP+CaCl2 or 0.3 ml of physiologic saline were injected (D15) into the rabbit's distracted mandibular areas of the experimental and control groups, respectively.

Consolidation period

The rabbits were kept in separate cages for 45 days and supplied with the appropriate food. Weight was measured every 2 weeks for all rabbits, only one rabbit from the experimental group showed a significant weight loss which led to its death in the 30th day of the consolidation period. The other rabbits showed a non significant ±200 g variation in their weight. The lost rabbit was not replaced. At the end of the consolidation period 5 rabbits remained in the experimental group and 6 in the control group.

Rabbits sacrificed

Following the consolidation period, the rabbits were sacrificed. The mandibles were removed. The extracted mandibles showed a 10 mm difference in length between the right and left mandibles which reflected the amount of distraction performed on the right mandible (Fig. 4).

The amount of distraction was measured on each removed mandible using calipers. One rabbit from the control group (N 5) was also after its removal excluded from the study for technical reasons.

Tests performed

Radiographic examination. The bone density and the amount of trabeculation within the regenerate area of each removed mandible were descriptively assessed on the radiographs and compared between both groups.

Regional dual X ray absorptiometry. Measurement of bone mineral density (BMD) and content of distracted areas was achieved using dual X-ray energy absorptiometry machine (Hologic Discovery, USA). Bone mineral content (BMC) and BMD for each rabbit were computed (4).

Mechanical test. The distracted mandibles were loaded in three-point bending test at the Faculty of Engineering, AUB. A force generated hits the middle area of the regenerate and causes its flexure and eventually leading into its breakage (Fig. 5).

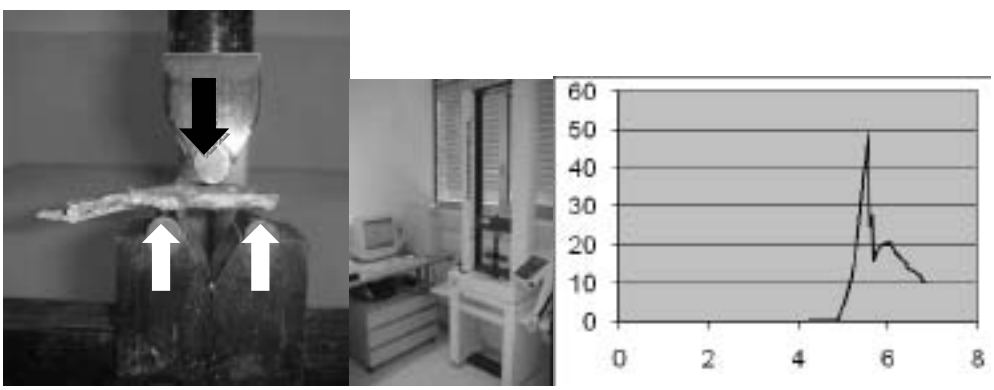

(a) (b) (c)

Fig. 5. ***A)*** *Mandible subjected to the three point bending test. Mandible seated on 2 points (white arrows) and a third point (black arrow) going down and hitting the regenerate middle area.* ***B)*** *Three point bending machine linked to a computer which represents the maximal flexural strength of the mandible on a graph.* ***C)*** *Maximal load of 49 N supported by the tested mandible.*

The generating force system was attached to a computer which represented the maximal flexural strength of the bone on a graph. The fracture strength was determined as the maximum load supported by each mandible before breakage; it was represented by the peak of the graph shown following the test. The X axis represented the flexion of the bone in mm and the Y axis represented the force corresponding to the flexure in Newton (N) (Fig. 5).

Histological test. Following the mechanical test, the regenerate area was sectioned. The first cutting area was medial to the pin previously placed medial to the mental nerve and the second cutting area distal to the pin; that is, placed distal to the mental nerve. The sectioned part contained the regenerate and the mandibular normal bone on both medial and distal sides. Following decalcification with a 0.5 mol/L ethylenediaminetetraacetic acid solution for 3 days, the bones were processed for routine microscopy according to established procedures. Five micrometer serial sections were cut from each block. Some were stained with Hematoxylin & Eosin (H&E) and some others with Masson Trichrome stain according to standard procedure for detection of collagen fibers within the tissue of the regenerate area.

RESULTS

The results were based on the treated mandibles of 10 rabbits. The control group consisted of 5 rabbits (3, 4, 7, 11 and 14) and the experimental group consisted also of 5 rabbits (2, 8, 10, 12 and 13). Rabbit 5 was excluded from the control group due to a lack of optimal distraction (7 mm) and rabbit 9 of the experimental group died on day 30th of the

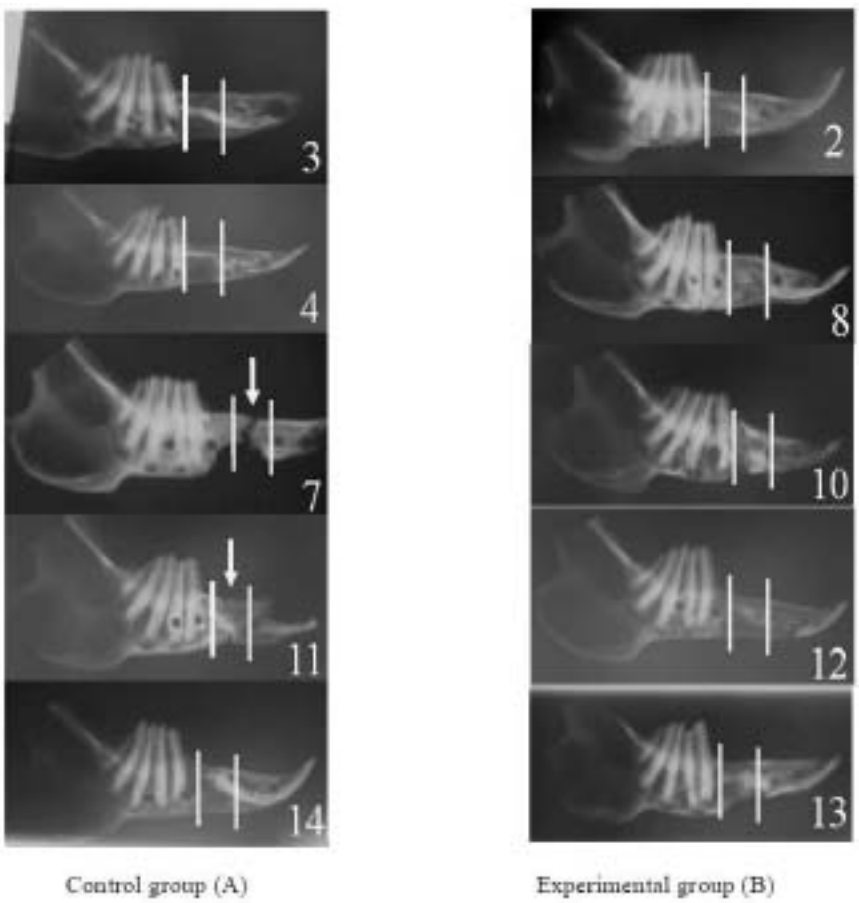

Fig. 6. *X-ray photos of the removed mandibles of both groups (Day 60). X-rays 3, 4, 7, 11 and 14 represent those of the control group (**A**) whereas 2, 8, 10, 12 and 13 represent the X-rays of the experimental group (**B**). Note the presence of gaps in 7 and 11 (White arrows) while no gaps existed in the experimental mandibles. The difference in trabeculaton and bone density between both groups was not significant. Note more predictable response in all experimental samples and more variations in the control group samples.*

Table I. *Regional dual x-ray absorptiometry (control group).*

Rabbits	Area (cm^2)	BMC (gm)	BMD (gm/cm^2)
N 3	1.21	0.27	0.224
N 4	1.21	0.18	0.152
N 7	0.92	0.14	0.150
N 11	1.19	0.28	0.24
N 14	1.03	0.16	0.156
Averages	**1.112**	**0.206**	**0.1844**
SEM	**0.101**	**0.086**	**0.080**
SD	**0.131**	**0.064**	**0.043**

BMC: Bone mineral content; BMD: Bone mineral density

Table II. *Regional dual x-ray absorptiometry (experimental group).*

Rabbits	Area (cm^2)	BMC (gm)	BMD (gm/cm^2)
N 2	1.32	0.21	0.162
N 8	1.16	0.17	0.147
N 10	1.09	0.35	0.32
N 12	1.13	0.12	0.111
N 13	1.06	0.19	0.176
Averages	**1.152**	**0.208**	**0.1832**
SEM	**0.101**	**0.086**	**0.080**
SD	**0.101**	**0.086**	**0.081**

consolidation period.

Macroscopic examination of the regenerate

A significant difference was noted between both groups concerning the amount of soft tissue in the middle area of the regenerate. In the experimental group, the regenerate area showed less soft tissue. In all control animals injected with saline, the relative amount of soft tissue was relatively more than controls. However, in 3 to5 animals of the control group; the soft tissue was significantly more abundant at the interface resulting in breakage of 2 of them at that site during manipulation of the mandibles.

Radiographic analysis

As shown in Fig. 6, all 5 mandibles of the experimental group showed complete ossification while 2 in the control mandibles showed clear gaps in the center of the regenerate areas. On the other hand, bone density and trabeculations did not show any significant difference.

Regional dual x-ray absorptiometry analysis

Although ossification was faster in the experimental group, no statistically significant difference has been noted, at this advanced stage of 45 days, between both control and experimental groups in the parameters tested, namely, BMC and BMD (Tables I and II).

Biomechanical testing

Mandibles of samples 7 and 11 from the control group were broken during manipulation. The experimental group samples showed a greater statistically significant strength as compared to control group samples. It might pertinent to note that, if the 2 outliers in both control and experimental

Table III. *Biomechanical test results.*

Experimental group	Maximal load (N)	Control group	Maximal load (N)
N 2	56.3	N 3	119.5
N 8	92	N 4	74.2
N 10	64	N 7	0
N 12	67.4	N 11	0
N 13	48.8	N 14	10.9
Averages	**65.7**		**40.9**
SD	**16.36**		**53.7**

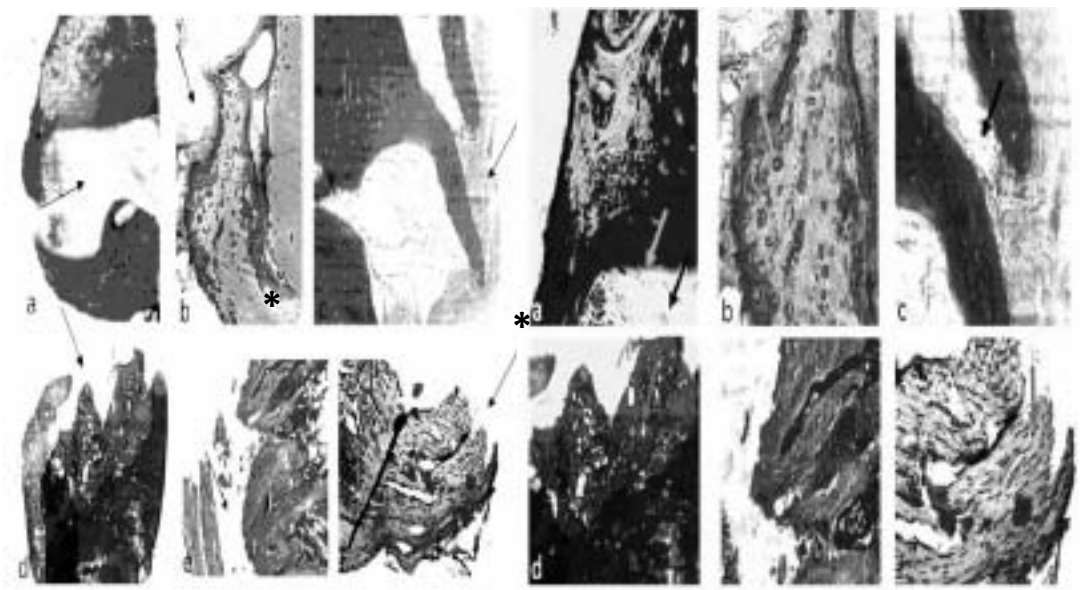

Fig. 7. *(Left panel) Photos of the histological cuts of the regenerate areas at 100 X magnification of the 3 samples of the control group (**a, b** and **c**) and 3 samples of the experimental group (**d, e** and **f**). Black arrows indicate the interface areas. The slides **a**, **b** and **c** clearly showed a great amount of green stained areas (black star) which corresponded to soft tissue and collagen fibers presence, reflecting a lack, or low level of calcification and bone maturation. The slides d and e were highly eosinophilic and did not show any green stained areas but more osteoid tissue and trabeculations which can be explained by the maturation of the woven non-calcified bone into a mature cortical bone. The slide f showed, still at the level of the interface, minor areas of green stain indicating incomplete ossification, however, much less than the control group. (Right panel) Photos of the histological sections at 200 magnifications of the regenerate areas of the 3 samples of the control group (a, b and c) and 3 samples of the experimental group (**d, e** and **f**). Black arrows represent the blood vessels in the interface area of the sections of the control groups. Yellow arrows represent the osteoblasts lining the interface area of the sections of the control group. Blue arrows represent the embedded osteocytes shown in the sections of the experimental group.*

groups were excluded (N3 and N8); one would detect a more significant difference between the experimental 59.12 Newton (N)±8.3 N versus 21.3N±35.65 N (Table III).

Histological study

The comparison between control and experimental groups was performed with respect to the amount of trabeculation, osteoid bone formation, and collagen

fibers presence. At low magnification (100 X) (Fig. 7, right), the regenerate areas of 3 animals from of the control group (a, b and c) and 3 samples of the experimental group (d, e & f) exhibited significant differences. The control group samples showed, at the level of the interface, a greater area of green stain for connective tissue than the experimental group. They indicated the presence of more collagen fibers and soft tissue at the interface level, thus, creating a weak point in the bone that corresponded to the area of least resistance.

Moreover, significant histological differences were noted between the sections from both study groups upon comparison at a higher magnification (200 X) (Fig. 7 left). First, blood vessels (black arrows) in large marrow cavities were noted in the interface areas of the control group sections (a and c) reflecting a bone regeneration activity going on in contrast to the experimental group sections (d, e, f) whereby the marrow spaces were already filled with bones trabeculae and osteoid bones.

Second, a large amount of soft tissue stained areas were noted in all sections of the control group (a, b and c), whereas, only one section of the experimental group showed some small green stained areas (f).

Third, the control group sections (a and b) showed at the interface border elongated cells, high cuboidal to columnar, lining its border (yellow arrows) which are bone forming cells (osteoblasts) generating new bone and replacing woven bone into mature cortical bone. Furthermore, the experimental group samples (D and F) showed osteocytes with their lacunae (blue arrows) embedded between the trabeculations of the mature cortical bone.

The fourth difference was related to the amount of trabeculation. The trabeculae were denser and greater in number in the experimental group sections.

DISCUSSION

Distraction osteogenesis is gaining more use as the treatment of choice for the surgical correction of congenital craniofacial skeletal anomalies. However, a long duration for bone consolidation is usually required. Platelet-rich plasma (PRP) can be easily prepared from autologous blood and is considered as a reservoir for growth factors that can stimulate osteoblastic activity and, therefore, speed up the regeneration process (24, 25).

In this study, we injected autologous PRP, locally in the distraction gap, following the distraction phase because, at that point, the colonization of the formed callus by stem cells is at its peak and that PRP has a great role in enhancing the differentiation of stem cells into osteoblasts and osteoclasts, thus, accelerating bone remodeling and regeneration (26).

The results in this study showed that PRP yielded a more predictable healing as shown in Fig. 6 where the radiographs of all experimental samples are alike, while more variations were encountered throughout the control samples. Two samples (7 and 11) from the control group showed soft tissue in the middle area of the regenerates reflecting the presence of immature woven bone at the interface, which caused their breakage during manipulation.

The unpredictable nonconsistent healing in the control group samples was noted in both the mechanical and the histological tests. As shown in Table III, a wide variation in the results of the control group samples (10.9N to 119.5N) was noted compared to results with less variation (48.8N to 92N) in the experimental group samples. A large amount of soft tissue was present in samples b and c of the control group, in addition to less green stained collagen reflecting a variation in the amount of immature woven bone still present (Fig. 7 right and left).

On the other hand, the samples d, e and f of the experimental group showed a mature bone and well defined trabeculations with minor amounts of soft tissue. These results indicate that PRP played a major role in decreasing variability between samples.

The macroscopic examination of the mandibles showed a great difference between both experimental and control groups concerning the presence of soft tissue at the middle area of the regenerate. In the experimental group, the regenerate area showed a well calcified area with little presence of soft tissue, thus indicating an accelerated rate of ossification.

Furthermore, in 3 to 5 samples of the control group there was a higher amount of soft tissue at the interface level and not enough ossification resulting into breakage of 2 of them at that site during manipulation and the breakage of the third sample at a very low load of 10.9N during the mechanical test. Hence, the middle area of the regenerate was

the last to calcify. Our macroscopic observations could be explained by the fact that during 45 days of consolidation period, 3 to 5 samples of the control group did not have enough time to fully calcify and, therefore, they showed relatively abundant soft tissue in the middle area and were easily broken at that site. On the other hand, all the experimental samples were fully calcified and, therefore, PRP, due to probably multiple growth factors present, accelerated bone remodeling at the regenerate area and helped newly formed bone to gain maturity in a faster timeframe.

In addition, the data emanating from the dual X-ray absorptiometry assessing the bone mineral content and density showed a trend of grossly stronger experimental mandibles treated with PRP without any gaps left at interfaces. However, the number of animals per group was small with wide variation in values leading to no significant statistical differences between groups. Such results could be explained by the fact that after 45 days, the proximal areas of the regenerates were ossified in both groups to different extents and leaving gaps in the controls filled with connective tissue elements. An intermediate time point of 30 days could have been very useful. So, for that reason, data in Tables I and II showed no significant differences between both groups. To detect such differences, a dual x-ray absorptiometry test should be restricted on the interface area of 0.2 mm and not on all the regenerate; this couldn't be achieved with the conventional dual x-ray absorptiometry machines present in our current facilities.

Our results are in line with the study Swennem et al. (25). The nonsignificant difference found between the control and experimental groups concerning the bone mineral density of the regenerate was concomitant with our findings (Tables I, II). The main difference between the 2 studies consisted of an increase in the bone density at the proximal areas of the regenerate in the experimental group where PRP was injected directly before the distraction phase as compared to the control group. It is important to note that the main difference was found at the interface area, the middle area of the regenerate, whereby, 3 samples of our control group showed, upon the macroscopic examination, a large amount of soft tissue in that area. Two of these samples were broken during harvesting at that site and one of them showed a very low flexural strength during the mechanical test (Table III). In addition, two of them clearly showed great amount of trichrome stained collagen fibers at the interface area as compared to the experimental group which did not show soft tissue.

However, in the experimental PRP treated group, after 45 days of consolidation period, it was shown that the proximal areas were completely calcified and the middle areas were the least calcified and consequently the last areas to complete ossification (26). These findings could explain our results indicating the presence of immature bone at the interface level in the control group as reflected by the extra time needed by this group to complete its ossification compared to the experimental group, receiving PRP, who had completed its full ossification during the same time frame.

The results in Table III showed a significant statistical difference between both groups. If we exclude 2 outliers from the control and experimental groups, the results showed a greater strength of the experimental samples as compared to the control group samples. This can be explained by the fact that the presence of soft tissue at the interface area in samples of the control group reflected a lack of ossification in these samples that compromised their flexural strength as compared to the experimental group samples which did not show soft tissue at the interface level reflecting their complete ossification. In conclusion, PRP, added to the experimental samples offered a greater strength for these samples.

Moreover, the histological study of the regenerate areas of both groups showed the presence of a relatively large amount of soft tissue at the interface level in the samples of the control group while there was little amount of soft tissue noted in the experimental sections. This finding reflected less ossification of the interface area in the control group samples and consequently the positive role of PRP in speeding bone remodeling in the experimental group.

Mandibular distraction osteogenesis proved its efficacy in treating various pediatric craniofacial deformities but with the disadvantage of requiring a long consolidation period which corresponds to a long immobilization period with the subsequent adverse events including mainly bone fractures and feeding disorders. As shown in this study, the use of platelet-

rich plasma played an important role in accelerating the ossification following distraction, especially at the interface, which is the last area to gain maturity; thus reducing this long consolidation period and accelerating bone remodeling and regeneration. After 45 days, full maturity was gained in the experimental samples injected with PRP as opposed to less maturation in the control samples. A larger sample size and more time points are needed for statistical analysis to ascertain the specific role of PRP.

REFERENCES

1. McCarthy JG, Schreiber J, Karp N, Thorne CH, Grayson BH. Lengthening the human mandible by gradual distraction. Plast Reconstr 1992; 89(1):1-8.
2. Bertelè G, Mercanti M, Stella F, Albanese M, De Santis D. Osteodistraction in the craniofacial region. Minerva Stomatol 2005; 54(4):179-98.
3. Cascone P, Gennaro P, Spuntarelli G, Iannetti G. Mandibular distraction: evolution of treatment protocols in hemifacial microsomia. J Craniofac Surg 2005; 16(4):563-71.
4. Cho BC, Moon JH, Chung HY, Park JW, Kweon IC, Kim IS. The bone regenerative effect of growth hormone on consolidation in mandibular distraction osteogenesis of a dog model. J Craniofac Surg 2003; 14(3):417-25.
5. Aleksyniene R, Eckardt H, Bundgaard K, Lind M, Hvid I. Effects of parathyroid hormone on newly regenerated bone during distraction osteogenesis in a rabbit tibial lengthening model. A pilot study. Medicina Kaunas 2006; 42(1):38-48.
6. Seebach C, Skripitz R, Andreassen TT, Aspenberg P. Intermittent parathyroid hormone (1-34) enhances mechanical strength and density of new bone after distraction osteogenesis in rats. J Orthop Res 2004; 22(3):472-8.
7. Raschke MJ, Bail H, Windhagen HJ, et al. Recombinant growth hormone accelerates bone regenerate consolidation in distraction osteogenesis. Bone 1999; 24(2):81-8.
8. Bail HJ, Raschke MJ, Kolbeck S, et al. Recombinant species-specific growth hormone increases hard callus formation in distraction osteogenesis. Bone 2002; 30(1):117-24.
9. Takushima A., Kitano Y., Harii K. Osteogenic potential of cultured periosteal cells in a distracted bone gap in rabbits. J Surg Res 1998; 78(1):68-77.
10. Shao Z, Liu B, Peng Q, Liu W, Liu Y, Liu R, Xu Y, Liu L. Transplantation of osteoblast-like cells to the distracted callus in the rabbit mandible. Plast Reconstr Surg 2007; 119(2):500-7.
11. Kokoroghiannis C, Papaïoannou N, Lyritis G, Katsiri M, Kalogera P. Calcitonin administration in a rabbit distraction osteogenesis model. Clin Orthop Relat Res 2003; 415:286-92.
12. Sen C, Gunes T, Erdem M, Koseoglu RD, Filiz NO. Effects of calcitonin and alendronate on distraction osteogenesis. Int Orthop 2006; 30(4):272-7.
13. Gandhi A, Bibbo C, Pinzur M, Lin SS. The role of platelet-rich plasma in foot and ankle surgery. Foot Ankle Clin 2005; 10(4):621-37.
14. Blumenfeld I, Srouji S, Lanir Y, Laufer D, Livne E. Enhancement of bone defect healing in old rats by TGF-beta and IGF-1. Exp Gerontol 2002; 37(4):553-65.
15. Abdallah Hajj Hussein I, Dali Balta N, Jurjus RA, et al. Rat model of burn wound healing: effect of Botox. J Biol Regul Homeost Agents 2012; 26(3):389-400.
16. Zhang, CQ, Yuan, T., Zeng, BF. Experimental study on effect of platelet-rich plasma in repair of bone defect. Reparative and reconstructive surgery 2003; 17(5):355-8.
17. Mazor Z, Peleg M, Garg AK, Luboshitz J. Platelet-rich plasma for bone graft enhancement in sinus floor augmentation with simultaneous implant placement: patient series study. Implant Dent 2004; 13(1):65-72.
18. Gigante A, Cappella M, Manzotti S, Cecconi S, Greco F, Di Primio R, Mattioli-Belmonte M. Osteoinduction properties of different growth factors on cells from non-union patients: in vitro study for clinical application. J Biol Regul Homeost Agents 2010; 24(1):51-62.
19. Marx RE, Carlson ER, Eichstaedt RM, Schimmele SR, Strauss JE, Georgeff KR. Platelet-rich plasma: Growth factor enhancement for bone grafts. Oral Surg Oral Med Oral Pathol Oral Radiol Endod. 1998 Jun; 85(6):638-46.
20. Nash TJ, Howlett CR, Martin C, Steele J, Johnson KA, Hicklin DJ. Effect of plateletderived growth factor on tibial osteotomies in rabbits. Bone 1994; 15(2):203-8.

21. Coviello V, Peluso F, Dehkhargani SZ, Verdugo F, Raffaelli L, Manicone PF, D' Addona A. Platelet-rich plasma improves wound healing in multiple myeloma bisphosphonate-associated osteonecrosis of the jaw patients. J Biol Regul Homeost Agents 2012; 26(1):151-5.
22. Gigante A, Del Torto M, Manzotti S, Cianforlini M, Busilacchi A, Davidson PA, Greco F, Mattioli-Belmonte M. Platelet rich fibrin matrix effects on skeletal muscle lesions: an experimental study. J Biol Regul Homeost Agents 2012; 26(3):475-84.
23. Luengo Gimeno F, Gatto S, Ferro J, Croxatto JO, Gallo JE.. Preparation of platelet-rich plasma as a tissue adhesive for experimental transplantation in rabbits. Thromb J 2006; 4:18
24. Kitoh H, Kitakoji T, Tsuchiya H, Katoh M, Ishiguro N. Transplantation of culture expanded bone marrow cells and platelet-rich plasma in distraction osteogenesis of the long bones. Bone 2007; 40(2):522-8
25. Swennen GR, Schutyser F, Mueller MC, Kramer FJ, Eulzer C, Schliephake H. Effect of platelet-rich-plasma on cranial distraction osteogenesis in sheep: preliminary clinical and radiographic results. Int J Oral Maxillofac Surg 2005; 34(3):294-304.
26. Yasui N, Sato M, Ochi T, Kimura T, Kawahata H, Kitamura Y, Nomura S. Three modes of ossification during distraction osteogenesis in the rat. J Bone Joint Surg Br 1997; 79(5):824-30.

ERYTHROPOIETIN DOES NOT AFFECT TNF AND IL-6 PRODUCTION DIRECTLY

I. CERVELLINI, S. SACRE, P. GHEZZI, and M. MENGOZZI

Brighton and Sussex Medical School, Falmer, United Kingdom

Received November 7, 2012 - Accepted January 22, 2013

The tissue-protective action of erythropoietin (EPO) in animal models is often associated with reduced inflammation. However, there are many contrasting reports of the effect of EPO on the production of inflammatory cytokines induced by lipopolysaccharide (LPS) *in vitro*, with different papers reporting an inhibition, an upregulation, or a lack of effect. Negative results are likely underestimated by a publication bias. As EPO has anti-inflammatory actions in models associated with tissue injury, we hypothesized that EPO could specifically inhibit the induction of inflammatory cytokines by danger signals associated with cell death, and investigated its effect on the induction of IL-6 or TNF by high-mobility group-box 1 protein (HMGB1) or by necrotic cells. We did not observe any significant effect of EPO in these models; neither EPO affected the response induced by TLR agonists different from LPS, or by extracellular ATP-mediated activation of the inflammasome. We conclude that the inhibition of inflammation by EPO is likely to be an indirect effect, secondary to its tissue-protective activity, or that it requires a prior priming induced by the injury.

EPO has been reported to have a protective effect that is associated with a decrease in inflammatory cytokines, in various tissues including the brain (1) and kidney (2). However, whether or not EPO directly affects production of inflammatory cytokines is a controversial issue. While we found that EPO treatment decreases brain TNF, IL-6 and MCP-1 induced by cerebral ischemia in rats *in vivo*, *in vitro* addition of EPO to human peripheral blood mononuclear cells (PBMC) or primary rat glial cells stimulated with endotoxin (lipopolysaccharide, LPS) did not have any effect (1). Likewise, EPO did not affect TNF production induced *in vivo* in the brain by injection of LPS (1, 3) or circulating cytokines in rats treated with LPS (4).

This work was aimed at investigating whether EPO has a direct inhibitory action on the production of inflammatory cytokines *in vivo* and *in vitro* using stimuli of inflammation more relevant to tissue injury than LPS.

Activation of the cytokine cascade can take place not only with molecules bearing pathogen associated molecular patterns, such as the commonly-used LPS, acting on various pattern recognition receptors including Toll-like receptors (TLRs), but also with endogenous molecules and proteins acting as danger signals (5). Products released by necrotic cells stimulate cytokine production (6, 7) through a number of danger signals such as HMGB1 (8, 9) or heat-shock proteins (6). In addition, danger signals such as ATP are able to induce K+ efflux and activate caspase-1, a requirement for the secretion of cytokines of the IL-1 family, including IL-1β, from macrophages activated with LPS (10, 11).

We first used the human monocytic cell line Mono Mac 6 (MM6) to investigate the effect of EPO

Key words: Inflammation, HMGB1, necrosis, tissue-protective cytokines, LPS

Mailing address: Prof Pietro Ghezzi,
Chair in Experimental Medicine,
Head Division of Clinical and Laboratory Investigations,
Brighton & Sussex Medical School, Trafford Centre,
Falmer, BN19RY, United Kingdom
Tel.: +44 1273 873112 Fax: +44 1273 873112
e-mail: p.ghezzi@bsms.ac.uk

0393-974X (2013)

DISCLOSURE: ALL AUTHORS REPORT NO CONFLICTS OF INTEREST RELEVANT TO THIS ARTICLE.

on IL-6 production *in vitro* induced by HMGB1 or by a necrotic cell lysate obtained from the SH-SY5Y human neuronal cell line, and on IL-1β secretion induced by LPS and ATP. Secondly, the effect of EPO on TNF production induced by various TLRs agonists was investigated in primary human macrophages. Finally, because one of the tissue-protective mechanisms of EPO is the mobilization of circulating bone marrow-derived endothelial precursor cells (EPC) *in vivo* (12, 13), which may indirectly affect cytokine production, we investigated whether pretreatment of mice with EPO using a schedule known to mobilize EPC affected *ex vivo* TNF production by whole blood.

Despite the broad range of models investigated, no inhibitory effect of EPO could be demonstrated in any of these systems; conversely, there was an upregulation of cytokine production in some of these models.

MATERIALS AND METHODS

Reagents

Erythropoietin (EPO, Creative Dynamics); Lipopolysaccharide (LPS, E. coli 055:B5, Sigma); High-mobility group protein-1 (HMGB-1, kind gift of Kevin J. Tracey, North Shore University Hospital, Manhasset, NY); IL-1α (Peprotech); R-848 (Invitrogen); Pam3Cys (Alexis); ATP (Sigma) was dissolved at 50 mg/ml in Hepes 100 mM (Invitrogen) diluted 1:10 (vol/vol) in RPMI 1640 and then neutralized with NaOH 1M.

Cells and necrotic cell lysate

The human monocytic Mono Mac 6 (MM6) cell line was cultured in RPMI 1640 (PAA Laboratories) supplemented with 10% (vol/vol) heat-inactivated FBS (Invitrogen), 1% L-glutamine (Invitrogen), 1% penicillin/streptomycin (P/S, Invitrogen), 1% OPI (Sigma; oxaloacetate, pyruvate and insulin) and 1% non essential amino acids (NEAA, Invitrogen). For experiments, MM6 cells were plated at the concentration of $4x10^5$ cells/well in 24 well plates.

The human neuroblastoma cell line SH-SY5Y was cultured in DMEM with high glucose and sodium pyruvate (PAA), supplemented with 10% heat-inactivated FBS, 1% L-glutamine and 1% P/S, and used to obtain necrotic cell lysate (NCL), as described (El Mezayen, 2007).

Human peripheral blood was purchased from the National Health Service Blood and Transplant (NHSBT). All donors gave written informed consent. The study was approved by the local Research Governance and Ethics Committee. Blood was diluted with Hanks balanced salt solution (HBSS, PAA) and layered onto Lympholite-H (Cedarlane), then centrifuged at 2,000 rpm for 25 m. Peripheral blood mononuclear cells (PBMC) were collected. Monocytes were isolated from PBMC by density gradient centrifugation on iso-osmotic Percoll at 700x g for 15 m. Iso-osmotic Percoll was prepared by mixing one volume of 1.5 M NaCl with nine volumes of Percoll-Plus (GE Healthcare). The gradient was then prepared by mixing 1:1 (vol/vol) iso-osmotic Percoll with PBS/citrate. Monocytes were collected, washed with HBSS, resuspended in complete RPMI supplemented with 100 ng/ml macrophage colony-stimulating factor (M-CSF, Peprotech). After 4 days in culture, macrophages were harvested, plated at $2x10^5$ cells/well in 96 well plates and left to adhere for 6 h before treatments.

Mice treatment and whole blood cultures

Experiments were carried out in accordance with the UK Animals (Scientific Procedures) Act 1986.

CD1 male mice (Harlan Laboratories; 4-6 weeks old) were treated with EPO (50 μg/Kg) or vehicle (saline) i.p., daily, for 3 days to mobilize EPC in the circulation, as reported (12). Three h after the last injection, peripheral blood was collected by intracardiac puncture into heparinized syringes.

For whole blood cultures, 200 μl of blood were diluted 1:3 (vol/vol) with RPMI-1640 (PAA Laboratories), incubated in Eppendorf tubes at 37°C, 5% CO_2 for 24 h with or without LPS, then centrifuged at 5,000 rpm, 4°C for 20 min. The plasma was collected and frozen at -20°C to measure TNF by ELISA.

Real time qPCR

For quantification of EPC, expressing CD34 (12), CD34 mRNA was measured in mouse PBMC by qPCR. Analysis of rare cell types, in particular of CD34+ cells, by qPCR has been reported (14). PBMC were separated by gradient centrifugation (Lympholite-Mammals, Cedarlane) and total RNA was extracted with TRIzol, following the manufacturer's instructions (Invitrogen). Reverse transcription and real time qPCR to measure CD34 and HPRT1 (housekeeping) expression was carried out as reported (15), using Taqman gene expression assays (Applied Biosystems). Relative gene expression was quantified using the ΔΔCt method, following Applied Biosystems guidelines.

The same method was used to quantify EPOR mRNA in human PBMC and MM6 cells, using Taqman gene expression assays for huEPOR and huGAPDH (housekeeping) from Applied Biosystems.

Cytokine ELISA

Human IL-6, IL-1β, and TNF-α, and murine TNF-α were assayed by ELISA, using DuoSet kits from R&D Systems.

RESULTS

Effect of EPO on IL-6 production induced by HMGB1 or necrotic cells

We first investigated whether EPO modified IL-6 response to danger signals associated with cell death. Stimulation of MM6 cells with 1 µg/ml HMGB1 was unaffected by 0.1 ng-1,000 ng/ml EPO (Fig. 1A). In this dose-response experiment, EPO was added 30 min before HMGB1 and IL-6 production was measured 24 h later. Although EPO has protective effects when given 30 min before injury or later, and does not require a longer pre-treatment (16), we investigated the effect of an 18 h pre-treatment with 80 ng/ml EPO on IL-6 induced by 1 µg/ml HMGB1. This concentration of EPO was the same as previously shown to protect neuronal cells from apoptosis (17). Also with this longer pre-treatment time, EPO had no effect on IL-6 production (Fig. 1B).

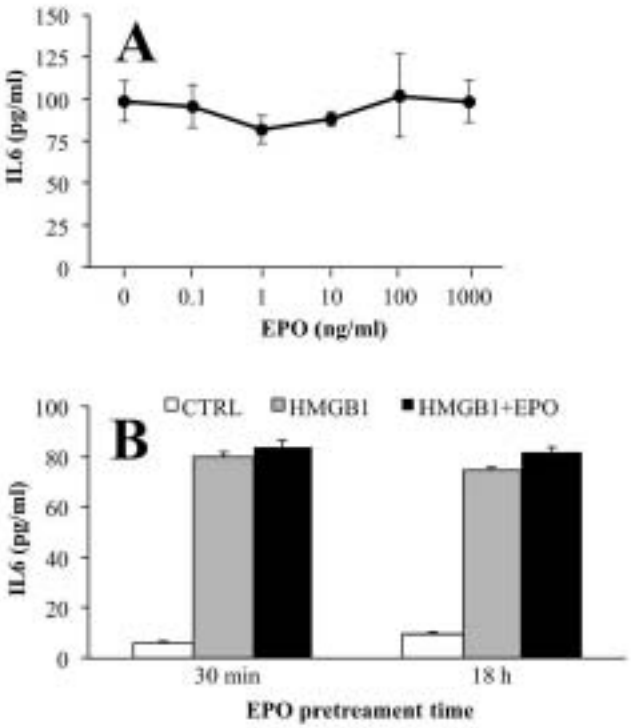

Fig. 1. *EPO does not affect HMGB1-induced IL-6 production in vitro.* ***A****) Mono Mac 6 (MM6) cells were pretreated for 30 min with EPO at the indicated concentration, and then 1 µg HMGB1 was added and IL-6 production evaluated 24 h later. Data are mean±SD of triplicate samples. In the absence of HMGB1, baseline production of IL-6 was undetectable.* ***B****) MM6 cells were pre-treated for 18 h or 30 m with 80 ng/ml EPO, then 1 µg HMGB1 was added and IL-6 production evaluated 24 h later. Data are mean±SD of triplicate samples.*

Human PBMC express EPOR (18), but EPOR levels in MM6 cells had never been measured. By real time qPCR, we found that MM6 cells expressed higher levels of EPOR mRNA than human PBMC (EPO mRNA, fold induction±SD of MM6 *vs* PBMC: 1.7±0.3, $P<0.05$). Therefore, the lack of an EPO effect in MM6 cells was not due to the absence of EPOR expression.

We then investigated the effect of a necrotic cell lysate (NCL) on IL-6 production (Fig. 2A). NCL alone significantly induced IL-6 (NCL 50% vol/vol, 11.5±0.1 pg/ml *vs* 1.1±0.2 without NCL; $P<0.01$ by Student's *t*-test) and synergized with 0.1 ng/ml LPS (NCL 50%+LPS, 49.3±2.2 pg/ml *vs* 26.2±3.4 pg/ml for LPS 0.1 ng/ml alone; $P<0.01$ by Student's *t*-test). At the lower dose of 0.01 ng/ml, LPS did not synergize with NCL (NCL 50%+LPS, 11.7±1.6 pg/ml *vs* 11.5±0.1 for NCL 50% alone). For this reason, the induction with NCL alone or in association with LPS 0.1 ng/ml was chosen for studying the effect of EPO in this model. EPO, at the concentration of 80 ng/ml, did not affect IL-6 production induced by 50% NCL, with and without 0.1 ng/ml LPS (Fig. 2B).

Effect of EPO on IL-1β secretion induced by LPS and ATP

Although high doses of LPS can induce secretion of mature IL-1β from fresh monocytes, secretion of IL-1β (and other cytokines of the IL-1 family) from macrophages requires a second stimulus, like ATP, that can induce K+ release. This mechanism activates caspase-1 through the inflammasome, inducing the cleavage of the pro-IL-1β into the mature cytokine (10, 11).

Since EPO had no effect on cytokine secretion induced *in vitro* by LPS, we reasoned that it might decrease cytokine production by acting at some level downstream to LPS induction, for instance inhibiting

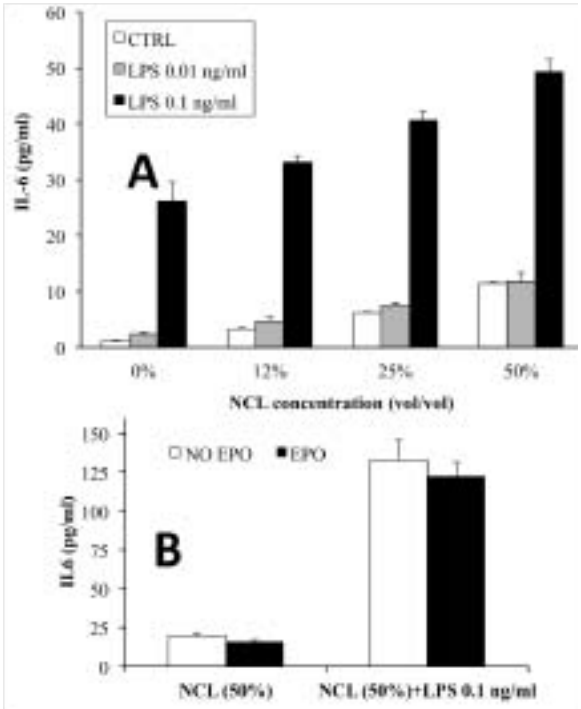

Fig. 2. *EPO does not affect in vitro IL-6 induction by necrotic cell lysate. **A)** MM6 cells were cultured with the indicated concentration (vol/vol) of NCL from SH-SY5Y, in the presence or absence of 0.01 or 0.1 ng/ml LPS. IL-6 production was evaluated 24 h later. Data are mean±SD of triplicate samples. **B)** MM6 cells were cultured with 50% (vol/vol) of NCL, in the presence or absence of 0.1 ng/ml LPS and 80 ng/ml EPO. IL-6 production was evaluated 24 h later. Data are mean±SD of triplicate samples.*

K+ efflux induced by ATP. MM6 cells primed with 40 ng/ml LPS for 6 h secreted IL-1β when further stimulated with 2 mM ATP for 1 h. However EPO, either added 10 min before LPS or before ATP, did not affect the induction of IL-1β (Fig. 3).

Effect of EPO on activation of different TLRs

To assess the effect of EPO on TLR induced TNF production, primary human M-CSF derived macrophages were used from three independent donors. The cells were stimulated with 1 ng/ml LPS (TLR4 agonist), 20 ng/ml IL-1α (IL-1 Receptor agonist), 1μg/ml R-848 (TLR7/8 agonist) and 100 ng/ml Pam3 (TLR2 agonist) for 24 h. IL-1α was chosen as an alternative activator of the MyD88 pathway shared by most of the TLRs. However, no inhibition of TNF production was observed in the presence of 80 ng/ml EPO (Table I).

Effect of in vivo EPO treatment on LPS-induced TNF production ex vivo

Pre-treatment of mice with EPO causes mobilization of EPC, which may affect cytokine response. To investigate this possibility, we treated mice with EPO (50 μg/Kg) for three days, as reported (12). Blood was collected 3 h after the last EPO injection. To assess whether, in our experimental conditions, EPO had actually increased mobilization of EPC, 3 h after the last injection blood was taken, mononuclear cells isolated and CD34 mRNA was measured by real time qPCR (Fig. 4A). As expected, CD34 mRNA increased more than two-fold with

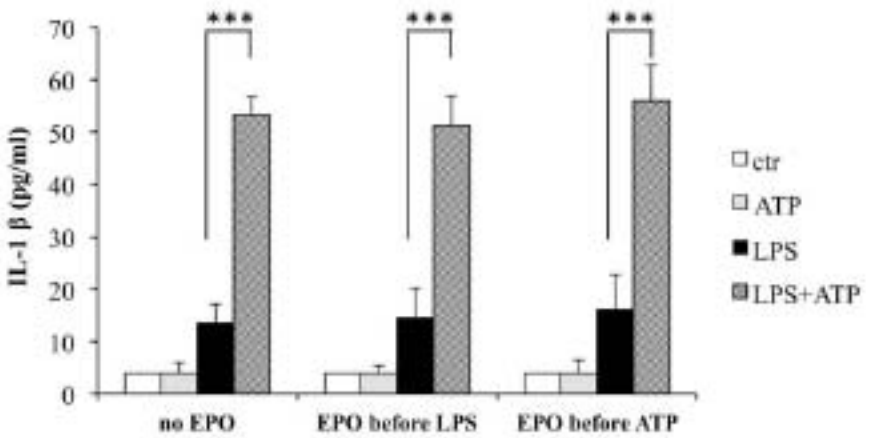

Fig. 3. *Effect of EPO on IL-1β secretion induced by inflammasome activation with ATP. MM6 cells were treated with 40 ng/ml LPS for 6 h followed by 2 mM ATP. When indicated, 80 ng/ml EPO was added 10 min either before LPS or before ATP. Control samples (ctrl) received no LPS or ATP. IL-1β was measured in the supernatants 1 h after ATP. Data are mean±SD of triplicate samples. ***P<0.0001 vs respective LPS alone by Student's t-test.*

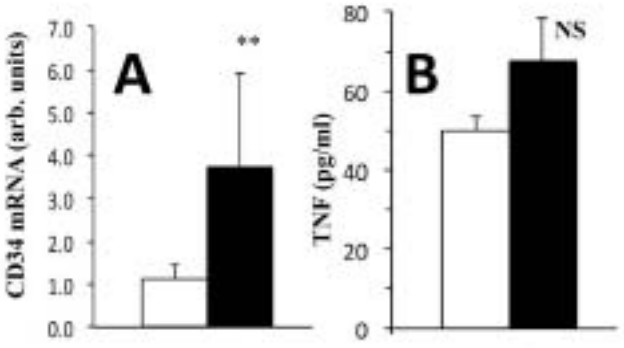

Fig. 4. *Ex vivo TNF production in whole blood from EPO-pre-treated mice. Mice were treated i.p. for 3 days with saline (open bars) or 50 µg/kg EPO (closed bars), then blood was taken.* ***A)*** *CD34 mRNA in circulating PBMC is expressed as arbitrary units, and is the mean*±SD *of 11 samples.* ***B)*** *TNF production by whole blood stimulated for 4 h with 1 µg/ml LPS, mean±SD of 5 mice per group, each analysed independently. No TNF was detectable in the absence of LPS. ** P < 0.001; NS, not significant vs saline, by Student's t-test.*

EPO. However, despite the presence of an increased number of EPC, *ex vivo* EPO treatment did not affect LPS-induced TNF production in whole blood (Fig. 4B).

DISCUSSION

The published studies investigating whether EPO has a direct effect on the production of inflammatory cytokines *in vitro* and *in vivo* report controversial results pointing at different answers to the research question.

We could not find inhibition in human PBMC or rat glial cells or in rats injected intra-cerebrally with LPS (1), and Wilms et al. reported no inhibition of LPS-induced TNF in murine microglial cells (19), while two papers reported that injection of EPO decreases TNF levels in the cecal ligation and puncture-model of peritoneal sepsis (20, 21). The negative data published are probably underestimated, because of the well known publication bias by which only papers showing an effect are published. Others reported that addition of EPO increases production of TNF, IL-12 or IL-1 in human PBMC (22, 23, 24) or mouse bone marrow-derived macrophages (25) while inhibiting production of anti-inflammatory IL-10 (25). More importantly, in view of the clinical implications, EPO administration to dialyzed patients increases levels of IL-1α (26) and IL-1β (27), and a study on healthy human volunteers injected with LPS with and without EPO administration found markedly augmented TNF and IL-6 levels (28). On the other hand, Nairz et al. reported that EPO inhibits *in vitro* TNF production in LPS-stimulated primary mouse peritoneal macrophages or RAW264.7 macrophage-like cells (29), confirming and extending a study by Yazihan et al. reporting that EPO inhibits LPS-induced TNF in the human monocytic cell line U937

Table I. *Effect of EPO on TNF induction by different TLR agonists in primary human macrophages.*

Stimulus	TNF (pg/ml)	
	Control	EPO
None	<15	<15
LPS	4718 ± 674	4138 ±461
IL-1α	97 ±31	63 ±18
R-848	4782 ±181	4102 ±342
PAM3	835 ±90	781 ±59

When indicated, 80 ng/ml EPO was added 30 min before the stimulus. The stimuli used were: LPS (TLR4 agonist; 1 ng/ml), IL-1α (IL-1 receptor agonist; 20 ng/ml), R-848 (TLR7/8 agonist; 1 µg/ml), PAM3 (TLR2 agonist; 100 ng/ml). Data are the mean±SD of triplicate samples from one donor and are representative of 3 donors.

(30).

The issue of the effect of EPO on inflammatory cytokines is not only important for the mechanism of action of EPO as a tissue-protective cytokine but has important safety implications. Nairz et al. reported that while the anti-inflammatory action of EPO was protective in a model of inflammatory colitis, it had a worsening effect in Salmonella infection (29).

Our hypothesis was that the reason for these conflicting results could be that EPO inhibited inflammatory cytokine production when this was induced by danger signals associated with cell death, not directly by LPS. In fact, we previously reported that EPO, while not inhibiting TNF production by glial cells exposed to LPS, inhibited TNF production induced in the same cells by co-culture with neurons undergoing cell death (1). Furthermore, in monocytes, inhibition of LPS-induced TNF production by EPO is associated with protection of the same cells from the toxic effect of LPS (30).

However, we could not demonstrate any effect of EPO on IL-6 production when induced by HMGB1 or by a necrotic cell lysate. In our experimental condition, EPO did not inhibit TNF production stimulated by various TLR agonists. It should be mentioned that the same preparation/batch of rhuEPO induced other responses in our laboratory, including activation of early growth response genes, in experiments performed at the same time as those reported here (15).

Altogether these data suggest that EPO does not act as a direct inhibitor of TNF and IL-6 production, unlike "classical" anti-inflammatory cytokines such as IL-10 that, for this reason, was originally called "cytokine synthesis inhibitory factor (31). We cannot exclude that EPO might inhibit cytokine production induced by danger signals different from those that we used. The question remains on which experimental details can explain why some investigators reported a direct inhibitory effect and others a lack of effect or even an up-regulation.

The consistent anti-inflammatory effect in disease models *in vivo* but not *in vitro* might be explained in different ways. For instance, a number of physiological mechanisms can limit the inflammatory responses and take place only *in vivo*, such as the activation of the hypothalamus-pituitary-adrenal axis with the release of glucocorticoids (32), the production of neurosteroids (33), or the stimulation of the vagus nerve (34). Another possibility could be that EPO only acts in a disease context, when the inflammatory signal is associated with a second stimulus present in disease conditions that prime the cells to respond to EPO. This has been originally postulated by Brines and Cerami (35) who, to explain the more consistent tissue-protective activity of EPO *in vivo* than *in vitro*, suggested that EPO requires upregulation of specific tissue-protective receptors by an injury (35).

We could not show any direct effect of EPO on the production of inflammatory cytokines, even when these were induced by danger signals. This leaves the question of the mechanism of the decrease in inflammatory cytokines observed *in vivo* by tissue protective doses of EPO open. Further studies on the anti-inflammatory action of EPO will be required, not only to better define its mechanism of action and the receptors involved, but also its safety implications.

ACKNOWLEDGEMENTS

Supported by the European Regional Development Fund (PG), the R.M. Phillips Trust (PG).

REFERENCES

1. Villa P, Bigini P, Mennini T, et al. Erythropoietin selectively attenuates cytokine production and inflammation in cerebral ischemia by targeting neuronal apoptosis. J Exp Med 2003; 198:971-5.
2. Souza AC, Volpini RA, Shimizu MH, et al. Erythropoietin prevents sepsis-related acute kidney injury in rats by inhibiting NF-kappaB and upregulating endothelial nitric oxide synthase. Am J Physiol Renal Physiol 2012; 302:F1045-54.
3. Spreer A, Gerber J, Hanssen M, Nau R. No neuroprotective effect of erythropoietin under clinical treatment conditions in a rabbit model of Escherichia coli meningitis. Pediatr Res 2007; 62:680-3.
4. Mitra A, Bansal S, Wang W, Falk S, Zolty E, Schrier RW. Erythropoietin ameliorates renal dysfunction during endotoxaemia. Nephrol Dial Transplant 2007; 22:2349-53.
5. Gallucci S, and Matzinger P. Danger signals: SOS to the immune system. Curr Opin Immunol 2001;

13:114-9.
6. El Mezayen R, El Gazzar M, Seeds MC, McCall CE, Dreskin SC, Nicolls MR. Endogenous signals released from necrotic cells augment inflammatory responses to bacterial endotoxin. Immunol Lett 2007; 111:36-44.
7. Li M, Carpio DF, Zheng Y, Bruzzo P, Singh V, Ouaaz F, Medzhitov RM, Beg AA. An essential role of the NF-kappa B/Toll-like receptor pathway in induction of inflammatory and tissue-repair gene expression by necrotic cells. Journal of Immunology 2001; 166:7128-35.
8. Scaffidi P, Misteli T, Bianchi ME. Release of chromatin protein HMGB1 by necrotic cells triggers inflammation. Nature 2002; 418:191-5.
9. Wang H, Bloom O, Zhang M, et al. HMG-1 as a late mediator of endotoxin lethality in mice. Science 1999; 285:248-51.
10. Kahlenberg JM, Lundberg KC, Kertesy SB, Qu Y, Dubyak GR. Potentiation of caspase-1 activation by the P2X7 receptor is dependent on TLR signals and requires NF-kappaB-driven protein synthesis. J Immunol 2005; 175:7611-22.
11. Mariathasan S, Weiss DS, Newton K, et al. Cryopyrin activates the inflammasome in response to toxins and ATP. Nature 2006; 440:228-32.
12. Heeschen C, Aicher A, Lehmann R, et al. Erythropoietin is a potent physiologic stimulus for endothelial progenitor cell mobilization. Blood 2003; 102:1340-6.
13. Westenbrink BD, Lipsic E, van der Meer P, et al. Erythropoietin improves cardiac function through endothelial progenitor cell and vascular endothelial growth factor mediated neovascularization. European heart journal 2007; 28:2018-27.
14. Molesh DA, Hall JM. Quantitative analysis of CD34+ stem cells using RT-PCR on whole cells. PCR Methods Appl 1994; 3:278-84.
15. Mengozzi M, Cervellini I, Villa P, et al. Erythropoietin-induced changes in brain gene expression reveal induction of synaptic plasticity genes in experimental stroke. Proceedings of the National Academy of Sciences of the United States of America 2012; 109:9617-22.
16. Brines ML, Ghezzi P, Keenan S, Agnello D, de Lanerolle NC, Cerami C, Itri LM, Cerami A. Erythropoietin crosses the blood-brain barrier to protect against experimental brain injury. Proc Natl Acad Sci U S A 2000; 97:10526-31.
17. Siren AL, Fratelli M, Brines M, et al. Erythropoietin prevents neuronal apoptosis after cerebral ischemia and metabolic stress. Proc Natl Acad Sci U S A 2001; 98:4044-9.
18. Lisowska KA, Debska-Slizien A, Bryl E, Rutkowski B, Witkowski JM. Erythropoietin receptor is expressed on human peripheral blood T and B lymphocytes and monocytes and is modulated by recombinant human erythropoietin treatment. Artif Organs 2010; 34:654-62.
19. Wilms H, Schwabedissen B, Sievers J, Lucius R. Erythropoietin does not attenuate cytokine production and inflammation in microglia--implications for the neuroprotective effect of erythropoietin in neurological diseases. J Neuroimmunol 2009; 212:106-11.
20. Vachharajani V, Vital S, Russell J. Modulation of circulating cell-endothelial cell interaction by erythropoietin in lean and obese mice with cecal ligation and puncture. Pathophysiology 2010; 17:9-18.
21. Rodrigues CE, Sanches TR, Volpini RA, Shimizu MH, Kuriki PS, Camara NO, Seguro NC, Andrade L. Effects of continuous erythropoietin receptor activator in sepsis-induced acute kidney injury and multi-organ dysfunction. PLoS One 2012; 7:e29893.
22. Takemasa A, Yorioka N, Ito T, Yamashita K, Oda H, Yamakido M. Recombinant human erythropoietin increases interleukin-1 beta production in cultured peripheral blood mononuclear cells from patients resistant to recombinant human erythropoietin therapy. Nephron 1994; 67:245-7.
23. Takemasa A, Yorioka N, and Yamakido M. Investigation of the influenza-like symptoms associated with recombinant human erythropoietin therapy. J Int Med Res 1997; 25:127-34.
24. Takemasa A, Yorioka N, and Yamakido M. Stimulation of interleukin-1 beta production may be involved in unresponsiveness to erythropoietin therapy. Int J Artif Organs 1996; 19:633-7.
25. Lifshitz L, Tabak G, Gassmann M, Mittelman M, Neumann D. Macrophages as novel target cells for erythropoietin. Haematologica 2010; 95:1823-31.
26. Buemi M, Allegra A, Aloisi C, Privitera M,

Morabito N, Frisina N. Influence of the treatment with recombinant human erythropoietin on plasma concentration of interleukin-1-alpha and tumour necrosis factor-alpha in hemodialyzed subjects. Nephron 1993; 64:333-4.
27. Sayinalp N, Erdem Y, Haznedaroglu IC, Dundar S, Caglar S, Kirazli S. Effect of recombinant human erythropoietin on interleukin-1 beta and interleukin-6 in patients on maintenance hemodialysis. Clin Nephrol 1995; 44:404.
28. Hojman P, Taudorf S, Lundby C, Pedersen BK. Erythropoietin augments the cytokine response to acute endotoxin-induced inflammation in humans. Cytokine 2009; 45:154-7.
29. Nairz M, Schroll A, Moschen AR, et al. Erythropoietin contrastingly affects bacterial infection and experimental colitis by inhibiting nuclear factor-kappaB-inducible immune pathways. Immunity 2011; 34:61-74.
30. Yazihan N, Karakurt O, Ataoglu H. Erythropoietin reduces lipopolysaccharide-induced cell Damage and midkine secretion in U937 human histiocytic lymphoma cells. Adv Ther 2008; 25:502-14.
31. de Waal Malefyt R, Abrams J, Bennett B, Figdor CG, de Vries JE. Interleukin 10(IL-10) inhibits cytokine synthesis by human monocytes: an autoregulatory role of IL-10 produced by monocytes. J Exp Med 1991; 174:1209-20.
32. Fantuzzi G, Di Santo E, Sacco S, Benigni F, Ghezzi P. Role of the hypothalamus-pituitary-adrenal axis in the regulation of TNF production in mice. Effect of stress and inhibition of endogenous glucocorticoids. J Immunol 1995; 155:3552-5.
33. Di Santo E, Sironi M, Mennini T, Zinetti M, Savoldi G, Di Lorenzo D, Ghezzi P. A glucocorticoid receptor-independent mechanism for neurosteroid inhibition of tumor necrosis factor production. Eur J Pharmacol 1996; 299:179-86.
34. Tracey KJ. Reflex control of immunity. Nature reviews. Immunology 2009; 9:418-28.
35. Brines M, Cerami A. Erythropoietin-mediated tissue protection: reducing collateral damage from the primary injury response. J Intern Med 2008; 264:405-32.

MECHANISMS OF OCULAR NEUROPROTECTION BY ANTIOXIDANT MOLECULES IN ANIMAL MODELS

M. NEBBIOSO[1], G. SCARSELLA[2], M. TAFANI[3] and N. PESCOSOLIDO[4]

[1]Department of Sense Organs, Sapienza University of Rome, Rome, Italy; [2]Department of Biology and Biotechnology Charles Darwin, Sapienza University of Rome, Rome, Italy; [3]Department of Experimental Medicine, Sapienza University of Rome, Rome, Italy; [4]Department of Cardiovascular, Respiratory, Nephrology, Geriatric, and Anesthetic Sciences, Sapienza University of Rome, Rome, Italy

Received November 26, 2012 – Accepted January 24, 2013

This work was conducted to evaluate the efficacy of a treatment on retinal ganglion cells (RGC) and on astrocytes of the optic nerve of glaucomatous eyes, using a combination of α-lipoic acid (ALA) and superoxide dismutase (SOD). Thirty-two male Wistar rats were fed with a diet supplemented with ALA, SOD, ALA and SOD or with no product for 8 weeks. Ocular hypertension was induced with 2% methylcellulose (MTC) and then rats were sacrificed. TUNEL assay showed a marked fluorescence in the ganglion cells and astrocytes of MTC-treated rats evidencing induction of apoptosis. In contrast, sections of eyes pretreated with ALA and SOD showed a lack of fluorescence quite similar to that of the controls. Similarly, eyes sections from rats pre-treated with ALA and SOD showed reduced differential expression of inducible nitric oxide synthase (iNOS) and of caspase-3 in compared to normally-fed/ MTC-inoculated cases. An increase of ALA and SOD exerts an antiapoptotic effect and protects against oxidative stress and hence against the structural remodelling of the RGCs and astrocytes of the optic nerve in the presence of an ischemic and pressure stress.

The human body is constantly exposed to oxidative stress, due to alterations occurring at tissue and cellular level, and therefore at macromolecular level when biological structures are exposed to an excess of oxidizing agents (1, 2).

The oxidizing agents may be either endogenous, such as those produced in areas affected by inflammation or in tumor cells, or exogenous, such as those due to environmental, chemical or physical toxins (eg pesticides or ionizing radiation) (1-3).

Oxidative stress usually derives from the action of chemicals, primarily free radicals, such as reactive oxygen species (ROS) and reactive nitrogen species (RNS) (4-6) causing tissue damage that is counteracted by so-called "scavenger activity", a defence system made up of enzymes and other mechanisms to defend cells against free radicals (5-8). An appropriate balance between oxidants and antioxidants, or redox balance, is essential for the proper functioning of physiological activities, which are sensitive to even slight alterations in this balance (6-8).

If the antioxidant defences of the cells cannot counteract the pro-oxidant effect then different macromolecules of the cells can be damaged (8-11). Among those macromolecules more sensitive

Key words: α-lipoic acid (ALA), animal models, antioxidants, glaucoma, inducible nitric oxide synthase (iNOS), superoxide dismutase (SOD)

Mailing address: Marcella Nebbioso, M.D.,
Department of Sense Organs,
Centre of Ocular Electrophysiology,
Sapienza University of Rome
viale del Policlinico 155, 00161 Rome, Italy
Tel.: +39 06 49975422 Fax: +39 06 49975425
e-mail: marcella.nebbioso@uniroma1.it

0393-974X (2013)

to oxidative damage there are the phospholipids of biological membranes, leading to loss of structure and selective transport mechanisms, the nucleic acids, leading to mutations and alterations in gene expression, and the proteins, with amino acid oxidation and loss of enzyme function, transport, receptor capacity, etc.

Significant imbalances can thus produce dysfunctions, cell damage, genomic mutations, apoptosis or cell necrosis (6-13).

Oxidative stress reactions play a part in a wide variety of conditions so as in inflammatory, auto-immune, neurodegenerative, cardiovascular, respiratory, and metabolic diseases (10-17). In recent years, their role has come to light (4,7-17) in aging, kidney, liver, and pancreas disorders; likewise in disorders of the eye, such as glaucoma, cataract and retinal degeneration.

Some antioxidants, for example α-lipoic acid (ALA), have dual solubility, both in water and in lipids, may be ubiquitous and be found in the cytoplasm, in cell membranes, in the interstitial fluid and plasma (18-20). ALA, also known as thioctic acid or vitamin N, as it has a low redox potential can act as an antioxidant against ROS and RNS and can regenerate the reduced (i.e. active) form, of many antioxidants that would otherwise be lost (20). ALA is the cofactor of several enzymes involved in the process of converting glucose, fatty acids and other energy sources into ATP and is a powerful antidote because it is a chelator of heavy metals, such as manganese, mercury, copper, arsenic, zinc and lead (18-20). ALA is present in mitochondria-rich animal and plant tissues; it is abundant in potatoes, tomatoes, cabbage, broccoli, spinach and red meat. The properties of ALA can therefore be useful in limiting oxidative damage. Thus, it can be used to reduce local inflammatory reactions, hyperalgesia, and to control the evolution of neuropathy. This has been demonstrated in clinical trials such as: Aladin I-II-III and Sydney 1-2. In fact, ALA inhibits the production of arachidonic acid, the substrate for the formation of inflammation mediators such as prostaglandin, leukotrienes and thromboxane (18-21).

The main enzymes responsible for cell redox homeostasis are superoxide dismutase (SOD), catalase and glutathione peroxidase (22, 23). SODs include a group of enzymes that may be found in the cytosol or in the nucleus, in which case they require copper, zinc or iron as cofactors. Otherwise they can be found in mitochondria where they use manganese (MnSOD) as cofactor (24). SODs catalyze the breakdown of the superoxide anion into oxygen and hydrogen peroxide and are present in nearly all aerobic cells and extracellular fluids (23, 24). The mitochondrial isoenzyme MnSOD seems to be the most important from a biological point of view, as mice lacking this enzyme die soon after birth (23-26).

In the light of these considerations, we aimed to study the mechanisms through which antioxidant factors and enzymes are able to protect cells from the damaging effects of the production of free radicals, such as ROS and RNS, during pathologies or ageing. In particular, aim of this project was to assess the efficacy of an eye tissue treatment using a combination of ALA and SODs, in laboratory rats with induced ocular hypertension. A specific analysis was performed on cells and on typical molecular markers, both at the level of the axons of the optic nerve head close to the lamina cribrosa with damage to the astrocytes, as well as at retinal level on the ganglion cells (RGCs).

MATERIALS AND METHODS

Animals, treatments, and experimental procedures

All experimental procedures were in accordance with the ARVO Statement for the Use of Animals in Ophthalmic and Vision Research, the guidelines of the European Communities Council Directive of 24 November 1986 (86/609/EEC), Italian Health Ministry guidelines, and EU Directive 2010/63/EU for animal experiments.

The experimental model of ocular hypertension used in this study is based on inoculation with methylcellulose 2% (MTC) in the anterior chamber of the animal eyes. MTC is a molecule capable of mechanically blocking the outflow of aqueous humor, leading to ocular hypertension (27).

A group of 32 animals were used for our research: they were fed for 8 weeks and then sacrificed. Eight adult male Wistar rats for the 4 groups, average weight 250-300 g and age between 180 and 210 days, were housed in controlled light and temperature. Contralateral eye was used as control. The rats were fed with a diet which was the same each day, supplemented with ALA, SOD, ALA + SOD or with no supplement. The dosage of the product per kilogram of body weight was equal to 8.57 mg/day for ALA and 2 IU/day for SOD, i.e. corresponding to the human diet, equal to 600 mg/day of ALA and 140 IU/day

of SOD (ALA600 SOD®, Alfa Wassermann, Bologna, Italy).

After local anesthesia by administration of eye drops of 0.4% oxibuprocaine (Novesine, Novartis, Basel, Switzerland) and after induction with ether, animals were injected in the anterior chamber of the right eye with 15 µl of MTC 2% (SIGMA-Aldrich, St. Louis, MO, USA) in physiological solution. The intraocular pressure was monitored by tonometry (Tonopen XL, Automated Ophthalmics, Ellicott City, MD, USA). The degree of animal sufferance was evaluated by the behavioural Irwin test and by the recovery of body weight (27). The ocular hypertension reached a maximum of 55-60 mmHg within 3 to 6 h after injection, and then stabilized within 24 h at intermediate values, that were nonetheless high, of 25-30 mmHg. This method reproduced the whole series of clinical and histopathological signs typical of human glaucoma (27).

Twenty-four h after the intraocular injection, the animals were given general anaesthesia by intra-peritoneal injection of 500 µl sodium-thiopental solution (Farmotal, Pharmacia & Upjohn, USA) in phosphate buffered saline (PBS). They were then sacrificed by carotid bleeding, after which the eyeballs were removed.

The studies were conducted using both immunohistochemical techniques and western blot. We looked for the following on the rat retina and optic nerve head: glial activation markers, alterations of the cell cycle, apoptotic cell damage, damage caused by oxidative stress.

Morphological, molecular analysis of tissue sections and of retina total protein extracts - morphology techniques and sample preparation

The eyes were enucleated, the corneas were rapidly cut vertically, and the crystalline lens and vitreous humour were removed. We then carried out the following procedures on the residual tissues: fixation in paraformaldehyde 4% for 6 h at 4°C; rapid wash with 1X PBS pH 7.4; immersion in a 30% sucrose solution in 1X PBS pH 7.4 at 4°C overnight; embedding in Killik embedding medium (Bio-Optica, Milan, Italy) in order to perform the cryostat cut into 10 µm sections, horizontally, to allow longitudinal observation of the optic nerve. The sections were placed on microscope slides and stored at -20°C.

Immunohistochemistry

This method was used to localize inducible nitric oxide synthase (iNOS) and caspase-3 in the retina and the optic nerve head.

Fluorescence immunolocalization

iNOS expression was detected with a rabbit primary polyclonal anti-iNOS antibody (Santa Cruz) (1:50), followed by a green fluorescent goat anti-rabbit IgG Alexa Fluor (Molecular Probes) secondary antibody.

Caspase-3 expression was detected with a rabbit primary polyclonal anti-caspase-3 antibody (Santa Cruz) (1:100), followed by a green fluorescent goat anti-rabbit IgG Alexa Fluor (Molecular Probes) secondary antibody.

The sections, left to dry at room temperature for 30 min, were subjected to various treatments: washes in 1X PBS for 5 min; post-fixation with alcohol at increasing volumes (70°, 95°, 100°) for 2 min; washes in 1X PBS for 5 min; block with serum (NRS or NGS), 10% in PBS, 1 h in a moist chamber; incubation with the primary antibody diluted in 1X PBS + BSA 1% for 1 h; fast washes in 1X PBS; incubation with the secondary antibody diluted 1:200 in 1X PBS + 1% of the serum of the animal in which the antibody was produced, for 30 min at room temperature; washes in 1X PBS for 5 min; mounting of the slides with Eukitt.

The observations were made under a fluorescence microscope and pictures taken by computerized image acquisition.

Preparation of protein extracts

After weighing the rat retinas, they were immersed in lysis buffer, and protein extracted. The test-tubes were kept for 10 min on ice, then centrifuged at 13000 rpm for 5 s and transferred back to the ice for another 10 min. Finally, they were centrifuged for 10 min, at 13000 rpm. Subsequently, the supernatant was collected and used in the study.

Western blotting and immunodetection

An equal amount of proteins was loaded, separated on an SDS PAGE gel and then iNOS and caspase-3 presence was identified by Western blotting. α-tubulin was used s a loading control to normalize protein expression. The Bradford assay was used to estimate protein concentration.

TUNEL assay

At an advanced stage of the apoptosis cascade, the cell presents extensive DNA degradation which leads to the production of molecules 180-200 bp in length and their multiples. The *in situ* fragments of DNA are highlighted by fluorescent nucleotide conjugation using terminal deoxynucleotidyl transferase or the TUNEL technique.

The TUNEL technique (Terminal deoxynucleotidyl transferase mediated dUTP Nick End Labeling) consists of in situ labelling of DNA fragments by fluoresceinated nucleotide conjugation using terminal deoxynucleotidyl transferase, iNOS and caspase-3.

Tissue sections with a thickness of 10 µm were subjected to DNA terminal staining using nucleotides

linked to a fluorescent chromophore, fluorescein. Nuclei with degraded DNA showed greater fluorescence than nuclei in which the degenerative process was absent, because the terminal transferase specifically incorporates fluorescent nucleotides onto the free 3'OH ends of fragmented DNA.

The sections, left to dry at room temperature for 30 min, were subjected to the following treatments: rehydration through a descending alcohol series (100°, 95°, 75°; 2 min each); incubation with protease 20 µg/mL in Triton X-100 to 0.1% at 37°C for 30 min; washes with 1X PBS for 2 min; incubation with the TUNEL reagent (In Situ Cell Death Detection Kit, AP/ROCHE), containing 1/10 in volume of terminal deoxynucleotidyl transferase and the remaining fraction of nucleotides labeled with a fluorescent chromophore, 10 µl per section at 37°C for 1 h. On each slide, one of the sections was always used as the negative control, i.e. incubated without terminal transferase but only with the nucleotides in order to detect any non-specific staining of the sections; washes with 1X PBS for 5 min; mouting of the slides with Eukitt. The observations were made under a fluorescence microscope and pictures taken by computerized image acquisition.

Statistical analysis

All the experiments were repeated at least four times. Statistical analysis of the results was performed using the ANOVA test. The significance of the result was determined by the Student's *t*-test. P-values <0.05 were considered significant.

RESULTS

Cellular morphology is maintained by ALA and SOD treatment

The cell morphology differed between control cases and those with induced ocular hypertension. Indeed, in the controls, there were Müller cells and RGCs (Fig. 1A, B). By contrast, cells in which a condition of oxidative/hypoxic stress had been induced via ocular hypertension with MTC showed some vacuolated RGCs, with dispersed and fragmented chromatin; Müller cells had a similar appearance. However, after pretreatment with ALA and SOD, the appearance of the cell was similar to that of the control cases (Fig. 1C). The optic nerve astrocytes in the control cases maintained their elongated shape (Fig. 1D), while in conditions of ocular hypertension this shape was lost (Fig. 1E). Whereas, tissue treated with ALA and SOD maintained a more regular organization of astrocyte cells (Fig. 1F).

ALA and SOD prevent DNA damage

Analysis of the state of DNA degradation in the retina and in the optic nerve can be studied using TUNEL (Terminal deoxynucleotidyl transferase mediated dUTP Nick End Labeling). This technique labels the nucleus of cells in an advanced stage of death, where endonucleases have fragmented the DNA due to apoptosis or cell necrosis.

The sections of eyes from MTC-treated rats showed marked fluorescence in the RGCs and astrocyte cells of the optic nerve (Fig. 2A, B) due to DNA fragmentation. The sections of eyes of ALA-treated rats showed a slight positive fluorescence compared with MTC-treated eyes (Fig. 2A-C). The fluorescence in the sections treated with SOD was slightly more evident (Fig. 2A-D). The sections of eyes of rats treated with ALA and SOD (Fig. 2E) had slight fluorescence, quite similar to that of the control cases (Fig. 2A).

ALA and SOD reduce iNOS expression

An ischemic insult at retinal level activates the expression of iNOS with the production of high levels of nitric oxide (NO). High NO concentrations are cytotoxic because they rapidly react with radical molecules, causing lipid peroxidation (27-30).

In pathological conditions, almost all the cells are able to express iNOS 6-8 h after induction. This is the time needed for the expression of the gene and the synthesis of the enzyme that produces a large amount of NO (28-30).

Twenty four h after treatment with MTC, there was high iNOS positivity in the RGCs and astrocytes of the optic nerve (Fig. 3A-D). In the sections of animals treated with MTC and ALA (Fig. 3E, F) there was reduced staining and therefore lower iNOS expression compared to the sections treated with MTC and SOD (Fig. 3G, H). A barely detectable staining was observed in MTC cases treated with ALA + SOD, (Fig. 3I, J). Subsequently, a western blot of total protein extracts of the retina was performed, in order to obtain quantitative data for the differential expression of iNOS (130kDa). Normalization was performed through localization of α-tubulin. Western blot analsyis of iNOS confirmed what had previously been seen by immunolocalization (Fig.

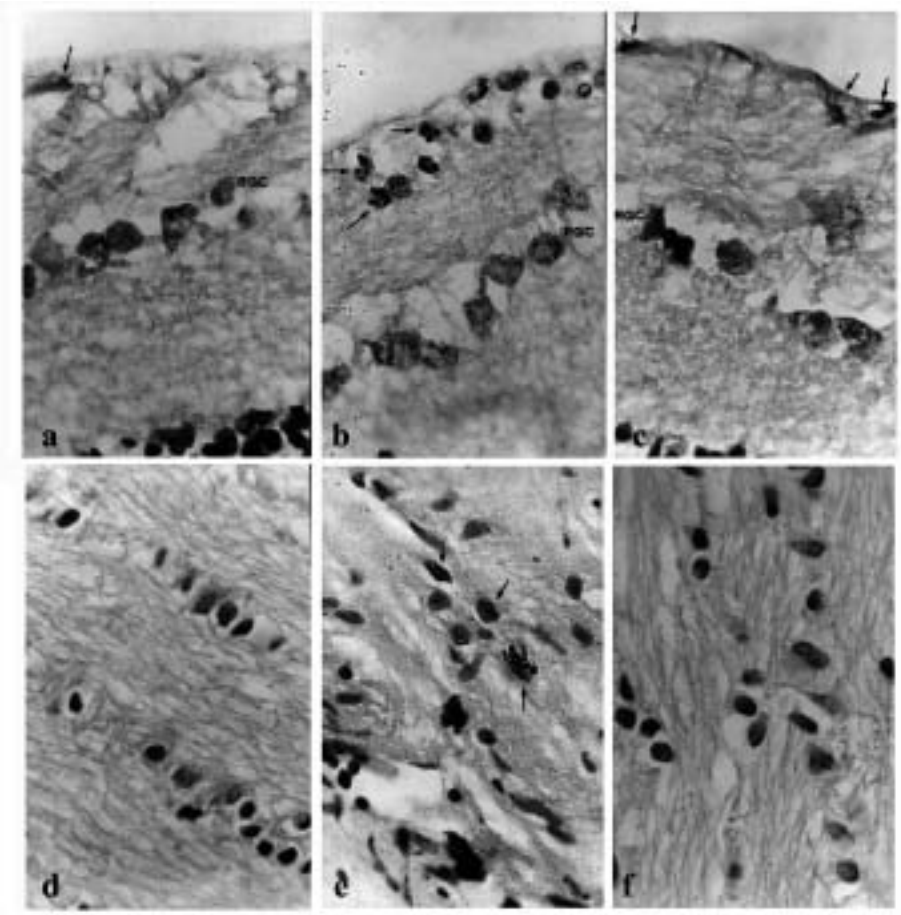

Fig. 1. *Panel A. Retinal ganglion cells (RGCs) stained with haematoxylin-eosin. RGCs or infiltrating leucocytes (arrows).* ***a****) Control Section;* ***b****) Section of eye treated with methylcellulose 2% (MTC);* ***c****) Section of MTC eye treated with α-lipoic acid (ALA) + superoxide dismutase (SOD). Panel B. Astrocyte cells of the optic nerve stained with haematoxylin-eosin.* ***d****) Control Section.* ***e****) Section of eye treated with MTC. The astrocytes have lost their elongated shape. The arrows indicate vacuolated nuclei.* ***f****) Section of MTC eye treated with ALA + SOD. The elongated shape of the cells remains partially intact.*

4). The band detectable at approximately 130kDa was larger when the treatments were carried out with either ALA or SOD than with ALA + SOD together. Table I and Fig. 5 represent quantification of iNOS expression after α-tubulin normalization.

ALA and SOD reduce caspase-3 activation

Caspase-3 is an executor molecules responsible for the final stages of the apoptotic cascade. After 24 h, MTC-treated eyes showed high expression of activated caspase-3 due to the process of cell death both in the retina and in the optic nerve (Fig. 6 A-D). In the sections of animals treated with MTC and ALA (Fig. 6 E,F) there was reduced immunofluorescence and therefore lower caspase-3 expression compared to the sections treated with MTC and SOD (Fig. 6 G, H). A faint immunofluorescence occurred in MTC cases treated with ALA + SOD, (Fig. 6 I, J). Again, in order to obtain quantitative data for the differential expression of caspase-3, a western blot of protein extracts of the retina was performed (Fig. 7). Normalization was carried out by detection of α-tubulin. Western blot confirmed an increase in caspase-3 expression in ocular tissues treated with MTC and a decrease in the expression of the same protease in eyes treated simultaneously with ALA and SOD. This shows that the apoptotic cascade is less activated when the two free radical scavengers

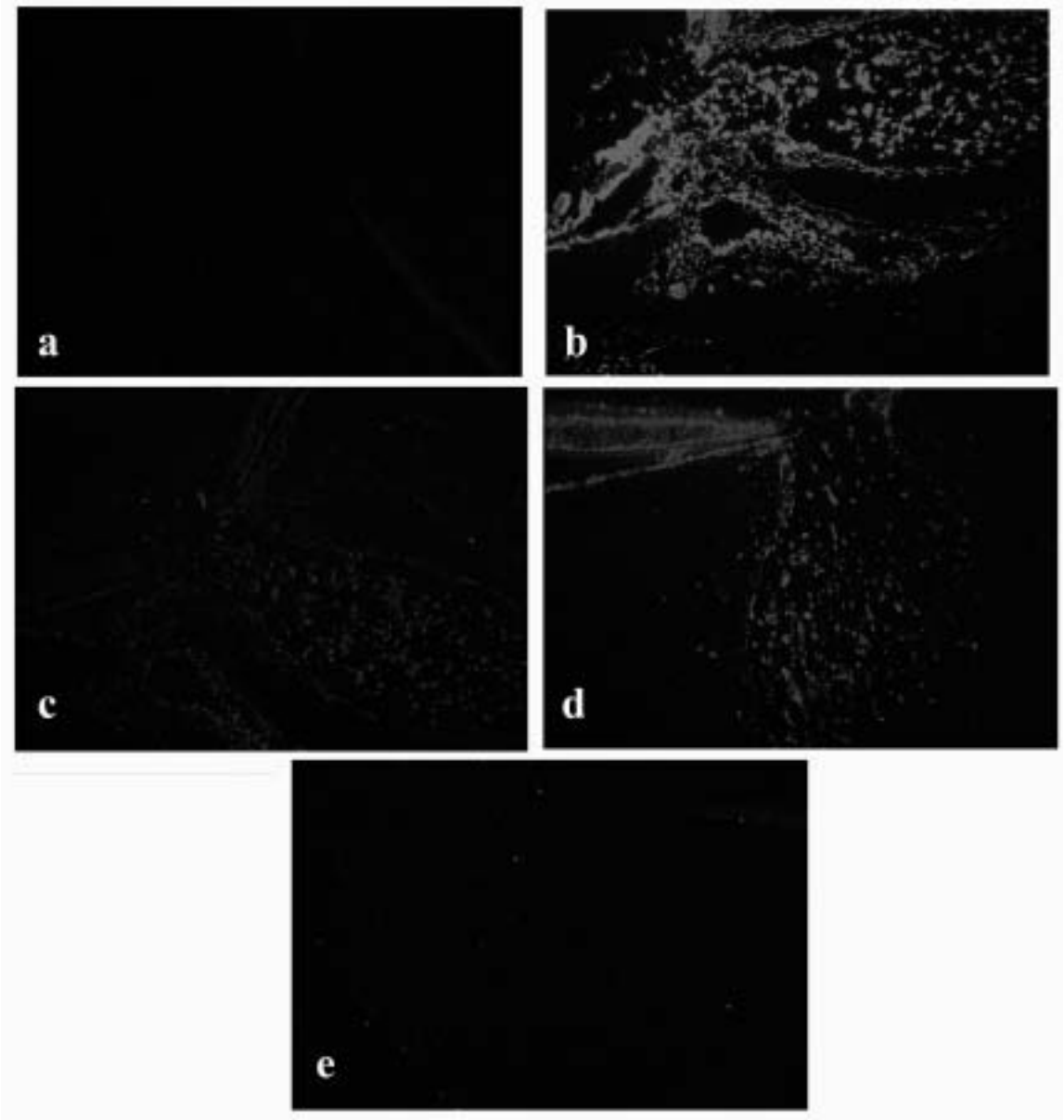

Fig. 2. *Fluorescence after TUNEL technique in sections of the optic nerve and retina after 24 h.* ***a)*** *Control Section;* ***b)*** *Section 24 h after treatment with methylcellulose 2% (MTC);* ***c)*** *Section 24 h after treatment with MTC + α-lipoic acid (ALA);* ***d)*** *Section 24 h after treatment with MTC + superoxide dismutase (SOD);* ***e)*** *Section 24 h after treatment with MTC and ALA + SOD*

are combined (Table II and Fig. 8).

DISCUSSION

Some studies have already shown that oxidative stress can lead to a series of structural alterations, only partially reversible, thus compromising the correct operation of many cellular components (1-3, 5-7). Starting from this premise, we wished to improve our knowledge in this area using young adult rats subjected to ischemic-oxidative stress after induction of ocular hypertension in the presence or absence of two oxidant scavengers such as ALA and SOD.

The parameters we observed revealed that ALA reduced markers of apoptosis and oxidative

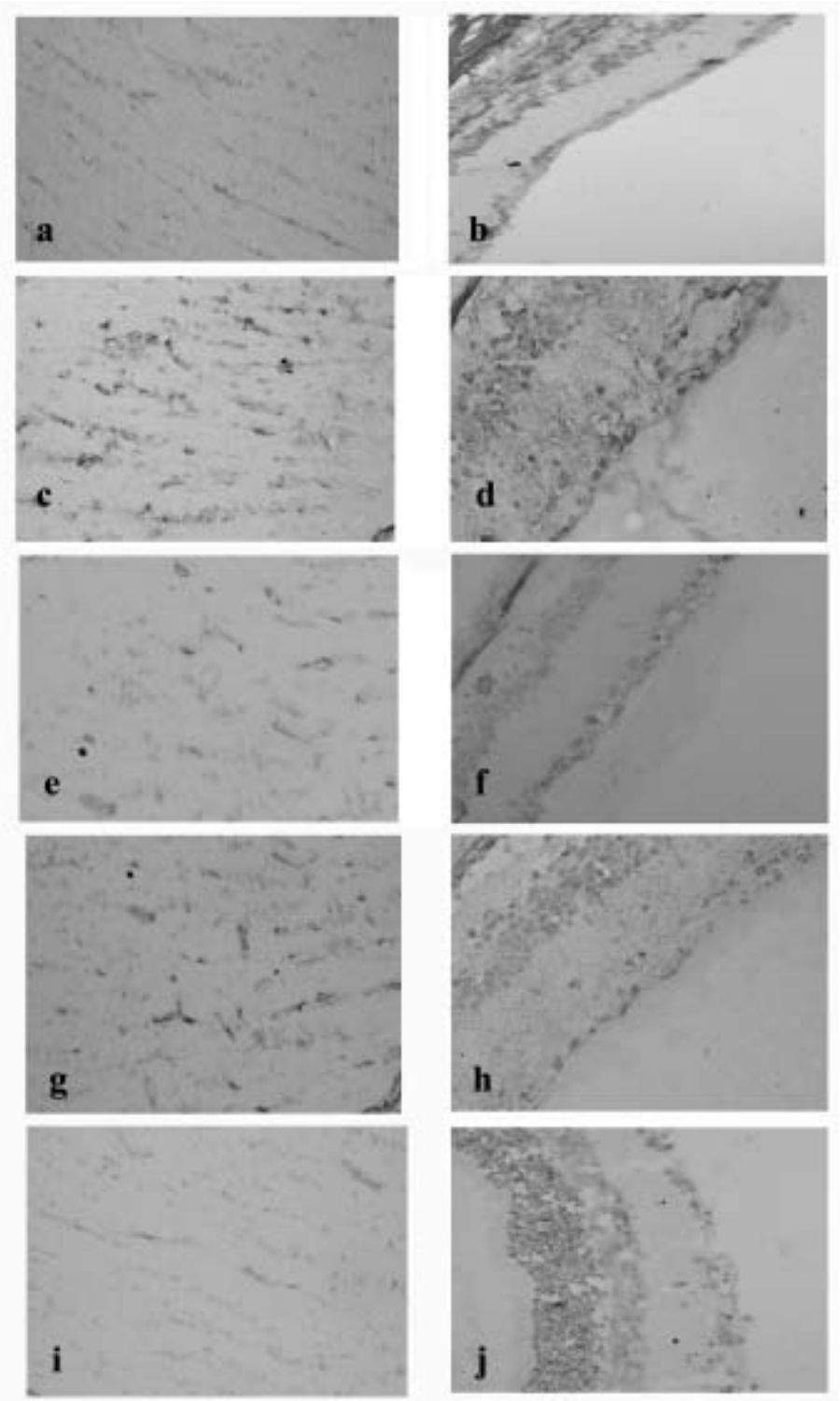

Fig. 3. *Immunolocalization of inducible nitric oxide synthase (iNOS). All images are at x500.* ***a-b****) Longitudinal section of the optic nerve and retina (control).* ***c-d****) Longitudinal section of the optic nerve and retina of the eye treated with methylcellulose 2% (MTC).* ***e-f****) Longitudinal section of the optic nerve and retina of the MTC-treated eye + α-lipoic acid (ALA).* ***g-h****) Longitudinal section of the optic nerve and retina of the MTC-treated eye + superoxide dismutase (SOD).* ***i-j****) Longitudinal section of the optic nerve and retina of the MTC-treated eye with ALA + SOD.*

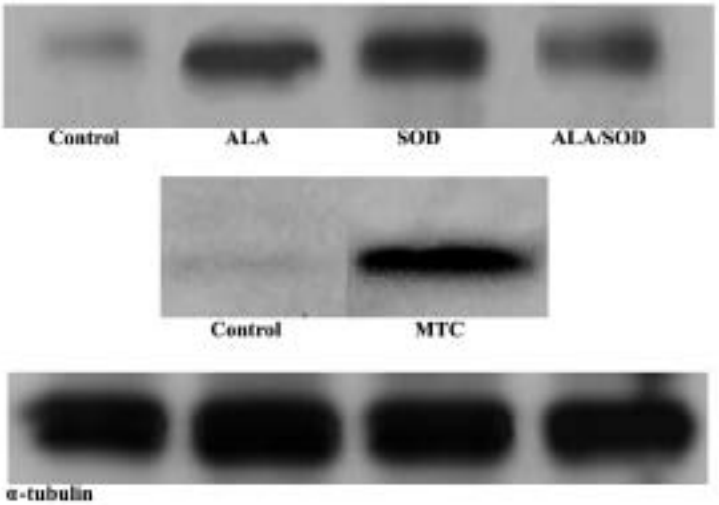

Fig. 4. *Western blot analysis of inducible nitric oxide synthase (iNOS).*

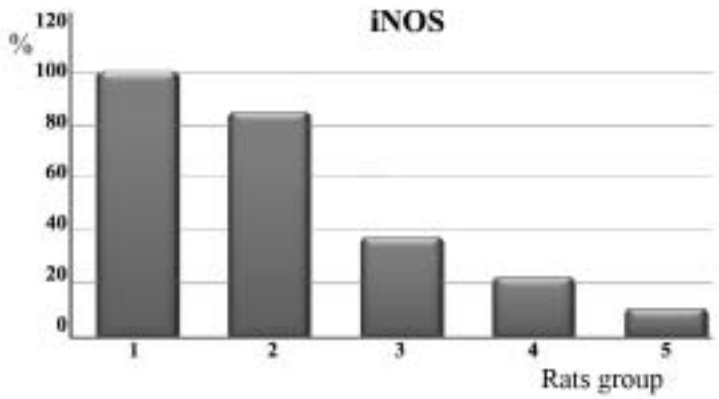

Fig. 5. *Quantization of the inducible nitric oxide synthase (iNOS) bands obtained by western blot. Values are expressed as percentages. 1: treatment with methylcellulose 2% (MTC); 2: treatment with MTC + superoxide dismutase (SOD); 3: treatment with MTC + α-lipoic acid (ALA); 4: treatment with MTC + ALA + SOD; 5: control.*

stress more significantly than SOD. These effects seemed particularly relevant when treatment was administered concomitantly with ALA and SOD, probably due to the presence of synergistic mechanisms of action (21, 26, 28). Our assays would seem to confirm that ocular hypertension causes the onset of the programmed cell death cascade, for a large number of cells, within 24 h.

We know that the mitochondrion is a major site of ROS production in the cell (5-7). As such, the mitochondrion is also an important site for the initiation and progression of apoptosis (8, 14, 15). This would lead to an increase in the lipid peroxidation reaction in tissues following pressure-mediated trauma and oxidative stress (14, 15, 20). Excessive ROS production can damage different components of mitochondrial metabolic pathways, resulting in altered mitochondrial function and an imbalance in cellular homeostasis (12,14-17). Thereafter, the destabilization of mitochondrial membranes would be responsible for the release of pro-apoptotic factors. Upon mitochondrial dysfunction, many molecules are released from mitochondria to initiate and propagate apoptosis (11, 12). Cytochrome c, when released into the cytoplasm, interacts with Apaf-1 to form a protein complex called the apoptosome,

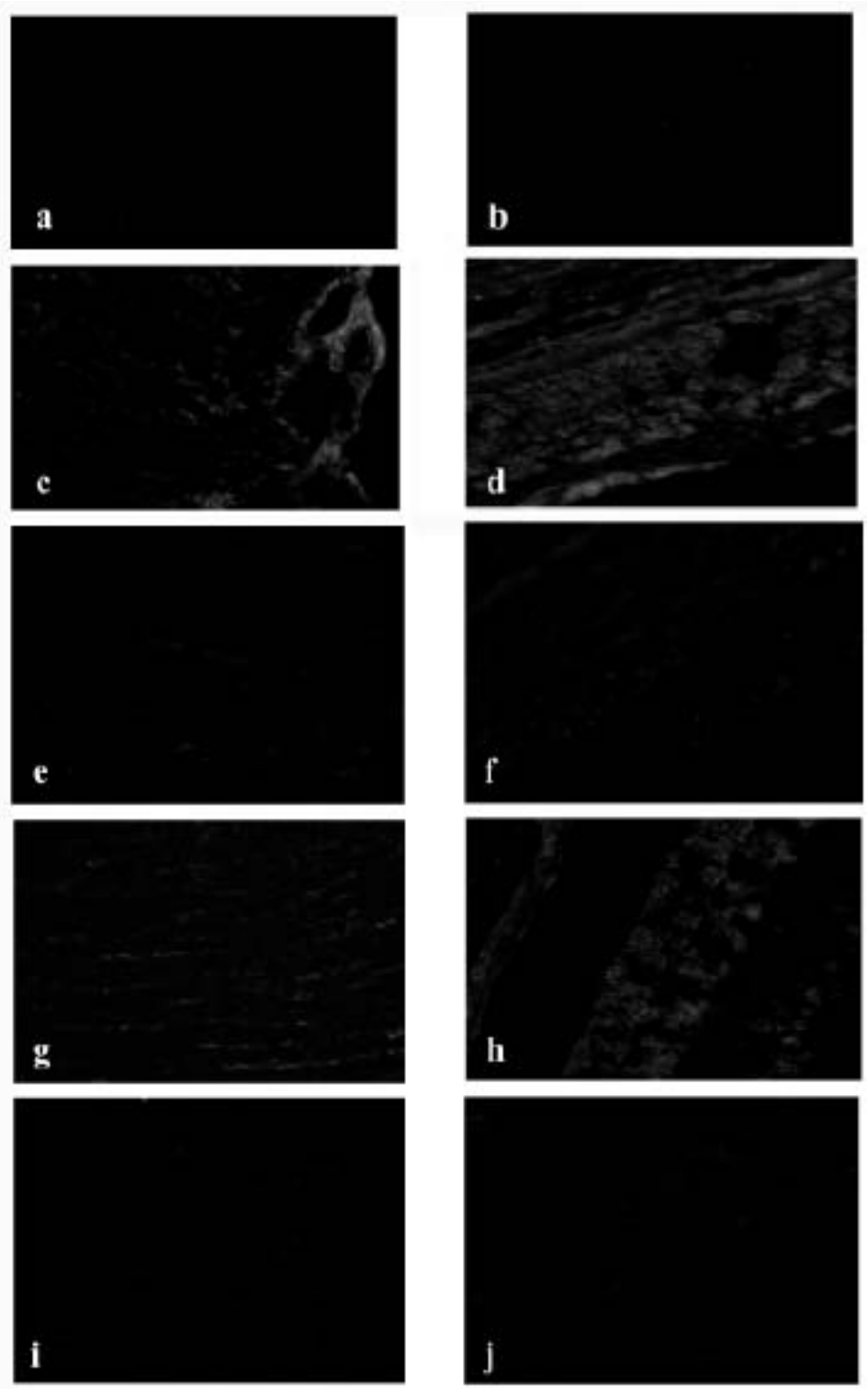

Fig. 6. *Immunolocalization of caspase-3 in rats. All images are at x500.* ***a-b****) Longitudinal section of the control optic nerve and retina.* ***c-d****) Longitudinal section of the optic nerve and retina of the eye treated with methylcellulose 2% (MTC).* ***e-f****) Longitudinal section of the optic nerve and retina of the MTC-treated eye + α-lipoic acid (ALA).* ***g-h****) Longitudinal section of the optic nerve and retina of the MTC-treated eye + superoxide dismutase (SOD).* ***i-j****) Longitudinal section of the optic nerve and retina of the MTC-treated eye with ALA + SOD.*

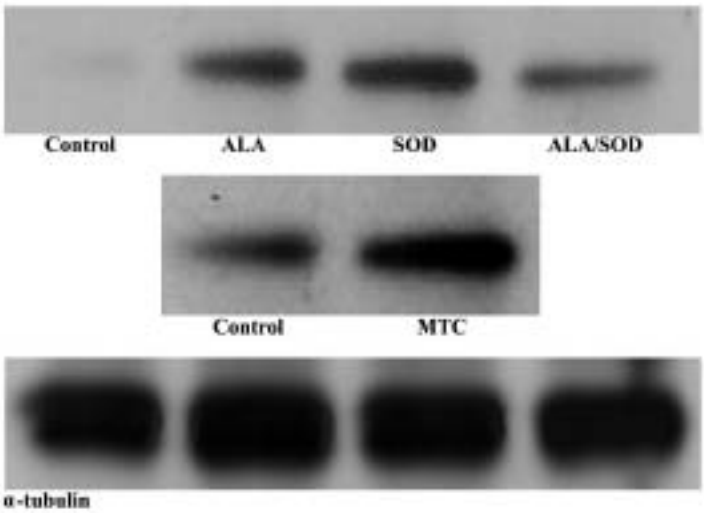

Fig. 7. *Western blot analysis of caspase-3.*

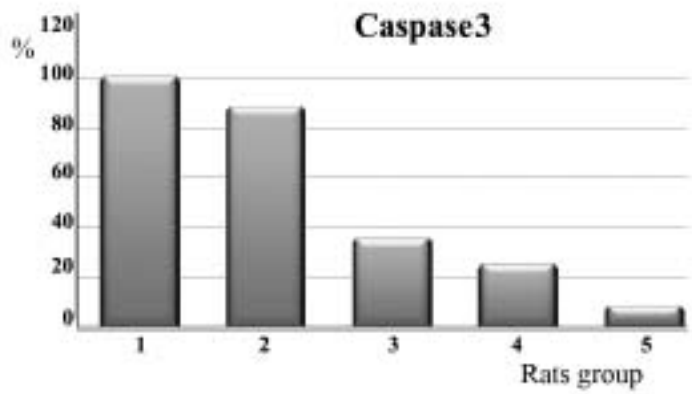

Fig. 8. *Quantization of Caspase-3 bands obtained by western blot. Values are expressed as percentages. 1: treatment with methylcellulose 2% (MTC); 2:treatment with MTC + superoxide dismutase (SOD); 3:treatment with MTC + α-lipoic acid (ALA); 4:treatment with MTC + ALA + SOD; 5: control.*

which promotes activation of caspase. So in cases of animals pretreated with antioxidants and inoculated with MTC, there would be a decrease in the presence of free radicals and therefore in the apoptotic death cascade, due to the reduction in the expression of the protease following the improvement in the indirect stability of mitochondrial membranes, proteins and cellular DNA.

Furthermore, it should be remembered that some clinical trials have reported that ALA can directly inhibit membrane phospholipase A_2 (PLA_2) which is activated by the free radicals produced, in turn, by the mitochondria responsible for the damage to cellular structures (11, 12, 20, 21).

On the other hand, SODs, as already mentioned in the introduction, comprise a group of cellular enzymes that use different cofactors depending on the site of action (22-25). SOD introduced via food would probably reach the blood by pinocytosis and seems, at our concentrations, able to reach the tissues despite the high level of metabolization by the liver. At tissue level, SOD could cross the barriers present (i.e. blood-retinal barrier) and would then act outside the cell on the free superoxides, which in turn are in equilibrium with those produced inside the cell. Mitochondrial MnSODs have manganese as a cofactor and would

Table I. *Quantization of the inducible nitric oxide synthase (iNOS) bands obtained by western blot. Values are expressed as percentages. 1: treatment with MTC; 2: treatment with MTC + SOD; 3: treatment with MTC + ALA;4: treatment with MTC + ALA + SOD; 5: control.*

MTC	MTC+SOD	MTC+ALA	MTC+ALA+SOD	Control
100	85 ± 4 %	37 ± 3 %	22 ± 3 %	10 ± 1 %
	$P_{1.2} < 0.5$ $P_{2.3} < 0.1$	$P_{2.3} < 0.1$ $P_{3.4} < 0.5$	$P_{4.5} < 0.1$	

The values are means ± standard error (n = 8). MTC: methylcellulose 2%; SOD: superoxide dismutase; ALA: α-lipoic acid.

Table II. *Quantization of Caspase-3 bands obtained by western blot. Values are expressed as percentages. 1: treatment with MTC; 2: treatment with MTC + SOD; 3: treatment with MTC + ALA; 4: treatment with MTC + ALA + SOD; 5; control.*

MTC	MTC+SOD	MTC+ALA	MTC+ALA+SOD	Control
100	88 ± 3 %	35 ± 3 %	25 ± 2 %	8 ± 2 %
	$P_{1.2} < 0.5$ $P_{2.3} < 0.1$	$P_{2.3} < 0.1$ $P_{3.4} < 0.5$	$P_{4.5} < 0.1$	

The values are means ± standard error (n = 8). MTC: methylcellulose 2%; SOD: superoxide dismutase; ALA: α-lipoic acid.

seem to be the most important types. Numerous studies in different model systems demonstrate the indispensable role for MnSOD in protecting aerobic life from the deleterious effects of oxygen (23, 24). Methods to increase the expression or activity of MnSOD may prove to be valuable strategies for the treatment of various disease conditions involving aberrant mitochondrial ROS production, including numerous neurological conditions, cardiovascular disease, and cancer (22, 24, 28). These various adaptive responses may protect cells from apoptosis caused by numerous toxic agents (8, 28-30).

Our research has found that ALA and SOD cause: i) a negative modulation of the enzyme iNOS and reduced production of free radicals; ii) a down regulation of caspase-3 expression, iii) lower degradation of DNA, iv) reduction in extra- and intracellular oxidative stress.

We can thus conclude that an increase in the cellular and extracellular pool of ALA and SOD, obtained through exogenous administration, would be able to prevent degenerative tissue phenomena and antiapoptotic effects in rat retinal cells, subjected to ischemic and pressure-related stress. Additional studies will be needed to clarify the biochemical processes and their connections with environmental and

genetic factors.

ACKNOWLEDGEMENTS

This research was supported by the following grants: Alfa Wasserman S.p.A.

REFERENCES

1. Avery SV. Molecular targets of oxidative stress. Biochem J 2011; 434:201-10.
2. Halliwell B. Biochemistry of oxidative stress. Biochem Soc Trans 2007; 35:1147-50.
3. Poli G, Leonarduzzi G, Biasi F, Chiarpotto E. Oxidative stress and cell signaling. Curr Med Chem 2004; 11:1163-82.
4. Valko M, Leibfritz D, Moncol J, et al. Free radicals and antioxidants in normal physiological functions and human disease. Int J Biochem Cell Biol 2007; 39:44-84.
5. Boonstra J, Post JA. Molecular events associated with reactive oxygen species and cell cycle progression in mammalian cells. Gene 2004; 337:1-13.
6. Murphy MP. How mitochondria produce reactive oxygen species. Biochem J 2009; 417:1-13.
7. Matés JM, Segura JA, Alonso FJ, Márquez J. Intracellular redox status and oxidative stress: implications for cell proliferation, apoptosis, and carcinogenesis. Arch Toxicol 2008; 82:273-99.
8. Evans MD, Dizdaroglu M, Cooke MS. Oxidative DNA damage and disease: induction, repair and significance. Mutat Res 2004; 567:1-61.
9. MacNee W. Oxidative stress and lung inflammation in airways disease. Eur J Pharmacol 2001; 429:195-207.
10. Droge W. Free radicals in the physiological control of cell function. Physiol Rev 2002; 82: 47-95.
11. Kroemer G, Galluzzi L, Brenner C. Mitochondrial membrane Permeabilization in cell death. Physiol Rev 2007; 87:99-163.
12. Paradies G, Petrosillo G, Paradies V, Ruggiero FM. Oxidative stress, mitochondrial bioenergetics, and cardiolipin in aging. Free Radic Biol Med 2010; 48:1286-95.
13. Griffiths HR. ROS as signalling molecules in T cells – evidence for abnormal redox signalling in the autoimmune disease, rheumatoid arthritis. Redox Rep 2005; 10:273-80.
14. Moreno MC, Campanelli J, Sande P, et al. Retinal oxidative stress induced by high intraocular pressure. Free Radic Biol Med 2004; 37:803-12.
15. Chrysostomou V, Rezania F, Trounce IA, et al. Oxidative stress and mitochondrial dysfunction in glaucoma. Curr Opin Pharmacol 2012; pii:S1471-92.
16. Pescosolido N, Cavallotti C, Rusciano D, Nebbioso M. Trabecular Meshwork in Normal and Pathological Eyes. Ultrastruct Pathol 2012; 36:102-7.
17. Nebbioso M, Pascarella A, Cavallotti C, et al. Monoamine oxidase-enzymes and oxidative stress in the rat optic nerve: Age-related changes. Int J Exp Path 2012; 93(6):401-5.
18. Ha H, Lee J-H, Kim H-N, et al. α-Lipoic acid inhibits inflammatory bone resorption by suppressing prostaglandin E2 synthesis. J Immunol 2006; 176:111-7.
19. Cameron NE, Jack AM, Cotter MA. Effect of α-lipoic acid on vascular responses and nociception in diabetic rats. Free Radical Biol Med 2001; 31:125-35.
20. Gorąca A, Huk-Kolega H, Piechota A, Kleniewska P, Ciejka E, Skibska B. Lipoic acid-biological activity and therapeutic potential. Pharmacological report 2011; 63:849-58.
21. Ziegler D, Ametov A, Barinov A, et al. Oral treatment with α-lipoic acid imroves symptomatic diabetic polyneuropathy. The Sydney 2 trial. Diabetes Care 2006; 29:2365-70.
22. Miao L, St Clair DK. Regulation of superoxide dismutase genes: Implications in disease. Free Radic Biol Med 2009; 47:344-56.
23. Strange RW, Antonyuk SV, Hough MA, et al. Variable metallation of human superoxide dismutase: atomic resolution crystal structures of Cu-Zn, Zn-Zn and As-isolated wild-type enzymes. J Mol Biol 2006; 356:1152-62.
24. Holley AK, Bakthavatchalu V, Velez-Roman JM, et al. Manganese Superoxide Dismutase: Guardian of the Powerhouse. Int J Mol Sci 2011; 12:7114-62.
25. Giuca MR, Giuggioli E, Metelli MR, Pasini M, Iezzi G, D'Ercole S, Tripodi D. Effects of cigarette smoke on salivary superoxide dismutase and glutathione peroxidase activity. J Biol Regul Homeost Agents. 2010; 24(3):359-66.

26. Yasui K, Baba A. Therapeutic potential of superoxide dismutase (SOD) for resolution of inflammation. Inflamm Res 2006; 55:359-63.
27. Scarsella G, Nebbioso M, Stefanini S, Librando A, Pescosolido N. Degenerative effects in rat eyes after experimental ocular hypertension. European Journal of Histochemistry 2012; 56:e42:265-71.
28. Bertolotto F, Massone A. Combination of Alpha Lipoic Acid and Superoxide Dismutase Leads to Physiological and Symptomatic Improvements in Diabetic Neuropathy. Drugs R D 2012; 12:29-34.
29. Sennlaub F, Courtois Y, Goureau O. Inducible nitric oxide synthase mediates retinal apoptosis in ischemic proliferative retinopathy. J Neurosci 2002; 22:3987-93.
30. Sharpe MA, Ollosson R, Stewart VC, et al. Oxidation of nitric oxide by oxomanganese-salen complexes: a new mechanism for cellular protection by superoxide dismutase/catalase mimetics. Biochem J 2002; 366:97-107.

ALTERATIONS OF ROS PATHWAYS IN SCLERODERMA BEGIN AT STEM CELL LEVEL

M. ORCIANI[1], S. SVEGLIATI[2], S. GORBI[3], T. SPADONI[2], R. LAZZARINI[1], F. REGOLI[3], R. DI PRIMIO[1] and A. GABRIELLI[2]

[1]Department of Clinical and Molecular Sciences and Histology, Università Politecnica delle Marche, Ancona, Italy; [2]Department of Clinical and Molecular Sciences and Clinical Medicine, Università Politecnica delle Marche, Ancona, Italy; [3]Department of Life and Environmental Science, Università Politecnica delle Marche, Ancona, Italy

Received September 4, 2012 – Accepted February 4, 2013

Scleroderma is a chronic systemic autoimmune disease (primarily of the skin) characterized by fibrosis (or hardening), vascular alterations and autoantibodies production.There are currently no effective therapies against this devastating and often lethal disorder. Despite the interest for the immunomodulatory effects of mesenchymal stem cells (MSCs) in autoimmune diseases, the role of MSCs in scleroderma is still unknown. A pivotal role in scleroderma onset is played by oxidative stress associated with the accumulation of great amounts of reactive oxygen species (ROS). This study depicts some phenotypic and functional features of MSCs isolated from the skin of healthy and scleroderma patients; the ROS production and accumulation, the expression of ERK1/2 and the effects of the stimulation with PDGF, were analyzed in MSCs; results were compared to those observed in primary fibroblasts (Fbs) isolated from the same subjects. We found that the pro-oxidant environment exerted by scleroderma affects MSCs, which are still able to counteract the ROS accumulation by improving the antioxidant defenses. On the contrary, scleroderma fibroblasts show a disruption of these mechanisms, with consequent ROS increase and the activation of the cascade triggered by scleroderma auto-antibodies against PDGFR.

Scleroderma is a systemic autoimmune disease of unknown origin, characterized by microvascular injury, autoimmune inflammatory responses, severe and often progressive fibrosis (1-3).

The disease can occur in a localized form confined to the skin (limited scleroderma, lSSc) to diffuse cutaneous sclerosis with severe internal organ involvement (diffuse sclerosis, dSSc).

Even if its aetiology is unidentified, excessive collagen deposit in affected tissues is a key for the pathogenesis of the disease and comprises most of the clinical manifestations, determining its development and prognosis; concurrently, numerous treatments attempt target these collagen deposits (4).

In recent years, most of the attention has been focused on mesenchymal stem cells (MSCs) in order to understand if the physiopathological events leading to SSc start early at staminal level or not. It is not clear if the immunosuppressive properties exerted by MSCs may offer a potentially attractive therapeutic modality for this autoimmune disease or if, on the contrary, MSCs may be involved in the pathogenesis of scleroderma.

Some authors reported that autologous stem cell-

Key words: scleroderma, stem cells, ROS, PDGFR

Mailing address: Dr Roberto Di Primio,
Department of Clinical and Molecular Sciences -Histology,
Università Politecnica delle Marche,
Via Tronto 10/A, 60020 Ancona, Italy
Tel.: +39 071 2206076
Fax: +39 071 2206076
e-mail: r.diprimio@univpm.it

0393-974X (2013)

based therapies by topical application or systemic delivery may be effective for the treatment of peripheral vascular complications, including healing of digital ulcers and gangrene of the extremities (5). These therapeutic advantages may be correlated to the paracrine effect of MSCs, which secrete a broad panel of bioactive molecules, such as growth factors and cytokines, with proangiogenic and immunomodulatory effects. Conversely, other researches (5-7) found that bone marrow-derived mesenchymal stem cells (BM-MSCs) from SSc patients showed serious impairment in differentiation and release of bioactive proangiogenic factors.

Therefore, the comprehension of the role/effect of MSCs in scleroderma is still matter of debate; among the others, an important question to be addressed is the response of MSCs to PDGFR (Platelet Derived Growth Factor Receptor) stimulation. Previously we reported the presence of agonistic anti-PDGFR auto-antibodies (auto-abs) in the serum of patients affected by SSc (8, patent WO/2007/013124). Such SscIgG stimulate PDGFR and convert *in vitro* normal human fibroblasts (Fbs) into SSc-like cells characterized by overproduction of reactive oxygen species (ROS) and collagen. The oxidative stress caused by ROS overproduction has a pivotal role in scleroderma, where an alteration of antioxidant enzyme activities and/or oxyradical scavenging capacity has been reported in biological samples (9-11).

It is now well accepted that bone marrow, peripheral blood, amniotic fluid and cord blood (12-15) are only some of the reservoirs of MSCs, which can be successfully isolated also from skin (16-19).

Stem cells derived from adult skin have properties common to all stem cells: capability to proliferate for many passages in culture maintaining a relatively unspecialized phenotype and potential to differentiate into specialized cell types. As Fbs are the main cellular population to be involved in scleroderma and the skin fibrosis is one of its most common and recognizable symptoms, we decided to isolate MSCs and Fbs from skin of patients affected by scleroderma (healthy subjects were enrolled as controls); susceptibility to ROS, at basal level and after PDGF or immunoglobulinsG (IgG) stimulation, was compared in MSCs and Fbs to investigate a potential involvement of stem cells in the pathogenesis of scleroderma. In addition, we evaluated the ERK1/2/HaRas pathway (by phospho- ERK1/2 analysis) and the α1 (I) and α 2 (I) collagen gene expression, which are key markers of scleroderma.

MATERIALS AND METHODS

The study, approved by Politechnic Marche University Ethic Commitee and conducted in accordance with the Declaration of Helsinsky, enrolled three caucasian patients who fulfilled the criteria for the diagnosis of SSc and classified in diffuse SSc and limited SSc as suggested (20). Control group included age, sex and race matched healthy volunteers.

The demographic and clinical characteristics of the study populations are presented in Table I.

Isolation and cell culture of MSCs and primary Fbs

Human skin Fbs and MSCs were obtained from punch biopsies taken from the forearms of normal volunteers and from the involved skin of scleroderma patients (20).

The skin samples were divided into two pieces, one cultured in Mesenchymal Stem Cell Growth Medium bullet kit (Lonza Group Ltd, Basel, Switzerland) for MSCs isolation (18), the other in DMEM with 1 g/l glucose supplemented with 10% fetal bovine serum (FBS), 2 mM L-glutamine, 100 IU/ml penicillin and 100 µg/ml streptomycin (all from Euroclone, Milan, Italy) for Fbs culture. Cells were grown under standard conditions at 37°C in 5% CO_2. After 14 days of culturing, non-adherent cells and dermal tissue were removed, and the medium was changed twice a week. Cells between the fourth and the sixth subpassage were used for all experiments.

Characterization of MSCs and Fbs by cytofluorimetric and Real Time PCR analyses

Cells isolated from healthy and scleroderma subjects were examined for surface antigens that are reported as specific for stem cells (21), through staining with fluorescin isothiocyanate (FITC)-conjugated antibodies (Becton-Dickinson, Franklin Lakes, NJ USA) against: HLA-DR, CD19, CD14, CD34, CD45, CD73, CD90 and CD105. Flow cytometry analysis was performed with a Becton Dickinson FACScan instrument equipped with an argon ion laser tuned to 488 nm. The data acquisition was carried out with the CellQUEST software (Becton Dickinson). The cells were gated according to their light scattering, and the fluorescence intensity distribution histograms were analyzed.

Since it is reported (22) that many of the mesenchymal markers are also found in fibroblasts, we analyzed the level of CD9 (Becton Dickinson), which is differently

expressed by the two cellular subsets.

In addition, RNA transcripts of stem genes linked to self-renewal, such as Oct4, Sox2, Nanog and KLF4, were analyzed by real-time PCR in the two cellular populations. Total RNA was isolated using Aurum total RNA mini kit (BioRad Laboratories, CA, USA). cDNA was reverse transcribed from 0.5 μg of total RNA each sample, using IScript cDNA synthesis kit (BioRad). Complementary DNAs were mixed with SYBR-Green PCR IQ Super mix (BioRad) and primers (200nM, for the sequences see Tab.2), and real-time PCR was performed. GAPDH gene was used as internal control. The condition used for PCR were 10 min at 95°C and then 45 cycles of 15 s at 95°C and 1 min 60°C. Each reaction was performed in triplicate.

The PCR products were electrophoresed on 2% agarose gels, stained with ethidium bromide, and photographed. Subsequently, a densitometric analysis of the mRNA expression levels (quantified as arbitrary units, AU) was done.

All subsequent experiments were carried out on MSCs as well as in Fbs, isolated from healthy donors and scleroderma patients.

Antibody purification

ImmunoglobulinsG (IgG) were purified from serum of normal (NIgG) and scleroderma subjects (SScIgG) using gravity-flow column packed with protein A/G agarose following manufacturer instruction (Pierce, Thermo Fisher Scientific, Meridian Rd, Rockford, IL USA). Elution was performed at low-pH and then the samples were neutralized with 1/10th volume of 1M Tris –HCl ph 7,5-9. Concentration of all samples was calculated reading the absorbance at 280 nm. The eluted IgG fractions, characterized by the highest absorbance, were subjected to buffer exchange with PBS using desalting column, a size-exclusion chromatography with an average molecular weight exclusion limit of 5KDa (Pierce). Purity of IgG preparations was checked by Coomassie blue staining and immunoblotting with specific anti-cytokine antibodies.

ROS detection

For ROS detection, cells (30000 cells/w) were cultured in 24 well plates, starved 24 hours in medium containing 0.2% FCS and stimulated with PDGF-BB (20ng/ml, Peprotech, Rocky Hill, NJ) or SScIgG (200 μg/ml) for 15 min. Then they were loaded with DCHF-DA (10 μM) for 10 min at 37°C before assessing DCF fluorescence level (23) with multilabel counter (Victor 2 Perkin-Elmer ex: 485 nm; em. 530 nm).

Cell lysis and immunoblotting

After an overnight starvation (0.2% FCS), cells were stimulated with PDGF-BB (20ng/ml) or IgG (200 μg/ml, NIgG or SScIgG) for 15 min and lysed with 0.3 ml of cold RIPA buffer (1x PBS, 1% Nonidet P-40, 0.5% sodium deoxycholate, 0.1% SDS, 2 mM sodium orthovanadate, 2 μg/ml aprotinin, 1mM PMSF). The cells were kept for 30 min at 4°C and centrifugated at 10000 rpm for 10 min at 4°C. Equal amount of proteins were resolved by 10% SDS-PAGE and transferred to nitrocellulose membranes. The membranes were probed with anti phospho ERK1/2 (pERK1/2) antibody (Santa Cruz Biotechnology, Santa Cruz, CA, USA) and then with specific secondary peroxidase linked antibody (Santa Cruz Biotechnology); protein bands were revealed by enhanced Chemiluminescence (ECL system detection kit, Roche Diagnostic GmbH, Mannheim, Germany). Anti ERK2 antibody was used for normalization.

α1 (I) and α 2 (I) collagen gene expression

Levels of α1 and α2 type I collagen RNA transcripts were analyzed by real-time PCR. Total RNA isolation, cDNA synthesis, and Real-Time PCR program were carried out as described in "Stemness assessment" paragraph. Sequence primers, reported in table 2, derived from NCBI database (NCBI, http://www.ncbi.nlm.nih.gov/entrez/query.fcgi?CMD=search&DB= nucleotide; accession numbers GAPDH: BC013310; COL α 1(I): BC036531; COL α 2(I): BC054498).

To calculate the relative expression levels we used the $2^{-\Delta\Delta CT}$ method.

Biochemical analyses

Antioxidant responses were measured in cell lysates as the activities of two antioxidant enzymes (Glutathione S-Transferase and Glutathione Reductase, respectively GST and GR), and as the levels of glutathione (GSH) and of total oxyradical scavenging capacity (TOSC) towards peroxyl (ROO•) and hydroxyl radicals (HO•). The cells were resuspended in PBS (0.5-1.0 mg protein/ml) and aprotinin (1 μg/ml), freeze-thawed in liquid nitrogen three times, and centrifuged in an Eppendorf microcentrifuge at 12,000× *g* for 10 min at 4 °C. Detergents were not used for this cell lysate preparation because they have been shown to interfere with the TOSC determinations (24). The cell lysates were stored at -80 °C until analyzed.

GSTs were assayed using 1-chloro-2,4-dinitrobenzene (CDNB) as substrate at 340 nm. The assay was carried out in 100 mM K-phosphate buffer, pH 6.5, 1.5 mM CDNB, 1 mM GSH ($\varepsilon = 9.6\ mM^{-1}\ cm^{-1}$).

GR was determined following the decrease of absorbance due to NADPH oxidation during the reduction of oxidized glutathione, GSSG (λ =340 nm, $\varepsilon = -6.22\ mM^{-1}\ cm^{-1}$). The final assay conditions were 100 mM K-phosphate buffer, pH 7.0, 1 mM GSSG, 60 μM NADPH.

The levels of GSH were measured in 200,000 cells suspended in 100 µl PBS which were deproteinized in 5% sulfosalicylic acid and 4 mM EDTA (1:1 w/v ratio); the samples were maintained for 45 min on ice and centrifuged at 37,000× *g* for 15 min; the resulting supernatants were assayed spectrophotometrically by following the GR-catalyzed reaction of GSH with 5,5'-dithiobis-2-nitrobenzoic acid, and comparing this rate with a standard GSH curve.

The TOSC assay measured the overall ability of cellular antioxidants to absorb different forms of artificially generated oxyradicals, like ROO• and HO•, thus inhibiting the oxidation of α-keto-γ-methiolbutyric acid to ethylene gas (25-27). Ethylene formation was followed by gas-chromatography analysis, and the TOSC values were quantified from the equation: TOSC = 100-(∫SA/∫CA × 100), where ∫SA and ∫CA are the integrated areas calculated under the kinetic curves for the control (CA) and sample (SA) reactions (27). For each of the samples, a specific TOSC (normalized to the protein content) was calculated according to Regoli and Winston (28). The protein content of the cell lysates was determined by the Lowry method (28).

The DNA integrity was evaluated as single-strand breaks by the Comet assay. Control and H_2O_2-treated cells were resuspended in 100 µl 0.6% (w/v) low melting point agarose in PBS, pH 7.4 at 37°C, and immediately pipetted onto microscope slides precoated with 1% (w/v) normal melting point agarose in PBS. After gel solidification (10 min at 4°C), the slides were immersed in lysing solution (2.5 M NaCl, 100 mM EDTA, 1% Triton X-100, 10% DMSO, in 10 mM Tris buffer, pH 10.0) for 90 min at 4°C, to remove cell protein. DNA was unwound in 75 mM NaOH, 10 mM EDTA for 10 min at 4°C, which was followed by electrophoresis in the same buffer at 1 V cm^{-1} for 10 min at 4°C. The slides were washed 3 times for 10 min with 0.4 M Tris-HCl, pH 7.5, at 4°C, and fixed in methanol for 3 min at -20°C and dried. The slides were stained with 1 µg/ml 4',6-diamidino-2-phenylindole, and 100 randomly selected "nucleoids" per slide, and two replicates per sample, were examined under fluorescence microscopy (200×magnification; Olympus BX-51). The captured images underwent image analysis (Image- Pro-Plus) and were analyzed with the Comet Score software. The percentage of DNA in the tail was used to estimate the level of DNA fragmentation.

All experiments were repeated at least three times, and the results were expressed as the mean±SD. Significant differences of scleroderma respect to control group were determined using the paired-sample *t*-test. Statistical difference was accepted if $p<0.05$.

RESULTS

Isolation, culture and characterization of MSCs and Fbs

MSCs and Fbs were obtained from punch biopsies of normal volunteers and from the involved skin of

Table I. *Clinical and serological characteristics of patients and controls.*

	SSc1	SSc2	SSc3	CTRL1	CTRL2
AGE (yrs)	60	58	50	64	60
SEX	F	F	F	F	F
RAYNAUD'S FENOMENON DURATION (yrs)	5	5	2		
DISEASE DURATION (yrs)	1	5	1		
DISEASE SUBSET	lSSc	dSSc	dSSc		
ORGAN INVOLVMENT	DIGESTIVE TRACT	LUNG	DIGESTIVE TRACT-LUNG		
ANTINUCLEAR ANTIBODIES	+	+	+		
ANTI-CENTROMER ANTIBODIES	-	-	-		
ANTI Scl-70	+	+	-		
SCORE	9	28	24		

SSc1-2-3: scleroderma patients number 1-2-3
CTRL1-2: healthy subjects number 1-2

Table II. *Primer sequences used for PCR analyses*

GAPDH FW	5'-CCCTTCATTGACCTCAACTACATG-3'
GAPDH REV	5'- TGGGATTTCCATTGATGACAAGC-3'
Oct4 FW	5'-AGCGAACCAGTATCGAGAAC-3'
Oct4 REV	5'-TTACAGAACCACACTCGGAC-3'
Sox2 FW	5'-ACACCAATCCCATCCACACT-3'
Sox2 REV	5'-GCAAACTTCCTGCAAAGCTC-3'
Nanog FW	5'-TGAACCTCAGCTACAAACAG-3'
Nanog REV	5'-CTGGATGTTCTGGGTCTGGT-3'
KLF4 FW	5'-CCCACACAGGTGAGAAACCT-3'
KLF4 REV	5'-ATGTGTAAGGCGAGGTGGTC-3'
α1 (I) COL FW	5'-AGGGCCAAGACGAAGACATC-3'
α1 (I) COL REV	5'-AGATCACGTCATCGCACAACA-3'
α2 (I) COL FW	5'-AGGTCAAACAGGAGCCCGTGGG-3'
α2 (I) COL REV	5'-GCACCTGGGAAGCCTGGAGGG-3'

scleroderma patients.

Cells began to appear near to the explants after 7 days. Adherent cells started to divide rapidly, reaching confluence within 7 more days, and both cell populations appeared morphologically homogeneous (Fig. 1). No significant differences in morphology were observed between scleroderma and control cells.

Cells were then subjected to cytofluorimetric analysis; control and scleroderma MSCs and Fbs appeared to be positive for CD73, CD90 and CD105 and negative for HLA-DR, CD14, CD19, CD34 and CD45 (Fig. 2A). CD9 was used as a distinguishing marker between Fbs and MSCs. Inside the cellular subsets positive for CD73 and CD105, the expression of CD9 was higher in Fbs than in MSCs (36% *vs* 15% in $CD73^+$ cells; 54% *vs* 25% in $CD90^+$ cells), as shown by dot-plots in Fig. 2B, both from control or pathological subjects.

The expression of Oct4, Sox2, Nanog and KLF4 was tested in control and pathological MSCs and Fbs (Fig. 3). As expected, MSCs showed higher levels of gene transcripts than Fbs. In detail, inside each cellular type, SSc cells exhibited an enhanced expression of the analyzed genes with respect to healthy counterparts.

ROS assay

We previously demonstrated (Svegliati et al., 2005) that Fbs isolated from scleroderma skin lesions release increased amounts of free radicals *in vitro*, at basal level. Moreover we found that SScIgG selectively interact with PDGF receptor and increase ROS production (Baroni et al., 2006). To investigate whether PDGF induces intracellular ROS generation also in MSCs, cells were stimulated with PDGF-BB or SScIgG and intracellular ROS levels were determined using DCF-DA fluorescence-based assay (Fig. 4). No significant changes were found in the levels of intracellular ROS at basal conditions between normal and scleroderma MSCs. Stimulation with PDGF-BB or SScIgG induced an increase in ROS production, more detectable in SSc than in control MSCs. The analysis on Fbs confirmed our previous results, showing an increase in ROS release after PDGF or IgG stimulation in control cells, and a higher stable production of ROS in scleroderma fibroblasts.

Intracellular signaling

The effect of PDGF or IgG on Ras/ERK1/2 pathway was analyzed in MSCs and Fbs isolated from control and pathological donors. Starved cells were stimulated with PDGF-BB, NIgG and SScIgG and total lysates were subjected to western blot analysis. The basal expression of pERK1/2 was significantly higher in pathological than healthy MSC samples. In addition, ERK1/2 pathway in MSCs appeared to be activated by PDGF and SScIgG stimulation, while

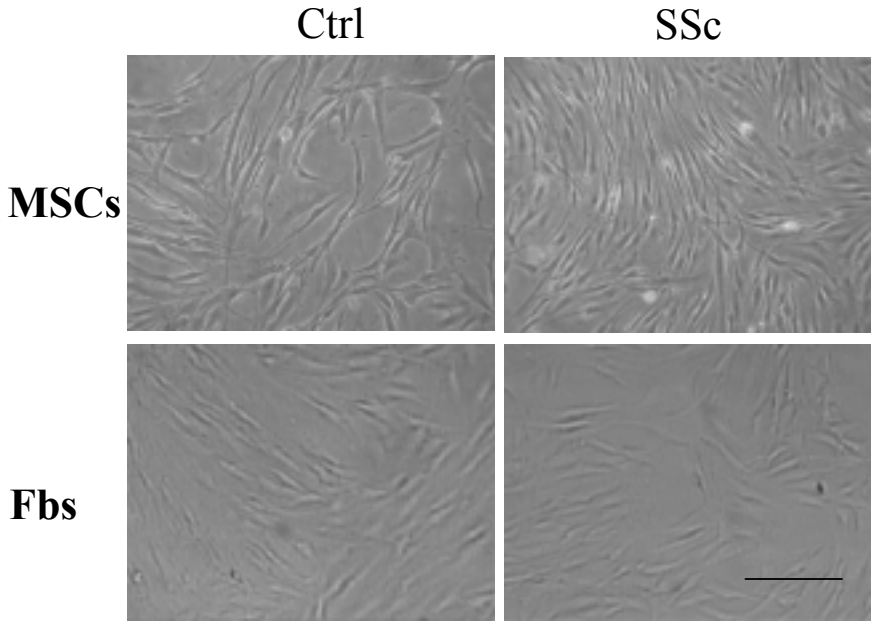

Fig. 1. *Phase contrast microscopy images of control and scleroderma cells. Homogeneous cell monolayer after 14 days of culture of control (Ctrl) and scleroderma (SSc) MSCs (top, left and right respectively) and Fbs (bottom, left and right respectively); bar=100 μm.*

incubation with NIgG produced a slight increment (no detectable in pathological MSCs) (Fig 5). Healthy Fbs displayed the same results evidenced in healthy MSCs, while the expression of pERK1/2 in SSc Fbs did not change after stimulation. It is important to note that the level of pERK 1-2 in SSc Fbs was already high at baseline (Fig. 5).

Collagen production

The gene expression of α1 (I) and α 2 (I) collagen were quantitated by real-time PCR in MSCs and Fbs from healthy and pathological subjects. Scleroderma MSCs showed a down regulation of mRNA collagen expression with respect to control MSCs. On the contrary, the mRNA collagen expression was higher in scleroderma than in healthy Fbs (Fig. 6).

Biochemical analyses

The GST and GR activities were significantly induced in scleroderma MSCs respect to healthy ones; an opposite trend was observed for Fbs in which these antioxidant activities were inhibited in pathological counterparts (Fig. 7A, B). The level of GSH was higher in scleroderma than in healthy MSCs, while its level decreased in scleroderma Fbs compared to control cells (Fig. 7C).

Results on single antioxidant system were confirmed by the level of TOSC towards both peroxyl and hydroxyl radicals. In fact, scleroderma MSCs displayed higher values of TOSC HO• and TOSC •OOR than control MSCs; on the contrary, in pathological Fbs, the TOSC HO• and TOSC •OOR values were lower than those detected in control samples. The variations were significative only for ROO• (Fig. 8A) in both cellular type. Finally, the DNA damage was greatest in pathological Fbs, and gradually decreased in control Fbs, scleroderma MSCs up to healthy MSCs (Fig. 8B); these variations ranged from about 25% to 10% of fragmented DNA, therefore remaining to low level of damage.

DISCUSSION

Scleroderma is a chronic systemic autoimmune disease (primarily of the skin) characterized by fibrosis, vascular alterations and autoantibodies production. In spite of significant effort, the aetiology and the pathogenesis of SSc remain undefined.

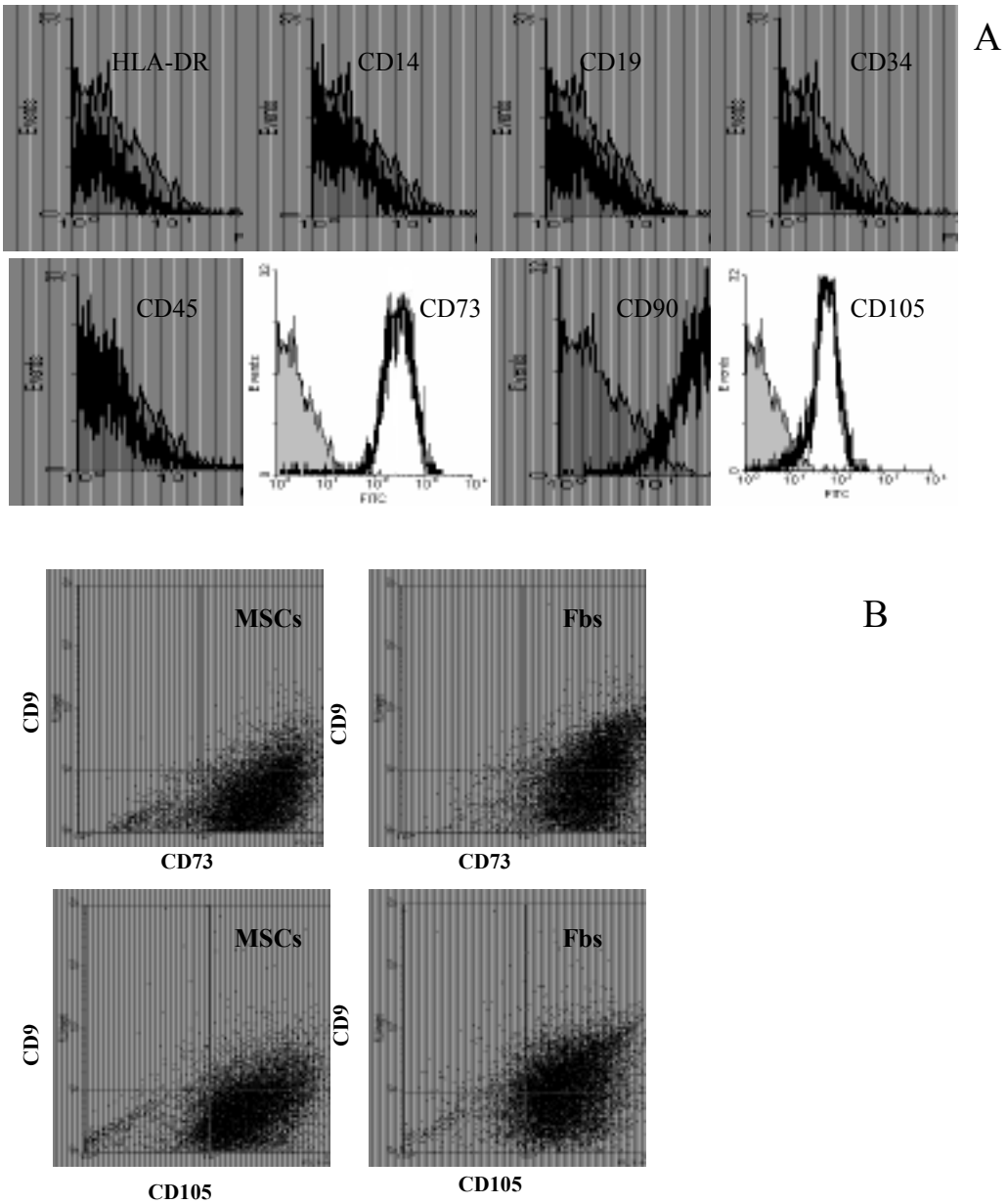

Fig. 2. *Immunophenotypical characterization of Fbs and MSCs.* ***A)*** *Representative FACScan analyses of cell-surface antigen expression, as indicated. Solid grey histograms refer to the negative control (IgG1 isotype control-FITC labeled). The data are representative of control and sclerodermic MSCs and Fbs.* ***B)*** *Dot plots of CD73/CD9 (top) and CD105/CD9 (bottom) expression in MSCs (left) and Fbs (right). Graphs are representative of analyses carried out on healthy and pathological cells, whose expression pattern was equivalent.*

The role of MSCs in scleroderma is still not clear; beside the interest for the immunomodulatory effects of MSCs in autoimmune diseases, it must be clear whether MSCs are yet affected by the pathology.

This study depicts some phenotypic and functional features of MSCs isolated from the skin of healthy and scleroderma patients; these marks were compared to those observed in fibroblasts (Fbs) isolated from the same subjects.

Firstly, we successfully isolated two different

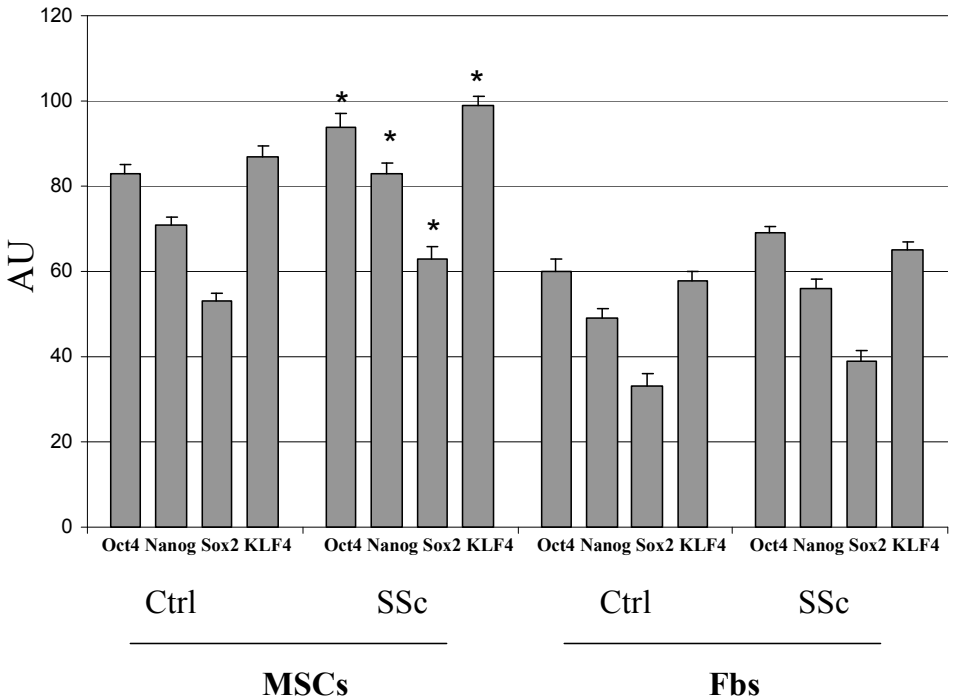

Fig. 3. *Expression of stem genes by Real-Time PCR. Representative densitometric analysis of the mRNA expression levels (quantified as arbitrary units, AU) from different cultures of MSCs and Fbs isolated from control (Ctrl) and scleroderma (SSc) subjects; data are means±standard deviations.*

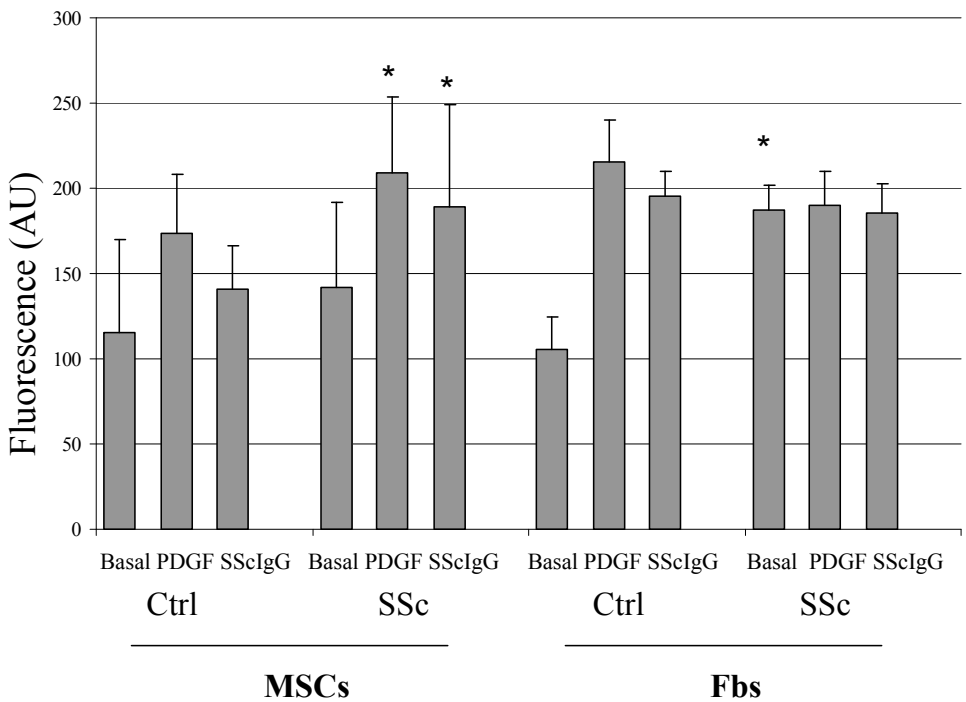

Fig. 4. *ROS detection. ROS production in control (Ctrl) and scleroderma (SSc) cells, at basal level and after incubation with PDGF-BB (20ng/ml) or IgG from three patients with systemic sclerosis (SScIgG, 200 μg/ml for 15 min). The ROS production was measured as arbitrary units (AU) as mean±standard deviations.*

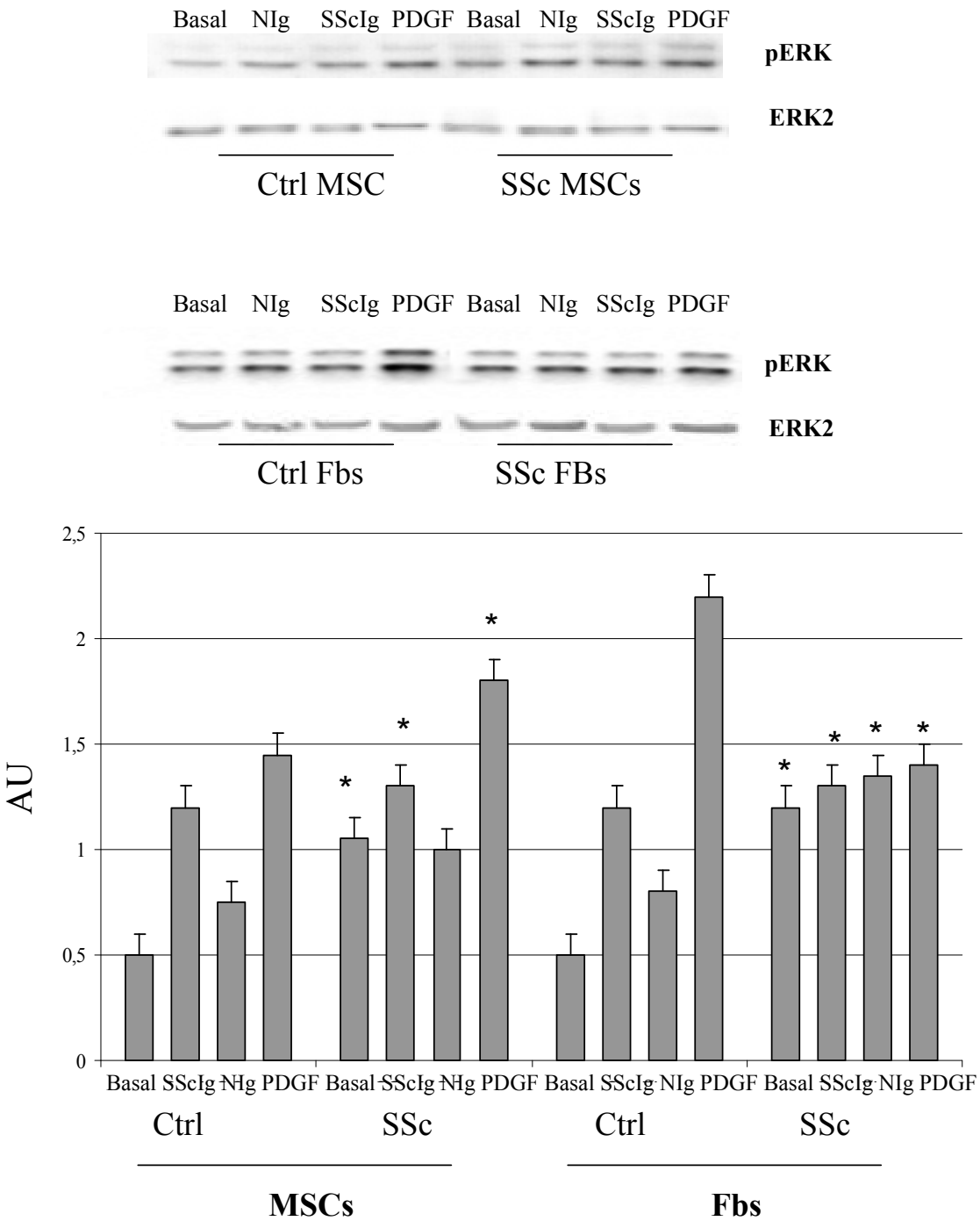

Fig. 5. *Expression of pERK1/2 in control and scleroderma MSCs and Fbs. Immunoblot analysis was performed before and after stimulation with IgG from three patients with systemic sclerosis (SScIgG, 200 µg/ml for 15 min), or with IgG from two normal controls (NIgG, 200 µg/ml for 15 min) or with PDGF-BB (20ng/ml for 15 min). Densitometric analysis of pERK1/2 level is reported in the lower part of the figure; the results of three experiments were normalized using ERK2 and represented in arbitrary unit (AU) as mean±standard deviations.*

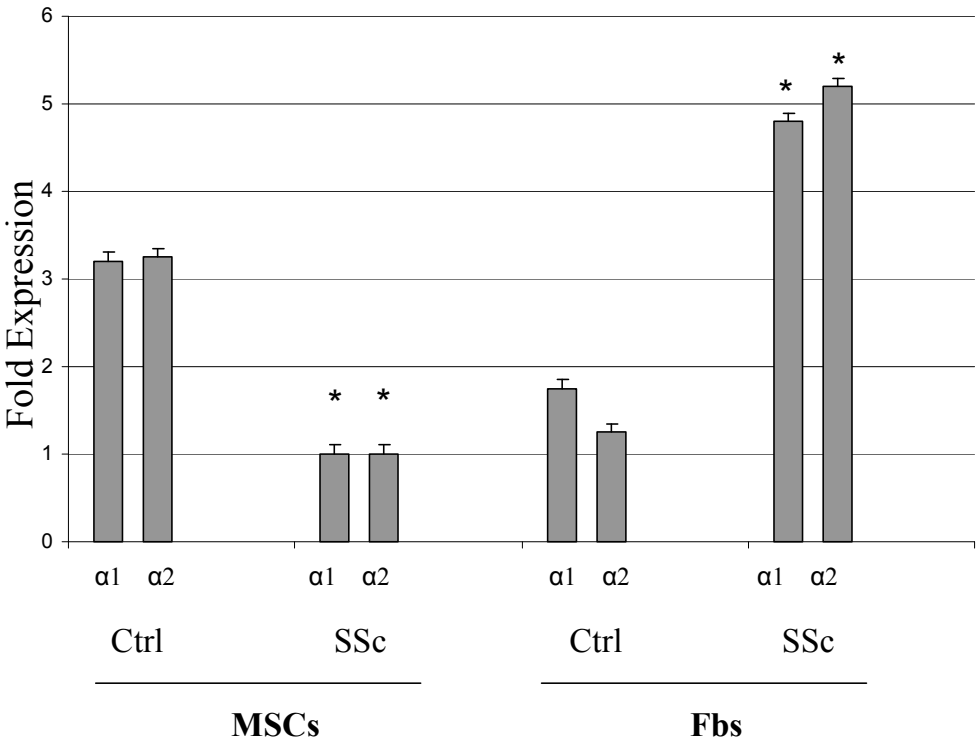

Fig. 6. *Type 1 collagen (α1 and α2) gene expression by Real Time PCR. mRNA expression levels in MSCs and Fbs from control (Ctrl) and scleroderma (SSc) patients was quantified by real-time PCR. The transcripts were normalized to GAPDH. Data are the average of three independent experiments. Values represent the fold-increase in gene expression. α1: type 1 collagen, α1; α2: type 1 collagen, α2.*

cellular populations, as proved by the analysis of the immunophenotype and the expression of genes related with the stemness and self-renewal. The selected genes (Oct4, Nanog, Sox2 and KLF4) were more expressed in MSCs than in Fbs. Interestingly, inside each cellular type, the expression was higher in scleroderma than in control cells. This is in agreement with the observation that scleroderma cells are *in vitro* more proliferative than healthy counterparts. A pivotal role in scleroderma onset is played by oxidative stress associated with the accumulation of great amounts of reactive oxygen species (ROS), which are in turn implicated in different cellular mechanisms: i) are part of a pathway linking the signaling proteins Ha-Ras and the growth-factor–activated extracellular- signal-regulated kinases 1 and 2 (ERK1/2), amplified in fibroblasts from patients with scleroderma; ii) enhance fibroblast proliferation and collagen-expression, mainly observed in scleroderma cells; iii) are stimulated by PDGF. PDGF is another key molecule in scleroderma, since serum from patients with scleroderma contains stimulatory IgG auto-antibodies directed toward the PDGF receptor (PDGFR). These auto-antibodies trigger PDGFR, with consequent induction of ROS and ERK1/2 signaling. The last event of this cascade is the fibroblast activation, which represents a distinctive feature of scleroderma. We not only investigated ROS production in undifferentiated cells of healthy and pathological samples, but we looked for a cause of ROS accumulation, testing variations of antioxidant defenses such as glutathione reductase, glutathione S-transferases, glutathione levels, integrated into the total oxyradical scavenging capacity (TOSC) towards peroxyl and hydroxyl radicals. Combining the results obtained about ROS accumulation and antioxidant defenses about scleroderma cells, we found that MSCs are still able to counteract the over-production of ROS (that characterizes scleroderma) by increasing the activity

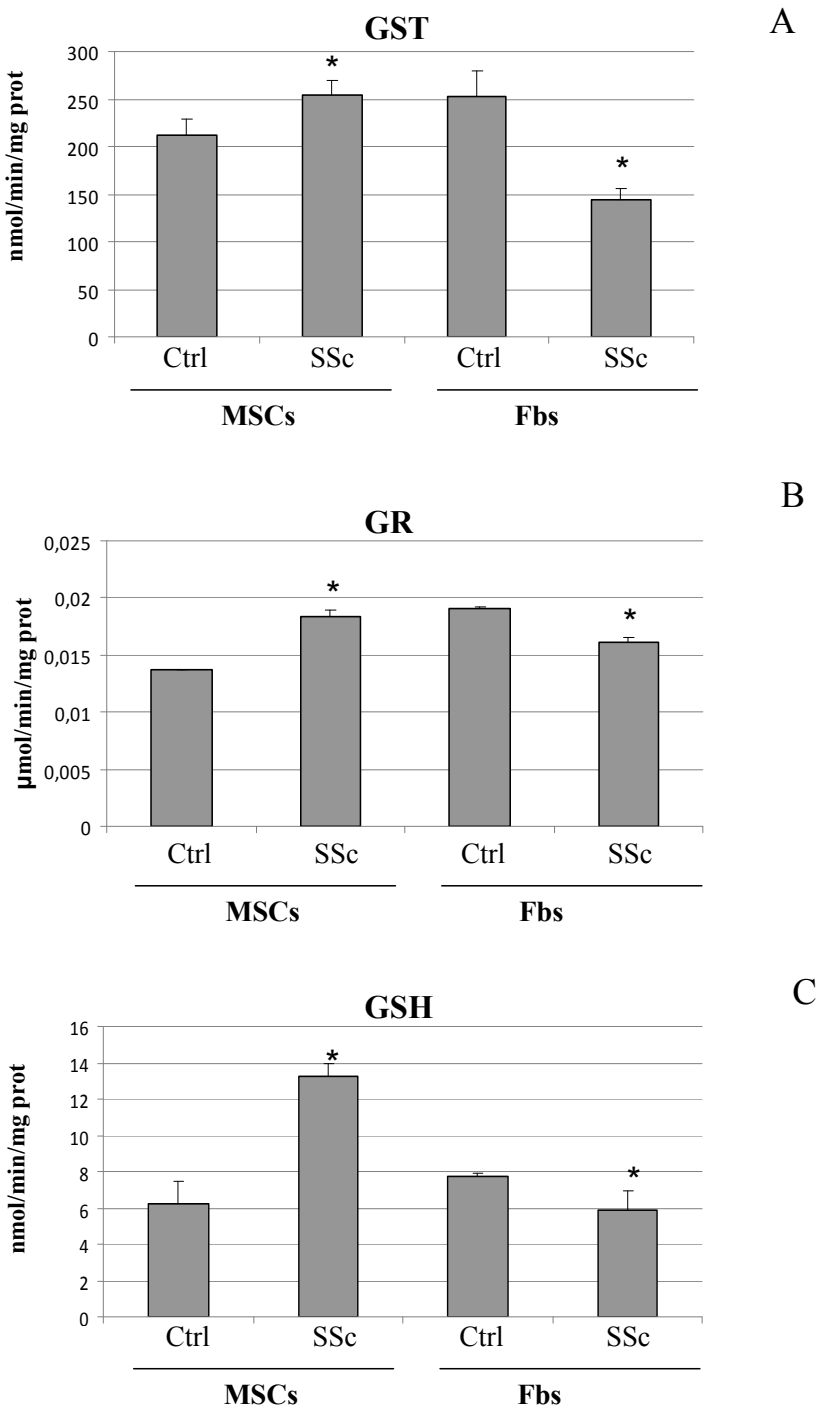

Fig. 7. *GST and GR activities and level of GSH in control and scleroderma MSCs and Fbs.* ***A****) GST: Glutathione S-Transferase;* ***B****) GR: Glutathione Reductase;* ***C****) GSH: levels of glutathione GSH. Data are showed as means ± standard deviations, from three individual experiments.*

of the antioxidant mechanisms-enzymes. The strong chronic pro-oxidant pressure exerted by scleroderma on fibroblasts damage the defense mechanisms, with consequent failure in ROS neutralization. These observations were confirmed by TOSC assay: higher levels of TOSC towards peroxyl and

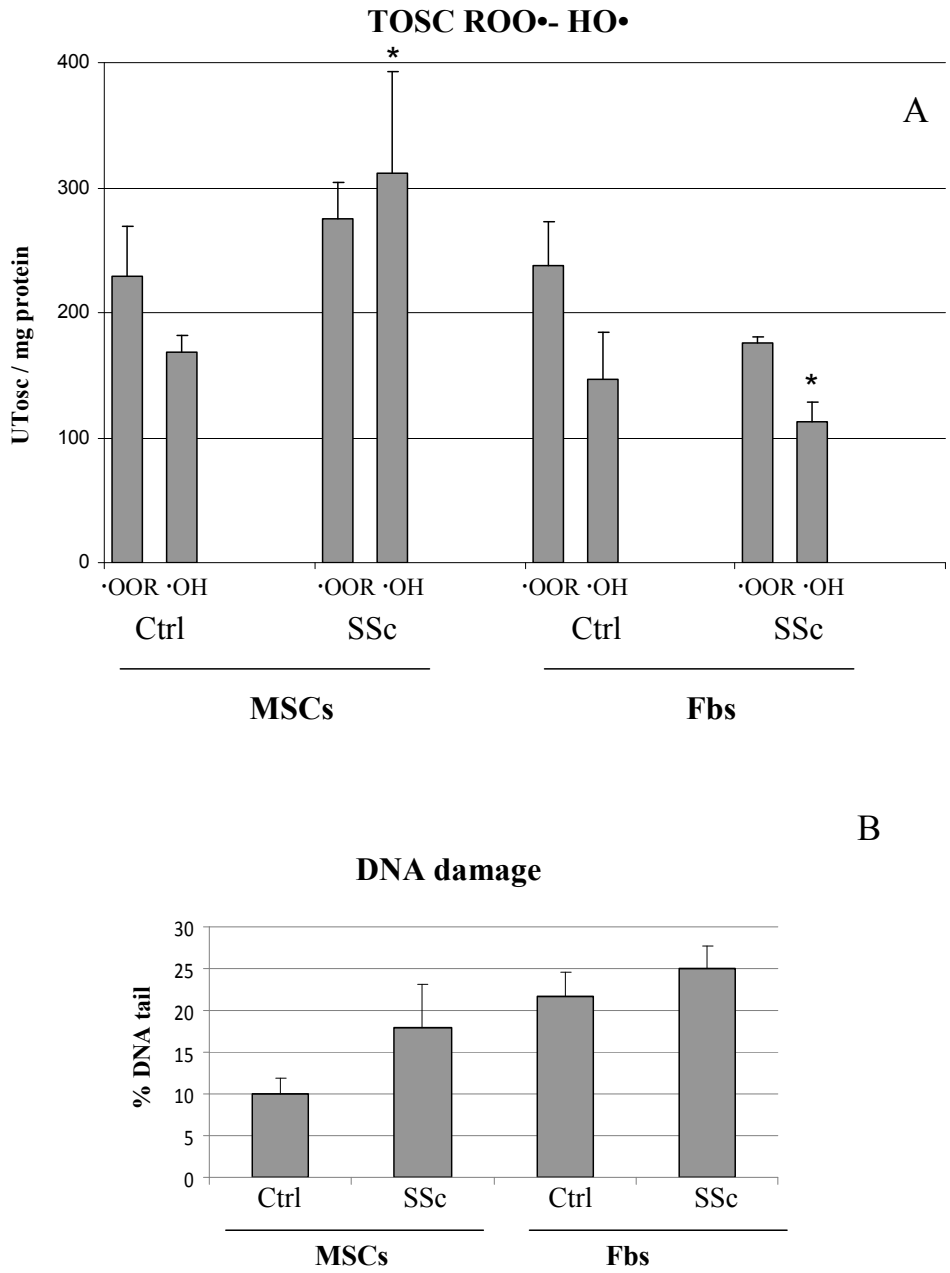

Fig. 8. *Levels of TOSC •OOR and HO•, and DNA damages in healthy and scleroderma MSCs and Fbs. **A**) TOSC •OOR: total oxyradical scavenging capacity toward peroxyl radicals; TOSC •OH: total oxyradical scavenging capacity toward hydroxyl radicals. Data are means±standard deviations, from three individual experiments. **B**) For DNA fragmentation assay, data are refers to percentages of DNA in the tail, as means±standard deviations, from three individual experiments.*

hydroxyl radicals were found in scleroderma MSC cells than in fibroblasts, confirming the ability of undifferentiated cells to improve the antioxidant mechanisms to counteract ROS production; on the other hand, fibroblasts showed less responsive mechanisms, damaged by the excessive pro-oxidant pressure. In normal condition, the levels of the antioxidant mechanisms-enzymes were lower than Fbs, confirming existing results (18). ROS overproduction is strictly linked to DNA damage;

our results reveal that the lower percentage of DNA fragmentation was found in control MSCs, whereas control fibroblasts showed a double percentage of DNA fragmentation. The increased percentage of DNA fragmentation observed in scleroderma cells (mostly in Fbs) is in agreement with the notion that the excess of ROS and the maintenance of active Ras-ERK1/2 pathways resulted in an enlarged DNA damage (29) and in stimulation of collagen-gene expression in scleroderma fibroblasts. According to this, we found a lower expression of collagen in scleroderma than in healthy MSCs; the circuit PDGFR-ROS-ERK1/2, resulting in collagen expression, is interrupted by the high activity of the antioxidant mechanisms of pathological MSCs, which avoids ROS accumulation. The minor responsiveness of healthy MSCs to oxidant pressure, together with a spontaneous expression of collagen gene found in mesemchymal stem cells (30), may explain the presence of collagen transcripts in these cells.

In conclusion, we found that the pro-oxidant environment exerted by scleroderma affects also MSCs, which counteracts the ROS accumulation by improving the antioxidant defenses; the elevated and chronic oxidant pressure experienced by scleroderma fibroblasts (which are not surrounding by a protective niche) leads to a disruption of these mechanisms which are not further able to neutralize ROS increase, with consequent activation of the cascade triggered by scleroderma auto-antibodies against PDGFR.

ACKNOWLEDGEMENTS

This work was supported by grant FIRB-RBAP10MLK7_003 from Ministero dell'Istruzione, dell'Università e della Ricerca, Rome, Italy

REFERENCES

1. Varga J, Abraham D. Systemic sclerosis: a prototypic multisystem fibrotic disorder. J Clin Invest 2007; 117:557-67.
2. Chen Y, Leask A, Abraham DJ, et al. Thrombospondin 1 is a key mediator of transforming growth factor β-mediated cell contractility in systemic sclerosis via a mitogen-activated protein kinase kinase (MEK)/extracellular signal-regulated kinase (ERK)-dependent mechanism. Fibrogenesis Tissue Repair 2011; 4:9.
3. Denton CP, Black CM, Abraham DJ. Mechanisms and consequences of fibrosis in systemic sclerosis. Nat Clin Pract Rheumatol 2006; 2:134-44.
4. Jimenez SA, Hitraya E, Varga J. Pathogenesis of scleroderma. Collagen. Rheum Dis Clin North Am 1996; 22:647-74.
5. Guiducci S, Manetti M, Romano E, et al. Bone marrow-derived mesenchymal stem cells from early diffuse systemic sclerosis exhibit a paracrine machinery and stimulate angiogenesis in vitro. Ann Rheum Dis 2011; 70:2011-21.
6. Cipriani P, Guiducci S, Miniati I, et al. Impairment of endothelial cell differentiation from bone marrow-derived mesenchymal stem cells: new insight into the pathogenesis of systemic sclerosis. Arthritis Rheum 2007; 56:1994-2004.
7. Del Papa N, Quirici N, Soligo D, et al. Bone marrow endothelial progenitors are defective in systemic sclerosis. Arthritis Rheum 2006; 54:2605-15.
8. Baroni SS, Santillo M, Bevilacqua F, et al. Stimulatory autoantibodies to the PDGF receptor in systemic sclerosis. N Engl J Med 2006; 354:2667-76.
9. Tikly M, Channa K, Theodorou P, Gulumian M. Lipid peroxidation and trace elements in systemic sclerosis. Clin Rheumatol 2006; 25:320-4.
10. Gabrielli A, Svegliati S, Moroncini G, Pomponio G, Santillo M, Avvedimento EV. Oxidative stress and the pathogenesis of scleroderma: the Murrell's hypothesis revisited. Semin Immunopathol 2008; 30:329-37.
11. Ogawa F, Shimizu K, Muroi E, Hara T, Sato S. Increasing levels of serum antioxidant status, total antioxidant power, in systemic sclerosis. Clin Rheumatol 2011; 30:921-5.
12. Salvolini E, Orciani M, Lucarini G, Vignini A, Tranquilli AL, Di Primio R. VEGF and nitric oxide synthase immunoexpression in Down's syndrome amniotic fluid stem cells. Eur J Clin Invest 2011; 41:23-9.
13. Gigante A, Manzotti S, Bevilacqua C, Orciani M, Di Primio R, Mattioli-Belmonte M. Adult mesenchymal stem cells for bone and cartilage engineering: effect of scaffold materials. Eur J Histoche 2008; 52:169-74.

14. Orciani M, Trubiani O, Vignini A, Mattioli-Belmonte M, Di Primio R, Salvolini E. Nitric oxide production during the osteogenic differentiation of human periodontal ligament mesenchymal stem cells. Acta Histochem 2009; 111:15-24.
15. Orciani M, Morabito C, Emanuelli M, et al. Neurogenic potential of mesenchymal-like stem cells from human amniotic fluid: the influence of extracellular growth factors. J Biol Regul Homeost Agents 2011; 25:115-30.
16. Orciani M, Campanati A, Salvolini E, et al. The mesenchymal stem cell profile in psoriasis. Br J Dermato 2011; 165:585-92.
17. Salvolini E, Lucarini G, Zizzi A, Orciani M, Di Benedetto G, Di Primio R. Human skin-derived mesenchymal stem cells as a source of VEGF and nitric oxide. Arch Dermatol Res 2010; 302:367-74.
18. Orciani M, Gorbi S, Benedetti M, et al. Oxidative stress defense in human-skin-derived mesenchymal stem cells versus human keratinocytes: Different mechanisms of protection and cell selection. Free Radic Biol Med 2010; 49:830-38.
19. Orciani M, Mariggiò MA, Morabito C, Di Benedetto G, Di Primio R. Functional characterization of calcium-signaling pathways of human skin-derived mesenchymal stem cells. Skin Pharmacol Physiol 2010; 23:124-32.
20. Sambo P, Jannino L, Candela M, et al. Monocytes of patients with systemic sclerosis (scleroderma) spontaneously release in vitro increased amounts of superoxide anion. A. J Invest Dermatol 1999; 112:78-84.
21. Dominici M, Le Blanc K, Mueller I, et al. Minimal criteria for defining multipotent mesenchymal stromal cells. The International Society for Cellular Therapy position statement. Cytotherapy 2006; 8:315-7.
22. Halfon S, Abramov N, Grinblat B, Ginis I. Markers distinguishing mesenchymal stem cells from fibroblasts are downregulated with passaging. Stem Cells Dev 2011; 20:53-66.
23. Cuda G, Paternò R, Ceravolo R, et al. Protection of human endothelial cells from oxidative stress: role of Ras-ERK1/2 signaling. Circulation 2002; 105:968-74.
24. Armeni T, Battino M, Stronati A, et al. Total antioxidant capacity and nuclear DNA damage in keratinocytes after exposure to H_2O_2. Biol Chem 2001; 382:1697-705.
25. Gorbi S, Regoli F. Total oxyradical scavenging capacity as an index of susceptibility to oxidative stress in marine organisms. Comments Toxicol 2003; 9:303-22.
26. Regoli F, Winston GW, Mastrangelo V, Principato G, Bompadre S. Total oxyradical scavenging capacity (TOSC) in mussel Mytilus sp. as a new index of biological resistance to oxidative stress. Chemosphere 1998; 37:2773-83.
27. Regoli F, Winston GW. Quantification of total oxidant scavenging capacity TOSC of antioxidants for peroxinitrite, peroxyl radicals and hydroxyl radicals. Toxicol Appl Pharmacol 1999; 56:96-105.
28. Lowry OH, Rosenbrough NJ, Farr A, Randall RJ. Protein measurement with the Folin Phenol reagent. J Biol Chem 1951; 193:266-75.
29. Svegliati S, Cancello R, Sambo P, et al. Platelet-derived growth factor and reactive oxygen species (ROS) regulate Ras protein levels in primary human fibroblasts via ERK1/2. Amplification of ROS and Ras in systemic sclerosis fibroblasts. J Biol Chem 2005; 280:36474-82.
30. Li Z, Liu C, Xie Z, et al. Epigenetic dysregulation in mesenchymal stem cell aging and spontaneous differentiation. PLoS One 2011; 6:e20526 PMID:21694780.

JOURNAL OF BIOLOGICAL REGULATORS & HOMEOSTATIC AGENTS Vol. 27, no. 1, 225-231 (2013)

LETTER TO THE EDITOR

INSULIN RESISTANCE IN FIRST-TRIMESTER PREGNANT WOMEN WITH PRE-PREGNANT GLUCOSE TOLERANCE AND HISTORY OF RECURRENT SPONTANEOUS ABORTION

Y. HONG[1], Q.X. XIE[2], C.Y. CHEN[2], C. YANG[2], Y.Z. LI[1], D.M. CHEN[1] and M.Q. XIE[1]

[1]Department of Obstetrics and Gynecology, The Second Affiliated Hospital of Sun Yat-sen University, Guangzhou, China; [2]Department of Gynecology, The Central Hospital, Chao-zhou, China

Received August 22, 2012 – Accepted November 26, 2012

The first two authors contributed equally to the manuscript

Insulin resistance (IR) has been reported to play an important role in recurrent spontaneous abortion (RSA) among patients with polycystic ovary syndrome (PCOS). However, scanted materials exist regarding the independent effect of IR on RSA. The aim of this study is to investigate the status of IR in first trimester pregnant patients with normal pre-pregnant glucose tolerance and history of RSA. This two-center case-control study enrolled totally 626 first trimester pregnant women including 161 patients with a history of recurrent spontaneous abortion, who were pre-pregnantly glucose-tolerant according to oral glucose tolerance test (OGTT), and 465 women with no history of abnormal pregnancies of any kind. Clinical, biochemical and hormonal parameters were simultaneously measured in all participants. Serum β-HCG, estradiol, progesterone, fasting plasma glucose and fasting plasma insulin levels, as well, the calculated homeostasis model assessment of insulin resistance index (HOMA-IR), fasting plasma glucose/insulin ratio(G/I) and pregnancy outcome were analyzed and compared. Serum β-HCG and progesterone were found to be significantly lower in RSA group compared to controls. Subjects in RSA group were found to have higher HOMA-IR and lower G/I ratio than those in control group. Serum β-HCG and progesterone were negatively correlated with HOMA-IR, and positively with G/I ratio even after adjustment for BMI. The spontaneous abortion rate within first trimester pregnancy of RSA patients was significantly higher than that in controls. In conclusion, woman with recurrent spontaneous abortion and normal pre-pregnant glucose metabolism tends to be more insulin resistant during first trimester pregnancy than healthy controls, no matter whether she has PCOS or not. Insulin resistance might be one of the direct causes that lead to recurrent abortion.

Recurrent spontaneous abortion (RSA) is defined as the loss of two or more consecutive pregnancies before viability or at a fetal weight of 500g or less, representing a significant pregnancy complication affecting around 0.5-5% couples trying to conceive and found to increase recently (1). The pathophysiology of RSA is complicated and poorly understood. A number of associated factors have been

Key words: recurrent spontaneous abortion, first trimester pregnancy, insulin resistance, metabolism, glucose intolerance

Mailing address: Dr. Meiqing Xie, M.D.,
Department of Obstetrics and Gynecology,
The Second Affiliated Hospital of Sun Yat-sen University,
Yanjiangxi Road #107, Guangzhou 510000, China
Tel.: +86 20 81332011
Fax: +86 20 81332011
e-mail: mqxiegz@hotmail.com

0393-974X (2013)

DISCLOSURE: ALL AUTHORS REPORT NO CONFLICTS OF INTEREST RELEVANT TO THIS ARTICLE.

identified to explain this heterogeneous disorder, including the areas of genetics (chromosome anomaly), anatomy (congenital or acquired uterine malformation, incompetent cervix), endocrinology (insufficient luteal function, hyperprolactinemia, thyroid dysfunction, polycystic ovary syndrome (PCOS)), infections (mycoplasma, ureaplasma, or chlamydia), immune defects (blocking antibody deficiency, anti-phospholipid syndrome), and psychological or idiopathetic causes as well.

Obesity has been identified as a risk factor of many pregnancy complications. A recent meta-analysis concluded that both overweight and obese patients (BMI $\geq$25kg/m^2) had a significantly higher risk of early pregnancy loss, regardless of the method of conception (2). In addition, a remarkable association between the presence of maternal obesity and RSA during first trimester was reported by Lashen (3). On the other hand, diabetes mellitus (DM) or abnormal glucose tolerance (AGT) were demonstrated to be possibly implicated as a cause for recurrent abortion (4). As we known, a common trait, namely Insulin resistance (IR), exists in various metabolic disorders including the illness mentioned above, plays an important role in the pathogenesis, and even acts as an independent etiologic factor. Actually, the endocrine evaluation of RSA has routinely involved plasma screening for TSH, PRL, mid-luteal progesterone. However, Insulin resistance (IR), as a possible etiology, has been underestimated in previous clinical and experimental research. And conclusions concerning IR associated RSA have mostly been drawn from studies that were performed in PCOS population or women in non-pregnant state. With IR as a prominent feature, prevailing in 30-75% sufferers (5), PCOS has been reported to be in relation to early RSA with an incidence of 21-56%. Meanwhile, 36-82% recurrent miscarriages are eventually diagnosed as PCOS on evaluation (6). In addition, administration of insulin sensitizer metformin, throughout the pregnancy or discontinued immediately after the confirmation of pregnancy, to women with PCOS was associated with a marked and significant reduction in the rate of early pregnancy loss (7). These findings reveal the correlation of IR and RSA in PCOS, whereas, after all, IR does not exist solely in PCOS. Thus it seems logical to hypothesize that insulin resistant patients without PCOS would be as well faced with the distressing issue of having increased risk for miscarriage during the first trimester. The current study was performed to investigate the status of insulin resistance in first trimester pregnant patients with RSA history compared to those without RSA history and its relationship with pregnancy-associated parameters and pregnancy outcome.

MATERIALS AND METHODS

Subjects

This was a retrospective case-control study, undertaken between January 2010 and August 2011 in Department of Obstetrics and Gynecology, The Second Affiliated Hospital of Sun Yat-sen University, Guangzhou, Guangdong, China and Department of Gynecology, Central Hospital of Chaozhou, Guangdong, China. 626 pregnant women attending our clinic for the first time in their first trimester pregnancy were selected as the study population. According to the guidelines from the American Society for Reproductive Medicine (ARSM), those who had $\geq$2 consecutive spontaneous miscarriages were classified as patients with RSA. 465 parous and currently pregnant women, on routine check-up, without history of abnormal pregnancies of any kind were selected as the controls. Informed consent was obtained from all subjects and the study was approved by the institutional review board of the hospital.

Before current pregnancy, the study patients have previously screened for chromosome anomaly (parental karyotype studies), uterine anomaly including cervical incompetence, antiphospholipid syndrome, PCOS (diagnosed according to the Rotterdam criteria (8)), infections including bacterial vaginosis, and endocrinological disorders (including hypothyroidism, diabetes mellitus, glucose intolerance, hyperprolactinaemia, hypothalamic/pituitary disorders). Those with positive findings have received relevant treatment if possible. Patients within 3 months of the study took medication that could have affected glucose metabolism were excluded from the study. All the study patients had normal pre-pregnant glucose metabolism diagnosed by oral glucose tolerance test (OGTT), and all controls had no diabetes mellitus by self-report or previous OGTT.

Once they were included in the study, all subjects were recorded about their immediate gestational ages and underwent anthropometric measurements, i.e. weight, height, and waist to hip circumference ratio (WHR). The BMI was calculated as body weight in kilograms divided by height in meters squared (kg/m2). Waist circumference

was obtained as the smallest circumference at the level of the umbilicus. Hip circumference was obtained as the widest circumference at the level of the buttocks.

Laboratory analysis

Blood was withdrawn from both the study patients and controls on their first visit specifically for the determination of the fasting blood glucose and fasting insulin levels. After a 12 h overnight fast, the blood was extracted between 8.00 and 10.00 a.m. on the day of the test. The fasting glucose was determined soon after the collection of the blood samples. The blood samples for fasting insulin were spun down immediately after collection and frozen at -80°C and analysis performed later. Plasma glucose was measured by the glucose oxidase method (Hitachi 7600) and plasma insulin was measured using a chemiluminescence immunometric assay and commercial kit (Immulite 2000 Analyzer; CPC). The fasting glucose to fasting insulin ratio (G/I ratio) was calculated for each subject. This ratio was equal to the insulin resistance for each subject. The HOMA for insulin resistance was also calculated as follows: FIN*FPG/22.5, where FIN = fasting insulin level (mU/l) and FPG = fasting glucose in SI units (mmol/l).

Hormones in serum were measured using commercially available kits. Estradiol was measured by a competitive immunoenzymatic assay (Immuno 1, Bayer, Tarrytown, NY, USA). The sensitivity of the assay was 10 pg/mL and the interassay coefficients of variation 5%. Progesterone was determined by a competitive chemiluminiscent immunoassay (Immulite, DPC, Los Angeles, CA, USA). The sensitivity of the method was 0.2 ng/mL and the interassay co-efficient of variation was 6.7%. Total ß-HCG was measured by a solid-phase, two site chemiluminiscent enzyme immunometric assay standardized against the Third International Standard 75/537 (Immulite, Diagnostic Products Co., Los Angeles, CA, USA), with a detection limit of 2 IU/l. The interassay coefficient of variation was 5.8%. Ultrasonic scans were performed using a 5 mHz vaginal transducer attached to an Aloka sector scanner (Model SSD-620; Aloka Co. LTD, Tokyo, Japan).

Statistical analysis

SPSS version 13.0 was used for statistical analysis. Student's t test was used if the variables between the groups complied with normal distributions and regular variances. If the variance was irregular, a corrected Student's t test was used. Variable descriptions are presented as mean±SD. Pearson correlation analyses were performed to determine correlations between parameters. The χ^2 test was used to determine the difference of pregnancy outcome between groups. A statistical significance level of $p<0.05$ was selected.

RESULTS

No significant differences between the RSA

Table I. *The demographic characteristics and pregnancy associated parameters of the population studied.*

	RSA group (n=161)	Control group (n=465)	*P* value
Age (years)	27.1±2.9	26.8±3.0	NS
BMI (kg/m^2)	21.8±2.0	21.4±2.1	NS
Family history of DM	10 (6.2%)	14 (3.0%)	NS
Gestational age (days)	60.4±12.7	62.9±13.1	NS
β-HCG, (IU/ml)	86141±10237	103321±14635	<0.05
E_2 (pg/ml)	1028±114	984±109	NS
P (ng/ml)	28.5±3.1	36.2±3.3	<0.01

Student's t-test and χ^2 test were used ; NS: not statistically significant, P>0.05

Table II. *Comparison of IR-associated parameters between RSA group and control group.*

	RSA group		Control group	
	PCOS（n=26）	non-PCOS（n=135）	PCOS（n=45）	non-PCOS（n=420）
FPG	5.12±0.43[a]	4.97±0.39[b]	4.79±0.41	4.69±0.40
（mmol/L）	10.01±5.17[a]	9.26±4.82[b]	8.14±4.52	7.57±4.35
FIN	2.24±1.02[a]	2.05±0.89[b]	1.87±0.98	1.59±0.93
（mU/ml）	0.50±0.08[a]	0.54±0.09[b]	0.58±0.09	0.62±0.10
HOMA-IR				
G/I				

Student's t-test was used ; a: compared with PCOS controls, P<0.05; b: compared with non-PCOS controls, P<0.05. FPG: fast plasma glucose; FIN: fast insulin; HOMA-IR: homeostasis model assessment of insulin resistance; G/I: glucose to insulin ratio.

Table III. *The Pearson Correlation Coefficient between IR-associated parameters and pregnancy-associated hormones after adjustments for BMI in the RSA group.*

	β-HCG		E_2		P	
	r	*P*	*r*	*P*	*r*	*P*
FPG	-0.153	0.072	-0.100	0.237	-0.141	0.116
FIN	-0.168	0.063	-0.088	0.331	-0.159	0.068
HOMA-IR	-0.205	**0.037**	0.095	0.284	-0.191	**0.047**
G/I	0.196	**0.042**	0.091	0.255	0.205	**0.037**

and control groups were found in terms of age, BMI, family history of DM, pregnancy weeks and serum estradiol level. However, serum β-HCG and progesterone levels of RSA group were found to be lower than those of the control group, and the differences were statistically significant (Table I).

Compared with controls, RSA patients with PCOS during first trimester pregnancy had higher fasting plasma glucose, fasting plasma insulin, HOMA-IR and lower G/I ratio (P<0.05). In addition, a similar tendency was shown in RSA patients without PCOS. (detailed in Table II) These findings demonstrated that IR status was worse in first trimester pregnant patients with RSA history than in controls.

Table IV. *The pregnancy outcome in two groups at the end of first trimester.*

	N	Spontaneous abortion	
		n	%
RSA group	161	30	18.6
Control group	465	31	6.7
P value		<0.01	

χ^2 test was used.

When analyzed in the RSA group, both β-HCG and P were found to be positively correlated with G/I ratio, and negatively correlated with HOMA-IR. Even after the adjustment for BMI, the significant correlations remained (Table III).

We observed the pregnancy outcome at the end of first trimester of each subject. The spontaneous abortion rate in RSA group was significantly higher than that in control group (18.6% *vs* 6.7%, χ^2 =19.473, *P*<0.01) (Table IV).

DISCUSSION

Insulin resistance as a common feature of various abnormal metabolism disorders has been extensively studied (9, 10). Noticing the high prevalence of pregnancy loss in patients with DM, IGT, obesity or PCOS, only recently, researchers have focused on systemic and local effects of IR and its secondary effects over recurrent spontaneous abortion (RSA). Most previous studies in this field were performed in PCOS population and almost all except few concluded that women with RSA have a significantly increased prevalence of IR when compared with matched fertile controls, and IR plays a role in the etiology of RSA (6). However, what warrants pointing out is that the subjects in these reports are all non-pregnant women. Within the context of physiological IR during pregnancy, whether pre-pregnancy IR would still exist and influence the maintenance of normal pregnancy or involve in the pathogenesis of early pregnancy loss remains to be elucidated. To our knowledge, our study was the first to investigate the correlation of IR with pregnancy associated hormones and pregnancy outcome specifically during first trimester.

Recent advances in genetics, immunology, and reproductive physiology accompanied with major improvements in pregnancy imaging, bioassay techniques, and new surgical and pharmaceutical treatments have all contributed to the great strides that have been made in characterizing the incidence and diversity of this heterogeneous disorder. However, a large proportion of RSA remains unexplained. In the literature, many endocrinological factors have been proposed to account for about 20-25% of this disorder. Very little attention has been paid on the doubt whether IR could be a causative factor in such problem. In general clinical procedure, only fasting plasma glucose is performed in women with RSA history. At most, OGTT is recommended for those who have high risks for DM, such as family history of DM and previous PCOS diagnosis. Nevertheless, it is noticeable that the reported rate of early pregnancy loss in general population was 10-15% (6, 11), while the rate in the population possessing high risks for IR was found to increase to various extents (2-4). Furthermore, metformin administration, an insulin

sensitizer, to pregnant women with PCOS throughout pregnancy or discontinuation immediately after the confirmation of pregnancy was associated with a marked and significant reduction in the incidence of early pregnancy loss (12-13); IR was demonstrated to be a risk factor independent of PCOS and obesity (14). These findings suggest the important role of IR in miscarriage.

Data relevant to the relationship between RSA and IR is quite limited. In a retrospective study, Craig et al. (15) selected 74 non-pregnant women with a history of RSA and determined their fast plasma glucose (FPG) and fast insulin (FIN) levels, showing an increased incidence of IR in that population compared with normal parous controls (27% *vs* 9.5%). Diejomaoh et al. (16) and most recently Celik et al. (17) performed further studies similar to Craig's, but did not suggest the association. On the other hand, some investigators believed that diabetes mellitus or abnormal glucose tolerance could be implicated as a cause for recurrent abortion (18), whereas others claimed that there was actually very little evidence to support the association between diabetes and abortion (19-20). All these studies involved subjects who were not currently in gestation. In a latest study involving first trimester pregnant women with and without RSA history, Wang et al. (21) concluded that women with a history of recurrent miscarriage are at an increased risk for insulin resistance during the first trimester of a new pregnancy. The current study adopted the most common-used parameters, namely HOMA-IR and G/I ratio, to evaluate the IR status of first trimester pregnant women. We found that, when compared with parous controls, RSA patients with PCOS during first trimester pregnancy were more insulin resistant according to the IR associated parameters including fasting plasma glucose, fasting plasma insulin, HOMA-IR and G/I ratio. In addition, the similar tendency was shown in RSA patients without PCOS. These findings suggested that woman with recurrent spontaneous abortion tends to be more insulin resistant in a new pregnancy than healthy controls, no matter whether she has PCOS or not.

In addition, the present study demonstrated that HOMA-IR was positively correlated with serum β-HCG and P levels, and the relationship remained statistically strong even after the adjustment for BMI. Progesterone has been negatively associated with glycemic control for over 50 years mostly due to its directly deleterious effects on peripheral insulin sensitivity during pregnancy (15). As we known, the elevation of progesterone level is simultaneously accompanied with the deterioration of physiological IR in the process of gestation. β-cells of pancreas islets in most pregnant women would undergo structural and functional accommodation to adapt to the increased insulin demand of maternal body so as to avoid glucose intolerance. We hypothesized that there might be some balance between progesterone and IR, which compensates the worsening of IR on the one hand, and provides enough progesterone to support the chorion trophoblast and maintain the pregnancy on the other hand. A worse degree than physiological IR might lead to the impairment of trophoblasts and gestational corpus luteum through some mechanism, followed by underdevelopment of embryo or even miscarriage.

In summary, woman with recurrent spontaneous abortion, no matter whether she has PCOS or not, tends to be more insulin resistant during first trimester pregnancy than healthy controls. Insulin resistance might be one of the reasons that lead to recurrent abortion. It is recommended to screen both fasting plasma glucose and insulin in all RSA patients in order to evaluate their insulin resistance status and better the clinical treatment on them. Meanwhile, it is important to point out the inevitable limitations of our study, including the absence of data regarding pre-pregnant IR among controls, as well the retrospective and cross-sectional design. Findings of us and other researchers demonstrate the need for more further studies to confirm and elucidate the correlation between IR and RSA.

ACKNOWLEDGEMENTS

This study was supported by the funds from The Science Technology Research Project of Guangdong Province (Grant 2007B020700003 and Grant 2009B060300019).

REFERENCES

1. Stephenson M, Kutteh W. Evaluation and management of recurrent early pregnancy loss. Clin

Obstet Gynecol 2007; 50:132-45.
2. Metwally M, Ong KJ, Ledger WL, Li TC. Does high body mass index increase the risk of miscarriage after spontaneous and assisted conception? A meta-analysis of the evidence. Fertil Steril 2008; 90:714-26.
3. Lashen H, Fear K, Sturdee DW. Obesity is associated with increased risk of first trimester and recurrent miscarriage: matched case-control study. Hum Reprod 2004; 19:1644-6.
4. Zolghadri J, Tavana Z, Kazerooni T, Soveid M, Taghieh M. Relationship between abnormal glucose tolerance test and history of previous recurrent miscarriages, and beneficial effect of metformin in these patients: a prospective clinical study. Fertil Steril 2008; 90:727-30.
5. ZheYi Cao. Chinese Obstetrics and Gynecology, ed 2. Beijing, People's Medical Publishing House 2004: p2453.
6. Ben-Haroush A, Yogev Y, Fisch B. Insulin resistance and metformin in polycystic ovary syndrome. Eur J Obstet Gynecol Reprod Biol 2004; 115:125-33.
7. Nawaz FH, Rizvi J. Continuation of metformin reduces early pregnancy loss in obese Pakistani women with polycystic ovarian syndrome. Gynecol Obstet Invest 2010; 69:184-9.
8. Rotterdam ESHRE/ASRM-Sponsored PCOS Consensus Workshop Group. Revised 2003 consensus on diagnostic criteria andlong-term health risks related to polycystic ovary syndrome. Fertil and Steril 2004; 81:19-25.
9. El-Mazny A, Abou-Salem N, El-Sherbiny W, El-Mazny A. Insulin resistance, dyslipidemia, and metabolic syndrome in women with polycystic ovary syndrome. Int J Gynaecol Obstet 2010; 109:239-41.
10. Hong Y, Yang D, Liu W, Zhao X, Chen X, Li L. Dyslipidemia in relation to body mass index and insulin resistance in Chinese women with polycystic ovary syndrome. J Biol Regul Homeost Agents 2011; 25:365-74.
11. Balen AH, Dresner M, Scott EM, Drife JO. Should obese women with PCOS receive treatment for infertility? BMJ 2006; 332:434-5.
12. Palomba S, Orio F, Nardo LG, Falbo A, Russo T, Corea D, et al. Metformin administration versus laparoscopic ovarian diathermy in clomiphene citrate-resistant women with polycystic ovary syndrome: A prospective parallel randomized double-blind placebo-controlled trial. J Clin Endocrinol Metab 2004; 89:4801-9.
13. Palomba S, Orio F, Falbo A, et al. Prospective parallel randomized, double-blind, double-dummy controlled clinical trial comparing clomiphene citrate and metformin as first-line treatment for ovulation induction in nonobese anovulatory women with polycystic ovary syndrome. J Clin Endocrinol Metab 2005; 90:4068-74.
14. Tian L, Shen H, Lu Q, Norman RJ, Wang J. Insulin resistance increases the risk of spontaneous abortion after assisted reproduction technology treatment. J Clin Endocrinol Metab 2007; 92:1430-3.
15. Craig LB, Ke RW, Kutteh WH. Increased prevalence of insulin resistance in women with a history of recurrent pregnancy loss. Fertil Steril 2002; 78:487-90.
16. Diejomaoh M, Jirous J, Al-Azemi M, Gupta M, Al-Jaber M, Farhat R, et al. Insulin resistance in women with recurrent spontaneous miscarriage of unknown aetiology. Med Princ Pract 2007; 16:114-8.
17. Celik N, Evsen MS, Sak ME, Soydinc E, Gul T. Evaluation of the relationship between insulin resistance and recurrent pregnancy loss. Ginekol Pol 2011; 82:272-5.
18. Carrington B, Sacks G, Regan L. Recurrent miscarriage: pathophysiology and outcome. Curr Opin Obstet Gynecol 2005; 17:591-7.
19. Crane JP, Wahl N. The role of maternal diabetes in repetitive spontaneous abortion. Fertil Steril 1981; 36:477-9.
20. Coulam CB, Stern JJ. Endocrine factors associated with recurrent spontaneous abortion. Clin Obstet Gynecol 1994; 37:730-44.
21. Wang Y, Zhao H, Li Y, Zhang J, Tan J, Liu Y. Relationship between Recurrent Miscarriage and Insulin Resistance. Gynecol Obstet Invest 2011; 72:245-51.

JOURNAL OF BIOLOGICAL REGULATORS & HOMEOSTATIC AGENTS Vol. 27, no. 1, 233-239 (2013)

LETTER TO THE EDITOR

IN VIVO LIVER EXPRESSION OF TLR2, TLR3 AND TLR7 IN CHRONIC HEPATITIS C

G. TARANTINO[1], A. DI CRISTINA[1], R. PIPITONE[1], P.L. ALMASIO[1], G. DI VITA[2], A. CRAXÌ[1] and S. GRIMAUDO[1]

[1]Sezione di Gastroenterologia and Epatologia, DIBIMIS, University of Palermo, Italy; [2]Dipartimento di Chirurgia, University of Palermo, Italy

Received September 28, 2011 - Accepted November 22, 2012

The role of innate immune response mediated by Toll-like receptors in HCV infection, is not yet well understood and there is a lack of data regarding liver tissue expression of these molecules in chronic hepatitis C (CHC). Our study is aimed to investigate *ex vivo*, liver expression of TLR2, TLR3 and TLR7, which are more involved in the immune-pathogenesis of CHC, and to explore possible correlations with features of disease. We obtained liver biopsies and collected peripheral blood mononuclear cells (PBMC) from 23 consecutive patients with CHC and from 6 patients of control, without liver disease, undergoing surgery for cholecystectomy. The levels of TLRs mRNA in the samples were determined using a real-time reverse transcription quantitative PCR (RT-qPCR). We found a significant high expression of TLR3 in the liver of CHC patients respect to controls (also higher than expression in the PBMC). Conversely no differences emerged in the TLR2 and TLR7 levels between cases and controls. Also we found a correlation of TLR2 and TLR7 levels with the grade of necro-inflammation in the liver. Furthermore TLR7 hepatic levels resulted related to a more advanced stage of liver fibrosis. Ours is the first study to provide data on tissue expression of TLRs during chronic hepatitis C and we believe that it could lead to a better understanding of the role of these molecules in the HCV-mediated liver damage.

A critical role of adaptive immunity in the hepatitis C virus infection has been largely proven to guide the outcome of clinical course in term of spontaneous recover or response to anti-viral therapy. In fact the strength of antigen-specific CD4+ and CD8+ T cells response constitutes the critical element in the eradication of HCV during both acute or chronic infection (1). The role of innate immune response, and in particular the Toll-like receptors mediated response is not yet well understood in HCV infection. HCV is a positive single-stranded RNA virus with several antigens, including HCV RNA and some structural and non structural proteins, able to trigger host defense through activation of TLRs, particularly TLR2, TLR3 and TLR7 (2), leading to a type 1 IFN-mediated response with anti-proliferative and immunomodulatory functions. HCV by itself interferes with these mechanisms by impairing signalling pathways and thus evading the immune-mediated response (3, 4).

Recently a number of studies have tried to find correlations between gene-expression of several TLRs in peripheral blood mononuclear cells (PBMC) and the clinical and histological features of patients with chronic hepatitis C. Overall, these analyses have shown a higher expression of some TLRs mRNA and inflammatory cytokines levels in HCV patients in respect to healthy controls (5-7).

Key words: TLR, HCV, Chronic Hepatitis C, liver biopsy

Mailing address: Dr. Giuseppe Tarantino (M.D. PhD), Clinica medica I, Sezione di Gastroenterologia & Epatologia, DIBIMIS, University of Palermo, p.zza delle Cliniche 2, Palermo 90100 Italy Tel.: +39 091 6552280 Fax: +39 091 6552280 e-mail: giutar@alice.it

0393-974X (2013)

DISCLOSURE: ALL AUTHORS REPORT NO CONFLICTS OF INTEREST RELEVANT TO THIS ARTICLE.

Individual studies confirm a TLR1-9 gene-expression in whole human liver although with low m-RNA levels respect to other tissues (8, 9). It was also shown that HepG2 cell line express greatly TLR1, TLR2, TLR3, TLR6 mRNA but, only minimal levels of TLR4, TLR7, and TLR9 (10). Studies using immunohistochemical techniques or flow cytometry have documented expression of TLR2 protein in the liver of patients with CHC (11) and of TLR7 in hepatocytes of HCV-infected subjects (12).

However there are no studies investigating, in the course of liver disease and particularly during chronic hepatitis C, the *in vivo* hepatic TLRs gene-expression.

Our study was hence aimed to investigate the liver and PBMC expression of TLR2, TLR3 and TLR7 genes in patients with chronic hepatitis C in comparison to their expression in healthy controls, and also to explore possible correlations with features of disease.

MATERIALS AND METHODS

Patients

We prospectively enrolled 23 consecutive, untreated patients with chronic hepatitis C who underwent liver biopsy at our Liver Unit between June and December 2009. We excluded patients with a co-infection with HBV and/or with HIV, with history of alcohol (>30 g ethanol/day) or intravenous drugs abuse and with clinical and serological signs of autoimmunity. Six patients with no stigmata of liver diseases undergoing elective surgical cholecystectomy for lithiasis, who gave informed consent for a liver biopsy performed during surgery, served as a control group.

The study was performed in accordance with the principles of Good Clinical Practice, the principles of the Declaration of Helsinki and its appendices, and local and national laws.

Clinical and laboratory assessment

Baseline clinical data were recorded at the time of admission to hospital. Blood samples for biochemical routine and virological assays were obtained from each patient. Moreover a 12 ml of venous blood was withdrawn in EDTA tubes and cells was separated with FICOLL, centrifuged and homogenized for PBMC collection.

Serum HCV-RNA was measured by a qualitative PCR assay (Cobas Amplicor HCV Test version 2.0; limit of detection: 50 IU/mL) at entry. Quantification of serum HCV-RNA levels was performed with Versant HCV-RNA 3.0 bDNA (Bayer Co., Tarrytown, NY) and expressed in IU/mL. Genotype was investigated with INNO-LiPA, HCV II (Bayer).

Assessment of liver biopsy

Percutaneous liver biopsies, performed with a 16-gauge needle, were formalin fixed and paraffin embedded. Portal, peri-portal and lobular necro-inflammatory activity (grading) and fibrosis (staging) were investigated by applying Scheuer's 1991 histological score (13). Liver steatosis was assessed as the percentage of hepatocytes containing macrovescicular fat droplets. A fragment of biopsy of approximately 0.5 cm of length was collected and frozen in liquid nitrogen at -80°C for molecular biology.

Molecular biology evaluations

Liver samples were stored at -80°C and distrupted/homogenized using the TissueRuptor apparatus (Qiagen) immediately before the acid nucleic extraction. DNA and RNA from biopsy, PBMC and cells cultures were extracted using the AllPrep DNA/RNA Micro Kit (Qiagen) according to the manufacture instructions. 0.5 µg of RNA were used for cDNA synthesis with QuantiTect Reverse Transcription Kit (Qiagen). The levels of TLR2, TLR3 and TLR7 mRNA in the samples were determined using a real-time reverse transcription quantitative PCR (RT-qPCR) (ABI PRISM 7500 Fast Real Time System, Applied Biosystems). The detection was performed using SYBR Green and Quantitect Primer Assays (Qiagen) that provide a PCR reaction with high efficiency and specificity. 18S rRNA was used as endogenous control gene. Results were expressed as N-fold difference in target gene expression relative to the 18S rRNA gene compared with the expression in HepG2 cell line for TLR2 and TLR3 and with the expression in patient 21 sample for TLR7 used as calibrator. Data analysis was performed using Sequence Detection Software Version 1.3-7500, Applied Biosystems.

Statistical methods

Continuous variables were summarized as mean±SD or median (range) when appropriate, and categorical variables as frequency and percentage. Significant differences were calculated using Student's t and Mann-Whitney tests for continuous variables, while a χ^2 test was used for categorical variables. Correlation coefficients were calculated by Spearman's test. Analysis was performed through SPSS software (SPSS Inc., Chicago, IL, USA).

The scatter plots were generated through GraphPad Prism® software (version 4.02; San Diego, CA, U.S.A). Differences were considered significant for p values of <0.05.

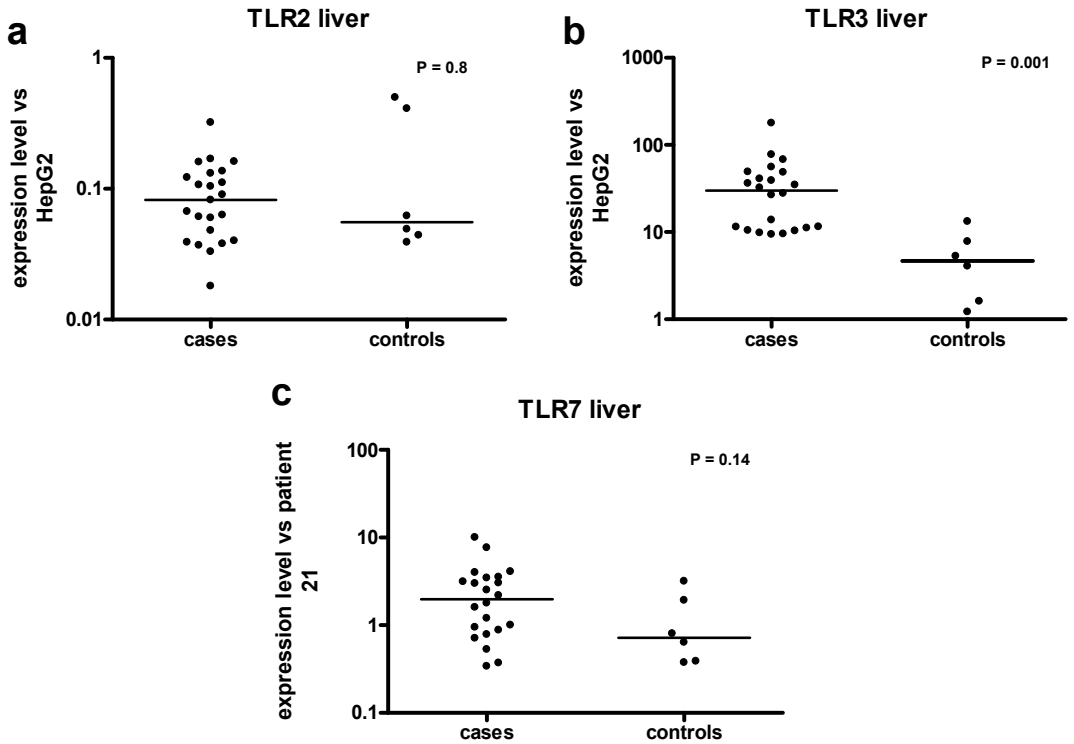

Fig. 1. *Scatter plots of m-RNA expression levels in the liver of TLR2 (**a**), TLR3 (**b**), and TLR7 (**c**), showing the comparison between patients with CHC and healthy controls.*

RESULTS

Demographic, biochemical, serological and histological features of patients are shown in Table I. Of the 23 patients, 20 were infected by HCV genotype 1. Mean age and gender were comparable between patients and controls. As expected liver enzymes resulted significantly higher in patients with CHC respect to healthy controls.

A moderate-severe grade of necro-inflammation and a moderate-severe stage of fibrosis in the liver biopsy was found in 13 patients (57%).

TLRs expression levels in the liver and in PBMC

The hepatic levels of TLR3 resulted significantly higher in patients with CHC respect to healthy controls, (30.02 *vs* 4.67 median of fold relative to HepG2 levels of expression; P=0.001). We found instead no significant differences in the TLR2 and TLR7 m-RNA liver expression between the two groups (0.08 *vs* 0.05 median of fold relative to HepG2 levels of expression with P=0.8 and 1.98 *vs* 0.72 median of fold relative to expression levels in P21; P=0.14, respectively) (Fig. 1).

TLR2 turned out to be significantly more expressed in PBMC than in liver tissue of patients (5.56 *vs* 0.08 median of fold relative to HepG2 levels of expression; P<0.001), while the levels of TLR3 were higher in the liver than PBMC (30.02 *vs* 13.53 median of fold relative to HepG2 levels of expression; P=0.01). No differences were observed for TLR7 levels of expression between PBMC and liver (Fig. 2).

TLRs expression and disease features

Possible correlations between the expression of TLRs and disease features were explored by Spearman rho analysis. The grade of necro-inflammation resulted to be significantly related to the hepatic expression of TLR2 and TLR7. In fact the median level of TLR2 in patients with mild histological grade was 0.06 *vs* 0.11 of those with a moderate-severe grade (P=0.05). Likewise median level of TLR7 in patients with a mild grade was

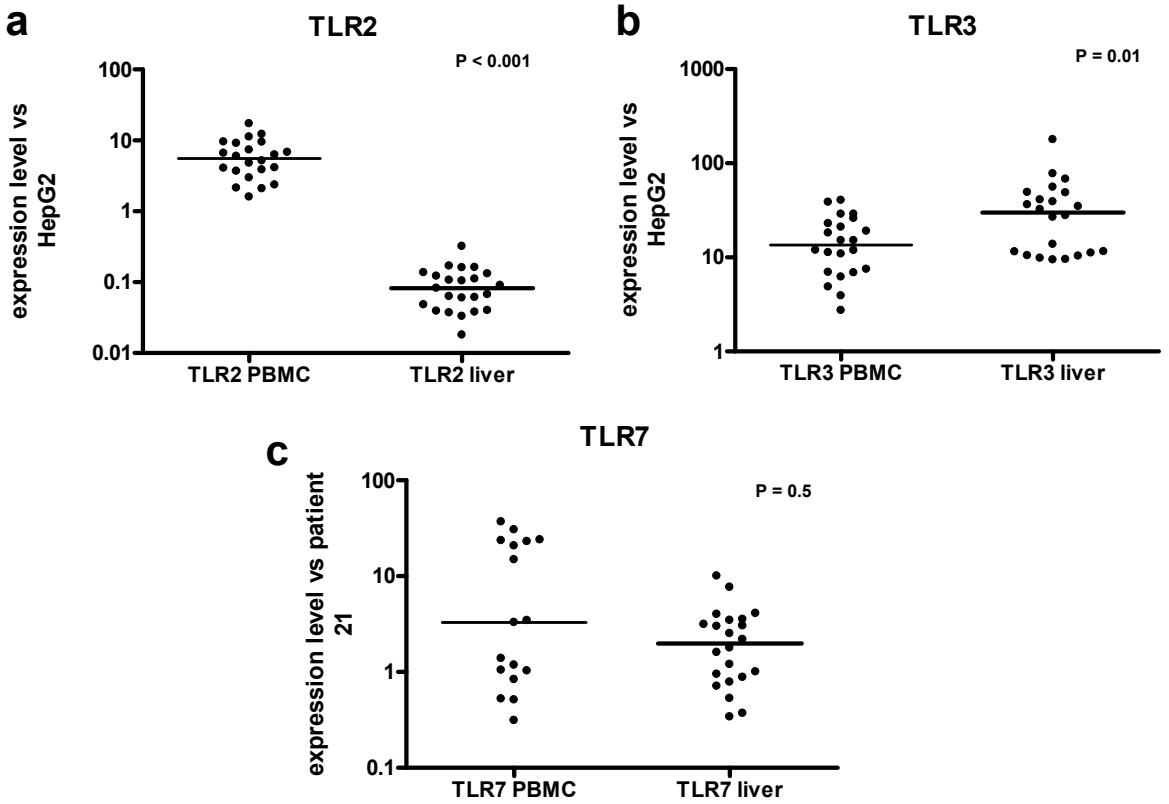

Fig. 2. *Scatter plots of m-RNA expression levels of TLR2 (**a**), TLR3 (**b**), and TLR7 (**c**), in the PBMC respect to liver tissue in patients with CHC.*

0.94 *vs* 3.04 of the patients with a moderate-severe grade (P=0.02). TLR7 liver expression was also significantly related to stage of fibrosis with a median level of 0.94 for patients with mild fibrosis *vs* 2.99 of those with a moderate-severe fibrosis, (P=0.03). No significant correlations was found between hepatic TLR3 expression nor between TLRs expression in PBMC with any clinical or histological features. (Fig. 3)

DISCUSSION

Ours is the first study that provides *ex vivo* data about liver expression of the TLRs more involved in the immune-pathogenesis of HCV hepatic disease: TLR2, TLR3 and TLR7. Double stranded RNA from HCV binds to TLR3 within the endosome, however HCV has developed strategies to avoid an efficient TLR3 signalling pathway through the degradation of Trif and the block of TBK1 by HCV NS3/4A and NS3 respectively, preventing the association between TBK1 and IRF3. TLR7 recognizes single-stranded RNA of virus and activates IRF7 through a series of MyD88-dependent phosphorylation mechanisms, but also HCV NS5A blocks TLR7-induced levels of MyD88 (2). The interference of HCV with these signal pathways impairs synthesis of type I IFNs thus the antiviral effect. At the same time, NS3 and core protein of HCV promote inflammatory signals through TLR2 and TLR4 activation and likely contribute to maintain an inflammatory state that causes persistent liver injury (14-16).

In the current study we found that hepatic m-RNA levels of TLR2 were lower than normal and did not appear to be influenced by HCV replication. In fact we observed analogous m-RNA levels in cases and controls. A relevant difference was instead observed in comparison with expression in PBMC, which turned out to be significantly higher than in the liver, akin to data from studies on healthy human tissues (8, 9). Likewise Sato et al. did not find an increase of TLR2 expression in monocytes of

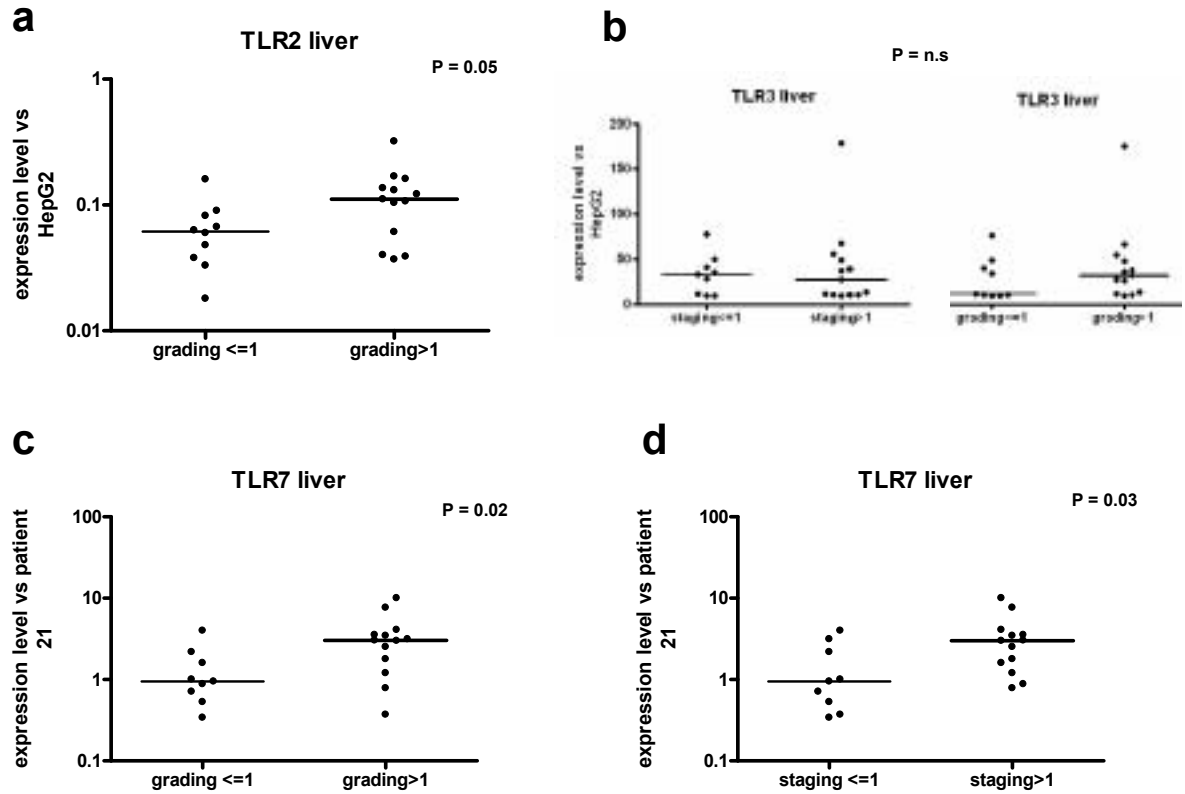

Fig. 3. *Scatter plots of m-RNA expression levels in the liver of TLR2, TLR3 and TLR7 in relation to the grade of necro-inflammation (**a, b, c**) and TLR3 and TLR7 in relation to the stage of fibrosis (**b, d**).*

patients with CHC in respect to controls, until after incubation of cells with HCV core protein (6). These reports indicate that activation of TLR2-mediated inflammatory response by HCV occur in the absence of a TLR2 up-regulation. TLR2 hyper-expression, highly correlated with serum levels of TNF-α, was found by Riordan et al. in patients with cirrhosis irrespective of aetiology, associated to evidence of gut-derived bacterial translocation typical of portal hypertension (17). None of our patients had advanced cirrhosis, and only two had stage 4 fibrosis at biopsy, hence we could not find any correlations between TLR2 expression level (specifically in PBMC) and stage of fibrosis, nor between TLR expression with laboratoristic parameters such as platelets count, aminotrasferases levels and bilirubin levels).

Levels of TLR3 m-RNA in the liver were higher than in the HepG2 cell line used as calibrator, and significantly more elevated in patients with CHC than in controls. Moreover, the hepatic expression of TLR3 m-RNA was higher than that in PBMC. Hence HCV seemingly acts by specifically increasing the expression of TLR3 in the liver. Previous studies did not show a peripheral over-expression of TLR3 in patients with CHC, while a suppressed TLR3 expression was found in HepG2 cells transfected with the entire HCV genome (6). We believe that our finding may be relevant in the pathogenesis of HCV mediated immune damage. In fact, the chronic inflammatory state associated to a block of the signalling cascade of TLR3 operated by HCV could up-regulate the transcription of TLR3-gene.

Levels of TLR7 m-RNA in HepG2 cells were almost undetectable, as already proven by other authors, so we had to choose a patient (n. 21) as calibrator that presented a low-medium expression level of TLR7. No significant difference of expression levels was observed between cases and controls nor between PBMC and liver. Our findings contrast with data from the study of Chang et al. showing a reduced expression of TLR7-RNA in the livers of 6 patients with chronic HCV infection compared with

Table I. *Clinical, biochemical and histological features of patients.*

VARIABLES	PATIENTS 23	CONTROLS 6	P
Mean age, (yrs)	45.17±12.84	47.4±17.25	0,7
Female gender (%)	10 (43.5)	2 (33.3)	0.6
Median HCV-RNA qt (IU/ml)	358,839.0 (102,000–13,500,000)		
HCV Genotypes			
▪ **1**	20 (87)		
▪ **3**	1 (4.3)		
▪ **4**	1 (4.3)		
▪ **N.a.**	1 (4.3)		
Leukocytes/mmc	6,766.5±2282.4		
AST (IU/ml)	47.30±26.9	20.2±3.3	0.03
ALT (IU/ml)	72.96±43.8	23.2±10.8	<0.001
GGT (IU/ml)	77.95±87.0	32.7±23.4	0.05
Alkaline phospathase (IU/ml)	79.48± 40.9		
Albumin (g/dl)	4.51±0.36		
Gamma-globulin (g/dl)	1.43±0.27		
Total bilirubin (mg/dl)	0.82±0.45	0.94±0.9	0.7
Cholesterol (mg/dl)	170.35±22.8		
Triglycerides (mg/dl)	91.05±33.0		
HISTOLOGICAL FEATURES (Scheuer score of 1991)			
Grading>1	13 (56.5)		
Staging>1	13 (56.5)		
Steatosis (>20%)	6 (26.1)		

Abbreviations: n.a. not available.

an unstated number of healthy, HBV and NAFLD controls. This was in line with *in vitro* experiments showing a reduction of TLR7 expression in HCV-replicating hepatoma cells, leading them to assert a role of HCV in the down regulation of TLR7 (18).

The correlations of TLR2 and TLR7 liver

expression and an higher grade of necro-inflammation may be due to a more substantial proportion of non-parenchymal cells constituting inflammatory infiltrate in the liver and expressing TLRs. Anyhow data such as the correlation between TLR7 and a more advanced stage of fibrosis, like we found, are difficult to interpret and new acquisitions on role in the immune pathogenesis of these molecules are yet required.

REFERENCES

1. Day CL, Lauer GM, Robbins GK, et al. Broad specificity of virus-specific CD4+ T-helper-cell responses in resolved hepatitis C virus infection. J Virol 2002; 76:12584-95.
2. Schwabe RF, Seki E, Brenner DA. Toll-like receptor signalling in the liver. Gastroenterology 2006; 130:1886-00.
3. Li K, Foy E, Ferreon JC, et al. Immune evasion by hepatitis C virus NS3/4A protease-mediated cleavage of the Toll-like receptor 3 adaptor protein TRIF. Proc Natl Acad Sci U S A 2005; 102:2992-7.
4. Foy E, Li K, Sumpter R Jr, et al. Control of antiviral defenses through hepatitis C virus disruption of retinoic acid-inducible gene-I signaling. Proc Natl Acad Sci USA 2005; 102:2986-91.
5. Riordan SM, Skinner NA, Kurtovic J, Locarnini S, McIver CJ, Williams R, Visvanathan K. Toll-like receptor expression in chronic hepatitis C: correlation with pro-inflammatory cytokine levels and liver injury. Inflamm Res 2006; 55:279-85.
6. Sato K, Ishikawa T, Okumura A, et al. Expression of Toll-like receptors in chronic hepatitis C virus infection. J Gastroenterol Hepatol 2007; 22:1627-32.
7. Machida K, Cheng KT H, Sung VMH, Levine AM, Foung S, Lai MMC. Hepatitis C Virus Induces Toll-Like Receptor 4 Expression, Leading to Enhanced Production of Beta Interferon and Interleukin-6. Journal of Virology 2006; 866-74
8. Zarember KA, Godowski PJ. Tissue expression of human Toll-like receptors and differential regulation of Toll-like receptor mRNAs in leukocytes in response to microbes, their products, and cytokines. J Immunol 2002; 168(2):554-61
9. Nishimura M, Naito S. Tissue-specific mRNA expression profiles of human toll-like receptors and related genes. Biol Pharm Bull 2005; 28(5):886-92.
10. Preiss S, Thompson A, Chen X, et al. Characterization of the innate immune signalling pathways in hepatocyte cell lines. Journal of Viral Hepatitis 2008; 15:888-900
11. Mozer-Lisewska I, Sluzewski W, Kaczmarek M et al. Tissue localization of Toll-like receptors in biopsy specimens of liver from children infected with hepatitis C virus. Scand J Immunol 2005; 62(4):407-12.
12. Lee J, Wu CC, Lee KJ et al. Activation of anti-hepatitis C virus responses via Toll-like receptor 7. Proc Natl Acad Sci USA 2006; 103(6):1828-33.
13. Scheuer PJ, Lefkowitch JH: Liver biopsy interpretation W.B. Saunders London 2000; 294.
14. Dolganiuc A, Oak S, Kodys K et al. Hepatitis C core and nonstructural 3 proteins trigger Toll-like receptor 2-mediated pathways and inflammatory activation. Gastroenterology 2004; 127:1513-24.
15. Ishii S, Koziel MJ. Immune responses during acute and chronic infection with hepatitis C virus. Clin Immunol 2008; 128:133-47.
16. Mencin A, Kluwe J and Schwabe RF. Toll-like receptors as targets in chronic liver diseases. Gut 2009; 58704-20.
17. Riordan SM, Skinner N, Nagree A et al. Peripheral blood mononuclear cell expression of Toll-like receptors and relation to cytokine levels in cirrhosis. Hepatology 2003; 37:1154–64.
18. Chang S, Kodys K, Szabo G. Impaired expression and function of toll-like receptor 7 in hepatitis C virus infection in human hepatoma cells. Hepatology 2010; 51(1):35-42.

LETTER TO THE EDITOR

ULTRASTRUCTURAL AGE-RELATED CHANGES IN THE SENSORY CORPUSCLES OF THE HUMAN GENITAL SKIN

A. TAMMARO[1], F.R. PARISELLA[2], C. CAVALLOTTI[3], S. PERSECHINO[1] and C. CAVALLOTTI[4]

[1]U.O.C. Dermatology, NESMOS Department, Sant'Andrea Hospital, Faculty of Medicine and Psychology, University "Sapienza", Rome, Italy; [2]Faculty of Medicine, University of Maryland, USA; [3]UOC of Dermatology, IRCS San Gallicano Hospital, Rome, Italy; [4]Department of Anatomy, University "Sapienza", Rome, Italy

Received July 30, 2012 - Accepted November 8, 2012

In human genital skin the majority of superficial sensory corpuscles is represented by glomerular corpuscles. These corpuscles show an own morphology. In this report the ultra-structure of the sensitive corpuscle in the penis skin of the younger and older subjects was compared, showing that the genital skin of the older humans contains more simple complexes than the younger ones. Our findings support the view that the age-related changes that can be observed in human glomerular genital corpuscles are consistent with an increase of the simple complexes and a strong decrease of the poly-lamellar one in the older people. These findings demonstrate that human genital corpuscles underwent age-related changes. Moreover our morphological findings can be correlated in relation to the clinical evolution of the sensitivity in the genital skin.

The human skin contains numerous sensitive corpuscles in which lamellar complexes consisted of a central zone (axon) and several surrounding lamellae formed by Schwann cells. Simple and/or complex sensory corpuscles in the genitals of mammals were first studied by Tinofeew in 1896, Dogiel in 1899 and Ruffini in 1902 (1-3). After these pioneering studies Malinovsky performed the evaluation and the classification of both simple and complex sensory nerve formations (4-6).

The ultra-structure of sensory nerve endings in the human genital organs were poorly studied. With the aid of the electron microscopy Malinovsky and Pac observed three main types of glomerular corpuscles (7). In the human genital skin of clitoris different types of glomerular nerve endings from simple to complicated genital corpuscles were found. Some of these receptors resemble the Meissner corpuscles structure. The complicated glomerular endings (the genital corpuscles) contain a number of lamellar complexes. Around the axon there are up to 10 lamellae of Schwann cells. As in the human glabrous skin rapidly adapting receptor units were observed in contrast to the fact that simple sensory corpuscles occur in the superficial layers of the dermis quite rarely and therefore it is concluded that the lamellar complexes in human genital corpuscles represent a morphological and functional equivalent of simple sensory corpuscles in other mammals (8).

It has been hypothesized that these genital

Key words: sensory corpuscles, genital skin, lamellar complexes, human, age-related changes

Mailing address: Tammaro Antonella MD,
U.O.C. Dermatology, NESMOS Department,
Sant'Andrea Hospital, Faculty of Medicine and Psychology,
University "Sapienza" Via di Grottarossa, 1035
00189 Rome, Italy
Tel.: +39 06 33775907 Fax: +39 06 33775378
e-mail: tammaroantonella@gmail.com

0393-974X (2013)

DISCLOSURE: ALL AUTHORS REPORT NO CONFLICTS OF INTEREST RELEVANT TO THIS ARTICLE.

corpuscles show same age related changes. For these reasons the aim of this study was to evaluate, by means of the electron microscopy, the age related changes of the human genital corpuscles.

MATERIALS AND METHODS

The ultra-structure of glomerular corpuscles was examined in the skin of the penis glans in 20 younger (mean age 24±3 years) and 20 older humans (mean age 71±5 years). Human material was taken from the skin of the penis glans during autopsies with informed consent of relatives.The penis glans of the enrolled subjects was exposed and a small part of the skin was harvested and immediately fixed in a 3% solution of glutaraldehyde in 0.1 M phosphate buffer (pH 7.4) for 2 h. The fixation was followed by treatment with 2% OsO4 in phosphate buffer. The material was then dehydrated with acetone and alcohol and embedded in Durcupan ACM. Semi-thin and ultrathin sections were cut with a Tesla BS 490 ultra-microtome and treated for electron microscopy.

RESULTS

The authors compared the ultra-structure of superficial sensory corpuscles in the penis skin of the younger and older subjects. Some information on the enrolled subjects are reported in Table I. The sensitive corpuscles are represented by glomerular corpuscles. In these corpuscles, lamellar complexes were described consisting of a central dendritic zone (axon) and several surrounding lamellae formed by Schwann cells (Fig. 1).

The axon of some complexes is en-sheathed with a spiral mesaxon and with spirally arranged Schwann cell cytoplasmatic lamellae. On some places of the lamellae pinocytotic vesicles occur. The surface of the lamellae is covered with a basement membrane. In the inter lamellar spaces collagenous fibrils are visible (Fig. 2).

A simple lamellar complex is characterized by a dendritic zone with mitochondria accumulation and en-sheathed with a small number of larger cytoplasmic lamellae of Schwann cells, the mesaxon is clearly evident (Fig 3, 4). Numerous collagenous fibrils are scattered among the lamellae. In a complicated lamellar complex the Schwann cell lamellae encircle the dendritic zone filled with numerous mithocondria. The width of this complex is about 6.5 μm. In the spaces between the lamellae of both sides a “cleft” is evident as a typical feature of the inner core of lamellar sensory corpuscles. The lamellae contain small pinocytotic vesicles. In the interlamellar spaces there are collagenous fibrils; in the areas with wider interlamellar spaces, a basement membrane covering the surface of the lamellae is well evident. These lamellar complexes do not have a capsule and structures are all located inside the glomerular corpuscles.

In the older subjects the lamellar complexes are simple and consist of a maximum of 5 lamellae of Schwann cells, the greatest width is about 4.5 μm. Some dendritic zones are almost encircled with lamellae of Schwann cells up to five. The dendritic zones contain numerous mitochondria; some of them are somewhat changed due to immersion and/or fixation. The lamellae are relatively thin and contain numerous clear vesicles. Over the lamellae a basement membrane is formed. The spaces among the Schwann cells lamellae are filled with fine filamentous material the width of the largest complexes is about 4 μm (between 3.6 and 4.5), depending on the number of lamellae. In the younger humans the genital skin shows simple glomerular as well as more complicated sensory corpuscles. In the second group (older humans) some dendritic areas are almost encircled with lamellae of up to five Schwann cells. The dendritic zones contain numerous mitochondria; some of them are somewhat changed to immersion and or fixation. The lamellae are relatively thin and contain numerous clear vesicles. Over the lamellae a basement membrane is formed. The spaces among the Schwann cells lamellae are filled with fine filamentous material the width of the largest complexes is about 4 μm (3,6-4,5 μm), depending on the lamellae number. Throughout all the complicated glomerular corpuscles (genital corpuscles) in the skin numerous and different types of lamellar complexes occur from quite simple formations to lamellar complexes with about 7 lamellae of Schwann cell cytoplasm. In the younger subjects the lamellar complexes have a maximun width of about 6.5μm and consist of a maximum of 7 lamellae. The interlamellar spaces are narrower than in the first case and are filled with fine filamentous material and collagenous fibrils. In some of these more complicated complexes an interlamellar cleft

Table I. *Information on the enrolled subjects. Small fragments of the skin glans were harvested during autopsies. All the enrolled subjects were dead from non skin and/or genital diseases.*

Subjects	Number	Mean age
Younger	20	24±3
Older	20	71±5

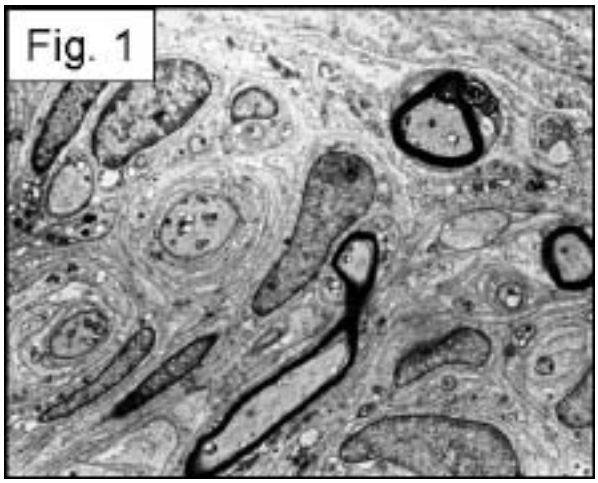

Fig. 1. *Section of a human genital corpuscle with two complex lamellar structures (in the left corner of the figure). Some Schwann cells are localized around the two lamellar corpuscles. The sample was harvested from a young subject (magnification 8,000x).*

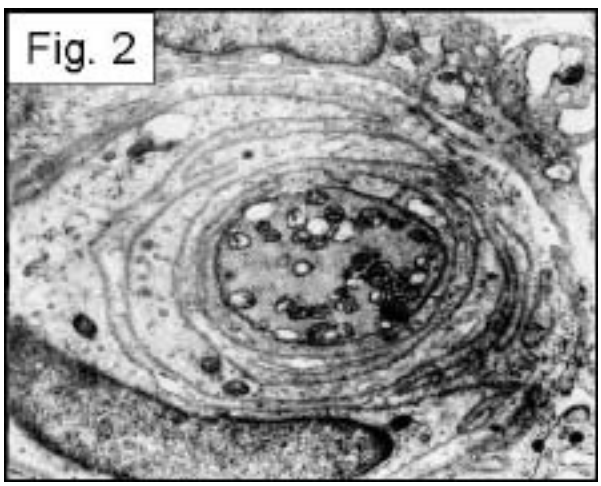

Fig. 2. *Complicated lamellar complex from a human genital corpuscle with inner core clefts at one of the opposite side of the axon pole. The sample was harvested from a young subject (magnification 12,000x).*

also occurs, resembling those in lamellar complexes, it approximately corresponds with the width of the inner core of simple lamellar corpuscles.

DISCUSSION

These findings support the view that the lamellar complexes of glomerular corpuscles are morphologically and functionally similar to the simple lamellar sensory corpuscles localized in the different areas of the human body. The glomerular corpuscles also contain a-myelin thin nerve fibres. The ultra-structure of axons in the endings of various types of mammals, including rats and humans, have been described (9, 10). The corium of the human penis glans contains many sensitive corpuscles. In the Meissner corpuscles the axons are almost completely enveloped in the cytoplasm of Schwann cells. Moreover they contain numerous mitochondria. Next, there are lamellar bodies, vesicles and further organelles. The papillar glomerular endings show an accumulation of Schwann cells. The axons are irregular in shape, eccentrically placed in the cytoplasm of the Schwann cell, either completely or partially surrounded by the cytoplasm of the Schwann cell. Finally we have found axons with a concentric system of lamellae up to five in number. In the complicated glomerular endings the axons vary in appearance and are enveloped in one to five lamellae of Schwann cells, which is typical of those formations. Around some of these lamellar systems there is a sign of a capsule formed by an elongated lamella of the endo-neural of peri-neural membrane. The cytoplasm of the Schwann cell covers the axons either partially or completely or it again forms around the axons a lamellar system amounting up to four layers. It is noticeable that these axons are very poor in organelles (3-8).

Sensory nerve endings were found also in the

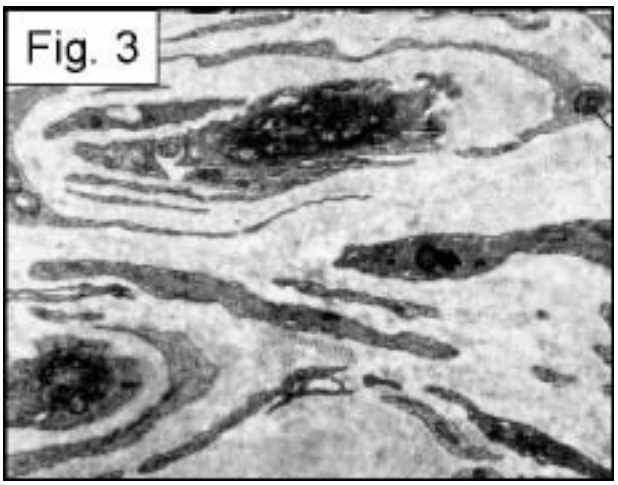

Fig. 3. *Some simple lamellar complexes in glomerular corpuscles of the genital skin of an older subject. The figure shows only simple lamellar systems while the complex lamellar structures are absent. (magnification 8,000 x).*

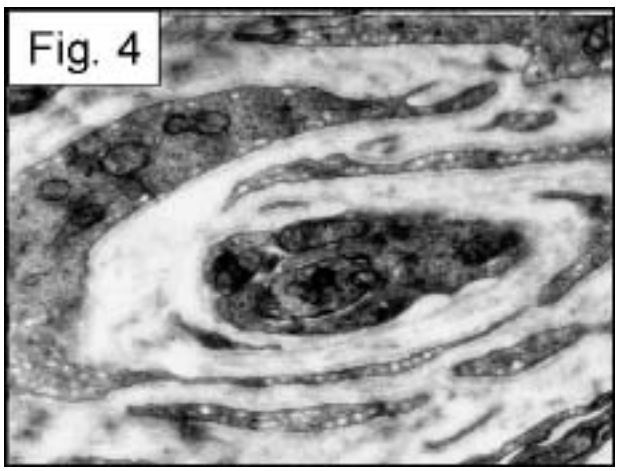

Fig. 4. *Details of a simple lamellar complex in a genital corpuscle harvested from the genital skin of an older subject. (magnification 12,000 x).*

glans penis of the rat by Johnson and Halata (11). With light and electron microscopy, these authors observered free nerve endings in the epidermis and numerous lamellated corpuscles in the superficial dermis while the dermal papillae are devoid of any neural structure. The same authors conclude that the penis glans of the rat contains a sensory receptor distribution similar to the human penis glans. Marquez and co-workers studied the changes in human cutaneous sensory corpuscles after spinal cord and/or peripheral nerve injury (12). On the basis of the results the authors conclude that the structural and functional cutaneous sensory axons are necessary to preserve the integrity of the related sensory corpuscles.

Considering the age-related changes, on the basis of our results, we can affirm that in younger subjects the complex lamellae system are prevalent while in the older ones we found only simple lamellar corpuscles. The sensitive genital corpuscles in older subjects are strongly decreased and modified. The decrease especially involved the complex lamellar system. The lamellar system only show a decrease of their intracellular elements.

The clinical evaluation of the sensitivity in the human genital skin is still little known and further studies are warranted to clarify this topic. Our results are consistent with an increase of the simple complexes and a strong decrease of the poli-lamellar complexes in the older subjects. These age-related changes in the genital corpuscles demonstrate that the human genital skin also shows strong changes in the older subjects.

REFERENCES

1. Timofeew T. Anat Anz 1895; 16:452.
2. Dogiel AS. Zur frage viber den Ban der Herbst'schen Korperchen. Z Wiss Zool 1899; 66:358-76.
3. Ruffini A. Sur les expansions nerveuses de la peau chez l'homme et quelques autres mammiferes. Rev Gen Histol 1985; 1:419-542.
4. Malinovsky L. Some problems connected with evaluation of skin receptors and their classification. Folia morphol 1967; 15:18-24.
5. Malinovsky L. Classification of sensory nerve endings in vertebrates brought up to date. Folia morphol 1986; 34:261-64.
6. Malinovsky L. System approach in the classification of sensory nerve formations. 5th Intern Theriol Congr Rome 1989; 992-93.
7. Malinovsky L, Pac L. Morphology of sensory corpuscles in mammals. Acta Fac Med Brno 1982;79-84
8. Haro JJ, Vega JA, del Valle ME, Calzada B, Zaccheo D, Malinovsky L. Immunohistochemical study of sensory nerve formations in human glabrous skin.

Eur J Morphol 1991; 29(4):271-84.
9. Malinovský L, Sommerová J. Sensory nerve endings in the penis in green monkey (Cercopithecus aethiops sabaeus). Z Mikrosk Anat Forsch 1977; 91:94-104.
10. Malinovský L. Ultrastructure of sensory nerve terminals in the penis in green monkey (Cercopithecus aethiops sabaeus). Z Mikrosk Anat Forsch 1977; 91:541-52.
11. Johnson RD, Halata Z. Topography and ultrastructure of sensory nerve endings in the glans penis of the rat. J Comp Neurol 1991; 312:299-310.
12. Marquez J, Perez-Perz M, Naves FJ, Vega JA. Effect of spinal cord and peripheral nerve injury on human cutaneous sensory corpuscles. An immunohistochemical study. J Peripher Nerv Syst 1997; 2:49-59.

JOURNAL OF BIOLOGICAL REGULATORS & HOMEOSTATIC AGENTS Vol. 27, no. 1, 247-251 (2013)

LETTER TO THE EDITOR

EVALUATION OF PATTERNS AND APPROPRIATE GASTRO PROTECTION IN ALBANIAN PRIMARY HEALTH CARE USERS

S. KELLICI[1], A. DIBRA[2], X.H. DRACINI[2], L. DEDA[3], M. FIDA[3] and G. BURAZERI[4]

[1]Pharmaceutical Department, Faculty of Medicine, University of Tirana, Albania; [2]First Clinic of Abdominal Surgery, Faculty of Medicine, University of Tirana, Albania; [3]Faculty of Medicine, University of Tirana, Albania; [4]Department of International Health, School for Public Health and Primary Care (CAPHRI), Faculty of Health, Medicine and Life Sciences, Maastricht University, Maastricht, The Netherlands

Received September 3, 2012 – Accepted January 7, 2013

Our aim was to assess the prevalence of gastro protection in the Albanian population using non-steroidal anti-inflammatory drugs (NSAIDs). A cross-sectional study, conducted in November-December 2011 in Albania, included 610 NSAIDs users (236 men and 374 women) who visited pharmacies to receive their NSAID medication. A structured questionnaire was administered to all participants including information on age, sex, educational status, pathology being treated with NSAID, presence of gastrointestinal ulcer or related complications, duration of NSAIDs therapy, type of drug used, and gastro protection therapy. Almost all participants (N=599) received NSAIDs to treat rheumatic and/or musculoskeletal disorders. Of these, 475 individuals were on chronic therapy with high daily doses of NSAIDs. Concomitant gastro protective therapy was found in 184 individuals (30% of the overall sample). Women and the more educated individuals received more gastro protection than men and the low educated counterparts, respectively (33.4% in women *vs* 25% in men; 47% in highly educated *vs* 18% in low educated). Appropriate use of gastro protective therapy for NSAID users needs to be promptly implemented in Albania, as its inappropriate use raises ethical and economic concerns. Prescriptions should follow clear guidelines for prevention of gastrointestinal damage following NSAIDs therapy among persons at high risk.

Non-steroidal anti-inflammatory drugs (NSAIDs) are one of the most widely prescribed medications in the world. One of the most important side effects for which NSAIDs are accused is the gastrointestinal damage, and this is the reason for their frequent co-prescription with gastro protective agents (1, 2). It is estimated that this gastrointestinal damage increases 2.5-5 fold to the NSAIDs users as compared to non NSAIDs users (3). The use of NSAID without gastro protective co-therapy is considered appropriate in patients <65 years, not taking anticoagulant and/or corticosteroid therapy and having no gastro-intestinal (GI) history. Co-prescription of gastro protective agents is recommended to the patients at high risk for developing GI damage after NSAIDs therapy. These risk factors according to actual guidance include: age ≥65 years, history of GI ulcer or ulcer complications, use of high doses and prolonged therapy of NSAIDs, concomitant therapy of anticoagulants or corticosteroids, use of more than one NSAID etc (4,

Key words: non-steroidal anti-inflammatory drugs, gastro protection, risk factors

Mailing address: Prof. Asc. Arvin Dibra,
Universiteti Zoja e Keshillit te Mire,
Rruga Dritan Hoxha,
Tirana, Albania
Tel.: +355 69 2082162
Fax: +355 42 273291
e-mail: a.dibra@unizkm.edu.al

0393-974X (2013)

DISCLOSURE: ALL AUTHORS REPORT NO CONFLICTS OF INTEREST RELEVANT TO THIS ARTICLE.

5). An option to the gastro protection would be the use of Coxib-s (selective NSAIDs) only when there is no cardiovascular risk (6-9).

The aim of this study is to assess the prevalence of gastro protection in the Albanian population that uses NSAIDs (including selective and non selective). There are no previous data on this topic regarding the Albanian population. As a consequence we undertook this survey to identify the determinants and trends of gastro protection in patients using NSAIDs in Albania.

MATERIALS AND METHODS

We performed a cross-sectional study through a questionnaire which was filled in by NSAIDs users (primary care populations) who visited the pharmacies to receive their NSAID medication. This study included 15 pharmacies in Tirana, the Albanian capital, and 15 pharmacies in other districts of Albania, selected randomly. There were no pharmacies which refused to participate in the survey. The questionnaires were completed under the supervision of the pharmacists in the Albanian territory. Data collection was carried out for 1 month (November- December 2011). These data were collected mostly in the Tirana area, but about 30% of data came from other cities covering almost all territory (all main cities). Data collection was focused to: age, gender, educational status, pathology that is being treated with NSAID, presence of gastrointestinal ulcer or related complications, NSAIDs therapy duration, type of drug used, gastro protection therapy (if applied). We took in consideration not only patients who presented to the pharmacy with a medical prescription but also patients who came for self medication. We evaluated the appropriateness of gastro protection within this patient group included in the study. We analyzed patients with one risk factor, patients with more than one risk factor and examined the presence of gastro protective measures. We examined for any association between gender, educational level and gastro protection therapy.

Chi-square test was used to assess the differences in gastro protection rates between groups defined by the presence of one, two, or three risk factors.

RESULTS

Six hundred and ten individuals were included in the study (236 males and 374 females). Five hundred and ninety nine patients received NSAIDs to treat rheumatic and/or musculoskeletal disorders. The rest still used NSAIDs but for different health conditions. 475 patients were on chronic therapy with NSAIDs and received high daily doses of these drugs. Most of the patients presented a medical prescription to receive the NSAIDs medication (92%) and only 8% of them received these drugs as self medication. The NSAIDs used consisted of 8 classes of drugs with the following ranking of their frequency of use: Diclofenac (29.5%), Piroxicam (16.1%), Ibuprofen (14.3%), Salicilates (11%), Ketoprofen (10.7%), Naproxen (8.5%), Cox-2 inhibitors (6.6%) and Mefenamic acid (3.4%).

Regarding the level of education, we noticed that 253 of the NSAIDs users had medium education, 179 of them had elementary education and 178 had higher education (university studies).

Overall in 184 patients in therapy with NSAIDs (out of 610) we found concomitant gastro protective therapy.

Based on investigating the relations between different factors and the gastro protection behaviors, it can be stated that women receive more gastro protection than men (33.4% of gastro protection in the women's group *vs* 25% of gastro protection in the men's group). The most gastro protected persons seems to be at the higher level of education (46.6% of the gastro protected patients are at the highest level of education (university), 26.9% are at medium level of education and 18.4% are at elementary level of education ($p < 0.001$).

If the medications are ranked in relation to the gastro protection, it can be seen that the higher score of gastro protection is seen with Naproxen, rather than with Diclofenac and Piroxicam (although these ratings do not show any statistical significance). There is small utilization of Cox-2 inhibitors therapy and this therapy is associated with gastro protection in 22.5% of the users. This is a high percentage of gastro protection in this group as compared to the 9.1% of gastro protection reported at other studies (10).

Regarding the risk factors for gastrointestinal side effects, data shows that 49 individuals that use NSAIDs had no risk factor that would suggest any gastro protective strategy. Nineteen of these individuals without any risk factor (38.7%) receive gastro protective agents.

The risk factors that we analyzed were: age,

Table I. *Gastro protection rates by presence of risk factors.*

No gastro protection	Gastro protection	Total
no risk factors		
30 (61.3 %)	19 (38.7 %)	49
at least 1 risk factor		
396 (70.6 %)	165 (29.4 %)	561
at least 1 risk factor: age over 65 years		
164 (78.8 %)	44 (21.2 %)	208
at least 1 risk factor: prolonged therapy at high doses		
333 (70.1 %)	142 (29.9 %)	475
at least 1 risk factor: history of gastric ulcers and related problems		
204 (69.9 %)	88 (30.1 %)	292
at least 2 risk factors: history of gastric ulcers and age over 65 years		
66 (73.3 %)	24 (26.7 %)	90
at least 2 risk factors: age over 65 years and prolonged therapy at high doses		
130 (78.8 %)	35 (21.2 %)	165
at least 2 risk factors: prolonged therapy at high doses and history of GI ulcers		
160 (69.3 %)	71 (30.7 %)	231
all the 3 risk factors (age, prolonged therapy and history of GI ulcers)		
51 (70.8 %)	21 (29.2 %)	72

history of gastrointestinal ulcers or related problems and prolonged therapy with high doses. Five hundred and sixty one subjects had at least one risk factor which would justify the use of gastro protective agents. Within this group of patients with at least one risk factor we found only 165 (or 29.4%) that received gastro protective therapy.

We analyzed separately each risk factor and examined the gastro protection strategy in patients having at least one risk factor [(I) prolonged use with high doses of NSAIDs; (II) age over 65 years; (III) history of ulcers or related gastrointestinal factors)]. We analyzed the combinations of two risk factors and the related gastro protection or not and the same analyses was performed for the group of patients presenting 3 risk factors. The range of gastro protection within these groups was similar (ranging from 21.2% to 30.7%). In the group of patients presenting 3 risk factors the gastro protective therapy was performed in 29.2%). All data regarding risk factors and gastro protection therapy are shown in the Table I.

DISCUSSION

We observed the lack of use of gastro protective strategies in 70.6% of the patients that require gastro protection and an overuse of these strategies in 38.7% of the patients that do not require such a treatment. This finding is similar with previous studies reported

in literature (11).

Within the description of risk factors, the cut age >65 years was defined based on some of the available guidelines. Instead could be also appropriate substitute this concept with "patients of older age".

No differences were noted in the percentage of patients receiving gastro protection who had 1, 2 or 3 risk factors at the same time. There is a difference between these data and those reported from other important studies in this field that demonstrate an increase in the gastro protective measures with the increase of the presence of risk factors (Hartnell et al, 2004) (Herings and Goettsch, 2004) (Abraham et al., 2005) (1). This shows a deficiency in the prescribing behavior as the majority of the enrolled patients received the medication following a medical prescription and only a small number was receiving NSAIDs as a self medication. These deficiency is probably the result of the lack of national guidelines for the prescription of these drugs, inadequate knowledge and/or the underestimation of the problem.

There is a strong correlation between the level of education and use of gastro protection, showing a higher use of gastro protective therapy in persons with higher level of education. This is probably due to the greater medical knowledge of these persons and to the requirement they make to their doctors to prescribe these gastro protective agents.

The most commonly used gastro protective agent was naproxen. This is a discrepancy with similar studies that have shown the lowest level of gastro protection through (12).

It is evident that the use of Cox-2 inhibitors is not yet a preferred therapy in Albania as compared with other countries (13). This is probably due to the lower availability of these drugs in the Albanian market and/ or because prescribers have few information about these drugs and their benefits in the clinical use.

The interventional gastro protective strategies in Albania actually consist on relatively low costs (approximate costs10-50 €/month). Instead the cost of treating gastrointestinal damage could be around €500.

It is necessary that prescribers follow clear guidance for the prevention of gastrointestinal damage following NSAIDs therapy in persons at risk and do not underestimate this measure.

Appropriate use of gastro protective therapy for NSAID users needs to be promptly implemented, as its inappropriate use raises ethical and economic concerns (14). An interventional measure could be a sensibility campaign that would raise awareness about the importance of the gastro protective strategies to prevent gastrointestinal damage in NSAIDs users at risk. This is suggested by the finding of higher use of gastro protective by the higher education group of patients who probably haves more information on this topic compared to the other groups.

In this study we analyzed the level of use of gastro protection among NSAIDs users in Albania. Our further objective is to evaluate the appropriateness of the use of gastro protection to see whether it is effective and correct and if adherence to its use is adequate.

REFERENCES

1. Moore RA, Derry S, Phillips CJ, McQuay HJ. Nonsteroidal anti-inflammatory drugs (NSAIDs), cyclooxygenase-2 selective inhibitors (coxibs) and gastrointestinal harm: review of clinical trials and clinical practice. BMC Musculoskelet Disord 2006; 7:79.
2. Garcia EB, Michaud K, Wolfe F, et al. Gastrointestinal prophylactic therapy among patients with arthritis treated by rheumatology specialists. J Rheumatol 2006; 33:779-84.
3. Arroyo M, Lanas A. NSAIDs-induced gastrointestinal damage. Review. Minerva Gastroenterol Dietol 2006; 52(3):249-59.
4. Laine L. The gastrointestinal effects of nonselective NSAIDs and COX-2-selective inhibitors. Semin Arthritis Rheum 2002; 32(1):25-32.
5. Vonkeman H, Klok R, Postma M. Brouwers J, Van de Laar M. Direct medical costs of serious gastrointestinal ulcers among users of NSAIDs. Drugs Aging 2007; 24:681-90.
6. Steinman MA, McQuaid KR, Covinsky KE. Age and rising rates of cyclooxygenase-2 inhibitor use. Results from a national survey. J Gen Intern Med 2006; 21:245-50.
7. White WB, Faich G, Borer JS, Makuch RW. Cardiovascular thrombotic events in arthritis trials of the cyclooxygenase-2 inhibitor celecoxib. Am J

Cardiol 2003; 92:411-8.

8. Hernandez-Diaz S. Varas-Lorenzo C. Garcia Rodriguez LA. Non-steroidal antiinflammatory drugs and the risk of acute myocardial infarction. Basic Clin Pharmacol Toxicol 2006; 98**:**266-74.
9. Rostom A. Muir K. Dubé C, et al. Gastrointestinal safety of cyclooxygenase-2 inhibitors: a Cochrane collaboration systematic review. Clin Gastroenterol Hepatol 2007; 5:818-28.
10. Bombardier C, Laine L, Reicin A, et al. Comparison of upper gastrointestinal toxicity of rofecoxib and naproxen in patients with rheumatoid arthritis. VIGOR Study Group. N. Engl J Med 2000; 343(21):1520-8.
11. Morini S, Zullo A, Oliveti D, et al. A very high rate of inappropriate use of Gastroprotection for nonsteroidal anti-inflammatory drug therapy in primary care: a cross-sectional study. J Clin Gastroenterol 2011; 45(9):780-4.
12. Raghavendra B, Narendranathsanji S, Ullal SD, et al. Trends in prescribing gastroprotective agents with non steroidal anti-inflammatory drugs in an orthopaedic outpatient unit of a tertiary care hospital. Journal of Clinical and Diagnostic Research 2009; 3:1553-6.
13. Arellano FM, Yood MU, Wentworth CE, Oliveria SA, Rivero E, Verma A, Rothman KJ. Use of cyclo-oxygenase 2 inhibitors (COX-2) and prescription non-steroidal anti-inflammatory drugs (NSAIDS) in UK and USA populations. Implications for COX-2 cardiovascular profile. Pharmacoepidemiol Drug Saf 2006; 15(12):861-72.
14. Wiklund I, Långström G, Hawkey C, et al. Upper GI symptoms reduce the quality of life for patients on long-term NSAID therapy. Ann Rheum Dis 2003; 62(1):150.

JOURNAL OF BIOLOGICAL REGULATORS & HOMEOSTATIC AGENTS Vol. 27, no. 1, 253-258 (2013)

LETTER TO THE EDITOR

IMMUNOMODULATING ACTIVITY OF PIDOTIMOD IN CHILDREN WITH DOWN SYNDROME

G.V. ZUCCOTTI[1], C. MAMELI[1], D. TRABATTONI[2], S. BERETTA[1], M. BIASIN[2], L. GUAZZAROTTI[1] and M. CLERICI[3]

[1]Department of Pediatrics, University of Milan, L. Sacco Hospital, Milan, Italy; [2]Department of Biomedical and Clinical Sciences, University of Milan, Milan, Italy; [3]Department of Physiopathology Medical-Surgery and Transplantation, University of Milan, Milan, and Don C. Gnocchi Foundation ONLUS, IRCCS, Milan, Italy

Received December 3, 2012 – Accepted January 31, 2013

Acute respiratory tract infections (ARTIs) are the most frequent illnesses in pediatric age, frequently experienced in children with Down Syndrome (DS) due to the associated immune defects of both specific and non-specific immunity. Pidotimod, a synthetic immunostimulant, was shown to reduce the rates of ARTIs in children with DS, however the mechanisms associated with this effect is currently unknown. We analyzed immune parameters in DS children who received the seasonal 2011–2012 virosomal-adjuvanted influenza vaccine. Eighteen children aged 3-10 years (mean age 7.1±2.6 years) were randomly assigned (1:1 ratio) to receive Pidotimod 400 mg, administered orally once a day for 90 days or placebo. At the recruitment (T0) all children received a single dose of virosomal-adjuvanted influenza vaccine (Flu). Blood samples were collected at T0 and 3 months after the recruitment (T3) in order to evaluate innate and adaptative immune responses pathway. Flu-specific IgG1 and IgG3 levels in plasma samples were determined at pre-vaccination (T0), and 1 (T1) and 3 months (T3) post-vaccination. The use of Pidotimod was associated with the upregulation of a number of genes involved in the activation of innate immune responses and in antimicrobial activity. Interestingly the ratio of Flu-specific IgG1/IgG3 was skewed in pidotimod-treated individuals, suggesting a preferential activation of complement-dependent effector mechanisms. Although preliminary these data suggest that Pidotimod can potentiate the beneficial effect of immunization, possibly resulting in a stronger activity of both innate and adaptive immune responses.

Acute respiratory tract infections (ARTIs) are the most frequent illnesses in pediatric age, leading to 20% of medical consultations, 30% of days lost from school, and 75% of antibiotics prescriptions (1). Down Syndrome (DS) is the most common chromosomal anomaly among live-born infants, with an incidence of 1 in out of 800 overall births, and a prevalence of nearly 6 in out of 10.000 births in Italy (2). Besides mental retardation and various congenital defects, immune defects are also associated to DS (3). Immunological alterations in DS include a reduction of circulating B cells, a decrease of CD4+ T lymphocytes and an increase of CD8+ T cells, with a resulting inversion of the CD4/CD8 ratio (4-7), T-helper functional defects, such as an augmented mitogen-stimulated production of IL-2, IL-7, IL-10,

Key words: pidotimod, Down syndrome, immunostimulant

Mailing address: Gian Vincenzo Zuccotti,
Department of Pediatrics,
University of Milan, Luigi Sacco Hospital,
Milan, Italy
Tel.: +39 02 39042269
Fax: +39 02 39042254
e-mail: gianvincenzo.zuccotti@unimi.it

0393-974X (2013)

TNFα, IFNγ (8-9), and defective antibody responses to immunization (10-11). As a consequence of these defects, children with DS usually experience an increased susceptibility to ARTIs and a prolonged course of respiratory infections that are also favored by DS-associated non-immunological factors, such as airways and ear anatomical abnormalities (12).

Pidotimod (3-L-pyroglutamyl-L-thiaziolidine-4carboxylic acid) is a synthetic dipeptide molecule with immunomodulatory properties; notably, *in vitro* and *in vivo* studies have shown that this compound has an immunomodulatory activity on both adaptive and innate immunity (13). Thus, Pidotimod induces dendritic cells (DCs) maturation, up-regulates the expression of HLA-DR and of co-stimulatory molecules CD83 and CD86, stimulates DCs to release pro-inflammatory molecules driving T-cell proliferation and differentiation towards a Th1 phenotype, enhances NK cell functions, and promotes phagocytosis (14-15). All these results notwithstanding, the effects of Pidotimod on immune responses are still not completely characterized; in particular, even if the efficacy of Pidotimod in reducing the rates of ARTIs in a population of children with DS was recently reported, the mechanisms associated with this effect were not examined (16).

In the attempt to shed light on the ability of Pidotimod to modulate immune responses, we analyzed immune parameters in DS children who received the seasonal 2011–2012 virosomal-adjuvanted influenza vaccine**.**

MATERIALS AND METHODS

A randomized controlled trial involving children with DS aged 3-10 years was designed. All children were enrolled in Winter 2011 through the Vivi Down Association in Milano, Italy. Vivi Down is a non-profit organization that supports individuals with DS and their families. All members with DS undergo a yearly complete clinical check-up.

Children having experienced ARTIs in the previous winter season and well being at the recruitment were considered as fulfilling the inclusion criteria. Having experienced therapy with immunostimulants in the preceding 6 months, use of an immunosuppressive regimen, being affected of immunological congenital or acquired diseases including viral infections such as measles, rubella and varicella within 6 months before the beginning of the study, ongoing antibiotic prophylaxis, congenital anatomical abnormalities of the respiratory tract, cystic fibrosis and previous adenotonsillectomy were considered as fulfilling the exclusion criteria.

The Ethics Committees of the Vivi Down Association approved the research protocol, and relatives of each individual enrolled in the study signed an informed consent.

Children were randomly assigned (1:1 ratio) to receive Pidotimod 400 mg, administered orally once a d for 90 d or placebo. Both compounds were identical in appearance and were presented in indistinguishable bottle.

At the recruitment (T0) all children underwent in-depth medical examinations and received a single dose of virosomal-adjuvanted influenza vaccine. Whole blood was collected in EDTA containing vacutainer tubes at T0 and 3 months after the recruitment (T3) in order to evaluate innate and adaptative immune responses pathway. Flu-specific IgG1 and IgG3 levels in plasma samples were determined at pre-vaccination (T0) , and 1 (T1) and 3 months (T3) post-vaccination.

Serological assays

Flu-specific IgG1 and IgG3 levels in plasma samples were measured by an ELISA method based on a wide range of synthetic peptides from the Influenza type A virus A/HK [A/Hong Kong/8/68-X-31 (H3N2)]. Samples were heat inactivated at 37°C for 1 h and therefore complement depleted. 96 well plates were coated overnight at 4°C with 100 µl of Influenza virus peptides diluted 1/250 in PBS. After washing the plates three times with Tween-20 0.1 % buffer (in PBS), plates were incubated for 2 h at 37°C 5% CO2 or 4°C for IgG1 and IgG3 detection, respectively, with PBS containing 3% of bovine serum albumin (BSA) (Sigma, St Louis, MO) to block non-specific protein binding sites. Plasma dilutions 1/10 to 1/100 were incubated for 2 h at 37°C, 5% CO2. Plates were then washed three times and a goat biotin-conjugated γ-chain specific anti-human IgG1 antibody (Sigma, St. Louise, MN) or a goat biotin-conjugated anti-human IgG3 antibody (Jackson Immuno-Research, West Grove, PA) was added to the plates diluted 1:2000 or 1:1000 in PBS/BSA, respectively. Following 1 h of incubation at 37°C, 5% CO_2, the plates were washed and incubated with HRP (horseradish peroxidase)-conjugated Streptavidin and tetramethylbenzidine (TMB, R&D Systems, Minneapolis, MN) substrate solution for 30 min at RT. The color reaction was stopped by adding H_2SO_4 2 N solution. The optical density was measured at an absorbance of $\lambda = 450$ nm and the concentrations of IgG1 or IgG3 were calculated from the established standard curve.

RNA extraction from PBMC

Whole blood was collected by venipuncture in Vacutainer tubes containing EDTA (Becton Dickinson),

and PBMC were separated on lymphocyte separation medium (Organon Teknica). RNA was extracted from PBMC at different time points using the acid guanidium thiocyanate–phenol–chloroform method, as previously described (17). The RNA was dissolved in RNase-free water, and purified from genomic DNA with RNase-free DNase (RQ1 DNase, Promega, Madison, Wisconsin, USA). One microgram of RNA was reverse transcribed into first-strand cDNA in a 20 µl final volume containing 1 µM random hexanucleotide primers, 1 µM oligo dT and 200 U Moloney murine leukemia virus reverse transcriptase (Promega, Madison, Wisconsin, USA).

Innate and adaptative immune responses pathway

Innate and Adaptative Immune Responses Pathway was analysed in a real-time PCR array including a set of optimized real-time PCR primers on 96-well plates (QUIAGEN, Crowley, UK). This approach permits to monitor mRNA expression of 96 genes involved in nearly all aspects of innate and adaptive immunity following the procedures suggested by the manufacturer. The experiments have been run on all of the subjects included in the study 90 days after Pidotimod/placebo administration, pooled according to the treatment. Thus, the results represent the mean value of the different targets analysed in each group. Furthermore, those targets showing marked differences between the two groups analyzed have been retested by real-time PCR on each individual sample confirming the data obtained in the array (data not shown). Reactions were performed using a SYBR Green PCR mix (RealMasterMix SYBR ROX, *5 PRIME,* Hamburg, Germany) and results were expressed as $^{\Delta\Delta}$Ct and presented as ratios between the target gene and the GAPDH and b-actin housekeeping mRNA.

Safety and tolerability of Pidotimod were also assessed: reports of adverse events, new-onset of medically significant conditions were gathered during the whole study period.

The study was conducted in accordance with the good clinical practices recommendations and ethical principles as explained and recommended in the Declaration of Helsinki.

RESULTS

Thirty-five children met the inclusion criteria for the study, however 17 caregivers refused to give consent to study enrollment. A final sample size of 18 children (4 females, 14 males) aged 3-10 years (mean age 7.1±2.6 years) were included in the study; 9 children received Pidotimod and 9 placebo. All children were compliant to the prescribed dose of Pidotimod.

Pidotimod was well tolerated in all subjects and no adverse events were reported during the whole study period.

Innate and adaptative immune responses genes expression levels

Innate and adaptive immune response gene expression levels were analyzed and compared between patients treated with Pidotimod or placebo 3 months post therapy initiation.

Data obtained 90 days post Pidotimod or placebo treatment showed that a number of genes involved in the generation of immune responses were significantly upregulated in the Pidotimod - compared to placebo-treated subjects (Fig. 1). Only those targets showing at least a 3-fold difference in the two groups were considered as those to be significantly modulated. Notably, the targets which were expressed at a higher transcriptional rate in pidotimod-treated patients control different aspects of both innate and adaptive immunity and include: TLR4, sensor of lipopolysaccharide from Gram-negative bacteria; S100-A12 which displays a regulatory effect on cytoskeletal components modulating various neutrophil activities; cAMP which shows antimicrobial activity including cell chemotaxis, immune mediator induction and inflammatory response regulation; CCL2 which displays chemotactic activity for monocytes and basophils; IL1RN which modulates a variety of interleukin 1 related immune and inflammatory responses; MIF, a lymphokine involved in cell-mediated immunity, immunoregulation, and inflammation; LTF an antimicrobial factor found in the secondary granules of neutrophils; and TNFRSF1A an activator of NF-kappaB, which mediates apoptosis, and functions as a regulator of inflammation.

Flu-specific IgG1 and IgG3 levels

Production of distinct isotype antibodies such as IgG1 and IgG3 is due to a different mechanism of immune system activation that leads to a prevalent synthesis of IL-4 or IFN-γ, respectively. The main effector functions of these two Ig isotypes are different as well, as IgG1 prevalently activates the complement cascade whereas IgG3 are considered

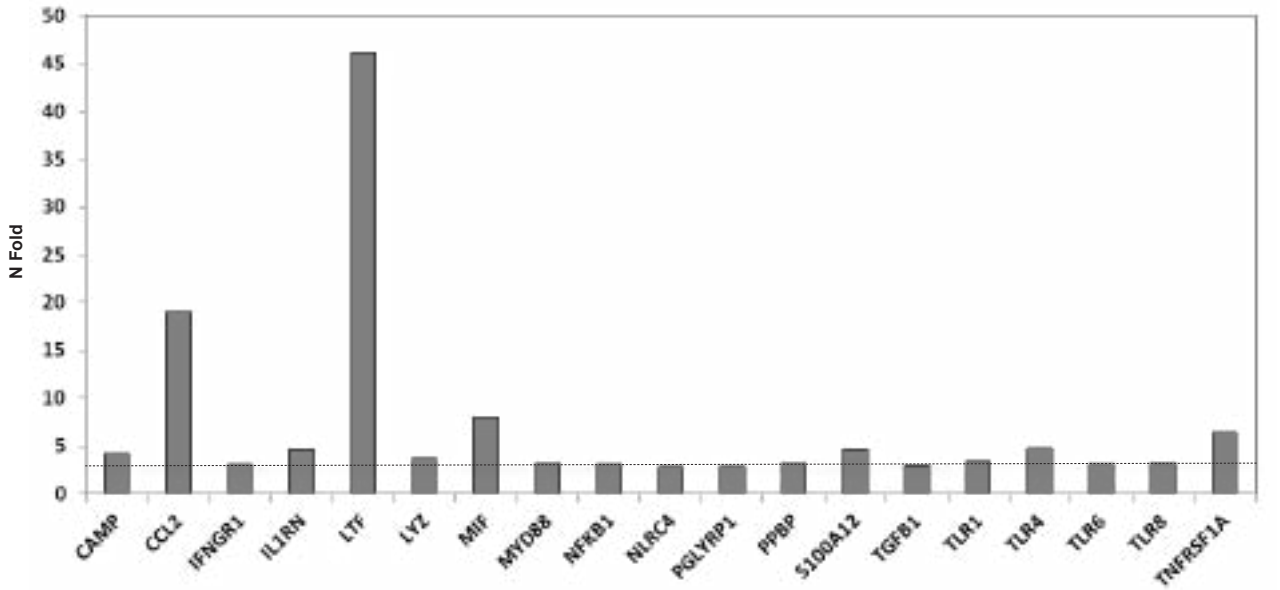

Fig. 1. *Innate and adaptive immune response gene expression levels in Pidotimod compared to control group 90 days post Pidotimod or placebo treatment. Only those targets showing at least a 3-fold difference between two groups are shown.*

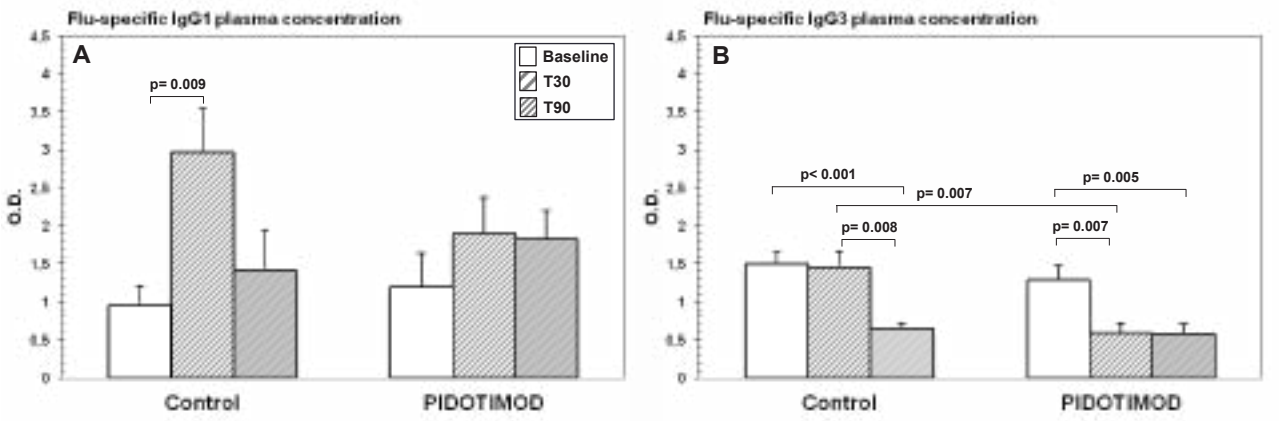

Fig. 2. *Flu-specific IgG1 (panel **A**) and IgG3 (panel **B**) plasma levels analysed at baseline and after 30 or 90 days of treatment. Mean values and standard error are shown. OD: optical density*

as better inducers of phagocytosis.

Plasma levels of Flu-specific IgG1 were increased in both the Pidotimod and the in control group 30 days after the immunization with the Flu vaccine; as compared to baseline these differences reached statistical significance for the control group (p=0.009). Increased plasma titers of Flu-specific IgG1 were seen as well 90 days after vaccination in both groups, even of the differences were not statistically significant (Fig. 2A). In contrast with these results, Flu-specific IgG3 were reduced 30 days after the immunization in both groups, with the differences being significant in Pidotimod-receiving children (p= 0.007); this effect was maintained at the 90 days time period (Fig. 2B).

DISCUSSION

The possible role of immunomodulants (IS) in preventing ARTIs in children is a heatedly debated

topic. Pidotimod was shown to have a beneficial effect in children reducing the number of ARTIs after treatment and, as consequence, decreasing the number of days of absence from kindergarten or school and the consumption of antibiotics and symptomatic drugs (18-20). However the heterogeneity of the included trials in terms of sample size, age of subjects recruited, confounding factors (e.g. concomitant asthma or allergy, number of siblings, smokers at home, seasons during the study, time and timing of attendance at daycare centre or school), duration of the intervention and misused statistical tests was high and the possibility of publication bias cannot be completely excluded. Further high-quality trials are required to confirm the true effect of IS and individual IS preparations in the prevention of ARTIs.

The ability of Pidotimod, a synthetic dipeptide molecule with immunomodulatory properties, to influence the immunogenicity of an influenza vaccine was analyzed in a group of children affected by DS, a genetic condition associated with mental retardation and immune defects.

Results showed that co-administration of the vaccine and Pidotimod, and supplementation with Pidotimod for an extended period resulted in a potentiation of immune responses and, in particular, in the strengthening of innate immunity. Thus, the use of Pidotimod induce a significant upregulation of genes involved in chemotaxis, antimicrobial activity, and inflammation. Thus, CCL2, a protein that chemoattracts numerous cell types including monocytes, neutrophils, and basophils, was upregulated by this compound. Notably, these later cells were also enhanced to produce antimicrobial compounds including, MIF and lactoferrin, as well as immune protein such as IL1RN, cAMP, and TNFRSF1A that play important roles in modulating the amplitude and the duration of inflammatory responses. These activities might have been optimally stimulated *via* a TLR4-mediated pathway, as was suggested by the observation that the transcription rate of this important innate immunity receptor was augmented as well in Pidotimod-receiving patients. These data, although preliminary, confirm that Pidotimod positively modulates innate immune responses, possibly resulting in a more effective control of the initial phases of infection.

As expected, vaccination resulted in an increase of antigen-specific antibodies; interestingly, the use of Pidotimod was possibly associated with the preferential stimulation of the generation of IgG1 vaccine-specific antibodies, as the IgG1/IgG3 ratio for these antibodies was skewed in Pidotimod-treated compared to control individuals. IgG1 and IgG3 are considered to be more indicative of Th2 and Th1 functionality, respectively. Notably, beside being preferentially correlated with Th1 and Th2 T cells subsets, IgG1 and IgG3 are also associated with the optimal activation of complement and phagocytosis by macrophages via ADCC, respectively. Results herein, thus suggest that this immunomodulator might favor the elimination of microorganisms via complement-associated mechanisms.

A limitation of our study was the relatively small sample size: the strict exclusion criteria of the study (children with DS are extremely prone to suffering with chronic diseases) and the little parental response contributed to reduce the number of eligible children. Moreover given to the small sample size the efficacy of Pidotimod in preventing ARTIs was impossible to be assessed.

In conclusion this study suggests that Pidotimod is indeed endowed with the ability to stimulate potentially beneficial innate and adaptive immune response *in vivo* and sustains its safety and tolerability in children; still further studies and a larger sample size are needed to evaluate clinical outcomes in DS affected children.

ACKNOWLEDGEMENTS

We thank Vivi Down Association, Cristiana Caprio and Silvia Fasan for their kind collaboration. We particularly extend our appreciation to the many parents and children without whose volunteerism this study would not have been possible.

REFERENCES

1. Del Rio Navarro BE, Espinosa Rosales F, Flenady V, Sienra Monge JJ. Immunostimulants for preventing respiratory tract infection in children. Cochrane Database Syst Rev 2006; 4:CD004974.
2. Cocchi G, Gualdi S. Prenatal diagnosis and Down Syndrome, 2004. ANNUAL Report 2006 with data

for 2004. Rome: International Clearinghouse for Birth Defects surveillance and Research 2006: 9-13. Anomalies ESoC. EUROCAT Website Database. University of Ulster, 2010, last update 03/04/2012.
3. Cruz NV, Mahmoud SA, Chen H, Lowery-Nordberg M, berlin K, Bahna SL. Follow up study of immune defects in patients with dysmorphic disorders. Ann Allergy Asthma Immunol 2009; 102:426-31.
4. Cossarizza A, Ortolani O, forti E, et al. Age-related expansion of functionally inefficient cells with markers of functionally inefficient cells with markers of natural killer activity in Down syndrome. Blood 1991; 77:1263-70.
5. Hing YC, van der Vossen PW, Gemen EF, Mulder AB, Hop WC, Brus F, de Vries E. Intrinsic abnormalities of lymphocyte counts in children witj Doen syndrome. J Ped 2005; 147:744-47.
6. Douglas SD. Down syndrome:immunologic and epidemiologic associations-Enigmas remain. J Ped 2005; 147:723-5.
7. Karttunen R, Nurmi T, Ilonen J, Surcell HM. Cell mediated immunodeficiency in Down syndrome: normal IL" production but inverted ratio of Tcell subsets. Clin Exp Immunol 1984; 55:257-63.
8. Franciotta D, Verri A, cardini E, Androni L, De Amici M, Moratti R, Nespoli L. Interferon-gamma and interleukin-4 producing T cells in Down syndrome. Neurosciences Letters 2006; 395:67-70.
9. Guazzarotti l, Trabattoni D, Castelletti E, et al. lymphocyte maturation is impaired in healthy young individuals carrying trisomy 21 (Down syndrome). Am J Intellect Dev Disabil 2009; 114:100-9.
10. Epstein L, Phillip R. Abnormalities in the immune response to influenza antigen in Down syndrome (trisomy 21). Prog Clin Biol Res 1987; 246:163-82.
11. Costa-Carvalho BT, Martinez RM, Dias AT, Kubo CA, Barros-Nunes P, Leiva L. Antibody response to pneumococcal capsular polysaccharide vaccine in Down syndrome patients. Braz J Med Biol Res 2006; 39:1587-92.
12. Ram G, Chinen J, Infections and immunodeficiency in Down syndrome. J Clin Exp Immunol 2001; 164:9-16.
13. Riboldi P, Gerosa M, Meroni PL. Pidotimod: a reappraisal. Int J Immunopathol Pharmacol 2009; 22:255-62.
14. Migliorati G, D'Adamio L, Coppi G, Nicoletti I, Riccardi C. Pidotimod stimulates natural killer cell activity and inhibits thymocyte cell death. Immunopharmacol Immunotoxicol 1992; 14:737-48.
15. Auteri A, Pasqui AL, Bruni F, Saletti M, Di Renzo M, Bova G Effect of Pidotimod, a new immunostimulating agent, on some aspects of immune response. In vitro study. Pharmacol Res. 1992; 26(S):196-7.
16. La Mantia I, Grillo C, Mattina T, Zaccone P, Xiang M, Di Mauro M, Meroni PL, Nicoletti F. Prophylaxis with the novel immunomodulator Pidotimod reduces the frequency and severity of upper respiratory tract infections in children with Down's syndrome. J Chemother 1999; 11:126-30.
17. Biasin M, Piacentini L, Lo Caputo S, et al. Apolipoprotein B mRNA-editing enzyme, catalytic polypeptide-like 3G: a possible role in the resistance to HIV of HIV-exposed seronegative individuals. J Infect Dis 2007; 195:960-4.
18. Burgio GR, Marseglia GL, Severi F, et al. Immunoactivation by Pidotimod in children with recurrent respiratory infections. Arzneimittelforschung 1994; 44:1525-9.
19. Careddu P, Mei V, Venturoli V, Corsini A. Pidotimod in the treatment of recurrent respiratory infections in paediatric patients. Arzneimittelforschung 1994; 44:1485-9.
20. Caramia G, Clemente E, Solli R, Mei V, Cera R, Carnelli V, Venturoli V, Corsini A. Efficacy and safety of Pidotimod in the treatment of recurrent respiratory infections in children. Arzneimittelforschung 1994; 44:1480-4.

LETTER TO THE EDITOR

INTERACTIONS AMONG PRO-INFLAMMATORY CYTOKINES, IGF SYSTEM AND THYROID FUNCTION IN PRE-PUBERTAL OBESE SUBJECTS

M.E. STREET[1], A. SMERIERI[1], L. MONTANINI[1], B. PREDIERI[2], L. IUGHETTI[2], M.VALENZISE[3], F. DE LUCA[3], M.C. VIGONE[4], G. WEBER[4], M. MAGHNIE[5] and S. BERNASCONI[1]

On behalf of the Italian study groups on growth, obesity, and thyroid disorders in childhood
[1]Department of Paediatrics, University Hospital of Parma, Parma, Italy; [2]Department of Paediatrics, University of Modena and Reggio-Emilia, Modena, Italy; [3]Department of Paediatrics, University of Messina, Messina, Italy; [4]Department of Paediatrics, Vita-Salute San Raffaele University, San Raffaele Scientific Institute, Milan, Italy; [5]Department of Paediatrics, IRCCS G. Gaslini, University of Genoa, Genoa, Italy

Received December 07, 2012 - Accepted January 29, 2013

Obesity is a state of chronic inflammation. Data on IGF system are often discrepant, and their relationships with mediators of inflammation are unknown. Furthermore, changes in thyroid function have been reported. We aimed at investigating the changes in these systems, and verify any relationships among cytokines, IGF system, thyroid function and insulin-insensitivity. Fifty obese pre-pubertal children, and 55 normal-weight subjects comparable for age and sex were enrolled. Serum IGF-I, IGF-II, IGFBP-1, IGFBP-2, IGFBP-3, IL-6 and TNF-α were assayed. In obese children insulin, TSH and FT4 were measured also, and the HOMA-IR index was calculated. Increased IGF-II, IL-6 and TNF-α, and decreased IGFBP-1 and IGFBP-2 concentrations were found in obese compared to normal-weight children. The IGF-I/IGFBP-3 molar ratio was also reduced in the obese subjects. In the obese children with high HOMA-IR index, IGFBP-1 and -2 serum concentrations were significantly decreased compared with those with normal insulin sensitivity, and in the obese subjects with increased TSH, IGFBP-2 concentrations were lower, and IGFBP-3 levels were higher compared to their counterparts with normal TSH levels. Among the significant correlations, BMISDS was correlated with IGF-II, and TSH. IGF-II concentrations showed a positive relationship with IL-6. TSH was correlated with IGFBP-2 also. The data showed interactions among IL-6, IGF system, insulin sensitivity, and thyroid function with changes being related to the degree of obesity. Chronic inflammation in obese children was confirmed. Some of the changes in the IGF system could be a consequence of insulin resistance and could account also for later complications in obese subjects.

Obesity is well recognised to date as a state of chronic inflammation, and data on IGF system peptides have been published but are often discrepant (1).

Cytokines are major regulators of adipose tissue metabolism, and adipocytes can synthesize tumour necrosis factor alpha (TNF-α), and interleukins (IL), notably IL-1 beta and IL-6 which are involved in

Key words: obesity, IGF-I, IGF-II, IGFBP-1, IGFBP-2, IGFBP-3, IL-6, TNF-α, TSH

Mailing Address: Maria E. Street, MD, PhD,
University Hospital of Parma,
Department of Paediatrics,
Via Gramsci, 14, 43100 Parma, Italy
Tel.: +39 0521 702723
Fax: +39 0521 702209
e-mail: mariaelisabeth.street@unipr.it

0393-974X (2013)

DISCLOSURE: ALL AUTHORS REPORT NO CONFLICTS OF INTEREST RELEVANT TO THIS ARTICLE.

the regulation of lipases, insulin stimulated glucose uptake, induction of apoptosis, regulation of cell size and de-differentiation (2).

With regard to the IGF system, insulin and IGFBP-3 have been reported to be significantly increased in children whereas IGF-I, free IGF-I, free IGF-I/total IGF-I and IGFBP-1 levels would not be significantly different from controls in some studies, while others reported significantly higher free IGF-I levels and normal or high total IGF-II levels (3). IGFBP-1 was reported both as suppressed, and increased (3).

Thyroid hormones are well known to be involved with control of energy homeostasis (4). In recent years changes in thyroid function have been reported in obese children (5).

Cytokine and growth factor interactions have been reported in recent years (6). Both cytokines and IGFs are related with the state of glucose tolerance. TNF-α, could reduce the function of the glucose transporter GLUT 4 (7), and studies have shown that IL-6 can interfere with insulin action (8). Furthermore, IGF-I serum concentrations seem to affect insulin sensitivity, and GH and IGF-I replacement seem to be capable of improving insulin sensitivity in diabetes (9).

Relationships among cytokines, IGF system, thyroid function and glucose metabolism have not been searched yet, as well as their possible clinical meaning in obese pre-pubertal subjects with respect to the development of later complications in adulthood.

The following study assessed changes in IGF system, IL-6, TNF-α, and thyroid function in obese pre-pubertal children compared with normal-weight healthy controls, and to assess relationships among these systems, and insulin sensitivity.

MATERIALS AND METHODS

Subjects

Fifty obese children (28 M, 22 F) above 5 years of age, and 55 normal-weight prepubertal subjects comparable for age and sex (29 M, 26 F) were enrolled in the study (Table I) from two different University Hospital settings in Italy (Modena and Messina). Normal-weight control subjects were a group of school children and scouts whose parents accepted to have their children measured at the paediatric endocrine clinic in Parma. All subjects were pre-pubertal and were enrolled consecutively. Children were defined as obese if their body mass index (BMI) was above the one indicated for age and sex by the IOFT criteria (10), and was also above the 90th centile according to the Italian reference data (11). Control subjects had a normal weight (BMI <75th centile) according to Italian reference data (11).

Endocrine disorders, chronic diseases and genetic syndromes or dysmorphic features were considered exclusion criteria. Coeliac disease, liver dysfunction, and diabetes were excluded by means of standard blood tests.

All obese children underwent thyroid function tests and had a normal thyroid ultrasound, and negative anti-thyroid antibodies.

At inclusion the following data were recorded in all subjects: gestational age, birth weight, family history of diabetes, obesity, hypertension, and dyslipidemia. All had normal birth weight and were term deliveries. Blood samples were taken just after the first visit, and therefore none of the obese subjects was yet on a standard diet nor on a standard exercise programme.

Auxological observations

Height (Ht) and weight were measured in all subjects using a Harpenden stadiometer , and an electronic scale, respectively. Ht and mid-parental height (MPHt) were expressed as standard deviation scores (SDS) using the Italian reference data (11).

BMI was calculated as weight/height^2 (Kg/m^2), and standardized according to the Italian (11) and to Cole's reference data (12). Auxological data of obese and normal-weight subjects are reported in Table I.

Biochemical assays

Blood was drawn after an overnight fast between 08:00 and 09:00 h in patients and controls. All patients were in good health at the moment of the study. Blood samples were centralized in Parma and Genoa.

Plasma glucose concentrations were assayed using a polarographic method (Synchron CX systems).

Insulin concentrations were measured using a chemiluminescence method by Diagnostic Products Corporation (Los Angeles, CA, USA) for reading by Immulite2000. The intra-assay CV was 6.5, the inter-assay CV 7.1%.

IGF-I was measured using an IRMA method (DSL-5600, Diagnostic System Laboratories, Inc. Webster, Texas, USA). The intra-assay coefficient of variation (CV) was 2.6%, and the inter-assay CV was 4.4%. Prior to assaying IGFBPs were precipitated by acid-ethanol extraction.

IGF-II was measured using an IRMA method (Diagnostic System Laboratories, Inc. Webster, Texas,

USA). The intra-assay and inter-assay CVs were 4.8 and 5.3%, respectively.

Total IGFBP-1 and IGFBP-3 were measured using IRMA methods (Diagnostic System Laboratories, Inc. Webster, Texas, USA). For IGFBP-1, the intra- and inter-assay CVs were 4.1 and 4.3 %, respectively. For IGFBP-3 the CVs were 2.9 and 1%, respectively.

IGFBP-2 was assayed using a RIA method (Diagnostic System Laboratories, Inc. Webster, Texas, USA). The intra-assay and inter-assay CVs were 6.4 and 6.3%, respectively.

To transform IGF-I, IGF-II, IGFBP-1, IGFBP-2 and IGFBP-3 from ng/mL to nmol/L we multiplied the single values by 0.131, 0.134, 0.035, 0.035 and 0.035 respectively. Molar ratios were subsequently calculated.

IL-6 was measured using an ultrasensitive ELISA method (Quantikine HS, R&D Systems, Minneapolis, MN, USA). The intra-assay and inter-assay CVs were 7.3 and 7.7%, respectively.

Serum TNF-α was measured using an ultrasensitive ELISA method (Biosource International Camarillo, CA, USA). The intra-assay and inter-assay CVs were 5.3 and 8.4%, respectively.

TSH was measured using a standard commercial kit (Immulite 2000; Diagnostic Products, Los Angeles, CA, USA).

FT4 was measured using a standard commercial kit (Immulite 2000; Diagnostic Products, Los Angeles, CA, USA).

Insulin resistance

From fasting glucose and insulin the homeostasis model assessment (HOMA)-IR, was calculated, according to the following formulas (13):

Homeostasis model assessment (HOMA)-IR: $\frac{G_0 \times I_0}{22.5}$

where G_0 and I_0 were basal fasting glucose and insulin, respectively. Glucose was expressed in mmoL/l and insulin in mIU/mL. An HOMA-IR index above 2.69 (97th centile) was considered abnormal, according to criteria for age and Tanner Stage 1 (14).

Ethical approval

Informed written consent was obtained from the parents as appropriate. The study was approved by the Ethical Committee of the University and Hospital of Parma.

Study design

The study was designed in order to compare obese and normal-weight prepubertal subjects, comparable for age, and sex. Differences were subsequently searched within the obese subjects considering two subgroups based on a normal or high HOMA-IR (> 97th centile) (27) as an index of insulin resistance, and in two subgroups based on normal and high TSH serum concentrations (normal range: 0.4-4.0 μU/mL).

Relationships among auxological observations, cytokines, IGF system peptides and thyroid function were then investigated in the group of obese subjects. Thyroid function was not measured in the control subjects at the moment of the study.

Statistical analysis

Statistical analysis was carried out using the SPSS package 17.0. Normal distribution of data was assessed by the Kolmogorov-Smirnov test. As no significant difference was detected in this series between males and females, subjects of both sexes were analysed together.

To analyze differences between obese and normal-weight subjects, and differences between subgroups of obese subjects we used Student's *t*-test for un-paired data. Non-parametric Spearman correlation test and Pearson's coefficient of correlation were used to measure associations between variables, as appropriate.

Data are expressed as mean±SEM unless otherwise stated. Only significant correlations are reported in the text.

RESULTS

Comparison between obese and normal-weight prepubertal subjects

IGF-I concentrations were lower, in obese children compared with normal-weight subjects (30.6±3.8 *vs* 49.2±9.7 nmol/L, P: 0.090, n.s.; Figure 1A).

IGF-II serum concentrations were increased in the obese compared with the normal-weight children (187.1±12.1 *vs* 150.2±9.1 nmol/L, P: 0.015, Figure 1B).

IGFBP-1 was lower in the obese compared with the normal-weight children (0.85±0.14 *vs* 1.77±0.38 nmol/L, P: 0.030, Figure 1C). Similarly, IGFBP-2 was also lower in the obese subjects (9.5±0.9 *vs* 15.4±1.7 nmol/L in normal-weight, P: 0.003, Figure 1D).

IGFBP-3 was similar in the obese subjects compared with the normal-weight children (181.9±8.3 *vs* 165.0±6.1 nmol/L, P: 0.102, n.s; Figure 1E).

The IGF-I/IGFBP-2 molar ratio was similar in the obese children compared with controls (3.22±0.41 *vs* 3.19±1.75, P: 0.240, n.s.) whereas the IGF-I/IGFBP-3 molar ratio was significantly lower in the

Table I. *Auxological data of obese and normal-weight prepubertal children, matched for sex and chronological age.*

	OBESE	NORMAL-WEIGHT
Number	50	55
(M/F)	(28 M / 22 F)	(29 M / 26 F)
Chronological Age (yr) (M/F)	10.16±0.63 / 8.24±0.67	9.40±0.41 / 9.42±0.42
Height SDS	1.42±0.17	1.12±0.16
Mid-parental height SDS	-0.57±0.44[a]	0.82±0.37
BMI (M/F)	30.49±1.05[a] / 31.75±1.36[a]	15.86±0.76 / 18.58±0.92
BMISDS (Cole)	3.53±0.12[a]	0.33±0.24
Birth weight (kg)	3.36±0.21	3.09±0.14

[a]*P<0.05 versus normal-weight subjects*

obese children (0.17±0.02 *vs* 0.30±0.06, P:0.007).

IL-6 was significantly increased in the obese children compared with the normal-weight (0.43±0.08 *vs* 0.17±0.08 IU/ml, P: 0.030, Figure 1F).

TNF-α was increased in the obese compared with the normal-weight children (0.20±0.08 *vs* 0.03±0.001 IU/ml, P: 0.027).

Comparison between obese children, based on insulin-resistance (HOMA index)

Twenty-one/50 obese (42%) subjects had an increased HOMA index, above the 97th centile for age and stage 1 of puberty (1.96±0.30 *vs* 4.43±0.35, n.s.).

Obese children with an increased HOMA index had lower IGFBP-1 (0.52±0.10 versus1.46±0.41 nmol/L, P: 0.060, n.s.) and IGFBP-2 concentrations compared with obese subjects with normal HOMA index (8.86±1.15 *vs* 13.91±1.43 nmol/L, P: 0.013).

The IGF-I/IGFBP-1, IGF-I/IGFBP-2 and IGF-II/IGFBP-1 molar ratios were also lower in the obese children with increased HOMA index (data not shown).

IGF-I, IGF-II, IGFBP-3, IL-6 and TNF-α serum concentrations were similar in the two subgroups based on the HOMA index.

Comparison between obese children, based on the TSH serum concentration

Fourteen out of 50 obese children had an increased TSH (28%) (5.30±0.22 *vs* 3.81±0.18 μU/ml). In this latter subgroup, IGFBP-2 concentrations were lower with respect to the group with normal serum TSH concentrations (7.02±1.08 versus 11.82±1.21 nmol/L, P: 0.02), whereas IGFBP-3 was increased (213.97±2.27 *vs* 172.35±7.77 nmol/L, P: 0.03).

IGF-I, IGF-II, IGFBP-1, IL-6 and TNF-α serum concentrations were similar in the two subgroups based on the TSH serum concentrations.

Correlation analysis

BMISDS was correlated with the IGF-II/IGFBP-1 molar ratio, IGF-II, IGFBP-1, HOMA index, and TSH (Table II).

Insulin levels were negatively correlated with IGF-I (R: -0.70; P: 0.002), and positively correlated with the IGF-II/IGFBP-1 molar ratio (R: 0.56; P: 0.020). Insulin was also negatively correlated with IGFBP-1 and IGFBP-2 (Table II). Relationships with indices of insulin sensitivity (HOMA) were

Table II. *Correlation coefficients(r) and P values of correlations between BMISDS, IGF system, thyroid function, insulin and HOMA index.*

PARAMETER	VARIABLE	r	P value
BMISDS	IGF-II/IGFBP-1 molar ratio	+0.47	0.044
	IGF-II	0.38	0.041
	IGFBP-1	-0.54	0.001
	TSH	+0.36	0.046
	HOMA index	+0.48	0.008
IGF-II	IL-6	+0.50	0.002
	IGFBP-1	+0.45	0.03
Insulin	IGFBP1	-0.61	0.0001
	IGFBP2	-0.39	0.052
HOMA index	IGF-II/IGFBP-1 molar ratio	+0.46	0.021
	IGF-I/IGFBP-2 molar ratio	+0.47	0.016
	IGFBP-1	-0.62	0.001
TSH	IGF-I	+0.65	0.001
	IGFBP-1	+0.52	0.005
	IGFBP-2	-0.46	0.03
	IGF-1/IGFBP-1 molar ratio	-0.56	0.046
	IGF-II/IGFBP-1 molar ratio	-0.43	0.057
FT4	IGF-II/IGFBP-2 molar ratio	-0.57	0.04
	IGFBP-2	0.72	0.005

found as expected (R: 0.78; P: 0.0001).

The HOMA index was correlated with positively with the IGF-II/IGFBP-1 and IGF-I/IGFBP-2 molar ratios, and negatively with IGFBP-1 serum concentration (Table II).

IGF-II concentrations showed a positive relationship with IL-6, and IGFBP-1 serum concentrations (Table II).

TSH levels were correlated also with IGF-I, IGFBP-1, IGFBP-2 , IGF-I/IGFBP-1, and IGF-II/IGFBP-1 molar ratios (Table II).

FT4 was negatively correlated with the IGF-II/IGFBP-2 molar ratio, and with IGFBP-2 (Table 2). No relationships with TNF-α were found.

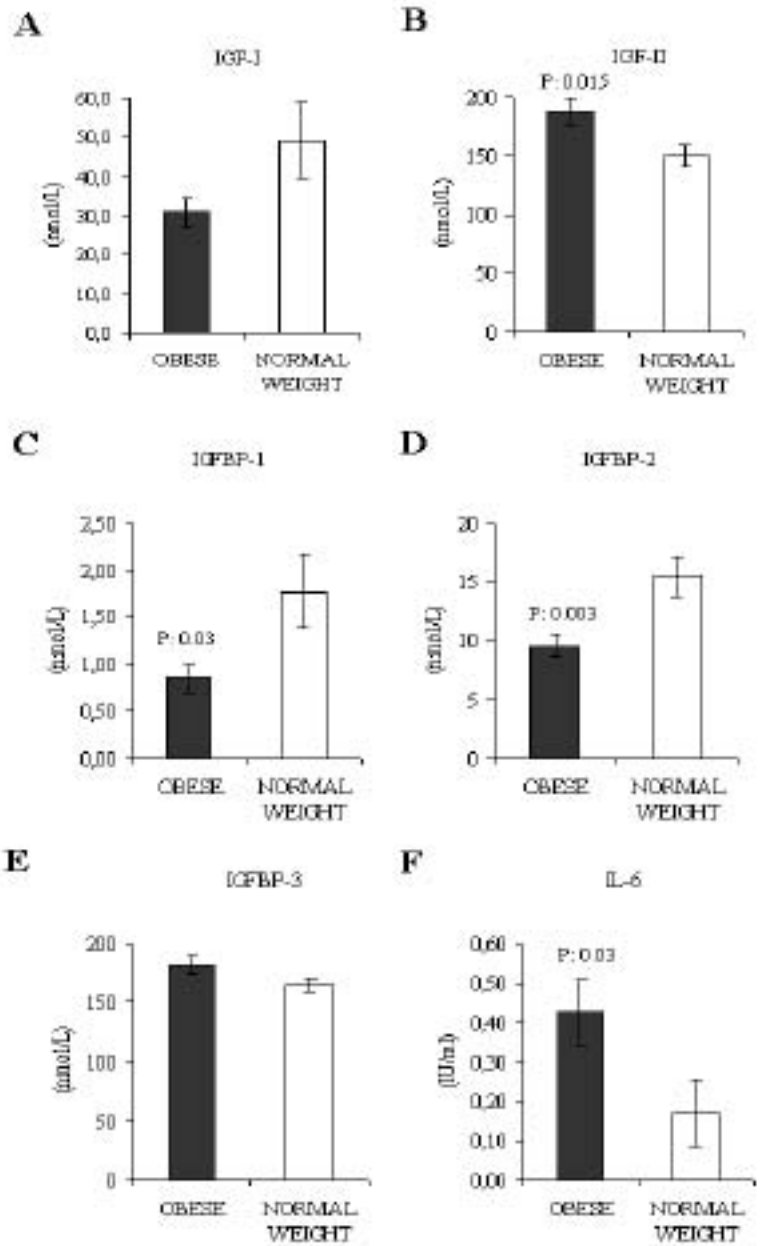

Fig. 1. *IGF-I (A), IGF-II (B), IGFBP-1 (C), IGFBP-2 (D), IGFBP-3 (E) and IL-6 (F) serum concentrations in obese and normal-weight prepubertal children matched for sex and age. Data are mean±SEM. Significant P values are reported in the figure (obese versus normal-weight subjects).*

DISCUSSION

Changes in the IGF system have been previously described in obese subjects, however, these studies evaluated only few peptides in the system (15). We described, in a homogeneous population, similar serum IGF-I concentrations compared with normal-weight, as in previous studies (15). The significantly reduced IGF-I/IGFBP-3 molar ratio stands in favour of reduced IGF-I bioavailability in obesity. We also described increased IGF-II serum concentrations as previously reported (15). This increase could be ascribed both to a compensatory mechanism, and to insulin resistance. Furthermore, the positive

relationship between IGF-II and IL-6 is of interest as it suggests that low grade chronic inflammation (2) could be responsible for the increase in IGF-II. This would confirm also previous published data showing interactions between inflammation and the IGF system (6). We did not find changes in IGFBP-3 concentrations at variance with one previous report (15). Few studies have described reduced IGFBP-2 serum concentrations as we find. Furthermore, we did not detect any correlations of IGFBP-2 with other IGFBPs and IGFs (15). The finding of decreased IGFBP-1 serum concentrations in obese children is in agreement with previously reported data (15). As expected, IGFBP-1 and IGFBP-2 showed negative relationships with insulin concentrations. The similar reduction in both IGFBP-1 and -2 could contribute to explain also the relative tall stature commonly observed in obese children as was seen also in our patients by modifying IGF bioavailability (Table 1). IGFBP-2 concentration is gaining increasing interest as studies using transgenic mice overexpressing IGFBP-2, have shown that this increase is associated with reduced susceptibility to obesity and improved insulin sensitivity (16). In addition, studies are looking at IGFBP-2 as a potential marker of metabolic and cardiovascular risk (17). The negative relationship between TSH and IGFBP-2 serum concentrations was an interesting finding in the light of recent advances on the understanding IGFBP-2 function in metabolism (18), however, is yet difficult to interpret. This study confirmed a direct relationship between TSH serum concentrations and BMI (19), and TSH was increased in 28% of obese subjects, as commonly reported in the Literature (20). Finally, attention should be drawn to IL-6 and TNF-α which were both increased in obese children confirming that inflammation is already present in childhood. In conclusion, childhood obesity is associated with changes in pro-inflammatory cytokine concentrations, IGF system peptides, and thyroid function. The correlations between these systems suggested active interactions and possible common links. Thyroid function changes were related with the degree of adiposity. The data supported the need for early intervention in childhood.

ACKNOWLEDGEMENTS

Grant support for this study was from the Department of Pediatrics, University of Parma, and from the the Ministry of Education and Research in Italy.

REFERENCES

1. Osborn O, Olefsky JM. The cellular and signalling networks linking the immune system and metabolism in disease. Nat Med 2012; 18:363-74.
2. Coppack SW. Pro-inflammatory cytokines and adipose tissue. Proc Nutr Soc 2001; 60:349-56.
3. Wabitsch M, Blum WF, Muche R, et al. Insulin-like growth factors and their binding proteins before and after weight loss and their associations with hormonal and metabolic parameters in obese adolescent girls. Int J Obes Relat Metab Disord 1996; 20:1073-80.
4. Iglesias P, Diez JJ. Influence of thyroid dysfunction on serum concentrations of adipocytokines. Cytokine 2007; 40:61-70.
5. Pacifico L, Anania C, Ferraro F, Andreoli GM, Chiesa C. Thyroid function in childhood obesity and metabolic comorbidity. Clin Chim Acta 2012; 413:396-405.
6. Street ME, Ziveri MA, Spaggiari C, et al. Inflammation is a modulator of the IGF-IGFBP system inducing reduced bioactivity of IGFs in Cystic Fibrosis. Eur J Endocrinol 2006; 154:1-7.
7. Stephens JM, Lee J, Pilch PF. Tumor necrosis factor-alpha-induced insulin resistance in 3T3-L1 adipocytes is accompanied by a loss of insulin receptor substrate-1 and GLUT 4 expression without a loss of insulin receptor-mediated signal transduction. J Biol Chem 1997; 272:971-6.
8. Klover PJ, Zimmers TA, Koniaris LG, Mooney RA. Chronic exposure to interleukin-6 causes hepatic insulin resistance in mice. Diabetes 2003; 52:2784-9.
9. Cusi K, DeFonzo R. Recombinant human insulin-like growth factor I treatment for 1 week improves metabolic control in type 2 diabetes by ameliorating hepatic and muscle insulin resistance J Clin Endocrinol Metab 2000; 85:3077-84.
10. Cole TJ, Bellizzi MC, Flegal KM, Dietz WH. Establishing a standard definition for child overweight and obesity worldwide: international survey. BMJ 2000; 320:1240-3.
11. Cacciari E, Milani S, Balsamo A, et al. Italian cross-sectional growth charts for height, weight and BMI (6-20yr). Eu J Clin Nutr 2002; 56:171-80.

12. Cole TJ. A chart to link child centiles of body mass index, weight and height. Eur J Clin Nutr 2002; 56:1194-9.
13. Uwaifo GI, Fallon EM, Chin J, Elberg J, Parikh SJ, Yanovski JA. Indices of insulin action, disposal, and secretion derived from fasting samples and clamps in normal glucose-tolerant black and white children. Diabetes Care 2002; 25:2081-7.
14. D' Annunzio G, Vanelli M, Pistorio A, et al. Insulin resistance and secretion indexes in healthy Italian children and adolescents: a multicentre study. Acta Biomed 2009; 80:21-8.
15. Argente J, Caballo N, Barrios V, et al. Multiple endocrine abnormalities of the growth hormone and insulin-like growth factor axis in pre-pubertal children with exogenous obesity: effect of short and long-term weight reduction. J Clin Endocrinol Metab 1997; 82:2076-83.
16. Wheatcroft SB, Kearney MT, Shah AM, et al. IGF-binding protein-2 protects against the development of obesity and insulin resistance. Diabetes 2007; 56:285-94.
17. De Kort SWK, van Doorn J, van de Sande AGM, Leunissen RWJ, Hokken-Koelega ACS. Serum Insulin-like growth factor-binding protein-2 levels and metabolic and cardiovascular risk factors in young adults and children born small for gestational age. J Clin Endocrinol Metab 2010; 95:864-71.
18. Sabin MA, Russo VC, Azar WJ, Yau SW, Kiess W, Werther GA. IGFBP-2 at the interface of growth and metabolism-implications for childhood obesity Pediatr Endocrinol Rev 2011; 8:382-93.
19. Radetti G, Kleon W, Buzi F, et al. Thyroid function and structure are affected in childhood obesity**.** J Clin Endocrinol Metab. 2008; 93:4749-54.
20. Stichel H, L'Allemand D, Gruters A. Thyroid function and obesity in children and adolescents. Horm Res 2000; 54:14-9.

LETTER TO THE EDITOR

INFLUENCE OF NIGHT-SHIFT AND NAPPING AT WORK ON URINARY MELATONIN, 17-β-ESTRADIOL AND CLOCK GENE EXPRESSION IN PREMENOPAUSAL NURSES

M. BRACCI[1], A. COPERTARO[2], N. MANZELLA[1], S. STAFFOLANI[1], E. STRAFELLA[1], L. NOCCHI[1], M. BARBARESI[2], B. COPERTARO[2], V. RAPISARDA[3], M. VALENTINO[1], and L. SANTARELLI[1]

[1]Occupational Medicine, Department of Clinical and Molecular Sciences, Polytechnic University of Marche, Ancona, Italy; [2]Healthcare Workers Service, ASUR area 2, Loreto Hospital, Loreto, Italy; [3]Section of Occupational Medicine, Department of Internal Medicine and Systemic Diseases, University of Catania, Catania, Italy

Received October 15, 2012 – Accepted February 6, 2013

Night-workers experience disruption of the sleep-wake cycle and light at night which may increase breast cancer risk by suppressing the nocturnal melatonin surge, resulting in higher levels of circulating estrogens. Night-work may also deregulate peripheral clock genes which have been found to be altered in breast cancer. This study investigated urinary 6-sulfatoxymelatonin (aMT6s), serum 17-β-estradiol levels in premenopausal shift nurses at the end of the night-shift compared to a control group of daytime nurses. Peripheral clock gene expression in lymphocytes were also investigated. All participants were sampled in the follicular phase of the menstrual cycle. The effect of nurses' ability to take a short nap during the night-shift was also explored. The shift-work group had significantly lower aMT6s levels than daytime nurses independently of a nap. Night-shift napping significantly influences 17-β-estradiol levels resulting in higher outcomes in nurses who do not take a nap compared to napping group and daytime workers. Peripheral clock genes expression investigated was not significantly different among the groups. Our findings suggest that shift nurses experience changes in aMT6s levels after a night-shift. Napping habits influence 17-β-estradiol levels at the end of a night-shift. These findings might be related to the increased cancer risk reported in night-shift workers and suggest that a short nap during night-shifts may exert a positive effect.

Shift-work involving night-shifts entails an occupational risk factor, since it induces a mismatch between the endogenous circadian clock and environmental synchronizers resulting in disrupted circadian rhythms and altered psycho-physiological functions. The International Agency for Research on Cancer (IARC) associated shift-work to breast cancer (1).

The circadian rhythm is kept by the suprachiasmatic nucleus (SCN), which regulates melatonin production and its release. The physiologic production of melatonin, the ''hormone of the dark'' follows a circadian rhythm that is heavily determined by day/night light exposure, with a peak of production in the middle of the night (between 2 and 5 am) and relatively low circulating levels during the day (2).

Key words: shift-workers, night-work, circadian rhythm, breast cancer, work schedule tolerance

Mailing address: Massimo Bracci, MD, PhD
Occupational Medicine, Department of Clinical and Molecular Sciences Polytechnic University of Marche
Via Tronto 10/a, 60020 Torrette, Ancona, Italy
Tel.: + 39 071 2206063
Fax: + 39 071 2206062
e-mail: m.bracci@univpm.it

0393-974X (2013)

DISCLOSURE: ALL AUTHORS REPORT NO CONFLICTS OF INTEREST RELEVANT TO THIS ARTICLE.

Melatonin modulates the secretion of hormones involved in carcinogenesis such as estrogens (3). Higher estrogen levels increase the risk of malignant transformation stimulating the turnover of mammary epithelial cells (4-5). The relation between melatonin, estrogens and light at night during night-work has been hypothesized as the following: exposure to light at night suppresses melatonin production and is paralleled by an increase in estrogen levels which may induce a higher breast cancer risk (4-6).

Exposure to artificial light at night and sleep-wake cycle alterations may affect not only the circadian rhythm kept by the SCN but also the intracellular clock of peripheral cells (7). Intracellular clocks consist of autoregulatory transcriptional-translational feedback loops that involve several genes (8). Since circadian clock genes are involved in cell proliferation, apoptosis and DNA damage response, defects in some core clock genes are associated with the risk of developing certain forms of malignancy such as breast cancer (9).

Some researchers have investigated the effects of night-shift napping as a night-shift countermeasure for the problem of sleepiness and fatigue in night-shift workers (10-11). According to these studies, night-shift napping could help to maintain circadian rhythms, and thereby have beneficial effects for worker's health. However, all the potential effects of nocturnal nap on circadian rhythms in shift nurses have not yet been investigated.

In this study we investigated nurses at the end of the night-shift to determine whether the shift nurses stratified according to the habit of night-shift napping showed alterations in variables related to breast cancer by evaluating urinary aMT6s, serum 17-β-estradiol and the expression of genes peripheral clock *BMAL1*, *NPAS2*, *CRY1, CRY2*, *PER2*, *PER3*, and *REVERBα* as compared to daytime nurses.

MATERIALS AND METHODS

Participants and sampling

A total of 184 registered female nurses working in NHS hospital wards in Ancona, Italy, underwent their periodic health monitoring between January and May 2011. Of these, 82 were shift-working (SW) nurses; from this group we recruited 31 nurses meeting the following criteria: fertile age, no current treatment with drugs, a negative history of psychiatric disorders, degenerative or cardiovascular disease, insomnia, chronic viral infections, tumor or autoimmune disease or conditions such as fibromatosis of the uterus and polycystic ovary. We also required nurses to have maintained the same assignment for at least two years without schedule breaks in the previous 6 months; nurses shift schedules involved at least 48 night-shifts/year; and no participant had experienced occupational exposure to ionizing radiation or involvement in antiblastic drug preparation. Among all nurses, 102 were daytime workers (DT) with a work schedule from 7:00 am to 2:00 pm. Only 56 DT nurses met the selection criteria of the SW nurses and had habitual sleep/wake schedule approximately between 23:00 pm and 6:00 am, and no episodes of sleep deprivation for at least 3 weeks prior to the study. Out of 56 DT nurses we randomly selected 31 nurses as control group.

A critical point in the studies about shift workers is represented by the different definitions used to select shift workers which led the IARC to convey a working group in 2009 to establish how to define night work (12). In accordance with this criteria the shift-work of the 31 SW nurses can be defined as a *"*clockwise rapidly rotating*"* type and the schedule was as follows: Day 1: 07:00 am-2:00 pm; Day 2, 02:00 pm -10:00 pm; Day 3: 10:00 pm - 07:00 am; 48 h of rest; resumption of the cycle.

The study was conducted in accordance with the Declaration of Helsinki's ethical standards. Being part of the standard occupational health surveillance it needed no formal approval by the local ethics committee, which was nevertheless consulted and which granted an informal authorization. Subjects gave their written informed consent to participate in the study.

Sampling was conducted at 7:00 am, i.e. at the beginning of the day nurses' shift. After sample collection participants filled in a questionnaire enquiring into their work schedule (including the opportunity of taking a short nap during night-shifts), reproductive physiology, physical exercise and other habits such as smoking and alcohol consumption.

SW nurses were further stratified into those who did/did not take a short nap with lights off or dimmed during the night-shift.

Urine and blood samples were collected between the 2nd and 5th day of the menstrual cycle (follicular phase), when stable estrogen levels enable comparisons between groups (13-14). The urine sampled was produced by the participants between the hours of 11:00 pm to 7:00 am and was collected in a container by the participants during the whole temporal interval. After delivery to the laboratory urine samples were stored at −80°C until melatonin and creatinine analysis.

Fasting blood samples (8 h) were drawn at 7.00 am and processed immediately after collection; they were

divided into two aliquots, one for serum 17-β-estradiol quantification and another for immediate lymphocyte separation, then stored at −80°C until RNA extraction.

Hormone assay

aMT6s was assayed using DRG Melatonin-Sulfate (DRG International Inc., Mountainside, USA), a commercially available solid-phase competitive ELISA kit. Variations in urine diluteness were adjusted by expressing aMT6s levels as ng of aMT6s per mg of urinary creatinine (aMT6s concentration divided by the creatinine concentration). Creatinine was measured using the Urinary Creatinine Detection Kit (Arbor Assays, Ann Arbor, USA).

Quantification of 17-β-estradiol was performed by an enzyme-linked fluorescent assay (SA, Marcy- l'Étoile, France) according to the manufacturer's instructions. All samples were measured in duplicate.

Expression of clock genes

Immediately after blood sampling, lymphocytes were isolated using a density gradient separation medium (Cedarlane Laboratories LTD, Hornby, Ontario, Canada) and stored at -80°C until RNA extraction.

The Isolation of total RNA was performed using the Vantage Total RNA Purification Kit (Origene, Rockville, USA) according to the manufacturer's instructions. RNA quality and quantification were evaluated with a Nanodrop 1000 spectrophotometer (Thermo Scientific, Wilmington, USA).

cDNA was synthesized according to the High-Capacity cDNA Reverse Transcription Kit protocol (Applied Biosystems, Foster City, USA).

Gene expression was analyzed by real-time quantitative PCR using the TaqMan Gene Expression Master Mix (Applied Biosystems, Foster City, USA). Specific primer sets were obtained from IDT (Integrated DBA Technologies Inc., Coralville, USA). To control for variation in the amount of cDNA available for PCR in the different samples, the gene expression levels of the target sequences were normalized to the expression of an endogenous control, glyceraldehyde-3-phosphate dehydrogenase (*GAPDH*).

The expression levels of clock genes were calculated as a ΔCt, where high ΔCt value corresponds to low gene expression.

Statistical analysis

Since quantitative variables were not normally distributed, a non-parametric approach was chosen. The Kruskal–Wallis one-way analysis of variance and the Wilcoxon-Mann-Whitney test were used to test differences among DT and SW nurses, and SW nurses napping or not napping during night-shifts. The *chi*-square test was used to test dichotomous or categorical parameters. Spearman's rho correlation test was applied to analyze relationships between continuous parameters. Multivariate linear regression analysis corrected for possible confounding variables was used to assess aMT6s, 17-b-estradiol and clock gene expression in the different groups. Statistical significance was set at $P<0.05$. The SPSS 15 statistical software package (SPSS Inc., Chicago, USA) was used for all calculations.

RESULTS

The socio-demographic characteristics of the 62 participants are reported in Table I. SW nurses were significantly younger, had lower job seniority, fewer children, and engaged to a greater proportion in physical exercise compared with DT nurses. However, the two groups did not differ in body mass index (BMI), prevalence of metabolic syndrome, alcohol consumption, cigarette smoking, menstrual cycle regularity, or number of miscarriages.

Among SW nurses 17 (54.8%) did not take a nap during the night-shift, either because they did not feel the need for one or because of lack of opportunity, whereas the other 14 did take a short (<60 min) nap if they managed, with the lights off or dimmed (<200 Lux). The two subgroups of SW nurses had significantly different age, BMI, physical exercise and smoking habits.

Results showed urinary aMT6s was significantly lower and serum 17-β-estradiol was higher, but not significantly, in SW nurses compared with DT nurses (Fig. 1). The relation between aMT6s and shift-work was investigated by multiple linear regression analysis with age, physical exercise and offspring as covariates. The results confirmed an effect of shift-work on aMT6s ($\beta=-0.321$, $p<0.05$).

In the crude analysis of circadian gene expression we observed significant up-regulation of *PER2* and *PER3* mRNA expression in SW nurses compared to DT nurses (Table II). However, when we adjusted *PER* gene expression for significant confounding factors such as age, job seniority, physical exercise and offspring, the association between rotating shift work and circadian gene expression disappeared.

Results also showed that no napping SW nurses did not have different aMT6 levels, but did have significantly higher serum 17-β-estradiol levels and

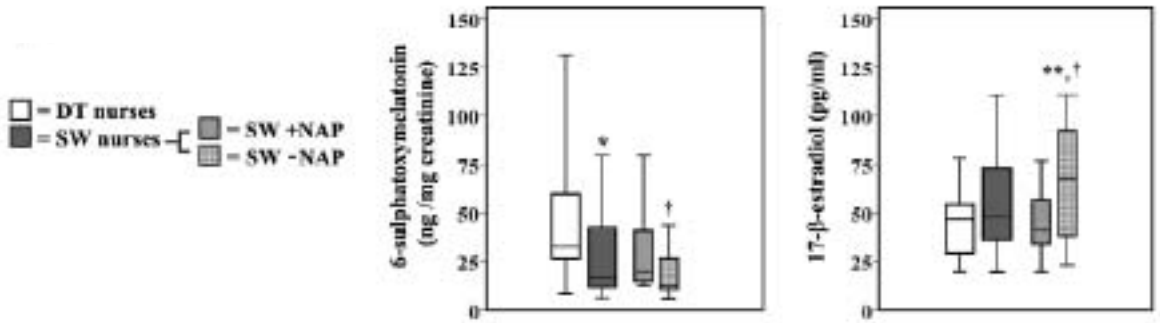

Fig. 1. *Levels of 6-sulphatoxymelatonin (aMT6s), 17-β-estradiol of daytime (DT) and shift-working (SW) nurses who did (+NAP) and did not (-NAP) take a short nap during the night-shift. * SW vs DT nurses; ** SW -NAP vs SW +NAP nurses; † SW -NAP vs DT nurses, P< 0.05*

Table I. *Socio-demographic characteristics of daytime (DT) and shift-working (SW) nurses who did (+NAP) and did not (-NAP) take a short nap during the night-shift.*

	DT nurses	SW nurses	SW +NAP nurses	SW -NAP nurses
Age (years): median (25^{th}–75^{th} percentile)	40.0 (38.0-46.0)	37.0 (35.0-41.0)*	39.0 (36.0-45.0)	36.0 (30.0-40.0)**, †
Job seniority (years): median (25^{th}–75^{th} percentile)	18.0 (16.0-25.0)	14.0 (9.5-18.0)*	16.5 (13.0-20.0)	12.5 (7.5-15.3) †
Shift-work seniority (years): median (25^{th}–75^{th} percentile)	-	13.0 (9.0-17.0)	16.0 (11.8-17.5)	12.0 (7.0-15.0)
BMI: median (25^{th}–75^{th} percentile)	23.4 (21.8-25.8)	22.0 (20.4-28.3)	23.5 (21.4-29.5)	21.5 (19.9-23.4)**, †
Incidence of metabolic syndrome (%)	6.5	9.7	14.3	6.7
Subjects taking physical exercise (%)	48.4	75.8	71.4	19.1**
Physical exercise (days/week): median (25^{th}–75^{th} percentile)	1.0 (.0-2.0)	2.0 (.8-3.0)*	2.0 (.0-3.0)	2.0 (.8-2.3)
Alcohol drinkers (%)	35.5	32.3	14.3	40.0
Smokers (%)	38.7	45.2	21.4	66.7**
Smoking habit among smokers (no. cigarettes/day): median (25^{th}–75^{th} percentile)	8.5 (5.3-15.0)	5.0 (1.0-10.0)	10.0 (8.0-15.0)	10.0 (5.0-12.5)
Irregular menstrual cycle (%)	51.6	54.8	42.9	60.0
With offspring (%)	87.1	38.7*	71.4	53.8
Miscarriages (%)	16.1	19.4	28.6	13.3

** SW vs DT nurses; ** SW -NAP vs SW +NAP nurses; † SW -NAP vs DT nurses, P<0.05*

PER3 expression compared to napping SW nurses; napping SW nurses show 17-β-estradiol and *PER3* expression levels similar to DT nurses.

In the multiple linear regression analysis adjusted for age, BMI, physical exercise and smoking, night-shift napping was confirmed to affect 17-β-estradiol

Table II. *Levels of clock genes expression of daytime (DT) and shift-working (SW) nurses who did (+NAP) and did not (-NAP) take a short nap during the night-shift.*

	DT nurses	SW nurses	SW +NAP nurses	SW -NAP nurses
BMAL **(ΔCt):** median (25^{th}–75^{th} percentile)	5.30 (4.43-6.41)	4.14 (3.07-5.69)	4.30 (3.62-6.79)	3.99 (2.68-5.65)
NPAS2 **(ΔCt):** median (25^{th}–75^{th} percentile)	5.97 (4.75-7.09)	6.21 (4.47-7.40)	6.21 (4.47-7.54)	6.14 (3.83-7.25)
PER2 **(ΔCt):** median (25^{th}–75^{th} percentile)	7.45 (6.62-8.00)	6.32 (5.97-7.21)*	6.14 (5.17-6.93)	6.32 (6.07-8.21)
PER3 **(ΔCt):** median (25^{th}–75^{th} percentile)	7.05 (5.77-7.42)	5.62 (4.89-7.21)*	6.98 (5.30-7.28)	4.99 (3.94-6.58)**, †
CRY1 **(ΔCt):** median (25^{th}–75^{th} percentile)	4.61 (3.21-5.74)	3.95 (3.12-5.35)	4.93 (3.64-6.00)	3.25 (2.46-4.64)
CRY2 **(ΔCt):** median (25^{th}–75^{th} percentile)	3.91 (2.32-4.55)	3.23 (1.87-4.49)	3.09 (2.11-4.83)	4.55 (1.62-4.43)
REVERBα **(ΔCt):** median (25^{th}–75^{th} percentile)	4.83 (2.51-5.36)	3.47 (2.14-5.00)	3.47 (2.03-4.96)	3.50 (2.08-4.62)

High ΔCt value corresponds to low gene expression.
** SW vs DT nurses; ** SW -NAP vs SW +NAP nurses; † SW -NAP vs DT nurses, P<0.05*

(β=-0.496 p<0.05) but not *PER3* expression although the significance was borderline (β=0.477, p=0.06).

As shown in Table III, *PER2*, *PER3* and *CRY2* expression and age correlated positively; *BMAL* and *PER3* expression correlated negatively with physical exercise. *PER2* and *PER3* expression correlated positively with smoking habits. All the clock genes examined correlated significantly with one another in all participants.

DISCUSSION

The findings of this study are consistent with the hypothesis that women who work on rotating night-shifts experience changes in melatonin and estrogens levels that may be associated with the increased cancer risk observed among night-shift workers (15-20). Night-shift napping results in lower 17-b-estradiol levels and thereby may have beneficial effects on worker's health.

Specifically, urinary aMT6s was lower in SW than in DT nurses and night-shift napping did not influence it; however the nap taken by nurses in our sample may have been too short to yield significant differences in aMT6s levels.

The role of age and physical exercise in promoting a reduction in melatonin production is controversial (21-24). We found no correlation between age or physical activity and aMT6s levels. Although alcohol consumption may induce a melatonin reduction (25), we found no evidence for it, possibly in relation to the low amount of alcohol consumed by participants (data not shown). Melatonin levels were not related to smoking habits according to previous evidences (26). Our data also evidenced no correlation between aMT6s levels and job seniority.

Despite the absence of significant differences in serum 17-β-estradiol levels between SW and DT nurses, the stratification of SW nurses by the night-shift napping habit highlighted significantly higher levels in SW without napping behavior. The levels of 17-β-estradiol found in napping SW nurses were similar to those found in DT nurses. Sleep times have been reported to affect estrogen production (27-

Table III. *Spearman rank-order correlation (Rho) between the variables examined in all participants.*

	aMT6s	**17-β-estradiol**	***BMAL***	***NPAS2***	***PER2***	***PER3***	***CRY1***	***CRY2***	***REVERBα***
Age	0.06	0.21	0.24	-0.09	**0.34***	**0.37***	0.22	**0.32***	0.21
BMI	-0.24	-0.11	0.04	0.11	-0.13	0.11	0.18	0.05	0.07
Shift-work seniority	-0.12	0.18	0.04	-0.02	-0.06	0.07	0.07	0.17	0.06
Physical exercise	-0.48	0.10	**-0.42***	0.11	0.01	**-0.29***	-0.23	-0.24	-0.12
Smoking habit	-0.19	0.01	0.44	-0.78	**0.53***	**0.52***	0.21	0.36	0.20
aMT6s	1	0.05	0.01	0.15	-0.10	-0.99	-0.82	-0.62	-0.19
17-β-estradiol	0.05	1	0.03	-0.26	0.25	0.12	0.05	0.12	0.01
BMAL	0.02	0.03	1	**-0.48***	**0.41***	**0.82***	**0.82***	**0.80***	**0.68***
NPAS2	0.15	-0.26	**-0.48***	1	**-0.44***	**-0.41***	**-0.43***	**-0.47***	**-0.52***
PER2	-0.10	0.25	**0.41***	**-0.44***	1	**0.46***	**0.35***	**0.32***	**0.38***
PER3	-0.99	0.12	**0.82***	**-0.41***	**0.46***	1	**0.83***	**0.72***	**0.62***
CRY1	-0.82	0.53	**0.82***	**-0.43***	**0.35***	**0.83***	1	**0.84***	**0.70***
CRY2	-0.62	0.12	**0.80***	**-0.47***	**0.32***	**0.72***	**0.84***	1	**0.81***
REVERBα	-0.19	0.01	**0.68***	**-0.52***	**0.38***	**0.62***	**0.70***	**0.81***	1

** P<0.05*

28); our findings suggest that a short nap during the night-shift could partly offset the potential endocrine imbalance induced by night-work.

Exposure to light and alteration of the sleep-wake cycle also seems to affect the expression of peripheral clock genes (7-8). In a univariate analysis our study reported a significantly greater expression of the *PER* genes in the SW nurses compared to the DT group in line with previous investigations (29); no napping nurses showed higher levels of *PER3* gene expression compared to napping nurses. The inclusion of age among the confounding factors in the multivariate analysis, resulted in the loss of significance for both shift-work and night-shift napping; however the significance of the night-shift nap effect on *PER3* expression was borderline (p=0.06) therefore a possible effect of night-shift napping is not to be excluded.

The analysis of participants' socio-demographic characteristics showed some significant differences among groups; specifically SW nurses were significantly younger, had lower job seniority, engaged more often in physical exercise, and had fewer children. However these findings were expected, since older nurses with greater job seniority tend to be assigned to daytime work by hospital management (30-31). The greater proportion of SW nurses taking exercise may be related to their younger age and to a work schedule enabling a better organization of leisure time. However the parameters resulted statistically different among groups were included in the multivariate analysis as covariates.

The study is limited by the small sample size but this limitation is an inevitable consequence of the stringent and accurate inclusion criteria of participants and the timing of sampling. In fact all participants had to be in first days of follicular phase of menstrual cycle and in particular, night-shift nurses had to be in this menstrual phase at the end of a night-shift. The numerous inclusion criteria limited the number of participants but constituted the necessary conditions to obtain comparable results. Our results refer to the end of the night-shift and should be considered in association with the specific work schedule of our nurses' groups since another time of sampling or type of shift-work may result in different findings.

In conclusion this study suggests that nurses employed in rotating shift-work undergo changes in aMT6s levels after night-shifts. Lack of night-shift napping results in higher 17-β-estradiol levels therefore napping during the night-shift should be encouraged, when manageable.

Since melatonin and 17-β-estradiol deregulation are associated with increased risk for breast carcinoma, the findings of this study need careful consideration but also further investigation in larger samples.

ACKNOWLEDGEMENTS

This study was in part supported by grants from the Italian Institute of Insurance against Professional illness and Injuries (INAIL). The authors thank Mrs. Megan Conner for kindly revising the English language.

REFERENCES

1. IARC Working Group on the Evaluation of Carcinogenic Risks to Humans. Painting, firefighting, and shiftwork. IARC Monogr Eval Carcinog Risks Hum 2010; 98:9-764.
2. Czeisler CA, Duffy JF, Shanahan TL, et al. Stability, precision, and near-24-hour period of the human circadian pacemaker. Science 1999; 284:2177-81.
3. Cos S, González A, Martínez-Campa C, Mediavilla MD, Alonso-González C, Sánchez-Barceló EJ. Melatonin as a selective estrogen enzyme modulator. Curr Cancer Drug Targets 2008; 8:691-702.
4. Costa G, Haus E, Stevens R. Shift work and cancer - considerations on rationale, mechanisms, and epidemiology. Scand J Work Environ Health 2010; 36:163-79.
5. Nelson R. Steroidal oestrogens added to list of known human carcinogens. Lancet 2002; 360:2053.
6. Stevens RG. Working against our endogenous circadian clock: Breast cancer and electric lighting in the modern world. Mutat Res 2009; 680:106-8.
7. Franken P, Dijk DJ. Circadian clock genes and sleep homeostasis. Eur J Neurosci 2009; 29:1820-9.
8. Reppert SM, Weaver DR. Coordination of circadian timing in mammals. Nature 2002; 418:935-41.
9. Rana S, Mahmood S. Circadian rhythm and its role in malignancy. J Circadian Rhythms 2010; 8:3.
10. Takeyama H, Kubo T, Itani T. The nighttime nap strategies for improving night shift work in workplace. Ind Health 2005; 43:24-9.
11. Ribeiro-Silva F, Rotenberg L, Soares RE, et al. Sleep on the job partially compensates for sleep loss in night-shift nurses. Chronobiol Int 2006; 23:1389-99.
12. Stevens RG, Hansen J, Costa G, et al. Considerations of circadian impact for defining 'shift work' in cancer studies: IARC Working Group Report. Occup Environ Med 2011; 68:154-62.
13. Small CM, Marcus M, Sherman SL, Sullivan AK, Manatunga AK, Feigelson HS. CYP17 genotype predicts serum hormone levels among pre-menopausal women. Hum Reprod 2005; 20:2162-7.
14. Eliassen AH, Missmer SA, Tworoger SS, Spiegelman D, Barbieri RL, Dowsett M, Hankinson SE. Endogenous steroid hormone concentrations and risk of breast cancer among premenopausal women. J Natl Cancer Inst 2006; 98:1406-15.
15. Schernhammer ES, Laden F, Speizer FE, Willett WC, Hunter DJ, Kawachi I, Colditz GA. Rotating night shifts and risk of breast cancer in women participating in the nurses' health study. J Natl Cancer Inst 2001; 93:1563-8.
16. Schernhammer ES, Rosner B, Willett WC, Laden F, Colditz GA, Hankinson SE. Epidemiology of urinary melatonin in women and its relation to other hormones and night work. Cancer Epidemiol Biomarkers Prev 2004; 13:936-43.
17. Davis S, Mirick DK, Stevens RG. Night shift work, light at night, and risk of breast cancer. J Natl Cancer Inst 2001; 93:1557-62.
18. Hansen J. Risk of breast cancer after night- and shift work: current evidence and ongoing studies in Denmark. Cancer Causes Control 2006;17:531-7.
19. Franzese E, Nigri G. Night work as a possible risk factor for breast cancer in nurses. Correlation between the onset of tumors and alterations in blood melatonin levels. Prof Inferm 2007; 60:89-93.
20. Leonardi GC, Rapisarda V, Marconi A, et al. Correlation of the risk of breast cancer and disruption of the circadian rhythm (Review). Oncol Rep. 2012; 28:418-28.
21. Skrinar GS, Bullen BA, Reppert SM, Peachey SE, Turnbull BA, McArthur JW. Melatonin response to exercise training in women. J Pineal Res 1989; 7:185-94.
22. Kennaway DJ, Lushington K, Dawson D, Lack L, van den Heuvel C, Rogers N. Urinary 6-sulfatoxymelatonin excretion and aging: new

results and a critical review of the literature. J Pineal Res 1999; 27:210-20.
23. Zeitzer JM, Daniels JE, Duffy JF, Klerman EB, Shanahan TL, Dijk DJ, Czeisler. Do plasma melatonin concentrations decline with age? Am J Med 1999; 107:432-436.
24. Escames G, Ozturk G, Baño-Otálora B, et al. Exercise and melatonin in humans: reciprocal benefits. J Pineal Res 2012; 52:1-11.
25. Stevens RG, Davis S, Mirick DK, Kheifets L, Kaune W. Alcohol consumption and urinary concentration of 6-sulfatoxymelatonin in healthy women. Epidemiology 2000; 11:660-5.
26. Grundy A, Sanchez M, Richardson H, Tranmer J, Borugian M, Graham CH, Aronson KJ. Light intensity exposure, sleep duration, physical activity, and biomarkers of melatonin among rotating shift nurses. Chronobiol Int 2009; 26:1443-61.
27. Merklinger-Gruchala A, Ellison PT, Lipson SF, Thune I, Jasienska G. Low estradiol levels in women of reproductive age having low sleep variation. Eur J Cancer Prev 2008; 17:467-72.
28. Nagata C, Nagao Y, Yamamoto S, Shibuya C, Kashiki Y, Shimizu H. Light exposure at night, urinary 6-sulfatoxymelatonin, and serum estrogens and androgens in postmenopausal Japanese women. Cancer Epidemiol Biomarkers Prev 2008; 17:1418-23.
29. Ando H, Ushijima K, Kumazaki M, et al. Influence of age on clock gene expression in peripheral blood cells of healthy women. J Gerontol A Biol Sci Med Sci 2010; 65:9-13.
30. Copertaro A, Bracci M, Barbaresi M, Santarelli L. Assessment of cardiovascular risk in shift healthcare workers. Eur J Cardiovasc Prev Rehabil 2008; 15:224-9.
31. Hasselhorn HM, Tackenberg P, Muller BH. Working conditions and intent to leave the profession among nursing staff in Europe. Working Life Research Report 7. Stockholm: National Institute for Working Life 2003.

LETTER TO THE EDITOR

ANTIPROLIFERATIVE EFFECTS OF 5-FLUOROURACIL AND OXALIPLATIN IN COLON CANCER CELL LINES: COMPARISON OF THREE DIFFERENT CYTOTOXICITY ASSAYS

A. FAILLI[1], A. LEGITIMO[1], G. ORSINI[2], M. CASTAGNA[3], R. SPISNI[2], P. MICCOLI[2] and R. CONSOLINI[1]

[1]Department of Reproductive Medicine and Child Development, Division of Pediatrics, Laboratory of Immunology, University of Pisa, Pisa, Italy; [2]Department of Surgery, University of Pisa, Pisa, Italy; [3]Section of Pathology III, Department of Surgery, University of Pisa, Pisa, Italy

Received September 29, 2011 – Accepted April 2, 2012

The first two authors contributed equally to this work

Adjuvant therapy in colorectal cancer has evolved to become the standard of care, whereas the tumor capability of activating effective mechanisms of defence against both chemical and physical cytotoxic agents represents a serious obstacle to the successful therapy of human tumors. Therefore, the possibility to have an assay useful to measure the drug sensitivity of tumor cells has a great importance. A number of cytotoxicity assays are currently available, each of them using a specific approach to detect different aspects of cell viability, such as cell integrity, proliferation and metabolic functions. The purpose of this study is to compare, under identical experimental conditions, three common cytotoxicity assays (ATP-lite, MTT and CCK-8 assays) in the assessment of the anti-proliferative effects of 5-fluorouracil (5-FU) and oxaliplatin (OHP) on three colon cancer cell lines (WiDr, SW620 and HT-29). Regarding 5-FU, the three assays were found to be significantly correlated with a moderate or high correlation coefficient, whereas in the case of OHP we found different outcomes among the assays. Our study demonstrates that the CCK-8 is the most sensitive assay for detecting changes of cell viability, suggesting that the viability measured in cells after drug exposure depends on several parameters like the drug used, the biological characteristics of the target cell and the specific approach employed by the method to detect distinct cell growth and metabolic functions.

Adjuvant therapy in colorectal cancer has evolved to become the standard of care, whereas the tumor capability of activating effective mechanisms of defence against both chemical and physical cytotoxic agents represents a serious obstacle to the successful therapy of human tumors (1). Therefore, the possibility to have an assay useful to measure the drug sensitivity of tumor cells has a great importance (2-4).

A number of cytotoxicity assays are currently available, each of them using specific approach to detect different aspects of cell viability, such as cell integrity, proliferation and metabolic functions (5). As primary human colon cancer cultures from fresh

Key words: ATP luminescence Assay, MTT Assay, CCK-8 assay, chemosensitivity, 5-fluorouracil, oxaliplatin, cell lines

Mailing address: Prof. Rita Consolini,
Department of Reproductive Medicine,
and Child Development, Division of Pediatrics,
Laboratory of Immunology,
University of Pisa, Via Roma 67, 56126 Pisa, Italy
Fax: +39 050 888622 Tel: +39 050 992222
e-mail: rita.consolini@med.unipi.it

0393-974X (2013)

tumor are technically difficult to obtain, experiments with human cancer cell lines remain essential to explore new adjuvant chemotherapy drugs as well to investigate the individual responsiveness to the known agents (2, 6, 7).

The purpose of this study is to compare, under identical experimental conditions, three common cytotoxicity assays (ATP-lite, MTT and CCK-8 assays) in the assessment of the anti-proliferative effects of 5-fluorouracil (5-FU) and oxaliplatin (OHP) on three colon cancer cell lines (WiDr, SW620 and HT-29).

As cellular ATP is the most important chemical energy reservoir in cells and is used for biological synthesis, signalling, transport, and movement processes, it represents one of the most sensitive end points in measuring cell viability (8-10). Its intracellular concentration rapidly decreases when the cell undergoes necrosis or apoptosis.

The MTT assay is based on the cleavage of the yellow tetrazolium salt MTT (3-[4,5-dimethylthiazol-2-yl]-2,5-diphenyltetrazolium bromide), an insoluble formazan, to purple formazan crystals by mitochondrial succinate dehydrogenases of metabolic active cells. This cellular reduction involves the pyridine nucleotide cofactors NADH and NADPH (11).

The Cell Counting Kit-8 (CCK-8) allows sensitive colorimetric assays for the determination of cell viability in cell proliferation and cytotoxicity assays. Dojindo's highly water-soluble tetrazolium salt, 2-(2-methoxy-4-nitrophenyl)-3-(4-nitrophenyl)-5-(2,4-disulfophenyl)-2H-tetrazoliummonosodium salt (WST-8), is reduced by dehydrogenase activities in cells to give a yellow-color formazan dye, which is soluble in the tissue culture media. The amount of the formazan dye, generated by the activities of dehydrogenases in cells, is directly proportional to the number of living cells. So, CCK-8 can be used in a similar way to MTT with the advantage of formation of water-soluble formazans (5).

All these methods, widely used, measure the metabolic activity of the cells, each of them using a different endpoint to assess cell viability: ATP, break down of ATP production; MTT and CCK-8, activity of mitochondrial dehydrogenases. In the literature, the choice of the cytotoxicity method seems to be a debatable issue.

In our work we demonstrate that the CCK-8 is the most sensitive assay for detecting changes of cell viability, suggesting that differences among the three assays depend on the mechanism of action of the drug employed, the type of cell and the fundamental physical properties measured by the assay used.

MATERIALS AND METHODS

Cell lines

WiDr, HT-29 and SW620 human colon cancer cell lines were a gift of Prof. Danesi R. (Department of Oncology and New Technology of Transplant, Pisa University). These cell lines differ in their malignant potential and their responsiveness to drugs: SW620 cell line isolated from metastasis of primary adenocarcinoma of colon into lymph node, has fully developed invasive and metastatic potential (5,12,13); HT-29 cell line, isolated from adenocarcinoma of colon grade 1, is moderately differentiated with low-metastatic potential (5,14,15); WiDr cells, established from a moderately differentiated primary rectosigmoid adenocarcinoma, are demonstrated non metastatic (15).

The cells were grown in monolayer cultures in RPMI-1640 medium (Gibco Loboratoire, Milano, Italy) supplemented with 10% fetal bovine serum (FBS), 2 mM L-glutamine (Cambrex BioScience Inc., Baltimore, USA), 100 IU/ml penicillin (Pharmacia & Upjohn SpA, Milano, Italy),100 µg/ml streptomycin (Bristol-Myers Squibb SpA, Sermoneta (LT), Italy). Cells were cultivated in 75 cm^2 tissue culture flasks (Greiner Bio-One, Germany), at 37°C in 5% CO_2. After reaching confluence, cells were detached with 0.05% trypsin-0.02% ethylenediaminetetraacetic acid (EDTA; Carlo Erba Reagents, Milano, Italy).

Drugs

5-FU and OHP were generous gifts from the Hospital Pharmacy (Santa Chiara, Pisa University).

5-FU and OHP stock solutions were prepared in physiological and 5% glucosate solutions respectively and stored at -20°C prior to use.

Individual drug cytotoxicity assays

The cytotoxicity was assessed using three commercially available kits: the ATP-lite (PerkinElmer, Boston USA), the MTT (Cell Proliferation Kit I; Roche Diagnostic GmbH, Germany) and the Cell Counting Kit-8 (CCK-8; BioChemika, Fluka Chemical Corp. Milwaukee, WI, USA). In order to reduce variability, cells were cultured under identical experimental conditions. Briefly, cells ($1x10^4$ cells/well) were seeded in 96-well Packard viewplate and incubated for 24 h at 37°C at 100% humidity

in 5% CO_2 atmosphere. After 24 h, cells were exposed to the individual drugs or to growth medium (controls) for three different times of continuous exposure (24, 48 and 72 h). We employed the drugs at six different doses, in order to obtain a good discrimination in the spectrum of growth inhibition (5-FU: 6, 12, 24, 48, 96, 192 μM and OHP: 0.01, 0.05, 0.1, 0.5, 1, 5 μM).

As the goal of the study was to compare the sensibility of three cytotoxic assays and not to put in evidence the known cytotoxic effect of OHP, we chose to perform the experiments using the above doses, which are the lowest ones reported in the literature (7, 16, 17).

Six experiments were performed using three replicated wells for each drug concentration and carried out independently three times.

At the end of the treatment periods (24, 48 and 72 h), the microplates were washed twice with Hank's balanced saline solution (HBSS, Cambrex) and the evaluation of cellular cytotoxicity was performed by comparing the following three assays.

ATP-lite assay. The ATP-lite is a luminescence assay based on the reaction of luciferin to oxyluciferin catalyzed by the enzyme luciferase in the presence of Mg^{2+} ions and ATP yielding a luminescent signal. Under aerobic condition, the luciferase catalyzes the reaction of luciferin and ATP which leads to the production of AMP and oxiluciferin; the resulting light has an emission maximum at 562 nm and the amount of light produced can be quantified in a microplate luminometer. In optimal conditions the relation between luminescence and ATP content is linear, so it can be used as an index of cell viability (10).

Cellular ATP was extracted by a detergent-based cell extraction reagent. A volume of 50 μl of luciferin-luciferase substrate buffer solution was then added. An ATP standard curve was performed for all studies using dilution series of the ATP standard solution (10 mM) from a concentration of 1 x 10^{-5} M down to blank.

MTT assay. The formazan product is impermeable to the cell membranes and therefore it accumulates in healthy cells. Therefore, the formazan crystals formed must be solubilized and the resulting colored solution is quantified using a scanning multiwell spectrophotometer. Since reduction of MTT can only occur in metabolically active cells the intensity of colour of the dissolved formazan is proportional to the number of viable cells (18).

At the end of the drug exposure, 10 μl of MTT solution was added to each well and incubated for 4 h at 37°C, 100% humidity, in 5% CO_2 atmosphere; then 100 μl of solubilizing buffer (10% sodium dodecyl sulphate dissolved in 0.01 M HCl) was added. After overnight incubation, the 96-well plate was read by an enzyme-linked immunosorbent assay (ELISA) reader at 570 nm for absorbance density values to determine the cell viability.

CCK-8 assay. The CCK-8 assay uses a formazan substrate, the WST-8 salt, that is highly water-soluble differing from MTT.

At the end of incubation, cells were exposed to medium with 10 μl of CCK-8, incubated for 4 h at 37°C at 100% humidity in 5% CO_2 atmosphere and the plate was read by an enzyme-linked immunosorbent assay (ELISA) reader at 450 nm for absorbance density values to determine the cell viability.

Since the absorbance at 460 nm is proportional to the number of viable cells in the medium, the viable cell number can be determined using the absorbance value of a previously prepared calibration curve.

Data obtained from each assay were transferred directly to a spreadsheet and elaborated using a data analysis program (Excel 2000, Microsoft). Results were expressed as percent cell viability. The percent cell viability for each drug concentration was calculated by the following formula: % viability= (reflection of the number of viable treated cells/ reflection of the number of viable control cells)x100.

Statistical analyses

All statistical calculations were performed using a personal computer (GraphPAD software, San Diego, CA). Correlations between ATP-lite and CCK-8, ATP-lite and MTT, MTT and CCK-8 were determined by linear regression analysis. Data were expressed as mean ± standard error of the mean (SEM). Statistical significance of the differences was evaluated by the paired (when compared with corresponding control) or unpaired 2-tailed Student's t-test. An association was considered statistically significant when the value was $p<0.05$.

RESULTS

Cell viability of WiDr, HT-29 and SW620 cells, exposed to six different concentrations of 5-FU for 24, 48 and 72 h, was determined with the ATP-lite, MTT and CCK-8 assay, in order to compare the different outcomes of the three cytotoxicity assays (Fig. 1 and Table I).

After 24-h exposure a weak loss of cell viability was notable with either CCK-8 or ATP-lite assay. After 48 h exposure, the IC50 values in all cell lines were restricted to the CCK-8 assay; on the contrary, by using the ATP-lite or the MTT assay the IC50 values were found only for the WiDr or the WiDr and HT-29 cells, respectively. The increase of the exposure time reduced cell viability and all the

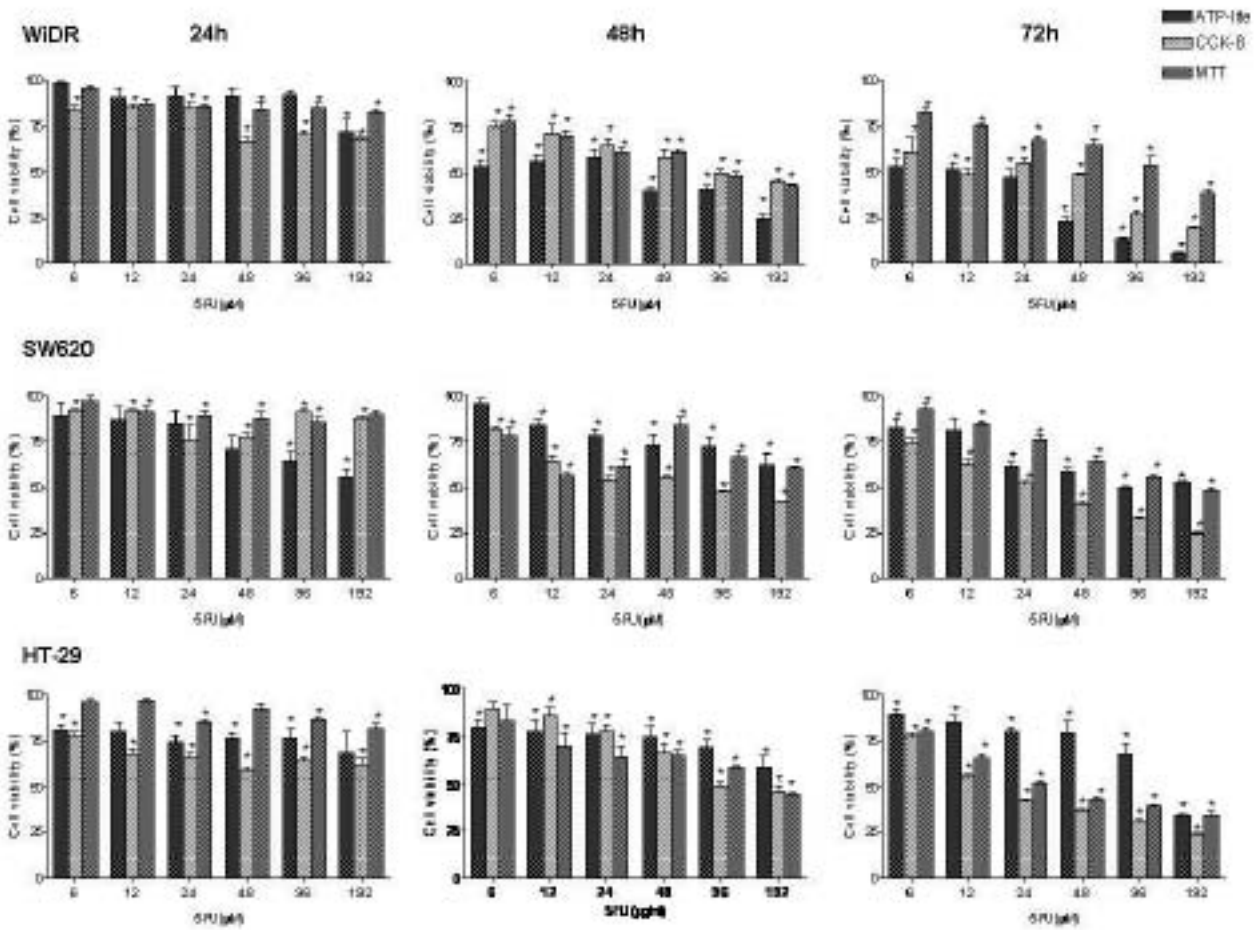

Fig. 1. *Effects of 5-FU at concentrations of 0.01-5 μM on WiDr, SW620 and HT-29 cells as measured by ATP-lite, CCK-8 and MTT assay. Data represent mean values ± standard error (SEM) of the percent cell survival at the different times of exposure. The percent cell viability was calculated by the following formula: % viability= (reflection of the number of viable treated cells/ reflection of the number of viable control cells)x100. Each experiment was performed using three replicated wells for each drug concentration and carried out independently three times. * represent statistically significant decrease of values compared to controls at p<0.05 with Student's t-test.*

assays provided IC50 values after a 72-h incubation period.

Following exposure of WiDr cells to 5-FU for 48 h and 72 h, the ATP assay appears to be more sensitive in detecting loss of viability compared to the other two assays employed. Moreover after a 72-h incubation period, the IC50 values obtained by the MTT assay were found to be about 6.7- and 3.97-fold increased respectively, compared to those found by the ATP and CCK-8 assays. On the contrary, the most significant decrease in cell viability in SW620 and HT-29 cells was observed with the CCK-8 assay compared to MTT or ATP assay. In particular, the IC50 values found with ATP and MTT assays were 3.6-, 5.9- and 7.5-, 1.7-fold increased in SW620 cells and HT-29 cells respectively.

When the inhibitions at six different 5-FU concentrations were analyzed to determine any correlation among the assays, it was found that the drug caused lower correlation coefficients in WiDr and HT-29 cells compared to SW620 cells; these values reached the same statistically significant level in all cell lines (Fig. 2). The study of the correlation between the assays was performed after 72 h of drug exposure, which is a time point often used in the literature. In WiDr cells the analysis showed a moderate/high degree of correlation between ATP and CCK-8 assays ($r=0.76$, $p<0.0001$) and a lower

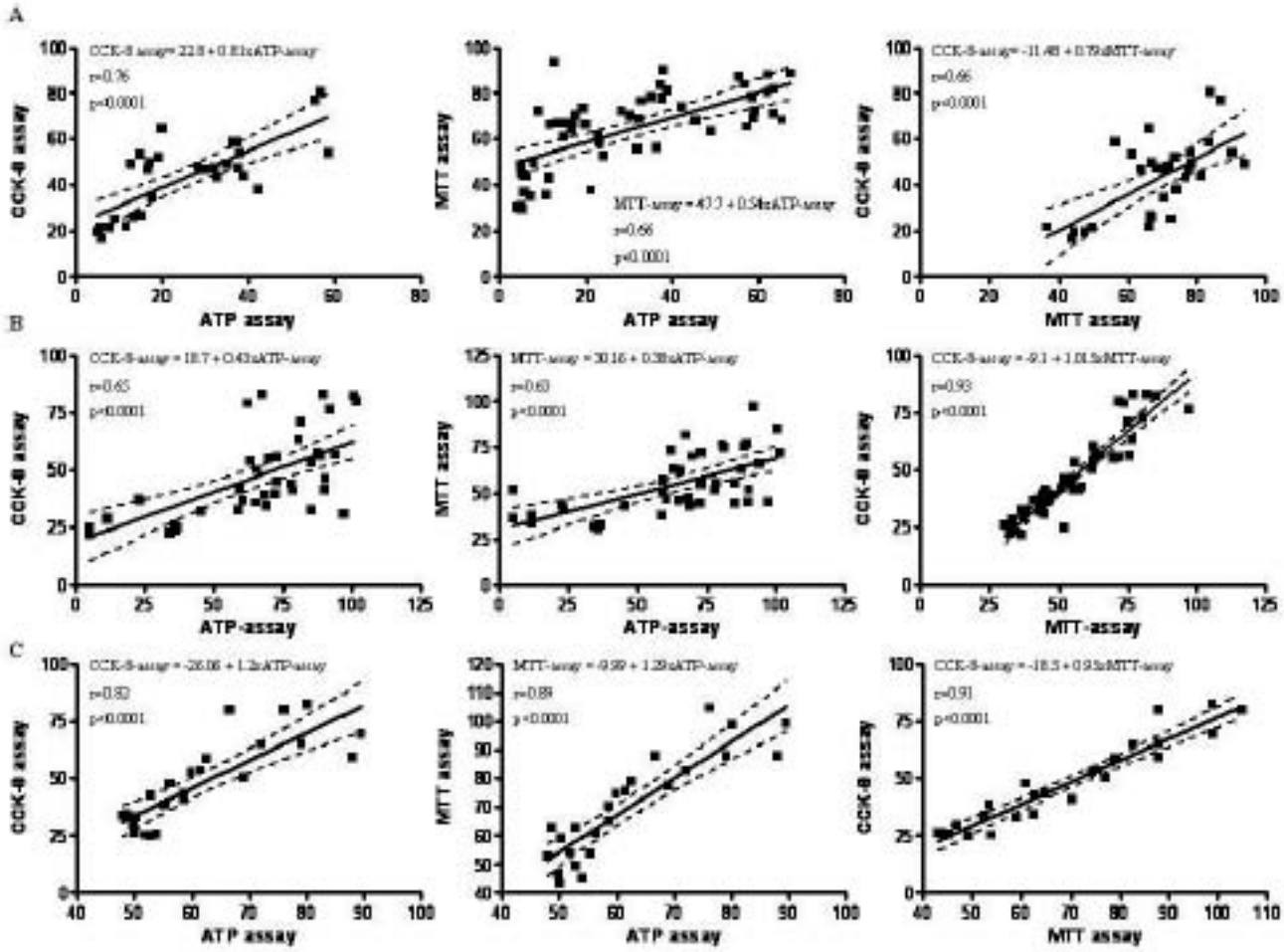

Fig. 2. *Correlation among the cytotoxic effect of ATP-lite, CCK-8 and MTT after 5-FU exposure of WiDr (**A**), HT-29 (**B**) and SW620 (**C**) cells. Dotted lines represent the 95% confidence intervals for the regression line.*

degree of correlation between ATP and MTT or between CCK-8 and MTT (r=0.66; p<0.0001). In HT-29 cells, a similar degree of correlation was observed between ATP and CCK-8 assay or between ATP and MTT assay (r=0.65 and 0.63, respectively; p<0.0001), whereas a high degree was observed between MTT and CCK-8 assay (r=0.93; p<0.0001). Finally, in SW620 cells the correlation among the assays was found to be always high (r>0.8 in all; p<0.0001).

Fig. 3 shows the different sensitivities of the three cell lines to OHP evaluated with ATP, CCK-8 and MTT-assay. Results indicated that the WiDr cells were scarcely sensitive to OHP exposure, being cell viability always higher than 50%. As shown in Table I, in SW620 cells either CCK-8 or MTT-assay showed an inhibitory effect after 72 h of continuous exposure reaching IC50 levels of 0.39 and 0.65 μM, respectively. In HT-29 cells the CCK-8 assay resulted the only assay giving an IC50 value at both 48 and 72 h of continuous exposure (3.63 and 3.55 μM, respectively).

We found no or low correlation among the assays when OHP was employed in the WiDr cell line; the correlation coefficient between either ATP and CCK-8 or ATP and MTT assays was moderate when the drug was employed in the HT-29 cells (r=-0.55 or r=-0.52 respectively), and in the SW620 cells (r=0.62 or

Table I. *IC50 values for WiDr, SW620 and HT-29 cells following continuous exposure either to 5-FU or to OHP for 48 and 72 h based on the dose-response curves as derived from the ATP-lite assay, the CCK-8 assay and the MTT assay.*

Cell line	Times	IC50 (μM)					
		ATP-lite		MTT		CCK-8	
		5-FU	OHP	5-FU	OHP	5-FU	OHP
WiDR	48h	35.48	-	89.12	-	104.7	-
	72h	16	-	107	-	26.9	-
SW620	48h	-	-	-	-	50.1	-
	72h	98	-	158.5	0.65	26.9	0.39
HT-29	48h	-	-	141.2	-	120.2	3.63
	72h	122	-	27.5	-	16.2	3.55

(-) indicates no IC50 values obtained for the corresponding incubation periods with the assay employed.

r=0.69). Conversely, a good correlation coefficiency (r=0.97 and r=0.72) was found between CCK-8 and MTT assay when OHP was used in SW620 and HT-29 cell lines respectively (Fig. 4).

DISCUSSION

The determination of cellular proliferation, viability and activation are key areas in a wide variety of cell biological approaches. Therefore the need for sensitive, quantitative, reliable and automated methods led to the development of standard assays for this proposal. In the particular field of cancer research, there are a number of tests to assess the anti-growth effects of chemotherapeutic agents *in vitro*. These current assays measure distinct cell growth and metabolism related endpoints such as the enzymatic activity, integrity of cellular membranes, DNA synthesis, ATP status, etc. (5). However, the expression, the cellular localization and the activity of intracellular enzymes may show profound changes in various cells. Thus, as many significant differences among the assays are reported, depending on the drug used, on the supposed cell death mechanism and on the type of cell, the choice of a cytotoxicity method represents a debatable issue in the literature.

Additionally, as the goal of chemotherapy is to utilize an agent that is the most effective in cell cancer destruction, while sparing patient toxicity, a diagnostic assay capable of determining the cytotoxic response also to a low drug concentration could help to improve the choice of the treatment.

The intention of the present study was to compare three common assays: the ATP-lite, the MTT and the CCK-8, in the evaluation of the cellular response of three different colon cancer cell lines, representing individual steps of tumorigenesis, to 5-FU and OHP. Thus, we used two chemotherapeutic drugs, whose cytotoxic effect is known, at the doses, which are the lowest ones reported in the literature (7, 16, 17).

The ATP serves as the principal immediate donor of energy and is present in all metabolically active cells. Measurement of ATP is fundamental to the study of living process. Multiple distinct anticancer drugs reduce the intracellular concentration of ATP before and during the manifestation of apoptotic characteristics such as the dissipation of the mitochondrial transmembrane potential and the exposure of phosphatidylserine residues on the plasma membrane. Indeed, as apoptosis progresses, intracellular ATP concentrations decrease, although even advanced-stage apoptotic cells still contain sizeable ATP levels. Only when cells enter secondary necrosis, the ATP concentration falls to undetectable

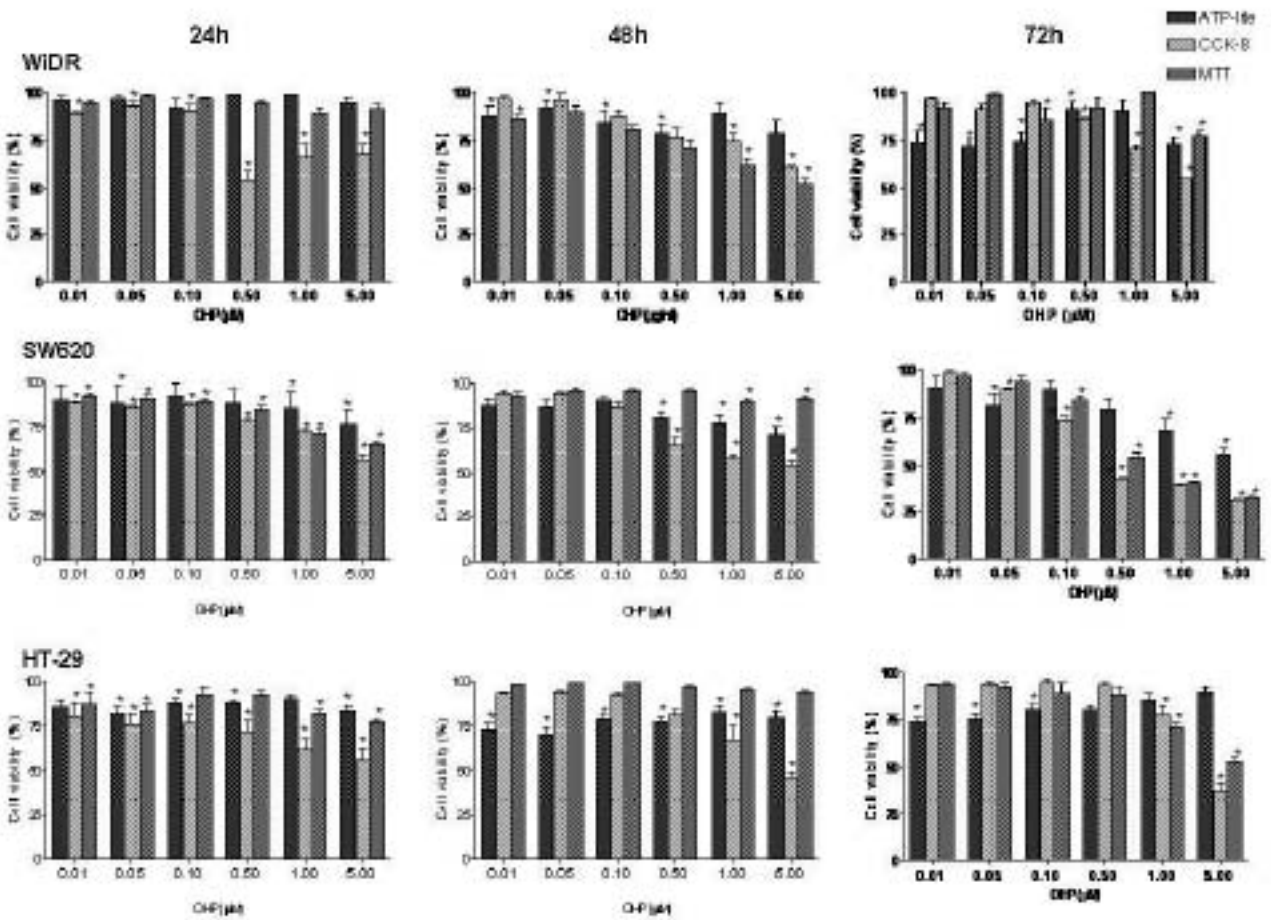

Fig. 3. *Effects of OHP at the concentrations of 0.01-5 μM on WiDr, SW620 and HT-29 cells as measured by ATP-lite, CCK-8 and MTT assay. Data represent mean values ± standard error (SEM) of the percent cell survival at the different times of exposure. The percent cell viability was calculated by the following formula: % viability= (reflection of the number of viable treated cells/ reflection of the number of viable control cells)x100. Each experiment was performed using three replicated wells for each drug concentration and carried out independently three times. * represent statistically significant decrease of values compared to controls at p<0.05 with Student's t-test.*

levels (19-21).

The MTT assay quantifies mitochondrial activity by measuring the formation of a dark blue formazan product formed by the reduction of the tetrazolium ring of MTT. The reduction of MTT was thought to mainly occur in the mitochondria through the action of succinate dehydrogenase but a number of other non-mitochondrial enzymes are implicated (22-24).

Comparing the cost of the two assays, the MTT is comparatively cheaper as well as the more frequently used, while ATP assay is technologically more advanced due to its luminescence-based methodology, and allows measurements of *in vitro* toxicity to be made with considerable precision (8, 21, 23).

In our study, ATP-lite assay failed to detect cytotoxic effect of OHP on all cell lines. These results were presumably related to the induced apoptotic effect of OHP, whereas the cells still maintain ATP concentration. The fact that OHP forms mainly intrastrand links between two adjacent guanine residues, disrupting DNA replication and transcription, as described by Nannizzi et al., can further explain this failure (25-27).

The CCK-8 assay uses a formazan substrate, the WST-8 salt, that is highly water-soluble differing

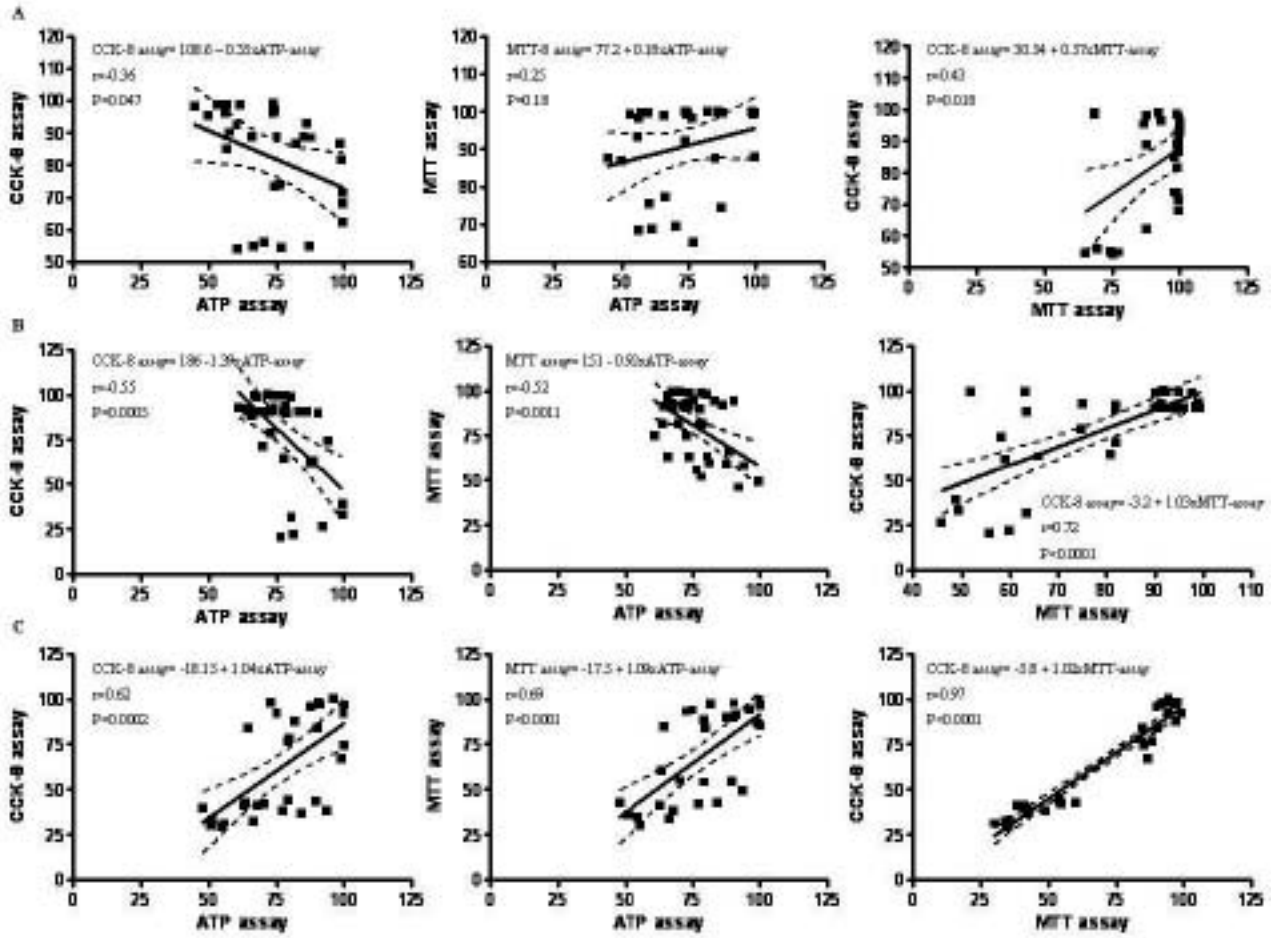

Fig. 4. *Correlation among the cytotoxic effect of ATP-lite, CCK-8 and MTT after OHP exposure of WiDr (**A**), HT-29 (**B**) and SW620 (**C**) cells. Dotted lines represent the 95% confidence intervals for the regression line.*

from MTT. Thus, the necessity of the extraction of the formed MTT formazan makes this method more laborious, time-consuming and less sensitive than CCK-8 assay.

Regarding 5-FU, the three assays were found in our study to be significantly correlated with a moderate or high correlation coefficient. The same results were previously described between the ATP and MTT assay (8, 28). Conversely, in the case of OHP we found different outcomes among the assays: the coefficiency correlation ranged from its absence (e.g. in the WiDr cells) to high value. We suggest that these discrepancies depend on the mechanism of action of the drug employed, the type of cell and the fundamental physical properties measured by the assay used, according to a previous report (8).

As the analysis of the correlation among the assays is not the sole parameter in comparing the methods, in our study we evaluated the differences in the growth inhibition. This aspect reflects the physical properties measured by the assay used. It has been reported that the dying cells lose relatively less dehydrogenase activity than ATP (8). Thus, the MTT assay may overestimate the viability as the cells still retain, to some extent, formazan although they are dying, which is evidenced by the decrease in the ATP level. This assumption may explain the relatively higher percentage of WiDr cell viability found in our study, when MTT assay was used to evaluate the responsiveness to 5-FU.

Although both MTT and CCK-8 measure the inhibition of dehydrogenase activity, our results

demonstrated substantial difference between the IC50 values. In fact, for the fluorouracil, the IC50 values calculated with MTT assay were higher then those ones calculated in CCK-8 assay.

In summary, our study demonstrates that the CCK-8 is the most sensitive assay for detecting changes of cell viability, suggesting that the cell viability measured after drug exposure depends on several parameters like the drug used, the biological characteristics of the target cell and the specific approach employed by the method to detect distinct cell growth and metabolic functions.

REFERENCES

1. Hatok J, Babusikova E, Matakova T, Mistuna D, Dobrota D, Racay P. In vitro assays for the evaluation of drug resistance in tumor cells. Clin Exp Med 2009; 9:1-7.
2. Failli A, Consolini R, Legitimo A, Spisni R, Castagna M, Romanini A, Crimaldi G, Miccoli P. The challenge of culturing human colorectal tumor cells: establishment of a cell culture model by the comparison of different methodological approaches. Tumori 2009; 95:343-47.
3. Luca T, Privitera G, Lo Monaco M, Prezzavento C, Castorina S. Validation study of a cell culture model of colorectal cancer. Ital J Anat Embryol 2007; 112:81-92.
4. Oikonomou E, Kothonidis K, Zografos G, Nasioulas G, Andera L, Pintzas A. Newly established tumourigenic primary human colon cancer cell lines are sensitive to TRAIL- induced apoptosis in vitro and in vivo. Br J Cancer 2007; 97:73-84.
5. Schröterová L, Králová V, Voráčová A, Hašková P, Rudolf E, Červinka M. Antiproliferative effects of selenium compounds in colon cancer cells: comparison of different cytotoxicity assays. Toxicol in Vitro 2009; 23:1406-11.
6. Dangles-Marie V, Pocard M, Richon S, et al. Establishment of human colon cancer cell lines from fresh tumors versus xenografts: comparison of success rate and cell line features. Cancer Res 2007; 67:398-407.
7. Failli A, Consolini R, Legitimo A, Orsini G, Romanini A, Spisni R, Castagna M, Miccoli P. Evaluation of in vitro cytotoxicity of oxaliplatin and 5-fluorouracil in human colon cancer cell lines: combination versus sequential exposure. J Biol Regul Homeost Agents 2011; 25:575-88.
8. Ulukaya E, Ozdikicioglu F, Oral AY, Demirci M. The MTT assay yields a relatively lower result of growth inhibition than the ATP assay depending on the chemotherapeutic drugs tested. Toxicol In Vitro 2008; 22:232-9.
9. Maehara Y, Anai, H, Tamada, R, Sugimachi, K. The ATP assay is more sensitive than the succinate-dehydrogenase inhibition test for predicting cell viability. Eur J Cancer Clin Oncol 1987; 23:273-6.
10. Zhang W, Liu ES, Fu J, Tian HM, Wu YJ, Pang SF. Suppression of primary breast, colon, gastric and bladder cancers cell growth in vitro by CKBM, a natural product. Invest New Drugs 2006; 24:181-7.
11. Berridge VM, Tan SA. Characterization of the cellular reduction of 3-(4,5-dimethylthiazol-2-yl)-2,5-diphenyltetrazolium bromide (MTT): subcellular localization, substrate dependence, and involvement of mitochondria electron transport in MTT reduction. Arch Biochem Biophys 1992; 303:474-82.
12. Leibovitz A, Stinson JC, McCombs 3rd WB, McCoy CE, Mazur KC, Mabry ND. Classification of human colorectal adenocarcinoma cell lines. Cancer Res 1976; 36:4562-69.
13. Subauste MC, Kupriyanova TA, Conn EM, Ardi VC, Quigley JP, Deryugina EI. Evaluation of metastatic and angiogenic potentials of human colon carcinoma cells in chick embryo model system. Clin Exp Metastasis 2009; 26:1033-47.
14. Fogh J, Trempe G. New Human Tumor Cell Lines. In Human Tumor Cells in Vitro. Plenum Press New York, 1975; 115-60.
15. Wang M, Vogel I, Kalthoff H. Correlation between metastatic potential and variants from colorectal tumor cell line HT-29. World J Gastroenterol 2003; 9:2627-31.
16. Kornmann M, Fakler H, Butzer U, Beger HG, Link KH. Oxaliplatin exerts potent in vitro cytotoxicity in colorectal and pancreatic cancer cell lines and liver metastases. Anticancer Res 2000; 20:3259-64.
17. Noordhuis P, Laan AC, van de Born K, Losekoot N, Kathmann I, Peters GJ. Oxaliplatin activity in selected and unselected human ovarian and colorectal cancer cell lines. Biochem Pharmacol 2008; 76:53-

61.
18. Mosmann T. Rapid colorimetric assay for cellular growth and survival: application to proliferation and cytotoxicity assays. J Immunol Methods 1983; 65:55-63.
19. Martins I, Tesniere A, Kepp O, et al. Chemotherapy induces ATP release from tumor cells. Cell Cycle 2009; 8(22):3723-8.
20. Cree IA, Kurbacher CM, Untch M, et al. Correlation of clinical response to chemotherapy in breast cancer with ex vivo chemosensitivity. Anticancer Drugs 1996; 7:630-35.
21. Cree IA, Andreotti PE. Measurement of cytotoxicity by ATP-based luminescence assay in primary cell cultures and cell lines. Toxicol In Vitro 1997; 11:553-6.
22. Lobner D. Comparison of the LDH and MTT assays for quantifying cell death: validity for neuronal apoptosis? Journal of Neuroscience methods 2000; 96:147-152.
23. Martinez-Martos JM, Ramirez-Exposito MJ, Mayas-Torres MD, Garcia-Lopez MJ, Ramirez-Sanchez M. Utility of the 3-(4,5-dimethylthiazol-2-yl)-2,5-diphenyl tetrazolium bromide (MTT) assay to measure mitochondrial activity in K+ and ATP-stimulated rodent cortex synaptosomes. Neurosci Res Commun 2000; 27:103-07.
24. Nakamura R, Saikawa Y, Kubota T, et al. Role of the MTT chemosensitivity test in the prognosis of gastric cancer patients after postoperative adjuvant chemotherapy. Anticancer Res 2006; 26:1433-37.
25. Nannizzi S, Veal GJ, Giovannetti E, Mey V, Ricciardi S, Ottley CJ, Del Tacca M, Danesi R. Cellular and molecular mechanisms for the synergistic cytotoxicity elicited by oxaliplatin and pemetrexed in colon cancer cell lines. Cancer Chemother Pharmacol 2009; 66:547-58.
26. Tanaka R, Ariyama H, Qin B, Takii Y, Baba E, Mitsugi K, Harada M, Nakano S. In vitro schedule-dependent interaction between paclitaxel and oxaliplatin in human cancer cell lines. Cancer Chemother Pharmacol 2005; 55:595-01.
27. Jennerwein MM, Eastman A, Khokhar A. Characterization of adducts produced in DNA by isomeric 1,2-diaminocyclohexane platinum(II) complexes. Chem Biol Interact 1989; 70:39-49
28. Hazary RC, Chaudhuri D, Wishart GJ. Application of an MTT reduction assay for assessing sperm quality and predicting fertilising ability of domestic fowl semen. Br Poult Sci 2001; 42:115-17.

Vol. 25, No 3, July - September 2012

ISSN 0394-6320/2012

IMPACT FACTOR 2.991

International Journal of Immunopathology and Pharmacology

Lorenzo Lotto - "Portrait of Giovane"

Published by Biolife

www.biolifesas.org

Vol. 10, No 3, September - December 2012

ISSN 1721-727X

IMPACT FACTOR 5.233

European Journal of Inflammation

Official Journal of the Italian Society of Oral Pathology and Medicine

Published by
Biolife

www.biolifesas.org